Contributions to multidisciplinary design optimization under uncertainty, application to launch vehicle design.

L. Brevault

École Nationale Supérieure des Mines de Saint-Étienne

Thèse de Doctorat

Spécialité: Mathématiques appliquées

présenté et soutenue publiquement par

Loïc BREVAULT

le 06 octobre 2015

à l'Office National d'Études et de Recherches Aérospatiales

Contributions à l'optimisation multidisciplinaire sous incertitudes, application à la conception de lanceurs

(Contributions to Multidisciplinary Design Optimization under uncertainty, application to launch vehicle design)

Jury

Président:	
Jean Antoine Désidéri	Directeur de recherche, *INRIA, Sophia-Antipolis*
Rapporteurs:	
Rajan Filomeno Coelho	Assistant Professor HDR, *Université libre de Bruxelles*
Joaquim R. R. A. Martins	Professor of Aerospace Engineering, *University of Michigan*
Examinateurs:	
Raphael T. Haftka	Professor of Aerospace Engineering, *University of Florida*
Rodolphe Le Riche	Directeur de recherche, *CNRS*
Mathieu Balesdent	Docteur ingénieur, *Onera*
Invités:	
Nicolas Bérend	Ingénieur, *Onera*
Olivier Deslandes	Ingénieur, *CNES*

Directeur de thèse:	Rodolphe Le Riche
Encadrants Onera:	Mathieu Balesdent et Nicolas Bérend
Laboratoires:	Office National d'Études et de Recherches Aérospatiales
	Institut Henri Fayol

NNT: 2015 EMSE 0792

Spécialités doctorales	Responsables :	Spécialités doctorales	Responsables
SCIENCES ET GENIE DES MATERIAUX	K. Wolski Directeur de recherche	MATHEMATIQUES APPLIQUEES	O. Roustant, Maître-assistant
MECANIQUE ET INGENIERIE	S. Drapier, professeur	INFORMATIQUE	O. Boissier, Professeur
GENIE DES PROCEDES	F. Gruy, Maître de recherche	IMAGE, VISION, SIGNAL	JC. Pinoli, Professeur
SCIENCES DE LA TERRE	B. Guy, Directeur de recherche	GENIE INDUSTRIEL	A. Dolgui, Professeur
SCIENCES ET GENIE DE L'ENVIRONNEMENT	D. Graillot, Directeur de recherche	MICROELECTRONIQUE	S. Dauzere Peres, Professeur

EMSE : Enseignants-chercheurs et chercheurs autorisés à diriger des thèses de doctorat (titulaires d'un doctorat d'État ou d'une HDR)

ABSI	Nabil	CR	Génie industriel	CMP
AVRIL	Stéphane	PR2	Mécanique et ingénierie	CIS
BALBO	Flavien	PR2	Informatique	FAYOL
BASSEREAU	Jean-François	PR	Sciences et génie des matériaux	SMS
BATTAIA-GUSCHINSKAYA	Olga	CR	Génie industriel	FAYOL
BATTON-HUBERT	Mireille	PR2	Sciences et génie de l'environnement	FAYOL
BERGER DOUCE	Sandrine	PR2	Sciences de gestion	FAYOL
BIGOT	Jean Pierre	MR(DR2)	Génie des Procédés	SPIN
BILAL	Essaid	DR	Sciences de la Terre	SPIN
BLAYAC	Sylvain	MA(MDC)	Microélectronique	CMP
BOISSIER	Olivier	PR1	Informatique	FAYOL
BONNEFOY	Olivier	MA(MDC)	Génie des Procédés	SPIN
BORBELY	Andras	MR(DR2)	Sciences et génie des matériaux	SMS
BOUCHER	Xavier	PR2	Génie Industriel	FAYOL
BRODHAG	Christian	DR	Sciences et génie de l'environnement	FAYOL
BRUCHON	Julien	MA(MDC)	Mécanique et ingénierie	SMS
BURLAT	Patrick	PR1	Génie Industriel	FAYOL
COURNIL	Michel	PR0	Génie des Procédés	DIR
DAUZERE-PERES	Stéphane	PR1	Génie Industriel	CMP
DEBAYLE	Johan	CR	Image Vision Signal	CIS
DELAFOSSE	David	PR0	Sciences et génie des matériaux	SMS
DELORME	Xavier	MA(MDC)	Génie industriel	FAYOL
DESRAYAUD	Christophe	PR1	Mécanique et ingénierie	SMS
DOLGUI	Alexandre	PR0	Génie Industriel	FAYOL
DRAPIER	Sylvain	PR1	Mécanique et ingénierie	SMS
FAVERGEON	Loïc	CR	Génie des Procédés	SPIN
FEILLET	Dominique	PR1	Génie Industriel	CMP
FRACZKIEWICZ	Anna	DR	Sciences et génie des matériaux	SMS
GARCIA	Daniel	MR(DR2)	Génie des Procédés	SPIN
GAVET	Yann	MA(MDC)	Image Vision Signal	CIS
GERINGER	Jean	MA(MDC)	Sciences et génie des matériaux	CIS
GOEURIOT	Dominique	DR	Sciences et génie des matériaux	SMS
GONDRAN	Natacha	MA(MDC)	Sciences et génie de l'environnement	FAYOL
GRAILLOT	Didier	DR	Sciences et génie de l'environnement	SPIN
GROSSEAU	Philippe	DR	Génie des Procédés	SPIN
GRUY	Frédéric	PR1	Génie des Procédés	SPIN
GUY	Bernard	DR	Sciences de la Terre	SPIN
HAN	Woo-Suck	MR	Mécanique et ingénierie	SMS
HERRI	Jean Michel	PR1	Génie des Procédés	SPIN
KERMOUCHE	Guillaume	PR2	Mécanique et Ingénierie	SMS
KLOCKER	Helmut	DR	Sciences et génie des matériaux	SMS
LAFOREST	Valérie	MR(DR2)	Sciences et génie de l'environnement	FAYOL
LERICHE	Rodolphe	CR	Mécanique et ingénierie	FAYOL
LI	Jean-Michel		Microélectronique	CMP
MALLIARAS	Georges	PR1	Microélectronique	CMP
MAURINE	Philippe	Ingénieur de recherche	Microélectronique	CMP
MOLIMARD	Jérôme	PR2	Mécanique et ingénierie	CIS
MONTHEILLET	Frank	DR	Sciences et génie des matériaux	SMS
MOUTTE	Jacques	CR	Génie des Procédés	SPIN
NEUBERT	Gilles	PR	Génie industriel	FAYOL
NIKOLOVSKI	Jean-Pierre	Ingénieur de recherche		CMP
NORTIER	Patrice	PR1		SPIN
OWENS	Rosin	MA(MDC)	Microélectronique	CMP
PICARD	Gauthier	MA(MDC)	Informatique	FAYOL
PIJOLAT	Christophe	PR0	Génie des Procédés	SPIN
PIJOLAT	Michèle	PR1	Génie des Procédés	SPIN
PINOLI	Jean Charles	PR0	Image Vision Signal	CIS
POURCHEZ	Jérémy	MR	Génie des Procédés	CIS
ROBISSON	Bruno	Ingénieur de recherche	Microélectronique	CMP
ROUSSY	Agnès	MA(MDC)	Génie industriel	CMP
ROUSTANT	Olivier	MA(MDC)	Mathématiques appliquées	FAYOL
ROUX	Christian	PR	Image Vision Signal	CIS
STOLARZ	Jacques	CR	Sciences et génie des matériaux	SMS
TRIA	Assia	Ingénieur de recherche	Microélectronique	CMP
VALDIVIESO	François	PR2	Sciences et génie des matériaux	SMS
VIRICELLE	Jean Paul	DR	Génie des Procédés	SPIN
WOLSKI	Krzystof	DR	Sciences et génie des matériaux	SMS
XIE	Xiaolan	PR1	Génie industriel	CIS
YUGMA	Gallian	CR	Génie industriel	CMP

ENISE : Enseignants-chercheurs et chercheurs autorisés à diriger des thèses de doctorat (titulaires d'un doctorat d'État ou d'une HDR)

BERGHEAU	Jean-Michel	PU	Mécanique et Ingénierie	ENISE
BERTRAND	Philippe	MCF	Génie des procédés	ENISE
DUBUJET	Philippe	PU	Mécanique et Ingénierie	ENISE
FEULVARCH	Eric	MCF	Mécanique et Ingénierie	ENISE
FORTUNIER	Roland	PR	Sciences et Génie des matériaux	ENISE
GUSSAROV	Andrey	Enseignant contractuel	Génie des procédés	ENISE
HAMDI	Hédi	MCF	Mécanique et Ingénierie	ENISE
LYONNET	Patrick	PU	Mécanique et Ingénierie	ENISE
RECH	Joël	PU	Mécanique et Ingénierie	ENISE
SMUROV	Igor	PU	Mécanique et Ingénierie	ENISE
TOSCANO	Rosario	PU	Mécanique et Ingénierie	ENISE
ZAHOUANI	Hassan	PU	Mécanique et Ingénierie	ENISE

Mise à jour : 29/06/2015

Acknowledgment

I owe a great amount of thanks to the people who contributed to the achievement of this thesis and I would like to thank them all.

This thesis has been accomplished in the System Design and Performance Evaluation Department (DCPS) at Onera, in collaboration with the CNES Launchers Directorate and the Department DEMO from the Fayol institute at Ecole Nationale Supérieure des Mines de Saint-Etienne. I would like to thank the director of DCPS, Dr. Donath, for giving me the opportunity to achieve this thesis in this stimulating department of Onera.

I would like to thank Prof. J-A. Désidéri who did me the honour of chairing my Ph.D. committee. I express my gratitude to Prof. J.R.R.A. Martins and Prof. R. Filomeno Coelho for reviewing this Ph.D. thesis and for all their remarks that allowed to improve this manuscript. I also thank Prof. R. T. Haftka for accepting to be part of my PhD committee. I would like to acknowledge Dr. Le Riche for agreeing to be my Ph.D. advisor during these three years despite the geographical distance between Ecole Nationale Supérieure des Mines de Saint-Etienne and Onera with teleconference communication cuts every twenty minutes. I thank them for the thought-provoking discussions and expertise that allowed this dissertation to come to fruition.

I would like to thank my Onera supervisor Mr. Bérend and my CNES supervisors, Mr. Oswald and Mr. Deslandes. I also would like to thank Dr. S. Lacaze and Prof. S. Missoum for the very stimulating, although brief, collaboration and for the opportunity to do an internship at the University of Arizona. I also would like to thank Mr. Chocat for his work on CMA-ES. I would like to thank Mr. Defoort for his help on the rocket modeling side and for the beers on the fun side. I would like to thank Mrs. F. Marie for her continuous assistance in navigating the mystifying ways of bureaucracy and paperwork.

I wish to thank my Onera advisor, Dr. M. Balesdent for his guidance and constant support through this difficult but enriching endeavor (both on the work side and the personal side). Mathieu was always available for our research discussions, and offered pointed and extremely helpful advice and guidance. Under his supervision, I have developed my critical thinking and my presentation and writing skills. I am also very grateful for all the opportunities he has given me, such as the collaboration with the University of Arizona and to co-advise an internship at Onera. He also gave me the exceptional opportunity to co-author several book chapters with him, and I am deeply grateful and proud of all these accomplishments and the *élan* that he gave me. Our discussions on personal aspects also help me to understand how important abnegation is.

My years as a graduate student would not have been as fun and interesting without my fellow labmates in DCPS: Arthur for his Sharknado attitude, Rata for her excitement about life, Damien for his coolness, Evrard for keeping the office quiet by sleeping, Pawit for his amazing thaï food, and all the others for their willingness to discuss research ideas, but also for the less serious sides of student life. Special thanks go to my office mate Christelle for accepting to share her office with me, for all her support on the work side and for all the long discussions about how complex but awesome life can be. Moreover, I would especially like to thank Ariane for her irreplaceable support, kindness, understanding and for giving me a new trajectory.

I could not forget to thank my friends Sandie, Audrey, Bruno, Charles, Juliette, Thomas (*gros*), Rémi, Guillaume G, Théo, Jigé, Clément, Arthur, Yves, Fabien, Guillaume A, Sibylline, Juan, Sarah, Alex, Maxou, Manu, Eliott, Julien, Benoit, Pif, Jeff for encouraging me up to the defense. Their contribution might not have been technical, yet it was one of the most crucial.

Last but not least, I would like to thank my parents, my sister and my grandparents, who believed in me and always encouraged me.

Contents

Acronyms

^{2}SMART	Subsets by Support vector Margin Algorithm for Reliability esTimation
AAO	All At Once
ACO	Ant Colony Optimization
ATC	Analytical Target Cascading
BLISS	Bi-Level Integrated System Synthesis
CDF	Cumulative Distribution Function
CE	Cross-Entropy
CEA	Chemical Equilibrium with Applications
(1+1)-CMA-ES	(1+1) - Covariance Matrix Adaptation - Evolution Strategy
CMA-ES	Covariance Matrix Adaptation - Evolution Strategy
CMC	Crude Monte Carlo
CO	Collaborative Optimization
CSSO	Concurrent SubSpace Optimization
CSSUA	Concurrent SubSystem Uncertainty Analysis
DoE	Design of Experiment
ESA	European Space Agency
FORM	First Order Reliability Method
FORM-UUA	First Order Reliability Method - Unified Uncertainty Analysis
FPI	Fixed Point Iteration
GLOW	Gross Lift-Off Weight
GMm	Generalized Max-min
GP	Gaussian Process
GTO	Geostationary Transfer Orbit
IA	Interval Analysis
IDF	Individual Discipline Feasible
IDF-PCE	Individual Discipline Feasible - Polynomial Chaos Expansion
IS	Importance Sampling

KDE	Kernel Density Estimation
LHS	Latin Hypercube Sampling
MCMC	Markov Chain Monte Carlo
MDA	MultiDisciplinary Analysis
MDF	Multi Discipline Feasible
MDO	Multidisciplinary Design Optimization
MHOU	Multi-level Hierarchical Optimization under Uncertainty
MPP	Most Probable failure Point
NAIS	Non parametric Adaptive Importance Sampling
NASA	National Aeronautics and Space Administration
PA	Probability Analysis
PCE	Polynomial Chaos Expansion
PDF	Probability Density Function
PSO	Particle Swarm Optimization
QSD	Quasiseparable Decomposition
RDBO	Reliability-based Design Optimization
RE	Relative Error
RMSE	Root Mean Squared Error
SORA	Sequential Optimization and Reliability Assessment
SORM	Second Order Reliability Method
SQP	Sequential Quadratic Programming
SS	Subset Simulation
SUA	System Uncertainty Analysis
SVM	Support Vector Machines
SWORD	Stage Wise decomposition for Optimal Rocket Design
UMDO	Uncertainty-based Multidisciplinary Design Optimization
iid	independent and identically distributed

Introduction

For many countries (United States of America, Russia, Europe, Japan, *etc.*), launch vehicles are cornerstones of an independent access to space. The space agency strategies for Solar system exploration, Earth monitoring and observation, human spaceflight are developed in accordance with their launch vehicle capabilities. Launch vehicle designs are long term projects (around 10 years) involving important budgets and requiring an intricate organization. NASA and ESA [Zeitlin et al., 2012] stress the need to reduce the cost and to improve the effectiveness of space missions and satellite launches. Ameliorating the design process for aerospace vehicles is essential to obtain low cost, high reliability, and effective launch capabilities [Blair et al., 2001]. This design is a complex multidisciplinary optimization process: the objective is to find the vehicle architecture and characteristics that provide the optimal performance [Jaeger et al., 2013] while satisfying design requirements and ensuring a certain level of reliability and safety.

The design of launch vehicles involves several disciplines and is customarily decomposed into interacting submodels for propulsion, aerodynamics, trajectory, mass and structure (Fig. 1). Each discipline may rely on computing-intensive simulations such as Finite Element analyses for the structure discipline or Computational Fluid Dynamics analyses for the aerodynamics discipline. The launch vehicle performance estimation which results from flight performance, safety, reliability and cost, demands coupled disciplinary analyses. The different disciplines are a primary source of trade-offs due to the antagonist disciplinary effects on launcher performance. The classical engineering design method (Fig. 2) consists of loops between different disciplinary optimizations (Fig. 2). At each iteration of this loop, each discipline is re-optimized based on the updated data from the previous discipline optimizations. Due to the possible antagonist discipline objectives, a difficult search for a compromise between these conflicting tasks needs to be performed. For instance, the aerodynamics discipline tends to decrease the diameter of the stages in order to decrease the drag during atmospheric flight, whereas the structure discipline tends to increase it for stability reasons. Such design is difficult because the couplings between disciplinary analyses generate large volumes of calculations, many heterogenous design variables need to be controlled and the compromise between disciplines needs to be formulated.

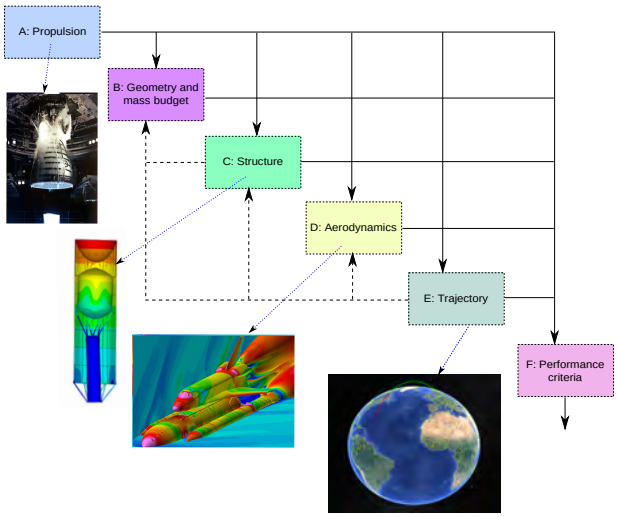

Figure 1: Example of launch vehicle design process

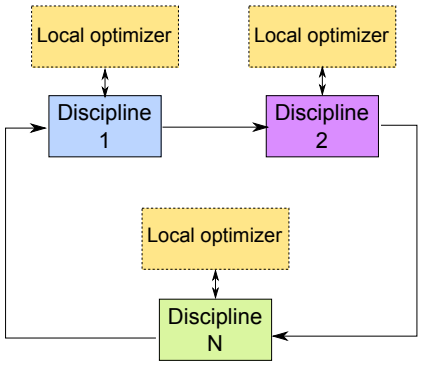

Figure 2: Traditional process for launch vehicle design

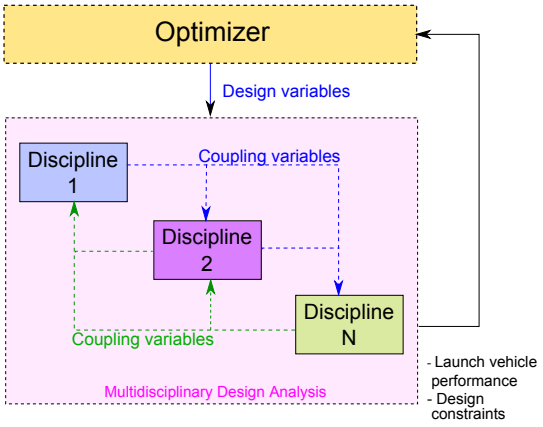

Figure 3: MDO design process

Consequently, the design of space transportation systems needs dedicated methodologies to manage the complexity of the problem to solve. It needs to handle the interdisciplinary couplings between the different disciplines to facilitate the research of compromises and to improve the efficiency of the overall design process. A family of adapted techniques, called Multidisciplinary Design Optimization (MDO), has been developed to help solve this problem. MDO is a set of engineering methods to handle complex design problems. MDO deals with the global design problem as a whole unlike classical engineering design methods. It provides an informed decision framework for system designers. MDO methods take advantage of the inherent synergies and couplings between the disciplines involved in the design process (Fig. 3) to decrease the computational cost and/or to

improve the quality of the global optimal design [Sobieszczanski-Sobieski and Haftka, 1997]. Unlike the sequential disciplinary optimizations performed with classical design methods, the interactions between the disciplines are directly incorporated in the MDO methods [Balesdent et al., 2012a]. However, the complexity of the problem is significantly increased by the simultaneous handling of all the disciplines. To subdue this complexity, various MDO formulations have been developed. In the 90's, several surveys classed MDO formulations into two general types of architectures: single-level methods [Cramer et al., 1994; Balling and Sobieszczanski-Sobieski, 1996], and multi-level methods [Alexandrov, 1997; Kroo, 1997]. Multi-level approaches introduce disciplinary level optimizers in addition to the system level optimizer present in single-level methods in order to facilitate the MDO problem convergence.

In the aerospace industry, a new system follows a development process involving several specific phases (Conceptual design, Preliminary design, Detailed design, Manufacturing) [Blair et al., 2001] (Fig. 4). For a launch vehicle, the conceptual design phase is decisive for the success of the whole design process. It has been estimated that at least 80% of the life-cycle cost of a vehicle is locked in by the chosen concept during the conceptual design phase [Blair et al., 2001] (Fig. 5). The design space at the conceptual phase is large since few characteristics of the system are fixed, and traditional design approaches lead to freeze some system characteristics to focus only on alternatives selected by experts [Zang et al., 2002]. MDO techniques are interesting for the conceptual design phase since they are able to handle large design spaces in a multidisciplinary environment. Martins *et al.* [Martins and Lambe, 2013] explains that designers may improve system performance and decrease design cycle cost and time by using MDO at the early design phases.

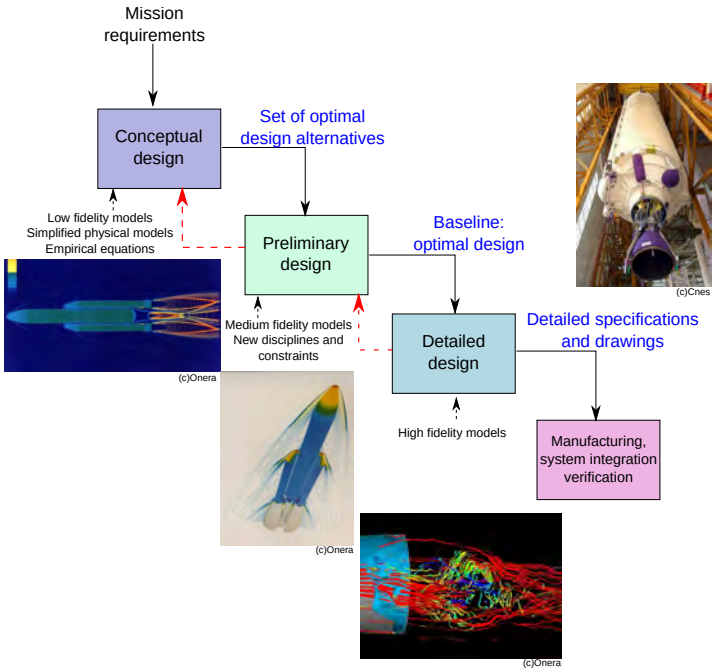

Figure 4: Design phases

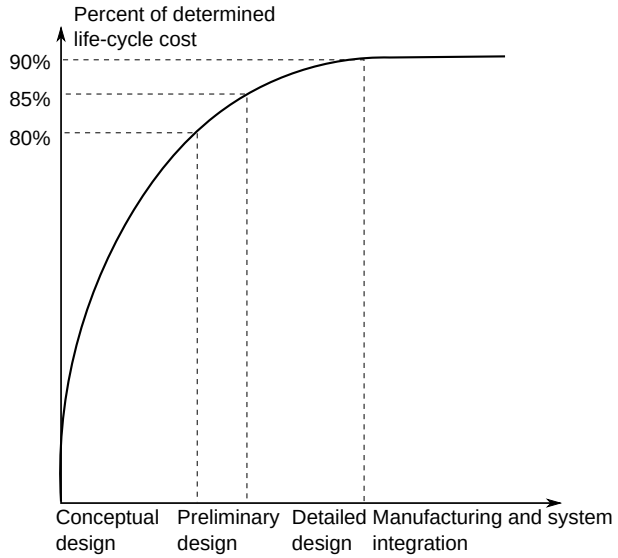

Figure 5: Evolution of the determined life cycle cost [Blair et al., 2001]

The early design phases are characterized by the use of low fidelity analyses as well as by the lack of knowledge about the future system design and performance. The low fidelity analyses are employed due to the non availability of these models in the early design phase and also the necessity to evaluate a high number of system architectures to explore the entire design space. This global exploration results in repeated discipline evaluations which is impossible to perform at an affordable computational cost with high fidelity models. On the other hand, computers and algorithms are getting faster, so it is also becoming more and more feasible to use higher fidelity models earlier in the design process. Moreover, to increase the performance of the launch vehicles and to decrease their costs, space agencies and industries introduce new technologies (new propellant mixture such as liquid oxygen and methane, reusable rocket engines) and new architectures (reusable first stage for launch vehicles) which present a high level of uncertainty in the early design phases. Incorporating uncertainties in MDO methodologies for aerospace vehicle design has thus become a necessity to offer improvements in terms of [Zang et al., 2002]:

- reduction of design cycle time, cost and risk,

- robustness of launch vehicle design to uncertainty along the development phase,

- increasing system performance while meeting the reliability requirements,

- robustness of the launch vehicle to aleatory events during a flight (*e.g.* wind gust).

If uncertainties are not taken into account at the early design phases, the detailed design phase might reveal that the optimal design previously found violates specific requirements and constraints. In this case, either the designers go back to the previous design phase to find a set of design alternatives, or they perform design modifications at the detailed design phase that could

result in loss of performance. Both options would result in a loss of time and money due to the re-run of complex simulations. Moreover, uncertainties are often treated with safety margins during the design process of launch vehicles which may result in very conservative designs therefore an adequate handling of uncertainty is essential [Jaeger et al., 2013]. Uncertainty-based Multidisciplinary Design Optimization (UMDO) aims at solving MDO problems under uncertainty. UMDO methods are recent and still under development and they have not reached sufficient maturity to efficiently estimate the final system performance and reliability [Zang et al., 2002; Yao et al., 2011].

Incorporating uncertainty in MDO methodologies raises a number of challenges which need to be addressed. Being able, in the early design phases, to design a multidisciplinary system taking into account the interactions between the disciplines and to handle the inherent uncertainties is often computationally prohibitive. In order to satisfy the designer requirements, it is necessary to find the system architecture which is optimal in terms of system performance while ensuring the robustness and reliability of the optimal system with respect to uncertainty. Three key challenges may be distinguished to efficiently solve UMDO problems.

- *Interdisciplinary coupling handling under uncertainty.*
  Most of the existing UMDO formulations are based on an adaptation of the single-level Multi-Discipline Feasible (MDF) formulation in the presence of uncertainty [Oakley et al., 1998; Koch et al., 2002; Jaeger et al., 2013]. In order to ensure the consistency of the interdisciplinary couplings, these methods involve a MultiDisciplinary Analysis (MDA) at the subsystem-level. MDA requires loops between the disciplines to converge to consistent couplings and guarantee multidisciplinary feasibility by finding the balance between the disciplines. Ensuring multidisciplinary system consistency is necessary to find an optimal solution that is physically realistic. However, MDA is computationally expensive and its combination with uncertainty propagation methods results in a computational burden. To avoid MDA loops, decomposition strategies of the design process have been proposed [Du and Chen, 2001; Du et al., 2008; Ghosh et al., 2014]. Nevertheless, these decompositions are not mature enough to adequately handle the interdisciplinary couplings in order to ensure the multidisciplinary feasibility whatever the unexpected event realization. The existing decoupled UMDO strategies only guarantee the multidisciplinary feasibility for some particular event realizations (*e.g.* most probable event realization leading to a system failure). However, in order to be equivalent to coupled design strategies, decoupled approaches must ensure multidisciplinary feasibility for all the possible unexpected events that may happen during the design and the system operational life.

  Furthermore, in literature all the examples of launch vehicle design under uncertainty consider a subdivision into disciplines such as propulsion, structure, trajectory, *etc.* Stage decomposition strategies [Balesdent, 2011] have been proposed to solve deterministic MDO problems but have not yet been adapted to handle uncertainty. A stage decomposition UMDO formulation for launch vehicle design could benefit from the same advantages as in deterministic MDO, that is introducing a multi-level process to facilitate the convergence of the system-level optimizer while decreasing the number of discipline evaluations by avoiding the disciplinary loops imposed by MDA-based formulations.

- *Reliability analysis for complex systems.*
  Another important topic induced by solving UMDO problems is to ensure the reliability of the optimal system with respect to the uncertainty. Reliability assessment consists of the

analysis of the probability of failure of the system regarding the exisiting uncertainties. It is used in the design of a system in order to ensure that the probability of failure is under a given requirement. Reliability assessments are often required in the UMDO constraint evaluation. This step is the most computationally intensive task in UMDO [Du et al., 2008] because it requires numerous discipline evaluations. At early design phases one has to cope with several uncertainties relative to the technology models (epistemic uncertainties) and aleatory uncertainties inherent to the physical phenomena occurring during the launch vehicle mission (*e.g.* wind gusts). These two types of uncertainty have to be considered in order to accurately estimate the reliability of the vehicle. The combination of both aleatory and epistemic uncertainties requires dedicated techniques to manage the computational cost induced by uncertainty propagation. Most of the UMDO reliability analysis methods are based on First Order Reliability Method (FORM) and Crude Monte Carlo (CMC) to compute a probability of failure of a system [Du et al., 2005; Du, 2008] which are easy to implement. FORM is computationally efficient, however, it is limited to systems presenting a unique zone in the input space leading to system failure. CMC may handle any type of reliability analysis but it is computationally expensive especially for low probability of failure ($\leq 10^{-4}$). Problems such as the determination of a safety zone for a launch vehicle stage fallout often involve multiple failure regions, non linear limit states and computationally intensive limit state function evaluations. Therefore, techniques dedicated to these kind of problems are essential within the context of launch vehicle design.

- *Constrained optimization in the presence of uncertainty with Evolutionary Strategy.*
  In order to solve UMDO problems, optimization algorithms should have at least two features. First, they have to be efficient despite the presence of uncertainty. Secondly, they have to handle constraints in order to take into account the design requirements. Classical optimization algorithms based on gradient calculation cannot be directly implemented for such problems and adaptations have been proposed to ensure algorithm convergence [Kiefer et al., 1952; Gardner, 1984]. Indeed, the presence of uncertainty makes the accurate estimation of the gradient that determines the search direction to converge to the optimal solution difficult. An alternative to the gradient-based optimizers are population-based algorithms. The latter are based on a set of search candidates for which the objective function is evaluated. Based on their values, the individuals are ranked and the population is accordingly modified in order to converge to the optimal solution. Population-based algorithms are interesting because of their ability to handle uncertain environments [Hansen et al., 2003; Jin and Branke, 2005], however, most of the existing algorithms do not intrinsically manage the constraints. Covariance Matrix Adaptation - Evolution Strategy (CMA-ES) is a population-based algorithm particularly competitive to solve complex optimization problems in the presence of uncertainty as highlighted in several extensive benchmarks [Auger and Hansen, 2009; Hansen, 2009]. However, this algorithm presents some limitations [Collange et al., 2010a] due to the constraint handling through a penalization approach which is problem dependent and requires a fine tuning of parameters.

This thesis is focused on the development of new Multidisciplinary Design Anaysis and Optimization methodologies in the presence of uncertainty enabling the design of complex systems such as launch vehicle at the early design phases.

Three contributions may be distinguished.

1. Firstly, two new UMDO formulations with interdisciplinary coupling satisfaction for all the realizations of the uncertain variables are elaborated. In order to ensure multidisciplinary feasibility, a new technique is proposed based on a parametric surrogate model (Polynomial Chaos Expansion) of the input coupling variables and a new interdisciplinary coupling constraint to guarantee the satisfaction of the interdisciplinary couplings for all the realizations of the uncertain variables. This technique enables the system-level optimizer to control the parameters defining the surrogate model of the input coupling variables in addition to the design variables. Therefore, it enables to decouple the disciplines while ensuring at the UMDO problem convergence that the functional relations between the disciplines are the same as if a coupled approach using MDA had been used. The two proposed formulations rely on this technique to handle interdisciplinary couplings. The first formulation is a single-level approach inspired from Individual Discipline Feasible (IDF) and adapted to the presence of uncertainty. This approach, called Individual Discipline Feasible - Polynomial Chaos Expansion (IDF-PCE), allows to ensure multidisciplinary feasibility for the optimal solution while reorganizing the design process through a decomposition strategy. It has been proposed in one conference and one journal article:

   - Decoupled UMDO formulation for interdisciplinary coupling satisfaction under uncertainty, L. Brevault, M. Balesdent, N. Bérend, R. Le Riche, 15^{th} *AIAA/ISSMO Multidisciplinary Analysis and Optimization Conference, Atlanta, GA, USA, June 2014*

   - Decoupled MDO formulation for interdisciplinary coupling satisfaction under uncertainty, L. Brevault, M. Balesdent, N. Bérend, R. Le Riche, *Accepted to AIAA Journal*, (July 2015)

   The second formulation is a multi-level approach inspired from the Stage-Wise decomposition for Optimal Rocket Design (SWORD) method [Balesdent et al., 2012a], which has been modified to take into account uncertainty and to maintain the equivalence with coupled approaches in terms of multidisciplinary feasibility. This formulation, named Multi-level Hierarchical Optimization under Uncertainty (MHOU), introduces multi-level optimization of the disciplines and is particularly adapted for launch vehicle design. It transforms the initial complex system design into an easier design process through a decomposition with individual stage optimizations. It has been proposed in a conference article:

   - Multi-level hierarchical MDO formulation with functional coupling satisfaction under uncertainty, application to sounding rocket design, L. Brevault, M. Balesdent, N. Bérend, R. Le Riche, *WCSMO-11, Sydney, Australia, June 2015*

2. Secondly, two new reliability analysis methods are developed to handle mixed aleatory/epistemic uncertainties for complex system. To solve this specific reliability analysis problem, adapted sampling-based methods combined with surrogate models and refinement strategies have been developed. These two methods differ in the effect of epistemic uncertainty. In the first one, epistemic uncertainty impacts the hyper-parameters of the joint Probability Density Function (PDF) which describes the aleatory uncertainty (*e.g.* the expected value of a Gaussian distribution is known only within an interval). In the second one, the epistemic uncertainty directly affects the limit state separating the failure domains from the safe one. These methods have been proposed in three journal papers and one conference article:

- Rare event probability estimation in the presence of epistemic uncertainty on input probability distribution parameters, M. Balesdent, J. Morio, L. Brevault, *Methodology and Computing in Applied Probability*, 2014, DOI 10.1007/s11009-014-9411-x, Springer,

- Kriging based sequential reliability analysis in the presence of mixed aleatory and epistemic uncertainties, L. Brevault, S. Lacaze, M. Balesdent, S. Missoum, *submitted to Structural Safety (Fev. 2015),*

- Probability of failure sensitivity with respect to decision variables, S. Lacaze, L. Brevault, M. Balesdent, S. Missoum, *Structural and Multidisciplinary Design Optimization*, DOI 10.1007/s00158-015-1232-1, April 2015, Springer,

- A sampling based RBDO algorithm with local refinement and efficient gradient estimation. S. Lacaze, S. Missoum, L. Brevault, M. Balesdent, 12^{th} *International Conference on Applications of Statistics and Probability in Civil Engineering, Vancouver, Canada, July 2015.*

3. Thirdly, a modification of CMA-ES algorithm is proposed to efficiently solve UMDO problem while handling constraints in an uncertain environment. This adaptation allows to avoid the traditional penalization-based methods which are problem dependent and require fine tuning. It is based on the modification of the covariance update mechanisms that enables the generation of a new population through a Gaussian distribution parameterized by the covariance matrix. The covariance matrix is modified in order to avoid the generation of individuals that could violate the constraints. This work has been proposed in one journal article:

   - Modified Covariance Matrix Adaptation - Evolution Strategy algorithm for constrained optimization under uncertainty, application to rocket design, R. Chocat, L. Brevault, M. Balesdent, S. Defoort, *Int. J. Simul. Multisci. Des. Optim.*, 2015, 6, A1. DOI: http://dx.doi.org/10.1051/smdo/2015001

In the three contributions, all the proposed approaches are compared to the existing reference methods on analytical test cases and on launch vehicle analysis or design problems.

This manuscript is organized into four parts according to the three contributions. The first part is devoted to drawing up a panorama of the UMDO methods and their applications to launch vehicle design. Chapter 1 presents the key concepts used to describe a deterministic MDO problem and the main formulations to solve it. In chapter 2 several aspects of uncertainty which are essential to lay the foundations of UMDO methodologies are presented. This chapter includes the uncertainty definition, the different mathematical modelings and the existing methods to propagate uncertainty into disciplines. Chapter 3 concerns the description of the existing UMDO formulations and the interdisciplinary coupling satisfaction in the presence of uncertainty. Chapter 4 is devoted to the presentation of reliability analysis techniques in the presence of mixed aleatory/epistemic uncertainties. Finally, chapter 5 details the different existing optimization algorithms employed to solve UMDO problems. In regards to this study, chapter 5 expresses some possible ways of improvement which will be detailed in parts II, III and IV.

The second part (Part II) of this thesis is related to the description and the analysis of the two proposed UMDO formulations. To this end, chapter 6 presents the Individual Discipline Feasible - Polynomial Chaos Expansion (IDF-PCE) formulation. A comparison with the most used UMDO method on an analytical test case is performed. Chapter 7 introduces the Multi-level Hierarchical

Optimization under Uncertainty (MHOU) formulation dedicated to launch vehicle design. Chapter 8 compares IDF-PCE and MHOU formulations on two launch vehicle test cases with MDF under uncertainty.

The third part (Part III) is devoted to reliability analysis for complex system design. Chapter 9 proposes a reliability analysis method to handle epistemic uncertainty in the hyper-parameter of the probability density function defining the input uncertainties. Chapter 10 introduces a new reliability method in the presence of mixed aleatory/epistemic uncertainty directly affecting the limit state function. Finally, in chapter 11, applications of the proposed methods to launch vehicle reliability analysis and, more specifically, to the determination of a safety zone for stage fallout are proposed. The methods are compared to the reference techniques.

The last part (Part IV) of this manuscript is devoted to the modification of CMA-ES algorithm in order to efficiently handle constraints in an uncertain environment to solve UMDO problem. In chapter 12, the modification of CMA-ES is described and a comparison of the proposed method with classical constraint handling techniques is performed on several analytical test cases. Finally, in chapter 13, an application to UMDO launch vehicle design is proposed and compared to MDF under uncertainty.

The appendices present the disciplinary models used in the different test cases. The last appendix consists of an extended abstract of this thesis written in French.

Part I

State-of-the-art of Uncertainty-based Multidisciplinary Design Optimization methods and numerical techniques

Chapter 1

Deterministic Multidisciplinary Design Optimization

Contents

Chapter goals

- Present the principal exisiting deterministic MDO formulations adapted to launch vehicle design,
- Introduce notations within the MDO context.

1.1 Introduction

Multidisciplinary Design Optimization (MDO) is a set of engineering methods to handle complex design problems involving several coupled disciplines. It provides an informed decision framework for system designers. In the MDO formalism, a system is described as a set of interconnected subsystems (called disciplines) in order to model its dynamics and to estimate its performance. MDO

approaches have been applied to a large panel of case studies in various fields such as: aircrafts [Henderson et al., 2012; Nguyen et al., 2013; Kenway et al., 2014], launch vehicles [Braun, 1996; Balesdent et al., 2012b; Breitkopf and Coelho, 2013], spacecrafts [Hwang et al., 2013; Huang et al., 2014], automotives [McAllister and Simpson, 2003], ships [Peri and Campana, 2003], buildings [Choudhary et al., 2005] and offer methods to solve complex design optimizations which are laborious to handle with the classical design methods [Alexandrov, 1997]. Classical design approaches (Fig. 1.1) consist of a sequence of discipline optimizations. However, in case of complex system design, disciplines often present antagonist objectives and classical design approaches have difficulty in the search for compromise between these conflicting disciplinary objectives [Balesdent et al., 2012b]. For instance, the aerodynamics discipline tends to decrease the diameter of the stages to decrease the drag during the atmospheric flight, whereas the structure discipline tends to increase it for stability reasons.

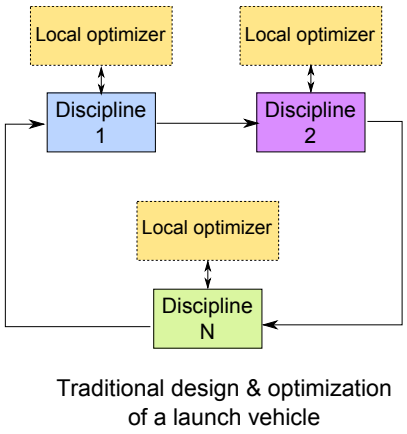

Figure 1.1: Classical design approaches

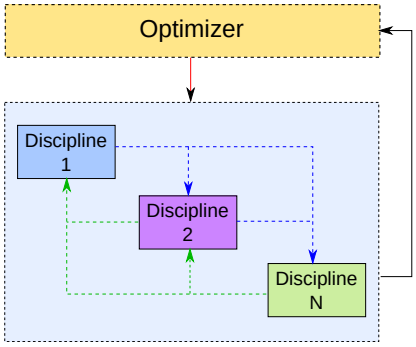

Figure 1.2: Multidisciplinary Design Optimization

Unlike the sequential disciplinary optimizations (Fig. 1.1), in MDO, the interactions between the disciplines are directly incorporated [Balesdent et al., 2012b]. The design of systems involves diverse fields of expertise and with the globalization of the industries, complex system design involve engineers distributed all over the world and data exchange between the teams is a crucial point to take into account in the design process. MDO approaches aims to facilitate discipline exchanges in order to faster find an optimal solution. MDO formulations take advantage of the inherent synergies and couplings between the disciplines involved in the design process to decrease the computational cost and/or to improve the quality of the global optimal design [Sobieszczanski-Sobieski and Haftka, 1997]. However, the complexity of the problem is significantly increased by the simultaneous handling of all the disciplines and their interdependence. To subdue the complexity introduced by MDO, various MDO formulations have been developed.

This chapter introduces the fundamental concepts, notations and methods required to describe a MDO process without the presence of uncertainty. In section 1.2, the concept of discipline and the general MDO formulation are introduced in addition to the appropriate notations to establish the preliminary bases. Section 1.3 details the interdisciplinary coupling handling methods existing in literature that may be distinguished into two categories: coupled and decoupled approaches. Section 1.4 presents an overview of the existing MDO formulations in order to describe their keys

steps and to highlight their main advantages and drawbacks. Moreover, a focus on MDO formulations used to solve launch vehicle design problem is proposed. Eventually, section 1.5 introduces the changes induced by the presence of uncertainty in MDO problems.

1.2 Mathematical formulation of the general deterministic MDO problem

In MDO, a discipline i is modeled by a function $c_i(\cdot)$ taking design variables and input coupling variables as inputs and calculating output coupling variables. A discipline i is illustrated in Figure 1.3.

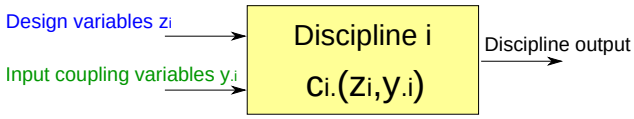

Figure 1.3: Discipline modeling

A general MDO problem can be formulated as follows [Balesdent et al., 2012b]:

$$
\begin{aligned}
&\min && f(\mathbf{z},\mathbf{y},\mathbf{x}) && (1.1)\\
&\text{w.r.t.} && \mathbf{z},\mathbf{y},\mathbf{x} &&\\
&\text{s.t.} && \mathbf{g}(\mathbf{z},\mathbf{y},\mathbf{x}) \leq 0 && (1.2)\\
& && \mathbf{h}(\mathbf{z},\mathbf{y},\mathbf{x}) = 0 && (1.3)\\
& && \forall (i,j) \in \{1,...,N\}^2 \; i \neq j, \; \mathbf{y}_{ij} = \mathbf{c}_{ij}(\mathbf{z}_i, \mathbf{y}_{.i}, \mathbf{x}_i) && (1.4)\\
& && \forall i \in \{1,...,N\}^2, \; \mathbf{r}_i(\mathbf{z}_i, \mathbf{y}_{.i}, \mathbf{x}_i) = 0 && (1.5)\\
& && \mathbf{z_{min}} \leq \mathbf{z} \leq \mathbf{z_{max}} && (1.6)
\end{aligned}
$$

All the variables and functions are described in the following sections. Three types of variables are involved in a deterministic MDO problem:

- $\mathbf{z}$ is the design variable vector. The design variables evolve all along the optimization process in order to find their optimal values with respect to the MDO problem (objective function and constraints). Design variables may be shared between several disciplines (noted $\mathbf{z_{sh}}$) or specific to the discipline i (noted $\bar{\mathbf{z}}_i$). We note $\mathbf{z}_i = \{\mathbf{z_{sh}}, \bar{\mathbf{z}}_i\}$ the input design variable vector of the discipline $i \in \{1,...,N\}$ with N the number of disciplines and $\mathbf{z} = \bigcup_{i=1}^{N} \mathbf{z}_i$ without duplication. Typical design variables in a launch vehicle design problem are stage diameters, pressures in the combustion chambers, propellant masses, *etc.*

- $\mathbf{x}$ is the state variable vector. Unlike $\mathbf{z}$, the state variables are not independent degrees of freedom but depend on the design variables, the coupling variables $\mathbf{y}$ and the state equations characterized by the residuals $\mathbf{r}$. These variables are often defined by implicit relations that require specific numerical methods for solving complex industrial problems. For instance, the guidance law (modeled for instance by pitch angle interpolation with respect to a set of way points) in a launch vehicle trajectory discipline has to be determined in order to ensure

payload injection into orbit. The guidance law is often the result of an optimization problem minimizing the discrepancy between the target orbit injection and the real orbit injection. In such modeling, the pitch angle way points are state variables for the trajectory discipline and $\mathbf{r}(\cdot)$ the residual to be minimized in the optimization problem.

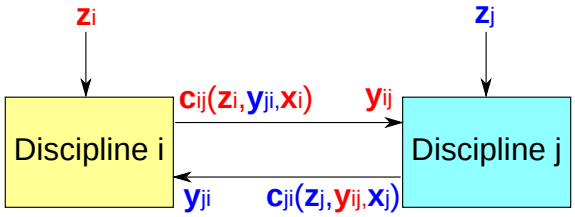

Figure 1.4: Couplings between the discipline i and the discipline j

- In a multidisciplinary environment, the disciplines exchange coupling variables, $\mathbf{y}$ (Fig. 1.4). The latter link the different disciplines to model the interactions between them. $\mathbf{c}_{ij}(\mathbf{z}_i, \mathbf{y}_{.i}, \mathbf{x}_i)$ is a coupling function used to compute the *output coupling* variable vector which is calculated by discipline i and input to discipline j. $\mathbf{y}_{.i}$ refers to the vector of all the *input coupling* variables of discipline i and $\mathbf{y}_{ij}$ is the *input coupling* variable vector which is input to discipline j and output from discipline i. We note $\mathbf{y} = \bigcup_{i=1}^{N} \mathbf{y}_{.i} = \bigcup_{i=1}^{N} \mathbf{y}_{i.}$ without duplication. From the design variables and the input coupling variables to the discipline i, the output coupling variables are computed with the coupling function: $\mathbf{c}_{i.}(\mathbf{z}_i, \mathbf{y}_{.i}, \mathbf{x}_i)$ and $\mathbf{y}_{i.} = (\mathbf{y}_{i1}, \ldots, \mathbf{y}_{iN})$ is the vector of the outputs of discipline i and the input coupling variable vector of all the other disciplines. For example, the sizing discipline computes the launch vehicle dry mass which is transferred to the trajectory discipline for a simulation of the launch vehicle flight. Another example is the classical aero-structure analysis (Fig. 1.5) [Coelho et al., 2009; El Majd et al., 2010; Kennedy and Martins, 2014; Kenway et al., 2014]. For a launch vehicle, aero-structure analysis involves coupled analyses between aerodynamics discipline (which requires the launch vehicle geometry and the deformations) and the structure discipline (which requires the aerodynamics loads on the launch vehicle structure). For coupled system, it is important to keep in mind that their design involves goals which are often conflicting with each other, for instance reducing weight may lead to higher stresses.

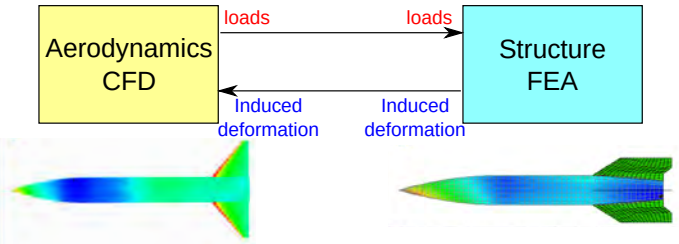

Figure 1.5: Couplings between aerodynamics and structure disciplines

In order to solve the MDO problem Eqs.(1.1-1.6), we are looking for:

- Inequality and equality constraint feasibility: the MDO solution has to satisfy the inequality constraints imposed by $\mathbf{g}(\cdot)$ and the equality constraints imposed by $\mathbf{h}(\cdot)$. These constraints translate the requirements for the system in terms of targeted performance, safety, flexibility, *etc.* For example, a target orbit altitude for a launch vehicle payload is an equality constraint to be satisfied.

- Individual disciplinary feasibility: the MDO solution has to ensure the disciplinary satisfaction through the equality constraints on the residuals $\mathbf{r}_i(\cdot)$. The residuals $\mathbf{r}_i(\cdot)$ quantify the satisfaction of the state equations in discipline i. The state variables $\mathbf{x}_i$ are the roots of the state equations of discipline i. For instance, state equations may translate thermodynamics equilibrium between the chemical components in rocket engine combustion. In the rest of the thesis, it is assumed that the satisfaction of the disciplinary feasibility is ensured by the disciplines, therefore, no more references to state variables and residuals will be done.

- Multidisciplinary feasibility: the MDO solution has to satisfy the interdisciplinary equality constraint between the input coupling variable vector $\mathbf{y}$ and the output coupling variable vector $\mathbf{c}(\cdot)$ resulting from the discipline simulations. The couplings between the disciplines i and j are said to be *satisfied* (also called *feasible* or *consistent*) when the following interdisciplinary system of equations is verified:

$$\begin{cases} \mathbf{y}_{ij} = \mathbf{c}_{ij}(\mathbf{z}_i, \mathbf{y}_{.i}) \\ \mathbf{y}_{ji} = \mathbf{c}_{ji}(\mathbf{z}_j, \mathbf{y}_{.j}) \end{cases} \tag{1.7}$$

  When all the couplings are satisfied, *i.e.* when Eqs.(1.7) are satisfied for all the couplings between all the disciplines, the system is said to be *multidisciplinary feasible*. The satisfaction of the interdisciplinary couplings is essential as it is a necessary condition for the modeled system to be physically realistic. Indeed, in the aero-structure example, if the aerodynamics discipline computes a load of 10MPa it is necessary that the structure discipline uses as input 10MPa and not another value otherwise the aero-structure analysis is not consistent. The existing method for coupling satisfaction in deterministic MDO are detailed in section 1.3.

- Optimal MDO solution: f is the objective function (also called performance) to be optimized. Multi-objective function may be used to quantify several performance to be optimized but is not considered in this thesis. This function characterizes the system and is a measure of its quality expressed with some metrics (*e.g.* launch vehicle life cycle cost in euros, Gross Lift-Off Weight (GLOW) in kg, *etc.*). In general, the objective function has to be minimized.

To summarize, in order to solve a MDO problem, it is necessary to ensure:

- Requirement feasibility: respect of the requirements asked by the designer,
- Multidisciplinary feasibility: respect of the physical relevance for the obtained design,
- Individual disciplinary feasibility: respect of the disciplinary state equations,
- MDO solution optimality.

The multidisciplinary feasibility is a specificity of multidisciplinary systems which involve coupled analyses and require specific methodologies to guarantee it. Classical methods to ensure interdisciplinary coupling satisfaction are detailed in the next section.

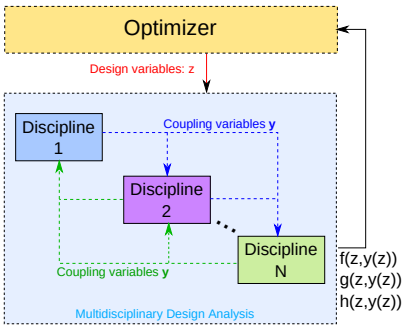

Figure 1.6: Multidisciplinary Design Optimization, **coupled** approach

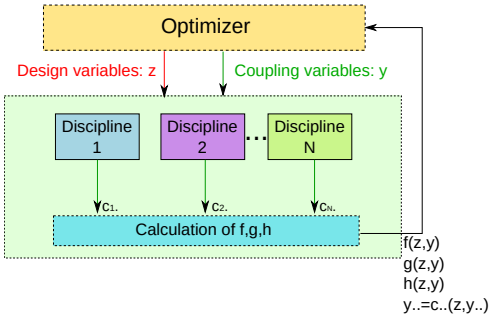

Figure 1.7: Multidisciplinary Design Optimization, **decoupled** approach

1.3 Multidisciplinary coupling satisfaction

In MDO, two categories of methods to satisfy the interdisciplinary couplings may be distinguished [Balling and Sobieszczanski-Sobieski, 1996]: the *coupled* approaches and the *decoupled* approaches.

1.3.1 Coupled approaches (MultiDisciplinary Analysis)

Coupled approaches (Fig. 1.6) perform a MultiDisciplinary Analysis (MDA) to ensure the interdisciplinary couplings at each iteration of the system-level optimization. MDA is an auxiliary analysis aiming to find an equilibrium between the disciplines by solving the system of interdisciplinary equations [Coelho et al., 2009]. In other words, MDA consists in finding the value of the input coupling variables $\mathbf{y}$ satisfying the system of interdisciplinary equations. An iterative scheme is required to solve the system of equations because of the coupled nature of the disciplines. Two classical MDA methods are distinguished: either the Fixed Point Iteration (FPI) or an auxiliary optimization process minimizing the residuals of the interdisciplinary equations [Coelho et al., 2009; Breitkopf and Coelho, 2013].

- **Fixed Point Iteration.** FPI is an iterative procedure involving a loop between the disciplines with no control on the coupling variables (excepted for the initialization) which directly result from the discipline simulations. FPI can be interpreted as a generalized Gauss-Seidel scheme for multidisciplinary analysis because of its links with the Gauss-Seidel algorithm for solving linear algebraic equations. It is important to note that FPI may not always converge, a theoretical analysis of conditions under which convergence can be guaranteed (for instance if the interdisciplinary set of equations defines a contraction mapping) may be found in [Ortega, 1973]. In the FPI approach, only one coupling vector is initialized (for instance y_{ij} in Fig. 1.8). A FPI algorithm for scalar coupling variable between two disciplines is described in Algorithm 1. The algorithm can be generalized to vector couplings with more than two disciplines.

- **Discrepancy minimization.** Alternatively, MDA may be solved by minimizing the discrepancy between the input coupling variable vector and the coupling output vector [Tedford and

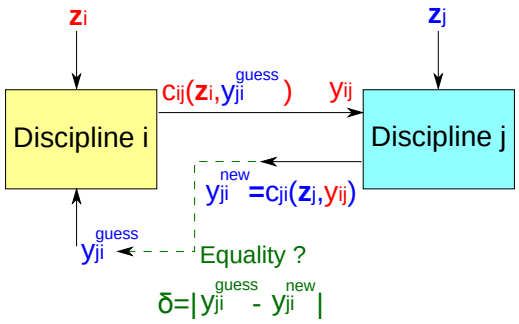

Figure 1.8: FPI between the discipline i and the discipline j

Martins, 2006]:

$$\begin{aligned} \min \quad & \| \mathbf{y}_{1.} - \mathbf{c}_{1.}(\mathbf{z}, \mathbf{y}_{.1}) \|^2 + ... + \| \mathbf{y}_{N.} - \mathbf{c}_{N.}(\mathbf{z}, \mathbf{y}_{.N}) \|^2 \\ \text{w.r.t.} \quad & \mathbf{y} \end{aligned} \tag{1.8}$$

with $\mathbf{y}_{i.}$ the input coupling variable vector of all the disciplines linked to the discipline i. The interdisciplinary coupling system is solved when the optimizer converges such that the discrepancy is equal to zero. An efficient auxiliary optimization algorithm often requires fewer calls to the discipline i than FPI, as the optimization process chooses the steps more freely than FPI [Sankararaman and Mahadevan, 2012]. Newton-Raphson or staggered solution approach [Felippa et al., 2001] are examples of root finding algorithms applied to MDA. More details on MDA can be found in [Keane and Nair, 2005]. MDO formulations satisfying the interdisciplinary equations with MDA ensure the system feasibility at each system-level optimization iteration.

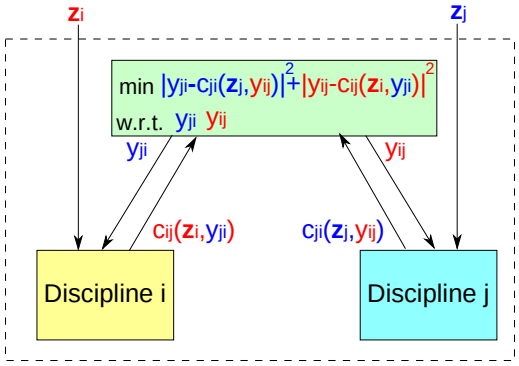

Figure 1.9: Discrepancy minimization for the discipline i and the discipline j

It is worth noting that whatever the numerical scheme employed to solve MDA, it is possible that the final couplings may depend on the initial guess. Indeed, a nonlinear system can have multiple equilibrium points resulting in several couplings satisfying the multidisciplinary feasibility. Even though such situations are rarely encountered in launch vehicle design, MDA must be performed carefully to ensure that the most physically meaningful solution is picked.

Algorithm 1 FPI algorithm for scalar coupling between two disciplines

Require: $\mathbf{z}_i$, $\mathbf{z}_j$, initial coupling guess y_{ji}^{guess}, convergence tolerance criterion δ_{ref}, maximum number of iterations $k_{\max}$
1) Initialize $k = 0$
2) Evaluate discipline i with: $c_{ij}(\mathbf{z}_i, y_{ji}^{guess}) = y_{ij}$
3) Evaluate discipline j with: $c_{ji}(\mathbf{z}_j, y_{ij}) = y_{ji}^{new}$
4) Compute the coupling error: $\delta = |y_{ji}^{guess} - y_{ji}^{new}|$
5) $k \leftarrow k + 1$
while $\delta > \delta_{ref}$ and $k < k_{\max}$ **do**
  6-1) Set $y_{ji}^{guess} = y_{ji}^{new}$
  6-2) Evaluate discipline i with: $c_{ij}(\mathbf{z}_i, y_{ji}^{guess}) = y_{ij}$
  6-3) Evaluate discipline j with: $c_{ji}(\mathbf{z}_j, y_{ij}) = y_{ji}^{new}$
  6-4) Compute the coupling error: $\delta = |y_{ji}^{guess} - y_{ji}^{new}|$
  6-5) $k \leftarrow k + 1$
end while
if $k < k_{\max}$ **then**
  return y_{ji}^{new}, y_{ij} and k
else
  return "not converged".
end if

1.3.2 Decoupled approaches

Decoupled approaches (Fig. 1.7) aim at removing MDA and to impose equality constraints on the coupling variables in the MDO formulation at the system-level (Eq.1.4) to ensure the interdisciplinary coupling satisfaction only for the optimal design. Instead of solving the system of interdisciplinary equations at each MDO process iteration in $\mathbf{z}$, equality constraints may be imposed between the input and the output coupling variables in the MDO formulation at the same level as the constraints $\mathbf{g}(\cdot)$ and $\mathbf{h}(\cdot)$: $\forall (i,j) \in \{1,...,N\}^2 \ \forall i \neq j, \ \mathbf{y}_{ij} = \mathbf{c}_{ij}(\mathbf{z}_i, \mathbf{y}_{.i})$. These constraints impose to the optimal design the multidisciplinary feasibility. The basic idea is to define the coupling variables $\mathbf{y}$ as optimization variables along with the design variables $\mathbf{z}$. Indeed, in the decoupled approaches, the system-level optimizer handles both the design variables and the input coupling variables. Hence, the additional degrees of freedom introduced by expanding the variables controlled by the system-level optimizer are removed by the coupling equality constraints. The equality constraints on coupling variables may not be satisfied at each iteration but guide the search of optimal design.

The coupled and decoupled approaches to handle the interdisciplinary couplings have been incorporated in various MDO formulations that are briefly presented in the following sections.

1.4 MDO formulations

A lot of MDO formulations have been proposed in literature to efficiently solve general and specific engineering problems. Some articles [Balling and Sobieszczanski-Sobieski, 1996; Alexandrov, 1997; Balesdent et al., 2012b; Martins and Lambe, 2013; Breitkopf and Coelho, 2013] provide a review

of the different methods and compare them qualitatively and numerically on a benchmark of MDO problems [Yi et al., 2008; Tedford and Martins, 2010].

This section presents the main MDO formulations that will be used in the following. Classical MDO formulations may be classified in four categories (Fig. 1.10) according to the *coupled* or *decoupled* and to the *single* or *multi-level* approaches:

- Single level approaches by application of MDA: *e.g. Multi Discipline Feasible* (MDF) [Balling and Sobieszczanski-Sobieski, 1996],
- Multi-level approaches by application of MDA: *e.g. Concurrent SubSpace Optimization* (CSSO) [Sobieszczanski-Sobieski, 1988], *Bi-Level Integrated System Synthesis* (BLISS)[Sobieszczanski-Sobieski et al., 1998],
- Single level approaches with equality constraints on the coupling variables: *e.g. Individual Discipline Feasible* (IDF) [Balling and Sobieszczanski-Sobieski, 1996], *All At Once* (AAO) [Balling and Sobieszczanski-Sobieski, 1996],
- Multi-level approaches with equality constraints on the coupling variables: *e.g. Collaborative Optimization* (CO) [Braun et al., 1996], *Analytical Target Cascading* (ATC) [Allison et al., 2005], Quasiseparable Decomposition (QSD) [Haftka and Watson, 2005].

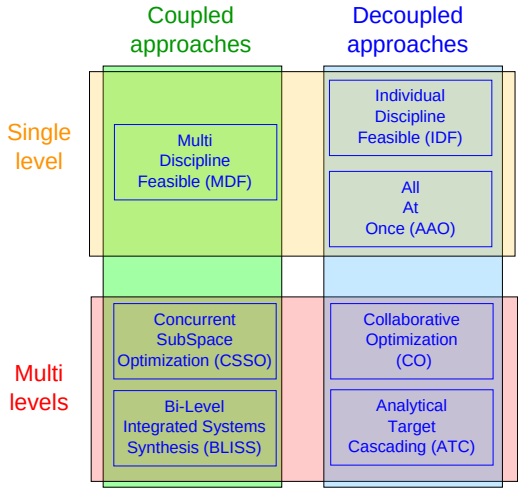

Figure 1.10: Classification of the main MDO formulations

The single level *vs.* multi-level formulations are differentiated by the number of optimizers. Single formulations have only one system optimizer to solve the MDO problem whereas in multi-level formulations, in addition to the system optimizer, discipline optimizers are introduced in order to distribute the problem complexity over different dedicated discipline optimizations. Among the formulations relying on MDA, MDF is the most usual [Balesdent et al., 2012b]. MDF is a single level optimization formulation in which the system performance is evaluated with a disciplinary iterative process. CSSO and BLISS formulations use MDA to ensure interdisciplinary couplings but enable decoupled discipline optimizations. IDF, CO, ATC and AAO are fully decoupled formulations

with satisfaction of the couplings by incorporating additional variables and equality constraints in the formulations. The decoupled MDO formulations offer several advantages compared to MDF [Balesdent et al., 2012b; Martins and Lambe, 2013]:

- The system-level optimization process allows parallel analyses of the disciplines, however load balancing has to be taken into account when some analyses or optimizations are much more expensive than others, such as in multifidelity optimization problem [Zadeh and Toropov, 2002], the decoupled approaches suffer because of the inactivity of the processors running the inexpensive analyses and optimizations which is waiting for updates from other processors.

- The number of calls to the computationally expensive discipline codes may be notably decreased by avoiding expensive MDA calculations,

- The multi-level methods facilitate the system optimization by distributing the problem complexity over the different dedicated discipline optimizations, however poor convergence rate may be observed due to the imbrication of several levels of optimization [DeMiguel and Murray, 2000; Martins and Lambe, 2013],

- In the multi-level approaches, the discipline optimizers handle local design variables (decreasing the system-level design space size) and the system-level optimizer only handles the shared design variables between several disciplines and the coupling variables.

However, compared to MDF, the decoupled MDO formulations require an appropriate interdisciplinary coupling handling and involve an optimization problem with more variables in total (the design variables plus the coupling variables that can be distributed among the system and the local disciplinary optimizers in the case of multi-level approaches) and more constraints. In the next sections, two single level formulations (one coupled and one decoupled) and two multi-level formulations (one coupled and one decoupled) are presented in order to highlight the coupling handling approaches in the main MDO formulations. First, the two single level approaches are introduced.

1.4.1 Multi Discipline Feasible (MDF)

The Multi Discipline Feasible (MDF) formulation (Fig. 1.11) is the most usual MDO method. This approach is described in [Cramer et al., 1994; Balling and Sobieszczanski-Sobieski, 1996]. MDF is a single level coupled deterministic approach which uses MDA to ensure interdisciplinary coupling satisfaction at each iteration of the system-level optimizer. All the subsystems (disciplines) are coupled in an analysis module which aims to determine the couplings satisfying the interdisciplinary system of equations ensuring multidisciplinary feasibility. Once the MDA is performed, design variables and converged couplings are used to compute the objective function and the constraints. The disciplines are in charge to find the state variables satisfying state equations consequently they do not intervene in the MDF formulation.

$$\begin{aligned} \min \quad & f(\mathbf{z}, \mathbf{y}(\mathbf{z})) && (1.9) \\ \text{w.r.t.} \quad & \mathbf{z} \\ \text{s.t.} \quad & \mathbf{g}(\mathbf{z}, \mathbf{y}(\mathbf{z})) \leq 0 && (1.10) \\ & \mathbf{h}(\mathbf{z}, \mathbf{y}(\mathbf{z})) = 0 && (1.11) \\ & \mathbf{z_{min}} \leq \mathbf{z} \leq \mathbf{z_{max}} && (1.12) \end{aligned}$$

with $\mathbf{y}(\mathbf{z})$ the coupling variable vector satisfying the system of interdisciplinary equations (Eqs.1.7). It is important to notice that, in MDF, due to the repeated calls to MDA, at each iteration, each found solution is multidisciplinary feasible. The main advantage of MDF is its simplicity of implementation which involves only one system optimizer and handles interdisciplinary couplings with MDA. Moreover, this formulation is general enough to be easily adapted to all types of multidisciplinary systems. MDF formulation is often considered as a reference due to its intrinsic interdisciplinary coupling satisfaction thanks to MDA. However, MDF presents also important drawbacks. MDA requires iterative loop between the disciplines and is computationally expensive. In the presence of computationally expensive disciplines, the repeated calls to MDA in MDF results in a prohibitive computational cost.

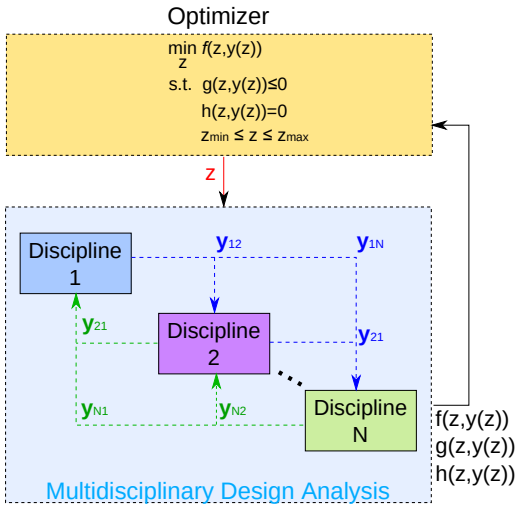

Figure 1.11: MDF method

For large scale industrial design problems, each subsystem may involve specialists and engineering teams distributed all over the world and performing MDA becomes a complicated task as it requires [Balesdent, 2011]:

- the definition of each subsystem autonomy and domain of action with respect to all the involved collaborators,
- the management of the exchanges of information and data transmissions between the different subsystems,
- the traceability of the exchanged information and the evaluated system design.

Moreover, the subsystem analyses are performed sequentially and each team has to wait for the previous one in order to perform its tasks (when FPI is used to solve MDA) which can be very time consuming.

1.4.2 Individual Discipline Feasible (IDF)

Individual Discipline Feasible [Cramer et al., 1994; Balling and Sobieszczanski-Sobieski, 1996] (Fig. 1.12) is a decoupled single level deterministic formulation Eqs.(1.13-1.17). It replaces the computationally expensive MDA by introducing additional degrees of freedom, the input coupling variables handled at the system-level, and by adding interdisciplinary coupling constraints in the formulation, Eq.(1.16):

$$\begin{aligned}
&\min && f(\mathbf{z},\mathbf{y}) && (1.13)\\
&\text{w.r.t.} && \mathbf{z},\mathbf{y} && \\
&\text{s.t.} && \mathbf{g}(\mathbf{z},\mathbf{y}) \leq 0 && (1.14)\\
& && \mathbf{h}(\mathbf{z},\mathbf{y}) = 0 && (1.15)\\
& && \forall (i,j) \in \{1,\ldots,N\}^2 i \neq j, \mathbf{y}_{ij} = \mathbf{c}_{ij}(\mathbf{z}_i, \mathbf{y}_{.i}) && (1.16)\\
& && \mathbf{z_{min}} \leq \mathbf{z} \leq \mathbf{z_{max}} && (1.17)
\end{aligned}$$

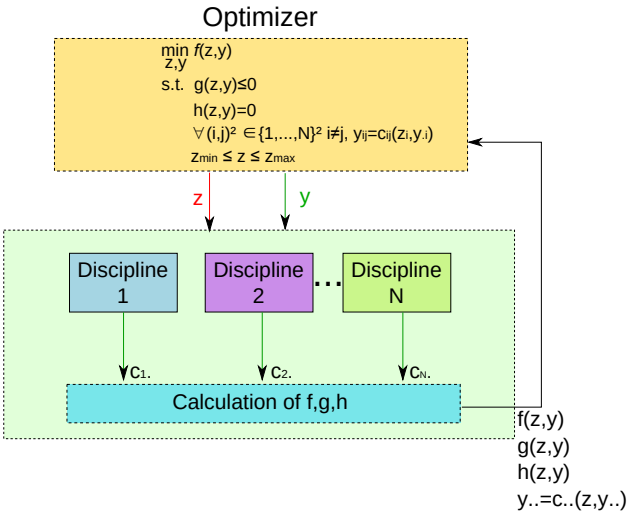

Figure 1.12: IDF method

This formulation allows to decompose the main problem into several subproblems by removing MDA. The input coupling variables are controlled by the system-level optimizer allowing to decouple the disciplines and to evaluate them in parallel. The optimizer exchanges coupling information with all the disciplines to coordinate them to a multidisciplinary feasible solution. In order to ensure the system consistency for the optimal solution, equality constraints Eq.(1.16) between the input and the output coupling variables are added compared to MDF formulation. In IDF, the

multidisciplinary feasibility is ensured only at the MDO problem convergence and the intermediate optimization solution consistency is not guaranteed. This decomposition approach increases the number of decision variables controlled by the system-level optimizer but the computational cost may be improved thanks to the discipline parallelization. Unlike MDF, at each system-level iteration, only one call to the disciplines is performed. For large scale applications, the management tasks are less restrictive than in MDF because each discipline only dialogues with the optimizer and does not need to wait the results of the other disciplines.

Multi-level approaches have been proposed in order to ease the system-level optimization by introducing dedicated subsystem-level optimizers. Bi-Level Integrated Systems Synthesis (BLISS) and Collaborative Optimization (CO) approaches are respectively coupled and decoupled multi-level formulations and are detailed in the next sections.

1.4.3 Bi-Level Integrated System Synthesis (BLISS)

Bi-Level Integrated System Synthesis (BLISS) [Sobieszczanski-Sobieski et al., 1998, 2000] is a multi-level deterministic MDO formulation (Fig. 1.13). It is an iterative method organized with a system-level optimizer and a set of disciplinary optimizers at the subsystem-level. The basic idea of BLISS is to create a path in the design space using a series of linear approximations to the original design problem, with bounds on the design variable steps defined by the designer, in order to avoid to the design point from moving so far away that the approximations are inaccurate. The concept is similar to trust region optimization algorithms [Conn et al., 2000]. BLISS is based on a gradient approach and optimizes successively the contributions of the individual design variables (subsystem optimization problems) and the shared design variables to the objective function (system-level optimization problem). In order to ensure multidisciplinary feasibility, BLISS relies on MDA as in MDF which is performed between the system and the subsystem optimization problems.

At the k^{th} iteration, the system-level optimizer solves the following problem:

$$\begin{aligned} \min \quad & f_k^* + \frac{\partial f_k^*}{\partial \mathbf{z_{sh}}} \Delta \mathbf{z_{sh}} && (1.18) \\ \text{w.r.t.} \quad & \Delta \mathbf{z_{sh}} \\ \text{s.t.} \quad & \Delta \mathbf{z_{sh_{min}}} \leq \Delta \mathbf{z_{sh}} \leq \Delta \mathbf{z_{sh_{max}}} && (1.19) \end{aligned}$$

The i^{th} subsystem optimization problem is given by:

$$\begin{aligned} \min \quad & f + \frac{\partial f}{\partial \bar{\mathbf{z}}_i} \Delta \bar{\mathbf{z}}_i && (1.20) \\ \text{w.r.t.} \quad & \Delta \bar{\mathbf{z}}_i \\ \text{s.t.} \quad & \mathbf{g}_i + \frac{\partial \mathbf{g}_i}{\partial \Delta \bar{\mathbf{z}}_i} \Delta \bar{\mathbf{z}}_i \leq 0 && (1.21) \\ & \mathbf{h}_i + \frac{\partial \mathbf{h}_i}{\partial \Delta \bar{\mathbf{z}}_i} \Delta \bar{\mathbf{z}}_i = 0 && (1.22) \\ & \Delta \bar{\mathbf{z}}_{i_{\mathbf{min}}} \leq \Delta \bar{\mathbf{z}}_i \leq \Delta \bar{\mathbf{z}}_{i_{\mathbf{max}}} && (1.23) \end{aligned}$$

with Δz the optimization variable increments at the current iteration k. In the system-level optimization problem Eqs.(1.18-1.19), the objective function f_k^* is a first order Taylor series expansion

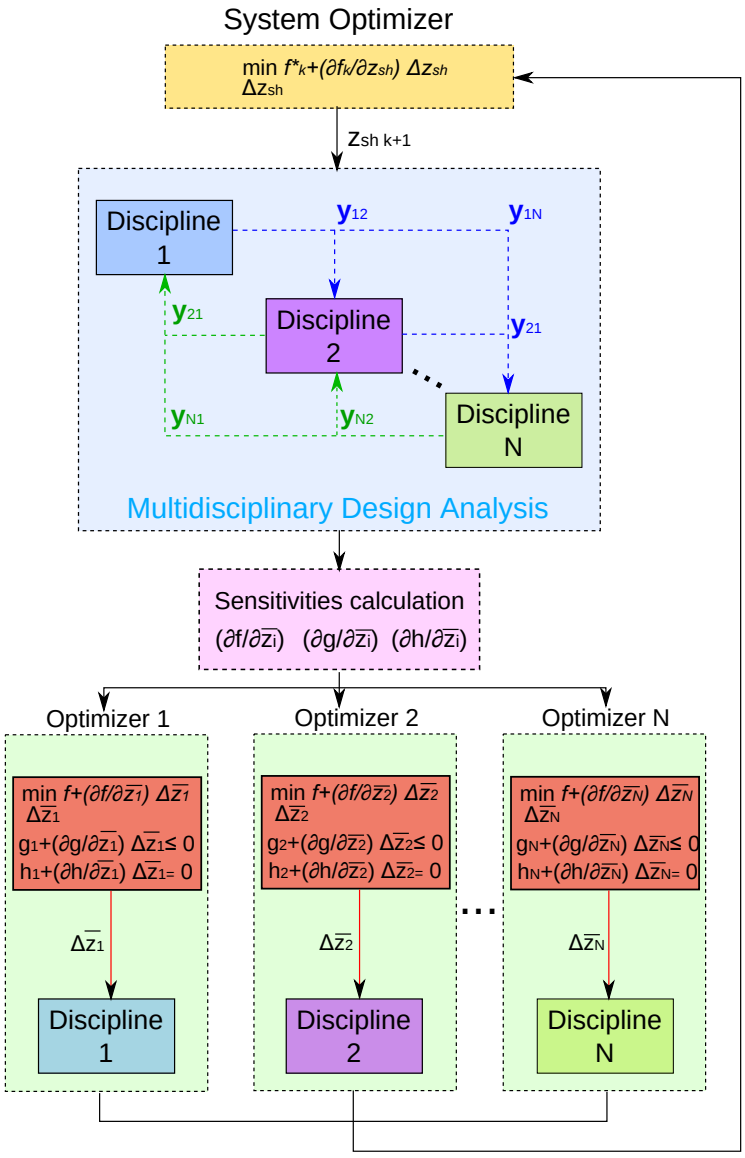

Figure 1.13: BLISS method

with the disicpline design variables $\mathbf{z}_i$ being fixed to their optimal values found at the subsystem-level. At the subsystem-level, the objective function and the constraints are first order Taylor series expansion with the shared variables being fixed to the optimal values found at the system-level. BLISS allows one to separate the system-level optimization and the optimizations of the different disciplines at the subsystem-level. Adapted optimization methods for each discipline is possible improving the system convergence. The reliance of BLISS on linear approximations may introduce

diffuculties if the underlying problem is highly nonlinear, the algorithm may converge slowly. The user-defined variable bounds may help the convergence if these bounds are correctly chosen, *e.g.*, through a trust-region framework. Variants of BLISS have been developed such as BLISS2000 using approximate models to replace the original disciplines to decrease the computational cost.

1.4.4 Collaborative Optimization (CO)

Collaborative Optimization (CO) [Braun et al., 1996] is a decoupled bi-level deterministic formulation (Fig. 1.14). This formulation has been developed to offer more autonomy to the subsystems to satisfy the interdisciplinary couplings. CO formulation may be resumed as follows:

$$\begin{aligned} \min \quad & f(\mathbf{z}, \mathbf{y}) && (1.24)\\ \text{w.r.t.} \quad & \mathbf{z}, \mathbf{y} \\ \text{s.t.} \quad & \hat{J}_{i.}(\hat{\mathbf{z}}_i, \mathbf{z}_i, \mathbf{y}) = 0, \forall i \in \{1, \ldots, N\} && (1.25)\\ & \mathbf{z_{min}} \leq \mathbf{z} \leq \mathbf{z_{max}} && (1.26) \end{aligned}$$

with $\hat{J}_{i.}$ the optimized objective function of the i^{th} discipline and $\hat{\mathbf{z}}$ the local copies of $\mathbf{z}$ controlled by the subsystem optimizer. The i^{th} subsystem optimization problem is given by:

$$\begin{aligned} \min \quad & J_{i.} = \| \hat{\mathbf{z}}_i - \mathbf{z}_i \|_2^2 + \| \mathbf{y}_{i.} - \mathbf{c}_{i.}(\mathbf{y}_{.i}, \hat{\mathbf{z}}_i) \|_2^2 && (1.27)\\ \text{w.r.t.} \quad & \hat{\mathbf{z}}_i \\ \text{s.t.} \quad & \mathbf{g}_i(\hat{\mathbf{z}}_i, \mathbf{y}_{.i}) \leq 0 && (1.28)\\ & \mathbf{h_i}(\hat{\mathbf{z}}_i, \mathbf{y}_{.i}) = 0 && (1.29)\\ & \hat{\mathbf{z}}_{i_{\mathbf{min}}} \leq \hat{\mathbf{z}}_i \leq \hat{\mathbf{z}}_{i_{\mathbf{max}}} && (1.30) \end{aligned}$$

CO presents important advantages compared to single level MDO formulations. Indeed, CO allows to employ the most adapted optimization method to each discipline with possible actions of the disciplinary experts. Moreover, the design process offers modularity and flexibility to add or remove disciplines without modifying the entire design process. However, theoretical and practical convergence issues with respect to the quadratic constraint formulation have been observed by some researchers [Alexandrov and Lewis, 2000] due to instabilities at the convergence. Several adaptations of CO have been proposed in order to overcome this difficulty [DeMiguel and Murray, 2006]. Nevertheless, this approach has been shown to be valid and to provide good results for some MDO problems [Braun et al., 1996].

For more details on deterministic MDO formulations one can refer to [Balling and Sobieszczanski-Sobieski, 1996; Alexandrov, 1997; Balesdent et al., 2012b; Martins and Lambe, 2013]. Launch vehicles are complex systems and their design involve an MDO problem [Braun, 1996; Gang et al., 2005; Brown and Olds, 2006; Balesdent et al., 2012a; Breitkopf and Coelho, 2013]. In literature, a large number of papers applied the general deterministic MDO formulations (MDF, IDF, AAO, CO, BLISS, ATC) to launch vehicle design problems. These formulations are general enough to be adapted to the design of launch vehicles. Moreover, dedicated deterministic MDO formulations have been proposed to design launch vehicle to improve the design process efficiency. In the next section, a focus on deterministic MDO formulations for the design of launch vehicle is proposed.

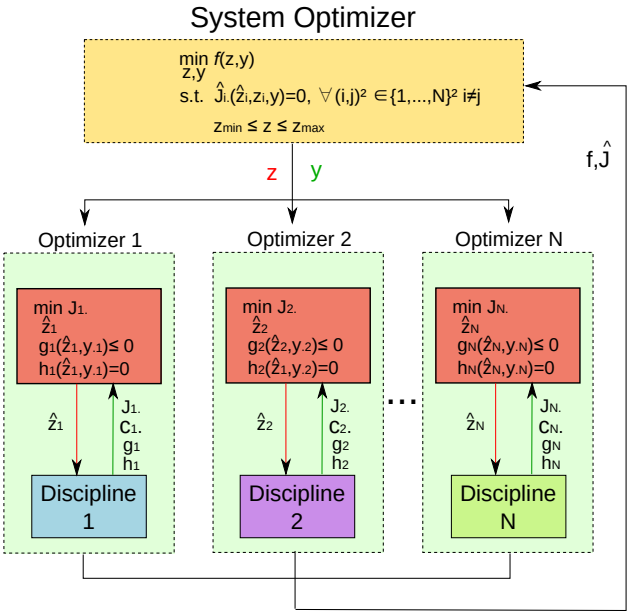

Figure 1.14: CO method

1.4.5 Deterministic MDO for launch vehicle design

Multi-Discipline Feasible (MDF) method appears to be the most used MDO method to design a launch vehicle [Balesdent et al., 2012a; Breitkopf and Coelho, 2013]. MDF formulation is the easiest formulation to implement explaining its popularity in the launch vehicle community. Some articles used other MDO formulations such as IDF [Braun and Kroo, 1995] , AAO [Braun, 1996; Brown and Olds, 2006], CO [Braun, 1996; Cormier et al., 2000; Gang et al., 2005; Brown and Olds, 2006] and BLISS [Brown and Olds, 2006]. In [Balesdent et al., 2012a] the authors performed a detailed review on MDO formulations applied to launch vehicle design. These MDO formulations are flexible enough to be adapted to the design of any complex systems such as launch vehicle. However, launch vehicle design present particularities, notably the importance of the trajectory discipline compared to the other disciplines. Exploiting these specificities in a MDO formulation might improve the launch vehicle design process. Dedicated formulations for launch vehicle design have been proposed such as the Stage Wise decomposition for Optimal Rocket Design (SWORD) [Balesdent et al., 2012a]. The next paragraph focuses on this dedicated formulation.

Stage Wise decomposition for Optimal Rocket Design 3rd formulation (SWORD). In literature, the classical approach to design a launch vehicle is to decompose the design process according to the involved disciplines (propulsion, aerodynamics, sizing, trajectory, *etc.*). In SWORD formulations [Balesdent et al., 2012a], the design process of a launch vehicle is decomposed according to the different stages in order to improve the efficiency of the MDO process. In these formulations, the subsystems are not the disciplines but instead the different stage optimizations incorporating all the required disciplines to the stage design. SWORD decompositions are multi-level decoupled MDO formulations. Four different formulations have been proposed depending on

the decomposition process and the interdisciplinary coupling constraint handling. According to their comparison on launch vehicle application cases implemented by Balesdent *et al.* [Balesdent et al., 2012a], the third formulation is more efficient to solve MDO problems (with respect to the number of discipline evaluations) due to its hierarchical decomposition of the design process and is detailed in the following. In SWORD, the objective function $f(\cdot)$ is assumed to be decomposed such as $f(\cdot) = \sum_{j=1}^{n} f_j(\cdot)$ with n the number of stages. In practice, the Gross Lift-Off Weight (GLOW) is often minimized in launch vehicle design process [Balesdent et al., 2012b; Castellini, 2012] and it can be decomposed as the sum of the stage masses plus the fairing and payload masses. The different stage masses are coupled, a change in the upper stage mass would introduce a modification of the lower stage masses in order to ensure mission success. Also, the cost of launch vehicle follows the same decomposition (sum of the stage cost).

The formulation at the system-level is given by:

$$\begin{aligned} &\min && f(\mathbf{z}, \mathbf{y}) && (1.31)\\ &\text{w.r.t.} && \mathbf{z_{sh}}, \mathbf{y} && \\ &\text{s.t.} && \mathbf{g_0}(\mathbf{z}, \mathbf{y}) && (1.32)\\ & && \mathbf{z_{min}} \leq \mathbf{z} \leq \mathbf{z_{max}} && (1.33) \end{aligned}$$

At the subsystem-level:
$i = n$
While $i > 0$
For the i^{th} **stage:**
Given $\mathbf{z_{sh}}, \mathbf{y}$ and the optimal masses of the stages $i+1$ to n:

$$\begin{aligned} &\min && f_i(\mathbf{z_{sh}}, \bar{\mathbf{z}}_i, \mathbf{y}) && (1.34)\\ &\text{w.r.t.} && \bar{\mathbf{z}}_i && \\ &\text{s.t.} && \mathbf{g}_i(\mathbf{z_{sh}}, \bar{\mathbf{z}}_i, \mathbf{y}) \leq 0 && (1.35)\\ & && \mathbf{h}_i(\mathbf{z_{sh}}, \bar{\mathbf{z}}_i, \mathbf{y}) = 0 && (1.36)\\ & && \mathbf{y}_{i.} = \mathbf{c}_{i.}(\mathbf{z_{sh}}, \bar{\mathbf{z}}_i, \mathbf{y}_{.i}) && (1.37)\\ & && \bar{\mathbf{z}}_{i_{\min}} \leq \bar{\mathbf{z}}_i \leq \bar{\mathbf{z}}_{i_{\max}} && (1.38) \end{aligned}$$

$i \leftarrow i - 1$

where $\mathbf{g_0}(\cdot)$ are system-level inequality constraints and Eq.(1.36) is only considered for $i = n$ and Eq.(1.37) for $i \neq n$. This formulation allows to separately optimize each stage in a hierarchical process. The last stage is optimized first and the first stage is optimized last. The result of the previous optimization is passed to the next launch vehicle stage optimization (Fig. 1.15). Furthermore, this formulation ensures to the user to have multidisciplinary feasible solution even if the system-level optimizer has not converged yet. The different optimizations of the stages cannot be performed in parallel which may be a drawback when parallelization is possible in terms of computational cost. This formulation has been applied to the design of a three-stage-to-orbit launch vehicle [Balesdent et al., 2012a] and compared to MDF. The 3$^{\text{rd}}$ SWORD formulation appears to be the best formulation among the SWORD formulations and succeed to reduce the number of calls to the disciplines compared to MDF. For more details on SWORD see [Balesdent et al., 2012a].

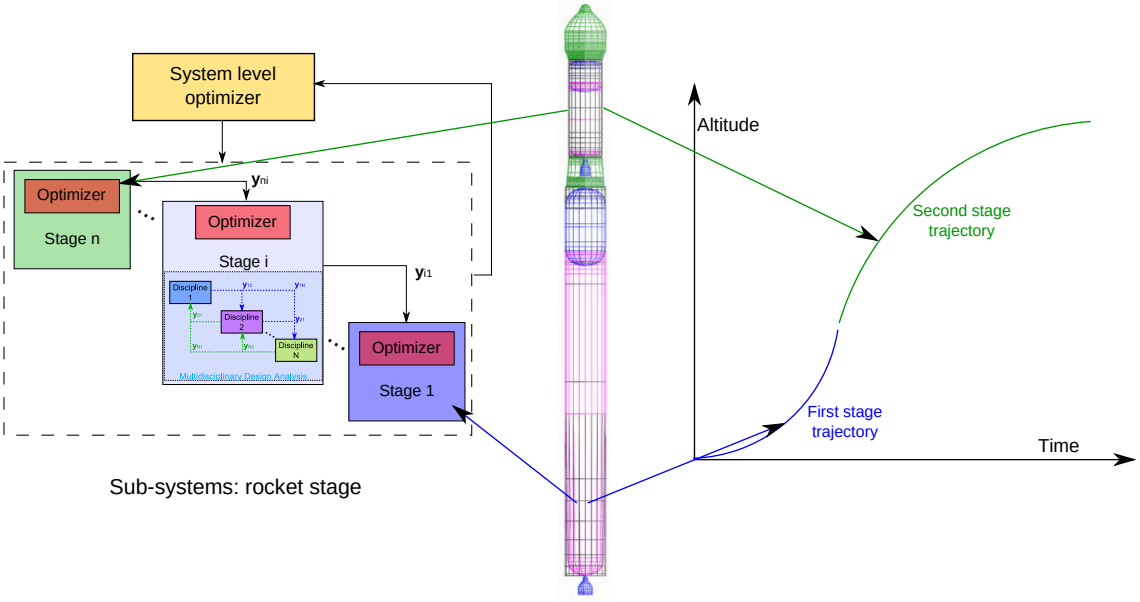

Figure 1.15: 3rd SWORD formulation

1.5 Conclusion

Several existing deterministic MDO formulations have been presented in this chapter. These formulations might be classified according to the interdisciplinary coupling handling techniques (coupled or decoupled approaches) and according to the number of level of optimization (single or multi). Decomposition strategies of the design process can offer autonomy to the engineering teams of each discipline but they make the MDO problem to solve more complex. Deterministic MDO methods have been applied to solve launch vehicle design problem involving mostly the single-level MDF formulation. More adapted formulations such as SWORD have been developed in order to facilitate the decomposition of the design process according to the stages of the launch vehicle.

Since the last decade, space agencies such as NASA [Zang et al., 2002] stress upon the need for the development of design methods allowing launch vehicles to have better performance, higher reliability at lower cost and risk. To efficiently address these objectives, designers use modeling, simulation and optimization methods and include all the relevant aspects of the launch vehicle life-cycle from the conceptual design to its industrialization. However, in practice, the life-cycle is affected by various uncertainties arising from the launch vehicle itself, its environment or its operational conditions. These uncertainties may modify or introduce fluctuations in the system performance or even may cause system failures due to unexpected deviation from nominal expected conditions. Therefore, taking into account the various uncertainties in the early design phases is essential to avoid unexpected design failure and to ensure optimal performance. The introduction of uncertainty in MDO formulations would offer the possibility to enhance the design of complex systems by taking into account potential synergistic uncertain phenomena thanks to coupled discipline analysis. Uncertainty-based Multidisciplinary Design Optimization (UMDO) aims at solving MDO problem under uncertainty.

Taking into account uncertainties in MDO require a number of new thematics to accurately treat uncertainty. These new thematics will be introduced in the following chapters.

First, the definition of uncertainty, its classification into different types has to be discussed in order to identify the potential sources of uncertainty (section 2.2.1). Then, an appropriate modeling of uncertainty is a premise in UMDO. Mathematical representation of the uncertainty modeled allows to incorporate uncertainty in the MDO framework. Different formalisms of uncertainty exist and the appropriate choice of modeling is essential as it affects all the UMDO process (section 2.2.2). Moreover, the propagation of uncertainty is another essential thematic which involves the calculation of the measure of uncertainty of the objective function and of the inequality constraints (section 2.3). The calculation of uncertainty measures for the constraints may involve reliability assessment for the systems and dedicated methods are needed. The existing methods are presented in chapter 4. Furthermore, an appropriate handling of the interdisciplinary coupling is required to ensure the multidisciplinary feasibility of the system. The existing approaches are detailed in chapter 3. Eventually, optimization algorithms in noisy environment are needed to find a robust and reliable solution while ensuring its optimality (see chapter 5).

Rich literature has been published to cover this large specter of thematics linked to UMDO methodologies. In the following chapters 2 to 5, the key aspects, methods and formulations existing in literature are presented in order to provide a comprehensive overview of the UMDO methods.

Chapter 2

Uncertainty formalisms and reliability analyses

Contents

Chapter goals

- Present the principal existing approaches to handle uncertainty (modeling, propagation, reliability assessment, surrogate modeling),
- Introduce unified notations within the framework of uncertainty.

2.1 Introduction

The description of several characteristics of uncertainty is essential to lay the foundation of UMDO methodologies: the definition of uncertainty, the identification of sources of uncertainty, their mathematical representations, their propagation in the disciplines and in the system, *etc.* The main goal of this chapter is to review the elementary notions on these subjects which will be used in the following of the thesis.

In this chapter, in section 2.2.1, the definition, taxonomy and classification of uncertainty are introduced in order to identify different types of uncertainty and their appropriate mathematical representations (section 2.2.2). Then, in section 2.3, classical methods to propagate uncertainty through input-output functions are reviewed. The uncertainty propagation methods are essential to characterize the uncertainty of a system performance and reliability based on input disciplinary uncertainties. In section 2.4, a particular type of uncertainty propagation is reviewed, the reliability analysis. For that purpose, the main existing approaches for rare event probability estimation are introduced. Finally, in section 2.5, surrogate models used for reliability analysis are reviewed. They allow to decrease the computational cost of rare event probability estimation by approximating the exact limit state function defining the failure domain by a metamodel less computationally intensive.

2.2 Uncertainty modeling

2.2.1 Uncertainty definition and classification

Engineering problems are solved inside the boundaries of a model universe. A model is a representation of the reality under specific assumptions [Kiureghian and Ditlevsen, 2009]. Due to simplification hypotheses, lack of knowledge and inherent uncertain phenomena, models represent reality with uncertainty.

Modern approaches of uncertainty handling have emerged with the Reactor Safety Study (WASH-1400) in 1974 conducted by Rasmussen [Rasmussen, 1974] and the different extensive reviews by the risk and safety community [Pate-Cornell, 1986]. Different taxonomies and classifications of uncertainty have been proposed since the Reactor Safety Study [Krause and Clark, 1993; Bouchon-Meunier and Nguyen, 1996; Klir, 2005] reflecting the various visions of uncertainty and their evolution for the last 20 years. In more recent years, a consensus has been established on two main categories: **aleatory** and **epistemic** uncertainty. Thunnissen [Thunnissen, 2003] presented a review of uncertainty classification for various fields (social sciences, physical sciences, engineering, *etc.*). Specificities for aleatory and epistemic uncertainties exist depending on the field of application and the granularity of the studied phenomena. For aerospace vehicles at the conceptual design phase, aleatory and epistemic uncertainties are classically distinguished [Thunnissen, 2003; Yao et al., 2011] and these two categories are adopted in this thesis. Definitions and examples of these two types of uncertainty are detailed in the following.

Aleatory uncertainty.
It corresponds to the inherent variability of a physical system and/or its environment under consideration. Aleatory uncertainty cannot be reduced by collecting more information or data. It is also referred as variability, stochastic uncertainty, randomness, irreducible uncertainty. Classical examples of aleatory uncertainties are: the presence, the direction and the amplitude of a wind

gust during a rocket launch (Fig. 2.1), the exact mass of propellant introduced in the rocket before the launch, *etc.*

Epistemic uncertainty.
The epistemic uncertainty arises from any lack of knowledge or simplifications about modeled phenomena and may be reduced by collecting more information. It encompasses the model uncertainty which is associated to the precision of the chosen simplified mathematical models to represent the real physical phenomena. It is also referred as ignorance, subjective uncertainty, reducible uncertainty. For instance, the flow model built under simplification hypotheses such as an incompressible, without boundary layer, without turbulence flow in a rocket nozzle represents with a low fidelity the gas flow compared to real physical phenomena (Fig. 2.1).

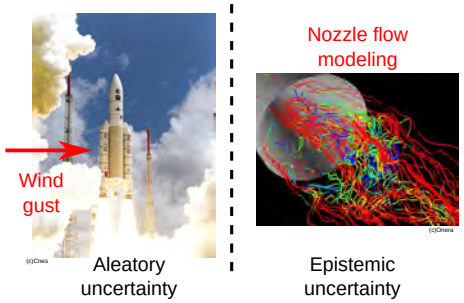

Figure 2.1: Examples of aleatory and epistemic uncertainties for launch vehicle design

The distinction between the two types of uncertainty is important because specific mathematical modeling exist for each type of uncertainty. Zhang *et al.* [Zhang and Huang, 2010] highlighted that in UMDO, improper modeling of uncertainty could engender greater degree of uncertainty than those introduced by physical phenomena. In order to propagate uncertainty through system models, an adequate representation of the input uncertainty is required in order to have to meaningful quantification of the uncertainty in the system response. The uncertainty modeling is a key step in the UMDO problem statement and overlooking could result in non robust solution to the real uncertainty [Choi et al., 2005]. Probability theory developed by Kolmogorov in 1934 [Kolmogorov, 1950] was the first advanced mathematical formalism dealing with uncertainty. With its important theoretical background, probability theory is traditionally used by engineers to model aleatory uncertainty. It is due to the possibility to access to large amount of information to accurately represent uncertainty. However, as pointed out by [Ferson et al., 1996; Helton et al., 2004; Zhang and Huang, 2010], when there are not enough sufficient data to construct precise statistical distributions of model inputs due to time, money, *etc*, the results of the probabilistic method will be unreliable or risky. Other more adapted formalisms such as interval [Moore et al., 2009] or Evidence theory [Dempster, 1967; Shafer, 1976] have been developed. In the next section, an overview of probability theory and interval formalism is presented in order to introduce key concepts required to solve UMDO problems described in parts II and III. For the sake of conciseness, other formalisms such as Evidence theory or Fuzzy logic will not be described. For more details, one can consult [Dempster, 1967; Klir, 2005]

2.2.2 Elements of probability theory

Definition 2.2.1. *A probability measure $\mathbb{P}$ on a measurable set $(\Omega, \mathcal{A})$, where Ω is the sample space with its σ-algebra $\mathcal{A}$, is a mapping from $\mathcal{A}$ to $[0,1]$ such that the two following point are satisfied [Kolmogorov, 1950]:*

- $\mathbb{P}(\Omega) = 1$
- *let $(A_i)_{i\in\mathbb{N}}$ be a countable collection of disjoint events in $\mathcal{A}$:* $\mathbb{P}\left(\bigcup_{i=0}^{+\infty} A_i\right) = \sum_{i=0}^{+\infty} \mathbb{P}(A_i)$

The triple $(\Omega, \mathcal{A}, \mathbb{P})$ is called a *probability space*.

Definition 2.2.2. *Let $(\Omega, \mathcal{A}, \mathbb{P})$ denote a probability space, a real-valued random variable U is a measurable application defined by:*

$$U : \begin{cases} \Omega \to \mathbb{R} \\ \omega \to U(\omega) \end{cases} \tag{2.1}$$

with w an outcome. For the sake of conciseness, in the rest of the thesis, a realization $U(\omega)$ is noted u.

Definition 2.2.3. *Let $(\Omega, \mathcal{A}, \mathbb{P})$ denote a probability space, a d-dimensional real-valued random variable vector $\mathbf{U}$ is a measurable application defined by:*

$$\mathbf{U} : \begin{cases} \Omega \to \mathbb{R}^d \\ \omega \to \mathbf{U}(\omega) \end{cases} \tag{2.2}$$

In the same way, a realization $\mathbf{U}(\omega)$ is noted $\mathbf{u}$. The i^{th} coordinate of the vector $\mathbf{U}$ is noted $U^{(i)}$ and $\mathbf{U} = \left[U^{(1)}, \ldots, U^{(d)}\right]$. For instance, let's consider the fall-out position of a launcher stage (*i.e.* latitude and longitude) which evolves in the 2-dimensional sample space space $\mathbf{\Omega} = [-90°, 90°] \times [-180°, 180°]$ (with '$\times$' the Cartesian product between the longitude and the latitude spaces). 150 trials of launcher stage fall-out positions obtained with a simulator are represented in Figure 2.2.

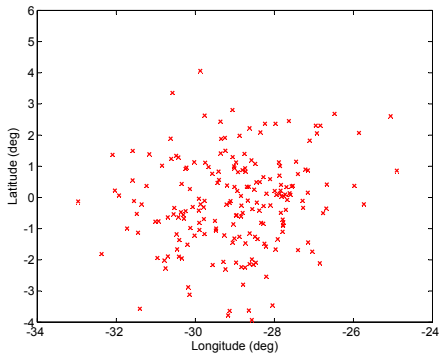

Figure 2.2: 150 trials of launcher stage fall-out position

Definition 2.2.4. *Let $(\Omega, \mathcal{A}, \mathbb{P})$ denote a probability space and U a variable that is a real-valued measurable mapping from $(\Omega, \mathcal{A})$ to $(\mathbb{R}, \mathfrak{B}(\mathbb{R}))$ with $\mathfrak{B}(\mathbb{R})$ the Borel algebra. The variable U is a continuous random variable if there exists a function $\phi : \Omega \to \mathbb{R}$ such that:*

- $\forall u \in \mathbb{R},\ \phi(u) \geq 0$
- *ϕ is a continuous function almost everywhere on Ω*
- $\displaystyle\int_{-\infty}^{+\infty} \phi(u)du = 1$
- $\mathbb{P}(U \in A) = \displaystyle\int_A \phi(u)du,\ \forall A \in \mathfrak{B}(\mathbb{R})$

The function $\phi(\cdot)$ is the Probability Density Function (PDF) of the random variable U. In Figures 2.3 and 2.4, a simple example of PDF $\phi(\cdot)$ defined on $\mathbb{R}$ and some random samples generated with this PDF are represented.

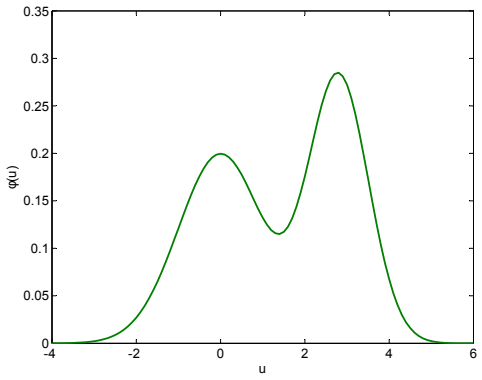

Figure 2.3: PDF $\phi(\cdot)$

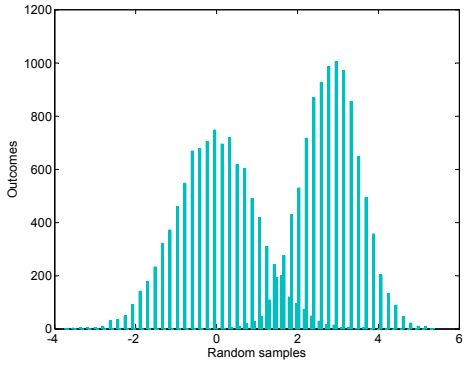

Figure 2.4: Corresponding iid random samples generated with PDF $\phi(\cdot)$

Definition 2.2.5. *Let U be a random variable and $\phi(\cdot)$ its PDF. The Cumulative Distribution Function (CDF) $\Phi(\cdot)$ of U is defined by:*

$$\Phi : \begin{cases} \mathbb{R} \to [0,1] \\ u \to \mathbb{P}(U \leq u) \end{cases} \tag{2.3}$$

The CDF may also be defined from the PDF by:

$$\forall u \in \mathbb{R},\ \Phi(u) = \int_{-\infty}^{u} \phi(t)\,dt \tag{2.4}$$

The CDF uniquely defines the probability law of a random variable. The cumulative distribution function $\Phi(\cdot)$ of the PDF $\phi(\cdot)$ proposed in Figure 2.3 is represented in Figure 2.5.

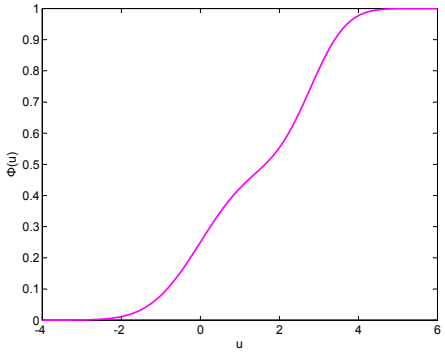

Figure 2.5: Cumulative distribution function $\Phi(\cdot)$ of the PDF $\phi(\cdot)$

Definition 2.2.6. *: Statistical moments*
A common way to characterize a random variable is to determine its statistical moments. The first order statistical moment is the mathematical expectation noted $\mathbb{E}[\cdot]$ and defined by:

$$\mathbb{E}[U] = \int_{\mathbb{R}} u\ \phi(u)\mathrm{d}u = \mu_U \tag{2.5}$$

if the integral convergence is ensured.

The centered second order statistical moment is the variance noted $\mathbb{V}[\cdot]$ and is defined by:

$$\mathbb{V}[U] = \int_{\mathbb{R}} (u - \mathbb{E}(U))^2\, \phi(u)\mathrm{d}u = \mathbb{E}\left[(U - \mathbb{E}[U])^2\right] \tag{2.6}$$

The standard deviation σ of U is defined based on the variance by: $\sigma[U] = \sqrt{\mathbb{V}[U]}$. Provided that the expected value is non null, the *coefficient of variation* of U is defined as the ratio between the standard deviation and the expected value: $\delta(U) = \frac{\sigma[U]}{|\mathbb{E}[U]|}$. Moreover, the covariance between two uncertain variables U_1 and U_2 is defined as follows:

$$\mathrm{Cov}(U_1, U_2) = \mathbb{E}\left[(U_1 - \mu_{U_1})(U_2 - \mu_{U_2})\right] \tag{2.7}$$

The p-order centered statistical moment ($p \geq 2$) is defined by:

$$\mathbb{M}_p(U) = \int_{\mathbb{R}} (u - \mathbb{E}[U])^p\, \phi(u)\mathrm{d}u = \mathbb{E}\left[(U - \mathbb{E}[U])^p\right] \tag{2.8}$$

if the integral convergence is ensured.

All these statistical moments may be easily generalized for random variable vector.

Theorem 2.2.1. *Transport theorem. Let* $\mathbf{U}$ *a continuous d-dimensional random vector with a joint PDF* $\phi(\cdot)$ *and* $c : \mathbb{R}^d \to \mathbb{R}$ *a measurable function, the expected value* $\mathbb{E}\left[c(\mathbf{U})\right]$ *is given by:*

$$\mathbb{E}\left[c(\mathbf{U})\right] = \int_{\mathbb{R}^d} c(\mathbf{u})\phi(\mathbf{u})\, d\mathbf{u} \tag{2.9}$$

if the integral convergence is ensured. This theorem allows one to define the probabilities of interest in an industrial context with $c(\cdot)$ an input-output function (also referred as black-box function) characterizing the studied system. Such function may be only evaluated, for a given input it provides the corresponding output.

Classical parameterized PDF distributions are often used to model aleatory uncertainties. Among these distributions, the Gaussian distribution (also called normal distribution) is the most used PDF to represent uncertainty. The Gaussian distribution is extensively used to represent uncertainty as it is the distribution that present the maximal entropy (measure of the information content) among all real-valued distributions with specified expectation μ and variance σ^2. The central limit theorem also justifies this PDF choice in several domains. A Gaussian variable U is represented by a PDF noted $\phi_{\mathcal{N}(\mu,\sigma^2)}$ with μ its mean value and σ^2 its variance. The so-called standard Gaussian distribution noted $\phi_{\mathcal{N}_{(0,1)}}$ is obtained for $\mu = 0$ and $\sigma^2 = 1$ (Fig. 2.6). The PDF of a Gaussian variable is given by:

$$\phi_{\mathcal{N}(\mu,\sigma^2)}(u) = \frac{1}{\sqrt{2\pi\sigma^2}} \exp\left(-\frac{(u-\mu)^2}{2\sigma^2}\right), \; u \in \mathbb{R} \tag{2.10}$$

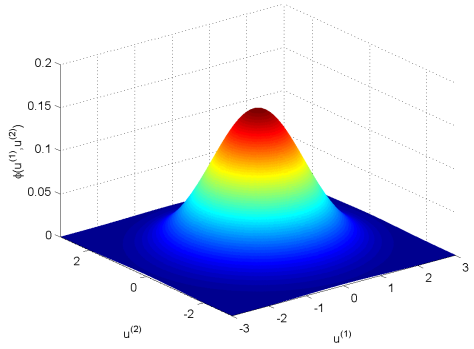

Figure 2.6: Two dimensional standard Gaussian distribution PDF

Another distribution intensively used is the uniform distribution. A uniform variable U is represented by a PDF noted $\phi_{\mathcal{U}(a,b)}$ with a the lower bound and b the upper bounds of the distribution. The uniform distribution assumes that each singleton inside the interval $[a, b]$ has the same probability to occur:

$$\phi_{\mathcal{U}(a,b)}(u) \begin{cases} \frac{1}{b-a} & \text{if } \; u \in [a,b] \\ 0 & \text{else} \end{cases}$$

Other classical parameterized distributions are Beta distribution, Gamma distribution, Lognormal distribution, *etc.*

2.2.3 Elements of interval analysis

Interval data are commonly encountered in practical engineering problems. Ferson *et al.* [Ferson et al., 2007] and Du *et al.* [Du et al., 2005] discussed such situations where interval data are

present. For instance, in early design phase, often the experts cannot provide a complete PDF of the uncertain variables U and the only information available is in the form of an expert opinion expressed through interval data which specify a range of possible values for the variable. Moreover, it appears that a uniform distribution might not be adapted in some cases because it requires to know that the samples are distributed with an iso-probability inside the interval to be appropriately used [Klir, 2005; Ferson et al., 2007]. In the following, a random variable is noted U with a capital letter whereas an epistemic variable is noted u.

A closed interval for a real valued continuous uncertain variable u is a set defined as:

$$\Upsilon = \{u \in \mathbb{R} | u_{\min} \leq u \leq u_{\max}\} \tag{2.11}$$

with $u_{\min}$ and $u_{\max}$ respectively the lower and upper bounds of the interval. An interval is denoted by its bounds $[u_{\min}, u_{\max}]$. For a d-dimensional uncertain variable $\mathbf{u} = \left[u^{(1)}, \ldots, u^{(d)}\right]$, its representation by an interval is given by:

$$\mathbf{\Upsilon} = \{\mathbf{u} \in \mathbb{R}^d | u^{(i)} \in \left[u^{(i)}_{\min}, u^{(i)}_{\max}\right] \ \forall i \in \{1, \ldots, d\}\} \tag{2.12}$$

As intervals are sets, the same arithmetical operations are possible such as intersection, unions, sums, *etc.* For more details on interval formalism, one can refer to [Moore et al., 2009].

When epistemic variables are modeled with probability theory, Bayesian theory [Soundappan et al., 2004; Bernardo and Smith, 2009] may be used to update our knowledge about uncertain parameters based on new simulations or experiments. It would offer the possibility to take into account the evolution of the knowledge about the uncertainty and its modeling along the different design phases (with the use of increase fidelity models). An approach based on Bayesian theory will be presented in chapter 3. In the rest of the thesis, epistemic uncertainty will be modeled with interval formalism. For more details about Bayesian theory see [Bernardo and Smith, 2009].

2.3 Uncertainty propagation

The uncertainty propagation consists in determining the impact of the disciplinary input uncertainty on the discipline output. Indeed, due to the presence of uncertainty, the discipline output is also an uncertain variable that need to be characterized. The output of the discipline is supposed to be a scalar variable in this chapter (except in section 2.3.1.3).

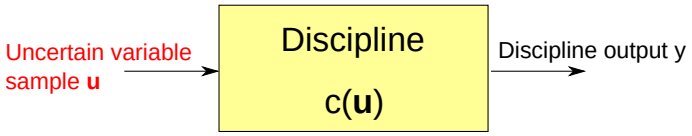

Figure 2.7: Discipline: input-output function

Let us consider a discipline represented as an input-output function by (Fig. 2.7):

$$c : \begin{cases} \mathbb{R}^d \to \mathbb{R} \\ \mathbf{u} \to y = c(\mathbf{u}) \end{cases} \tag{2.13}$$

Given input uncertainty $\mathbf{U}$ (either represented with the probability or the interval formalisms), the uncertainty propagation consists in characterizing the uncertain discipline output Y. Several

methods exist to represent the discipline output depending on the uncertainty formalism and are introduced in the following sections.

2.3.1 Uncertainty propagation within the probability framework

In this section, input uncertainty $\mathbf{U}$ is modeled with the probability theory and defined by its known joint PDF $\phi : \mathbb{R}^d \to \mathbb{R}$ (Fig. 2.8). Within the probability formalism, the output Y may be characterized by:

- Its statistical moments,
- Its PDF.

Another way to characterize the output is to study its distribution with respect to a threshold and to determine a probability to exceed (or to be underneath) this threshold. This study is called reliability analysis and will be detailed in section 2.4.

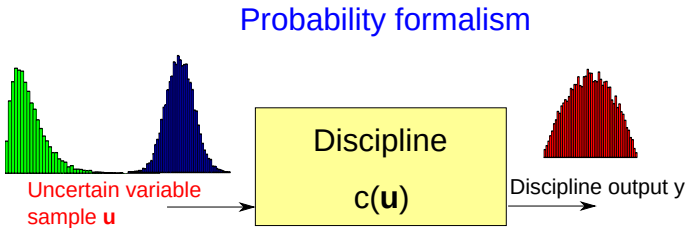

Figure 2.8: Uncertainty propagation with probability formalism

2.3.1.1 Statistical Moment Estimation

The statistical moment calculation of the discipline output consists in computing multidimensional integrals Eqs.(2.5,2.6,2.8) using the Transport theorem (see Theorem 2.2.1). In practice, analytical calculation of these integrals is impossible due to the presence of the black-box which can only be evaluated. These multidimensional integrals have to be numerically approximated. In the following paragraphs, classical methods to estimate the statistical moments are introduced.

Crude Monte Carlo (CMC)
One way to approximate a multivariate integral is to use CMC. This sampling method is easy to implement and often used to compute integrals. In CMC, M independent and identically distributed (iid) samples $\mathbf{u}_{(1)}, \ldots, \mathbf{u}_{(M)}$ are generated according to the joint PDF $\phi(\cdot)$ (Fig. 2.9). The discipline is evaluated on these inputs with the function $c(\cdot)$: $c\left(\mathbf{u}_{(1)}\right), \ldots, c\left(\mathbf{u}_{(M)}\right)$. Then, the mathematical expectation of the discipline output is numerical approximated by:

$$\mathbb{E}[Y] = \mathbb{E}[c(\mathbf{U})] \simeq \frac{1}{M} \sum_{k=1}^{M} c\left(\mathbf{u}_{(k)}\right) = \mathbb{E}^{CMC}[Y] \tag{2.14}$$

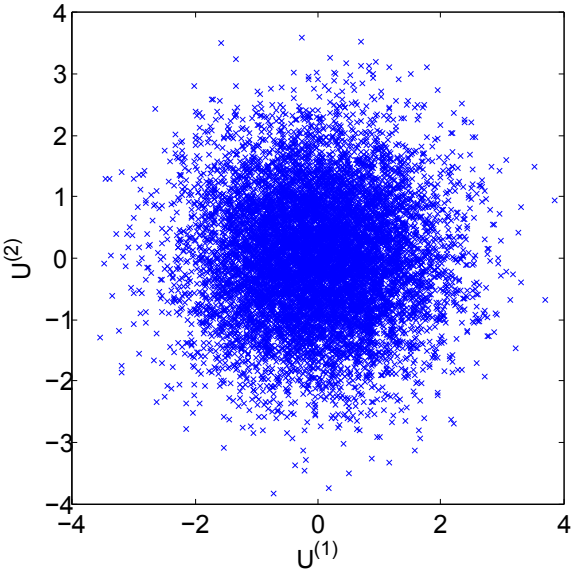

Figure 2.9: CMC samples input space

The estimator $\mathbb{E}^{CMC}[\cdot]$ is a random variable as it is an approximation based on the M iid selected samples. This estimation converges almost surely to the mathematical expectation as a consequence of the law of large numbers. Providing M is sufficiently large, according to the central limit theorem, the CMC estimator is unbiased and normally distributed meaning that

$$\left(\mathbb{E}^{CMC}[Y] - \mathbb{E}[Y]\right) \underset{M \to +\infty}{\longrightarrow} \phi_{\mathcal{N}(0, \sigma^2_{\mathbb{E}^{CMC}[Y]})} \tag{2.15}$$

The Relative Error (RE) of the CMC estimator is given by:

$$RE\left(\mathbb{E}^{CMC}[Y]\right) = \frac{\sigma_{\mathbb{E}^{CMC}[Y]}}{\mathbb{E}[Y]} = \frac{1}{\sqrt{M}} \frac{\sqrt{\mathbb{E}[Y] - \mathbb{E}[Y]^2}}{\mathbb{E}[Y]} \tag{2.16}$$

The CMC convergence speed only depends on M and $\mathbb{E}[Y]$ whatever the dimension d of the input space. The lower $RE(\cdot)$ the greater confidence in $\mathbb{E}^{CMC}[\cdot]$ with respect to the residual error in the estimation. CMC may reach any level of accuracy if enough samples are generated. Based on the same idea, p-order centered statistical moments may be approximated by CMC. It can be easily implemented but, when the discipline is computationally intensive as in case of the launch vehicle design, this method is computationally prohibitive. Other sampling methods such as Latin Hypercube Sampling (LHS) [Helton and Davis, 2003] have been developed to decrease the computational burden by a better sampling scheme.

Quadrature rules

Quadrature rules approximate integrals as a weighted sum of functions evaluated at specific points in the domain of integration [Davis and Rabinowitz, 2007] whereas in CMC the points are randomly

sampled according to the PDF $\phi(\cdot)$. The expected value of the discipline output is approximated by quadrature rules such that:

$$\mathbb{E}[Y] = \mathbb{E}[c(\mathbf{U})] \simeq \sum_{i_1=1}^{M_1} \sum_{i_2=1}^{M_2} \cdots \sum_{i_d=1}^{M_d} \left(w_{(i_1)} \otimes w_{(i_2)} \otimes \cdots \otimes w_{(i_d)} \right) c\left(u_{(i_1)}^{(1)}, u_{(i_2)}^{(2)}, \ldots, u_{(i_d)}^{(d)} \right) \quad (2.17)$$

where w are weights and $\otimes$ is the tensor product operator. The simplest approximation of the multidimensional integral is done through a tensor product quadrature (Fig. 2.10) with $M_1, ..., M_D$ the number of specific points in each dimension. The quadrature rules are based on interpolating function, generally polynomial functions. The interpolation points $u_{(i_1)}^{(1)}, u_{(i_2)}^{(2)}, \ldots, u_{(i_d)}^{(d)}$ and the weights w_i are selected according to the input variable PDF $\phi(\cdot)$. Table 2.12 presents a set of polynomial families which provide an optimal basis for different PDFs. The optimal basis is derived from the family of hypergeometric orthogonal polynomials known as the Askey scheme [Askey and Wilson, 1985]. The optimality of these polynomial basis results from their orthogonality with respect to weighting functions corresponding to the standard PDFs. The density and weighting functions differ by a constant factor because a PDF integral has to be equal to one over the support range. The selected points in the quadrature rules are the roots of the polynomials which are orthogonal to the weighting functions of the input variable PDF joint ϕ [Davis and Rabinowitz, 2007].

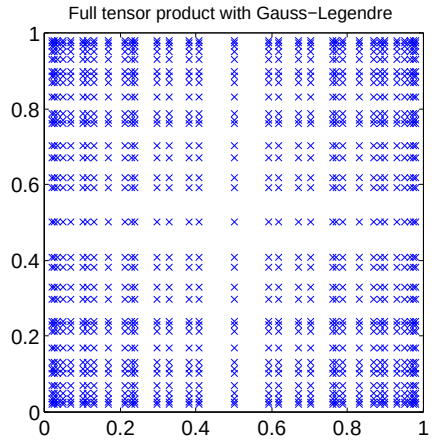

Figure 2.10: Full tensor product 2D

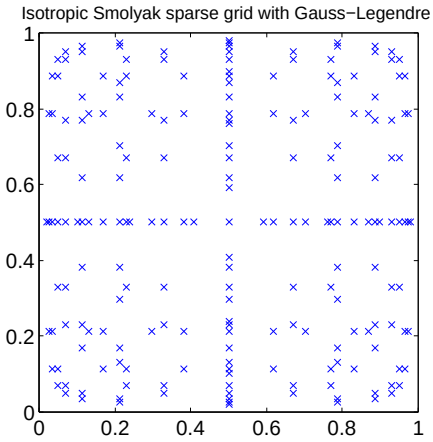

Figure 2.11: Smolyack sparse grid 2D

Table 2.12: Examples of orthogonal polynomial families [Eldred, 2009]

Distribution	Polynomial family	Weight function	Support range
Normal	Hermite	$e^{\frac{-u^2}{2}}$	$[-\infty, \infty]$
Uniform	Legendre	1	$[-1, 1]$
Exponential	Laguerre	e^{-u}	$[0, \infty]$
Beta	Jacobi	$(1-u)^{\alpha}(1+u)^{\beta}$	$[-1, 1]$

The quadrature rules require $\prod_{i=1}^{d} = M_i$ discipline evaluations to compute a statistical mo-

ment of the discipline output. Compared to CMC, the approximation based on tensor product is efficient for a small number of input uncertain variables, but the method suffers from the curse of dimensionality [Eldred, 2009]. Sparse grid approaches [Smolyak, 1963] can be implemented in order to decrease the number of function evaluations while preserving the accuracy for high dimensional integrals. An example of two dimensional full tensor product and Smolyak sparse grid based on Gauss-Legendre interpolation is illustrated in Figures (2.10,2.11). More details on quadrature rules may be found in [Davis and Rabinowitz, 2007].

Surrogate model

Approximation of the black-box function $c(\cdot)$ may be used to estimate the statistical moments of the discipline outputs [Vapnik and Vapnik, 1998; Hurtado, 2004a; Basudhar et al., 2012; Hosder, 2012; Balesdent et al., 2013]. In the following two surrogate models to propagate uncertainty are described as they will be later used in part II. Moreover, surrogate models used within the framework of reliability analysis will be introduced in section 2.4. The surrogate models offer the possibility to compute many discipline output samples cheaply in order to accurately estimate statistical moments. However, it is necessary to ensure the accuracy of the surrogate model and they often suffer from the curse of dimensionality.

Taylor series expansion

Taylor series expansion is often used to propagate uncertainty. Taylor series expansion allows one to locally approximate the function $c(\cdot)$ and the statistical moments of the output. For instance, with a first order Taylor series expansion, the function $c(\cdot)$ is approximated around a local realization $\mathbf{u}_0$ by:

$$c(\mathbf{u}) \simeq c(\mathbf{u}_0) + \sum_{k=1}^{d} \frac{\partial c(\mathbf{u}_0)}{\partial \mathbf{u}^{(k)}} \left(\mathbf{u}^{(k)} - \mathbf{u}_0^{(k)} \right) \tag{2.18}$$

Based on this local approximation, the expected value and standard deviation of the discipline output are estimated by:

$$\mathbb{E}[Y] = \mathbb{E}[c(\mathbf{U})] \simeq c(\mathbf{u}_0) \tag{2.19}$$

$$\mathbb{V}[Y] = \mathbb{V}[c(\mathbf{U})] \simeq \sum_{k=1}^{d} \left(\frac{\partial c(\mathbf{u}_0)}{\partial \mathbf{u}^{(k)}} \right)^2 \sigma^2_{\mathbf{U}^{(k)}} + \sum_{k=1}^{d} \sum_{j=k+1}^{d} \left(\frac{\partial c(\mathbf{u}_0)}{\partial \mathbf{u}^{(k)}} \right) \left(\frac{\partial c(\mathbf{u}_0)}{\partial \mathbf{u}^{(i)}} \right) \mathrm{Cov}\left(\mathbf{u}^{(k)}, \mathbf{u}^{(i)} \right) \tag{2.20}$$

where $\sigma_{\mathbf{U}^{(k)}}$ is the standard deviation of the k^{th} component of the vector uncertain $\mathbf{U}$. Taylor series expansion is only valid locally and requires the computation of partial derivatives that can be difficult for complex simulation models [Arras, 1998]. The first order approximation is only accurate for nearly linear functions. Higher order expansion may be used for nonlinear models but requires the computation of the Hessian. The estimation accuracy of the statistical moments decreases as the coefficient of variation of the input random variable increases [Arras, 1998].

Polynomial Chaos Expansion

Polynomial Chaos Expansion (PCE) is an polynomial approximation of the function $c(\cdot)$ [Wiener, 1938; Askey and Wilson, 1985; Eldred, 2009]. PCE consists of an expansion of a function $c(\cdot)$ such as $\mathbb{E}[c(\mathbf{U}^2)] < +\infty$ over a polynomial orthogonal basis [Hosder, 2012]:

$$c(\mathbf{U}) = a_0 + \sum_{k=1}^{\infty} a_k P_1\left(U_{(k)}^{(1)}\right) + \sum_{i=1}^{\infty}\sum_{j=1}^{i} a_{i,j} P_2\left(U_{(i)}^{(1)}, U_{(j)}^{(2)}\right) + ... \tag{2.21}$$

with $\{P_1, P_2, ..., P_r, ...\}$ a basis of orthogonal polynomials, with P_r of degree r and $\mathbf{a}$ the vector of the PCE coefficients. The choice of the polynomial basis is made consistently with the distribution of the input random variables in the same way than quadrature rules (see section 2.3.1.1). The polynomial basis is orthogonal to the weighting function [Askey and Wilson, 1985; Eldred, 2009] of the input uncertain variable distributions. Classical orthogonal polynmial families are given in Table 2.12. In practice, the expansion Eq.(2.21) is truncated to a degree d and is reorganized to have a one-to-one correspondence between the coefficients and the polynomials:

$$c(\mathbf{U}) \simeq \sum_{j=0}^{d_{\text{PCE}}} \alpha_j \Psi_j(\mathbf{U}) \equiv \hat{c}(\mathbf{U}, \boldsymbol{\alpha}) \tag{2.22}$$

where α_j and Ψ_j correspond to $a_{i,j,...,k}$ and $P_r\left(U_i^{(1)}, U_j^{(2)}, \ldots, U_k^{(r)}\right)$. Two types of truncation may be distinguished. The *total expansion order* includes a complete basis of polynomials up to a total order specification p. The number of PCE coefficients is given by: $d_{\text{PCE}} + 1 = \frac{(n+p)!}{n!p!}$ with n the number of uncertain variables and p the total order specification. The other approach, the *tensor product expansion*, does not bound the total expansion order but only truncates on a per-dimension basis [Askey and Wilson, 1985; Eldred, 2009]. It allows one to have different truncation orders p_i and therefore enables anisotropy in the polynomial order for each dimension. The number of PCE coefficients is given by: $d_{\text{PCE}} + 1 = \prod_{i=1}^{n}(p_i + 1)$.

The difficulty in PCE is the estimation of the polynomial coefficients [Poles and Lovison, 2009]. Intrusive and non intrusive approaches exist to compute the coefficients. The intrusive approaches require to modify the simulation code used to compute the function $c(\cdot)$ in order to determine the PCE coefficients. As only black-box functions to model the disciplines are considered, we focus on non intrusive methods. Two main techniques may then be employed: the orthogonal spectral projection or the regression [Xiong et al., 2011]. The orthogonal spectral projection consists in projecting the output $c(\cdot)$ on each polynomial basis function using the orthogonality [Eldred, 2009]:

$$\alpha_j = \frac{< c, \Psi_j >}{< \Psi_j^2 >} = \frac{1}{< \Psi_j^2 >} \int_{\mathbf{\Omega}} c(\mathbf{u}) \Psi_j(\mathbf{u}) \phi(\mathbf{u}) \mathrm{d}\mathbf{u} \tag{2.23}$$

with $< ., . >$ the inner product on functions, $< .^2 >$ the norm squared. The multivariate integral can be estimated by sampling or by other numerical integration methods [Eldred, 2009]. The regression method relies on a least squared fitting. Given M sample points $\{\mathbf{u}_{(1)}, ..., \mathbf{u}_{(M)}\}$, the PCE coefficient vector $\boldsymbol{\alpha} = [\alpha_0, ..., \alpha_{d_{\text{PCE}}}]^{\mathrm{T}}$ is determined by [Eldred and Burkardt, 2009]:

$$\boldsymbol{\alpha} = \underset{\mathbf{a} \in \mathbb{R}^{d_{\text{PCE}}}}{\operatorname{argmin}} \sum_{i=1}^{M} \left(c\left(\mathbf{u}_{(i)}\right) - \hat{c}\left(\mathbf{u}_{(i)}, \mathbf{a}\right)\right)^2 \tag{2.24}$$

Xiong *et al.*[Xiong et al., 2011] proposed to use the roots of the orthogonal polynomial basis as the sample points and to use a weighted least square regression to represent the higher contribution of sample points in the higher frequency region of the input random variables.

PCE metamodeling is interesting in the uncertainty context as it provides analytical statistical moment formula linking the PCE coefficients to the output statistical moments. For instance the expected value and the standard deviation of the PCE output are given by:

$$\mathbb{E}\left[\hat{c}(\mathbf{U})\right] = \mu_{\hat{c}} \simeq \sum_{j=0}^{d} \alpha_j < \Psi_j > \tag{2.25}$$

$$\mathbb{V}\left[\hat{c}(\mathbf{U})\right] = \sigma^2_{\hat{c}} \simeq \sum_{j=0}^{d} \alpha_j^2 < \Psi_j^2 > \tag{2.26}$$

These analytical statistical moments converge to the real moments as the truncation degree increases. Higher statistical moments also have analytical expressions [Eldred and Burkardt, 2009].

The assessment of the fitting property of a surrogate model is measured with a *loss function* [Vapnik, 2000a] $L(\cdot)$, which quantifies the error between the modeled function and the surrogate model for a particular $\mathbf{u}_0$. Different loss functions exist among which the commonly used square loss function [Vapnik, 2000a]:

$$L(\mathbf{u}_0, \boldsymbol{\alpha}) = \left[c(\mathbf{u}_0) - \hat{c}(\mathbf{u}_0, \boldsymbol{\alpha})\right]^2 \tag{2.27}$$

Statistical learning theory defines the *generalization error* J to quantify the error of the surrogate model as the expectation of the loss function [Vapnik, 2000a]:

$$J = \mathbb{E}\left[\left(c(\mathbf{U}) - \hat{y}(\mathbf{U}, \boldsymbol{\alpha})\right)^2\right] = \int_{\boldsymbol{\Omega}} \left[c(\mathbf{u}) - \hat{c}(\mathbf{u}, \boldsymbol{\alpha})\right]^2 \phi(\mathbf{u}) \mathrm{d}\mathbf{u} \tag{2.28}$$

Surrogate models may also be used instead of the exact function $c(\cdot)$ combined with CMC or quadrature rules to compute the statistical moments of the discipline output at an affordable computational cost.

A summary of the statistical moment estimation techniques for an output of a model with the advantages and drawbacks is provided in Table 2.13. CMC, quadrature rules and PCE techniques to compute statistical moments will be compared in chapters 7 and 8 for the propagation of uncertainty.

Table 2.13: Advantages and drawbacks of the main surrogate model techniques for reliability analysis

	Advantages	Drawbacks
CMC	Easy to implement	Computational cost (low convergence)
Quadrature rules	Low computational cost (Smolyak grid)	Curse of dimensionality
Taylor expansion	Easy to implement, low computational cost	Limited linearly approximated models
PCE	Low computational cost	Curse of dimensionality

2.3.1.2 Measure of uncertainty

To characterize a performance or a specification in the presence of uncertainty $c(\mathbf{u})$, uncertainty measures are required in order to take into account the uncertain nature of the input variable vector $\mathbf{u} \in \mathbf{\Omega}$. Classically, two types of measure are distinguished [Baudoui, 2012]:

- Robust measures: they involve statistical moments of the quantity of interest, for instance the expected value $\mathbb{E}[c(\mathbf{u})]$ and/or the standard deviation $\sigma[c(\mathbf{u})]$. It enables to characterize the discipline output taking into account the effect of uncertainty. In design, the measures of robustness allows to compare design solution based on the distributions of the performance and of the constraints. The distributions are parameterized by their statistical moments which are compared to find the optimal solution. Other metrics such as quantile may also be used as a measure of robustness [Baudoui, 2012].
- Reliability measures: see Sections 2.4 and 3.2.

2.3.1.3 PDF Estimation

Another way to characterize the discipline output is with its PDF. If the discipline output PDF belongs to a classical parameterized PDF family (*e.g.* Gaussian, Beta, Uniform), methods such as Maximum Likelihood Estimation techniques may be used to estimate the parameters that best fit the output distribution. However, in practice, for complex system models, the PDF of the discipline output does not belong to the classical parameterized PDF. Non parameterized methods have been developed such as with Kernel Density Estimation (KDE) [Wand and Jones, 1994] enables to approximate the output PDF.

2.3.2 Uncertainty propagation within the interval framework

In this section, input uncertainty $\mathbf{u}$ is modeled with the interval formalism and is defined by its lower and upper bounds $\mathbf{\Upsilon} = \{\mathbf{u} \in \mathbb{R}^d | u^{(i)} \in [u^{(i)}_{\min}, u^{(i)}_{\max}] \; \forall i \in \{1, \ldots, d\}\}$. Within the interval formalism, the output y may be characterized by its lower and upper bounds $\{y \in \mathbb{R} | y_{\min} \leq y \leq y_{\max}\}$ (Fig. 2.14). Several methods exist to compute the bounds of the output interval and are detailed in the following. Interval uncertainty propagation is also referred as Interval Analysis (IA).

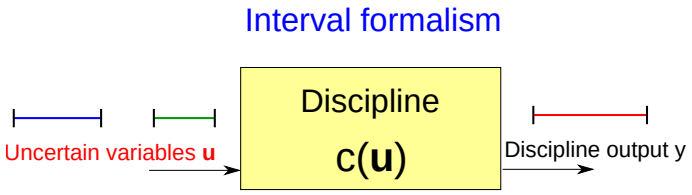

Figure 2.14: Uncertainty propagation with interval formalism

2.3.2.1 Sampling-based approaches

The sampling based approaches [Kreinovich and Ferson, 2004; Swiler et al., 2009] consist in treating interval with the probability framework to estimate the output interval bounds. First, the input

uncertainty intervals are substituted with uniform random variables $\mathbf{u} \sim \mathcal{U}(\mathbf{u}_{\min}, \mathbf{u}_{\max})$. Then, using CMC, M iid samples are generated according to the joint uniform distribution. The discipline is evaluated on these samples with the function $c(\cdot)$ giving $\{y_{(1)} = c(\mathbf{u}_{(1)}), \ldots, y_{(M)} = c(\mathbf{u}_{(M)})\}$. Finally, the probability information are discarded and only the support of the output distribution is considered to estimate the output interval bounds $[y_{\min}, y_{\max}]$. An example of interval bounds estimation by CMC is illustrated in Figure 2.15.

$$\begin{cases} y_{\min} = \min\limits_{i=1,\ldots,M} \; y_{(i)} \\ y_{\max} = \max\limits_{i=1,\ldots,M} \; y_{(i)} \end{cases} \tag{2.29}$$

Other sampling methods such as LHS may be used to sample in the input uncertain space. The

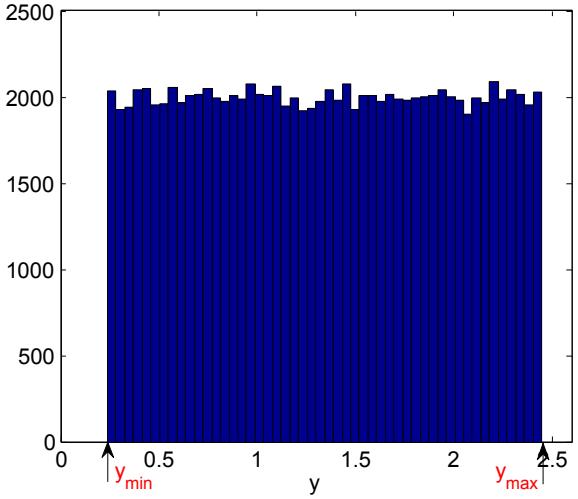

Figure 2.15: Interval bounds estimation by CMC

sampling-based approaches are easy to implement. However, these methods may be very costly and require a large number of discipline evaluations to precisely estimate the output interval bounds.

2.3.2.2 Optimization based approaches

Another approach to propagate interval uncertainty is to solve an optimization problem [Hansen and Walster, 2003; Bruns, 2006] to determine each output interval bound. This approach relies on global optimization techniques and the following optimization problems are solved

$$\begin{cases} y_{\min} = \min\limits_{\mathbf{u} \in \boldsymbol{\Upsilon}} \; c(\mathbf{u}) \\ y_{\max} = \max\limits_{\mathbf{u} \in \boldsymbol{\Upsilon}} \; c(\mathbf{u}) \end{cases} \tag{2.30}$$

The optimization methods to propagate interval bounds may be more efficient than sampling-based methods to precisely estimate the output interval bounds. However, the optimization problem might be complex to solve as it can involve a nonlinear and non convex problem.

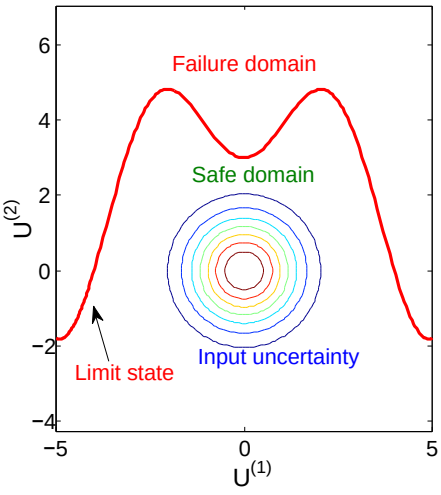

Figure 2.16: Example of reliability problem

2.4 Reliability analysis

The propagation of uncertainty is also necessary to estimate the system reliability with respect to the design constraints. Up to now, the presented uncertainty propagation methods focused on estimation of the statistical moments of the discipline output Y, the determination of its PDF or its interval bounds. Reliability analysis focuses on the tail of the discipline output distribution. It often consists in determining the probability that the output Y is underneath (or above) a given threshold S. Reliability analysis is also referred as Probability Analysis (PA). In this chapter it is assumed that $S = 0$ which can be easily obtain by considering the function $c(\cdot) - S$. Such probabilities are also called *probabilities of failure* in the system safety literature.
In the next sections, only aleatory uncertainty is considered (modeled with the probability theory). It is assumed that a failure occurs when $y = c(\mathbf{u}) > 0$. A probability of failure is determined by:

$$\mathbb{P}_f = \mathbb{P}(Y > 0) = \mathbb{P}\left(c(\mathbf{U}) > 0\right) = \int_{\mathbf{\Omega}_f = \{\mathbf{u} \in \mathbb{R}^d | c(\mathbf{u}) > 0\}} \phi(\mathbf{u}) \mathrm{d}\mathbf{u} \tag{2.31}$$

$$= \int_{\mathbb{R}^d} \mathbb{1}_{c(\mathbf{u})>0}\, \phi(\mathbf{u}) \mathrm{d}\mathbf{u} \tag{2.32}$$

$\mathbf{\Omega}_f$ is called the failure domain of $c(\cdot)$ and $\mathbb{1}(\cdot)$ the indicator function defined as follows:

$$\mathbb{1}_{c(\mathbf{u})>0} = \begin{cases} 1 & \text{if } c(\mathbf{u}) > 0 \\ 0 & \text{if } c(\mathbf{u}) \leq 0 \end{cases} \tag{2.33}$$

The calculation of Eq.(2.31) requires a multidimensional integral calculation. An example of limit state function for a 2 dimensional reliability problem is illustrated in Figure 2.16. The uncertain variables are distributed according to a 2 dimensional standard Gaussian distribution. This problem will be used all along this chapter.

Several reliability analysis techniques exist to compute rare event probability and the classical methods are presented in the following sections using the technique descriptions detailed in [Morio and Balesdent, 2015].

2.4.1 Crude Monte Carlo (CMC)

CMC presented in section 2.3.1.1 may also be used to compute a probability of failure [Silverman, 1986; Sobol, 1994; Kroese and Rubinstein, 2012a]. For that purpose, one generates M iid samples $\mathbf{u}_{(1)}, \ldots, \mathbf{u}_{(M)}$ with the joint PDF $\phi(\cdot)$ of $\mathbf{U}$ and computes their outputs $c\left(\mathbf{u}_{(1)}\right), \ldots, c\left(\mathbf{u}_{(M)}\right)$ (Fig. 2.17). The probability $\mathbb{P}_f$ is then assessed by

$$\hat{\mathbb{P}}^{CMC} = \frac{1}{M} \sum_{i=1}^{M} \mathbb{1}_{c(\mathbf{u}_{(i)})>0}$$

The implementation of CMC on input-output functions is simple, but CMC requires a significant simulation budget to accurately estimate a small probability. The required number of samples M to ensure that a failure probability is estimated with a given Relative Error (RE) dramatically increases as the probability gets lower. For example, the estimation of a probability of 10^{-k} (with $k > 2$) and a 10% coefficient of variation requires around 10^{k+2} simulations of $c(\cdot)$. Nevertheless, CMC is considered as a reference because its precision may be theoretically controlled (by addition of new samples) and is always compared to more advanced techniques detailed in the next sections.

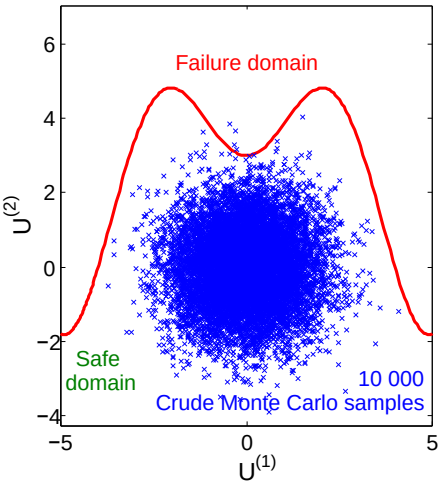

Figure 2.17: Exemple of CMC probability estimation

2.4.2 First/second-order reliability methods (FORM/SORM)

First/second-order reliability methods (FORM/SORM) [Madsen, 1986; Bjerager, 1990] are considered as efficient computational methods for structural reliability estimation. FORM/SORM rely on an analytical approximation of the limit state curve $\{\mathbf{u}|c(\mathbf{u}) = 0\}$ at the Most Probable Point of

failure (MPP) in the input space (Figs. 2.18,2.19). The MPP is the point on the limit state function curve which has the highest probability content. It is assumed that $\mathbf{U}$ follows a multivariate standard normal distribution. If it is not the case, different statistical transformations may be applied on the input distribution (such as Nataf [Nataf, 1962] or Rosenblatt [Rosenblatt, 1952] transformations). The MPP $\mathbf{u}^*$, also called most likely failure point, is obtained by solving the following optimization problem

$$\begin{aligned} \min \quad & \|\mathbf{u}\| && (2.34)\\ \text{w.r.t.} \quad & \mathbf{u} && (2.35)\\ \text{s.t.} \quad & c(\mathbf{u}) = 0 && (2.36) \end{aligned}$$

where $||.||$ is the Euclidean norm. The parameter $\zeta = \|\mathbf{u}^*\|$ is the reliability index. The constraint $c(\mathbf{u}) = 0$ defines the limit of failure space for input vector $\mathbf{u}$. Several algorithms have been proposed to compute $\mathbf{u}^*$ and to solve this optimization problem [Hasofer and Lind, 1974; Rackwitz and Flessler, 1978; Ditlevsen and Madsen, 1996]. Using Taylor series expansion, the surface $\{\mathbf{u}|c(\mathbf{u}) = 0\}$ at the solution $\mathbf{u}^*$ is approximated by an hyperplane in case of FORM. The failure probability is then estimated by:

$$\hat{\mathbb{P}}^{FORM} = \phi_{\mathcal{N}_{0,1}}(-\zeta)$$

where $\phi_{\mathcal{N}_{0,1}}(\cdot)$ is the CDF of a standard normal distribution.
Accuracy problems may happen when the limit state function surface is nonlinear due to the over or under estimation of the failure domain. SORM has been established as an attempt to improve the accuracy of FORM since SORM approximates the limit of failure space around the MPP by a quadratic surface. In SORM, the failure probability is given by [Breitung, 1984]

$$\hat{\mathbb{P}}^{SORM} = \phi_{\mathcal{N}_{0,1}}(-\zeta) \prod_{i=1}^{d-1} (1 - \zeta\kappa_i)^{-\frac{1}{2}}$$

where κ_i denotes the principal curvature of $c(\mathbf{u})$ at the MPP ζ. The term κ_i is defined by:

$$\kappa_i = \left. \frac{\partial^2 c(\mathbf{u})}{\partial^2 u^{(i)}} \right|_{\mathbf{u}=\mathbf{u}^*}$$

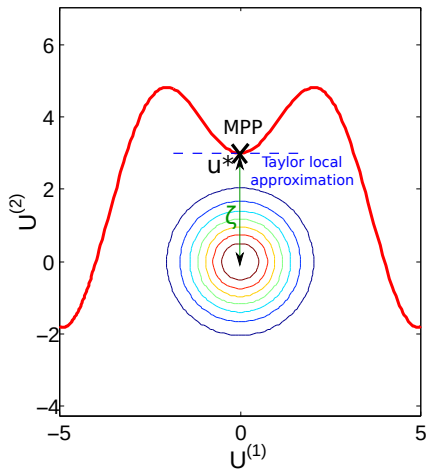

Figure 2.18: Example of FORM

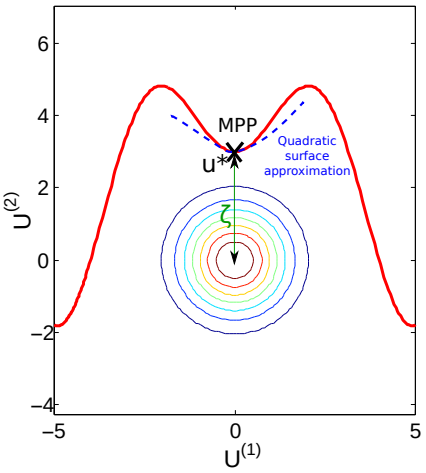

Figure 2.19: Example of SORM

Despite the different approximations, FORM and SORM give fairly accurate estimations of the failure probability when the MPP is unique. However, they may lead to very inaccurate results when several MPPs are involved. Moreover, another drawback of these approaches is that there is no control of the error in FORM/SORM compared to the exact probability of failure. For systems featuring multiple MPPs, Der Kiureghian and Dakessian [Der Kiureghian and Dakessian, 1998] proposed the restarted *iHLRF* algorithm. It aims to find several failure regions and take them into account in the calculation of the probability of failure. The method consists in penalizing previously found MPPs to force the algorithm to find a new MPP. Once these points are found, FORM or SORM surface approximations are constructed. The sought probability is computed as the probability of the union of the approximated events. However, the restarted approach shows lack of robustness [Dubourg, 2011b].

Variance reduction techniques aiming at deriving an estimator of the failure probability featuring a variance of estimation lower than for CMC have been developed. A focus on Importance Sampling (section 2.4.3) and Subset Simulation (section 2.4.4) is presented in the following sections. The Importance Sampling concepts are particularly detailed because they will be at the center of the chapter 9.

2.4.3 Importance Sampling (IS)

Remark 2.4.1. *For the sake of clarity, as the main idea of Importance Sampling (IS) is to change the sampling distribution, this latter is added in the expression of the statistical moments by a subscript determining the effective sampling distribution. For example $\mathbb{E}_\tau(\mathbf{U})$ means that the samples used for the estimation of the mathematical expectation have been generated with the PDF $\tau(\cdot)$.*

IS [Engelund and Rackwitz, 1993; L'Ecuyer et al., 2009; Kroese and Rubinstein, 2012b] starts from the premise that, around the threshold, the PDF $\phi(\cdot)$ takes value closed to zero. Therefore, generating samples in the regions closed to the threshold is difficult with the PDF $\phi(\cdot)$. The idea of IS is to substitute a more adapted PDF to $\phi(\cdot)$. IS uses an auxiliary distribution $\tau(\cdot)$ to generate more points $\mathbf{u}_{(1)}, \ldots, \mathbf{u}_{(M)}$ such that $c(\mathbf{u}) > 0$ than the original PDF $\phi(\cdot)$. A weight is then

introduced in the probability estimate to take into account the modification in the PDF generating the samples. IS takes advantage of the following re-writing:

$$\mathbb{P}_f = \mathbb{E}_\phi\left(\mathbb{1}_{c(\mathbf{U})>0}\right) = \mathbb{E}_\tau\left(\mathbb{1}_{c(\mathbf{U})>0}\frac{\phi(\mathbf{U})}{\tau(\mathbf{U})}\right)$$

The IS probability estimate $\hat{\mathbb{P}}^{IS}$ is then given by:

$$\hat{\mathbb{P}}^{IS} = \frac{1}{M}\sum_{i=1}^{M}\mathbb{1}_{c(\mathbf{u}_{(i)})>0}\frac{\phi(\mathbf{u}_{(i)})}{\tau(\mathbf{u}_{(i)})} \tag{2.37}$$

where $\mathbf{u}_{(i)}$ are iid samples generated with PDF $\tau(\cdot)$. For M sufficiently large, the central limit theorem ensures that $\hat{\mathbb{P}}^{IS}$ is an unbiased estimator of the quantity of interest and that:

$$\left(\hat{\mathbb{P}}^{IS} - \mathbb{P}_f\right) \underset{M\to+\infty}{\longrightarrow} \phi_{\mathcal{N}(0,\sigma^2_{IS})} \tag{2.38}$$

$\hat{\mathbb{P}}^{IS}$ variance is given by:

$$\mathbb{V}_\tau\left(\hat{\mathbb{P}}^{IS}\right) = \frac{\mathbb{V}_\tau\left(\sum_{i=1}^{M}\mathbb{1}_{c(\mathbf{u}_{(i)})>0}\frac{\phi(\mathbf{u}_{(i)})}{\tau(\mathbf{u}_{(i)})}\right)}{M^2} = \frac{\mathbb{V}_\tau\left(\mathbb{1}_{c(\mathbf{U})>0}w(\mathbf{U})\right)}{M} \tag{2.39}$$

with $w(\mathbf{U}) = \frac{\phi(\mathbf{U})}{\tau(\mathbf{U})}$. The term $w(\mathbf{U})$ is often referred as the Radon-Nykodin difference. The variance may be estimated using classical CMC formula as follows:

$$\hat{\mathbb{V}}_\tau\left(\hat{\mathbb{P}}^{IS}\right) = \frac{1}{M}\left(\frac{1}{M}\sum_{i=1}^{M}\mathbb{1}_{c(\mathbf{u}_{(i)})>0}w^2(\mathbf{u}_{(i)}) - \left(\hat{\mathbb{P}}^{IS}\right)^2\right) \tag{2.40}$$

The variance of $\hat{\mathbb{P}}^{IS}$ depends on the selected auxiliary PDF $\tau(\cdot)$. The IS estimate may present a much smaller variance than the CMC estimate if $\tau(\cdot)$ is chosen appropriately. IS purpose is to decrease the probability estimate variance. An optimal IS auxiliary density $\tau_{opt}(\cdot)$ may be defined as the result of the minimization of the variance $\mathbb{V}_\tau\left(\hat{\mathbb{P}}^{IS}\right)$. $\tau_{opt}(\cdot)$ is given by [Bucklew, 2004]

$$\tau_{opt}(\mathbf{U}) = \frac{\mathbb{1}_{c(\mathbf{U})>0}\ \phi(\mathbf{U})}{\mathbb{P}_f} \tag{2.41}$$

Unfortunately, in practice this optimal density is inaccessible because it involves the unknown quantity of interest $\mathbb{P}_f$. Nevertheless, $\tau_{opt}(\cdot)$ may be derived to determine an efficient sampling PDF. Indeed, an interesting auxiliary sampling PDF $\tau(\cdot)$ approaching the density $\tau_{opt}(\cdot)$ with regard to a given criterion may be used to estimate the sought probability. Different methods have been proposed to approach the optimal auxiliary density and may be classified in two categories: the parametric and the non parametric approaches.

Parametric IS methods Parametric IS methods aim at learning the optimal sampling density $\tau_{opt}(\cdot)$ assuming a parameterized auxiliary PDF family (for instance a Gaussian PDF). The objective is to determine the parameters of the auxiliary PDF $\tau_{\boldsymbol{\theta}}(\cdot)$ that minimize a given criterion.

Cross-Entropy (CE) optimization of the IS auxiliary density has been proposed [Rubinstein and Kroese, 2004]. CE method is an iterative procedure aiming at minimizing the Kullback-Leibler divergence between the unknown optimal auxiliary PDF and the parameterized PDF with respect to its parameters $\boldsymbol{\theta}$. Let P and Q be two probability distributions defined by their PDF $p(\cdot)$ and $q(\cdot)$ with support $\mathbb{R}^d$. The Kullback-Leibler divergence between P and Q is defined by:

$$D_{KL}(P,Q) = \int_{\mathbb{R}^d} \ln\left(\frac{p(\mathbf{u})}{q(\mathbf{u})}\right) p(\mathbf{u})\mathrm{d}\mathbf{u}.$$

D_{KL} is equal to 0 if and only if $P = Q$ almost everywhere. CE aims at finding the parameter vector $\boldsymbol{\theta}_{opt}$ minimizing the Kullback-Leibler divergence between $\tau_{\boldsymbol{\theta}}(\cdot)$ and $\tau_{opt}(\cdot)$ [de Mello and Rubinstein, 2002; Rubinstein and Kroese, 2004]. $\boldsymbol{\theta}_{opt}$ may be obtained by solving

$$\boldsymbol{\theta}_{opt} = \underset{\boldsymbol{\theta}\in\boldsymbol{\Delta}}{\operatorname{argmin}} \left\{D_{KL}(\tau_{opt}, \tau_{\boldsymbol{\theta}})\right\} \tag{2.42}$$

$\boldsymbol{\theta}_{opt}$ in Eq.(2.42) depends on the unknown PDF $\tau_{opt}(\cdot)$. However, it may be shown [Rubinstein and Kroese, 2004] that Eq.(2.42) may be re-written

$$\boldsymbol{\theta}_{opt} = \underset{\boldsymbol{\theta}\in\boldsymbol{\Delta}}{\operatorname{argmax}} \left\{\mathbb{E}_{\phi}\left[\mathbb{1}_{c(\mathbf{U})>0} \ln\left(\tau_{\boldsymbol{\theta}}(\mathbf{U})\right)\right]\right\} \tag{2.43}$$

where the expected value is computed with the PDF $\phi(\cdot)$.

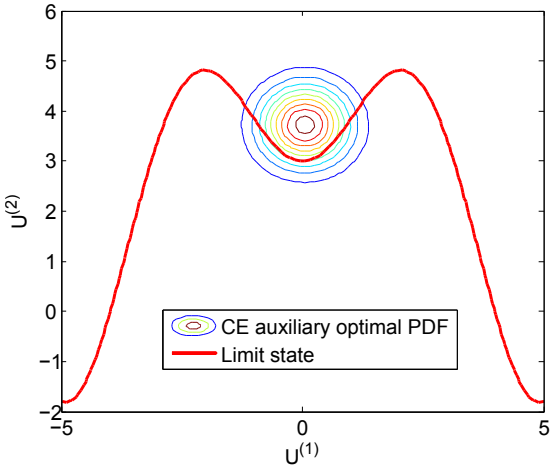

Figure 2.20: CE optimal auxiliary PDF iso-contour

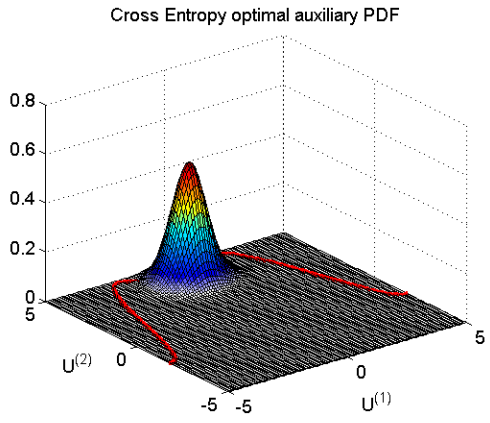

Figure 2.21: CE optimal auxiliary PDF

In practice, instead of directly solving Eq.(2.43), $\boldsymbol{\theta}_{opt}$ is determined by an iterative process involving optimization problem solving and a decreasing sequence of thresholds:

$$S_0 > S_1 > S_2 > \cdots > S_k > \cdots > 0$$

chosen adaptively using quantile definition. At the iteration [k] of the CE algorithm, the following optimization problem is solved:

$$\boldsymbol{\theta}_k = \underset{\boldsymbol{\theta}\in\boldsymbol{\Delta}}{\operatorname{argmax}} \left\{\mathbb{E}_{\tau_{\boldsymbol{\theta}_{k-1}}}\left[\mathbb{1}_{c(\mathbf{U})>S_k} \ln\left(\tau_{\boldsymbol{\theta}}(\mathbf{U})\right)\right]\right\} \tag{2.44}$$

where the expected value is computed with the intermediate auxiliary PDF $\tau_{\boldsymbol{\theta}_{k-1}}(\cdot)$ and S_k is the k^{th} intermediate threshold.
CE method is a parametric approach to determine a valuable auxiliary IS distribution. Nevertheless, the choice of a parametric density is not obvious and has to be done carefully *a priori* to fit the unknown optimal auxiliary IS distribution. Difficulties might be encountered for systems having multiple failure regions in the input uncertain space. Indeed, parametric PDF families are not well suited to take into account different failure modes. An example of CE determination of an auxiliary optimal PDF is illustrated in Figures 2.20 and 2.21. The auxiliary density is centered around the principal failure mode allowing to generate more failure samples and to improve the probability estimation. However, this test case has multiple failure modes and the parameterized Gaussian auxiliary density does not succeed to catch the three failure modes. For more details on CE algorithms one may refer to [Rubinstein and Kroese, 2004]. Other parametric methods for IS such as exponential twisting are described in [Morio and Balesdent, 2015]. Moreover, non parametric IS methods have been proposed to solve these problems and are briefly presented in the next section.

Non parametric IS methods Non parametric adaptive IS methods have also been proposed with the use of KDE. The objective of Non Parametric Adaptive Importance Sampling (NAIS) techniques [Zhang, 1996; Neddermeyer, 2009; Morio, 2012] is to approach the IS optimal auxiliary density given in Eq.(2.41) with kernel density function [Wand and Jones, 1994]. NAIS does not need a choice of a PDF family and is thus more flexible than the parametric methods. NAIS also relies on an adaptive principle similar to the CE method with a sequence of intermediate threshold and optimization problem solving. At each iteration of NAIS a new intermediate threshold is defined based on the generated samples and a quantile. A kernel-based sampling PDF is created based on the samples above the intermediate thresholds. The parameters of the kernel PDF are optimized according to the Asymptotic Mean Integrated Square Error between the kernel density of the samples and the exact density of the samples. Even if the exact density of the samples is not available, it is possible to derive an asymptotic estimate of this error when $M \to +\infty$.

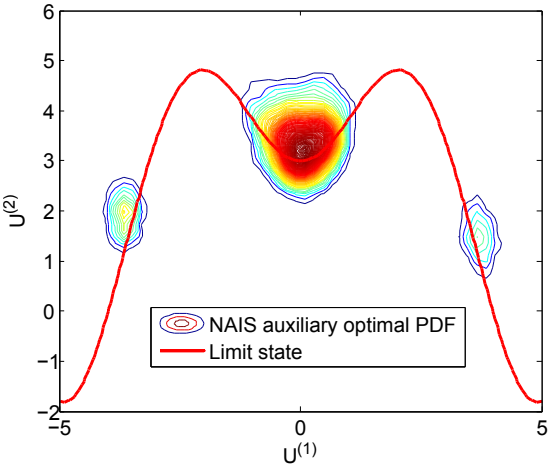

Figure 2.22: NAIS optimal auxiliary PDF iso-contour

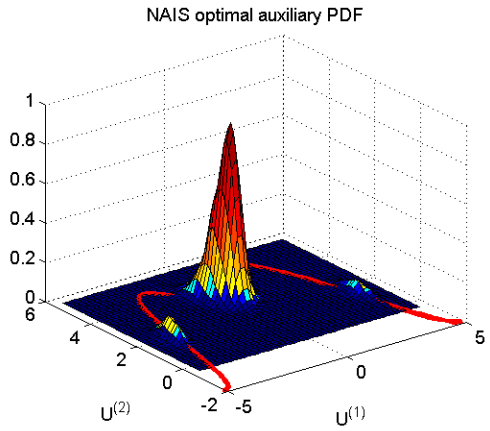

Figure 2.23: NAIS optimal auxiliary PDF

The use of kernel density function enables to approach various types of optimal auxiliary densities. NAIS is particularly adapted for systems presenting multiple failure regions. Figures 2.22 and 2.23 illustrate the optimal kernel density which presents three high content probability regions one around each failure modes. However, NAIS efficiency decreases with the increase of the input space dimension (above 10) due to the numerical cost induced by the use of kernel density [Morio, 2012] which highly suffers from the curse of dimensionality.

2.4.4 Subset Simulation (SS)

Subset Simulation (SS) [Au and Beck, 2001] (also called importance splitting) proposes to decompose the sought probability (Eq.2.31) into the product of conditional probabilities which are easier to calculate. The conditional probabilities involve more frequent events than the sought probability. Given a failure domain $\mathbf{\Omega}_f$, let $\mathbf{\Omega}_{f_0} \equiv \mathbf{\Omega} \supset \mathbf{\Omega}_{f_1} \supset \cdots \supset \mathbf{\Omega}_{f_m} \equiv \mathbf{\Omega}_f$ be a decreasing sequence of $m+1$ subset failure domains where $\forall i = \{1, \ldots, m\}$ $\mathbf{\Omega}_{f_i} = \{\mathbf{u} | c(\mathbf{u}) > S_i\}$. $S_{i \in \{1,\ldots,m\}}$ is a decreasing sequence of intermediate thresholds and $S_m = S = 0$. The sought probability can be expressed as:

$$\mathbb{P}_f = \mathbb{P}(\mathbf{U} \in \mathbf{\Omega}_f) = \prod_{i=1}^{m} \mathbb{P}\left(\mathbf{U} \in \mathbf{\Omega}_{f_i} | \mathbf{U} \in \mathbf{\Omega}_{f_{i-1}}\right), \tag{2.45}$$

with $\mathbb{P}\left(\mathbf{U} \in \mathbf{\Omega}_{f_i} | \mathbf{U} \in \mathbf{\Omega}_{f_{i-1}}\right)$ the conditional probability that $\mathbf{U} \in \mathbf{\Omega}_{f_i}$ knowing that $\mathbf{U} \in \mathbf{\Omega}_{f_{i-1}}$. Generating iid samples from the conditional PDFs is required to compute $\mathbb{P}\left(\mathbf{U} \in \mathbf{\Omega}_{f_i} | \mathbf{U} \in \mathbf{\Omega}_{f_{i-1}}\right)$ but is in most cases impossible as the conditional PDFs are unknown. In practice, these densities are built by Markov Chain Monte Carlo (MCMC) method for instance with the modified Metropolis-Hastings algorithm [Au and Beck, 2001]. MCMC techniques allow to generate samples following complex densities that do not belong to the classic density families. The method relies on a Markov process that will be approximately distributed according to the desired conditional PDFs over the long term, that is when the number of samples generated increases to infinity. This Markov process is defined with a proposal/refusal method. For more details on MCMC or Metropolis Hastings see [Metropolis et al., 1953; Hastings, 1970; Au and Beck, 2001]. Therefore, using the failure samples generated from the previous step (*i.e.* samples in $\mathbf{\Omega}_{f_i}$ whose values are lower than the threshold S_i), a new set of M samples is created according to Markov chains based on the modified Metropolis algorithm. The function $c(\cdot)$ is evaluated with the new generated samples and a new intermediate threshold is selected. In practice, the intermediate thresholds may be chosen in order to have all the intermediate conditional probabilities close to $\rho = 10^{-1}$ [Au and Beck, 2001; Balesdent et al., 2015]. The choice of the intermediate thresholds results from a trade-off between having intermediate probabilities involving frequent failure events and having a limited number of steps in the Subset Simulation algorithm. The conditional probability is evaluated with CMC.
SS is efficient to estimate rare event probability (*i.e.* $\mathbb{P}_f < 10^{-4}$) and SS does not highly suffer from the curse of dimensionality and may be employed for high dimensional systems. The SS budget is mainly dependent on the magnitude order of the sought probability and also on the ρ-quantile parameter. An example of SS probability estimation is illustrated in Figures 2.24,2.25,2.26 and 2.27. SS succeeds to capture the multiple failure modes and to generate failure samples to accurately estimate the probability.

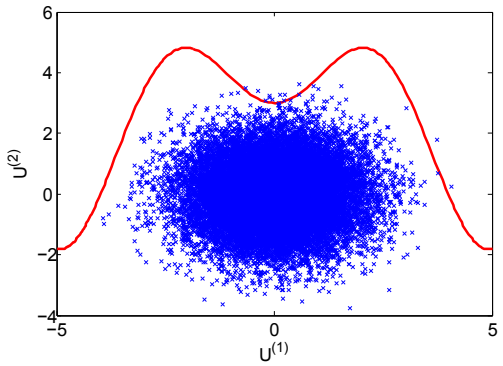

Figure 2.24: Example SS reliability analysis - step 1

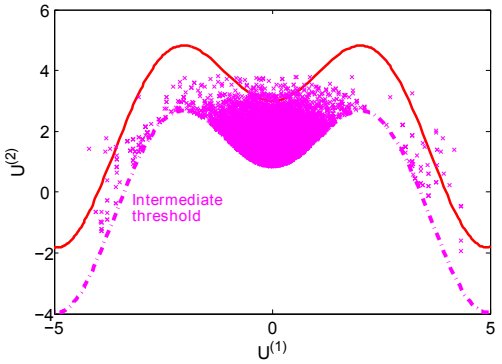

Figure 2.25: Example SS reliability analysis - step 2

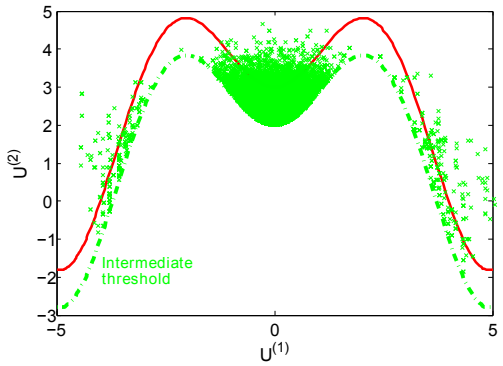

Figure 2.26: Example SS reliability analysis - step 3

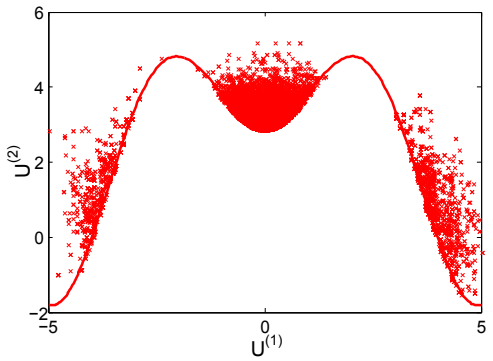

Figure 2.27: Example SS reliability analysis - step 4

Even if, SS or IS methods require less samples than CMC for the same level of accuracy, these methods still need an important number of calls to the computationally expensive limit state function $c(\cdot)$. In order to further reduce the number of calls to $c(\cdot)$, several works [Bichon et al., 2008a; Picheny et al., 2010; Dubourg et al., 2011, 2013] aim at replacing the exact limit state function by an approximate surrogate model less computationally intensive to evaluate.

A summary of the different reliability analysis techniques with the advantages and drawbacks of each methods is provided in Table 2.28. In chapter 9 of the thesis, because of the parametric approach of IS-CE, this estimation technique will be adapted to efficiently allow the estimation of the bounds of probability of failure in the presence of both aleatory and epistemic uncertainties. SS will be used in chapter 10 to estimate probability bounds when the limit state function is impacted by epistemic uncertainty as the estimation techniques multiple failure regions and coupled with an appropriate surrogate model it enables a probability of failure estimation at an affordable cost. Moreover, in chapter 10 sensitivities of the probability of failure with respect to decision variables will be derived based on SS.

Table 2.28: Advantages and drawbacks of the main reliability analysis techniques

	Advantages	Drawbacks
CMC	Easy to implement	Low estimator convergence
	Provide a variance of the estimator	High computational cost
FORM-SORM	Easy to implement	Limited to single failure problem
	Low computational cost	No estimation of the error
IS-CE	Simple optimization for Gaussian PDF family	Strong influence of the initial parametric density choice
	Fast computation	Limited to single failure problem
IS-NAIS	No choice of parametric density	High computational cost
	Handle multiple failure problem	Inapplicable for dimension higher than 10
SS	Applicable in high dimensions	Important simulation budget
	Handle multiple failure problem	More complex implementation

2.5 Surrogate model for reliability analysis

Complex simulation codes such as the ones used in aerospace are often computationally expensive and involve a large number of variables. These features markedly hamper the estimation of failure probabilities. To reduce the computational burden, a surrogate model of the computationally costly simulation code may be used to perform the probability estimation on this metamodel. Different surrogate models may be used to replace $c(\cdot)$ such as Response Surface Method [Faravelli, 1989; Hurtado, 2004a], Neural Network [Hurtado and Alvarez, 2001], Support Vector Machines [Bourinet et al., 2011a; Basudhar et al., 2012], Kriging [Kaymaz, 2005; Balesdent et al., 2013], *etc.* In this section, two main surrogate models are described in the context of reliability analysis: Kriging model and Support Vector Machine (SVM) as they will be later used in part III. These surrogate models may also be used in others contexts to replace computational expensive simulations.

2.5.1 Gaussian Process (GP)

Kriging [Matheron, 1963; Sasena, 2002] is a statistical surrogate model that may be used to approximate the limit state function $c(\cdot)$ on its input space $\mathbf{\Omega}$ by considering $c(\cdot)$ as a realization of a Gaussian process denoted by $C(\cdot)$. Kriging requires an initial Design of Experiments (DoE) with p samples $\mathcal{U} = \{\mathbf{u}_{(1)}, \ldots, \mathbf{u}_{(p)}\} \in \mathbf{\Omega}$. The exact limit state function $c(\cdot)$ is evaluated on the DoE

$\mathbf{c}_p(\mathcal{U}) = [c(\mathbf{u}_{(1)}), \ldots, c(\mathbf{u}_{(p)})]^T$. The Kriging model is a Gaussian process $C(\cdot)$ defined as:

$$C(\mathbf{u}) = m(\mathbf{u}) + Z(\mathbf{u}) \tag{2.46}$$

where $m(\cdot)$ is a regression model estimated from the DoE and $Z(\cdot)$ is a zero-mean Gaussian process. The covariance function $\text{cov}(\cdot,\cdot)$ of $Z(\cdot)$ is unknown and in practice is assumed to be expressed by

$$\text{cov}\left(Z(\mathbf{u}_{(i)}), Z(\mathbf{u}_{(j)})\right) = \sigma_Z^2 \text{Corr}\left(\mathbf{u}_{(i)}, \mathbf{u}_{(j)}\right) \tag{2.47}$$

with σ_Z^2 the process variance and $\text{Corr}(.,.)$ a parametric correlation function. A typical choice for the correlation function is

$$\text{Corr}\left(\mathbf{u}_{(i)}, \mathbf{u}_{(j)}\right) = \exp\left(-\sum_{k=1}^{d} \theta_k |u_{(i)}^{(k)} - u_{(j)}^{(k)}|^{q_k}\right) \tag{2.48}$$

where $u_{(i)}^{(k)}$ is the k^{th} coordinate of the vector $\mathbf{u}_{(i)}$, the parameter q_k reflects the smoothness of the interpolation and θ_k are scale factors which may be computed by Maximum Likelihood Estimation [Sasena, 2002]. The Kriging prediction for any $\mathbf{u} \in \mathbf{\Omega}$ is given by

$$\hat{c}(\mathbf{u},\mathcal{U}) = m(\mathbf{u}) + \mathbf{r}(\mathbf{u},\mathcal{U})^{\mathrm{T}} \mathbf{R}^{-1}(\mathcal{U})(\mathbf{c}_p(\mathcal{U}) - \mathbf{m}_p(\mathcal{U})) \tag{2.49}$$

where

$$\begin{cases} \mathbf{r}(\mathbf{u},\mathcal{U}) = \left[\text{Corr}(\mathbf{u}, \mathbf{u}_{(1)}), \ldots, \text{Corr}(\mathbf{u}\mathbf{u}_{(p)})\right]^{\mathrm{T}}, \\ \mathbf{R}_{|ij}(\mathcal{U}) = \text{Corr}(\mathbf{u}_{(i)}, \mathbf{u}_{(j)}) \\ \mathbf{m}_p(\mathcal{U}) = \left[m(\mathbf{u}_{(1)}), \ldots, m(\mathbf{u}_{(p)})\right]^{\mathrm{T}} \end{cases} \tag{2.50}$$

A confidence interval on the prediction $\hat{c}(\mathbf{u},\mathcal{U})$ may be determined as $C(\cdot)$ is a Gaussian process and the variance of the prediction is given by

$$\sigma^2(\mathbf{u},\mathcal{U}) = \sigma_Z^2\left(1 - \mathbf{r}(\mathbf{u},\mathcal{U})^{\mathrm{T}} \mathbf{R}^{-1}(\mathcal{U}) \mathbf{r}(\mathbf{u},\mathcal{U})\right) \tag{2.51}$$

This possibility to quantify the surrogate model prediction uncertainty will be further exploited in section 2.5.1.1 to find lower and upper bounds for the probability estimate.
An example of limit state approximation based on Kriging is presented in Figure 2.29. Kriging method presents some advantages in rare event probability estimation. Indeed, this surrogate model is based on a Gaussian process, that allows to estimate the variance of the prediction error and consequently to define a confidence domain of the surrogate model. This indicator may be directly used to refine the model, *i.e.*, to evaluate the exact function on new chosen points to improve the accuracy of the model. Kriging has been extensively used with CMC [Echard et al., 2011], IS [Schueremans and Van Gemert, 2005; Dubourg et al., 2013; Balesdent et al., 2013], or SS [Vazquez and Bect, 2009; Li et al., 2012; Bect et al., 2012a]. The way to refine the Kriging model is a key point and different strategies have been proposed [Picheny, 2009; Baudoui et al., 2012; Dubourg et al., 2013]. These techniques exploit the complete probabilistic description given by the Kriging in order to evaluate the minimal number of points on the exact function. The main methods are described in the following of this chapter. A numerical comparison of different Kriging based methods to estimate a probability of failure may be found in [Li et al., 2010a].

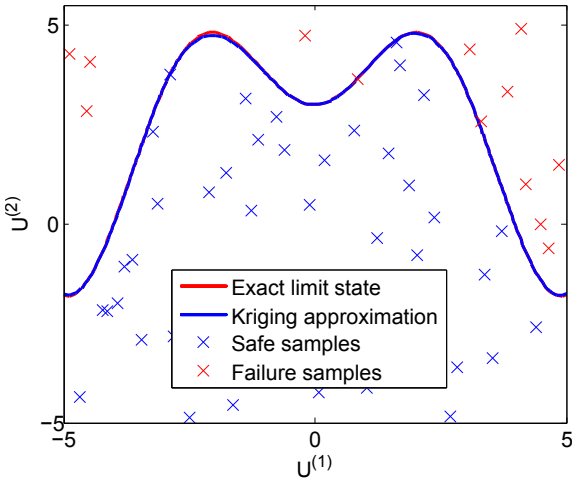

Figure 2.29: Example of Kriging approximation of a limit state function

2.5.1.1 Refinement strategies

In case of rare event probability estimation, the surrogate model has to be accurate in the zones of relevance *i.e.* in the vicinity of the threshold S and in the high probability content regions. The use of the exact function $c(\cdot)$ and its surrogate $\hat{c}(\cdot)$ in the probability calculation will lead to the same result if $\forall \mathbf{u} \in \mathbb{R}^d, \mathbb{1}_{c(\mathbf{u})>0} = \mathbb{1}_{\hat{c}(\mathbf{u},\mathcal{U})>0}$. In other words, the surrogate model might not be representative of the exact function outside the zones of interest as they do not take part of the probability estimation. From the initial training set $\mathcal{U}$, the Kriging properties (*i.e.* Gaussian process, estimation of the predicted error variance) are valuable to determine the additional samples which have to be evaluated on $c(\cdot)$ to refine its surrogate model. Different refinement strategies have been developed in the literature and are briefly described in the following. Two categories may be distinguished in the methods: the direct and one step look ahead methods. The first ones directly use the Kriging model to determine the sample to be added to the training set whereas the later estimate the influence of the training set candidate sample upon the updated surrogate model (*i.e.* kriging model built from the candidate point in addition to past training set samples). The refinement stopping criteria used in the different methods are based on the Kriging prediction error in order to evaluate the accuracy of the surrogate model and its impact on the rare event probability estimate.

Direct methods

The direct approaches solve an optimization problem to determine the new sample point $\mathbf{u}$ to add to the current training set $\mathcal{U}$ based on the exisiting Kriging model. The methods differ by the optimization criteria used in the optimization problem and they involve the estimation of the Kriging prediction variance at the potential candidate point. For instance, the active learning reliability method combining Kriging and probability estimation method [Echard, 2012] determines the new sample to be added to the training set minimizing the Kriging prediction distance to the

threshold multiplied by the inverse of the prediction error.

$$\min_{\mathbf{u}} \frac{|\hat{c}(\mathbf{u},\mathcal{U})|}{\sigma(\mathbf{u},\mathcal{U})} \tag{2.52}$$

The Efficient Global Reliability Analysis method [Ranjan et al., 2008; Bichon et al., 2008b] also solves an optimization problem which involve an integral over the uncertain space in the vicinity of the threshold in order to find the point to add to the training set. EGRA may be associated with simulation techniques for rare event estimation and has been for instance applied with IS [Bichon et al., 2008b].

One step look ahead

The *one step look ahead* methods differ from the direct methods as they use an estimation of the effect of the updated Kriging model (*i.e.* based on the training set augmented with the new candidate sample) to refine the surrogate model. For numerical tractability, to estimate the influence of an added sample in the training set, these methods consider that the variance of the Gaussian process σ_Z^2 in Eq.(2.51), the kernel parameters and the regression model do not change, and only the correlation matrix is updated. Classical *one step look ahead* methods are the Target Integrated Mean Squares Error [Picheny et al., 2010], the reduction of misclassification uncertainty for rare event simulation techniques [Balesdent et al., 2013], the Stepwise Uncertainty Reduction [Bect et al., 2012b] and K-means clustering strategy for Kriging refinement [Dubourg, 2011a]. The methods have been coupled with CMC, IS and SS estimation techniques. For more details on the Kriging refinement strategies for rare event probability estimation, one can refer to [Morio and Balesdent, 2015]. The reduction of misclassification uncertainty technique [Balesdent et al., 2013] will be used and detailed in chapter 9.

2.5.2 Support Vector Machine (SVM)

Support vector machines (SVM) is a machine learning technique [Vapnik and Vapnik, 1998] used in different domains such as reliability analysis [Basudhar and Missoum, 2008, 2010] or classification and pattern recognition [Tou and Gonzalez, 1974; Shawe-Taylor and Cristianini, 2004]. An adaptation of SVM may be derived as a regression tool and is referred to as support vector machine for regression [Clarke et al., 2005]. The main advantage of SVM lies in its ability to model complex limit state functions that optimally separate different classes of data samples. In probability estimation (*e.g.* [Hurtado, 2004b; Bourinet et al., 2011b]), SVM may be employed as a surrogate model of $c(\cdot)$ around the threshold $S = 0$. This type of surrogate is particularly suited for discontinuous limit state functions and high dimensional reliability problems. The aim of this section is to provide a brief overview of the SVM main features. For more details, see [Cristianini and Shawe-Taylor, 2000; Steinwart and Christmann, 2008]. In this section, the classical SVM characteristics are only presented. Extensions of SVM such as Probabilistic SVM [Platt, 1999; Gao et al., 2002] or Virtual SVM [Song et al., 2013] have been proposed in the literature but are not considered in this thesis. In its basic form, SVM is a binary classifier. In a reliability context, these classes correspond to the failure domain (referred to as the "-1" class) and the safe domain (referred to as the "$+1$" class). SVM may also be extended to multi-class classification problems [Duan and Keerthi, 2005].

Consider a training set $\mathcal{U} = \{\mathbf{u}_{(1)}, ..., \mathbf{u}_{(p)}\}$ of p training samples in a d-dimensional space. One of the two classes characterized by a value $r_i = \pm 1$ is associated to the samples depending on the output of the limit state function position with respect to the threshold S. The objective of the

SVM construction is to find the optimal boundary (limit state function) separating the training data into the two classes. SVM theory in case of a linearly separable data set is explained in the following. It is then extended to the case where the data is not linearly separable.

Linear decision function In case the data set is separable with a linear limit state function, this latter is defined by hyperplane such that:

$$\mathbf{w}^T.\mathbf{u} + b = 0,$$

where b is the bias and $\mathbf{w}$ is hyperplane coefficient vector. The limit state function lies "half way" between two hyperplanes (referred to as support hyperplanes) that separate the two classes of data. This pair of hyperplanes has to pass at least through one of the training samples of each class (called the support vectors). Moreover, no sample has to be found within the margin. The two hyperplanes are defined by

$$\mathbf{w}^T.\mathbf{u} + b = +1. \tag{2.53}$$

and

$$\mathbf{w}^T.\mathbf{u} + b = -1. \tag{2.54}$$

For separable data, there is an infinity of possible limit state functions. The optimal decision function is defined as the limit state function that maximizes the *margin* separating the support hyperplanes. The two support hyperplane equations and the fact that no sample should be in the margin may be combined into a single global constraint:

$$r_i(\mathbf{w}^T.\mathbf{u} + b) - 1 \geq 0. \tag{2.55}$$

The separation distance of the two support hyperplanes is $\frac{2}{\|\mathbf{w}\|}$. Therefore, finding the support hyperplanes (*i.e.* determining $\mathbf{w}$ and b) may be translated into an optimization problem as follows:

$$\begin{aligned} \min_{\mathbf{w},b} \quad & \tfrac{1}{2}\|\mathbf{w}\|^2 \\ \text{s.t.} \quad & r_i(\mathbf{w}^T.\mathbf{u}_{(i)} + b) - 1 \geq 0,\ 1 \leq i \leq p \end{aligned} \tag{2.56}$$

This optimization problem is a quadratic programming problem. It is a convex problem and may be efficiently solved with existing optimization algorithms (*e.g.* SQP algorithm [Schittkowski, 1986]). The optimal $\mathbf{w}$, b, and the Lagrange multipliers λ_i may be obtained. The classification of any point $\mathbf{u}$ in the failure or the safe domains is determined by the sign of the following function:

$$s(\mathbf{u},\mathcal{U}) = b + \sum_{i=1}^{p} \lambda_i r_i \mathbf{u}_{(i)}^T \mathbf{u}. \tag{2.57}$$

The Karush Kuhn Tucker conditions ensure that only the λ_i corresponding to the support vectors are strictly positive while the other ones are equal to zero. In general, only a small fraction of the total number of samples in $\mathcal{U}$ are support vectors . By taking only into account the support vectors NSV in Eq.(2.57) it becomes:

$$s(\mathbf{u},\mathcal{U}) = b + \sum_{i=1}^{NSV} \lambda_i r_i \mathbf{u}_{(i)}^T \mathbf{u}. \tag{2.58}$$

In case the data is non-separable, slack variables are used to solve a relaxed optimization problem [Vapnik, 2000b]. In case where the limit state function is nonlinear, the method is generalized through the use of kernels as described below.

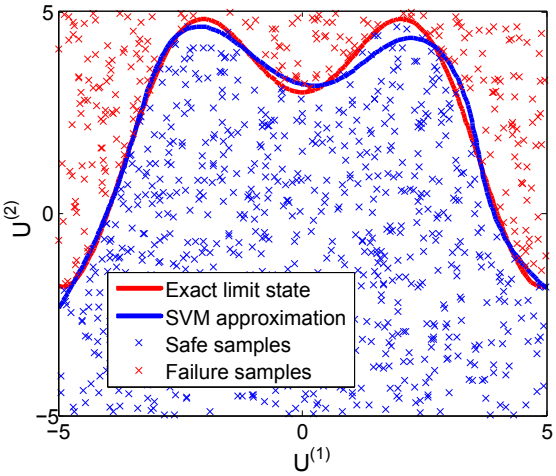

Figure 2.30: Example of SVM approximation of a limit state function

Nonlinear decision function In case of nonlinear limit state function, the initial set of variables is projected into a higher dimensional space called the *feature space*. In this n dimensional space, the new coordinates of a sample $\mathbf{u}$ are given by $(\psi_1(\mathbf{u}), \psi_2(\mathbf{u}), \ldots, \psi_n(\mathbf{u}))$ where ψ_i are the features. The general idea of SVM for nonlinear limit state function is to formulate a linear classification problem in the augmented feature space. The SVM classification of a new point $\mathbf{u}$ is given by the sign of

$$s(\mathbf{u}, \mathcal{U}) = b + \sum_{i=1}^{NSV} \lambda_i r_i < \boldsymbol{\psi}(\mathbf{u}_{(i)}), \boldsymbol{\psi}(\mathbf{u}) >, \tag{2.59}$$

where $\boldsymbol{\psi} = (\psi_1(\mathbf{u}), \psi_2(\mathbf{u}), \ldots, \psi_n(\mathbf{u}))$ and $<,>$ is the inner product. The inner product forms a kernel K, so that the limit state function is written

$$s(\mathbf{u}, \mathcal{U}) = b + \sum_{i=1}^{NSV} \lambda_i r_i K(\mathbf{u}_{(i)}, \mathbf{u}). \tag{2.60}$$

This approach is referred to as *kernel trick*. The Gaussian kernel is the most used in the literature and is defined as

$$K(\mathbf{u}_{(i)}, \mathbf{u}) = \exp\left(-\frac{\|\mathbf{u}_{(i)} - \mathbf{u}\|^2}{\sigma^2}\right), \tag{2.61}$$

where σ is the width of the Gaussian kernel.
An example of SVM approximation of a limit state function is illustrated in Figure 2.30.

2.5.2.1 Refinement strategies

In most applications of SVM, the model is based on a fixed training set which is built on the global input space [Li et al., 2006] or in specific zones such as those relevant to the Most Probable Point

(*e.g.* [Wang et al., 2012]). However, adaptive refinement strategies have been proposed to account for the input space zones relevant to rare event estimation. These refinement strategies take into account the spatial location of the samples in order to determine points to add to the existing training set.
In [Hurtado and Alvarez, 2010], the authors propose a refinement technique which consists in building a series of SVM models in order to approximate $\{\mathbf{u}|c(\mathbf{u}) = 0\}$. For that purpose, a sequence of optimization problems is solved. The optimization problem is solved with a Particle Swarm Optimization (PSO) algorithm [Eberhart and Kennedy, 1995]. Once this problem is solved, the optimal population found by PSO is used as the training set to build the SVM model. The next optimization problem solving uses the previous optimal PSO population as initialization. A parameter evolves at each step of the method to iteratively improve the accuracy of the SVM model, smoothing the curvature of the optimization problem objective function. At each sequence iteration, an estimation of the rare event probability is performed. Another approach called Subsets by Support vector Margin Algorithm for Reliability esTimation (^{2}SMART) [Deheeger and Lemaire, 2007; Bourinet et al., 2011b] is dedicated to the use of SS and consists in defining one SVM model at each adaptive SS threshold. For each intermediate threshold, a SVM model is constructed using a three stage-refinement approach (localization, stabilization and convergence) which allows to accurately represent the regions corresponding to the involved thresholds.
In the following section, two techniques to refine SVM models are briefly described because they will be at the center of the chapter 10.

Adaptive refinement of SVM using Max-min technique The "Max-min" technique, proposed in [Basudhar and Missoum, 2010] allows to sequentially add new samples to the current training set in order to refine the SVM model. This technique consists in solving the following optimization problem:

$$\begin{aligned} \max_{\mathbf{u}} \min_{\mathbf{u}_{(i)} \in \mathcal{U}} \quad & \|\mathbf{u}_{(i)} - \mathbf{u}\| \\ \text{s.t.} \quad & \hat{c}(\mathbf{u}) = 0, \end{aligned} \tag{2.62}$$

with $\mathbf{u}_{(i)},\ i \in \{1, \ldots, p\}$ the different samples of the current training set. This method allows to generate a sample located on the approximated iso-value $\hat{c}(\mathbf{u}) = 0$, and which is at the maximal distance of the current training set samples. This method has been applied with CMC method [Basudhar, 2011] but is applicable with any simulation techniques. Moreover, this method is not dedicated to SVM and may be applied to refine other surrogate models, such as Kriging. This method does not take into account the distribution of the input variables to refine the surrogate model in high probability content regions. To overcome this issue, an improvement of Max-min technique has been proposed and is described in the following.

Improvement of Max-min technique: Generalized Max-min (GMm) The generalized "Max-min" technique (GMm), proposed in [Lacaze and Missoum, 2014a] is based on the Max-min strategy but accounts for the PDF of the input random variables as follows:

$$\begin{aligned} \max_{\mathbf{u}} \min_{\mathbf{u}_{(i)} \in \mathcal{U}} \quad & \|\mathbf{u}_{(i)} - \mathbf{u}\| \phi(\mathbf{u})^{1/d} \\ \text{s.t.} \quad & \hat{c}(\mathbf{u}) = 0, \end{aligned} \tag{2.63}$$

with $\phi(\cdot)$ the joint PDF of the input variables and d the dimension of the input space. The main difference between the Max-min and generalized Max-min approaches comes from the weighting by the input variable joint PDF, which enables to refine the surrogate model in relevant regions to the sought probability estimation. As for the Max-min technique, the GMm approach is not dedicated to SVM and may be used to refine other surrogate models.

PCE presented in section 2.3.1.1 has also been used in reliability analysis and applied on different problems [Sudret and Der Kiureghian, 2002; Choi et al., 2004; Berveiller et al., 2005, 2006]. The limit state $\{\mathbf{u} \in \mathbf{\Omega} | c(\mathbf{u}) = 0\}$ is modeled by a PCE. The PCE surrogate model may be very efficient for parametric reliability studies and in [Sudret, 2007], the author recommends to use in general a third order expansion for reliability analysis problem. Different adaptive methods to build sparse PCE have been proposed [Blatman and Sudret, 2008, 2011; Hu and Youn, 2011]. Blatman *et al.* developed an adaptive sparse PCE methods based on least angle regression in order to automatically detect the significant PCE coefficients and to avoid to compute the non significant coefficients [Blatman and Sudret, 2008, 2011]. Hu *et al.* [Hu and Youn, 2011] also developed an adaptive sparse PCE approach based on a new projection method using dimension reduction techniques and also copula methods to handle nonlinear correlation of input random variables.

A summary of the different surrogate modeling methods with the advantages and drawbacks is provided in Table 2.31. In chapter 8, SVM will be used due to the discontinuous nature of the limit state function to ensure an accurate and cost efficient estimation of the probability of not injecting the payload of a launch vehicle to the target orbit. In chapters 9, 10 and 11, Kriging surrogate model will be used combined with two new refinement methods in order to compute the probability of failure bounds in the presence of aleatory and epistemic uncertainties. Kriging models are particularly adapted due to the use of prediction error in order to refine the surrogate model in the interesting regions for the probability estimations.

Table 2.31: Advantages and drawbacks of the main surrogate model techniques for reliability analysis

	Advantages	Drawbacks
Kriging	Provide an estimation of the prediction error	Limited to low dimensional problems (<10)
	Efficient refinement techniques	Do not handle discontinuous problem
SVM	Handle high dimensional problems	Do not provide an estimation of the prediction error
	Handle discontinuous problem	SVM is limited to classification

2.6 Conclusion

In this chapter, we have introduced the essential foundations to describe uncertainty and the main methods to characterize it using unified notations. Firstly, we have detailed the existing uncertainty definitions and classifications. Then, two mathematical formalisms to represent uncer-

tainty have been introduced: the probability and the interval formalisms. For each of formalism, uncertainty propagation methods have been presented while highlighting their advantages and drawbacks. The uncertainty propagation methods enable to characterize the uncertainty of a system performance based on input disciplinary uncertainties. A focus on reliability analysis methods has been made because guarantying the system reliability is a difficult task and dedicated uncertainty propagation techniques are required. In addition, two surrogate models (Kriging and Support Vector Machine) in the context of reliability analysis have been introduced to decrease the computational cost of reliability analysis.

In the context of design, reliability analysis methods were mainly limited to FORM and CMC techniques due to their low computational cost. However, more and more disciplinary design studies involving sampling-based techniques such as SS and IS coupled with surrogate modeling refinement approaches have been performed [Kaymaz, 2005; Bourinet et al., 2011a; Basudhar et al., 2012; Balesdent et al., 2013]. These approaches offer the possibility to handle complex failures (discontinuities, multiple failure regions, *etc.*) and accurate probability estimation while limiting the computational cost. However, most of these approaches still suffer from a curse of dimensionality and in the field of reliability analysis, works on high dimensional methods are expected in the near future.

The next logical steps on the thesis will be to focus on UMDO problems and for that to understand the differences and challenges introduced by uncertainty in MDO problem (see section 3.2). Then, existing methods for three different thematics of UMDO methodologies identified in the introduction will be studied:

- first, the existing UMDO formulations and the interdisciplinary coupling handling (chapter 3),
- then, the existing reliability analysis methods for multidisciplinary systems and also mono-disciplinary systems in the presence of mixed aleatory/epistemic uncertainties (chapter 4),
- finally, some existing optimization algorithms for constrained UMDO problems (chapter 5).

Chapter 3

Interdisciplinary coupling handling in existing UMDO formulations

Contents

Chapter goals

- Present the principal existing interdisciplinary coupling handling methods for coupled and decoupled UMDO formulations,
- Highlight the advantages and drawbacks of each technique.

3.1 Introduction

This chapter is devoted to the description of Uncertainty-based Multidisciplinary Design Optimization (UMDO) formulations and is focused on the interdisciplinary coupling satisfaction in the presence of uncertainty. The understanding of the importance of UMDO is spreading fast among academia and industry, but UMDO methodologies are still in the early stages of development and

are not mature enough to be applied to complex industrial cases. One of the key challenges in UMDO problem is the organizational procedures and the collaborative design process. Complex system design often involves teams spread all around the world and collaborative strategies have to be developed. UMDO formulations and interdisciplinary coupling handling are research branches focused on these issues. To understand the existing UMDO approaches, this chapter is organized as follows. In the second section, the differences between deterministic MDO and UMDO are highlighted and important notations are introduced. Section 3.3 is focused on the existing coupled UMDO formulations relying on MDA in the presence of uncertainty. Section 3.4 presents the existing decoupled UMDO formulations with a focus on the interdisciplinary coupling satisfaction. For each approach presented, we expose at first the principle of the approach, then its mathematical formulation accompanied by an explanatory scheme and finally the advantages and drawbacks relative to coupling satisfaction.

3.2 Differences between deterministic MDO and UMDO

In order to simplify the comprehension of the interdisciplinary coupling problem under uncertainty several hypotheses are made on the considered UMDO problem:

- Besides the interdisciplinary coupling equation Eq.(18.14), only inequality constraints are considered. In the design of launch vehicle, tolerances are often considered on equality constraints (such as orbit injection constraints) and therefore equality constraints may be transformed into inequality constraints involving the tolerances.
- State variables $\mathbf{x}$ and state equation residuals $\mathbf{r}(\cdot)$ are handled at the discipline-level and therefore do not appear in the UMDO formulations.

The introduction of uncertainty in a MDO problem leads to a new general UMDO problem [Yao et al., 2011] formulated as follows:

$$\begin{aligned}
&\min && \Xi\left[f(\mathbf{z}, \boldsymbol{\theta}_{\boldsymbol{Y}}, \mathbf{U})\right] && (3.1)\\
&\text{w.r.t.} && \mathbf{z}, \boldsymbol{\theta}_{\boldsymbol{Y}} && \\
&\text{s.t.} && \mathbb{K}\left[\mathbf{g}(\mathbf{z}, \boldsymbol{\theta}_{\boldsymbol{Y}}, \mathbf{U})\right] \leq 0 && (3.2)\\
& && \forall i \neq j, \forall \mathbf{u} \in \boldsymbol{\Omega},\ \mathbf{y}_{ij}(\boldsymbol{\theta}_{\boldsymbol{Y}ij}, \mathbf{u}_i) = \mathbf{c}_{ij}(\mathbf{z}_i, \mathbf{y}_{.i}(\boldsymbol{\theta}_{\boldsymbol{Y}.i}, \mathbf{u}_{.i}), \mathbf{u}_i) && (3.3)\\
& && \mathbf{z}_{\min} \leq \mathbf{z} \leq \mathbf{z}_{\max} && (3.4)
\end{aligned}$$

Important differences exist between the UMDO formulation and the deterministic MDO formulation presented in chapter 1. UMDO formulations require uncertainty modeling and measures, uncertainty propagation and optimization under uncertainty. In the following paragraphs, the main differences with deterministic MDO are detailed.

- First, $\mathbf{U}$ is the uncertain vector. We note $\mathbf{U}_i$, the input uncertain vector to the discipline i and $\mathbf{U} = \bigcup_{i=1}^{N} \mathbf{U}_i$ without duplication. In this chapter, it is assumed that the uncertain variables are modeled with the probability theory, and that the input variable distributions are known. To simplify the notations in the rest of the thesis, for all the uncertain variables, the realization $U(w)$ is noted u. The k^{th} sample generated for instance by CMC of the random vector $\mathbf{U}_i$ is noted $\mathbf{u}_{i(k)}$. The p^{th} coordinate of the k^{th} sample of the random vector

$\mathbf{U}_i$ is noted $\mathbf{u}_{i(k)}^{(p)}$. As highlighted in section 2.2.2, other uncertainty modelings exist such as evidence theory [Dempster, 1967], possibility theory [Zadeh, 1978] or interval analysis [Moore et al., 2009]. Moreover, it is assumed that the design variables $\mathbf{z}$ are deterministic variables, and all the uncertainties are represented by $\mathbf{U}$. We note $(\mathbf{\Omega}, \sigma_{\mathbf{\Omega}}, \mathbb{P})$ a probability space with $\mathbf{\Omega}$ a sample space for $\mathbf{U}$, $\sigma_{\mathbf{\Omega}}$ a sigma-algebra, and $\mathbb{P}$ a probability measure. We note $\phi(\cdot)$ the joint Probability Density Function (PDF) of the uncertain vector $\mathbf{U}$. If a design variable is considered as uncertain, then, its contribution is decomposed into two parts: one deterministic that is controlled by the optimizer and one aleatory that is propagated through the system. For instance, if the propellant mass m is considered as an uncertain design variable, therefore, the expected value of the propellant mass μ_m is the deterministic design variable controlled by the optimizer and the propellant mass uncertainty around the expected value is propagated through the system according to the propellant mass PDF.

- Secondly, Ξ denotes the objective function uncertainty measure. The measure Ξ quantifies the uncertainty in the objective function to be optimized. Within the probability formalism, the expected value $\mathbb{E}\left[f(\mathbf{z}, \boldsymbol{\theta}_{\boldsymbol{Y}}, \mathbf{U})\right]$ or an aggregation of the expected value and the standard deviation are commonly used to quantify the uncertainty in the objective function [Baudoui, 2012].

  Concerning the UMDO constraints, two classical measures of uncertainty exist. In the solving of UMDO problems, most computations are devoted to constraint evaluations [Du et al., 2008]. Depending on the choice of the constraint measures, two UMDO problems may be distinguished, the Robust-based UMDO and the Reliability-based UMDO [Yao et al., 2011]. Different definitions have been proposed, we consider in this thesis, that the difference between the two approaches results from the constraint uncertainty measures as illustrated in the following paragraphs.

Robust based UMDO

Eq.(18.13) is written $\mathbb{K}\left[\mathbf{g}(\mathbf{z}, \boldsymbol{\theta}_{\boldsymbol{Y}}, \mathbf{U})\right] = \mathbb{E}\left[\mathbf{g}(\mathbf{z}, \boldsymbol{\theta}_{\boldsymbol{Y}}, \mathbf{U})\right] + \eta\sigma\left[\mathbf{g}(\mathbf{z}, \boldsymbol{\theta}_{\boldsymbol{Y}}, \mathbf{U})\right]$ where $\mathbb{E}[\mathbf{g}(\cdot)]$ and $\sigma[\mathbf{g}(\cdot)]$ are the vector of the expected values and the vector of the standard deviations of the constraint function vector $\mathbf{g}(\cdot)$. The robust formulation is based on the statistical moments of the inequality function vector to ensure that despite the uncertainty, the system will stay feasible. η indicates the restriction of the feasible region to η standard deviations away from the mean value of the constraint function vector. In Robust-based UMDO, the formulation may be rewritten such as:

$$
\begin{aligned}
\min \quad & \Xi\left[f(\mathbf{z}, \boldsymbol{\theta}_{\boldsymbol{Y}}, \mathbf{U})\right] && (3.5)\\
\text{w.r.t.} \quad & \mathbf{z}, \boldsymbol{\theta}_{\boldsymbol{Y}} && \\
\text{s.t.} \quad & \mathbb{E}\left[\mathbf{g}(\mathbf{z}, \boldsymbol{\theta}_{\boldsymbol{Y}}, \mathbf{U})\right] + \eta\sigma\left[\mathbf{g}(\mathbf{z}, \boldsymbol{\theta}_{\boldsymbol{Y}}, \mathbf{U})\right] \leq 0 && (3.6)\\
& \forall i \neq j, \forall \mathbf{u} \in \mathbf{\Omega},\ \mathbf{y}_{ij}(\boldsymbol{\theta}_{\boldsymbol{Y}ij}, \mathbf{u}_i) = \mathbf{c}_{ij}(\mathbf{z}_i, \mathbf{y}_{.i}(\boldsymbol{\theta}_{\boldsymbol{Y}.i}, \mathbf{u}_{.i}), \mathbf{u}_i) && (3.7)\\
& \mathbf{z}_{\min} \leq \mathbf{z} \leq \mathbf{z}_{\max} && (3.8)
\end{aligned}
$$

For instance the approach Multidisciplinary Optimization and Robust Design Approaches applied to Concurrent Engineering (MORDACE) [Giassi et al., 2004] proposes to solve UMDO problems with a robust approach through concurrently design of subsystems ensuring effective

design work distribution. The method relies on surface response methods of each discipline in order to concurrently optimize them and then a compromise strategy (based on Pareto frontier analysis) in order to identify the potential optimal candidates of the different possible combination of subsystem optimization results.

Reliability based UMDO

Eq.(18.13) is written $\mathbb{K}\left[\mathbf{g}(\mathbf{z},\boldsymbol{\theta}_{\boldsymbol{Y}},\mathbf{U})\right] = \boldsymbol{\Lambda}\left[\mathbf{g}(\mathbf{z},\boldsymbol{\theta}_{\boldsymbol{Y}},\mathbf{U}) > 0\right] - \boldsymbol{\Lambda}_{\mathbf{t}}$ where $\boldsymbol{\Lambda}[\mathbf{g}(\cdot)]$ stands for the measure vector of uncertainty for the inequality constraint function vector. The vector of the uncertainty measures of the constraints have to be at most equal to $\boldsymbol{\Lambda}_{\mathbf{t}}$ [Agarwal et al., 2004]. The computation of the constraints involves reliability analysis methods such as the one presented in section 2.4. It reflects the requirement for the optimized system to lie in the feasible region with a given reliability despite the uncertainty. As the uncertain variables are modeled within the probability theory, we have for the i^{th} coordinate of the vector of the measures of uncertainty:

$$\mathbb{K}_i\left[g_i(\mathbf{z},\boldsymbol{\theta}_{\boldsymbol{Y}},\mathbf{U})\right] = \mathbb{P}\left[g_i(\mathbf{z},\boldsymbol{\theta}_{\boldsymbol{Y}},\mathbf{U}) > 0\right] - \mathbb{P}_{t_i} = \int_{\mathcal{I}_i} \phi(\mathbf{u})\mathrm{d}\mathbf{u} - \mathbb{P}_{t_i} \tag{3.9}$$

with g_i the i^{th} component of the inequality constraint vector, $\mathcal{I}_i = \{\mathbf{u} \in \boldsymbol{\Omega} | g_i(\mathbf{z},\boldsymbol{\theta}_{\boldsymbol{Y}},\mathbf{u}) > 0\}$ and $\mathbb{P}_{t_i}$ the maximal allowed failure probability. In Reliability-based UMDO, the formulation may be rewritten such as:

$$\begin{aligned}
\min \quad & \Xi\left[f(\mathbf{z},\boldsymbol{\theta}_{\boldsymbol{Y}},\mathbf{U})\right] && (3.10)\\
\text{w.r.t.} \quad & \mathbf{z},\boldsymbol{\theta}_{\boldsymbol{Y}} && \\
\text{s.t.} \quad & \mathbb{P}\left[\mathbf{g}(\mathbf{z},\boldsymbol{\theta}_{\boldsymbol{Y}},\mathbf{U}) > 0\right] - \mathbb{P}_t \leq 0 && (3.11)\\
& \forall i \neq j, \forall \mathbf{u} \in \boldsymbol{\Omega},\ \mathbf{y}_{ij}(\boldsymbol{\theta}_{\boldsymbol{Y}ij},\mathbf{u}_i) = \mathbf{c}_{ij}(\mathbf{z}_i,\mathbf{y}_{.i}(\boldsymbol{\theta}_{\boldsymbol{Y}.i},\mathbf{u}_{.i}),\mathbf{u}_i) && (3.12)\\
& \mathbf{z}_{\min} \leq \mathbf{z} \leq \mathbf{z}_{\max} && (3.13)
\end{aligned}$$

- Eventually, because of the presence of the uncertain vector $\mathbf{U}$, the coupling variable vector $\mathbf{Y}$ is also an uncertain vector Eq.(18.14). In the decoupled formulations (as in deterministic MDO), input coupling variables have to be controlled by the optimizer, however in the presence of uncertainty the optimizer cannot directly control the uncertain coupling variables. Indeed, as the input coupling variables are functions of $\mathbf{U}$ in order to avoid infinite dimension optimization problem, the optimizer does not directly control the uncertain coupling variables but rather deterministic parameters $\boldsymbol{\theta}_{\boldsymbol{Y}}$ modeling the uncertain input coupling vector $\mathbf{Y}$. These parameters may be some realizations of the uncertain variables, the statistical moments, the parameters of the PDF, *etc.*

As in deterministic MDO, in UMDO two types of formulations may be distinguished for the coupling handing:

- Interdisciplinary coupling satisfaction handled with a coupled approach (with MDA),

- Interdisciplinary coupling satisfaction handled with a decoupled approach.

In this chapter, the coupled and decoupled existing UMDO formulations are presented in the point of view of the interdisciplinary couplings in the presence of uncertainty. Several coupled and decoupled UMDO formulations have been proposed [Oakley et al., 1998; Koch et al., 2002; McAllister and Simpson, 2003; Liu et al., 2006; Jaeger et al., 2013; Ghosh et al., 2014]. Firstly, the existing coupled approaches are introduced. Then, in section 3.3 the existing decoupled formulations will be presented.

3.3 Coupled UMDO formulations

3.3.1 Multi Discipline Feasible under uncertainty

As in deterministic MDO, MDF under uncertainty [Koch et al., 2002] is the most used UMDO formulation. MDF under uncertainty is a single level coupled formulation. It takes advantages of the simplicity of the deterministic version and derives it in the presence of uncertainty. The most straightforward approach to ensure the coupling satisfaction in UMDO is to use Crude Monte Carlo simulations (CMC) to propagate uncertainty while solving the system of interdisciplinary equations by MDA for each realization of the CMC sample [Oakley et al., 1998; Koch et al., 2002; Jaeger et al., 2013] (Fig. 3.1). The MDF under uncertainty formulation is given by:

$$\begin{aligned} \min \quad & \Xi\left[f(\mathbf{z}, \mathbf{Y}(\mathbf{z}, \mathbf{U}), \mathbf{U})\right] && (3.14) \\ \text{w.r.t.} \quad & \mathbf{z} \\ \text{s.t.} \quad & \mathbb{K}\left[\mathbf{g}(\mathbf{z}, \mathbf{Y}(\mathbf{z}, \mathbf{U}), \mathbf{U})\right] \leq 0 && (3.15) \\ & \mathbf{z}_{\min} \leq \mathbf{z} \leq \mathbf{z}_{\max} && (3.16) \end{aligned}$$

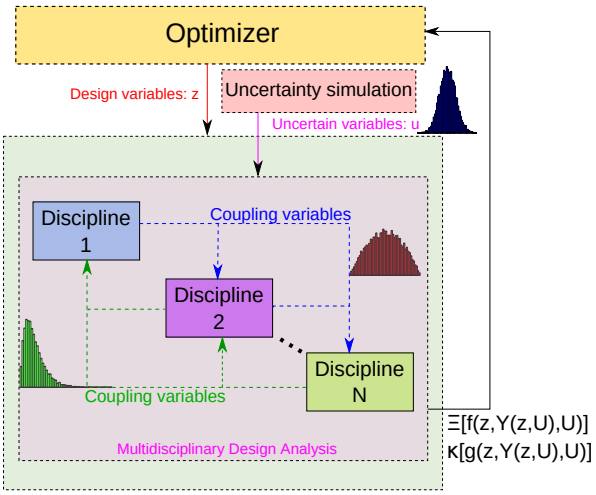

Figure 3.1: Multi Discipline Feasible under uncertainty

For a given design variable vector $\mathbf{z}_0$, to evaluate the objective function and the constraint functions, it is necessary to propagate the uncertainty in the entire system (through the different disciplines).

In the coupled formulations, $\mathbf{Y}$ (which some readers might prefer to read as $\mathbf{y}(\mathbf{z},\mathbf{U})$ but, for readability, the uppercase notation denoting random variables to $\mathbf{Y}$ is carried except to refer to realizations) is the coupling variable vector satisfying the following system of interdisciplinary equations:

$$\forall\ \mathbf{u}\in\mathbf{\Omega},\ \forall(i,j)\in\{1,...,N\}^2\ i\neq j,\ \mathbf{y}_{ij}=\mathbf{c}_{ij}(\mathbf{z}_i,\mathbf{y}_{.i},\mathbf{u}) \tag{3.17}$$

We assume that for a given realization of the uncertain vector $\mathbf{u}_0$, there exists a unique set of coupling variables such that the coupling variables satisfy:

$$\forall\ \mathbf{u}\in\mathbf{\Omega},\ \forall(i,j)\in\{1,...,N\}^2\ i\neq j,\exists!(\mathbf{y}_{ij},\mathbf{y}_{ji})|\ \mathbf{y}_{ij}=\mathbf{c}_{ij}(\mathbf{z}_i,\mathbf{y}_{.i},\mathbf{u}) \tag{3.18}$$

To compute the uncertainty measure of the performance $\Xi[f(\mathbf{z}_0,\mathbf{Y}(\mathbf{z}_0,\mathbf{U}),\mathbf{U})]$ and the constraints $\mathbb{K}\left[\mathbf{g}(\mathbf{z}_0,\mathbf{Y}(\mathbf{z}_0,\mathbf{U}),\mathbf{U})\right]$, repeated MDAs are performed for a set of uncertain variable realizations sampled by CMC.
MDF under uncertainty allows one to ensure interdisciplinary coupling satisfaction for all the realizations of the uncertain variables guarantying an appropriate estimation of the system performance and reliability. Indeed, at each iteration of the system-level optimizer in $\mathbf{z}$, for each realization of the uncertain variables, the system of interdisciplinary equations Eqs.(3.17) is solved by MDA. This approach ensures the multidisciplinary feasibility of the optimal design system and also all along the optimization process.
This formulation is computationally expensive due to the repeated evaluations of the disciplines. The computational cost of MDA under uncertainty with CMC corresponds to one MDA multiplied by the number of CMC samples [Mahadevan, 2000]. Therefore, the computational cost of MDF under uncertainty is amplified by the propagation of uncertainty and becomes intractable for the design of complex systems [Du et al., 2008]. MDF under uncertainty is considered as the reference UMDO formulation due to its intrinsic interdisciplinary coupling satisfaction. To reduce its computational cost, coupled approaches based on surrogate model have been proposed and are explained in the following section.

3.3.2 System Uncertainty Analysis (SUA) and Concurrent SubSystem Uncertainty Analysis (CSSUA)

To overcome the computational burden introduced by the repetitive MDAs, Du *et al.* [Du and Chen, 2002; Du et al., 2002] proposed a formulation called System Uncertainty Analysis (SUA) based on MDF in which MDA and the uncertainty propagation by CMC on the exact disciplines are replaced by a surrogate model approach (Fig. 3.2).

$$\begin{aligned}
&\min && \mathbb{E}\left[f(\mathbf{z},\hat{\mathbf{Y}}(\mathbf{z},\mathbf{U}),\mathbf{U})\right] && (3.19)\\
&\text{w.r.t.} && \mathbf{z} &\\
&\text{s.t.} && \mathbb{E}\left[\mathbf{g}(\mathbf{z},\hat{\mathbf{Y}}(\mathbf{z},\mathbf{U}),\mathbf{U})\right]+\eta\sigma\left[\mathbf{g}(\mathbf{z},\hat{\mathbf{Y}}(\mathbf{z},\mathbf{U}),\mathbf{U})\right]\leq 0 && (3.20)\\
& && \mathbf{z}_{\min}\leq\mathbf{z}\leq\mathbf{z}_{\max} && (3.21)
\end{aligned}$$

The surrogate model of the coupling relations $\hat{\mathbf{Y}}(\mathbf{z},\mathbf{U})$ is obtained by a first order Taylor series expansion and is used to estimate the first two statistical moments of the coupling variables. At the k^{th} system-level iteration for $\mathbf{z}=\mathbf{z}^{[k]}$, firstly a classical MDA by Fixed Point Iteration (FPI) for

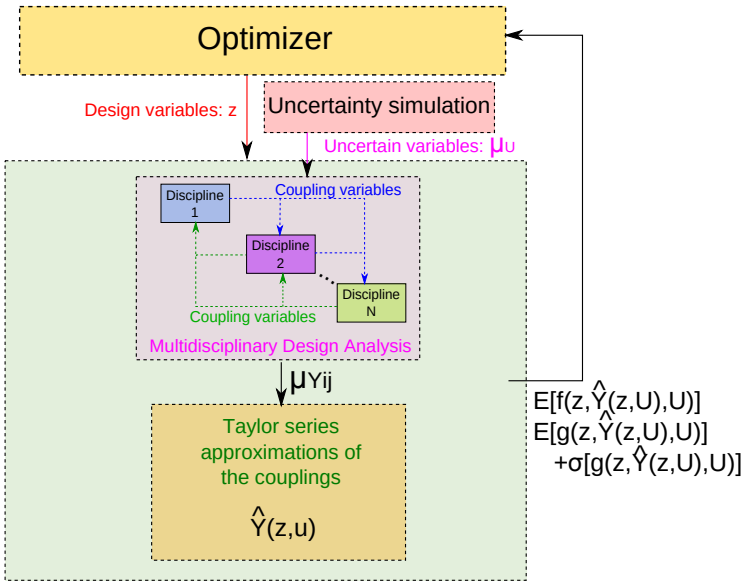

Figure 3.2: System Uncertainty Analysis (SUA)

the realization $\mathbf{u} = \boldsymbol{\mu}_{\mathbf{U}}$ is performed to compute the corresponding couplings:

$$\forall (i,j) \in \{1,...,N\}^2 \; i \neq j, \; \mathbf{y}_{ij}\left(\mathbf{z}_i^{[k]}, \boldsymbol{\mu}_{\mathbf{U}}\right) = \mathbf{c}_{ij}\left(\mathbf{z}_i^{[k]}, \mathbf{y}_{.i}, \boldsymbol{\mu}_{\mathbf{U}}\right) \tag{3.22}$$

A first linear approximation is made by assuming that:

$$\forall (i,j) \in \{1,...,N\}^2 \; i \neq j, \; \boldsymbol{\mu}_{\mathbf{Y}_{ij}} = \mathbf{y}_{ij}\left(\mathbf{z}_i^{[k]}, \boldsymbol{\mu}_{\mathbf{U}}\right) \tag{3.23}$$

Then, a first order Taylor series approximation around $\boldsymbol{\mu}_{\mathbf{U}}$ of the couplings between disciplines i and j is made:

$$\mathbf{Y}_{ij}\left(\mathbf{z}^{[k]}, \mathbf{Y}_{.i}, \mathbf{U}\right) = \boldsymbol{\mu}_{\mathbf{Y}_{ij}} + \left.\frac{\partial \mathbf{Y}_{ij}}{\partial \mathbf{U}}\right|_{\mathbf{U}=\boldsymbol{\mu}_{\mathbf{U}}} (\mathbf{U} - \boldsymbol{\mu}_{\mathbf{U}}) + \left.\frac{\partial \mathbf{Y}_{ij}}{\partial \mathbf{Y}_{.i}}\right|_{\mathbf{U}=\boldsymbol{\mu}_{\mathbf{U}}} (\mathbf{Y}_{.i} - \boldsymbol{\mu}_{\mathbf{Y}_{.i}}) \tag{3.24}$$

Then, by doing it for all the coupling variables between all the disciplines and reorganizing the system of equations, it is possible to have a first order approximation of the coupling variables as a function of the uncertain variables $\mathbf{U}$ around $\boldsymbol{\mu}_{\mathbf{U}}$ in a matrix form:

$$\hat{\mathbf{Y}}_{ij}\left(\mathbf{z}^{[k]}, \mathbf{U}\right) = \mathbf{A}\left(\mathbf{z}^{[k]}\right)^{-1} \mathbf{B}\left(\mathbf{z}^{[k]}\right)(\mathbf{U} - \boldsymbol{\mu}_{\mathbf{U}}) + \mathbf{C}\left(\mathbf{z}^{[k]}\right) \tag{3.25}$$

with $\mathbf{A}\left(\mathbf{z}^{[k]}\right)$ a matrix and $\mathbf{B}\left(\mathbf{z}^{[k]}\right), \mathbf{C}\left(\mathbf{z}^{[k]}\right)$ vectors detailed in [Du and Chen, 2002]. A first order Taylor series expansion of the objective function $f(\cdot)$ and the constraints $\mathbf{g}(\cdot)$ is used to propagate uncertainty and to estimate their first two statistical moments. It is possible therefore to estimate the expected value $\mathbb{E}[f(\cdot)]$ and $\mathbb{E}[\mathbf{g}(\cdot)] + \eta\sigma[\mathbf{g}(\cdot)]$. The first order Taylor series

expansion provides a functional model of the coupling dependency with respect to the uncertain variables. The method enables to find the optimal design while ensuring interdisciplinary couplings for all the uncertain variable realizations. However, the method has several limits: first order Taylor approximation is only valid for functions that can be locally approximated as linear functions and the method requires to perform a MDA to locally build the surrogate model.

In order to further improve SUA, Du *et al.* [Du and Chen, 2002; Du et al., 2002] proposed an amelioration named Concurrent SubSystem Uncertainty Analysis (CSSUA) to avoid the FPI to locally build the surrogate model (Fig. 3.3). An optimization problem replaces the required FPI in SUA to find the expected value of the coupling variables $\boldsymbol{\mu}_{\mathbf{Y}_{ij}}$ formulated as:

$$\begin{aligned} \min \quad & \sum_{i=1}^{N} \left|\left| \boldsymbol{\mu}_{\mathbf{Y}_{i.}} - \mathbf{c}_{i.}\left(\mathbf{z}_i^{[k]}, \boldsymbol{\mu}_{\mathbf{Y}_{.i}}, \boldsymbol{\mu}_{\mathbf{U}}\right) \right|\right|_2^2 \\ \text{w.r.t.} \quad & \boldsymbol{\mu}_{\mathbf{Y}} \end{aligned} \tag{3.26}$$

As in SUA, a linear approximation of the disciplines is made by assuming that:

$$\forall (i,j) \in \{1,...,N\}^2 \; i \neq j, \; \boldsymbol{\mu}_{\mathbf{Y}_{ij}} = \mathbf{y}_{ij}\left(\mathbf{z}_i^{[k]}, \boldsymbol{\mu}_{\mathbf{U}}\right) \tag{3.27}$$

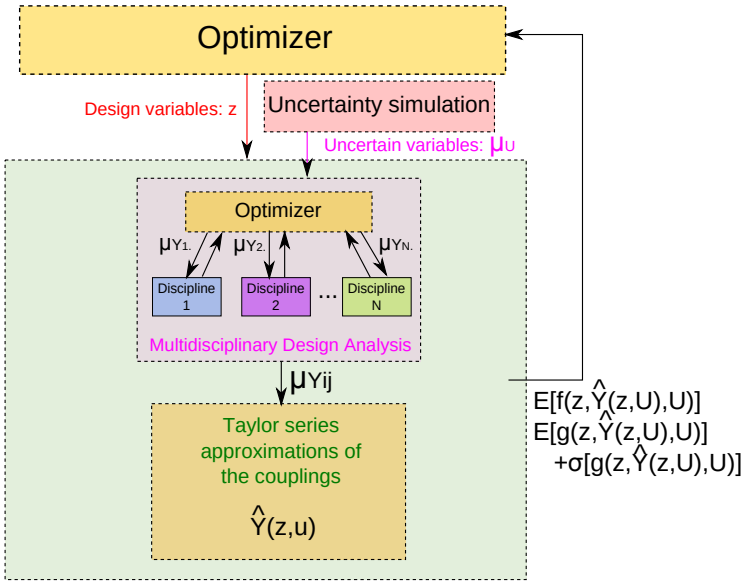

Figure 3.3: Concurrent SubSystem Uncertainty Analysis (CSSUA)

This optimization problem allows one to call the disciplines in parallel, reducing the computational cost compared to FPI. Once the expected value of the coupling variables are found, the same uncertainty propagation as in SUA is adopted. CSSUA suffers from the same drawbacks as SUA. In

launch vehicle design, some disciplines such as the aerodynamics and the trajectory involve highly non linear dynamics and the linearization hypothesis would introduce high errors compared to MDF under uncertainty.
In order to avoid performing MDA under uncertainty, an alternative way is to use the same approach as in deterministic MDO and to perform UMDO on decoupled multidisciplinary systems in order to further decrease the number of calls to the disciplines,. It would allow to benefit from the same advantages as the deterministic decoupled MDO formulations highlighted in chapter 1. Existing decoupled UMDO formulations are presented in the following sections.

3.4 Decoupled UMDO formulations

3.4.1 Statistical moment matching methods

In order to remove MDA, decoupled approaches inspired from CO [Braun et al., 1996] have been proposed [Du and Chen, 2001; McAllister and Simpson, 2003; Liu et al., 2006; Ghosh et al., 2014]. The idea is to extend CO framework to robust design. In these methods, the uncertain input coupling vector is replaced by its statistical moments. Therefore, the system-level optimizer only controls deterministic parameters. For instance Du *et al.* [Du and Chen, 2001] proposed the Hierarchical Approach to Collaborative Multidisciplinary Robust Design method in which the input coupling variables are characterized by their expected values $\boldsymbol{\mu}_Y$ and standard deviations $\boldsymbol{\sigma}_Y$. In this formulation, the system-level optimizer controls the design variable vector $\mathbf{z}$, the input coupling variable expected values $\boldsymbol{\mu}_Y$ and standard deviations $\boldsymbol{\sigma}_Y$.

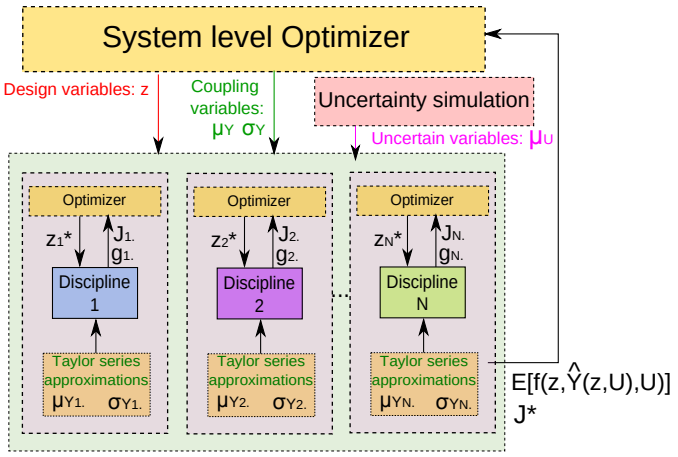

Figure 3.4: Hierarchical Approach to Collaborative Multidisciplinary Robust Design

As in SUA and CSSUA the disciplines, the objective function and the constraints are approximated by a first order Taylor series expansion to estimate their statistical moments. The subsystem-level objective is to modify its local design variables $\mathbf{z}_i^*$ in order to find an agreement with the other subsystems regarding to the coupling variables. The subsystem-level objective is a measure of the relative errors between the discipline outputs and the system-level instructions.

The formulation proposed by Du *et al.* [Du and Chen, 2001] (Fig. 3.4) is:

$$\begin{aligned}
&\min && \mathbb{E}\left[f(\mathbf{z},\hat{\mathbf{Y}}(\mathbf{z},\mathbf{U}),\mathbf{U})\right] && (3.28)\\
&\text{w.r.t.} && \mathbf{z},\boldsymbol{\mu}_{\mathbf{Y}},\boldsymbol{\sigma}_{\mathbf{Y}} &\\
&\text{s.t.} && \mathbf{J}^*_{i.}(\mathbf{z}^*_i,\mathbf{z}_i,\boldsymbol{\mu}_{\mathbf{Y}},\boldsymbol{\sigma}_{\mathbf{Y}})=0,\forall i\in\{1,\dots,N\} && (3.29)\\
& && \mathbf{z}_{\min}\leq\mathbf{z}\leq\mathbf{z}_{\max} && (3.30)
\end{aligned}$$

with $\mathbf{J}^*_{i.}$ the optimized objective function of the i^{th} discipline and $\mathbf{z}^*$ the local copies of $\mathbf{z}$ controlled by the subsystem optimizer. The i^{th} subsystem optimization problem is given by:

$$\begin{aligned}
&\min && \mathbf{J}_{i.}=\left|\left|\mathbf{z}^*_i-\mathbf{z}_i\right|\right|_2^2+\left|\left|\boldsymbol{\mu}_{\mathbf{Y}_{i.}}-\mathbf{c}_{i.}\left(\mathbf{z}^*_i,\boldsymbol{\mu}_{\mathbf{Y}_{.i}},\boldsymbol{\mu}_{\mathbf{U}}\right)\right|\right|_2^2 &\\
& && \quad+\left|\left|\boldsymbol{\sigma}^2_{\mathbf{Y}_{i.}}-\sum_{l=1}^{d}\left(\left.\frac{\partial c_{i.}}{\partial \mathbf{u}^{(l)}}\right|_{\mathbf{u}=\boldsymbol{\mu}_{\mathbf{U}}}\right)^2\sigma^2_{\mathbf{U}^{(l)}}\right|\right|_2^2 && (3.31)\\
&\text{w.r.t.} && \mathbf{z}^*_i &\\
&\text{s.t.} && \mathbb{E}\left[\mathbf{g}(\mathbf{z},\hat{\mathbf{Y}}(\mathbf{z},\mathbf{U}),\mathbf{U})\right]+\eta\sigma\left[\mathbf{g}(\mathbf{z},\hat{\mathbf{Y}}(\mathbf{z},\mathbf{U}),\mathbf{U})\right]\leq 0 && (3.32)\\
& && \mathbf{z}^*_{i_{\min}}\leq\mathbf{z}^*_i\leq\mathbf{z}^*_{i_{\max}} && (3.33)
\end{aligned}$$

This formulation relies on SUA and CSSUA approaches and does not involve any MDA offering the possibility for parallel discipline optimizations. The interdisciplinary coupling constraints at the system-level ensure that the input coupling variables and the output coupling variables have the same expected values and the same standard deviations. The first two statistical moments of the coupling variables are matched between the different disciplines to ensure the multidisciplinary feasibility.
This formulation has been extended in [Xiong et al., 2014] to avoid first order Taylor series approximation. CMC replaces Taylor series expansion to propagate uncertainty and to estimate the coupling variable statistical moments. To further improve the method, Ghosh *et al.* [Ghosh et al., 2014] proposed to capture the statistical dependence of the coupling variables by introducing the covariance matrix to model the correlations between them. The coefficients of the covariance matrix in addition to the expected values are controlled by the system-level optimizer. It increases the number of variables controlled by the system-level optimizer but it enhances the fidelity of the moment matching. Moreover, this approach has been extended to Reliability-based UMDO [Huang et al., 2010] to enable reliability analysis on the constraints instead of statistical moment estimations. Furthermore, moment matching approaches have been adapted in other UMDO formulations such as Probabilistic ATC [Liu et al., 2006] which presents similarities with CO. An important drawback of these approaches is the necessity for the disciplines to be differentiable with respect to the uncertain variables which might not be the case for complex simulation codes.

The moment matching formulations are interesting since they preserve some disciplinary autonomy *via* parallel sybsystem-level uncertainty propagation and optimizations. However, the interdisciplinary couplings is satisfied only in terms of statistical moments (expected value, standard deviation or covariance matrix) of the coupling variables.

3.4.2 Sequential Optimization and Reliability Assessment (SORA)

Du *et al.* [Du et al., 2008] proposed the Sequential Optimization and Reliability Assessment (SORA) for UMDO. The main idea is to separate the optimization and the reliability analysis. Indeed, reliability analysis is computationally expensive especially on multidisciplinary systems. To avoid to perform reliability analysis at each system-level iteration to compute the constraints, a sequential approach has been proposed. The UMDO problem is decomposed into a sequence of deterministic MDO problems and reliability analyses. SORA [Du and Chen, 2004] replaces the probabilistic reliability constraints by deterministic approximation of the reliability constraints evaluated at the Most Probable Point (MPP). Reliability analysis is performed by First Order Reliability Method (FORM) [Rackwitz, 2001] to find the MPP (noted $\boldsymbol{u}^*$). It is assumed here that the uncertain variables are given in the standard Gaussian space. If it is not the case, different statistical transformations may be applied on the input distributions (such as Nataf [Nataf, 1962] or Rosenblatt [Rosenblatt, 1952] transformations).

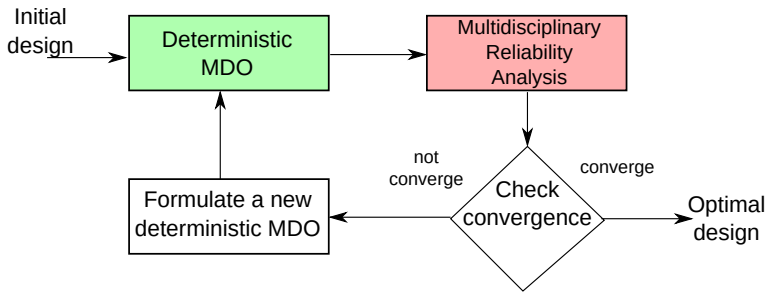

Figure 3.5: SORA procedure for UMDO [Du et al., 2008]

In SORA [Du et al., 2008], four steps are distinguished (Fig. 3.5):

- Step 1: At the k^{th} SORA iteration, deterministic MDO problem is solved with the uncertain variables fixed at their MPP found at the $[k-1]^{\text{th}}$ iteration.
- Step 2: Reliability analysis is performed to identify the MPP $\boldsymbol{u}^*_{(k)}$ of all the inequality constraints by FORM with the design variables fixed at the optimal design $\mathbf{z}^{*[k]}$ found in step 1. The objective function is computed: $f\left(\mathbf{z}^{*[k]}, \mathbf{y}\left(\mathbf{z}^{*[k]}, \boldsymbol{u}^{*[k]}\right), \boldsymbol{u}^{*[k]}\right)$, with $\mathbf{y}(\cdot)$ the coupling vector satisfying interdisciplinary couplings (see Eq.3.42) at the MPP.
- Step 3: the convergence is checked. If the inequality constraints ($\mathbb{P}\left[\mathbf{g}(\mathbf{z}, \mathbf{Y}(\mathbf{z}, \mathbf{U}), \mathbf{U}) > 0\right] - \mathbb{P}_t \leq 0$) are verified and the objective function becomes stable [Du et al., 2008], the solution is found.
- Step 4: if the convergence is not reached, or the inequality constraints are violated, a new deterministic MDO problem is formulated for $\mathbf{u} = \boldsymbol{u}^{*[k]}$, back to step 1.

Deterministic MDO: step 1

The deterministic MDO problem of step 1 may be solved with the classical decoupled MDO methods

(IDF, AAO, BLISS, ATC, *etc*). With the IDF method [Du et al., 2008], the deterministic MDO problem at the SORA k^{th}-cycle, $(k \geq 2)$, is formulated as follows :

$$
\begin{aligned}
&\text{given} && \boldsymbol{u}^{*[k-1]} && (3.34)\\
&\min && f\left(\mathbf{z}, \mathbf{y}, \boldsymbol{u}^{*[k-1]}\right) && (3.35)\\
&\text{w.r.t.} && \mathbf{z}, \mathbf{y} &&\\
&\text{s.t.} && \mathbf{g}\left(\mathbf{z}, \mathbf{y}, \boldsymbol{u}^{*[k-1]}\right) \leq 0 && (3.36)\\
& && \forall (i,j) \in \{1,...,N\}^2 \; i \neq j, \; \mathbf{y}_{ij} = \mathbf{c}_{ij}\left(\mathbf{z}_i, \mathbf{y}_{.i}, \boldsymbol{u}_i^{*[k-1]}\right) && (3.37)\\
& && \mathbf{z}_{\min} \leq \mathbf{z} \leq \mathbf{z}_{\max} && (3.38)
\end{aligned}
$$

The interdisciplinary couplings Eq.(3.37) are ensured for one particular realization of the uncertain variables corresponding to the MPP $\boldsymbol{u}^{*[(k-1)]}$.

Reliability analysis: step 2
The reliability analysis is performed for the design variables fixed at $\mathbf{z}^{*[k]}$ based on FORM [Chiralaksanakul and Mahadevan, 2007; Du et al., 2008] :

$$
\begin{aligned}
&\text{given} && \mathbf{z}^{*[k]} && (3.39)\\
&\min && \| \mathbf{u} \| && (3.40)\\
&\text{w.r.t.} && \mathbf{u}, \mathbf{y} &&\\
&\text{s.t.} && \mathbf{g}\left(\mathbf{z}^{*[k]}, \mathbf{y}, \mathbf{u}\right) = 0 && (3.41)\\
& && \forall (i,j) \in \{1,...,N\}^2 \; i \neq j, \; \mathbf{y}_{ij} = \mathbf{c}_{ij}\left(\mathbf{z}^{*[k]}, \mathbf{y}_{.i}, \mathbf{u}_i\right) && (3.42)
\end{aligned}
$$

This optimization provides the MPP value $\mathbf{u}^{*[k]}$ for the uncertain variables at the SORA k^{th}-cycle. Reliability analysis is performed on a decoupled multidisciplinary system and the interdisciplinary couplings are satisfied at the MPP in Eq.(3.42). By decoupling reliability analysis from the deterministic MDO, SORA tends to decrease the number of calls to the disciplinary functions compared to MDF under uncertainty [Du et al., 2008]. SORA has been implemented with various MDO formulations such as MDF [Chiralaksanakul and Mahadevan, 2007] IDF [Chiralaksanakul and Mahadevan, 2007], CO [Li et al., 2010b; Zhang and Zhang, 2013a], CSSO [Li et al., 2013; Zhang and Zhang, 2013b] or BLISS [Ahn and Kwon, 2006] but the coupling satisfaction relies on the same approach: satisfaction at the MPP of the coupling variables.

The interdisciplinary coupling satisfaction within SORA presents several advantages:

- Possibility to perform disciplinary analysis in parallel,
- Satisfaction of the interdisciplinary couplings at the MPP value for the coupling variables at the optimum,
- Reduction of the computational cost compared to MDF under uncertainty with CMC.

However, SORA has also several limitations. Reliability analysis is performed by FORM which locally linearizes the inequality constraints and may lead to inaccurate estimation of the probability of failure. FORM also assumes the uniqueness of the MPP which is a limiting hypothesis in practical applications [Dubourg et al., 2013]. Furthermore, in terms of interdisciplinary coupling satisfaction, the couplings are ensured only at the MPP which is the most likely failure to happen but another failure less likely may occur.

3.4.3 Likelihood-based MultiDisciplinary Analysis

The approach presented in this section is not an UMDO formulation but it focuses on decoupled uncertainty propagation methods for multidisciplinary systems. Sankararaman *et al.* proposed to satisfy the interdisciplinary couplings for all the realizations of the uncertain variables by constructing the input coupling PDF [Sankararaman and Mahadevan, 2012].
Let consider the system of Figure 3.6 representing a partially decoupled multidisciplinary system. The couplings from the discipline i to the discipline j are removed. For each realization of the uncertain vector $\mathbf{U}$ and the coupling vector $\mathbf{Y}_{ij}$, it is possible to compute: $\mathbf{c}_{ij}(\mathbf{z}_i, \mathbf{u}_i, \mathbf{c}_{ji}(\mathbf{z}_j, \mathbf{u}_j, \mathbf{y}_{ij}))$ and $\mathbf{e}_{ij}(\mathbf{z}, \mathbf{u}, \mathbf{y}_{ij}) = \mathbf{y}_{ij} - \mathbf{c}_{ij}(\mathbf{z}_i, \mathbf{u}_i, \mathbf{c}_{ji}(\mathbf{z}_j, \mathbf{u}_j, \mathbf{y}_{ij}))$. $\mathbf{E}_{ij}$ is the error between the input coupling variables and the corresponding output coupling variables. In this partially decoupled approach, $\mathbf{y}_{ji} = \mathbf{c}_{ji}(\mathbf{z}_j, \mathbf{u}_j, \mathbf{y}_{ij})$ results directly from the simulation of the discipline j. To simplify, we denote $\mathbf{c}_{ij}(\mathbf{z}_i, \mathbf{U}_i, \mathbf{c}_{ji}(\mathbf{z}_j, \mathbf{U}_j, \mathbf{Y}_{ij}))$ by $\mathbf{c}_{ij}(.)$.

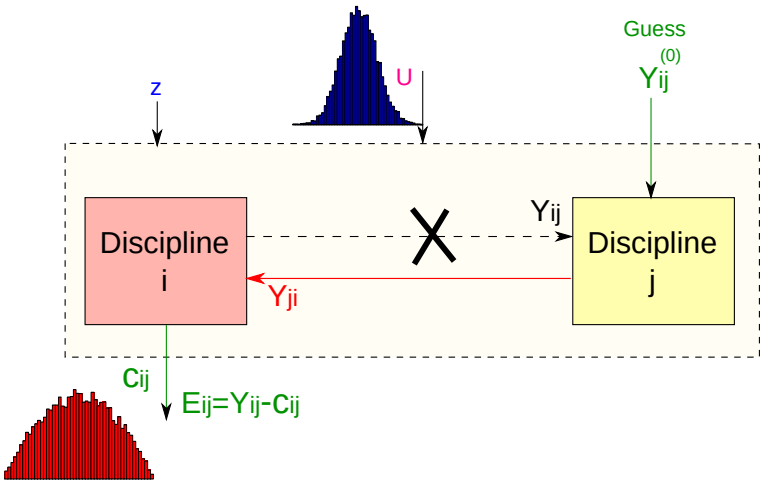

Figure 3.6: Partially decoupled multidisciplinary system [Sankararaman and Mahadevan, 2012] and related notations

The method is based on likelihood in order to construct the probability distribution the coupling variable $\mathbf{Y}_{ij}$. Then, the samples generated with this PDF are considered as an input uncertain variables in the same way as the variables $\mathbf{U}$. The uncertainty propagation is therefore carried out on the partially decoupled system. Considering Figure 3.6, an analysis is carried out on the partially decoupled system at a given design vector $\mathbf{z}$, with M CMC samples of $\mathbf{U}$ generated according to $\phi_{\mathbf{U}}(\cdot)$ and for a given fixed realization $\mathbf{y}_{ij(0)}$. Propagation of uncertainty is performed for the M

CMC samples of $\mathbf{U}$, generating M samples of the variables $\mathbf{c}_{ji}$ directly passed to discipline j which generate M samples of $\mathbf{c}_{ij}$. Among all the samples of $\mathbf{c}_{ij}$, the interdisciplinary coupling is satisfied when one sample of $\mathbf{c}_{ij}$ is equal to the realization $\mathbf{y}_{ij(0)}$ (*i.e.* $\mathbf{E}_{ij} = 0$). The likelihood $\mathcal{L}(\cdot)$ of $\mathbf{y}_{ij(0)}$ to satisfy the interdisciplinary is proportional to $\mathbb{P}\left(\mathbf{y}_{ij(0)} = \mathbf{c}_{ij}\right)$. The authors assume that this probability is equal to $\mathbb{P}\left(\epsilon \leq \mathbf{y}_{ij(0)} - \mathbf{c}_{ij} \leq \epsilon\right)$ for ϵ small enough

$$\mathcal{L}\left(\mathbf{y}_{ij(0)}\right) \propto \mathbb{P}\left(\epsilon \leq \mathbf{y}_{ij(0)} - \mathbf{c}_{ij} \leq \epsilon | \mathbf{y}_{ij(0)}\right) \tag{3.43}$$

The likelihood of different realizations of $\mathbf{Y}_{ij}$ is calculated based on the same principle. To sample $\mathbf{Y}_{ij}$ a uniform prior distribution is assumed. Based on these likelihoods and Bayes' theorem, an estimation of the conditional PDF of $\mathbf{Y}_{ij}$ satisfying the interdisciplinary couplings may be obtained by [Sankararaman and Mahadevan, 2012]:

$$\phi_{\mathbf{Y}_{ij}|\mathbf{E}_{ij}=0}(\mathbf{y}_{ij}) = \frac{\mathcal{L}(\mathbf{y}_{ij})}{\int \mathcal{L}(\mathbf{y}_{ij}) \mathrm{d}\mathbf{y}_{ij}} \tag{3.44}$$

Then, the conditional PDF $\phi_{\mathbf{Y}_{ij}|\mathbf{E}_{ij}=0}(\cdot)$ is used as an input distribution to propagate uncertainty on the partially decoupled system.
This approach is interesting because it allows to satisfy the couplings for all the realizations of the uncertain variables and not just at the MPP or at the expected value. Moreover, this method allows to propagate uncertainty on a partially decoupled system in order to avoid MDA. However, this approach has some limits in terms of interdisciplinary coupling satisfaction. First, the functional dependency between the uncertain variables $\mathbf{U}$ and the input coupling variables $\mathbf{Y}_{ij}$ is not considered in the construction of the input coupling probability density functions, only a statistical dependency is considered. Normally, $\mathbf{Y}$ depends on $\mathbf{z}$ and $\mathbf{U}$. This functional dependency is essential because it ensures that for a particular realization of the uncertain variables there exists a unique converged value for the coupling variables as with MDA under uncertainty. Secondly, in Bayes' theorem, a uniform prior distribution for $\mathbf{Y}_{ij}$ is assumed which may be a non valid assumption and introduce an error in the conditional PDF of the coupling variables. An extension for fully decoupled systems has been proposed based on the same principles, by constructing the PDF of the coupling variables by two semi-decoupled processes. However, it suffers from the same drawbacks as the semi-decoupled approach.
A summary of the main decoupled UMDO formulations is proposed in Table 3.7 .

Table 3.7: Advantages and drawbacks of the decoupled UMDO formulations

	Advantages	Drawbacks
Statistical moment matching	Easy to implement	Limited to parametric coupling distributions
SORA	Decoupling of the optimization from the reliability analysis	Coupling satisfaction only at the MPP
Likelihood-based MDA	Semi-decoupled approach	Do not ensure functional coupling satisfaction

3.5 UMDO methodologies dedicated to launch vehicle design

Most of the formulations presented in this chapter have been applied to analytical test cases and to some more complex engineering problems. However, in the literature only few papers formulate a complete UMDO problem for launch vehicle design. Most of the case studies focus on the robustness of the optimal space transportation system design and do not involve reliability assessment. Moreover, most of the UMDO formulations rely on MDF under uncertainty coupled with CMC to propagate uncertainty. In [Charania et al., 2002; Bettis et al., 2011], the authors quantify the uncertainty in the performance of a fixed launch vehicle configuration but no optimization is performed. Heuristic optimization methods (*e.g.* Genetic Algorithm, Particle Swarm Optimization) are compared in [Rafique et al., 2010] with a deterministic MDF formulation to design a launch vehicle. The robustness of the found deterministic solutions is studied with a probabilistic modeling of some uncertain parameters and CMC in order to select the most robust solutions.
Analysis of variance based on surrogate models is performed in [Yeniay et al., 2006] to determine the value of the design variables ensuring the minimal deviations from expected performance in launch vehicle weight and sizing analysis. MDF under uncertainty is used to optimize a function of the GLOW of a launch vehicle in [McCormick, 2001] and takes the propulsion, aerodynamics, sizing and trajectory disciplines into account. In [Zaman and Mahadevan, 2013], the authors used MDF under uncertainty to optimize the total power consumption of a satellite. Six design variables and three uncertain parameters are considered in this study. In [Zaman et al., 2011], the upper stage of a two-stage-to-orbit vehicle is optimized in the presence of uncertainty. The objective is to minimize a function of the dry mass of the upper stage with MDF. In [King et al., 2012], the weight of the wing of a reusable launch system is optimized based on MDF in the presence of uncertainty taking into account aero-elastic analysis.
Yao *et al.* [Yao et al., 2010, 2012] formulated a reliable and robust UMDO problem to design a satellite. The robustness is expressed by a weighted aggregation of the mean and the standard deviation of the satellite mass. In [Yao et al., 2010], the UMDO approach relies on CSSO which ensures the coupling satisfaction by MDA. The satellite system design is decomposed into different subsystem optimization problems which correspond to all the disciplines involved in the design process. The system robustness and reliability are computed with CMC and system performance is approximated by Taylor series. In [Yao et al., 2012], a MDF-CSSO decomposition is used with coupling satisfaction by MDA. A first optimum is found by a sequence of low fidelity surrogate model refinements combined with MDF under uncertainty. Then, based on the MDF optimal design, a local optimization under uncertainty with CSSO and high fidelity simulations is performed allowing disciplinary autonomy.

3.6 Conclusion

In this chapter, UMDO formulations have been described, presenting the main methods and their mathematical formulations using the unified notations introduced in the previous chapters. First, the differences between deterministic MDO and UMDO have been underlined and new notations have been presented. Then, the existing UMDO formulations have been introduced with a focus on the interdisciplinary coupling handling. The existing formulations either rely on computationally expensive MDA to rigorously ensure coupling satisfaction, or deal with incomplete coupling conditions (coupling in terms of statistical moments, at the MPP, *etc.*)

All the existing decoupled UMDO formulations do not allow to ensure the multidisciplinary feasibility for all the realizations of the uncertain variables used to compute the performance or the constraints. In the design of systems such as launch vehicles, it is necessary to ensure that the decoupled UMDO process implemented does not provide unfeasible solutions due to non satisfaction of the interdisciplinary coupling system of equations. The incomplete coupling condition satisfaction in the existing approaches motivate us to develop in chapters 6, 7 two new UMDO formulations in order to ensure multidisciplinary feasibility in the presence of uncertainty.
This chapter is focused on coupling management, however another important aspect in UMDO methodologies is the reliability assessment for complex systems. This analysis is a difficult task that requires dedicated techniques that will be presented in the next chapter. A focus on the existing methods for reliability analysis in the presence of mixed aleatory/epistemic uncertainties is proposed.

Chapter 4

Reliability analysis in the presence of mixed aleatory/epistemic uncertainties

Contents

Chapter goals

- Present the principal existing reliability assessment techniques in the presence of both aleatory and epistemic uncertainties,
- Highlight the advantages and drawbacks of each technique.

4.1 Introduction

This chapter is devoted to the presentation of reliability analysis techniques for the design of complex systems within the UMDO framework. In particular, the problematic of the presence of mixed aleatory/epistemic uncertainties in reliability assessment is essential in the early design phases. Indeed, in these phases, due to the lack of knowledge and the use of low fidelity models, epistemic

uncertainty arises in addition to aleatory uncertainty which results from the inherent variability in the system or its environment. In practice, as the design process progresses, the epistemic uncertainty is reduced, the knowledge is improved and the fidelity of the model used is increased. However, in the early design phases, epistemic uncertainty may induce important deviations from future nominal conditions and taking into account both types of uncertainties is essential. To avoid computational burden, the UMDO context imposes to estimate probabilities of failure at a low computational cost limiting at the maximum the number of discipline evaluations. In this chapter, existing methods to deal with mixed aleatory and epistemic uncertainties in UMDO are presented. For each approach, we expose at first the principle of the method, then its mathematical formulation and finally the advantages and drawbacks.

4.2 Problem description

Consider a reliability-based UMDO formulation based on a coupled approach in the presence of both aleatory and epistemic uncertainties:

$$\begin{aligned} \min \quad & \Xi\left[f(\mathbf{z}, \mathbf{Y}(\mathbf{z}, \mathbf{U}, \mathbf{e}), \mathbf{U}, \mathbf{e})\right] && (4.1) \\ \text{w.r.t.} \quad & \mathbf{z} \\ \text{s.t.} \quad & \mathbb{K}\left[\mathbf{g}(\mathbf{z}, \mathbf{Y}(\mathbf{z}, \mathbf{U}, \mathbf{e}), \mathbf{U}, \mathbf{e})\right] \leq 0 && (4.2) \\ & \mathbf{z}_{\min} \leq \mathbf{z} \leq \mathbf{z}_{\max} && (4.3) \end{aligned}$$

where $\mathbf{e} = [e^{(1)}, \ldots, e^{(w)}]^{\mathrm{T}} \in \mathbb{R}^w$ a parameter vector which suffers from epistemic uncertainty. The described methods in this chapter are devoted to the computation of Eq.(5.2). The solving of this UMDO problem requires reliability analysis to compute the inequality constraints. To focus on the reliability analysis problem in the presence of mixed uncertainties, a simplified problem is considered which consists in computing:

$$\mathbb{K}\left[\mathbf{g}(\mathbf{U}, \mathbf{e})\right] \leq 0$$

The uncertainty measure $\mathbb{K}$ has to handle both aleatory uncertainty (modeled within the probability formalism) and epistemic uncertainty. In this chapter, we focus on interval formalism to represent epistemic uncertainty which is easier to work with and to interpret for engineers than other more recent formalisms such as evidence theory [Dempster, 1967; Shafer, 1976] or imprecise probability theory [Walley, 1996]. Moreover, the probability formalism is used to represent the aleatory uncertainty and the probability measure $\mathbb{P}(\cdot)$ is used as measure for the failure.
In literature, the impact of epistemic uncertainty on the system may be classified into two categories:

- Either the hyper-parameters of the joint PDF of the aleatory uncertainty are affected by epistemic uncertainty (*e.g.* the expected value of a Gaussian PDF is not known exactly but only within an interval) (section 4.3),
- Either the limit state functions are directly affected by epistemic uncertainty (section 4.4).

These two cases are considered in the following sections.

4.3 Epistemic uncertainty on the hyper-parameters of the joint input PDF

4.3.1 Problem statement

Let consider a d-dimensional random vector $\mathbf{U}$ defined on the sample space $\mathbf{\Omega}$ by a joint PDF $\phi^{\mathbf{e}}(\cdot)$ indexed by a parameter vector $\mathbf{e} = [e^{(1)}, \ldots, e^{(w)}]^{\mathrm{T}} \in \mathbb{R}^w$. $\mathbf{e}$ suffers from epistemic uncertainties and only the variation domains of its components are known $\mathbf{\Upsilon} = \{\mathbf{e} \in \mathbb{R}^w | e^{(i)} \in [e^{(i)}_{\min}, e^{(i)}_{\max}] \; \forall i \in \{1, \ldots, w\}\}$. Consider a system characterized by a limit state function $g : \mathbf{\Omega} \to \mathbb{R}$ assumed to be a deterministic continuous input-output function. $g(\cdot)$ is assumed to be computationally expensive to evaluate in order to provide the output for a given input. Moreover, due to the complexity of the physical phenomena involved in the simulation of $g(\cdot)$, it is supposed that $g(\cdot)$ is non linear and presents multiple failure regions. In the presence of mixed aleatory and epistemic uncertainties impacting the system, the failure probability is not unique and depends on the values taken by $\mathbf{e}$ (Figs. 4.1,4.2). To characterize the probability of failure, it is possible to determine its domain of variation by finding the lower and upper bounds:

$$\begin{cases} \mathbb{P}_{\min} = \min\limits_{\mathbf{e} \in \mathbf{\Upsilon}} \; \mathbb{P}_{\mathbf{e}}(g(\mathbf{U}) \leq 0) \\ \mathbb{P}_{\max} = \max\limits_{\mathbf{e} \in \mathbf{\Upsilon}} \; \mathbb{P}_{\mathbf{e}}(g(\mathbf{U}) \leq 0) \end{cases} \tag{4.4}$$

The determination the epistemic values leading to the failure probability bounds requires optimization problem solvings and reliability analyses (*i.e.* probability estimation) The optimization problem is also referred as Interval Analysis (IA) and one evaluation of the objective function in the optimization problems Eqs.(4.4) requires one reliability analysis (also referred as Probability Analysis - PA).

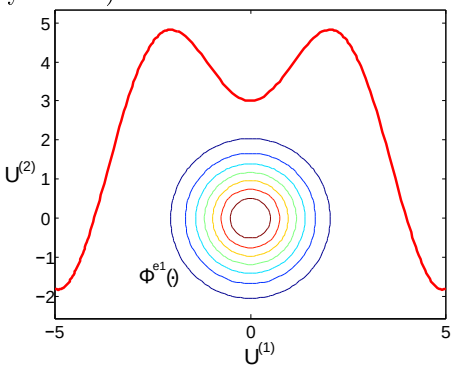

Figure 4.1: Reliability analysis with $\phi^{\mathbf{e1}}(\cdot)$

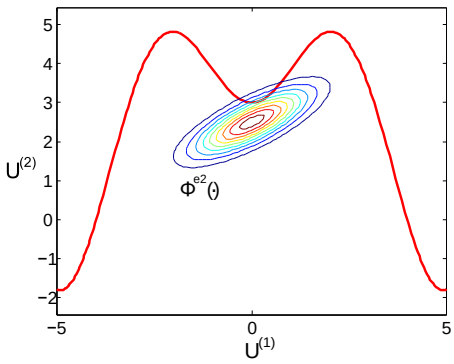

Figure 4.2: Reliability analysis with $\phi^{\mathbf{e2}}(\cdot)$

4.3.2 Existing methods

Approaches based on sampling [Zhang et al., 2010] or on FORM [Qiu et al., 2008] have been proposed to solve these optimization problems. A classical engineering approach to solve this problem with CMC could consist in a double loop. On the outer loop, one generates CMC samples in the epistemic uncertain space according to a uniform PDF and for each epistemic value, a CMC estimation of the

probability of failure is performed. The issue with this approach is the computational cost induced by the double CMC loops.
However, CMC method has been extended [Zhang et al., 2010] to an interval CMC method to propagate interval parameter uncertainty in reliability assessment. For a given $\mathbf{e}$, CMC estimates the probability of failure according to:

$$\mathbb{P}_{\mathbf{e}}\left[g(\mathbf{U}) \leq 0\right] = \int_{\mathbb{R}^d} \mathbb{1}_{g(\mathbf{U})\leq 0}\, \phi^{\mathbf{e}}(\mathbf{u})\mathrm{d}\mathbf{u} \tag{4.5}$$

$$\simeq \frac{1}{M}\sum_{k=1}^{M} \mathbb{1}_{g\left(\mathbf{u}_{(k)}[\phi^{\mathbf{e}}]\right)\leq 0} \tag{4.6}$$

with $\mathbf{u}_{(k)}[\phi^{\mathbf{e}}]$, $k \in \{1,\ldots,M\}$ samples generated with $\phi^{\mathbf{e}}(\cdot)$. The variation of $\mathbf{e}$ generates an ensemble of CDFs (also called p-box [Ferson et al., 2002]) (Fig. 4.3).

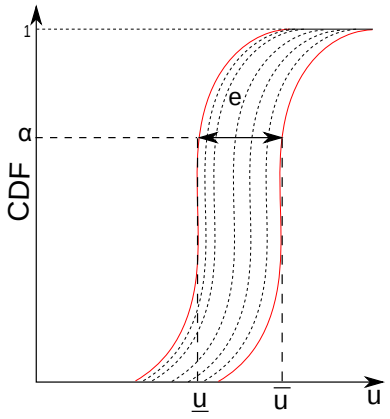

Figure 4.3: Probability boxes

The interval CMC method assumes that the epistemic variables may take different values depending on the aleatory uncertainty. In this approach, for each aleatory uncertainty CMC sample, the upper and lower values of the constraints $g(\cdot)$ are determined by an optimization problem to find the corresponding $\mathbf{e}$. Then, the maximal and minimal values of $g(\cdot)$ for each CMC sample are used to compute the lower and upper probability bounds by CMC. This method allows to handle interval uncertainty in the parameters of input joint PDF. However, it aggregates in the probability bounds calculation aleatory realization sampled from different epistemic parameter values. Moreover, the computational cost engendered by interval analysis for each CMC sample is large. This method has been applied with interval Finite Element Method in structural reliability to take advantage of interval method dedicated to structural responses within Finite Element analyses [Zhang et al., 2010]. This approach has also been extended to IS [Zhang, 2012] in which the auxiliary density is centered on the MPP. In order to decrease the computational cost, FORM method has been adapted to the presence of interval uncertainty in reliability analysis. In [Qiu et al., 2008] the authors modified FORM based on interval arithmetic to handle interval uncertainty on the expected value and standard deviation of the input joint PDF. Hurtado [Hurtado, 2013] developed a new method based on the technique of reliability plot.

4.4 Epistemic uncertainty affecting the limit state function

4.4.1 Problem statement

Let consider a d-dimensional random vector $\mathbf{U}$ defined on the sample space $\mathbf{\Omega}$ by a joint PDF $\phi(\cdot)$ and a w-dimensional vector $\mathbf{e} = [e^{(1)}, \ldots, e^{(w)}] \in \mathbb{R}^w$. $\mathbf{e}$ represents epistemic uncertainties defined using intervals: $\mathbf{e} \in \mathbf{\Upsilon} = \{\mathbf{e} \in \mathbb{R}^w | \ e^{(i)} \in [e^{(i)}_{\min}, e^{(i)}_{\max}] \ \forall i \in \{1, \ldots, w\}\}$. $g : \mathbf{\Omega} \times \mathbf{\Upsilon} \to \mathbb{R}$ is deterministic a scalar continuous input-output function. The reliability analysis of the system consists in determining its probability of failure defined as $\mathbb{P}(g(\mathbf{U}, \mathbf{e}) \leq 0)$. To characterize the probability of failure, it is possible to determine its domain of variation by finding the lower and upper bounds:

$$\begin{cases} \mathbb{P}_{\min} = \min\limits_{\mathbf{e} \in \mathbf{\Upsilon}} \ \mathbb{P}(g(\mathbf{U}, \mathbf{e}) \leq 0) \\ \mathbb{P}_{\max} = \max\limits_{\mathbf{e} \in \mathbf{\Upsilon}} \ \mathbb{P}(g(\mathbf{U}, \mathbf{e}) \leq 0) \end{cases} \tag{4.7}$$

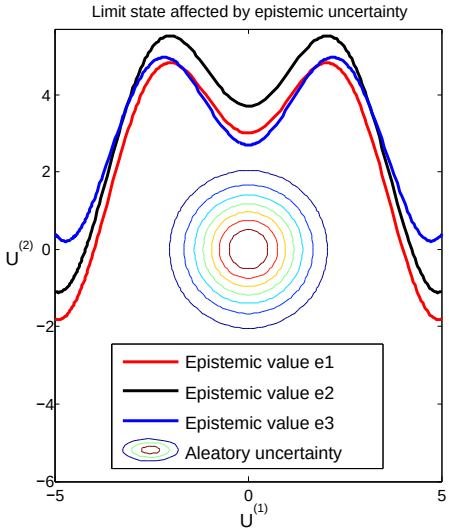

Figure 4.4: Limit state affected by epistemic uncertainty

This problem is different from the previous one because the epistemic uncertainty does not affect the input joint PDF but it affects directly the limit state function $g(\cdot)$ (Fig. 4.4). Dedicated methods based on sampling approaches or FORM have been proposed and are presented in the next section.

4.4.2 Existing methods

As in the previous section, reliability assessment in the presence of mixed uncertainties involves a two layer nested IA and PA processes. Since the solving of Eqs.(4.7) needs many optimization iterations and each iteration requires several limit state evaluations, the total number of discipline evaluations is very high [Du et al., 2005]. To avoid this nested process, Du *et al.* [Du et al., 2005;

Du, 2008] proposed a sequential approach named FORM-UUA (First Order Reliability Method - Unified Uncertainty Analysis). The flowchart of FORM-UUA is represented in Figure 4.5. The two solved optimization problems are:

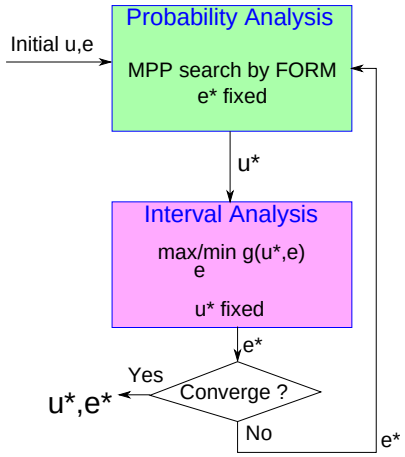

Figure 4.5: Flowchart of FORM-UUA method [Du, 2008]

Probability Analysis

$$\begin{aligned} \text{given} \quad & \mathbf{e}^* && (4.8)\\ \min \quad & \| \mathbf{u} \| && (4.9)\\ \text{w.r.t.} \quad & \mathbf{u} \\ \text{s.t.} \quad & \mathbf{g}(\mathbf{u}, \mathbf{e}^*) = 0 && (4.10)\\ & && (4.11) \end{aligned}$$

Interval Analysis

$$\begin{aligned} \text{given} \quad & \mathbf{u}^* && (4.12)\\ \max/\min \quad & g(\mathbf{u}^*, \mathbf{e}) && (4.13)\\ \text{w.r.t.} \quad & \mathbf{e} \in \boldsymbol{\Upsilon} \\ & && (4.14) \end{aligned}$$

The sequential approach consists of a sequence of PA with the epistemic uncertainty being fixed and IA with the aleatory uncertainty fixed at the MPP (Figure 4.5). However, as this approach relies on FORM for the reliability analysis, it does not handle multiple failure regions or non linear limit state function. Methods have been developed to locally linearize $g(\cdot)$ by CMC rather than by a first order Taylor series expansion at the MPP [Xiao et al., 2011] or to use a restarted FORM approach in case of multiple failure regions [Jiang et al., 2012]. FORM-UUA has been extended [Yao et al., 2013] with general optimization solvers to find the MPP.

A recent method [Yang et al., 2014] based on CMC and Kriging surrogate model has been developed in case of the presence of aleatory and epistemic uncertainties but not restricted to the hyper-parameters. It relies on a nested procedure with IA and PA which first needs the construction of a Kriging model to replace the exact limit state function. In order to have an accurate Kriging surrogate model in the vicinity of the threshold, the authors developed a refinement strategy inspired from the Expected Improvement function [Jones et al., 1998]. The refinement is performed on the entire epistemic uncertain space. The method allows one to take into account both aleatory and epistemic uncertainties. However, the definition of the probability bounds is different and it results in a different system of optimization problem.

$$\begin{cases} \mathbb{P}_{\min} = \mathbb{P}\left(\min\limits_{\mathbf{e}\in\boldsymbol{\Upsilon}} \ (g(\mathbf{U},\mathbf{e}) \leq 0)\right) \\ \mathbb{P}_{\max} = \mathbb{P}\left(\max\limits_{\mathbf{e}\in\boldsymbol{\Upsilon}} \ (g(\mathbf{U},\mathbf{e}) \leq 0)\right) \end{cases} \tag{4.15}$$

In this definition, it is assumed that the epsitemic variables may take different values depending on the aleatory uncertainty. This is not the case in the problem that we are considering.

4.5 Conclusion

In this chapter, reliability analysis methods involved in the design of complex systems in the presence of mixed aleatory/epistemic uncertainties within the UMDO context have been reviewed. To estimate failure probability in this context, existing techniques based on CMC and FORM have been described in this chapter. These methods have the advantage to be easily implementable. CMC is adaptable to any type of failure probability estimation problem but induces a computational cost that is not tractable for rare events. On the other hand, FORM based methods are computationally efficient but are limited to problem in which the limit state involves only one failure region which can be linearly approximated.
In addition to reliability analysis, to resolve the different UMDO formulations introduced in section 3.2, an optimization algorithm is needed. The latter should be able to optimize functions in the presence of noise (coming from the approximation of the uncertainty measure in the objective function or the constraints) under constraints. Several optimization algorithms have been proposed and have to be described in order to comprehend all the aspects involved in an UMDO problem. This is the purpose of chapter 5.

Chapter 5

Numerical optimization of noisy functions with constraint handling

Contents

Chapter goals

- Describe the main optimization algorithms dealing with the presence of uncertainty and constraints in the optimization problem solving,
- Highlight the advantages and drawbacks of each algorithm,
- Assess some possible ways of improvement based on the state of the art presented in part I

5.1 Introduction

This chapter is dedicated to the presentation of the optimization algorithms used to solve UMDO problems. In order to find the optimal solution, optimization algorithms are required and should have at least two features. First, they have to be efficient despite the presence of uncertainty. Indeed, uncertainty measure estimators (such as CMC, IS, *etc.*) are needed to compute the objective function and the constraints. These estimators are often random variables and introduce noise in the optimization problem. Secondly, UMDO problems often involve constraints to ensure the system multidisciplinary feasibility and the respect of the designer requirements. UMDO for complex systems needs nonlinear constrained optimization algorithms. The determination of the optimal system architecture requires a global exploration of the design space involving repeated evaluations of computationally expensive black box functions used to model the different disciplines. Let consider the following UMDO problem:

$$\begin{aligned}
\min \quad & \Xi\left[f(\mathbf{z}, \boldsymbol{\theta}_{\boldsymbol{Y}}, \mathbf{U})\right] && (5.1)\\
\text{w.r.t.} \quad & \mathbf{z}, \boldsymbol{\theta}_{\boldsymbol{Y}} && \\
\text{s.t.} \quad & \mathbb{K}\left[\mathbf{g}(\mathbf{z}, \boldsymbol{\theta}_{\boldsymbol{Y}}, \mathbf{U}) \leq 0\right] \leq 0 && (5.2)\\
& \forall i \neq j, \forall \mathbf{u} \in \boldsymbol{\Omega},\ \mathbf{y}_{ij}(\boldsymbol{\theta}_{\boldsymbol{Y}ij}, \mathbf{u}_i) = \mathbf{c}_{ij}(\mathbf{z}_i, \mathbf{y}_{.i}(\boldsymbol{\theta}_{\boldsymbol{Y}.i}, \mathbf{u}_{.i}), \mathbf{u}_i) && (5.3)\\
& \mathbf{z}_{\min} \leq \mathbf{z} \leq \mathbf{z}_{\max} && (5.4)
\end{aligned}$$

Solving this optimization problem is challenging due to the presence of both the uncertainty and the constraints. An overview of the existing algorithms used to solve this type of problems is provided in this chapter. In section 5.2, the most commonly used methods to handle noise in optimization are presented. Deterministic optimization algorithms based on gradient cannot be directly implement for such problems. Indeed, the presence of uncertainty makes difficult the accurate estimation of the gradient used to converge to the optimal solutions. Solutions have been proposed to adapt gradient based algorithms to the presence of noise and are presented in section 5.3. Alternatives in the presence of uncertainty are the population-based algorithms which are based on a population of individuals for which the objective function is evaluated. Based on their values, the individuals are ranked and the population is accordingly modified in order to converge to the optimal solution. Population-based algorithms are interesting because of their ability to handle uncertain environment [Hansen et al., 2003; Jin and Branke, 2005]. Two population-based algorithms are presented: the ant colony algorithm (section 5.4) and the Covariance Matrix Adaptation - Evolution Strategy algorithm (section 5.5) as they present advantages within the context of constrained optimization in the presence of noise. Moreover, these two algorithms are detailed as they will be either used or modified in the following of the thesis.

5.2 Noise handling in optimization algorithms

The presence of noise in the optimization problem results from the estimation of the measures of uncertainty (Ξ and $\mathbb{K}$). In order to numerically handle the presence of noise in optimization, several general approaches have been proposed:

- Re-sampling [Branke and Schmidt, 2003; Jin and Branke, 2005]: the re-sampling method consists of repeated evaluations of the objective and the constraint uncertainty measures for

the same design variable value $\mathbf{z}$. Then, a statistics of the repeated samples is used instead of the single evaluation of the objective and the constraint measures to decrease the impact of noise. The main drawback of this approach is the increase of the computational cost due to the repeated evaluations of objective and constraint functions.

- Surrogate model [Branke and Schmidt, 2003; Jin, 2005]: surrogate models of the objective function measure Ξ (and/or the constraint measures $\mathbb{K}$) are built from several evaluations. In general, surrogates smooth the noisy functions and decrease the impact of uncertainty in the optimization. A comprehensive review of the use of surrogate model in optimization is proposed in [Jin, 2005]. The main drawback lies in the difficulty to build accurate surrogate models in high dimensions and for highly non linear functions.

- Population-based algorithms [Nissen and Propach, 1998; Hansen et al., 2003; Jin and Branke, 2005]: to address uncertainty, optimization algorithms relying on a population of candidates allow to increase the size of the population to enlarge its spread and to obtain more information and smooth the noise. Because in population-based algorithms there are usually similar solutions in the population, the influence of noise in evaluating an individual is compensated by other similar individuals. This effect may be view as an *implicit averaging*. For instance, the size of a population for genetic algorithms has been studied in [Rattray and Shapiro, 1998] and it has been shown that increasing the population size reduces the effects of noise. The main drawback of population-based algorithms is the computational cost induced by the number of function evaluations which is often important with such algorithms to converge.

Moreover, another way to directly take into account the presence of noise and the constraints in optimization is to modify the deterministic gradient-based algorithms. Several adaptations have been proposed and a stochastic gradient algorithm is briefly presented in the following paragraph.

5.3 Stochastic gradient algorithms

The most used gradient-based algorithm suited for noise handling is the stochastic gradient descent algorithm [Kiefer et al., 1952; Gardner, 1984]. It is a descent algorithm combined with a Lagrangian approach to handle the constraints. Descent-based algorithms are efficient for deterministic convex optimization problems and are essentially based on the gradient estimation. In the presence of uncertainty, the estimation of the gradient by finite difference is not accurate enough to be used. Indeed, the gradients of the objective function or the constraint functions are noisy resulting in possible erroneous descent directions. An adaptation [Andrieu et al., 2007] of the Arrow-Hurwicz algorithm [Arrow et al., 1958] has been proposed to optimize an objective function under constraints in a noisy environment. Instead of computing $\Xi[f(\cdot)]$ and $\mathbb{K}[g(\cdot)]$, at each optimization iteration, the gradient estimation of the objective and the constraint functions is done for only one realization of the uncertain variables $\mathbf{u}_{(k)}$. The iterative equations in $\mathbf{z}$ of Arrow-Hurwicz method are modified to include the presence of uncertainty. The step size $\epsilon^{[k]}$ between two iterations has to follow the Robbins Monroe [Culioli and Cohen, 1995] conditions to ensure the convergence to the optimum:

$$\sum_{k\in\mathbb{N}} \epsilon^{[k]} = +\infty, \quad \sum_{k\in\mathbb{N}} \left(\epsilon^{[k]}\right)^2 < +\infty \tag{5.5}$$

The same conditions have to be imposed for the step size associated to the Lagrangian multipliers. The Robbins Monroe conditions on the step size ensure that the gradient estimation of the augmented Lagrangian objective using only one realization of the uncertain variable is asymptotically unbiased. The interest for this algorithm results from its facility of implementation because it is close to the deterministic version. Moreover, due to the Robbins Monroe conditions, only few parameters are needed to tune the algorithm. However, this approach requires some hypothesis such as the capability to project candidate solution on the feasible space which is most of the time unknown.

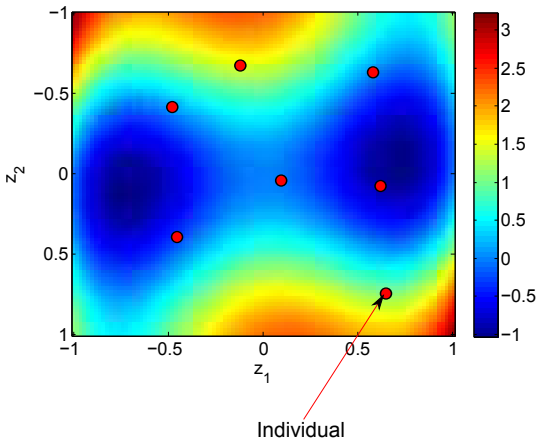

Figure 5.1: Population based algorithm example

Diverse derivative-free algorithms have been proposed in the literature to solve optimization under uncertainty problems [Larson, 2012]. These algorithms may present some interest in MDO because industrial simulations and disciplines may not have been developed to provide sensitivity information along with their evaluations. These algorithms handle non differentiable functions whereas gradient-based methods require appropriate differentiability and smoothness conditions. Among the derivative-free algorithms, the population based optimization algorithms (Fig. 5.1) seem promising [De Melo and Iacca, 2014]. Swarm Intelligence (Particle Swarm Optimization [Eberhart and Kennedy, 1995], Artificial Bee Colonies [Karaboga, 2005], Ant Colony [Dorigo and Birattari, 2010] *etc.*), Differential Evolution [Price et al., 2006], Evolutionary Algorithms (Genetic Algorithm [Holland, 1975]), Auto-adaptative Multi-Agent System [Jaeger et al., 2015] or Evolution Strategies (Covariance Matrix Adaptation - Evolution Strategy [Hansen et al., 2003]) have been investigated to solve noisy optimization problems. In the next sections, two of them are presented: the Ant Colony Optimization (ACO) and the Covariance Matrix Adaptation - Evolution Strategy (CMA-ES) as they will be latter used in the thesis (chapters 8, 12, 13). These two algorithms have been selected because CMA-ES present good convergence in the presence of noise as illustrated in several papers [Hansen, 2009; Auger and Hansen, 2009] and it has been used within the context of launch vehicle design [Breitkopf and Coelho, 2013]. Moreover, an academic benchmark of constrained optimization problem under uncertainty at the beginning of the thesis illustrated the efficiency of ACO and CMA-ES) algorithms available at Onera.

5.4 Ant colony optimization algorithms

Ant Colony Optimization (ACO) [Corne et al., 1999; Dorigo and Birattari, 2010] is inspired from the food research by biological ants and the pheromone trails used as a communication means. Biological ants first explore randomly the regions around their nest to find food. If an ant discovers a food source, it will come back to the nest laying down a chemical pheromone in order to mark the followed path. By the means of pheromone, this trail will attract other ants to use it to find food again. If the paths found by the ants are not used, over time the pheromones start to evaporate reducing the interest of these tracks. On the other hand, the paths frequently used are updated with new pheromones and remained attractive to the other ants. The most attractive trails are the ones with the shortest distance between the food and the nest. As a final result, a very short path will be discovered by the ant colony. This biological analogy inspired ACO algorithms. They are based on indirect communication between a colony of artificial ants through artificial pheromone trails. These latter are used to distribute and exchange information between the colony to stochastically find an optimal solution.

Each ant of the colony evolves along a path to find the optimal solution. Although each ant is a simple element, a colony is able to perform complex tasks. Considering the j^{th} ant a^j of the colony, it moves through intermediate solutions. At each algorithm iteration, each ant moves from an intermediate solution $\mathbf{z}^{[k]}$ to $\mathbf{z}^{[k+1]}$. At iteration $[k]$, the ant a^j defines a set of feasible new positions $\mathcal{Z}^{[j]}$ from $\mathbf{z}_{a^j}^{[k]}$ and goes to one of these according to a certain probability. The probability $\mathbb{P}_{\mathbf{z}_{a^j}^{[k]} \to \mathbf{z}_{a^j}^{[k+1]}}$ of moving from $\mathbf{z}_{a^j}^{[k]}$ to $\mathbf{z}_{a^j}^{[k+1]}$ for the ant a^j depends on the attractiveness of the displacement noted $\tau_{\mathbf{z}_{a^j}^{[k]} \to \mathbf{z}_{a^j}^{[k+1]}}$ and the pheromone deposit $\pi_{\mathbf{z}_{a^j}^{[k]} \to \mathbf{z}_{a^j}^{[k+1]}}$ reflecting the efficiency of this move in the past which corresponds to the amount of pheromone deposited for this transition. The probability may be calculated by:

$$\mathbb{P}_{\mathbf{z}_{a^j}^{[k]} \to \mathbf{z}_{a^j}^{[k+1]}} = \frac{\left(\tau_{\mathbf{z}_{a^j}^{[k]} \to \mathbf{z}_{a^j}^{[k+1]}}\right)^{\alpha} \left(\pi_{\mathbf{z}_{a^j}^{[k]} \to \mathbf{z}_{a^j}^{[k+1]}}\right)^{\beta}}{\sum_{\mathbf{z}_{a^j}^{[k+1]} \in \mathcal{Z}_j} \left(\tau_{\mathbf{z}_{a^j}^{[k]} \to \mathbf{z}_{a^j}^{[k+1]}}\right)^{\alpha} \left(\pi_{\mathbf{z}_{a^j}^{[k]} \to \mathbf{z}_{a^j}^{[k+1]}}\right)^{\beta}} \tag{5.6}$$

where $\alpha \geq 0$ and $\beta \geq 1$ are user-defined weight parameters and $\tau_{\mathbf{z}_{a^j}^{[k]} \to \mathbf{z}_{a^j}^{[k+1]}}$ is a function of the distance between the two positions.

Once all the ants have moved to a new intermediate solution, the trails are updated by:

$$\pi_{\mathbf{z}^{[k]} \to \mathbf{z}^{[k+1]}} \leftarrow (1-\eta)\pi_{\mathbf{z}^{[k]} \to \mathbf{z}^{[k+1]}} + \sum_{j=1}^{N_{\text{ant}}} \Delta\pi_{\mathbf{z}_{a^j}^{[k]} \to \mathbf{z}_{a^j}^{[k+1]}} \tag{5.7}$$

with η the coefficient of pheromone evaporation and N_{ant} the number of ants in the colony. More complex expressions of pheromone evaporation or modification (named daemon actions) are possible [Dorigo and Birattari, 2010]. $\Delta\pi_{\mathbf{z}_{a^j}^{[k]} \to \mathbf{z}_{a^j}^{[k+1]}}$ represents the sum of the contributions of all ants that used the displacement $\mathbf{z}_{a^j}[k] \to \mathbf{z}_{a^j}^{[k+1]}$ to construct their intermediate solution:

$$\Delta\pi_{\mathbf{z}_{a^j}^{[k]} \to \mathbf{z}_{a^j}^{[k+1]}} = \begin{cases} \frac{Q}{L_j} & \text{if the ant } a^j \text{ has used this displacement at iteration } [k] \\ 0 & \text{otherwise} \end{cases} \tag{5.8}$$

where L_j is the length covered by a^j and Q is a tuned parameter. ACO algorithms differ in the way the pheromone update is implemented [Dorigo and Birattari, 2010]. At the beginning, ACO has been developed for combinatorial discrete optimization problems but it has been extended to continuous optimization problems [Socha and Dorigo, 2008].
One of the current issues with the derivative-free algorithms is the constraint handling which relies mainly on heuristic approaches and is problem dependent [Mezura-Montes and Coello, 2011]. A comprehensive overview of constraint handling in derivative-free algorithms is presented in the survey [Mezura-Montes and Coello, 2011]. The most commonly applied methods to handle the constraints are:

- Death penalty [Schwefel and Rudolph, 1995]: it is the simplest method to handle constraints. The solution that does not satisfy the constraints is rejected and another potential solution is re-evaluated until one candidate solution satisfies the constraints. The advantage of the approach is that it does not modify the optimization algorithm. The method is very expensive because no information is learned from an unfeasible solution (a solution which does not satisfy the constraints) to characterize the non feasible space. Furthermore, if the feasible space is restricted compared to the design space, the computational cost becomes prohibitive because a high number of samples has to be generated to obtain feasible solutions.

- Penalization [Collange et al., 2010b; De Melo and Iacca, 2014]: this approach consists in replacing the objective function $\Xi[f(\cdot)]$ by a combination of the objective function and a penalization function Π such as: $\Xi[f(\cdot)] + \Pi(\mathbb{K}[\mathbf{g}(\cdot)])$. The penalization function may be fixed or may change as a function of the number of iterations. When a solution violates the constraints, the objective function is deteriorated by a factor proportional to the penalization function and the value of the constraints. Despite its simplicity, the main drawback of this approach lies in the determination of a suitable penalization function which depends on the objective function and the constraints and is thus problem dependent.

A new penalization, called Oracle Penalization approach [Schlüter and Gerdts, 2010] has been proposed to be coupled with ACO and stochastic metaheuristics algorithms such as Particle Swarm Optimization [Eberhart and Kennedy, 1995] or Genetic Algorithms [Holland, 1975]. The method is an advanced approach that only requires one parameter to be tuned. Oracle penalization transforms the optimization problem by modifying the objective function and adding a new constraint, $|\Xi[f(\cdot)] - \Theta| = 0$, depending on the objective function and an oracle parameter Θ. The oracle parameter is supposed to be the optimal objective function value. Dynamic weight factors balance the penalty function value in respect to the relationship between the new constraint and original ones. Moreover, in the proposed approach it is not necessary to know the value of the optimal objective function. Only two conditions have to be followed by the oracle parameter, it as to be superior or equal to the optimal objective function value and at least one feasible solution exist.

- Multi-objective [Coello, 2000]: this method transforms the optimization problem into a multi-objective optimization problem by considering the minimization of the violation of the constraints as an objective. Dedicated multi-objective optimization algorithms may be used, however, it often results in an increase of the computational cost [Mezura-Montes and Coello, 2011].

- Surrogate model [Kramer et al., 2009]: this approach builds a surrogate model based on the unfeasible solutions in order to approximate the non feasible zones. However, this approach

requires enough unfeasible solutions to construct accurate surrogate models. Moreover, it may be difficult to build the surrogates in high dimension or if the constraints are highly non linear.

A review of the method to handle noisy optimization with ACO is proposed in [Bianchi et al., 2009]. Re-sampling based methods have been proposed for ACO [Gutjahr, 2003, 2004; Birattari et al., 2005] in order to numerically handle the presence of a high level of noise. Moreover, due to the population-based strategy and the aggregation of information from different candidates, the ACO algorithms are robust to the presence of uncertainty.

Among the derivative-free algorithms, the Covariance Matrix Adaptation - Evolution Strategy (CMA-ES) [Hansen et al., 2003] is particularly competitive for real-valued black-box functions as highlighted in several extensive benchmarks [Hansen, 2009; Hansen et al., 2010]. Moreover, a treatment of uncertainty has been proposed for CMA-ES and has been successfully tested in a benchmark of optimization under uncertainty problems [Hansen, 2009]. CMA-ES is detailed in the following section.

5.5 Covariance Matrix Adaptation - Evolution Strategy

5.5.1 CMA-ES(λ, μ) algorithm

The Covariance Matrix Adaptation - Evolution Strategy (CMA-ES) introduced by Hansen *et. al.* [Hansen et al., 2003] belongs to the Evolutionary Strategy algorithm family. A brief overview of CMA-ES(λ, μ) is provided in this section, for more information on the algorithm see [Hansen et al., 2003]. CMA-ES(λ, μ) is used to solve unconstrained optimization problems. It relies on a distribution model of a candidate population (parametrized multivariate normal distribution) in order to explore the design space. It is based on a selection and an adaptation process of the candidate population. In CMA-ES(λ, μ), at each generation, λ offspring candidates are generated from μ parents. At the next generation, to select the new parents from the offspring candidates, a (λ, μ)-selection is used, the μ best offspring candidates are chosen with respect to their ranking according to the objective function. The multivariate normal distribution has an infinite support, but an iso-probability contour (for instance at ± 3 standard deviation of the mean) is characterized by an ellipsoid delimiting a probable search hypervolume (Fig. 18.8). Throughout the generations, the search hypervolume is updated in order to converge and to shrink around the global optimum. CMA-ES(λ, μ) generates the population by sampling a multivariate normal distribution:

$$\mathbf{z}_t^{[k+1]} \sim \mathbf{m}^{[k]} + \sigma^{[k]} \mathcal{N}\left(0, \mathbf{C}^{[k]}\right), \text{ for } t = 1, ..., \lambda \tag{5.9}$$

with $\mathbf{z}_t^{[k+1]} \in \mathbb{R}^n$ an offspring candidate generated from a mean vector $\mathbf{m}^{[k]}$, a step size $\sigma^{[k]}$ and a multivariate normal distribution $\mathcal{N}(0, \mathbf{C}^{[k]})$ with zero mean and a covariance matrix $\mathbf{C}^{[k]} \in \mathbb{R}^n \times \mathbb{R}^n$. λ is the size of the population generated at each iteration $[k]$. The normal distribution is characterized by a positive definite covariance matrix $\mathbf{C}^{[k]}$ in order to allow homothetic transformations and rotations of the probable search hypervolume (Fig. 18.8). The update of the covariance matrix incorporates dependence between the past generations and between the μ best candidates from the previous generation [Hansen et al., 2003]. The mean vector characterizes the center of the next population and is determined by a combination process through the weighting of the μ best

candidates: $\mathbf{m}^{[k+1]} = \sum_{i=1}^{\mu} w_i \mathbf{z}_{\{i\}}^{[k+1]}$ with $\sum_{i=1}^{\mu} w_i = 1$, $w_1 > w_2 > \cdots > w_\mu > 0$ the weighting coefficients and $(\mathbf{z}_{\{1\}}, ..., \mathbf{z}_{\{\mu\}})$ the best candidates among the offspring ranked according to the objective function value. The weighting coefficients are determined based on the number of μ best candidates according to [Hansen et al., 2003]. A simplified version of CMA-ES(λ, μ) is described in Algorithm 2. A detailed description of the selection and update mechanisms may be found in [Hansen et al., 2003].

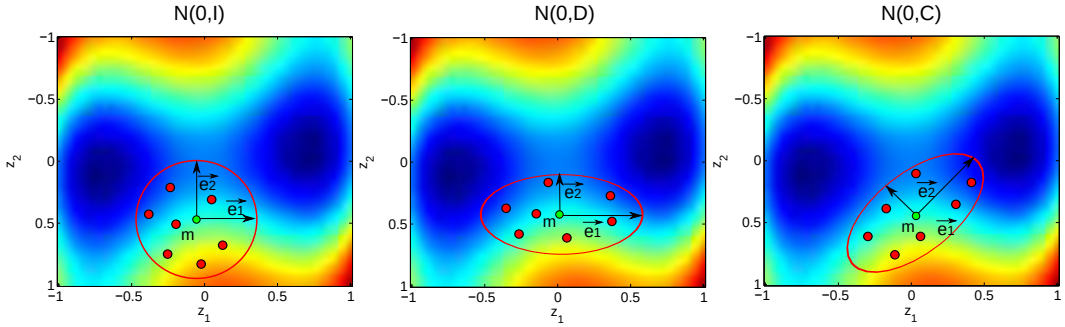

Figure 5.2: Three ellipsoids, depicting three different normal distributions, where $\mathbf{I}$ is the identity matrix, $\mathbf{D}$ is a diagonal matrix, and $\mathbf{C}$ is a positive definite covariance matrix.

Algorithm 2 CMA-ES(λ, μ) [Hansen et al., 2003]

1) Initialize the covariance matrix $\mathbf{C}^{[0]} = \mathbf{I}$, the step size $\sigma^{[0]}$ and the selection parameters [Hansen et al., 2003]
2) Initialize the mean vector $\mathbf{m}^{[0]}$ to a random candidate, $k \leftarrow 0$
while CMA-ES convergence criterion is not reached **do**
  3-1) Generate λ new offspring candidates according to: $\mathbf{z}_t^{[k+1]} \sim \mathbf{m}^{[k]} + \sigma^{[k]} \mathcal{N}(0, \mathbf{C}^{[k]})$, $t \in \{1, ..., \lambda\}$
  3-2) Evaluate candidates and rank them based on the objective function
  3-3) Determine the mean vector given the weighting coefficients of the μ best candidates: $\mathbf{m}^{[k+1]} = \sum_{i=1}^{\mu} w_i \mathbf{z}_{\{i\}}^{[k+1]}$
  3-4) Update covariance matrix $\mathbf{C}^{[k+1]}$ and the step size $\sigma^{[k+1]}$ according to [Hansen et al., 2003], $k \leftarrow k + 1$
end while
4) **return** best candidate $\mathbf{z_{best}}$

CMA-ES has already been used to design launch vehicles[Breitkopf and Coelho, 2013] with an MDF formulation. The convergence criteria may be either based on the maximum number of iterations (function evaluations), the objective function value, the standard deviation of the current population smaller than a given tolerance, or the covariance matrix $\mathbf{C}$ which becomes numerically not positive definite. ACO and CMA-ES algorithms are able to handle optimization problem with up to 30 design variables, based on the implemented benchmark used to select the algorithms in this thesis, but the solving of the optimization problem become complex. Indeed, the convergence rate

is small for high dimensional problems and they require in the order of ten thousand to hundred thousand calls to the functions to converge.

5.5.2 CMA-ES(λ, μ) algorithm for optimization under uncertainty

Several features ensure the CMA-ES robustness with respect to the presence of uncertainty in the objective function: the population-based approach, the weighted averaging in the recombination process avoiding information for one noisy source, the rank based and the non-elitist selection which is not based on the best offspring candidate that could be an outlier. However, if the noise is too high compared to the objective function (signal to noise ratio too low) it perturbs the algorithm convergence. An appropriate handling of uncertainty has been proposed by Hansen *et. al.* [Hansen et al., 2009] to overcome this issue. Modified selection and update mechanisms are performed when the noise is above a given threshold. It is based on a re-sampling approach and involves re-evaluation of the objective function. Because CMA-ES(λ, μ) is only based on the rank of the candidates, the effective noise is evaluated by monitoring changes or stability of the offspring candidate ranking. If the offspring candidate ranking is changed after the re-evaluation of the objective function, the ranking change of the offspring candidates is aggregated into a metric quantifying the uncertainty level [Hansen et al., 2009]. If the noise is higher than a given uncertainty level threshold, the step size σ is increased. The increase of σ ensures that despite the noise, sufficient selection information is available [Hansen et al., 2009].
A benchmark of algorithms dealing with optimization under uncertainty has been performed and the treatment of uncertainty with CMA-ES(λ, μ) allows to obtain accurate results [Hansen, 2009; Auger and Hansen, 2009]. CMA-ES is an unconstrained optimization algorithm. The test problems used in the benchmark [Hansen, 2009] to evaluate the performance of CMA-ES are unconstrained optimization problems and only few studies focus on the application of CMA-ES to constrained problems [Collange et al., 2010b; Beyer and Finck, 2012; De Melo and Iacca, 2014]. An adaptive penalty function has been proposed to update the penalty coefficient as a function of the sum of the violated constraint values [De Melo and Iacca, 2014]. CMA-ES(λ, μ) algorithm has been used [Collange et al., 2010a,b] to solve a deterministic MDO problem consisting in the design of a launch vehicle. CMA-ES(λ, μ) has been combined with a penalization method in this study. The algorithm presented efficient results however a feasible solution was not always found depending on the initialization. CMA-ES is a promising algorithm for UMDO problem solving but its main drawback concerns the constraint handling strategy. Arnold *et. al.*[Arnold and Hansen, 2012] proposed a new approach to handle the constraints for a simplified version of CMA-ES: (1+1)-CMA-ES which involves one offspring candidate generated from one parent and is detailed in the next section.

5.5.3 (1+1)-CMA-ES with constraint handling

(1+1)-CMA-ES [Arnold and Hansen, 2012] is a simplified version of CMA-ES(λ, μ) with only one offspring generated from one parent, $''+''$ means that the selection is done between the parent and the offspring. As in CMA-ES(λ, μ), the offspring candidate solution is generated as:

$$\mathbf{z}^{[k+1]} \sim \mathbf{z}^{[k]} + \sigma^{[k]} \mathcal{N}\left(0, \mathbf{C}^{[k]}\right) \tag{5.10}$$

(1+1)-CMA-ES is easier to implement as only one offspring $\mathbf{z}^{[k+1]}$ is generated from one parent $\mathbf{z}^{[k]}$ at each generation and the selection is between the parent and the offspring. The update mechanisms for (1+1)-CMA-ES are detailed in [Arnold and Hansen, 2012].

To incorporate the handling of constraints, Arnold *et. al.* [Arnold and Hansen, 2012] proposed to reduce the covariance of the distribution of the offspring candidate in the approximated directions of the normal vectors of the constraint boundaries in the vicinity of the current parent candidate solution. For that purpose, the matrix $\mathbf{A}^{[k]}$, which is the Cholesky decomposition of $\mathbf{C}^{[k]}$: $\mathbf{A}^{(k)}\mathbf{A}^{[k]^T} = \mathbf{C}^{[k]}$, is updated in case of constraint violations in order to avoid generating candidates in the next generations that will violate the constraints. $\mathbf{A}^{[k]}$ is used as it is easier to compute its inverse than for $\mathbf{C}^{[k]}$. A vector characterizing the constraints $\mathbf{v}_j^{[k]} \in \mathbb{R}^n$ is defined, initialized to be zero, and updated according to:

$$\mathbf{v}_j^{[k]} \leftarrow (1 - c_c)\mathbf{v}_j^{(k)} + c_c\mathbf{A}^{[k]}\mathbf{z}^{[k]} \; \forall j \in \{1, ..., \kappa\} \tag{5.11}$$

where $\mathbf{v}_j^{[k]}$ is an exponentially fading record of steps that have violated the constraints and c_c a parameter characterizing how fast the information present in $\mathbf{v}_j^{[k]}$ fades. In the generations in which the offspring candidate is unfeasible, the Cholesky matrix is updated according to:

$$\mathbf{A}^{[k]} \leftarrow \mathbf{A}^{[k]} - \frac{\beta}{\sum_{j=1}^{\kappa} \mathbb{1}_{g_j(\mathbf{z}^{[k]})>0}} \sum_{j=1}^{\kappa} \mathbb{1}_{g_j(\mathbf{z}^{[k]})>0} \frac{\mathbf{v}_j^{[k]}\mathbf{w}_j^{[k]^T}}{\mathbf{w}_j^{[k]^T}\mathbf{w}_j^{[k]}} \tag{5.12}$$

with $\mathbf{w}_j^{[k]} = \mathbf{A}^{[k]^{-1}}\mathbf{v}_j^{[k]}$, the indicator function associated to the constraint g_j: $\mathbb{1}_{g_j(\mathbf{z}^{[k]})>0}$ and β a parameter controlling the reduction of the covariance of the distribution. For $\beta = 0$, the algorithm is identical to the standard (1+1)-CMA-ES. The update of the matrix $\mathbf{A}^{[k]}$ allows one to modify the

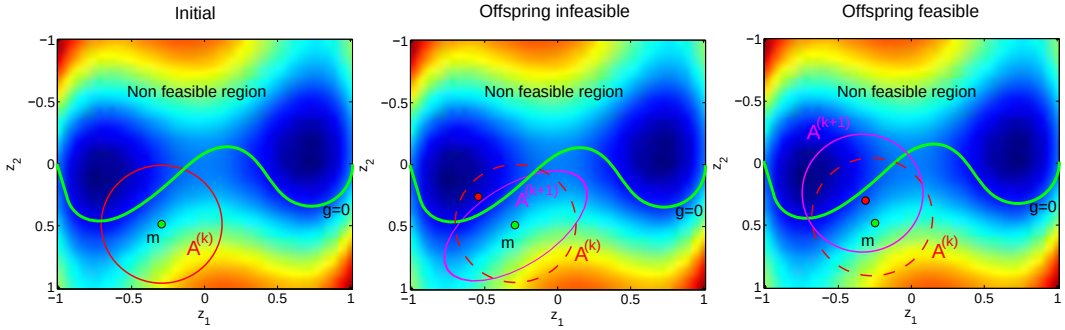

Figure 5.3: The green dot is the parent, the red dot is the generated offspring. On the left, the solid line circle is characterized by $\mathbf{A}^{[k]}$ defining the ellipsoid delimiting an iso-probability search hypervolume. At the center, the pink ellipsoid represents the update of $\mathbf{A}^{[k+1]}$ in order to take into account the constraint violation by the offspring. On the right figure, the offspring does not violate the constraint resulting in a standard covariance matrix update.

scale and the orientation of the search hypervolume in order to be tangential to the constraints and to avoid its violation (Fig. 5.3). Modified (1+1)-CMA-ES for constraint handling is interesting because it is not problem dependent. Experimental evaluations have been performed highlighting its efficiency for unimodal constrained optimization problems. However, as (1+1)-CMA-ES, it presents difficulties to optimize multimodal functions and becomes inefficient in high dimensions

[Arnold and Hansen, 2012].

It is important to notice that, in the presence of uncertainty, deterministic gradient-based algorithms are not adapted, however gradient-free approaches are not adapted to solve large dimensional optimization problems (40 variables or more) due to the induced computational cost. Stochastic-gradient based algorithms might be a good alternative for high dimensional problems. A summary of the advantages and drawbacks of the different algorithms is presented in Table 5.4.

Table 5.4: Advantages and drawbacks of the main optimization algorithms in the presence of uncertainty

	Advantages	Drawbacks
Stochastic gradient	Adapted to large scale problems	Convergence and constraint handling in the presence of uncertainty
ACO	Robustness to the presence of uncertainty	Constraint handling methods (penalization)
(1+1)-CMA-ES	Constraint handling technique	Limited to low dimension problems (<10)
CMA-ES	Robustness to the presence of uncertainty	Constraint handling methods (penalization)

5.6 Conclusion

In this chapter we have briefly described some algorithms used in the UMDO processes. The presence of uncertainty and of constraints complicate the solving of the optimization problem and dedicated methods have to be employed. Population-based algorithms such as Covariance Matrix Adaptation - Evolution Strategy algorithm seem particularly promising for UMDO problem solving but the constraint handling is not robust.
At the early design phase, launch vehicle design problems only involve macroscopic design variables (propellant masses, chamber pressures, *etc*) in dimension under 30. Moreover, these problems often present multiple optimal regions and deterministic gradient-based algorithms present some limits to find global optimum as illustrated in [Balesdent, 2011]. CMA-ES has been used to deterministically design launch vehicles in previous studies [Breitkopf and Coelho, 2013] and its efficiency in the presence of noise has been illustrated over several benchmarks [Hansen, 2009; Auger and Hansen, 2009], that is why, this algorithm is a good candidate for further investigations to solve UMDO problems in the presence of constraints and uncertainty.

5.7 General conclusion of part I and ways of improvement

In the light of this state-of-the-art presented in chapters 1 to 5, we may identify several ways of improvement relating to the use of UMDO methods. These ways of improvement instigate the proposed methods in the rest of the thesis to solve some of the current limitations highlighted in the state-of-the-art on the three main topics.

5.7.1 UMDO formulations and interdisciplinary coupling handling

Almost all the examples of launch vehicle designs with UMDO methods in literature rely on coupled approaches to ensure interdisciplinary coupling satisfaction. Decomposition strategies have been proposed, but the introduction of uncertainties require an adequate treatment of the coupling variables. The existing formulations either rely on computationally expensive MDA to rigorously ensure coupling satisfaction, or deal with incomplete coupling conditions (coupling in terms of statistical moments, at the MPP, *etc.*). To maintain the mathematical equivalence between coupled and decoupled strategies, it is necessary to ensure the interdisciplinary coupling satisfaction for all the realizations of the uncertain variables in the UMDO formulation. This kind of decomposition method could ensure the system multidisciplinary consistency whatever the uncertain event. Surrogate model of the functional coupling relations could be constructed during the optimization process in order to represent, at the UMDO problem convergence, the coupling relations as would do MDA.
Moreover, all the examples of the launch vehicle design problem under uncertainty in literature consider a subdivision into the disciplines such as propulsion, structure, trajectory, *etc.* Stage decomposition strategies have been proposed to solve deterministic MDO problem but are not adapted to handle uncertainty. A stage decomposition UMDO formulation for launch vehicle design could benefit from the same advantages as in deterministic MDO, that is introducing multi-level processes to facilitate the convergence of the system-level optimizer while decreasing the number of discipline evaluations by avoiding the disciplinary loops imposed by MDA-based formulations.
The proposed methods related to these thematics will be developed in Part II.

5.7.2 Reliability analysis for complex systems

Reliability analysis is one of the most important tasks in the solving of an UMDO problem and almost all the proposed approaches in literature are based on CMC or FORM which present some limitations for the design of complex systems. In particular the problematic of the presence of mixed aleatory/epistemic uncertainties seems interesting in the context of early design phases where modeling uncertainties are present. In order to handle both aleatory and epistemic uncertainties, dedicated reliability assessment methods are needed. Epistemic uncertainty may affect the aleatory uncertainty modeling or directly the limit state function. Moreover, launch vehicle design involves complex reliability analysis problem such as the determination of a safety zone for a stage fallout which often involves multiple failure regions and non linear limit states. To perform this type of reliability analysis in the presence of both uncertainties it appears essential to use methods more efficient than CMC in terms of computational cost and more adapted to complex failure regions than FORM. Sampling methods such as Subset Sampling based on surrogate models combined with a dedicated refinement strategy may be an interesting alternative to solve this problem. Surrogate models would allow to decrease the number of calls the the limit state function and the sampling

method would enable to handle multiple MPPs.
The proposed methods related to these thematics will be developed in Part III.

5.7.3 Constraint handling for Evolution Strategy algorithms in the presence of noise

In order to have a robust and reliable optimal UMDO solution, efficient optimization algorithms are required. Evolution Strategy algorithms such as Covariance Matrix Adaptation - Evolution Strategy have dedicated techniques to handle the noise in the optimization process. Moreover, the efficiency of CMA-ES(λ, μ) has been illustrated on several benchmarks in noisy environments [Auger and Hansen, 2009]. However, this algorithm does not intrinsically manage constraints and all the applications in literature use penalization methods [Collange et al., 2010a]. The penalization approach requires a fine tuning process which is problem dependent and may result in non convergence to the optimal solution. An adaptation of CMA-ES(λ, μ) algorithm to efficiently handle the constraints in the presence of noise could be an improvement to solve UMDO problems.
The proposed methods related to these thematics will be developed in Part IV.

Part II

UMDO formulations with functional interdisciplinary coupling satisfaction, applications to launch vehicle design

Chapter 6

Individual Discipline Feasible - Polynomial Chaos Expansion

Contents

Chapter goals

- Formulate the conditions to ensure mathematical equivalence between coupled and decoupled UMDO strategies,
- Develop a single-level UMDO formulation ensuring interdisciplinary coupling satisfaction for all the realizations of the uncertain variables,
- Apply and compare the proposed approach to MultiDisciplinary Feasible formulation on an analytical test case.

6.1 Introduction

This part of the thesis is devoted to the multidisciplinary feasibility in the presence of uncertainty for decoupled formulations. One of the main concluding remarks of the previous part concerns the UMDO process organization and the handling of interdisciplinary couplings in the presence of uncertainty. Indeed, it emerges from the analysis of the existing UMDO methods that ensuring multidisciplinary feasibility of the optimal design is a challenging task. One of the major requirements is to ensure the system consistency whatever the unexpected event realization. Decoupled strategies under uncertainty could benefit from the same advantages as in the deterministic case, however it must not be to the detriment of the multidisciplinary feasibility. In order to maintain the mathematical equivalence between the classical coupled approaches and the decoupled formulations, interdisciplinary couplings have to be satisfy for all the realizations of the uncertain variables. The existing decoupled UMDO formulations ensure coupling satisfaction for some particular values such as the expected value of the coupling variables or the MPP [Du and Chen, 2001; Liu et al., 2006; Du et al., 2008]. Surrogate models have been used to represent the coupling variables either in coupled approach (Taylor series [Du and Chen, 2002; Du et al., 2002]) or in decoupled approach to compute the coupling variables statistical moments (Taylor series [Du and Chen, 2001; Liu et al., 2006], Polynomial Chaos Expansion [Xiong et al., 2012]). However, the use of the surrogate was limited to an efficient statistical moment computation. Surrogate models used to represent the interdisciplinary coupling mappings at the UMDO convergence could offer the possibility to organize the design process with a decomposition strategy while guaranteeing the multidisciplinary consistency of the optimal system.

This part is organized in three chapters. In the first chapter (chapter 6), we present a single-level formulation called Individual Discipline Feasible - Polynomial Chaos Expansion (IDF-PCE) derived from IDF. This chapter is based on an iterative construction along the UMDO process of surrogate models (PCE) of the coupling functional relations. At the optimum, the surrogate models have to represent these mappings as would an MDA under uncertainty do. In the proposed UMDO processes, the disciplines are decoupled and the system-level optimizer handles both the design variables and the surrogate model parameters. Three approaches are proposed to propagate uncertainty in IDF-PCE leading to the three variants. Eventually, the latter are applied on an analytical test case and compared to MDF under uncertainty.

In the second chapter, a Multi-level Hierarchical MDO formulation under Uncertainty (MHOU) is proposed. This formulation is derived from the stage-wise decomposition formulations [Balesdent et al., 2012a] to take into account uncertainties while ensuring coupling satisfaction. The proposed approach is a semi-decoupled formulation which removes the feedback couplings while guaranteeing the multidisciplinary feasibility. This approach is particularly adapted for launch vehicle design. Indeed, instead of classically decomposing the process into the disciplines propulsion, aerodynamics, trajectory, *etc.*, the process is decomposed into the different launch vehicle stages. The subsystem-level optimizers are in charge of the design and optimization of the different stages. The system-level optimizer manages the optimization of the entire vehicle and the satisfaction of the interdisciplinary couplings.

In the third chapter, both single and multi-level formulations are applied to two different launch vehicle test cases and compared to a reference approach. This work has been performed in collaboration with Mathieu Balesdent (Onera), N. Bérend (Onera) and R. Le Riche (EMSE, CNRS).

6.2 Foundations for decoupled and consistent UMDO formulations

In order to avoid the repeated MDA used in MDF under uncertainty, decoupled approaches aim at propagating uncertainty on decoupled disciplines allowing one to evaluate them in parallel and to ensure coupling satisfaction by introducing equality constraint in the UMDO formulation. However, two main challenges are faced to decouple the design process:

- Uncertain input coupling variable vector $\mathbf{Y}$ has to be controlled by the system-level optimizer. Uncertain variables are function and infinite-dimensional problem are complex to solve and dedicated methods have to be used.
- Equality constraints between the input coupling variables $\mathbf{Y}$ and the output coupling variables computed by $c(\cdot)$, which are two uncertain variables, have to be imposed. Equality between two uncertain variables corresponds to an equality between two functions which is difficult to implement.

In order to understand these two challenges and the proposed approaches, a focus on decoupled deterministic MDO formulation is necessary. Consider two disciplines i and j and one scalar feedfor-

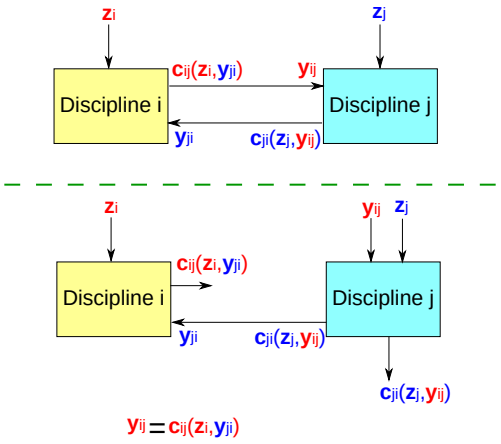

Figure 6.1: Two discipline coupling handling approaches

ward coupling y_{ij} and one scalar feedback coupling y_{ji} as illustrated in Figure 6.1. In deterministic decoupled MDO approach, to remove the feedforward coupling, there is only one equality constraint that has to be imposed at the system-level in the optimization formulation, Eq.(6.1), between the input coupling variable y_{ij} and the output coupling variable $c_{ij}(\mathbf{z}_i, y_{ji})$:

$$y_{ij} = c_{ij}(\mathbf{z}_i, y_{ji}) \tag{6.1}$$

However, in the presence of uncertainty, coupling satisfaction involves an equality constraint between two **uncertain variables**. An uncertain variable is a function (see section 2.2.2). Two uncertain variables are equals, if and only if the two corresponding functions have the same initial

and final sets and the same mappings. To ensure coupling satisfaction *in realizations*, an infinite number of equality constraints, Eq.(6.2), have to be imposed, one for each realization of the uncertain variables used to compute the objective and constraint functions:

$$\forall \mathbf{u} \in \mathbf{\Omega}, \;\; y_{ij} = c_{ij}(\mathbf{z}_i, y_{ji}, \mathbf{u}_i) \tag{6.2}$$

where $c_{ij}(\cdot)$ is a function of the uncertain variable realizations $\mathbf{u}$. However, it is important to notice that even if the coupling variables are random variables, for one realization $\mathbf{u}_0$ there is in general only one converged coupling realization that satisfies $y_{ij_0} = c_{ij}(\mathbf{z}_i, y_{ji_0}, \mathbf{u}_0)$ ensuring multidisciplinary feasibility. Indeed, the disciplines are modeled with deterministic functions, all the uncertainties arise in the discipline inputs.
Solving an optimization problem with an infinite number of constraints is a challenging task. To overcome this issue, considering an UMDO problem of N disciplines, we propose to introduce a new integral form for the interdisciplinary coupling constraint:

$$\forall (i,j) \in \{1,...,N\}^2, \; i \neq j, \; \mathbf{J}_{ij} = \int_{\mathbf{\Omega}} \left[\mathbf{c}_{ij}(\mathbf{z}_i, \mathbf{y}_{.i}, \mathbf{u}_i) - \mathbf{y}_{ij}\right]^2 \phi(\mathbf{u}) \mathrm{d}\mathbf{u} = 0 \tag{6.3}$$

In order to have the integrals in Eq.(6.3) equal to zero, the input coupling variables must be equal to the output coupling variables for each realization of the uncertain variables almost surely (except maybe over null measure sets). The interdisciplinary coupling constraints $\mathbf{J}_{ij}$ may be viewed as the integration of a loss function (the difference between the input and the output coupling variables) over the entire sample space (see section 2.3.1.1). If the new interdisciplinary coupling constraints Eq.(6.3) are satisfied, therefore a mathematical equivalence is maintained with the coupled approach because, as by using MDA, the couplings verify the following system of equations:

$$\forall \; \mathbf{u} \in \mathbf{\Omega}, \; \forall (i,j) \in \{1,...,N\}^2, \; i \neq j, \; \mathbf{y}_{ij} = \mathbf{c}_{ij}(\mathbf{z}_i, \mathbf{y}_{.i}, \mathbf{u}_i) \tag{6.4}$$

Nevertheless, to decouple the disciplines, the uncertain input coupling variables **$\mathbf{Y}$ have to be controlled by the optimizer**. Uncertain variables are functions and finding a function that is a solution to an infinite-dimensional optimization problem is a complex task. Several methods focus on these types of problems such as calculus of variations [Noton, 2013], optimal control [Zhou et al., 1996] and shape optimization [Sokolowski and Zolesio, 1992]. To avoid to directly solve an infinite-dimensional problem, most of the time the function is discretized and the discretization points are controlled by the optimizer [Devolder et al., 2010]. The discretization strategy has to be done in concordance with the optimization problem. In the proposed formulations, the considered scalar coupling variable y_{ij} is replaced by a surrogate model representing the coupling functional relations:

$$y_{ij} \rightarrow \hat{y}_{ij}\left(\mathbf{u}, \boldsymbol{\alpha}^{(ij)}\right) \tag{6.5}$$

The surrogate model, written $\hat{y}_{ij}\left(\mathbf{u}, \boldsymbol{\alpha}^{(ij)}\right)$, provides a functional representation of the dependency between the uncertain variables $\mathbf{U}$ and the input coupling variables with $\boldsymbol{\alpha}^{(ij)}$ the metamodel parameters. This approach ensures that the functional dependency between the uncertain variables and the coupling variables is taken into account. In the proposed formulations, each coupling that is removed is replaced by a surrogate model. The surrogate models are also functions, represented by parameters that may be used to decouple the UMDO problem by letting the system-level optimizer having the control on the surrogate model coefficients. Therefore, the infinite-dimensional

optimization problem is transformed into a q-dimensional optimization problem with q the number of coefficients required to model all the removed coupling variables.
We propose to model the coupling functional relations with Polynomial Chaos Expansion (PCE) because this surrogate model presents advantages in terms of uncertainty analysis and propagation [Eldred, 2009]. PCE are particularly adapted to represent the input coupling variables as they are dedicated to model functions that take as input uncertain variables as illustrated in section 2.3.1.1. The scalar coupling y_{ij} is modeled by:

$$\hat{y}_{ij}\left(\mathbf{u}, \boldsymbol{\alpha}^{(ij)}\right) = \sum_{k=1}^{d_{\text{PCE}}} \alpha_{(k)}^{(ij)} \Psi_k(\mathbf{u}) \tag{6.6}$$

where $q = d_{\text{PCE}}$ is the degree of PCE decomposition and Ψ_k is the basis of orthogonal polynomials chosen in accordance to the input uncertainty distributions.
Note that, in order to keep $\hat{y}_{ij}(\cdot)$ simple, the dependency between $\hat{y}_{ij}(\cdot)$ and $\mathbf{z}$ is not present here: $\hat{y}_{ij}(\cdot)$ is not a function of $\mathbf{z}$, it is learned for the specific $\mathbf{z}^*$ where the optimization converges. Interdisciplinary coupling satisfaction ensured for all the realizations of the uncertain variables enables to guaranty that the system is *multidisciplinary feasible*. Furthermore, the proposed technique transforms the complex original infinite-dimensional problem into a finite-dimensional problem, allowing to solve it in practice while guarantying the mathematical equivalence between coupled and decoupled formulations in terms of coupling satisfaction.
The proposed methods rely on the iterative construction of the PCE models of the coupling functional relations along with the system-level UMDO optimization. At the UMDO optimum, the metamodels of the coupling functional relations simulate these mappings as would MDA under uncertainty do (Fig. 6.2). Moreover, the proposed approaches do not require any MDA, allowing to reduce the number of calls to the computationally expensive disciplines. First, in the next section, a single-level formulation is proposed and applied to an analytical test case. Then, in chapter 7 a multi-level formulation is proposed based on the same coupling handling strategy.

6.3 Proposed single-level formulation: Individual Discipline Feasible - Polynomial Chaos Expansion (IDF-PCE)

IDF-PCE is a single-level decoupled UMDO formulation relying on a functional representation of the coupling variables. IDF-PCE is formulated as follows:

$$\begin{aligned}
\min \quad & \Xi\left[f(\mathbf{z}, \boldsymbol{\alpha}, \mathbf{U})\right] && (6.7)\\
\text{w.r.t.} \quad & \mathbf{z}, \boldsymbol{\alpha} \\
\text{s.t.} \quad & \mathbb{K}\left[\mathbf{g}(\mathbf{z}, \boldsymbol{\alpha}, \mathbf{U})\right] \leq 0 && (6.8)\\
& \forall (i,j) \in \{1, ..., N\}^2,\ i \neq j, \\
& \mathbf{J}_{ij} = \int_{\boldsymbol{\Omega}} \left[\mathbf{c}_{ij}\left(\mathbf{z}_i, \hat{\mathbf{y}}_{.i}\left(\mathbf{u}, \boldsymbol{\alpha}^{(.i)}\right), \mathbf{u}_i\right) - \hat{\mathbf{y}}_{ij}\left(\mathbf{u}, \boldsymbol{\alpha}^{(ij)}\right)\right]^2 \phi(\mathbf{u}) \mathrm{d}\mathbf{u} = \mathbf{0} && (6.9)\\
& \mathbf{z}_{\min} \leq \mathbf{z} \leq \mathbf{z}_{\max} && (6.10)
\end{aligned}$$

with $\mathbf{J}_{ij}$ the interdisciplinary constraint vector for the couplings from the discipline i to the dis-

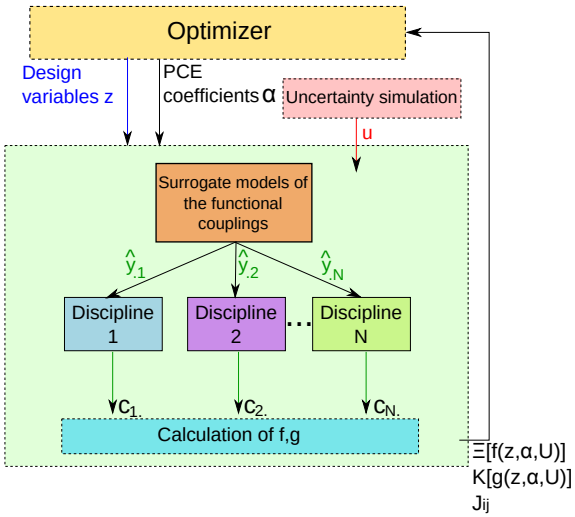

Figure 6.2: IDF-PCE with the surrogate models of the coupling functional relations

cipline j and $\hat{\mathbf{y}}_{.i}\left(\mathbf{u}, \boldsymbol{\alpha}^{(.i)}\right)$ the PCEs of all the input coupling variables of the discipline i. In this formulation, the system-level optimizer handles the design variables $\mathbf{z}$ and the PCE coefficients of the coupling variables $\boldsymbol{\alpha}$. The handling of the PCE coefficients at the system-level allows to decouple the disciplines and to evaluate them in parallel (Fig. 6.2). In comparison to the coupled formulations, the dimension of the design space is therefore increased by the number of parameters $\boldsymbol{\alpha}$. To ensure the multidisciplinary feasibility at the optimum, equality constraints involving the generalization error are imposed Eq.(6.9). These constraints involve the input coupling variables modeled by PCE and the output coupling variables resulting from the discipline simulations. The constraints have an integral form to ensure the coupling satisfaction for all the possible realizations of the uncertain variables. If we have: $\forall (i,j) \in \{1,...,N\}^2 \; \forall i \neq j, \; \mathbf{J}_{ij} = 0$, then the couplings are satisfied for all the realizations $\mathbf{u} \in \boldsymbol{\Omega}$ almost surely.
The vector $\mathbf{J}(\cdot)$ stands for the distances with respect to the MDA coupling satisfaction. Indeed, in the MDA approach, $\mathbf{J}(\mathbf{z}) = 0, \forall \mathbf{z} \in [\mathbf{z}_{\min}, \mathbf{z}_{\max}]$. In IDF-PCE, $\mathbf{J}(\mathbf{z}) = 0$, has to be satisfied only at the UMDO optimum $\mathbf{z} = \mathbf{z}^*$. The interdisciplinary feasibility is not ensured all along the optimization. In IDF-PCE, either the Robust-based UMDO or the Reliability-based UMDO problem may be considered (see section 3.2). The measures of uncertainty for the inequality constraint functions Eq.(6.8) may be distinguished by:

$$\mathbb{K}\left[\mathbf{g}(\mathbf{z}, \boldsymbol{\alpha}, \mathbf{U})\right] = \mathbb{E}\left[\mathbf{g}(\mathbf{z}, \boldsymbol{\alpha}, \mathbf{U})\right] + k\sigma\left[\mathbf{g}(\mathbf{z}, \boldsymbol{\alpha}, \mathbf{U})\right] \leq 0 \tag{6.11}$$

$$\mathbb{K}\left[\mathbf{g}(\mathbf{z}, \boldsymbol{\alpha}, \mathbf{U})\right] = \mathbb{P}_{\mathbf{g}(\mathbf{z}, \boldsymbol{\alpha}, \mathbf{U}) \leq 0} - \mathbb{P}_t \leq 0 \tag{6.12}$$

with $\mathbb{P}_t$ the admissible target probability. The first measure, Eq.(6.11), is based on the statistical moments of the inequality constraint functions and the second Eq.(6.12) is based on the probability of failure, *i.e.*, the probability for the inequality constraint function to be underneath a threshold. In practice, the multidimensional integrals associated to the statistical moments (expectations, standard deviations), to the coupling constraints $\mathbf{J}$ or to the probability of failure are difficult to

compute. We use three techniques to estimate the statistical moments and the coupling constraints (CMC, quadrature rules and decomposition of the output coupling variables over a PCE) and one to estimate the probability of failure by Subset Sampling using Support Vector Machines. Depending on the technique used to propagate uncertainty, this lead to three variants of IDF-PCE detailed in the following sections. These propagation techniques will be compared on an academic test cases to highlight their impacts on IDF-PCE formulation.

6.3.1 Uncertainty propagation by Crude Monte Carlo

CMC approximation of multidimensional integrals such that Eq.(6.9) relies on repeated sampling in the input uncertain space $\mathbf{\Omega}$ (Fig. 6.3). The integral in Eq.(6.9) is approximated by:

$$\mathbf{J}_{ij} \simeq \mathbf{J}_{ij}^{\mathrm{CMC}} = \frac{1}{M} \sum_{k=1}^{M} \left[\mathbf{c}_{ij} \left(\mathbf{z}_i, \hat{\mathbf{y}}_{.i} \left(\mathbf{u}_{(k)}, \boldsymbol{\alpha}^{(.i)} \right), \mathbf{u}_{i(k)} \right) - \hat{\mathbf{y}}_{ij} \left(\mathbf{u}_{(k)}, \boldsymbol{\alpha}^{(ij)} \right) \right]^2 \tag{6.13}$$

with M the number of CMC samples. Similar estimations are carried out for the expectations and standard deviations in Eqs.(6.7) and (6.8). $\mathbf{J}_{ij}^{\mathrm{CMC}}$ is called the *empirical error* [Vapnik, 2000a] and is related to the Root Mean Squared Error (RMSE) metric by:

$$RMSE = \sqrt{\mathbf{J}_{ij}^{\mathrm{CMC}}} \tag{6.14}$$

The smaller the RMSE, the better the interdisciplinary couplings are satisfied. The uncertain variables are sampled at the system-level and are propagated in the decoupled subsystems ($\hat{\mathbf{y}}(\cdot)$ and $\mathbf{c}(\cdot)$). CMC is easy to implement and it can reach any level of accuracy if enough samples are calculated. The convergence of CMC to the integral value is in order of $\frac{1}{\sqrt{M}}$. The convergence is slow and if the disciplines are computationally expensive, CMC becomes intractable. However, CMC does not suffer from the curse of dimensionality.

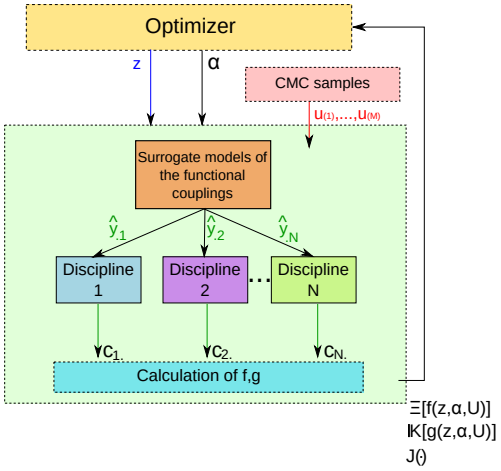

Figure 6.3: IDF-PCE with CMC propagation method

6.3.2 Uncertainty propagation by Quadrature rules

Quadrature rules approximate integrals as a weighted sum of functions evaluated at specified points within the domain of integration [Davis and Rabinowitz, 2007]. For a surrogate model $\hat{y}_{ij} : \boldsymbol{\Omega} \times \boldsymbol{\mathcal{A}} \to \mathbb{R}$ of the scalar coupling y_{ij}, with $\dim(\boldsymbol{\Omega}) = d$ and $\boldsymbol{\mathcal{A}}$ the PCE coefficient set, instead of sampling randomly as with CMC, a set of specific points is used to approximate the multivariate integral:

$$\int_{\boldsymbol{\Omega}} \hat{y}_{ij}(\mathbf{u}, \boldsymbol{\alpha}^{(ij)})\phi(\mathbf{u})\mathrm{d}\mathbf{u} \simeq \sum_{k_1=1}^{M_1}\sum_{k_2=1}^{M_2}\ldots\sum_{k_d=1}^{M_d}(w_{(k_1)}\otimes w_{(k_2)}\ldots\otimes w_{(k_d)})\hat{y}_{ij}(u_{(k_1)}, u_{(k_2)}, \ldots, u_{(k_d)}, \boldsymbol{\alpha}^{(ij)}) \tag{6.15}$$

where w are weights and $\otimes$ is the tensor product operator. Although the proposed formulation stands for any uncertainty measure $\Xi[\cdot]$, an example is given for the expected value of the objective function $\Xi\left[f(\mathbf{z}, \boldsymbol{\alpha}, \mathbf{U})\right] = \mathbb{E}\left[f(\mathbf{z}, \boldsymbol{\alpha}, \mathbf{U})\right]$. The approximation of the objective function and the interdisciplinary coupling constraints with quadrature rules are given by:

$$\begin{aligned}\mathbb{E}\left[f(\mathbf{z}, \boldsymbol{\alpha}, \mathbf{U})\right] &= \int_{\boldsymbol{\Omega}} f\left(\mathbf{z}, \boldsymbol{\alpha}, \mathbf{u}\right)\phi(\mathbf{u})\mathrm{d}\mathbf{u} &(6.16)\\ &\simeq \sum_{k_1=1}^{M_1}\ldots\sum_{k_d=1}^{M_d}(w_{(k_1)}\otimes\ldots\otimes w_{(k_d)})\times \\ &\qquad f\left(\mathbf{z}, \hat{\mathbf{y}}\left([u_{(k_1)}, \ldots, u_{(k_d)}], \boldsymbol{\alpha}\right), [u_{(k_1)}, \ldots, u_{(k_d)}]\right) &(6.17)\end{aligned}$$

$$\begin{aligned}\mathbf{J}_{ij} &= \int_{\boldsymbol{\Omega}}\left[\mathbf{c}_{ij}\left(\mathbf{z}_i, \hat{\mathbf{y}}_{.i}\left(\mathbf{u}, \boldsymbol{\alpha}^{(.i)}\right), \mathbf{u}_i\right) - \hat{\mathbf{y}}_{ij}\left(\mathbf{u}, \boldsymbol{\alpha}^{(ij)}\right)\right]^2\phi(\mathbf{u})\mathrm{d}\mathbf{u} &(6.18)\\ &\simeq \sum_{k_1=1}^{M_1}\ldots\sum_{k_d=1}^{M_d}(w_{(k_1)}\otimes\ldots\otimes w_{(k_d)})\left[\mathbf{c}_{ij}\left(\mathbf{z}_i, \hat{\mathbf{y}}_{.i}\left([u_{(k_1)}, \ldots, u_{(k_d)}], \boldsymbol{\alpha}^{(.i)}\right), [u_{(k_1)}, \ldots, u_{(k_d)}]_i\right)\right. \\ &\qquad \left. - \hat{\mathbf{y}}_{ij}\left([u_{(k_1)}, \ldots, u_{(k_d)}], \boldsymbol{\alpha}^{(ij)}\right)\right]^2 &(6.19)\end{aligned}$$

The quadrature rule requires $\prod_{i=1}^{d} M_i$ discipline evaluations to propagate the uncertainty. Compared to CMC, the approximation based on tensor product is efficient for a small number of input uncertain variables, but the method suffers from the curse of dimensionality [Eldred, 2009]. Sparse grid approaches may be used to decrease the number of function evaluations while preserving the accuracy for high dimension integrals (see section 2.3.1.1).

6.3.3 Uncertainty propagation by Polynomial Chaos Expansion of the output coupling variables

In this approach, the quadrature rules are used to compute the statistical moments involved in the objective function or the constraints, however, the coupling constraint expression is modified. Another way to impose coupling constraints and to benefit from the PCE uncertainty propagation is to decompose the output coupling variables with another PCE with respect to $\mathbf{U}$ (Fig. 6.4).

As at the UMDO problem convergence the input coupling variables must be equal to the output coupling variables, it is possible to decompose them over the same polynomial basis. We denote by *input PCE*, $\hat{\mathbf{y}}_{.i}\left(\mathbf{u}, \boldsymbol{\alpha}^{(.i)}\right)$, the PCEs of the coupling variables whose coefficients are controlled by the system-level optimizer. We also denote by *output PCE*, the PCE of the output coupling variables $\mathbf{c}_{ij}\left(\mathbf{z}_i, \hat{\mathbf{y}}_{.i}\left(\mathbf{u}, \boldsymbol{\alpha}^{(.i)}\right), \mathbf{u}_i\right)$ whose coefficients are calculated by orthogonal spectral projection. Two further assumptions allow to simplify the expression of the output PCE: like the input PCE, the effect of the design variables $\mathbf{z}$ is not present (so the output PCE is valid only for the converged design variables); $\mathbf{Y}_{.\mathbf{i}}$ is approximated by the input PCE, $\hat{\mathbf{y}}_{.i}\left(\mathbf{u}, \boldsymbol{\alpha}^{(.i)}\right)$. Therefore, once $\boldsymbol{\alpha}$ are chosen, the output PCE $\tilde{\mathbf{c}}_{ij}\left(\mathbf{u}, \tilde{\boldsymbol{\alpha}}^{(ij)}\right)$ is only a function of the uncertainties and its own coefficients $\tilde{\boldsymbol{\alpha}}^{(ij)}$. For one scalar coupling between the disciplines i and j:

$$c_{ij}\left(\mathbf{z}_i, \hat{\mathbf{y}}_{.i}\left(\mathbf{u}, \boldsymbol{\alpha}^{(.i)}\right), \mathbf{u}_i\right) \simeq \sum_{k=0}^{d_{\mathrm{PCE}}} \tilde{\alpha}_{(k)}^{(ij)} \Psi_k(\mathbf{u}) = \tilde{c}_{ij}\left(\mathbf{u}, \tilde{\boldsymbol{\alpha}}^{(ij)}\right) \tag{6.20}$$

The output PCE coefficients $\tilde{\boldsymbol{\alpha}}^{(ij)}$ are computed by orthogonal spectral projection:

$$\tilde{\alpha}_{(k)}^{(ij)} = \frac{< c_{ij}, \Psi_k >}{< \Psi_k^2 >} = \frac{1}{< \Psi_k^2 >} \int_{\boldsymbol{\Omega}} c_{ij}\left(\mathbf{z}_i, \hat{\mathbf{y}}_{.i}\left(\mathbf{u}, \boldsymbol{\alpha}^{(.i)}\right), \mathbf{u}_i\right) \Psi_k(\mathbf{u}) \phi(\mathbf{u}) \mathrm{d}\mathbf{u} \tag{6.21}$$

Eq.(6.9) may be approximated by:

$$\begin{aligned} J_{ij} &= \int_{\boldsymbol{\Omega}} \left[c_{ij}\left(\mathbf{z}_i, \hat{\mathbf{y}}_{.i}\left(\mathbf{u}, \boldsymbol{\alpha}^{(.i)}\right), \mathbf{u}_i\right) - \hat{y}_{ij}\left(\mathbf{u}, \boldsymbol{\alpha}^{(ij)}\right)\right]^2 \phi(\mathbf{u}) \mathrm{d}\mathbf{u} && (6.22) \\ &\simeq \int_{\boldsymbol{\Omega}} \left[\tilde{c}_{ij}\left(\mathbf{u}, \tilde{\boldsymbol{\alpha}}^{(ij)}\right) - \hat{y}_{ij}\left(\mathbf{u}, \boldsymbol{\alpha}^{(ij)}\right)\right]^2 \phi(\mathbf{u}) \mathrm{d}\mathbf{u} && (6.23) \\ &\simeq \int_{\boldsymbol{\Omega}} \left[\sum_{k=0}^{d} \left(\tilde{\alpha}_{(k)}^{(ij)} - \alpha_{(k)}^{(ij)}\right) \Psi_k(\mathbf{u})\right]^2 \phi(\mathbf{u}) \mathrm{d}\mathbf{u} && (6.24) \end{aligned}$$

To ensure the coupling satisfaction at the optimum between the disciplines i and j for all the uncertain variable realizations and to avoid the calculation of the multivariate integral, Eq.(6.24) is replaced by:

$$\forall (i,j) \in \{1, ..., N\}^2,\ i \neq j,\ \| \boldsymbol{\alpha}^{(ij)} - \tilde{\boldsymbol{\alpha}}^{(ij)} \|^2 = 0 \tag{6.25}$$

If Eq.(6.25) is satisfied then the integral (6.24) is equal to zero and Eq.(6.9) is quasi satisfied. Indeed, if the input and output PCE coefficients are equals, therefore the sum in the integral of Eq.(6.24) is composed of terms equal to zero. The constraints on the input and output PCE coefficients ensure the coupling satisfaction between the disciplines i and j for each uncertainty realization at the UMDO optimum under two conditions:

Condition 1: $\forall\, \mathbf{u} \in \boldsymbol{\Omega},\ \| \mathbf{c}_{ij}\left(\mathbf{z}^*, \mathbf{u}_i, \hat{\mathbf{y}}_{.i}\left(\mathbf{u}, \boldsymbol{\alpha}^{(.i)}\right)\right) - \tilde{\mathbf{c}}_{ij}\left(\mathbf{u}, \tilde{\boldsymbol{\alpha}}^{(ij)}\right) \| < \epsilon$, with ϵ a tolerance and $\mathbf{u}$ a realization of the uncertain variables (accurate approximation of the coupling variables by the output PCE),

Condition 2: Eq. (6.25) is verified.

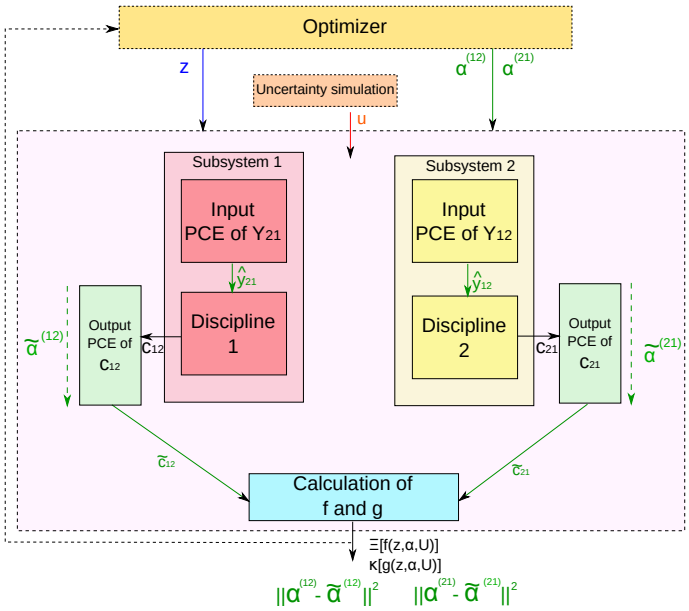

Figure 6.4: IDF-PCE with the numerical evaluation of the generalization errors by PCE

In this case, as the two uncertain functions $\tilde{\mathbf{c}}_{ij}(\cdot)$ and $\hat{\mathbf{y}}_{ij}(\cdot)$ have the same polynomial chaos expansion, for any uncertainty realization: $\tilde{\mathbf{c}}_{ij}(\cdot) \simeq \hat{\mathbf{y}}_{ij}(\cdot) \simeq \mathbf{c}_{ij}(\cdot)$. The statistical moments of the objective function and the constraint functions are calculated by quadrature rules as in the previous section with the discipline outputs.

The important difference of IDF-PCE-PCE with IDF-PCE (quadrature) lies in the expression of the coupling constraints Eq.(6.25) which only involve the PCE coefficients and could facilitate the optimizer convergence. This technique allows to avoid the propagation of the uncertainty for a large number of uncertain variable realizations as in CMC, and to decrease the number of calls to the disciplines. A numerical comparison of these three methods is performed in Section 6.4.

6.3.4 Reliability analysis with Subset Sampling and Support Vector Machine

Within the framework of Robust-based UMDO, CMC, quadrature rules or output couplings PCE decomposition may be used to approximate the multidimensional integrals involved in the calculation of the statistical moments of the constraints. Within the framework of Reliability-based UMDO, the measure of uncertainty for the inequality constraint functions in Eq.(6.8) involves a probability of failure as in Eq.(6.12). As highlighted in section 2.5, its computation requires specific methods. Indeed, CMC estimator of the probability of failure is asymptotically unbiased and converges to the exact value according to the law of large number, however the convergence is slow. CMC estimation technique is intractable for real world engineering problems for which the limit state functions involve expensive black-box functions. Dedicated methods such as FORM

(First Order Reliability Method) [Kuschel and Rackwitz, 1997], SORM (Second Order Reliability Method) [Kuschel and Rackwitz, 1997], Importance Sampling [Melchers, 1989], Subset Sampling [Au and Beck, 2001], *etc.*, have been developed in order to reduce the number of function evaluations required to compute the failure probability while decreasing the variance of the probability estimator. Moreover, these approaches have been combined with surrogate models [Dubourg et al., 2013] (PCE, Kriging, SVM) to replace the expensive functions by surrogate models which are less expensive to evaluate (section 2.5). In IDF-PCE formulation, any of these approaches may be used to compute the inequality constraints.
However, in case of launch vehicle design, the limit state functions often involve a launcher trajectory optimization code which is expensive to run. In order to limit the computational cost of the failure probability estimation, a sampling-based method (Subset Simulation, section 2.4.4) combined with an adaptive refinement strategy (Generalized Max-min [Lacaze and Missoum, 2014b], section 2.5.2.1) of a surrogate model (SVM) is implemented. The construction and refinement of the SVM $\hat{\mathbf{g}}(\cdot)$ is implemented in order to be representative around the failure zones of the limit state functions $\mathbf{g}(\cdot)$. Subset Sampling is used to compute the probability of failure combined with the surrogate model. For one scalar constraint function $g(\cdot)$:

$$\mathbb{P}_{g(\mathbf{z},\boldsymbol{\alpha},\mathbf{U})\leq 0} \simeq \mathbb{P}_{\hat{g}(\mathbf{z},\boldsymbol{\alpha},\mathbf{U})\leq 0} = \mathbb{P}(\mathbf{U} \in \boldsymbol{\Omega}_f) = \prod_{i=1}^{m} \mathbb{P}\left(\mathbf{U} \in \boldsymbol{\Omega}_{f_i} | \mathbf{U} \in \boldsymbol{\Omega}_{f_{i-1}}\right) \tag{6.26}$$

where $\forall i = \{1, \ldots, m\}$ $\boldsymbol{\Omega}_{f_i} = \{\mathbf{u} | \hat{g}(\mathbf{u}) \leq S_i\}$ is a decreasing sequence of intermediate subset failure domains and $S_m = S = 0$. SVM is used due to the complexity of the limit state functions (non linearity, possible discontinuities and multiple failure regions). In launch vehicle design problems, due to the presence of multiple failure regions and non linear limit state functions, Subset Simulation is adapted to estimate the probability of failure. Moreover, due to the presence of discontinuities in the limit state function (output of optimization trajectory which may present several optima), SVM are adapted to model discontinuous limit state function. Other approaches may be used to efficiently compute the probability of failure, for more details see [Dubourg et al., 2013]. The adopted approach has been proposed in [Lacaze and Missoum, 2014b] and consists in adding a selected number of sample points in the SVM training set according to the GMm sample selection.

The different steps of the IDF-PCE algorithm are summarized in Figure 6.5. Note that the proposed formulation is developed for deterministic design variables and all the uncertainty is assumed to be represented by $\mathbf{U}$. However, the proposed approach could be extended to uncertain design variables by letting the optimizer controlling the expected value of the design variables and propagating the uncertainty through the system as done in [Liu et al., 2006; Lin and Gea, 2013]. For instance the propellant mass could be considered as an uncertain design variable and the expected value of the propellant mass could be controlled by the optimizer while propagation the uncertainty through the system (according to the propellant mass uncertainty modeling). Moreover, PCE surrogate model is used to represent the functional relations between the coupling variables at the UMDO problem convergence because PCE are dedicated to model functions which take as input uncertain variables. However, the approach to handle interdisciplinary couplings could be extended to any parametric surrogate model. These parameters would have to be controlled by the system-level optimizer in addition with the design variables.
In conclusion, IDF-PCE presents several advantages. IDF-PCE solves a finite-dimensional problem

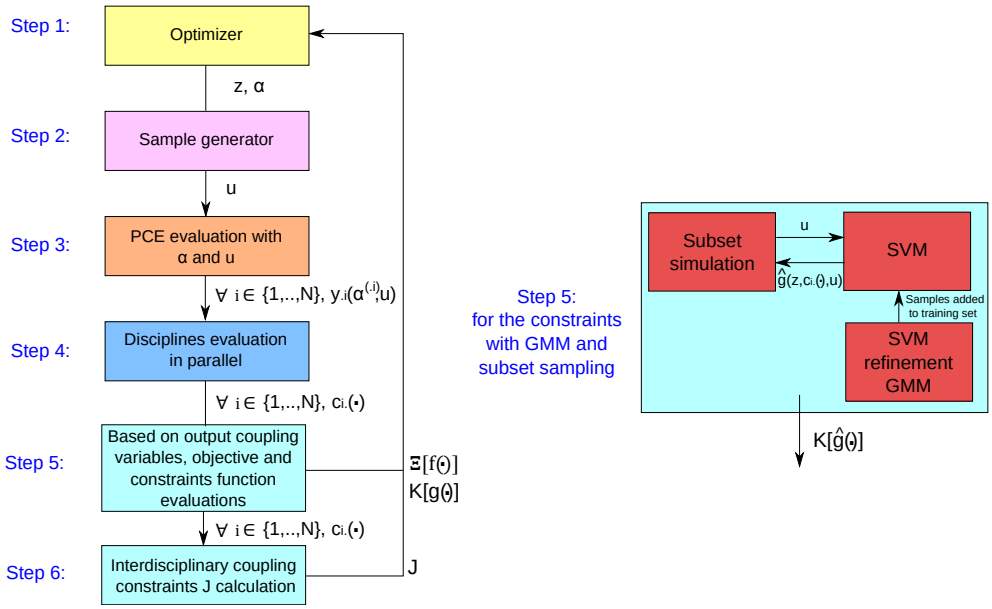

Figure 6.5: Steps of the IDF-PCE algorithm

which is manageable in practice compared to infinite-dimensional problems which are hard to handle. One of the principal advantages is that this formulation ensures the coupling satisfaction at the UMDO optimum for each uncertain variable realization. In that purpose, it models the functional dependency between the uncertain variables, the design variables and the coupling variables, which may be useful beyond optimization, *e.g.* for a post-optimality sensitivity analysis. IDF-PCE is a decoupled single-level UMDO formulation allowing to decompose the UMDO problem and to simulate in parallel the disciplines and it does not require any complete MDA. This decomposition of the UMDO process allows to reduce the management tasks compared to coupled formulations because each discipline just converses with the system-level and not more interdisciplinary information exchange are required during the subsystem-level uncertainty propagation. The different engineering teams do not have to wait the results from the other teams to start the analyses and the uncertainty propagation. Furthermore, the quadrature and the decomposition of the discipline outputs overs PCE allow to propagate uncertainty more efficiently (using less calls to the disciplines) compared to CMC.
However, this formulation presents some drawbacks as in deterministic IDF. Indeed, it increases the number of variables controlled by the system-level optimizer (design variables plus PCE coefficients). The increase in the design space makes more complex the UMDO problem to be solved. Moreover, PCE decomposition order has to be chosen *a priori* based on the coupling linearity knowledge (see section 6.5). The increase in PCE decomposition order may highly increase the size of the design space. Furthermore, IDF-PCE increases the number of equality constraints at the system-level in the optimization formulation which also makes more complex the optimization problem solving.
In the next paragraph, in order to assess the efficiency of IDF-PCE, it is applied to an analytical test case composed of two coupled disciplines and compared to MDF under uncertainty.

6.4 Application on an analytical test case

Numerical comparisons between the reference MDF under uncertainty (using MDA and CMC) and the proposed single level formulation are provided for an analytical test problem. First the mathematical problem is presented, then the coupled and the three variant decoupled UMDO formulations are described and finally the results are analyzed.
The mathematical UMDO problem presented in Figure 6.6 is a constrained optimization problem composed of:

- discipline 1: $y_{12} = c_{12}(\mathbf{z}, \mathbf{u}) = c_{13}(\mathbf{z}, \mathbf{u}) = -z_{sh}^{0.2} + u_{sh} + 0.25 \times u_1^{0.2} + z_1 + y_{21}^{0.58} + u_1^{0.4} \times y_{21}^{0.47}$

- discipline 2: $y_{21} = c_{21}(\mathbf{z}, \mathbf{u}) = c_{23}(\mathbf{z}, \mathbf{u}) = -z_{sh} + u_{sh}^{0.1} - z_2^{0.1} + 3 \times y_{12}^{0.47} + u_2^{0.33} + y_{12}^{0.16} \times u_2^{0.05} + y_{12}^{0.6} \times u_2^{0.13} + 100$

- calculation of f and g:

$$f = \frac{1}{5}\left[(z_{sh} - 5)^2 + (z_1 - 3)^2 + (z_2 - 7)^2 + (y_{21} + z_1 \times z_2)^{0.6} + (u_{sh} + 9)^2\right]$$
$$g = 150 + \exp(-0.01 \times u_1^2) \times z_{sh} \times z_1 - 0.02 \times z_2^3 \times u_2^5 + 0.01 \times y_{12}^{2.5} \times z_2 \times \exp(-0.1 u_{sh})$$

- 3 design variables: $z_1 \in [0, 1]$, $z_2 \in [0, 1]$ and the shared variable $z_{sh} \in [0, 1]$, we note: $\mathbf{z} = [z_{sh}, z_1, z_2]$,

- 3 uncertain variables: $U_1 = \mathcal{U}(-1, 1)$, $U_2 = \mathcal{N}_{(0,1)}$ and the shared uncertain variable $U_{sh} = \mathcal{N}_{(0,1)}$, we note: $\mathbf{U} = [U_{sh}, U_1, U_2]$,

- 2 coupling variables: $\mathbf{Y} = [Y_{12}, Y_{21}]$,

- 1 objective function: $\Xi[f(\mathbf{z}, \mathbf{Y}, \mathbf{U})] = \mathbb{E}[f(\mathbf{z}, \mathbf{Y}, \mathbf{U})]$, the expected value of the function f,

- 1 constraint function: $\mathbb{K}[g(\mathbf{z}, \mathbf{Y}, \mathbf{U})] = \mathbb{E}[g(\mathbf{z}, \mathbf{Y}, \mathbf{U}))] + 3\sigma[g(\mathbf{z}, \mathbf{Y}, \mathbf{U}))] \leq 0$

This analytical UMDO problem has been created and implemented because the disciplines are non linear and provide non gaussian coupling variable distributions in order to illustrate non linear problems. Moreover, it has been numerically verified for all $\mathbf{z}$ and $\mathbf{u}$ values tried that this problem is such that the MDA converges (it is a contraction mapping by FPI), and it converges to a unique coupling value.

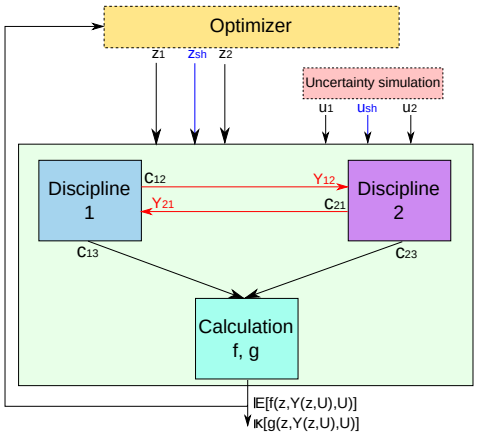

Figure 6.6: Analytical test case of a multidisciplinary coupled system

6.4.0.1 MDF under uncertainty

The MDF under uncertainty approach is formulated as follows:

$$\begin{aligned} \min \quad & \mathbb{E}[f(\mathbf{z}, \mathbf{Y}(\mathbf{z}, \mathbf{U}), \mathbf{U})] && (6.27) \\ \text{w.r.t.} \quad & \mathbf{z} \\ \text{s.t.} \quad & \mathbb{E}[g(\mathbf{z}, \mathbf{Y}(\mathbf{z}, \mathbf{U}), \mathbf{U}))] + 3\sigma[g(\mathbf{z}, \mathbf{Y}(\mathbf{z}, \mathbf{U}), \mathbf{U})] \leq \epsilon_g && (6.28) \\ & \mathbf{z} \in [0,1]^3 && (6.29) \end{aligned}$$

The dimension of the design space is 3. Uncertainties are propagated with CMC on MDA for each realization of the uncertain variables with a sample size $M = 150000$ in order to have an error lower than 10^{-3} on the estimation of the statistical moments. Because the means and the standard deviations are estimated by CMC, the objective function is noisy, therefore gradient based optimizers are not appropriate for this test case. Diverse derivative-free algorithms have been proposed in the literature, such as population based algorithms to handle such problems [Larson, 2012]. To compare the three proposed methods to MDF an Ant Colony optimizer (ACOmi) from the Matlab DOTcvp toolbox [Hirmajer et al., 2008] is used, as it is a population based algorithm that handles constraints with a penalization method [Schlüter and Gerdts, 2010]. Optimizations are stopped if there is no progress in 50 consecutive objective function evaluations with a tolerance of 10^{-3} on the objective function and the constraint. The MDA convergence criterion for the Fixed Point Iteration has been set to 10^{-4} as it corresponds to a variation in the objective and constraint functions smaller than 10^{-3}. Based on the numerical experimentation, 5 iterations are in general necessary to converge under the tolerance with the FPI methods. $\epsilon_g = -0.004$ is a conservative tolerance due to the estimation of the mean and the standard deviation of the constraint by CMC to ensure that the constraint is inferior or equal to 0.

6.4.0.2 IDF-PCE formulation

The general proposed IDF-PCE formulation (Fig 6.7) is given by

$$\begin{aligned}
\min \quad & \mathbb{E}\left[f\left(\mathbf{z}, \boldsymbol{\alpha}, \mathbf{U}\right)\right] && (6.30)\\
\text{w.r.t.} \quad & \mathbf{z}, \boldsymbol{\alpha}^{(12)}, \boldsymbol{\alpha}^{(21)} \\
\text{s.t.} \quad & \mathbb{E}[g(\mathbf{z}, \boldsymbol{\alpha}, \mathbf{U})] + 3\sigma[g(\mathbf{z}, \boldsymbol{\alpha}, \mathbf{U})] \leq \epsilon_g && (6.31)\\
& J_{12} = \int_{\mathbf{\Omega}} \left[c_{12}\left(z_{sh}, z_1, u_{sh}, u_1, \hat{y}_{21}\left(\mathbf{u}, \boldsymbol{\alpha}^{(21)}\right)\right) - \hat{y}_{12}\left(\mathbf{u}, \boldsymbol{\alpha}^{(12)}\right)\right]^2 \phi(\mathbf{u})\mathrm{d}\mathbf{u} \leq \epsilon && (6.32)\\
& J_{21} = \int_{\mathbf{\Omega}} \left[c_{21}\left(z_{sh}, z_2, u_{sh}, u_2, \hat{y}_{12}\left(\mathbf{u}, \boldsymbol{\alpha}^{(12)}\right)\right) - \hat{y}_{21}\left(\mathbf{u}, \boldsymbol{\alpha}^{(21)}\right)\right]^2 \phi(\mathbf{u})\mathrm{d}\mathbf{u} \leq \epsilon && (6.33)\\
& \mathbf{z} \in [0,1]^3 && (6.34)
\end{aligned}$$

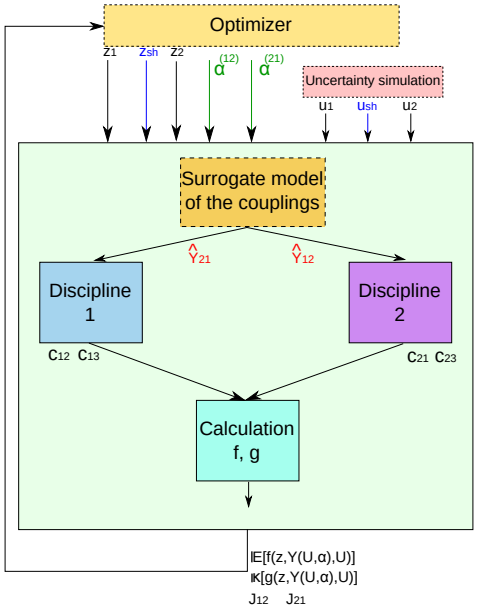

Figure 6.7: IDF-PCE design process

The system-level coupling variables are decomposed according to: $\hat{y}_{ij}(\mathbf{U}, \boldsymbol{\alpha}^{(ij)}) = \sum_{k=0}^{19} \alpha_k^{(ij)} \Psi_k(\mathbf{U})$, with $\Psi_k(\cdot)$ the product of Hermite and Legendre polynomials with a total expansion order of degree 3 in order to take into account the non linearity of the problem (see section 6.5 for a study of the PCE decomposition order). These polynomial bases are orthogonal to the input density distributions (Gaussian and uniform). As there are three uncertain variables for the decomposition, $\dim\left(\boldsymbol{\alpha}^{(12)}\right) = \dim\left(\boldsymbol{\alpha}^{(21)}\right) = \frac{(3+3)!}{3!3!} = 20$. The design space is of dimension 43. The methods to compute the multivariate integrals are detailed in the next paragraph.

IDF-PCE (CMC) formulation. In IDF-PCE with CMC, the interdisciplinary constraints are computed with:

$$J_{ij} \simeq \frac{1}{M}\sum_{k=1}^{M}\left[c_{ij}\left(z_{sh}, z_1, u_{sh(k)}, u_{1(k)}, \hat{y}_{.i}\left(\mathbf{u}_{(k)}, \boldsymbol{\alpha}^{(.i)}\right)\right) - \hat{y}_{ij}\left(\mathbf{u}_{(k)}, \boldsymbol{\alpha}^{(ij)}\right)\right]^2 \tag{6.35}$$

The mean of the objective function and the mean and the standard deviation of the constraint g are computed by CMC. The uncertainties are propagated with CMC on the decoupled system with a sample size of $M = 150000$. The interdisciplinary constraints on the couplings are such that $\epsilon = 10^{-3}$ in order to have on average a coupling error under ϵ. Another alternative to avoid a fixed ϵ value set by the designer is to convert the equality constraint of $J_{ij} = 0$ into an inequality constraint $J_{ij} \leq \epsilon$ where ϵ is a small positive real number, and use an additional dynamic slack variable to carry out the optimization process in order to minimize the value of ϵ to be as close as possible to 0.

IDF-PCE (quadrature) formulation. In the proposed decoupled formulation IDF-PCE with quadrature rules, the coupling constraints are computed as follows:

$$\begin{aligned} J_{ij} \quad = \quad & \sum_{k=1}^{M_{sh}}\sum_{l=1}^{M_1}\sum_{m=1}^{M_2}(w_{sh(k)} \otimes w_{1(l)} \otimes w_{2(m)})\left[c_{ij}\left(z_{sh}, z_1, u_{sh(k)}, u_{1(l)}, \hat{y}_{.i}\left(u_{sh(k)}, u_{1(l)}, u_{2(m)}, \boldsymbol{\alpha}^{(.i)}\right)\right)\right. \\ & \left. - \hat{y}_{ij}\left(u_{sh(k)}, u_{1(l)}, u_{2(m)}, \boldsymbol{\alpha}^{(ij)}\right)\right]^2 \end{aligned} \tag{6.36}$$

The expected value of $f(\cdot)$ and the mean and the standard deviation of the constraint $g(\cdot)$ are computed as explained in the quadrature rules paragraph (section 2.3.1.1). The quadrature rules used to compute the multidimensional integrals correspond to the tensor product of the one dimensional Gauss-Hermite and Gauss-Legendre quadratures. The number of sampling points in each direction is: $M_{sh} = M_2 = 8$ and $M_1 = 10$, resulting in a tensor product of 640 discipline evaluations to compute the multivariate integrals. This number of quadrature points is selected in order to have an error less than 10^{-3} compared to a CMC computation of the integrals with 1 000 000 points. The decomposition of the coupling variables is the same as in IDF-PCE with CMC formulation.

IDF-PCE (PCE) formulation. In this approach, the output PCE coefficients $\tilde{\boldsymbol{\alpha}}^{(ij)}$ are computed by orthogonal spectral projection based on Eq.(6.21) in which the multivariate integrals are computed by quadrature rules. The interdisciplinary constraints J_{12} and J_{21} are replaced by:

$$\| \boldsymbol{\alpha}^{(12)} - \tilde{\boldsymbol{\alpha}}^{(12)} \|^2 \leq \epsilon_\alpha \tag{6.37}$$

$$\| \boldsymbol{\alpha}^{(21)} - \tilde{\boldsymbol{\alpha}}^{(21)} \|^2 \leq \epsilon_\alpha \tag{6.38}$$

To compute the output PCE coefficients, we use the same quadrature rules as in IDF-PCE (quadrature) formulation: $M_{sh} = M_2 = 8$ and $M_1 = 10$. The constraints on the couplings are such that $\epsilon_\alpha = 0.5$ as it generates an error on average smaller than 10^{-3} compared to CMC approximation of the integral. The main difference with IDF-PCE quadrature formulation is in the coupling constraints to ensure the interdisciplinary couplings in realizations. In IDF-PCE (PCE) the quadratic constraints only involve the PCE coefficients and could facilitate the optimizer convergence.

6.4.0.3 Results

Due to the presence of uncertainty and the use of a stochastic optimizer, each optimization is repeated 10 times and the results given in Table 6.10 are the averages of the 10 optimizations. The ratio of the standard deviation over the expected value of the results is added in parenthesis in order to quantify the robustness of the results.

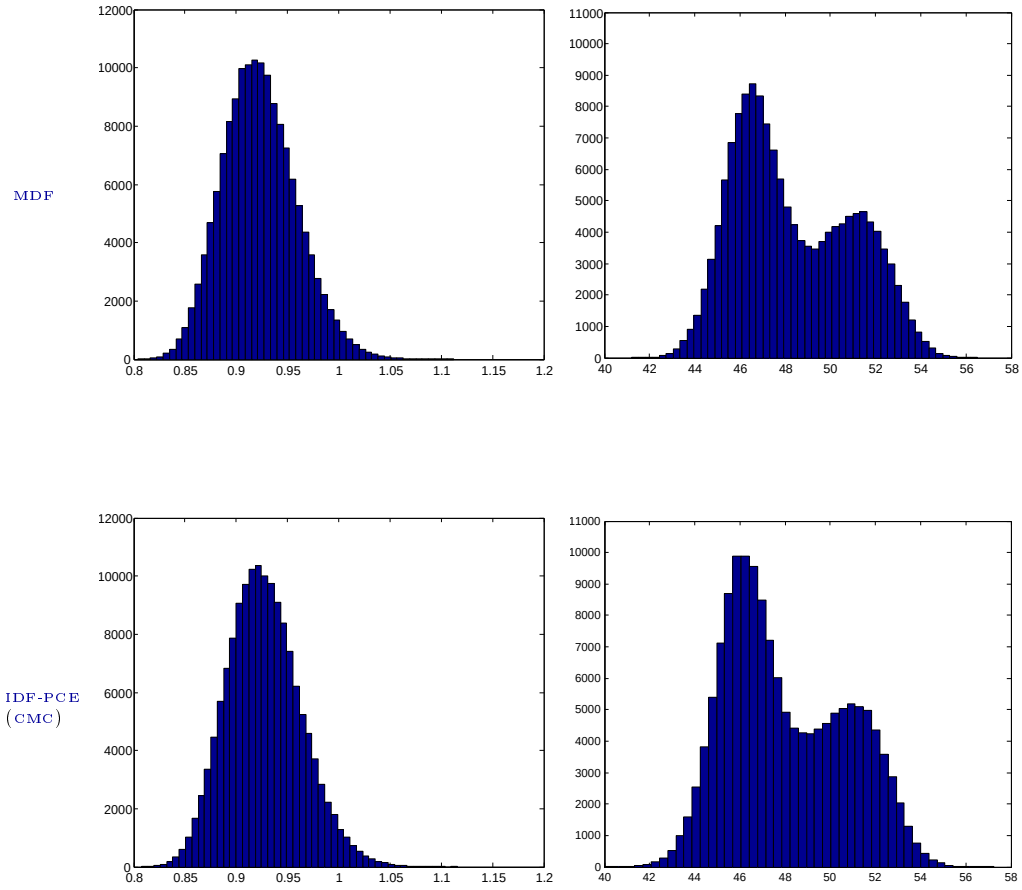

Figure 6.8: Distribution of the performance $f(\cdot)$ (left column) and the coupling variable Y_{12} (right column) estimated from 150000 $\mathbf{U}$ samples with MDF and IDF-PCE (CMC)

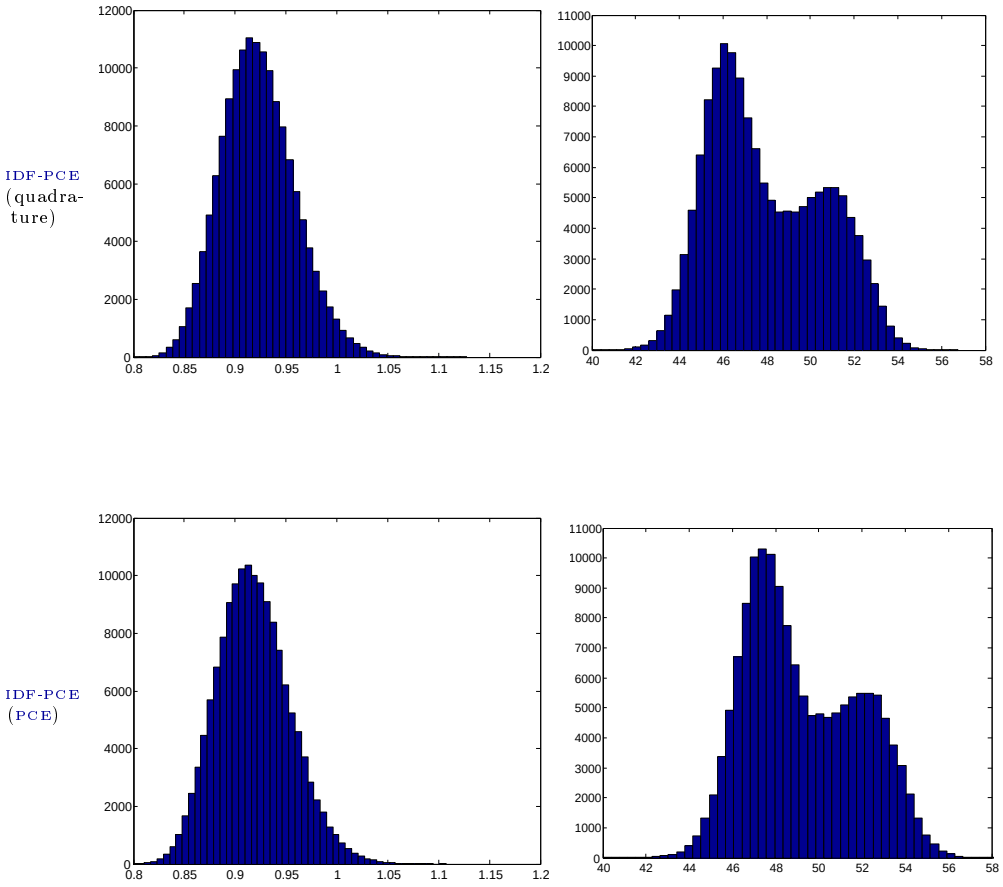

Figure 6.9: Distribution of the performance $f(\cdot)$ (left column) and the coupling variable Y_{12} (right column) estimated from 150000 $\mathbf{U}$ samples with IDF-PCE (quadrature) and IDF-PCE (PCE)

Table 6.10: Analytical test case results for the different proposed IDF-PCE formulations. In parenthesis, standard deviation over average of each result.

Results	MDF (ref)	IDF-PCE (CMC)	IDF-PCE (quadrature)	IDF-PCE (PCE)
Objective	$\mu_f = 0.928$ (0.64%)	$\mu_f = 0.926$ (0.65%)	$\mu_f = 0.926$ (0.70%)	$\mu_f = 0.914$ (0.49%)
Design variables	$z_{sh} = 0.520$ (0.63%) $z_1 = 0.340$ (1.13%) $z_2 = 0.658$ (1.55%)	$z_{sh} = 0.511$ (0.86%) $z_1 = 0.339$ (1.11%) $z_2 = 0.661$ (1.30%)	$z_{sh} = 0.514$ (1.34%) $z_1 = 0.340$ (1.27%) $z_2 = 0.661$ (1.68%)	$z_{sh} = 0.523$ (1.03%) $z_1 = 0.349$ (1.13%) $z_2 = 0.649$ (0.95%)
Coupling constraints	$\lvert c_{12} - y_{12}\rvert^2 \leq 0.0001$ $\lvert c_{21} - y_{21}\rvert^2 \leq 0.0001$	$J_{12} = 0.00067$ (1.23%) $J_{21} = 0.00057$ (1.15%)	$J_{12} = 0.00054$ (1.08%) $J_{21} = 0.00074$ (1.12)%	$\parallel \boldsymbol{\alpha}^{(21)} - \tilde{\boldsymbol{\alpha}}^{(21)} \parallel^2 = 0.48$ (1.56%) $\parallel \boldsymbol{\alpha}^{(21)} - \tilde{\boldsymbol{\alpha}}^{(21)} \parallel^2 = 0.3$ (2.13%)
Constraint $\mathbb{K}$ value	-0.001 (1.87%)	-0.002 (1.43%)	-0.001 (2.04%)	-0.002 (2.53%)
Design space dimension	3	43	43	43
Number of optimization iterations	$N_i = 2016$ (5.34%)	$N_i = 5608$ (14.5%)	$N_i = 5501$ (9.56%)	$N_i = 5262$ (8.10%)
Calls to each discipline	$N_d = \mathbf{1512 \times 10^6}$	$N_d = \mathbf{841.2 \times 10^6}$	$N_d = \mathbf{3.52 \times 10^6}$	$N_d = \mathbf{3.37 \times 10^6}$
Number of calls reduction factor	**1** (Ref)	**1.80**	**429.55**	**448.66**

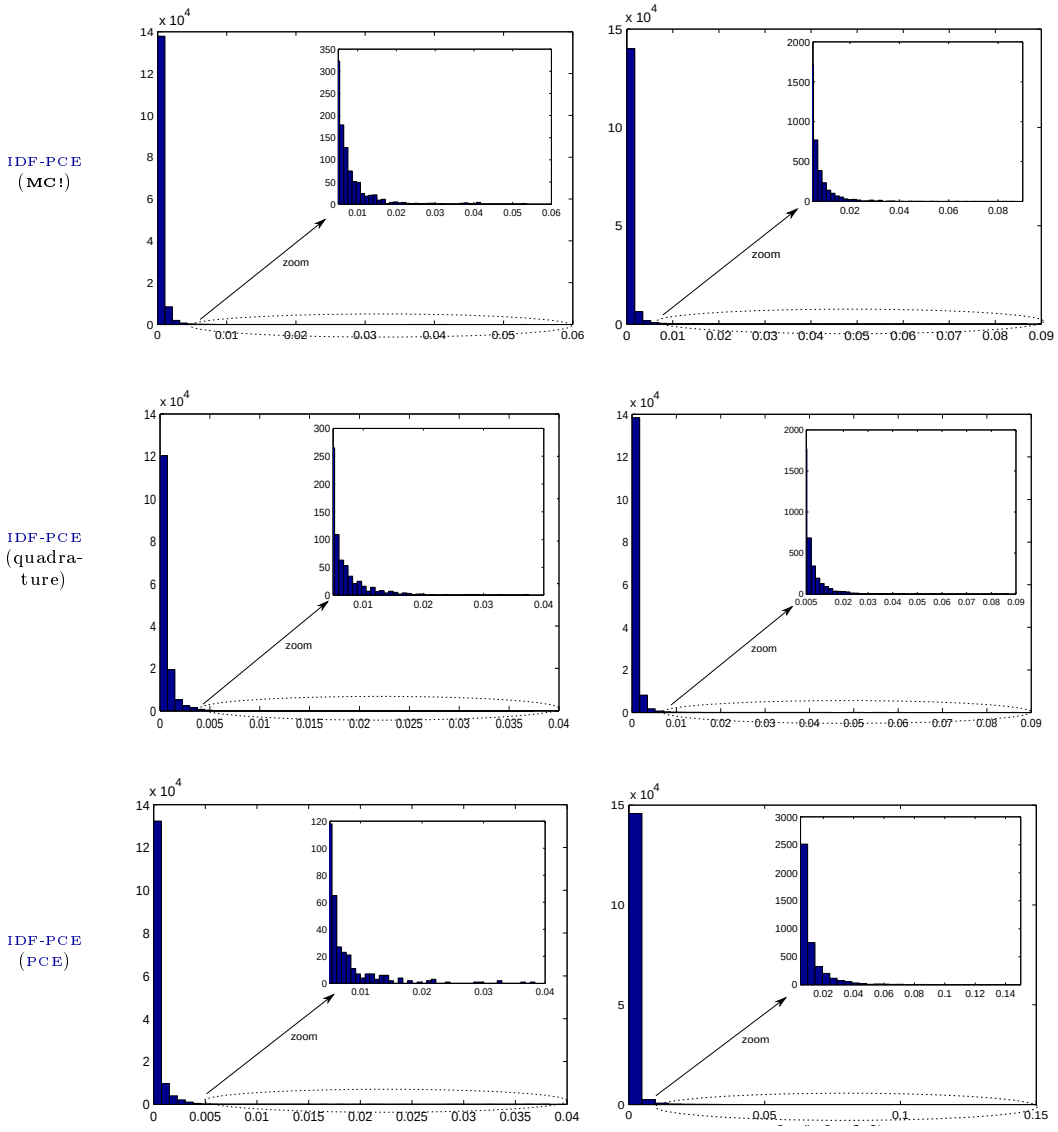

Figure 6.11: Distribution of the coupling errors $\mathbf{J}$. Left column, estimations of J_{12} , right column, estimations of J_{21}, from 150000 $\mathbf{U}$ samples.

In order to highlight the importance of incorporating uncertainty in MDO problems, a deterministic MDF optimization with the uncertain variables set to their mean values is performed. The optimal objective value is 0.466, the set of optimal design variables is: $z_{sh} = 0.504$, $z_1 = 0.452$, $z_2 = 0.682$ and the constraint is saturated. A propagation of uncertainty based on the found deterministic optimum $\mathbf{z}^*$ results in a violation of the constraint $\mathbb{E}[g(\mathbf{z}^*, \mathbf{Y}(\mathbf{z}^*, \mathbf{U}), \mathbf{U}))] +$

$3\sigma[g(\mathbf{z}^*, \mathbf{Y}(\mathbf{z}^*, \mathbf{U}), \mathbf{U})] = 2.73 > 0$ and the performance is decreased compare to the deterministic value $\mathbb{E}[f(\mathbf{z}^*, \mathbf{Y}(\mathbf{z}^*, \mathbf{U}), \mathbf{U}))] = 0.831$. For this analytical test case, the presence of uncertainty modifies both the optimal objective and the set of optimal design variables, but it results in a non robust deterministic solution.
The MDF under uncertainty formulation is considered as the reference for interdisciplinary coupling satisfaction as the couplings are satisfied for each uncertain variable realization. MDF and the proposed formulations converge to the same design variable $\mathbf{z}$ with errors inferior to 2.04% in terms of distance to MDF results. IDF-PCE (quadrature) provides the smaller error. The higher error stems from IDF-PCE (PCE) due to the approximations introduced by the output coupling PCEs $\tilde{\mathbf{c}}(\cdot)$. In terms of objective values, the relative error compared to MDF is of 0.21% for IDF-PCE (CMC) and IDF-PCE (quadrature) and 1.5% for IDF-PCE (PCE). The design space dimension is 3 in the MDF approach whereas it is 43 in the proposed formulations. The number of constraints is 1 in MDF whereas it is 3 in the proposed formulations. The increase in number of design variables and constraints leads to more optimization iterations. The number of calls to each discipline is 1512×10^6 for MDF. It is divided by 1.80 for IDF-PCE (CMC) formulation. Compared to MDF, the number of calls to each discipline decreases by a factor of 430 in IDF-PCE (quadrature) and by 449 in IDF-PCE (PCE). The reduction of the number of calls to the disciplines is due to the absence of complete MDA and the uncertainty propagation technique (quadrature and PCE) instead of CMC. While the absence of MDA decreases the number of calls to the disciplines, it generates higher errors in the interdisciplinary coupling satisfaction: the couplings are satisfied with a precision of 10^{-4} in MDF for all the realizations of the uncertain variables and with a precision of 6.7×10^{-4} on average in IDF-PCE (CMC). The replacement of CMC in IDF-PCE enables to decrease the number of calls to the disciplines while ensuring coupling satisfaction with a precision of 7.4×10^{-4} on average. The distribution of the performance values given by MDF and by the proposed approaches are similar (Figs. 6.8,6.9). The distributions of the coupling variable Y_{12} have the same tendencies for MDF and the decoupled approaches. Moreover, it can be noted that the proposed approaches succeed to handle multimodal probability density for the coupling variables. However, differences may be noted in the distribution tails (Figs. 6.8,6.9). This is due to the error introduced by the PCE metamodeling of the coupling relations. All the distributions of the coupling errors $\mathbf{J}$ for the proposed formulation are given Figure 6.11. The distributions have a small dispersion around 0, and the higher dispersion arises for IDF-PCE (PCE).
It is important to note that derivatives of the interdisciplinary coupling constraints could be used to ensure multidisciplinary feasibility. In practice, in numerical implementations, we use:

$$\mathbf{J}_{ij} = \int_{\mathbf{\Omega}} \left[\mathbf{c}_{ij} \left(\mathbf{z}_i, \hat{\mathbf{y}}_{.i} \left(\mathbf{u}, \boldsymbol{\alpha}^{(.i)} \right), \mathbf{u}_i \right) - \hat{\mathbf{y}}_{ij} \left(\mathbf{u}, \boldsymbol{\alpha}^{(ij)} \right) \right]^2 \phi(\mathbf{u}) \mathrm{d}\mathbf{u} \leq \boldsymbol{\epsilon} \tag{6.39}$$

For conciseness, we note $\left[\mathbf{c}_{ij} \left(\mathbf{z}_i, \hat{\mathbf{y}}_{.i} \left(\mathbf{u}, \boldsymbol{\alpha}^{(.i)} \right), \mathbf{u}_i \right) - \hat{\mathbf{y}}_{ij} \left(\mathbf{u}, \boldsymbol{\alpha}^{(ij)} \right) \right]^2 = \mathbf{j}_{ij} \left(\mathbf{z}_i, \boldsymbol{\alpha}^{(ij)}, \boldsymbol{\alpha}^{(.i)}, \mathbf{u} \right)$. Another way to ensure multidisciplinary feasibility could be to use:

- a robust approach:

$$\begin{aligned} \mathbf{J}_{ij} \quad = \quad & \int_{\mathbf{\Omega}} \mathbf{j}_{ij} \left(\mathbf{z}_i, \boldsymbol{\alpha}^{(ij)}, \boldsymbol{\alpha}^{(.i)}, \mathbf{u} \right) \phi(\mathbf{u}) \mathrm{d}\mathbf{u} \\ & + \boldsymbol{\eta} \left(\int_{\mathbf{\Omega}} \left[\mathbf{j}_{ij} \left(\mathbf{z}_i, \boldsymbol{\alpha}^{(ij)}, \boldsymbol{\alpha}^{(.i)}, \mathbf{u} \right) - \mathbb{E} \left[\mathbf{j}_{ij} \left(\mathbf{z}_i, \boldsymbol{\alpha}^{(ij)}, \boldsymbol{\alpha}^{(.i)}, \mathbf{u} \right) \right] \right]^2 \phi(\mathbf{u}) \mathrm{d}\mathbf{u} \right)^{\frac{1}{2}} \leq \boldsymbol{\epsilon} \end{aligned}$$

with $\boldsymbol{\eta}$ indicating the restriction of the feasible region to $\boldsymbol{\eta}$ standard deviations away from the expected value.

- a reliability approach:

$$\mathbf{J}_{ij} = \int_{\boldsymbol{\Omega}} \mathbb{1}_{\left[\frac{\mathbf{j}_{ij}\left(\mathbf{z}_i, \boldsymbol{\alpha}^{(ij)}, \boldsymbol{\alpha}^{(.i)}, \mathbf{u}\right)}{\mathbf{c}_{ij}\left(\mathbf{z}_i, \hat{\mathbf{y}}_{.i}\left(\mathbf{u}, \boldsymbol{\alpha}^{(.i)}\right), \mathbf{u}_i\right)^2}\right] > k} \phi(\mathbf{u}) \mathrm{d}\mathbf{u} \leq \mathbb{P}_t \tag{6.40}$$

where $\mathbb{P}_t$ is a maximal target probability of failure and k is a scalar value. The reliability constraint ensures that the probability that the relative error between the input coupling variables and the output coupling variables to be superior to $k\%$ is lower than $\mathbb{P}_t$.

However, in practice, Eq.(6.40) and Eq.(6.40) require an important computational effort compared to Eq.(6.39) and further investigations are needed to reduce the computational cost in order to use them.

6.5 Influence of the PCE degree decomposition

One of the difficulties with the proposed approach is to choose *a priori* the degree of decomposition of the PCE used to represent the coupling relations. Depending on the degree of truncation, PCE may model very different dynamics. In Figure 6.12, the first five Hermite based PCE for a one dimensional function are plotted. The zero order PCE may model constant dynamics whereas the first order models linear functions and the second order represent quadratic dynamics, and higher order more complex mappings.

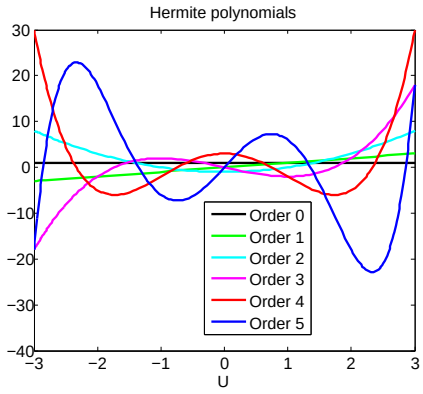

Figure 6.12: The first five Hermite polynomials for one dimensional function

The decomposition order influences the interdisciplinary coupling modeling at the convergence of the UMDO problem. Higher degrees of decomposition may capture more complex coupling relations however it comes to a cost, the increase in the number of PCE coefficients that have to be controlled by the system-level optimizer. A trade-off has to be made between the accuracy of the coupling modeling (increase in the PCE degree decomposition improves the accuracy of the

coupling modeling) and the complexity of the IDF-PCE solving (higher dimensional problem to solve).
For the previous analytical problem, we study the influence of the PCE degree decomposition by fixing the design variables to the optimum found in the previous section: $\mathbf{z}^* = [0.520, 0.340, 0.658]^{\mathrm{T}}$ and by evaluating the coupling error J_{12} for different PCE degrees of decomposition.
Figure 6.13 presents the distribution of the coupling Y_{12} for different PCE decomposition order. With a degree of 1, the coupling distribution is similar to a Gaussian distribution. The mean value of $\hat{Y}_{12}$ is close to the one resulting from a coupled analysis ($\mu_{Y_{12}} = 48.07$), however the coupling error is large between 0% and 12% and the distribution of $\hat{Y}_{12}$ does not present the two modes around $\hat{y}_{12} = 46$ and $\hat{y}_{12} = 52$ as in the coupled approach. The number of PCE coefficients are $\dim\left(\boldsymbol{\alpha}^{(12)}\right) = \frac{(3+1)!}{3!1!} = 4$. With a decomposition degree of 2, the coupling variable distribution is non Gaussian and present one mode around $\hat{y}_{12} = 46$ but not around 52. The coupling error is still large but now around 0% and 8% with more samples between 0% and 2% compared to the order 1. The number of PCE coefficients are $\dim\left(\boldsymbol{\alpha}^{(12)}\right) = \frac{(3+2)!}{3!2!} = 10$. The decomposition order of 3 provide accurate results compared to coupled approaches with a coupling relative error between 0% and 2%, however it requires 20 PCE coefficients. A decomposition order of 3 seems appropriate to model the coupling functional relation of Y_{12}.

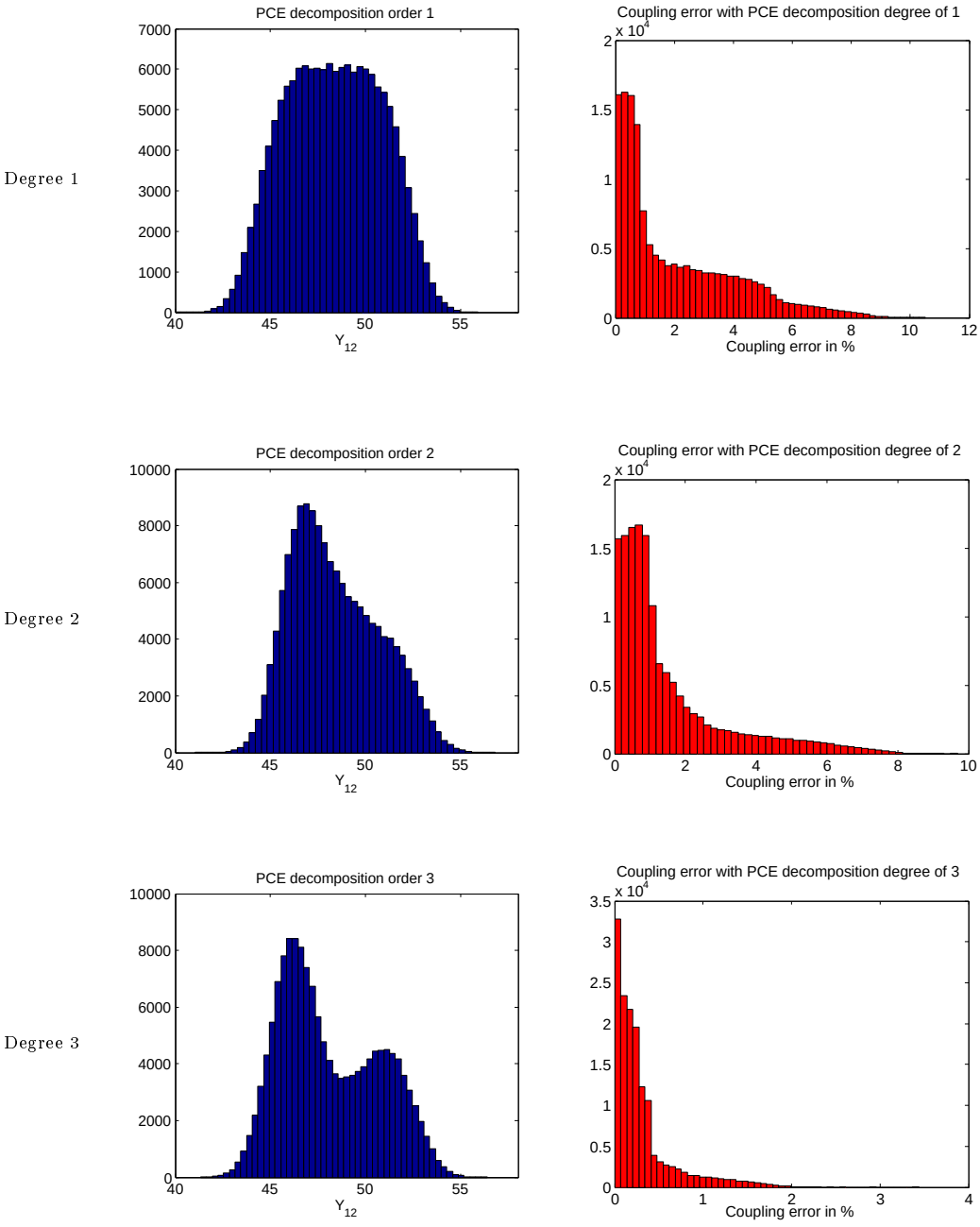

Figure 6.13: PCE decomposition order and coupling error. Left column, distribution of Y_{12}, right column, coupling relative error, from 150000 $\mathbf{U}$ samples.

In order to efficiently use IDF-PCE, the designer in collaboration with the discipline experts has to know for some design architectures, the degree of linearity of the coupling relations in order to correctly choose the PCE orders. If, based on a decomposition order assumption, at the UMDO convergence, the interdisciplinary couplings are not satisfied according to the requirements, a new problem may be solved with a higher degree of decomposition to capture more complex mappings between the disciplines. Moreover, adapted degree of decomposition for the couplings could be assessed based on information provided by MDA if such coupled analyses are affordable for some design variable values. Other alternatives in terms of degree of decomposition of PCE could be to use Least Angle Regression [Efron et al., 2004] method or to use Sparse PCE approaches [Blatman and Sudret, 2011]. However, in order to use Sparse PCE technique, it is necessary to run the exact function (in our case a MDA) which is not the philosophy of the proposed approach. However, future investigations should explore that possibility.

6.6 Conclusion

A new single-level decoupled UMDO formulation has been detailed in this chapter. The proposed *Individual Discipline Feasible - Polynomial Chaos Expansion* formulation ensures the system *multidisciplinary feasibility* for all the realizations of the uncertain variables. The satisfaction of the interdisciplinary couplings *in realizations* is important to ensure the physical relevance of the obtained designs and makes the proposed decoupled approach equivalent to a coupled formulation. IDF-PCE is based on the iterative construction of surrogate models (Polynomial Chaos Expansion) of the functional coupling relations. The PCE coefficients are controlled by the system-level optimizer and integral coupling constraints are imposed to ensure the interdisciplinary coupling satisfaction. This method allows to decompose the design process and to let engineering teams spread all over the world work in parallel. Three techniques have been used to compute the multidimensional integrals involved in the statistical moment calculations and the coupling constraints: CMC, quadrature rules and output coupling decomposition over PCE. Numerical comparisons between the reference MDF formulation and the proposed formulations have been performed on an analytical test case. It shows a decrease in the number of calls to the disciplines for the same accuracy of the optimal design. Moreover, for a same degree of numerical accuracy, IDF-PCE-PCE and and IDF-PCE (quadrature) enable to decrease by a factor of 400 the computational cost compared to MDF. Moreover, the numerical integration by quadrature and the discipline output decomposition over a PCE decrease by a factor of 240 the number of calls to the disciplines compared to CMC for the same level of accuracy.
In the following chapter 7, a new multi-level hierarchical UMDO formulation is proposed and derived from SWORD formulation [Balesdent et al., 2012a] in order to facilitate the design process of the system-level optimizer. The future work will naturally consists in applying the proposed formulations on a launch vehicle design test case. This is the purpose of chapter 8.

Chapter 7

Multi-level Hierarchical MDO formulation with functional coupling satisfaction under Uncertainty

Contents

Chapter goals

- Develop a multi-level UMDO formulation ensuring interdisciplinary coupling satisfaction for all the realizations of the uncertain variables,
- Develop a UMDO formulation adapted to launch vehicle design process.

7.1 Introduction

This chapter is devoted to the description of a new UMDO formulation called Multi-level Hierarchical Optimization under Uncertainty (MHOU) ensuring the coupling satisfaction for all the realizations of the uncertain variables. The proposed approach relies on two levels of optimization and on surrogate models in order to ensure, at the convergence of the system optimization problem, the coupling functional relations between the disciplines. The formulation is inspired from SWORD (Stage-Wise decomposition for Optimal Rocket Design) which is a formulation dedicated to launch vehicle design. Traditionally, in literature the design process of a launch vehicle is decomposed according to the different involved disciplinary analyses (*e.g.* propulsion, aerodynamics, *etc.*). Balesdent *et al.* [Balesdent et al., 2012a] proposed a new deterministic MDO formulation that decomposes the design problem according to the different stages of the rocket. This decomposition

has been compared to MDF and numerical comparisons showed it improves the efficiency of the MDO process. The authors proposed four variants of SWORD depending on the handling of the coupling variables. This chapter is focused on the generalization of one of the variant to the design of any system in the presence of uncertainty. It is a semi-decoupled formulation which removes the feedback couplings of a multidisciplinary design process while ensuring the multidisciplinary feasibility. It relies on the same idea as for the single-level IDF-PCE formulation for the interdisciplinary coupling handling but it introduces several levels of optimization. In section 7.2, MHOU is detailed with the design process. The mathematical formulation and explanatory scheme are provided. In Chapter 8, MHOU formulation will be applied to a launch vehicle design test case.

7.2 Proposed multi-level formulation: Multi-level Hierarchical Optimization under Uncertainty (MHOU)

The aim of MHOU is to ease the system-level optimizer by introducing a susbsystem-level optimization (Fig. 7.1). It is based on the same interdisciplinary coupling handling method as IDF-PCE. MHOU is a semi-decoupled hierarchical method that removes all the feedback interdisciplinary couplings in order to avoid the expensive disciplinary loops through MDA. Due to the curse of dimensionality of the surrogate model-based decoupling technique proposed in IDF-PCE (≤ 5 uncertain variables and ≤ 5 coupling variables), only the feedback couplings are removed in MHOU. It allows a hierarchical design process without any loops between the subsystems. This type of decomposition is proposed in the context of launch vehicle design, but it may be generalized to a set of problems. Indeed, the formulation assumes that the system-level objective $\Xi[f(\cdot)]$ is decomposable into a sum of subsystem contributions $\Xi[f(\cdot)] = \sum_{k=1}^{N} \Xi[f_k(\cdot)]$ where $\Xi[f_k(\cdot)]$ is the k^{th} subsystem objective function. For instance, the Gross Lift-Off Weight (GLOW) of a launch vehicle is decomposable as the sum of the stage masses. Other systems may also be decomposed according to the contribution of the subsystems (contributions of the subsystem costs, of the subsystem sizes, *etc.*).

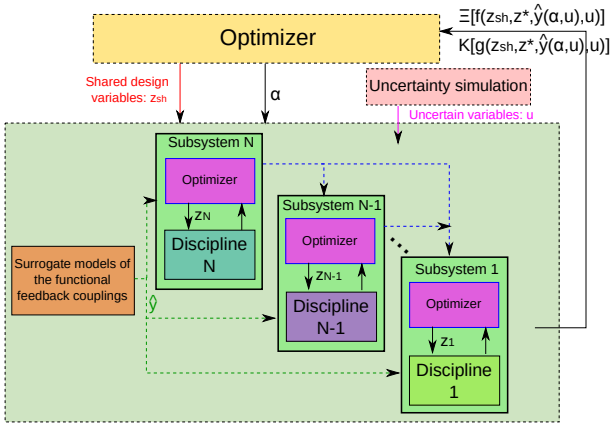

Figure 7.1: Multi-level Hierarchical Optimization under Uncertainty (MHOU)

In MHOU, the system-level and subsystem-level formulations are given by:

- System-level:

$$\begin{aligned}
\min \quad & \sum_{k=1}^{N} \Xi\left[f_k(\mathbf{z}_{sh}, \mathbf{z}_k^*, \boldsymbol{\alpha}, \mathbf{U})\right] && (7.1)\\
\text{w.r.t.} \quad & \mathbf{z}_{sh} \in \mathcal{Z}_{sh}, \boldsymbol{\alpha} \\
\text{s.t.} \quad & \mathbb{K}\left[\mathbf{g}(\mathbf{z}_{sh}, \mathbf{z}_k^*, \boldsymbol{\alpha}, \mathbf{U})\right] \leq 0 && (7.2)\\
& \forall (k,j) \in \{1,...,N\}^2,\ j \neq k\ \mathbf{J}_{kj}(\mathbf{z}_{sh}, \mathbf{z}_k^*, \boldsymbol{\alpha}) = 0 && (7.3)\\
& \forall k \in \{1,...,N\},\ \mathbb{K}\left[\mathbf{g}_k(\mathbf{z}_{sh}, \mathbf{z}_k^*, \boldsymbol{\alpha}, \mathbf{U})\right] \leq 0 && (7.4)
\end{aligned}$$

- Subsystem-level:

$k = N$

$$\begin{aligned}
\text{While} \quad & k > 0 \\
\text{Given} \quad & \mathbf{y}_{Nk}, \ldots, \mathbf{y}_{(k+1)k} \\
& \text{For the } k^{\text{th}} \text{ subsystem} \\
\min \quad & \Xi\left[f_k(\mathbf{z}_{sh}, \mathbf{z}_k, \boldsymbol{\alpha}, \mathbf{U})\right] && (7.5)\\
\text{w.r.t.} \quad & \mathbf{z}_k \in \mathcal{Z}_k \\
\text{s.t.} \quad & \mathbb{K}\left[\mathbf{g}_k(\mathbf{z}_{sh}, \mathbf{z}_k, \boldsymbol{\alpha}, \mathbf{U})\right] \leq 0 && (7.6)\\
& \forall j \in \{1,...,N\},\ j \neq k\ \mathbf{J}_{kj} = \\
& \int_{\boldsymbol{\Omega}} \left[\mathbf{c}_{kj}\left(\mathbf{z}_{sh}, \mathbf{z}_k, \hat{\mathbf{y}}_{.k}\left(\mathbf{u}, \boldsymbol{\alpha}^{(.k)}\right), \mathbf{u}_k\right) - \hat{\mathbf{y}}_{kj}\left(\mathbf{u}, \boldsymbol{\alpha}^{(kj)}\right)\right]^2 \phi(\mathbf{u}) \mathrm{d}\mathbf{u} = \mathbf{0} && (7.7)\\
& k \leftarrow k - 1
\end{aligned}$$

$\mathbf{z}_k$ is the local design variable vector of discipline k and it belongs to the set $\mathcal{Z}_k$ and $\mathbf{z}_{sh}$ is the shared design variable vector between several disciplines. $\mathbf{z}_k^*$ is the optimal design variables found by the subsystem-level optimizer. This formulation allows one to optimize each subsystem separately in a hierarchical process. The system-level optimizer handles $\mathbf{z}_{sh}$ and the PCE coefficients $\boldsymbol{\alpha}$ of the feedback coupling variables. The handling of PCE coefficients at the system-level allows one to remove the feedback couplings and to optimize the subsystems in sequence. The surrogate models of the functional feedback couplings provide the required input couplings to the different subsystems. The k^{th} subsystem-level optimizer handles $\mathbf{z}_k$ and the corresponding problem aims at minimizing the subsystem contribution to the system objective while satisfying the subsystem-level constraints $\mathbb{K}\left[\mathbf{g}_k(\cdot)\right]$. The interdisciplinary coupling constraint Eq.(7.7) guarantees the couplings whatever the realization of the uncertain variables. In MHOU formulation, Eq.(7.7) is only considered for $k \neq N$. This formulation is particularly suited for launch vehicle in order to decompose the design process into the different stage optimizations. The decreasing order of the discipline optimization, from N to 1 is more convenient for a launch vehicle (the last stage is optimized first, then the intermediate stages and the first one is optimized last), however, in general case any order may be adopted. In practice, the disciplines are organized to have the minimal number of feedback coupling variables in order to decrease the number of coupling variables controlled at the system-level and therefore

the complexity of the optimization problem. For the launch vehicle design problems, with SWORD and MHOU, the feedforward coupling variables are the masses of the different stages (the mass is passed from stage i to stage $i-1$) and the feedback couplings are the separation conditions (altitude, velocity, flight path angle) and trajectory loads.

7.3 Conclusion

MHOU is a semi-decoupled, multi-level, hierarchical UMDO approach. MHOU is not limited to launch vehicle system but to any system whose system-level objective may be decomposed according to subsystem contributions. The proposed formulation is derived from SWORD formulations [Balesdent et al., 2012a] and based on the same interdisciplinary coupling handling approach as IDF-PCE. It offers an autonomy to engineering teams to optimize their own subsystem in coordination with a system-level designer. The surrogate models provide a representation of the feedback coupling mappings at the convergence of the UMDO problem as would MDA do. In the next chapter, both IDF-PCE and MHOU formulations will be applied to launch vehicle design problems.

Chapter 8

Applications of the proposed UMDO formulations to launch vehicle design

Contents

Chapter goals

- Apply the developed formulations in chapters 6 and 7 to launch vehicle test cases,
- Compare the results with respect to classical Multi Disciplinary Feasible formulation.

8.1 Introduction

This chapter is devoted to the comparison of IDF-PCE and MHOU formulations with respect to the classical MDF under uncertainty. MDF is the reference formulation to evaluate the efficiency of the proposed methods as it is the most commonly used formulation for launch vehicle design as highlighted in section 3.5. Two design problems are considered. Section 8.2 focuses on the design of a launch vehicle composed of two stages aiming at injecting a payload into a Geostationary Transfer Orbit. MDF and IDF-PCE formulations are compared on this test case. Then, section 8.3 focuses on the design of a two stage sounding rocket for experimental purposes with a required minimal apogee altitude. MDF, IDF-PCE and MHOU formulations are compared on this second test case.

8.2 IDF-PCE for launch vehicle design

This launch vehicle test case consists in designing a launch vehicle composed of two stages to inject a payload of 4000kg into a Geostationary Transfer Orbit (GTO) from Kourou (French Guyana). The target orbit is 250×35786 km. At the early design phase, to comply with the request in payload mass, it is necessary to take into account the uncertainties due to the disciplinary models and the physical phenomena that are not well known at the beginning of the design effort. In this test case, we are interested in designing a two stage launch vehicle with UMDO methodologies and in comparing MDF and the proposed IDF-PCE formulations. Four disciplines are involved: propulsion, mass budget and geometry design, aerodynamics and trajectory (Fig. 8.1).

8.2.1 Design and uncertain variables

The objective of the UMDO problem is to minimize the expected value of the Gross Lift-Off Weight (GLOW) of the launch vehicle. The problem has seven design variables (Table 8.5). The optimization problem is initialized at an existing baseline (Table 8.5) that has to be optimized. The problem also incorporates three aleatory uncertain variables modeled according to typical level of uncertainty in early design phases [Gordon and McBride, 1996; Castellini, 2012]:

- 1^{st} stage specific impulse error: $Isp_{v1} \sim Isp_{v10} + \mathcal{N}(0, 0.6)$ (Fig. 8.2),
- 2^{nd} stage dry mass error: $Me \sim Me_0 + \mathcal{N}(0, 100)$ (Fig. 8.3),
- 2^{nd} stage thrust error: $T_2 \sim T_{20} + \mathcal{N}(0, 600)$ (Fig. 8.4).

These errors are additional terms to the nominal value of specific impulse (Isp_{v10}), of dry mass (Me_0) and thrust (T_{20}). We note: $\mathbf{z} = [D_1, Mp_1, T_1, OF_1, D_2, Mp_2, Der]^{\mathrm{T}}$ and $\mathbf{U} = [Isp_{v1}, T_2, Me]^{\mathrm{T}}$.

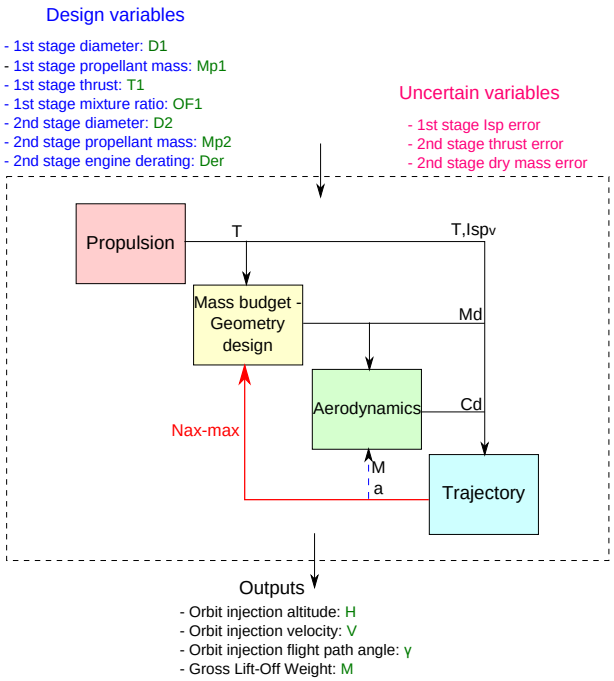

Figure 8.1: Design Structure Matrix for the two stage launch vehicle

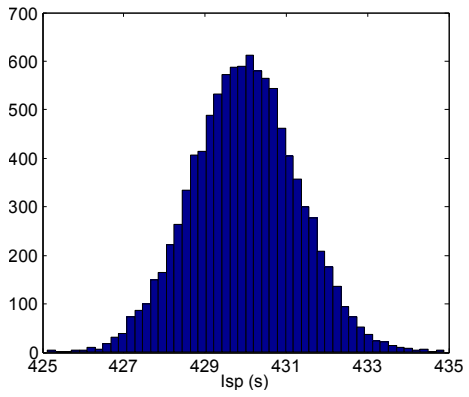

Figure 8.2: Distribution of the Isp uncertainty

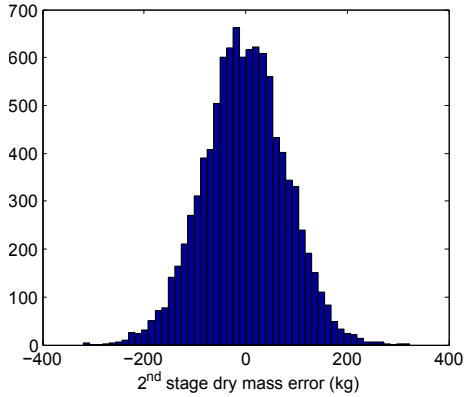

Figure 8.3: Distribution of the dry mass error uncertainty

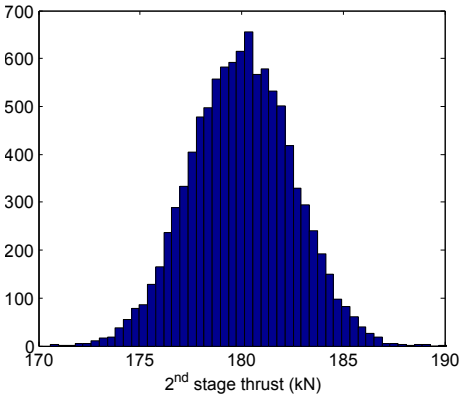

Figure 8.4: Distribution of the thrust uncertainty

Table 8.5: Design variables for the two stage launch vehicle

Variables	Symbol	Domain of definition	Baseline
1^{st} stage diameter	D_1	$[2.5, 5.5]$ (m)	$4.3m$
1^{st} stage propellant mass	M_{p1}	$[100000, 150000]$ (kg)	$125000kg$
1^{st} stage thrust	T_1	$[2500, 3400]$ (kN)	$3000kN$
1^{st} stage mixture ratio	OF_1	$[2.7, 6.5]$	4.2
2^{nd} stage diameter	D_2	$[2.5, 5.5]$ (m)	$3.5m$
2^{nd} stage propellant mass	M_{p2}	$[20000, 35000]$ (kg)	$30000kg$
2^{nd} stage engine derating	Der	$[92, 100]\%$	97%

The UMDO problem includes one inequality constraint which is the probability of failure of the mission (incorporating the altitude h, velocity v and flight path angle γ of the injection point) that has to be inferior to 5×10^{-2}.
For the injection into orbit, a failure occurs when the payload is injected outside a closed ball around the target injection point defined in the rotating frame by: $h_t = 250$km, $v_t = 9.713$km/s and $\gamma_t = 0°$. The radius of the ball corresponds to the injection tolerances and is set to be at 1% of the target altitude, at 0.5% of the target velocity and at 0.4° of the target flight path angle. To be feasible, the launch vehicle must have at least a probability of 95% to reach the target injection point (within the tolerances). In the next sections the involved disciplines are briefly detailed. For more information on the discipline models see the appendices.

8.2.2 Disciplinary models

8.2.2.1 Propulsion

In this test case, all the stages use liquid oxygen (LOx) and liquid hydrogen (LH2) cryogenic propulsion. The propulsion discipline is based on the NASA computer program CEA (Chemical Equilibrium with Applications [Gordon and McBride, 1996]) which computes chemical equilibrium compositions and properties of complex mixtures but also the dynamics of the expansion of gases

through the engine nozzle. The aim of the propulsion discipline is to compute the specific impulse in vacuum Isp_v(s) based on mixture ratio between LOx and LH2 and thermochemical data [Sutton and Biblarz, 2010]. For that, CEA computes the characteristic velocity (c^*) and the coefficient of thrust (c_τ) with shifting equilibrium until the nozzle throat and frozen expansion after. Isp_v and thrust T are coupling variables for the trajectory and mass budget disciplines.

8.2.2.2 Mass budget and geometry design

The mass budget and geometry design discipline aims at estimating the mass of the launcher and its geometry. The 1st and the 2nd stages are LOx/LH2 stages with common bulkhead. The dry mass of the stages (M_{di} for stage i) is the sum of the masses of the tanks, turbopumps, combustion chamber, nozzle, pressurization system, structural masses and avionics. The mass and geometry models are derived from the engineering models for the conceptual design of launch vehicle developed by Castellini [Castellini, 2012]. Interdisciplinary coupling between the mass budget and geometry design discipline and the trajectory is required to model the dependencies between the dry mass and the loads undergone during the flight. The maximal axial load factor Nax_{max} is the feedback coupling variable (Fig. 8.1).

8.2.2.3 Aerodynamics

The aerodynamics discipline consists in computing the aerodynamics coefficients such as the drag and lift coefficients required to compute the aerodynamics loads during the rocket atmospheric flight. A zero-lift model is used. The calculations of the drag coefficients are based on the US Air Force computer program MissileDATCOM [Blake, 1998] which relies on an experimental data base to determine the aerodynamics forces and coefficients of complex rocket geometries. A drag coefficient table as a function of the Mach is directly given to the trajectory discipline allowing to remove the feedback loop between the trajectory and the aerodynamics. This model is generally sufficient in the early design studies.

8.2.2.4 Trajectory

A three dimensional model with rotating round Earth (radius 6371km) is used. The trajectory discipline consists in solving an optimization problem. The objective of trajectory optimization is to minimize the distance between the injection point and the given target. In order to take the uncertainties into account, trajectory optimization is performed for each realization of the uncertain variables involved in the computation of the objective or the constraints. First, an optimization problem solving (using a pattern search algorithm [Audet and Dennis Jr, 2002]) yields a nominal feasible trajectory where the uncertain variables are set to their expected values. Then, for the uncertainty propagation, local trajectory optimizations (using a SQP algorithm) are performed for each realization of the uncertain variables. The trajectory optimization consists in defining crossing points (in dimension 13) for the pitch angle and modifying them to satisfy the specifications of the mission. The pitch angle is calculated by piecewise linear functions. The trajectory discipline computes the load $c_{Nax_{max}}$ required to simulate the mass budget and geometry design discipline.

All the models have been integrated inside a Matlab environment. CEA and MissileDATCOM have been reuse with some adaptations for interfaces with Matlab. Mass budget and geometry design

and the trajectory discipline have been completely redeveloped based on the given references. The test case has been performed with a desktop computer with 4 processors Intel Xeon CPU E5-1603 2.80GHz. A single run of MDA is in the order of few minutes. The parallel computing Matlab toolbox has been used in order to propagate uncertainty in parallel over all the processors.

8.2.3 Application of MDF under uncertainty

MDF is the reference formulation as the interdisciplinary system of equations is solved for each uncertain variable realization. The system is solved by FPI with a convergence criterion $|c_{N_{ax_{max}}} - y_{N_{ax_{max}}}|^2 \leq 10^{-4} m^2 s^{-4}$ between the input coupling variable $y_{N_{ax_{max}}}$ and the output coupling variable $c_{N_{ax_{max}}}$. Based on the numerical experimentation, 3 iterations are in general necessary to converge under the tolerance with the FPI methods. The uncertainty is propagated with CMC to estimate the objective function with $M_s = 100$ samples in order to have at most an error of 250kg in the GLOW expected value approximation. The probability of failure is computed by the approach described in section 6.3. The initial DoE is based on a Latin Hypercube Sampling of 100 samples. The GMm refinement strategy adds 96 new samples in order to accurately represent the limit state function in high probability density regions. A pattern search optimization algorithm [Audet and Dennis Jr, 2002] is used to solve both MDF and IDF-PCE (CMC) problems in order to uniquely compare the advantages of the formulation independently from the optimization algorithm. The MDF formulation is given by:

$$\begin{aligned}
\min \quad & \mathbb{E}\left[\text{GLOW}\left(\mathbf{z}, \mathbf{U}\right)\right] && (8.1)\\
\text{w.r.t.} \quad & \mathbf{z} = \left[D_1, M_{p1}, T_1, OF_1, D_2, M_{p2}, Der\right]^{\mathrm{T}} && \\
\text{s.t.} \quad & \mathbb{P}_f(\mathbf{z}, \mathbf{U}) \leq 5 \times 10^{-2} && (8.2)\\
& \mathbf{z}_{\min} \leq \mathbf{z} \leq \mathbf{z}_{\max} && (8.3)
\end{aligned}$$

with: $\mathbb{P}_f(\mathbf{z}, \mathbf{U}) = 1 - \mathbb{P}\left[(247.5 \leq h_t \leq 252.5) \cap (9.703 \leq v_t \leq 9.723) \cap (-0.4 \leq \gamma_t \leq 0.4)\right]$.

8.2.4 Application of IDF-PCE (CMC)

In order to compare the formulations with the same uncertainty propagation method, IDF-PCE (CMC) is implemented. The objective function is computed with the same approach as MDF and the interdisciplinary coupling constraint is computed by CMC with the same samples as the objective function. The interdisciplinary coupling satisfaction criterion ϵ is set to $10^{-4} m^2 s^{-4}$. The feedback loop is decoupled to avoid MDA and loops between the disciplines. The load factor coupling variable is decomposed according to a product of Hermite polynomials with a total expansion order of degree 2 resulting in $\dim(\boldsymbol{\alpha}) = \frac{(3+2)!}{3!2!} = 10$. IDF-PCE (CMC) formulation is given by:

$$\begin{aligned}
\min \quad & \mathbb{E}\left[\text{GLOW}\left(\mathbf{z}, \mathbf{U}\right)\right] && (8.4)\\
\text{w.r.t.} \quad & \mathbf{z} = \left[D_1, M_{p1}, T_1, OF_1, D_2, M_{p2}, Der\right]^{\mathrm{T}}, \boldsymbol{\alpha} && \\
\text{s.t.} \quad & \mathbb{P}_f(\mathbf{z}, \mathbf{U}) \leq 5 \times 10^{-2} && (8.5)\\
& J^{\text{CMC}} = \sum_{k=1}^{M_s} \left[c_{N_{ax_{max}}}\left(\mathbf{z}, \hat{y}_{N_{ax_{max}}}\left(\mathbf{u}_{(k)}, \boldsymbol{\alpha}\right)\right) - \hat{y}_{N_{ax_{max}}}\left(\mathbf{u}_{(k)}, \boldsymbol{\alpha}\right)\right]^2 \leq \epsilon && (8.6)\\
& \mathbf{z}_{\min} \leq \mathbf{z} \leq \mathbf{z}_{\max} && (8.7)
\end{aligned}$$

8.2.5 Results and conclusion

The results are presented in Table 8.21. MDF and IDF-PCE (CMC) converge to the same optimum in terms of design variable and objective function values. The expected value of the optimal launch vehicle GLOW is approximately 163.7t. The mission constraints in the two approaches are satisfied with a probability of failure under 5%. The interdisciplinary coupling constraint J^{CMC} is satisfied in IDF-PCE (CMC) and the expected value of the error between the input and the output load factors is of 0.1% (Fig. 8.20). The distributions of GLOW and the load factor for MDF and IDF-PCE (CMC) are similar (Figs. 8.16 - 8.19). The proposed approach converges faster ($\sim$ 11 times) than MDF to the optimum as it does not require loops between the disciplines (Figs. 8.6, 8.7). For the optimal launch vehicle, the results of uncertainty propagation for trajectory altitude, velocity and flight path angle are represented in Figures 8.10 to 8.15. A three dimensional representation of some of these trajectories with injection into GTO orbit is illustrated in Figure 8.25. These trajectories correspond to the result of the optimization for each realization of the uncertain variables in order to inject the payload into the targeted orbit. The optimal IDF-PCE launch vehicle geometry is represented in Figures 8.23 and 8.24. To conclude, the proposed approach allows to find the same optimal launch vehicle as the coupled approach while decreasing by a factor 11 the number of calls to the expensive disciplines, especially the trajectory which involves an optimization problem.
In order to highlight the importance of taking into account the uncertainties in the early design phase, the deterministic MDO problem is solved considering the uncertainties fixed to their mean values and an optimal GLOW of 158.21t is found. For the deterministic optimal launch vehicle, a propagation of uncertainty is performed by CMC and MDA with the same uncertainties as in the UMDO problem. In Figure 8.8, the nominal trajectory altitude which injects the payload at 250km is represented. In Figure 8.9, the trajectory altitude is represented for CMC uncertain variable realizations. The deterministic optimal launch vehicle is not robust to the presence of uncertainty as the injection altitude is scattered between 250km and 200km due the lack of propellant to reach the injection point. The Figure 8.10 highlights the robustness of the found solution compared to the deterministic one. The deterministic MDF and the MDF under uncertainty optimal launch vehicle dimensions are represented in Figure 8.22. MDF under uncertainty solution has a larger first stage diameter to carry more propellant however it is less higher than the deterministic solution.

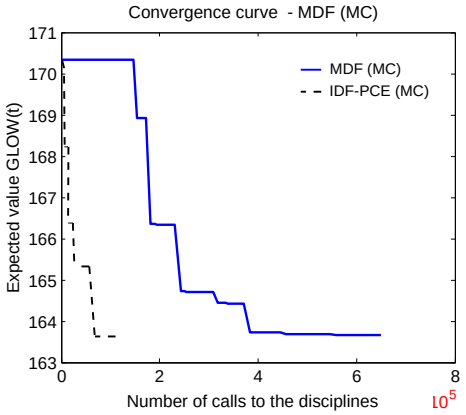

Figure 8.6: Convergence curves with the points satisfying the constraints

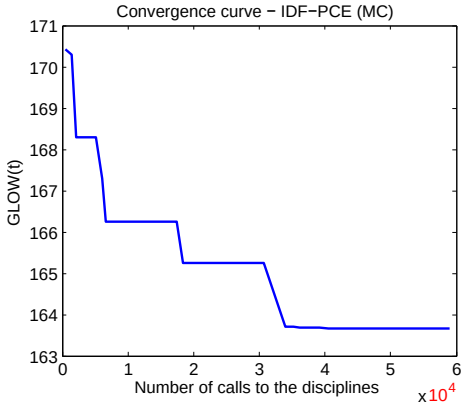

Figure 8.7: Convergence curve with the points satisfying the constraints

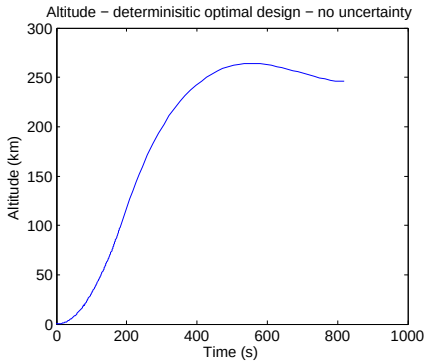

Figure 8.8: Trajectory altitude for the deterministic optimal launch vehicle, no uncertainty

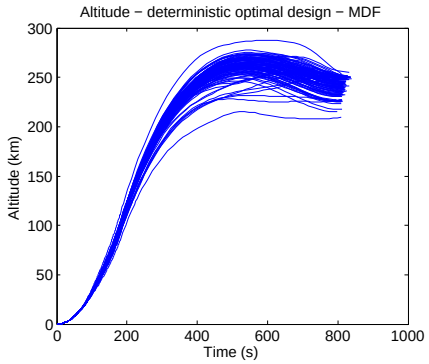

Figure 8.9: Uncertainty propagation - trajectory altitude - deterministic optimal launch vehicle

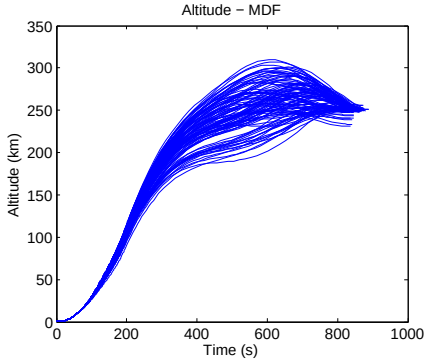

Figure 8.10: Optimal trajectory altitude under uncertainty - MDF

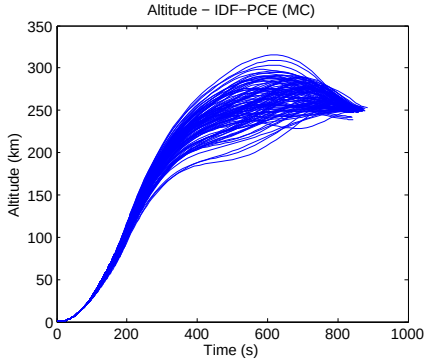

Figure 8.11: Optimal trajectory altitude under uncertainty - IDF-PCE (CMC)

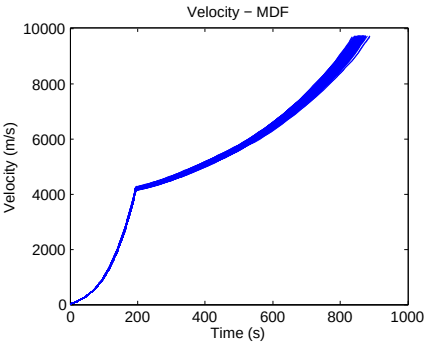

Figure 8.12: Optimal trajectory velocity under uncertainty - MDF

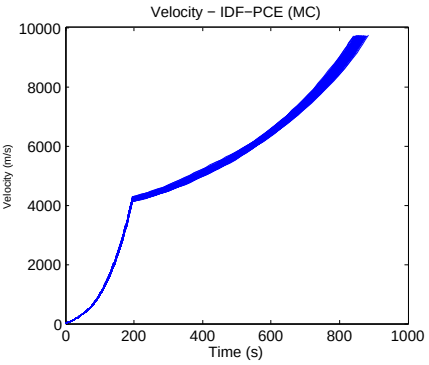

Figure 8.13: Optimal trajectory velocity under uncertainty - IDF-PCE (CMC)

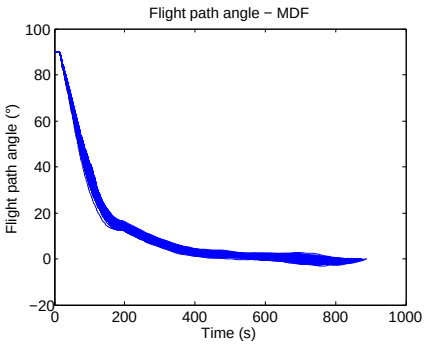

Figure 8.14: Optimal trajectory flight path angle under uncertainty - MDF

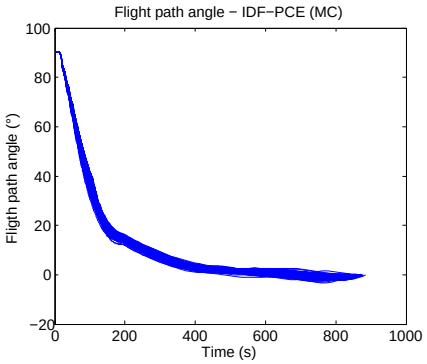

Figure 8.15: Optimal trajectory flight path angle under uncertainty - IDF-PCE (CMC)

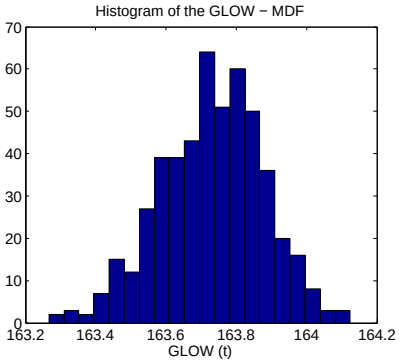

Figure 8.16: GLOW distribution - MDF

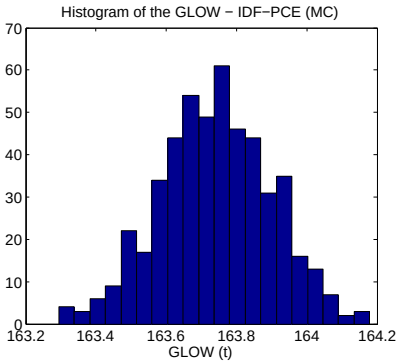

Figure 8.17: GLOW distribution - IDF-PCE (CMC)

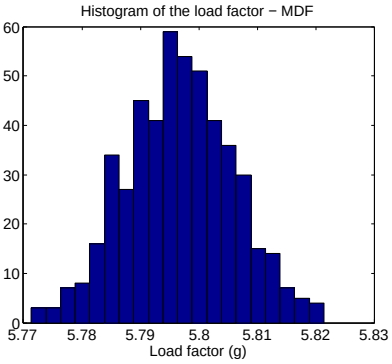

Figure 8.18: Load factor distribution - MDF

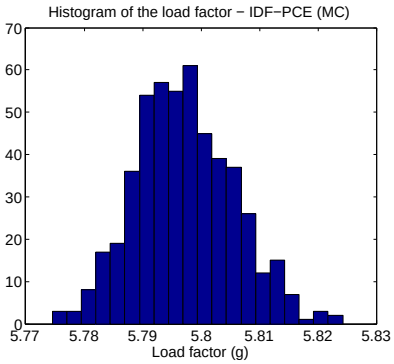

Figure 8.19: Load factor distribution - IDF-PCE (CMC)

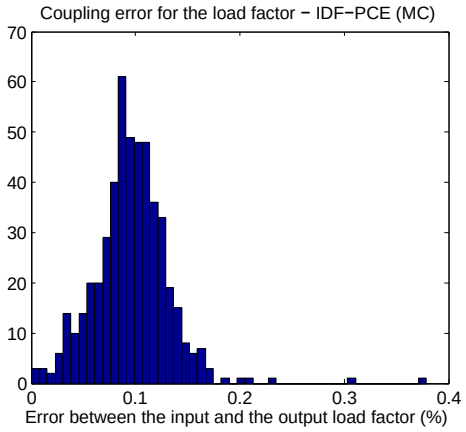

Figure 8.20: Distribution of the error between the input and the output couplings of the load factor

Table 8.21: Two stage rocket design results for MDF and IDF-PCE (CMC) formulations

Results	MDF	IDF-PCE (CMC)
$\mathbb{E}$[GLOW]	**163.74t**	**163.78t**
Design variables	$D1 = 3.957$m $Mp_1 = 115274$kg $T_1 = 2730.3$kN $OF_1 = 3.46$ $D_2 = 3.263$m $Mp_2 = 2507$kg $Der = 95.5\%$	$D1 = 3.914$m $Mp_1 = 115234$kg $T_1 = 2726.1$kN $OF_1 = 3.37$ $D_2 = 3.337$m $Mp_2 = 2514$kg $Der = 95.9\%$
Coupling constraints	$\lvert c_{N_{axmax}} - y_{N_{axmax}}\rvert^2 \leq 10^{-4} m^2 s^{-4}$	$J_{N_{axmax}} = 9.7 \times 10^{-5} m^2 s^{-4}$
Mission constraint $\mathbb{P}_f$	4.95×10^{-2}	4.93×10^{-2}
Design space dimension	7	17
Calls to each discipline	$N_d = 6.49 \times 10^5$	$N_d = 5.91 \times 10^4$
Computational reduction factor	1 (ref)	**11**

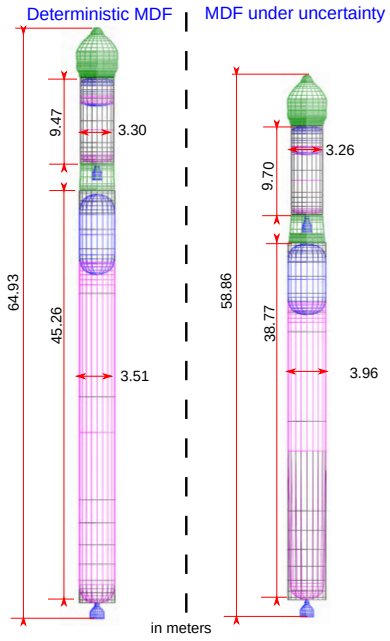

Figure 8.22: Comparison of optimal deterministic MDF and MDF under uncertainty launch vehicles

Figure 8.23: optimal IDF-PCE launch vehicle

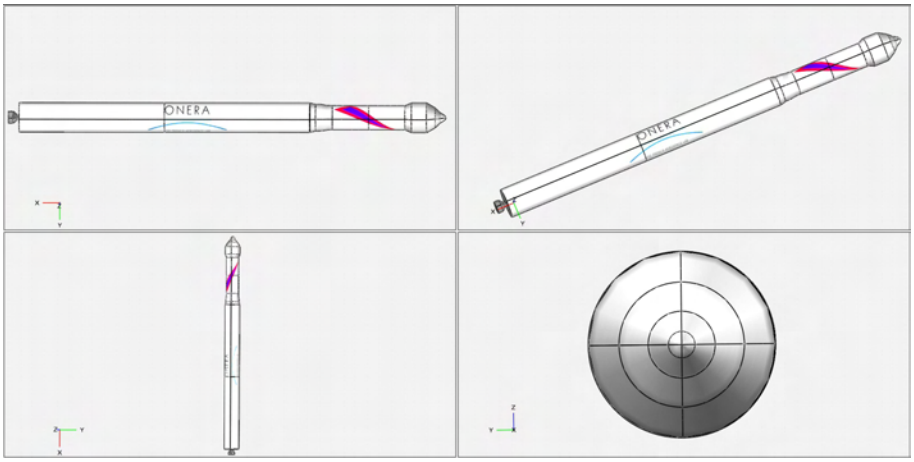

Figure 8.24: Different views of the optimal IDF-PCE launch vehicle

Figure 8.25: Visualization of 3 dimensional trajectories under uncertainty

8.3 MHOU for sounding rocket design

This launch vehicle design test case consists in designing a sounding rocket with two solid stages to launch a payload of 800kg from Kourou that has to reach at least an altitude of 300km. Sounding rockets carry scientific experiments into space along a parabolic trajectory. Their overall time in space is brief and the cost factor makes sounding rockets an interesting alternative to heavier launch vehicles as they are sometimes more appropriate to successfully carry out a scientific mission and are less complex to design. Four disciplines are involved in the considered test case, the propulsion, the mass budget and geometry design, the aerodynamics and the trajectory (Fig. 8.26). The sounding rocket design is decomposed into two subsystems, one for each stage. MHOU formulation enables a hierarchical design process decomposed into two teams, one for each sounding rocket stage.

8.3.1 Design and uncertain variables

The objective of the UMDO problem is to minimize a function of the GLOW of the sounding rocket. The k^{th} subsystem objective is to minimize a function of the stage mass $\mathbb{E}[M_k(\cdot)] + 2 \times \sigma[M_k(\cdot)]$

(with σ the standard deviation) and M_k the stage mass. The system-level objective is to minimize the contribution to the GLOW of the two stages. The problem has ten design variables summarized in Table 8.27. The uncertainty measure for the constraints $g_k(\cdot)$ is the probability measure $\mathbb{P}[\cdot]$. The required feedback couplings for the 2^{nd} stage design are $\mathbf{y}_{12} = [h_{f1}, v_{f1}]^{\text{T}}$ which are the separation altitude h_{f1} and velocity v_{f1} between the 1^{st} and 2^{nd} stages (Fig. 8.26). The design constraints for the i^{th} stage are $\mathbf{g}_i = [P_{ei}, h_{fi}, N_{fi}]^{\text{T}}$ which involve:

- the avoidance of the breakaway of the jet in the divergent skirt ($P_{ei} \leq 0.4 P_a(h)$, Summerfield criterion [Summerfield, 1951]) which ensures that the jet will stay along the nozzle to avoid turbulence flow and chocs in the nozzle. P_e is the pressure at the nozzle exit and P_a is the atmospheric pressure at the altitude h,
- the apogee altitude ($h_{fi} \geq 300$km) for the 2^{nd} stage,
- the maximal axial load factor ($N_{fi} \leq 15g$).

The apogee altitude constraint is not considered for the 1^{st} stage.

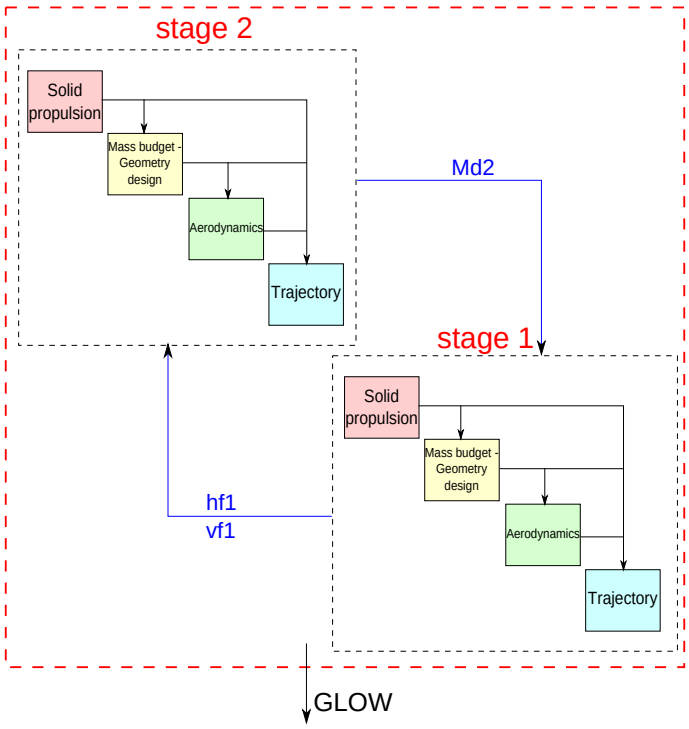

Figure 8.26: Design Structure Matrix for the two stage sounding rocket

Table 8.27: Design variables for the two stage sounding rocket.

Variables	Symbol	Domain of definition
1^{st} stage diameter	D_1	$[0.5, 1.0]$ (m)
1^{st} stage propellant mass	M_{p1}	$[1000, 3000]$ (kg)
1^{st} stage nozzle expansion ratio	ϵ_1	$[1, 20]$
1^{st} stage grain relative length	RL_1	$[30, 80]$ $(\%)$
1^{st} stage combustion depth	W_1	$[30, 80]$ $(\%)$
2^{nd} stage diameter	D_2	$[0.5, 1.0]$ (m)
2^{nd} stage propellant mass	M_{p2}	$[1000, 3000]$ (kg)
2^{nd} stage nozzle expansion ratio	ϵ_2	$[1, 20]$
2^{nd} stage grain relative length	RL_2	$[30, 80]$ $(\%)$
2^{nd} stage combustion depth	W_2	$[30, 80]$ $(\%)$

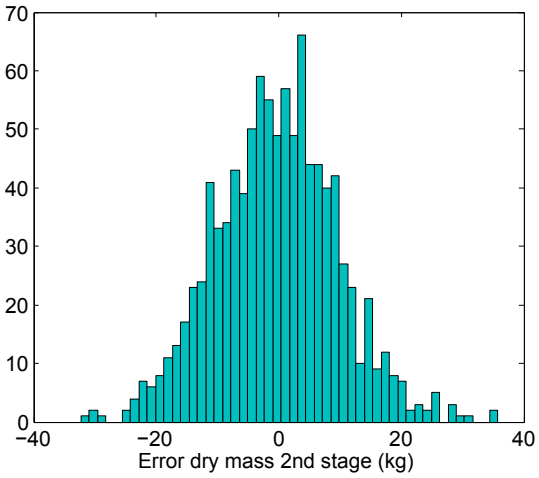

Figure 8.28: 2^{nd} stage dry mass uncertainty

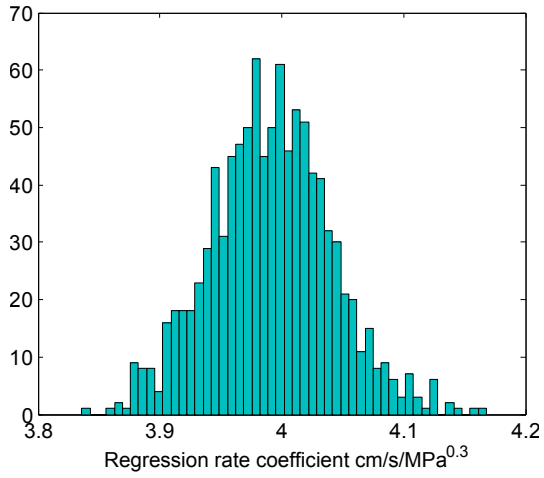

Figure 8.29: 1^{st} stage regression rate coefficient uncertainty for the baseline

The uncertain variables taken into account are the 1^{st} stage combustion regression rate coefficient $\mathcal{N}(3.99, 0.05)$ in $cm/s/MPa^{0.3}$ and the 2^{nd} stage dry mass error $\mathcal{N}(0, 50)$ in kg. The uncertainty on the combustion model through the combustion regression rate results in uncertainty on the 1^{st} stage thrust for the baseline sounding rocket (Fig. 8.30). The mission has to ensure that the payload reaches at least an altitude of 300km (with a probability of failure of 3×10^{-2}). In the next sections, the involved disciplines are briefly detailed. For more information on the discipline models see the appendices.

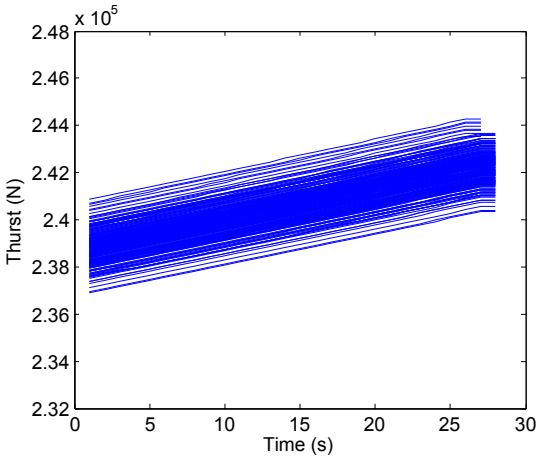

Figure 8.30: 1st stage thrust uncertainty

8.3.2 Disciplinary models

8.3.2.1 Propulsion

In this test case, all the stages use solid propellant TP-H-3340 composed of 18% of Aluminum, 71% of Ammonium Perchlorate (AP) and 11% of Hydroxyl-terminated Polybutadiene (HTPB). The propulsion discipline is based on CEA. Moreover, the simulations are based on a geometrical model of the solid propellant grain (circular or star grains). The dynamics of combustion coupled with the evolution of the combustion surface are derived from [Ricciardi, 1992]. A shifting equilibrium is assumed in the combustion chamber and up to the nozzle throat and a frozen equilibrium after the throat. Figures 8.31 and 8.32 illustrate the dynamics of the combustion surface for a circle and a star grain. The iso-combustion depth curves are represented.

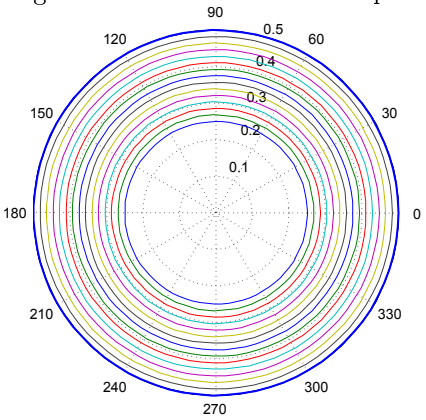

Figure 8.31: Curves of iso-combustion depth for the circle grain

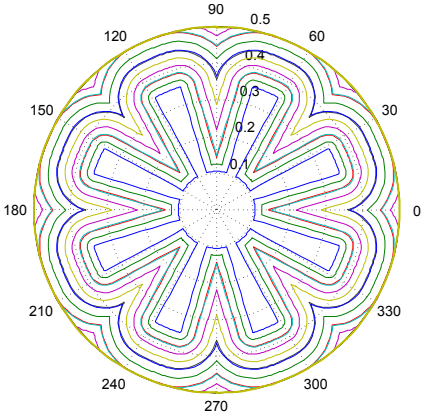

Figure 8.32: Curves of iso-combustion depth for the star grain

8.3.2.2 Mass budget and geometry design

The mass budget and geometry design discipline aims at estimating the mass of the sounding rocket and its geometry. The two stages are solid propellant stages. The dry mass of the stages (M_{di} for stage i) is the sum of the masses of the case, the nozzle, the thermal protection and the igniter. The mass and geometry models are derived from the engineering models for the conceptual design of launch vehicle [Castellini, 2012]. A solid rocket motor is mainly designed based on the maximal chamber pressure and the trajectory loads are not critical as in the case of liquid rocket. However, the maximal axial load factor is considered as a constraint to ensure the comfort of the payload during the flight. Each stage is composed of two grains, one circular and one star. The ratio of the two grains (RL) and the combustion depth (W) are design variables.

8.3.2.3 Aerodynamics

The same models as in IDF-PCE test case are used for the aerodynamics (see section 8.2.2.3).

8.3.2.4 Trajectory

A three dimensional model with rotating round Earth (radius 6371km) is used. The trajectory discipline consists of the simulation of a vertical launch and a pitch maneuver in order to reach an altitude of 300km. No control of the sounding rocket is offered. The simulation is stopped at the apogee of the trajectory (when the vertical velocity is equal to zero) which is compared to the requirement.
All the models have been integrated inside a Matlab environment. CEA and MissileDATCOM have been reuse with some adaptations for interfaces with Matlab. Mass budget and geometry design, solid propellant model and the trajectory discipline have been completely redeveloped based on the given references. The test case has been performed with a desktop computer with 4 processors Intel Xeon CPU E5-1603 2.80GHz. A single run of MDA is in the order of few minutes. The parallel computing Matlab toolbox has been used in order to propagate uncertainty in parallel over all the processors.
In the following, the proposed multi-level decoupled MHOU formulation, IDF-PCE and MDF under uncertainty are compared on this sounding rocket test case.

8.3.3 Application of MDF under uncertainty

MDF is the reference approach as the interdisciplinary system of equations is solved for each uncertain variable realization. The system is solved by FPI with a convergence criterion resulting in a relative error between the input and the output coupling variables of 1%. Based on the numerical experimentation, 4 iterations are in general necessary to converge under the tolerance with the FPI methods. The uncertainty is propagated with CMC to estimate $\Xi[\cdot]$ and $\mathbb{P}[\cdot]$ based on a fixed set of 10^3 random samples. The uncertain samples are considered as fixed in order to be compared to the multi-level approach which requires a fixed uncertain set. Gradient based optimizer (Sequential Quadratic Programming) is used at the system-level in both formulations as no noise is present in the optimization problem. Both system-level optimizers are stopped when 5.6×10^6 evaluations of the disciplines is reached. The MDF formulation is given by:

$$\begin{aligned}
\min \quad & \mathbb{E}\left[\text{GLOW}\left(\mathbf{z}, \mathbf{U}\right)\right] + 2\sigma\left[\text{GLOW}\left(\mathbf{z}, \mathbf{U}\right)\right] && (8.8)\\
\text{w.r.t.} \quad & \mathbf{z} = \left[D_1, M_{p1}, \epsilon_1, RL_1, W_1, D_2, M_{p2}, \epsilon_2, RL_2, W_2\right]^{\mathrm{T}} && \\
\text{s.t.} \quad & \mathbb{P}[-h_{f2}(\mathbf{z}, \mathbf{U}) > -300] \leq 3 \times 10^{-2} && (8.9)\\
& \mathbb{P}[P_{e2}(\mathbf{z}, \mathbf{U}) - 0.4P_a(h) > 0] \leq 3 \times 10^{-2} && (8.10)\\
& \mathbb{P}[N_{f2}(\mathbf{z}, \mathbf{U}) > 15] \leq 3 \times 10^{-2} && (8.11)\\
& \mathbb{P}[P_{e1}(\mathbf{z}, \mathbf{U}) - 0.4P_a(h) > 0] \leq 3 \times 10^{-2} && (8.12)\\
& \mathbb{P}[N_{f1}(\mathbf{z}, \mathbf{U}) > 15] \leq 3 \times 10^{-2} && (8.13)\\
& \mathbf{z}_{\min} \leq \mathbf{z} \leq \mathbf{z}_{\max} && (8.14)
\end{aligned}$$

8.3.4 Application of MHOU

The MHOU formulation is:

- System-level

$$\begin{aligned}
\min \quad & \sum_{k=1}^{2} \Xi\left[M_k(z_{sh}, \mathbf{z}_k^*, \boldsymbol{\alpha}, \mathbf{U})\right] + 2 \times \sigma\left[M_k(z_{sh}, \mathbf{z}_1^*, \mathbf{z}_2^*, \boldsymbol{\alpha}, \mathbf{U})\right] && (8.15)\\
\text{w.r.t.} \quad & z_{sh} \in \mathcal{Z}_{sh}, \boldsymbol{\alpha} \\
\text{s.t.} \quad & \mathbf{J}_{h_{f1}}^*(z_{sh}, \mathbf{z}_1^*, \boldsymbol{\alpha}) \leq \epsilon && (8.16)\\
& \mathbf{J}_{v_{f1}}^*(z_{sh}, \mathbf{z}_1^*, \boldsymbol{\alpha}) \leq \epsilon && (8.17)\\
& \mathbb{P}[-h_{f2}(z_{sh}, \mathbf{z}_2^*, \mathbf{U}) > -300] \leq 3 \times 10^{-2} && (8.18)\\
& \mathbb{P}[P_{e2}(z_{sh}, \mathbf{z}_2^*, \mathbf{U}) - 0.4P_a(h) > 0] \leq 3 \times 10^{-2} && (8.19)\\
& \mathbb{P}[N_{f2}(z_{sh}, \mathbf{z}_2^*, \mathbf{U}) > 15] \leq 3 \times 10^{-2} && (8.20)\\
& \mathbb{P}[P_{e1}(z_{sh}, \mathbf{z}_1^*, \mathbf{U}) - 0.4P_a(h) > 0] \leq 3 \times 10^{-2} && (8.21)\\
& \mathbb{P}[N_{f1}(z_{sh}, \mathbf{z}_1^*, \mathbf{U}) > 15] \leq 3 \times 10^{-2} && (8.22)
\end{aligned}$$

- Subsystem-level

For the 2nd stage

$$\begin{aligned}
\min \quad & \Xi\left[M_2(z_{sh}, \mathbf{z}_2, \boldsymbol{\alpha}, \mathbf{U})\right] + 2 \times \sigma\left[M_2(z_{sh}, \mathbf{z}_2, \boldsymbol{\alpha}, \mathbf{U})\right] && (8.23)\\
\text{w.r.t.} \quad & \mathbf{z}_2 = [M_{p2}, \epsilon_2, RL_2, W_2]^{\mathrm{T}} \in \mathcal{Z}_2 \\
\text{s.t.} \quad & \mathbb{P}\left[\mathbf{g}_2(z_{sh}, \mathbf{z}_2, \boldsymbol{\alpha}, \mathbf{U})\right] \leq 3 \times 10^{-2} && (8.24)\\
& && (8.25)
\end{aligned}$$

Given $\mathbf{y}_{21}$

For the 1st stage

$$\begin{aligned}
\min \quad & \Xi\left[M_1(z_{sh}, \mathbf{z}_1, \boldsymbol{\alpha}, \mathbf{U})\right] + 2 \times \sigma\left[M_1(z_{sh}, \mathbf{z}_1, \boldsymbol{\alpha}, \mathbf{U})\right] && (8.26)\\
\text{w.r.t.} \quad & \mathbf{z}_1 = [D_1, M_{p1}, \epsilon_1, RL_1, W_1]^{\mathrm{T}} \in \mathcal{Z}_1 \\
\text{s.t.} \quad & \mathbb{P}\left[\mathbf{g}_1(z_{sh}, \mathbf{z}_1, \boldsymbol{\alpha}, \mathbf{U})\right] \leq 3 \times 10^{-2} && (8.27)\\
& J_{h_{f1}} = \\
& \int_{\mathbf{\Omega}} \left[h_{f1}\left(z_{sh}, \mathbf{z}_1, \mathbf{y}_{21}, \mathbf{u}_1\right) - \hat{h}_{f1}\left(\mathbf{u}, \boldsymbol{\alpha}^{(12)}\right)\right]^2 \phi(\mathbf{u}) \mathrm{d}\mathbf{u} \leq \epsilon && (8.28)\\
& J_{v_{f1}} = \\
& \int_{\mathbf{\Omega}} \left[v_{f1}\left(z_{sh}, \mathbf{z}_1, \mathbf{y}_{21}, \mathbf{u}_1\right) - \hat{v}_{f1}\left(\mathbf{u}, \boldsymbol{\alpha}^{(12)}\right)\right]^2 \phi(\mathbf{u}) \mathrm{d}\mathbf{u} \leq \epsilon && (8.29)
\end{aligned}$$

where $z_{sh} = D_2$ is the 2nd stage diameter, $\mathbf{g}_2(\cdot) = [P_{e2}(\cdot), h_{f2}(\cdot), N_{f2}(\cdot)]^{\mathrm{T}}$ and $\mathbf{g}_1(\cdot) = [P_{e1}(\cdot), N_{f1}(\cdot)]^{\mathrm{T}}$. The set of the 2nd stage mass realizations for the optimal solution of the 2nd stage optimization problem is the feedforward coupling $\mathbf{y}_{21}$ of the 1st stage optimization. In order to hierarchically optimize the second stage and then the first stage, the feedforward coupling has to be passed from stage 2 to stage 1. In order to keep the consistency between the two optimizations, a fixed set of uncertain variable realizations has been used all along the optimization process. The set has also been used for MDF for consistent comparison. The altitude and the velocity at the moment of separation between the two stages are the feedback coupling variables from stage 1 to stage 2 that are decoupled. These variables are decomposed according to a product of Hermite polynomials with a total expansion order of degree 2 resulting in $\dim(\boldsymbol{\alpha}) = \frac{(2+2)!}{2!2!} = 6$. Therefore, the design space dimension is 13 at the system-level, 4 for the 2nd stage and 5 for the 1st stage. The interdisciplinary coupling constraint $J_{h_{f1}}$ and $J_{v_{f1}}$ have to be inferior to $\epsilon = 1\%$ in order to ensure interdisciplinary coupling satisfaction as in MDF.

8.3.5 Application of IDF-PCE

The IDF-PCE formulation is similar to MHOU in terms of interdisciplinary coupling handling (same degree of decomposition, same feedback couplings) but it is a single-level formulation given by:

$$\begin{aligned}
\min \quad & \mathbb{E}\left[\mathrm{GLOW}\left(\mathbf{z}, \boldsymbol{\alpha}, \mathbf{U}\right)\right] + 2\sigma\left[\mathrm{GLOW}\left(\mathbf{z}, \boldsymbol{\alpha}, \mathbf{U}\right)\right] && (8.30)\\
\text{w.r.t.} \quad & \mathbf{z}, \boldsymbol{\alpha} \\
\text{s.t.} \quad & \mathbf{J}_{h_{f1}}(\mathbf{z}, \boldsymbol{\alpha}) \leq \epsilon && (8.31)\\
& \mathbf{J}_{v_{f1}}(\mathbf{z}, \boldsymbol{\alpha}) \leq \epsilon && (8.32)\\
& \mathbb{P}[-h_{f2}(\mathbf{z}, \mathbf{U}) > -300] \leq 3 \times 10^{-2} && (8.33)\\
& \mathbb{P}[P_{e2}(\mathbf{z}, \mathbf{U}) - 0.4P_a(h) > 0] \leq 3 \times 10^{-2} && (8.34)\\
& \mathbb{P}[N_{f2}(\mathbf{z}, \mathbf{U}) > 15] \leq 3 \times 10^{-2} && (8.35)\\
& \mathbb{P}[P_{e1}(\mathbf{z}, \mathbf{U}) - 0.4P_a(h) > 0] \leq 3 \times 10^{-2} && (8.36)\\
& \mathbb{P}[N_{f1}(\mathbf{z}, \mathbf{U}) > 15] \leq 3 \times 10^{-2} && (8.37)\\
& \mathbf{z}_{\min} \leq \mathbf{z} \leq \mathbf{z}_{\max} && (8.38)
\end{aligned}$$

All the design variables $\mathbf{z}$ for the two stages are controlled by the system design variables in addition with the PCE coefficients $\boldsymbol{\alpha}$.

8.3.6 Results

CMA-ES optimization algorithm is used at the subsystem-level for MHOU formulation. The three problems start from the same feasible baseline to be optimized. The baseline corresponds to the deterministic optimal solution of the two stage sounding rocket problem (Fig. 8.35) found by a deterministic MDF approach. However, as illustrated in Figure 8.37, this solution is not robust to the presence of uncertainty. Indeed, the deterministic optimal solution does not succeed to reach with a probability of failure lower than 3×10^{-2} an altitude of 300km, the failure rate is around 70%.
Based on this baseline, MDF under uncertainty, IDF-PCE and MHOU are implemented. The results of the sounding rocket problem are summarized in Table 8.33. MHOU (6.68t) and IDF-PCE (6.88t)

Table 8.33: Two stage sounding rocket design results for MDF, MHOU and IDF-PCE formulations

Results	MDF	MHOU	IDF-PCE
$\mathbb{E}$[GLOW] + 2σ[GLOW]	**7.07t**	**6.68t**	**6.88t**
Design variables	$D_1 = 0.75$m $M_{p1} = 2850$kg $\epsilon_1 = 4.4$ $RL_1 = 69.4\%$ $W_1 = 66.0\%$	$D_1 = 0.79$m $M_{p1} = 2659$kg $\epsilon_1 = 9.24$ $RL_1 = 30.7\%$ $W_1 = 43.5\%$	$D_1 = 0.72$m $M_{p1} = 2729$kg $\epsilon_1 = 12.7$ $RL_1 = 42.3\%$ $W_1 = 41.8\%$
	$D_2 = 0.76$m $M_{p2} = 2395$kg $\epsilon_2 = 9.97$ $RL_2 = 69.5$ % $W_2 = 65.9$ %	$D_2 = 0.75$m $M_{p2} = 2287$kg $\epsilon_2 = 17.4$ $RL_2 = 41.0$ % $W_2 = 63.9$ %	$D_2 = 0.79$m $M_{p2} = 2402$kg $\epsilon_2 = 12.3$ $RL_2 = 40.5$ % $W_2 = 61.1$ %
Coupling constraints	$\lvert c_{hf1} - y_{hf1}\rvert / c_{hf1} \leq 1\%$ $\lvert c_{vf1} - y_{vf1}\rvert / c_{vf1} \leq 1\%$	$J_{hf1} = 0.31\%$ $J_{vf1} = 0.24\%$	$J_{hf1} = 0.42\%$ $J_{vf1} = 0.19\%$
Mission constraint $\mathbb{P}_f$	2.8×10^{-2}	2.9×10^{-2}	2.9×10^{-2}
Design space dimension	10	$22(13 + 4 + 5)$	22

presents better characteristics in terms of quality of objective function than MDF (7.07t) for a fixed discipline evaluation budget (Fig. 8.34). MDF, IDF-PCE and MHOU solutions satisfy the constraints especially the apogee altitude of 300km as illustrated in Figure 8.36 for MDF and MHOU. Only 2.9% of the trajectories do not reach the required apogee altitude. Moreover, MHOU ensures interdisciplinary coupling satisfaction for the feedback couplings as illustrated by the comparison of the couplings found respectively by the coupled approach and the decoupled approach for the optimal solution found by MHOU. The same coupling satisfaction are found for IDF-PCE. The separation altitude and velocity distributions for the optimal MHOU found solution are similar by using MDA or MHOU (Fig. 8.38-8.41). Moreover, the interdisciplinary coupling error for the separation altitude and velocity are represented in Figures 8.42 and 8.43. The coupling error is always lower than 2% and concentrated around 0%-0.5%. The design space dimension for the system-level is increased from 10 for MDF to 13 for MHOU, however it enables multi-level optimization where each stage subsystem handles its local design variables. For IDF-PCE, the dimension of the system-level design space is 22. Thanks to the two levels of optimization, MHOU allows a convergence to a better optimum than IDF-PCE in this test case while enabling decoupled design strategy and autonomy to each engineering team working on each stage. 3 dimensional trajectories with MHOU results are illustrated in Figure 8.44.

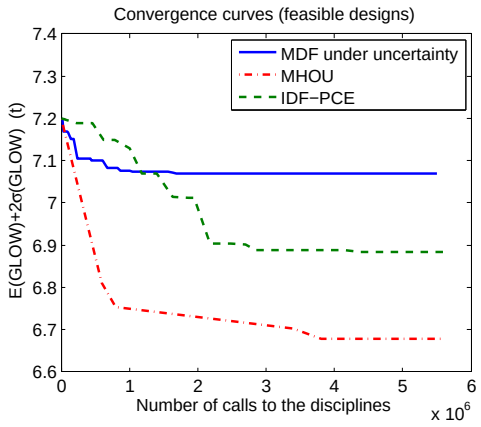

Figure 8.34: Convergence curves with the points satisfying the constraints

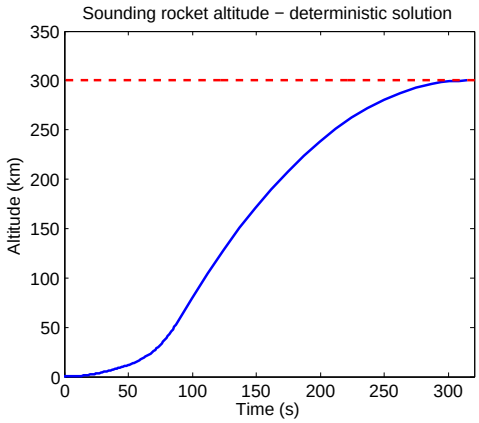

Figure 8.35: Optimal sounding rocket altitude without uncertainty

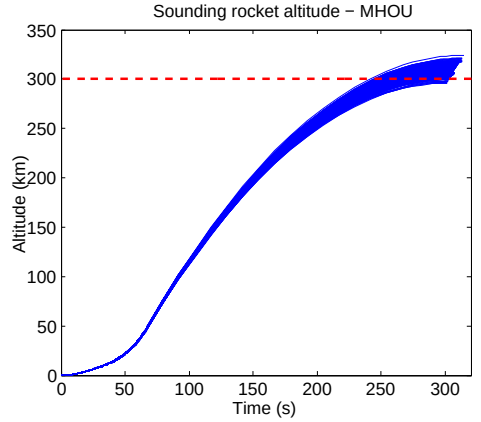

Figure 8.36: Optimal sounding rocket altitude

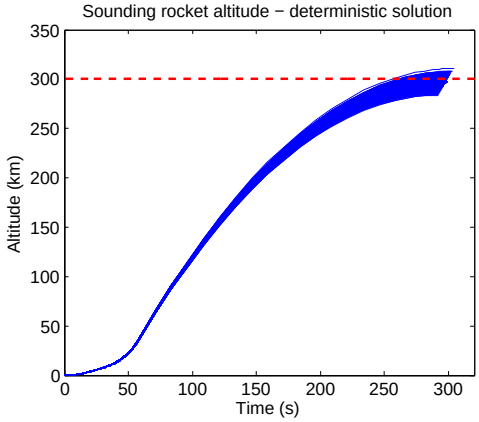

Figure 8.37: Deterministic optimal sounding rocket altitude in the presence of uncertainty

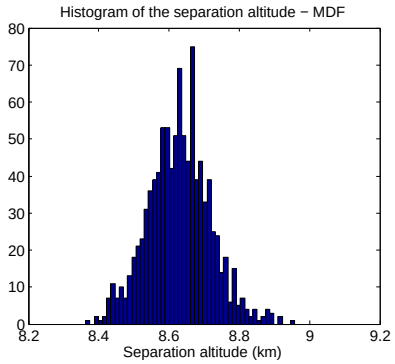

Figure 8.38: Distribution of the separation altitude for the optimal MHOU solution - by MDA

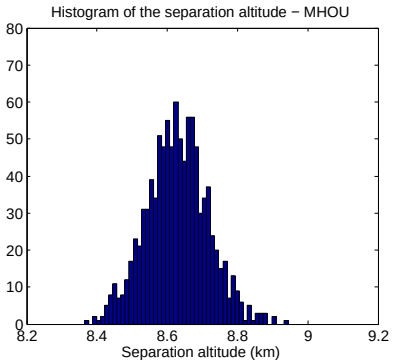

Figure 8.39: Distribution of the separation altitude for the optimal MHOU solution

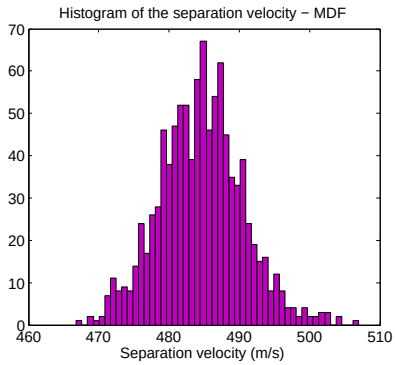

Figure 8.40: Distribution of the separation velocity for the optimal MHOU solution - by MDA

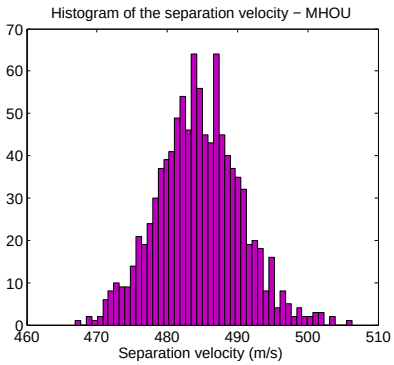

Figure 8.41: Distribution of the separation velocity for the optimal MHOU solution

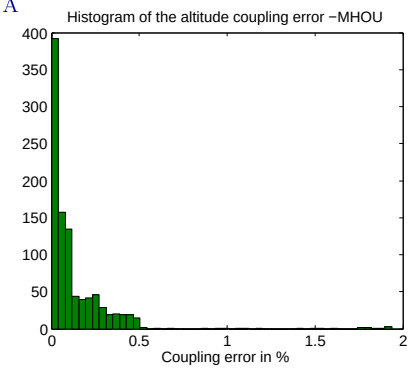

Figure 8.42: Distribution of the altitude coupling error MHOU

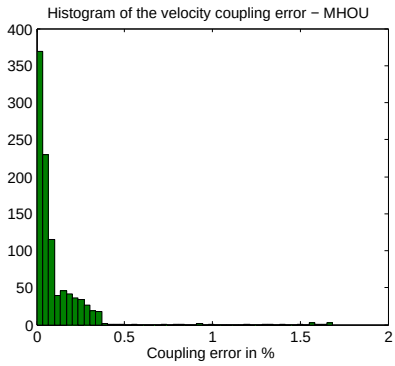

Figure 8.43: Distribution of the velocity coupling error MHOU

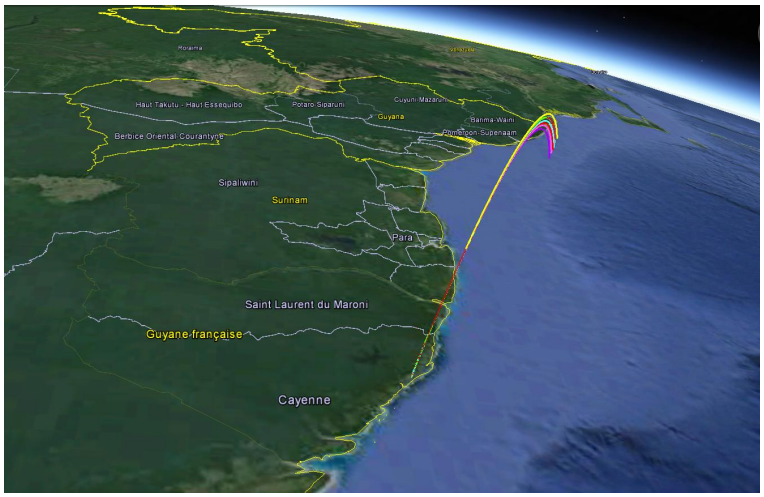

Figure 8.44: Visualization of 3 dimensional trajectories under uncertainty for the optimal sounding rocket

8.4 Limitations of the numerical comparisons

For the two test cases, the achieved numerical comparisons (in a Matlab environment) are based on local approaches initialized at a baseline. The computational cost induced by the repeated discipline simulations, the uncertainty propagation and the optimization results in limited comparison capability. For instance, the trajectory discipline for the test case of IDF-PCE which involved an auxiliary optimization problem to find the optimal trajectory resulted in a very computationally expensive discipline in the context of UMDO. Using a computer with 2.80GHz CPU (4 cores) and 8Go memory with all the cores in parallel (with the Matlab toolbox), the IDF-PCE comparison lasted 432 hours and the MHOU comparison lasted 617 hours. With a higher computation capability a global analysis with several initializations for IDF-PCE and MHOU would be interesting but could not be performed in the framework of this study. Moreover, an extended comparison of the two proposed approaches over other launch vehicle design test cases could be performed to further illustrate the interest of multi-level formulations.

8.5 Conclusion of part II

In this part, based on the reasoning on interdisciplinary coupling handling in the presence of uncertainty, we have proposed one single-level decoupled formulation named IDF-PCE and one multi-level formulation called MHOU. Both formulations are based on a surrogate model construction of the interdisciplinary coupling relations all along the UMDO process in order to represent at the convergence the functional coupling relations as would MDA do. The surrogate models are based on Polynomial Chaos Expansion as they are particularly adapted to functions affected by uncertainty and offer tools to efficiently propagate uncertainty. Ensuring multidisciplinary feasibility in the presence of uncertainty is essential to ensure the physical relevance of the

obtained design. The test cases illustrate that the proposed decoupled formulations numerically ensure an identical level of accuracy of the interdisciplinary couplings compared to the coupled strategies. Decomposition-based design processes allow to offer autonomy to engineering team and to decouple the design process according to disciplines or to subsystems. In practice, industrial companies in charge of the design of launch vehicles are often divided according to different department highlighting various fields of competence (propulsion, aerodynamics, structure, *etc.*). Therefore, a decomposition design strategy is particularly adapted to the actual configuration of these companies. Moreover, decoupled strategies enables to avoid loops between the disciplines through MDA reducing the computational cost. Several uncertainty propagation techniques have been adapted within IDF-PCE framework to overcome the computational burden of CMC. The multi-level MHOU formulation is particularly adapted to launch vehicle design as it decomposes the design process according to each stage of the rocket.

The numerical comparisons have highlighted the efficiency of the proposed formulations with respect to MDF. The analytical test case has highlighted the capability of PCE to model complex interdisciplinary coupling relations if an appropriate decomposition degree is chosen. Moreover, uncertainty propagation with quadrature rules or the decomposition of the discipline output over another PCE is very efficient in terms of number discipline evaluations. Indeed, these approaches decrease by a factor of 400 the number of discipline evaluations compared to CMC for the same level of accuracy. The numerical study with IDF-PCE for the design of a launch vehicle highlighted the interest of a decomposition strategy to reduce the computation cost compared to a coupled MDF approach while maintaining an equivalence in terms of interdisciplinary coupling satisfaction. IDF-PCE allowed to reduce by a factor of 11 the number of discipline evaluations on this test case. The comparative study with MHOU has showed the advantages of the stage-wise decomposition formulation that improve the design process with respect to MDF which is the most commonly used method in literature. The design process strategy considering the decomposition according to the stages instead of traditional disciplines presents the same advantages as in deterministic SWORD and offers the possibility to faster find optimal launch vehicle architecture. This decomposition is in accordance with the importance of the trajectory discipline in the design of a launch vehicle.

Two main ideas have to be retained:

- The importance of taking into account the uncertainty in the design of a launch vehicle at the early design phases. As highlighted in the two test cases, the deterministic optimal launch vehicle configuration is not robust to the presence of uncertainties. Once this optimal system is subjected to uncertainty, it does not succeed to fulfill the requirements imposed by the designer. However, taking into account the uncertainty from the beginning of the design allows to find an optimal launch vehicle which is robust and reliable to the presence of uncertainty.
- The importance of interdisciplinary coupling handling in MDO in the presence of uncertainty. Due to the coupled nature of the disciplines, strategies either coupled or decoupled have to be used to solve the system of interdisciplinary coupling equations. These strategies have to be adapted to the presence of uncertainty. Decoupled approaches are interesting to decrease the computational cost but the efficiency of these approaches must not be to the detriment of the interdisciplinary coupling satisfaction. Maintaining a mathematical equivalence between coupled and decoupled strategies in terms of multidisciplinary feasibility is essential.

As highlighted in the two design test cases, evaluating the reliability of the optimal system is a complex task but essential to ensure the satisfaction of the designer requirements. In the context of launch vehicle it may consist to guarantee the precision of the orbit injection or the stage fallout in a safe zone. As highlighted in section 4, for complex systems, existing reliability assessment methods present some drawbacks and ways of improvement have been outlined (see section 5). Dedicated reliability analysis techniques for multidisciplinary system in the presence of aleatory and mixed aleatory/epistemic uncertainties are developed in the next Part III.

- Context:
  - Interdisciplinary coupling handling in UMDO formulation,
  - Decomposition strategy of the design process,
  - State-of-the-art decoupled UMDO methods only deal with incomplete coupling conditions.
- Contributions:
  - Development of a new single level UMDO formulation inspired from Individual Discipline Feasible formulation with interdisciplinary coupling satisfaction for all the realizations of the uncertain variables,
  - Development of a new multi-level UMDO formulation inspired from Stage-Wise Decomposition for Optimal Rocket Design with interdisciplinary coupling satisfaction for all the realizations of the uncertain variables,
  - Maintaining of the mathematical equivalence between coupled and decoupled strategies in the presence of uncertainty,
  - Application of the proposed formulations to the design of launch vehicles, highlighting the importance of taking into account uncertainty in MDO process in early design phases to ensure the robustness and reliability of the system.
- Actionable information:
  - Appropriate for problems that have to be solved with a decomposition strategy involving different engineering teams to offer autonomy,
  - Useful to perform uncertainty propagation in parallel over multiple processors,
  - Ensure system design consistency and reliability with an integrated process,
  - Other applications: conceptual design of aircraft, ships, automobiles, *etc.*
- Perspectives:
  - Develop a method to appropriately determine *a-priori* the surrogate model decomposition degree for the modeling of the functional coupling relations,
  - Further reduce the computational cost induced by the number of calls to the disciplines (surrogate models of the disciplines, other formulations, *etc.*),
  - Perform test cases with increased dimension and complexity design problems.

Part III

Reliability analysis in the presence of mixed aleatory/epistemic uncertainties, applications to launch vehicle design

Chapter 9

Reliability analysis in the presence of epistemic uncertainty on the hyper-parameters of PDF distributions

Contents

Chapter goals

- Develop a reliability analysis method in the presence of epistemic uncertainty on the hyper-parameters of PDF distributions,
- Apply and compare the proposed approach to reference techniques on two analytical test cases.

9.1 Introduction

In the previous part II, a focus on the interdisciplinary coupling handling in UMDO problem has been made, highlighting the importance of dedicated techniques to coordinate the design process when decomposition strategies are adopted. Another important task in designing of a complex system is the assessment of its reliability. Estimating failure probabilities is important for systems involving safety issues. In the presence of mixed aleatory and epistemic uncertainties impacting the system, the failure probability is not unique and depends on the values taken by epistemic uncertainty. One way to characterize the probability of failure is to determine its domain of variation in order to have an estimation of the rare event probability variation domain (see chapter 4). The determination of the probability bounds induces intricate problem optimization solving and numerous probability estimations in order to determine the upper and lower bounds of the probability estimate. Moreover, reliability analysis often involves system simulations which are supposed to require a considerable computational effort. Complex systems may present multiple failure regions and non linear limit state functions. The existing methods reviewed in chapter 4 are not suited for launch vehicle design problems as they mostly rely on CMC or FORM resulting in intractable or restrained applications.
Let us consider a model of the system defining a limit state. This model allows to determine if the system is in a failure state or a safe state depending on uncertain inputs. The reliability analysis consists in estimating the probability for the system to be in a failure state considering aleatory input uncertainty affecting the system. In literature, two categories of problems exist for the impact of epistemic uncertainty in reliability analysis:

- epistemic uncertainty affects the hyper-parameters defining the PDF of the aleatory uncertainty (for instance the expected value of the PDF is only known in an interval),
- epistemic uncertainty directly affects the disciplinary models impacting the limit state.

These two types of problems are different and require dedicated techniques. The part III of the thesis is devoted to the presentation of two methods dedicated to reliability analysis for complex systems in the presence of both aleatory and epistemic uncertainties. Chapter 9 presents a method developed in collaboration with Mathieu Balesdent (Onera) and Jerome Morio (Onera) to handle epistemic uncertainty on the hyper-parameters of the aleatory uncertainty PDF. The method proposes to estimate the bounds of the rare event probability using Kriging-based adaptive Importance Sampling. It relies on an improvement of Cross Entropy algorithm (section 2.4.3) used in Importance Sampling coupled with a Kriging model [Matheron, 1963] of the limit state function, a refinement strategy of the surrogate model and CMA-ES optimization algorithm to account for epistemic uncertainty and to avoid expensive limit state function evaluations.
Chapter 10 describes a method developed in collaboration with Mathieu Balesdent (Onera), Sylvain Lacaze (University of Arizona) and Samy Missoum (University of Arizona) to handle epistemic uncertainty directly affecting the system failure state. To compute the bounds of the failure probability, a sequential approach is proposed. Because an estimation of a probability of failure involving rare events cannot be estimated by a classical method such as CMC due to the numerical cost induced, Subset Simulation is used. Subset Simulation is efficient to estimate rare event probability [Au and Beck, 2001] and is able to handle multiple failure regions and non linear limit state function. Moreover, it is assumed that the limit state function is computationally expensive to evaluate, hence in order to further reduce the number of calls to the simulation codes, a Kriging

surrogate model is used. A dedicated refinement strategy of the Kriging model is proposed to ensure the accuracy of the probability bound estimation while limiting the number of calls to the expensive limit state function.
In chapter 11, the two proposed reliability analysis methods are applied on two launch vehicle stage fallout problems. The launch vehicle designers have to take into account the non controlled re-entry of the launch vehicle first stages (booster, first and sometimes second stages) and to ensure that the fallout does not present risk for the populations. The estimation of the probability for a stage to fall at a certain distance of the nominal impact point is an essential study that as to be taken into account as early as possible. If this study is performed too late in the design process and it appears that the stage falls into an inadequate region, it will force the designers to modify the launch vehicle ascent trajectory which may degrade its performance.

The current chapter describes the method for estimating the probability of failure using Kriging-based adaptive Importance Sampling in the presence of epistemic uncertainty on the input parameter distributions and is organized as follows. In section 9.2, the rare event probability estimation problem is presented and the adaptive Importance Sampling (IS) is briefly reviewed to introduce the subsequent notations. Section 9.3 describes the proposed method and details the different steps of the algorithm. Finally, in section 9.4, the approach is applied and compared to reference techniques on two analytical test cases to demonstrate its effectiveness.

9.2 Formulation of the uncertainty propagation problem and description of adaptive Importance Sampling

9.2.1 Problem description

Consider a d-dimensional random vector $\mathbf{U}$ defined on the sampling space $\mathbf{\Omega}$ by a joint PDF $\phi^{\mathbf{e}}(\cdot)$ which depends on a parameter vector $\mathbf{e} = \left[e^{(1)}, \ldots, e^{(w)}\right]^{\mathrm{T}} \in \mathbb{R}^w$. $\mathbf{e}$ suffers from epistemic uncertainties and only the variation domains of its components are known $\mathbf{\Upsilon} = \{\mathbf{e} \in \mathbb{R}^w | e^{(i)} \in [e^{(i)}_{\min}, e^{(i)}_{\max}]\ \forall i \in \{1, \ldots, w\}\}$. Consider a system characterized by a limit state function $g : \mathbf{\Omega} \to \mathbb{R}$ assumed to be a deterministic continuous input-output function. Moreover, due to the complexity of the physical phenomena involved in the simulation of $g(\cdot)$, it is supposed that $g(\cdot)$ is non linear. In the presence of mixed aleatory and epistemic uncertainties impacting the system, the failure probability is not unique and depends on the values taken by $\mathbf{e}$ (Figs. 4.1,4.2). To characterize the probability of failure, it is possible to determine its domain of variation by finding the lower and upper bounds:

$$\begin{cases} \mathbb{P}_{\min} = \min\limits_{\mathbf{e} \in \mathbf{\Upsilon}} \ \mathbb{P}_{\mathbf{e}}(g(\mathbf{U}) > 0) \\ \mathbb{P}_{\max} = \max\limits_{\mathbf{e} \in \mathbf{\Upsilon}} \ \mathbb{P}_{\mathbf{e}}(g(\mathbf{U}) > 0) \end{cases} \tag{9.1}$$

$g(\cdot)$ is a function that may be calculated through a complex industrial system simulation, so is supposed to require a considerable computational effort to provide the output for a given input.
For a given $\mathbf{e}$, a classical method to estimate the probability of interest is to perform CMC simulations (section 2.4.1) [Niederreiter and Spanier, 2000]. In that way, one generates independent and identically distributed samples $\mathbf{u}_{(1)}[\phi^{\mathbf{e}}], \ldots, \mathbf{u}_{(M)}[\phi^{\mathbf{e}}]$ according to $\phi^{\mathbf{e}}(\cdot)$ and estimates the

probability in the following manner:

$$\mathbb{P}_{\boldsymbol{e}}^{\mathrm{CMC}} = \frac{1}{M}\sum_{k=1}^{M} \mathbb{1}_{g(\mathbf{u}_{(k)}[\phi^{\mathbf{e}}])>0} \tag{9.2}$$

Concerning the estimation of rare events in an industrial context (*e.g.* estimation of a probability of failure, determination of safety zone, *etc.*), it is well known that the use of classical methods such as CMC is unadapted. Different methods have been proposed to accurately estimate the probability of rare events, such as Importance Sampling, Importance Splitting, *etc.* (see section 2.4). In this chapter, we focus on Importance Sampling and propose a method to propagate the epistemic uncertainty on the input parameter distributions $\mathbf{e}$ to the Importance Sampling probability estimate.

9.2.2 Adaptive Importance Sampling by Cross-Entropy

In this section, we briefly recall the Cross-Entropy (CE) algorithm [Rubinstein and Kroese, 2004] for estimating the probability of rare events with an initial fixed PDF (section 2.4.3). Let us consider $\boldsymbol{e}_0$, a given parameter vector defining the input density $\phi^{\mathbf{e}_0}(\cdot)$ (*e.g.* the expected value if $\phi^{\mathbf{e}_0}(\cdot)$ is modeled by a Gaussian law). CE consists in introducing a parametric density $\tau_{\boldsymbol{\theta}}^{\mathbf{e}_0}(\cdot)$, with $\boldsymbol{\theta} \in \boldsymbol{\Theta}$ a parameter vector which is optimized in order to minimize the Kullback-Leibler divergence between the unknown optimal auxiliary density $\tau_{\mathrm{opt}}(\cdot)$ and $\tau_{\boldsymbol{\theta}}^{\mathbf{e}_0}(\cdot)$ in order to minimize the variance of the probability estimate (section 2.4.3).
The adaptive CE algorithm for the IS probability estimation is [Rubinstein and Kroese, 2004]:

1. $k = 1$, define $\tau_{\boldsymbol{\theta}_0}^{\mathbf{e}_0}(\cdot) = \phi^{\mathbf{e}_0}(\cdot)$ and set $\rho \in]0,1[$
2. Generate the samples $\mathbf{u}_{(1)}[\tau_{\boldsymbol{\theta}_{k-1}}^{\mathbf{e}_0}], \ldots, \mathbf{u}_{(M)}[\tau_{\boldsymbol{\theta}_{k-1}}^{\mathbf{e}_0}]$ according to the PDF $\tau_{\boldsymbol{\theta}_{k-1}}^{\mathbf{e}_0}(\cdot)$ and apply the function $g(\cdot)$ in order to have $\upsilon_{(1)} = g\left(\mathbf{u}_{(1)}[\tau_{\boldsymbol{\theta}_{k-1}}^{\mathbf{e}_0}]\right), \ldots, \upsilon_{(M)} = g\left(\mathbf{u}_{(M)}[\tau_{\boldsymbol{\theta}_{k-1}}^{\mathbf{e}_0}]\right)$
3. Compute the empirical ρ-quantile $q_k = \min(0, \upsilon_{\lfloor \rho M \rfloor})$, where $\lfloor z \rfloor$ denotes the largest integer that is smaller than or equal to z
4. Optimize the parameter vector $\boldsymbol{\theta}$ of the auxiliary PDF family as :

$$\boldsymbol{\theta}_k = \underset{\boldsymbol{\theta}\in\boldsymbol{\Theta}}{\mathrm{argmax}} \left\{ \frac{1}{M}\sum_{i=1}^{M} \left[\mathbb{1}_{g(\mathbf{u}_{(i)}[\tau_{\boldsymbol{\theta}_{k-1}}^{\mathbf{e}_0}])>q_k} \frac{\tau_{\boldsymbol{\theta}_0}^{\mathbf{e}_0}(\mathbf{u}_{(i)}[\tau_{\boldsymbol{\theta}_{k-1}}^{\mathbf{e}_0}])}{\tau_{\boldsymbol{\theta}_{k-1}}^{\mathbf{e}_0}(\mathbf{u}_{(i)}[\tau_{\boldsymbol{\theta}_{k-1}}^{\mathbf{e}_0}])} \ln\left[\tau_{\boldsymbol{\theta}}^{\mathbf{e}_0}(\mathbf{u}_{(i)}[\tau_{\boldsymbol{\theta}_{k-1}}^{\mathbf{e}_0}])\right] \right] \right\}$$

5. If $q_k \leq 0$, $k \leftarrow k+1$, go to Step 2
6. Estimate the probability

$$\mathbb{P}_{\mathbf{e}_0}^{\mathrm{CE}}(g(\mathbf{U}) > 0) = \frac{1}{M}\sum_{i=1}^{M} \mathbb{1}_{g(\mathbf{u}_{(i)}[\tau_{\boldsymbol{\theta}_k}^{\mathbf{e}_0}])>0} \frac{\tau_{\boldsymbol{\theta}_0}^{\mathbf{e}_0}(\mathbf{u}_{(i)}[\tau_{\boldsymbol{\theta}_k}^{\mathbf{e}_0}])}{\tau_{\boldsymbol{\theta}_k}^{\mathbf{e}_0}(\mathbf{u}_{(i)}[\tau_{\boldsymbol{\theta}_k}^{\mathbf{e}_0}])}$$

ρ is a parameter which is used to define the intermediary thresholds and has to be chosen carefully. Typical values for this parameter are given in [Boer et al., 2005].

9.3 Kriging-based adaptive Importance Sampling in the presence of epistemic uncertainty on input probability distributions

The uncertain parameters $e^{(i)}, i = 1, \ldots, w$ of the input PDF $\phi^{\mathbf{e}}(\cdot)$ are described using intervals: $e^{(i)} \in \left[e^{(i)}_{\min}, e^{(i)}_{\max}\right]$. In order to propagate this uncertainty to the probability of interest, one has to determine the probability bounds defined in Eqs.(9.1). Unfortunately, these optimizations are numerically expensive because they induce nested optimization and probability calculation steps, involving the input-output function $g(\cdot)$ which is also computationally expensive to evaluate. In order to tackle this problem, two techniques to perform fast CE probability calculations during the optimization process have been developed. The first one (section 9.3.1) aims to estimate a new probability due to a change of $\boldsymbol{e}$, based on preceding IS estimations, in order to reduce the number of samples that have to be generated to determine the probabilities of interest during the optimization. The second approach (section 9.3.2) aims at reducing the number of samples that have to be evaluated on the exact function $g(\cdot)$ by building a metamodel dedicated to adaptive IS, as proposed in [Balesdent et al., 2013]. Moreover, as the probability estimate is a random variable, the optimization process has to be robust to noisy objective functions. As described hereinafter, CMA-ES algorithm (section 5.5) is used to perform the optimization because it is able to efficiently handle noisy functions, as illustrated in several benchmarks [Hansen, 2009] (see chapter 5). An alternative gradient-based technique to optimize the bounds of the probability of failure based on its sensitivities will be proposed in the next chapter 10.

9.3.1 Method for estimating a new probability based on preceding Importance Sampling estimations

9.3.1.1 Description of the approach

In this section, we present the proposed method for estimating a new probability based on the preceding IS estimations. Let us consider the model described in the previous section, with the PDF of the input variables depending on a fixed parameter vector $\boldsymbol{e}$. Let us assume that an estimation of the probability of interest has been computed for a "nominal value" $\boldsymbol{e}_0$ of the uncertain parameter vector $\mathbb{P}^{\mathrm{CE}}_{\boldsymbol{e}_0}(g(\mathbf{U}) > 0)$. The problem to address is the evaluation of this probability when the input distribution parameters vary $\mathbb{P}^{\mathrm{CE}}_{\boldsymbol{e}}(g(\mathbf{U}) > 0)$, without having to carry out a complete CE estimation from the beginning, in order to reduce the computational cost.
The CE algorithm performed for the estimation of $\mathbb{P}^{\mathrm{CE}}_{\boldsymbol{e}_0}(g(\mathbf{U}) > 0)$ provides the CE optimal auxiliary density at the final iteration k: $\tau^{\mathbf{e}_0}_{\boldsymbol{\theta}_k}(\cdot)$ and the corresponding samples: $\mathbf{u}_{(1),\ldots,(M)}[\tau^{\mathbf{e}_0}_{\boldsymbol{\theta}_k}]$ for the initial vector $\boldsymbol{e}_0$. These samples and this density may be used as the initialization of the CE algorithm for estimating the probability of interest considering a new $\boldsymbol{e}$: $\mathbb{P}^{\mathrm{CE}}_{\boldsymbol{e}}(g(\mathbf{U}) > 0)$, in order to speed up the convergence of CE. Indeed, considering the definition of the IS probability estimate (Eq. 2.37), the density $\tau^{\mathbf{e}_0}_{\boldsymbol{\theta}_k}(\cdot)$ is able, whatever $\boldsymbol{e}$, to generate samples over the threshold which are relevant to estimate the probability of interest. Consequently, knowing $\tau^{\mathbf{e}_0}_{\boldsymbol{\theta}_k}(\cdot)$ for the estimation of $\mathbb{P}^{\mathrm{CE}}_{\boldsymbol{e}_0}(g(\mathbf{U}) > 0)$, we may propose $\tau^{\boldsymbol{e}}_{\boldsymbol{\theta}_0} = \tau^{\mathbf{e}_0}_{\boldsymbol{\theta}_k}$ as the initialization of the CE algorithm in order to estimate more quickly $\mathbb{P}^{\mathrm{CE}}_{\boldsymbol{e}}(g(\mathbf{U}) > 0)$. This distribution will be then reconfigured using the CE mechanisms in order to provide the optimal CE density for the considered $\boldsymbol{e}$ until the termination criterion of the algorithm is reached (estimation of the relative standard deviation of the probability

estimate under a given threshold Λ).

9.3.1.2 Proposed algorithm

Let us consider the density distribution $\tau_{\boldsymbol{\theta}_k}^{\mathbf{e}_0}(\cdot)$ and the corresponding samples $\mathbf{u}_{(1),\dots,(M)}[\tau_{\boldsymbol{\theta}_k}^{\mathbf{e}_0}](\cdot)$. The proposed algorithm considers $\tau_{\boldsymbol{\theta}_k}^{\mathbf{e}_0}$ as the initialization of CE and performs the classical CE algorithm considering as the termination criterion not the quantile ρ but the convergence of the probability estimate:

1. Define $\boldsymbol{e}$ the new value of the input distribution parameter vector, set $j = 1$, define the value of the termination criterion Λ, and consider $\tau_{\boldsymbol{\theta}_k}^{\mathbf{e}_0}(\cdot)$, $\mathbf{u}_{(1),\dots,(M)}[\tau_{\boldsymbol{\theta}_k}^{\mathbf{e}_0}]$ from the previous CE final iteration
2. Set $\tau_{\boldsymbol{\theta}_0}^{\boldsymbol{e}} = \tau_{\boldsymbol{\theta}_k}^{\mathbf{e}_0}$, $\mathbf{u}_{(1),\dots,(M)}[\tau_{\boldsymbol{\theta}_0}^{\boldsymbol{e}}] = \mathbf{u}_{(1),\dots,(M)}[\tau_{\boldsymbol{\theta}_k}^{\mathbf{e}_0}]$
3. Find the optimal parameter $\boldsymbol{\theta}_j$ according to the CE optimization process:

$$\boldsymbol{\theta}_j = \underset{\boldsymbol{\theta}\in\boldsymbol{\Theta}}{\operatorname{argmax}} \left\{ \frac{1}{M} \sum_{i=1}^{M} \left[\mathbb{1}_{g(\mathbf{u}_{(i)}[\tau_{\boldsymbol{\theta}_{j-1}}^{\boldsymbol{e}}])>0} \frac{\tau_{\boldsymbol{\theta}_0}^{\boldsymbol{e}}(\mathbf{u}_{(i)}[\tau_{\boldsymbol{\theta}_{j-1}}^{\boldsymbol{e}}])}{\tau_{\boldsymbol{\theta}_{j-1}}^{\boldsymbol{e}}(\mathbf{u}_{(i)}[\tau_{\boldsymbol{\theta}_{j-1}}^{\boldsymbol{e}}])} \ln \left[\tau_{\boldsymbol{\theta}}^{\boldsymbol{e}}(\mathbf{u}_{(i)}[\tau_{\boldsymbol{\theta}_{j-1}}^{\boldsymbol{e}}]) \right] \right] \right\}$$

4. Generate the population $\mathbf{u}_{(1)}[\tau_{\boldsymbol{\theta}_j}^{\boldsymbol{e}}], \dots, \mathbf{u}_{(M)}[\tau_{\boldsymbol{\theta}_j}^{\boldsymbol{e}}]$ according to the PDF $\tau_{\boldsymbol{\theta}_j}^{\boldsymbol{e}}(\cdot)$ and apply the function $g(\cdot)$ in order to have $\upsilon_{(1)} = g(\mathbf{u}_{(1)}[\tau_{\boldsymbol{\theta}_j}^{\boldsymbol{e}}]), \dots, \upsilon_{(M)} = g(\mathbf{u}_{(M)}[\tau_{\boldsymbol{\theta}_j}^{\boldsymbol{e}}])$
5. Compute the CE probability estimate

$$\mathbb{P}_j^{\mathrm{CE}} = \frac{1}{M} \sum_{i=1}^{M} \mathbb{1}_{g(\mathbf{u}_{(i)}[\tau_{\boldsymbol{\theta}_j}^{\boldsymbol{e}}])>0} \frac{\tau_{\boldsymbol{\theta}_0}^{\boldsymbol{e}}(\mathbf{u}_{(i)}[\tau_{\boldsymbol{\theta}_j}^{\boldsymbol{e}}])}{\tau_{\boldsymbol{\theta}_j}^{\boldsymbol{e}}(\mathbf{u}_{(i)}[\tau_{\boldsymbol{\theta}_j}^{\boldsymbol{e}}])}$$

6. Estimate $\mathbb{V}(\mathbb{P}_j^{\mathrm{CE}})$ according to Eq.(2.40). If $\frac{\sqrt{\mathbb{V}(\mathbb{P}_j^{\mathrm{CE}})}}{\mathbb{P}_j^{\mathrm{CE}}} > \Lambda$, set $j \leftarrow j+1$ and go to Step 3
7. Estimate the probability $\mathbb{P}_{\boldsymbol{e}}^{\mathrm{CE}}(g(\mathbf{U}) > 0) = \frac{1}{M} \sum_{i=1}^{M} \mathbb{1}_{g(\mathbf{u}_{(i)}[\tau_{\boldsymbol{\theta}_j}^{\boldsymbol{e}}])>0} \frac{\tau_{\boldsymbol{\theta}_0}^{\boldsymbol{e}}(\mathbf{u}_{(i)}[\tau_{\boldsymbol{\theta}_j}^{\boldsymbol{e}}])}{\tau_{\boldsymbol{\theta}_j}^{\boldsymbol{e}}(\mathbf{u}_{(i)}[\tau_{\boldsymbol{\theta}_j}^{\boldsymbol{e}}])}$

In this section, a method to limit the number of iterations of CE and consequently the number of samples of $\mathbf{U}$ that have to be generated to estimate the probability of interest has been developed. In the following section, we describe an approach to reduce the number of points that have to be physically simulated on $g(\cdot)$ at Step 4 of the described algorithm.

9.3.2 Kriging-based adaptive Cross Entropy

9.3.2.1 Description

In this section, a Kriging-based method to the adaptive IS is described. The main idea of this method is to build the surrogate model only in the area of interest *i.e.* in the vicinity of the threshold and in high probability content regions. Indeed, let $\widehat{g}(\cdot)$ be the surrogate model of $g(\cdot)$, the estimated probability is the same using $g(\cdot)$ or $\widehat{g}(\cdot)$ if the two indicator functions $\mathbb{1}_{g(\cdot)>0}$ and

$\mathbb{1}_{\widehat{g}(\cdot)>0}$ take the same values over the input variable variation domain.
Kriging surrogate modeling [Matheron, 1963; Sasena, 2002] is based on Gaussian process. It allows to estimate the variance of the surrogate prediction (section 2.5.1). This entity may be used to select the points to evaluate on $g(\cdot)$ to improve the accuracy of the surrogate model. The way to update the model is the critical point in Kriging-based modeling and different strategies may be applied (see section 2.5.1.1). In the following, a method developed in [Balesdent et al., 2013] to update the surrogate model dedicated to the adaptive IS is presented and will be used in the proposed method.

Let us briefly describe the Kriging model used to approximate $g(\cdot)$ on its input space $\mathbb{R}^d$. Let $\mathcal{X} = \{\mathbf{x}_{(1)}, \ldots, \mathbf{x}_{(p)}\}$, $\mathcal{X} \in \mathbf{\Omega}^p$ be an initial training set composed of p samples for which $g(\cdot)$ has been evaluated $\boldsymbol{g}_p(\mathcal{X}) = \left[g\left(\mathbf{x}_{(1)}\right), \ldots, g\left(\mathbf{x}_{(p)}\right)\right]^{\mathrm{T}}$. Kriging model is a Gaussian process $G(\cdot)$, expressed for any input vector $\mathbf{u} \in \mathbb{R}^d$, as:

$$G(\mathbf{u}) = m(\mathbf{u}) + Z(\mathbf{u}), \tag{9.3}$$

with $m(\cdot)$ a regression model estimated from available data and $Z(\cdot)$ a zero-mean Gaussian process. As presented in section 2.5.1, the Kriging predictor at any $\mathbf{u} \in \mathbb{R}^d$ is defined as:

$$\widehat{g}(\mathbf{u}, \mathcal{X}) = m(\mathbf{u}) + \mathbf{r}\left(\mathbf{u}, \mathcal{X}\right)^{\mathrm{T}} \mathbf{R}^{-1}(\mathcal{X}) \left(\boldsymbol{g}_p(\mathcal{X}) - \mathbf{m}_p(\mathcal{X})\right) \tag{9.4}$$

A confidence interval of the prediction may be computed through the variance of the Kriging prediction given by:

$$\widehat{\sigma}^2(\mathbf{u}, \mathcal{X}) = \sigma_Z^2 \left(1 - \mathbf{r}(\mathbf{u}, \mathcal{X})^{\mathrm{T}} \mathbf{R}^{-1}(\mathcal{X}) \mathbf{r}(\mathbf{u}, \mathcal{X})\right). \tag{9.5}$$

9.3.2.2 Method used to update the Kriging model

In this section, we describe the method used to update the Kriging model depending on the current iteration (l) of CE and the value of the ρ-quantile q_l. The method has been proposed in [Balesdent et al., 2013] and is dedicated to the refinement of Kriging model for IS. At the l^{th} iteration of CE, let $\mathcal{X} = \{\mathbf{x}_{(1)}, \ldots, \mathbf{x}_{(p)}\}$ be the current design of experiments, $\mathbb{U}^l$ the population generated by the auxiliary PDF (for conciseness, we do not mention the sampling distribution in the notation of this section : $\mathbb{U}^l = \{\mathbf{u}_{(1)}[\tau^{\boldsymbol{e}}_{\boldsymbol{\theta}_l}], \ldots, \mathbf{u}_{(M)}[\tau^{\boldsymbol{e}}_{\boldsymbol{\theta}_l}]\}$. Let $\tilde{\mathbb{U}}^l$ be the points that may be potentially misclassified (*i.e.* their predictions by Kriging model are above the current threshold q_l while the true values $g(\tilde{\mathbb{U}}^l)$ are below and conversely). Using the Kriging properties, $\tilde{\mathbb{U}}^l$ is defined as:

$$\tilde{\mathbb{U}}^l = \{\mathbf{u}_{(i)} \in \mathbb{U}^l, i = 1, \ldots, M | \widehat{g}(\mathbf{u}_{(i)}, \mathcal{X}) - \eta\widehat{\sigma}(\mathbf{u}_{(i)}, \mathcal{X}) < q_l < \widehat{g}(\mathbf{u}_{(i)}\mathcal{X}) + \eta\widehat{\sigma}(\mathbf{u}_{(i)}, \mathcal{X})\}, \tag{9.6}$$

where η is a parameter that defines the confidence level of the Kriging model (*e.g.* $\eta_S = 1.96$ defines a confidence level of 95%). Only these samples (and not the total population $\mathbb{U}^l$) have to be precisely determined in order to compute the auxiliary density (intermediate iterations of CE) of the probability estimate (final iteration). This is performed by appending new sampled points in the current training set according to a criterion in order to improve the accuracy of the surrogate model.
Since CE is an adaptive IS method, the surrogate model has to be defined not only for the final threshold $S = 0$ but also for each of the intermediary thresholds q_l. Defining the Kriging model with the same accuracy (η_S) at all of the IS intermediate thresholds is not an efficient strategy because it requires to compute $g(\cdot)$ on many points which do not intervene directly in the probability

estimation (points that define the intermediate thresholds but that are not involved directly in the probability computation). In order to adjust the accuracy of the surrogate model to the adaptive IS, η is defined for each iteration as a function of the current $\rho-$quantile q_l and the final threshold $S = 0$, in such a way that at the l^{th} iteration of the adaptive IS method, we have:

$$\eta_l = \eta_S \left(\frac{1}{q_l + 1} \right) \tag{9.7}$$

The new point which has to be added to the current design of experiments at this iteration $[l]$ should be the one that best reduces the uncertainty on $\tilde{\mathbb{U}}^l$. Let $AN(\mathcal{X}, \mathbf{x}, \tilde{\mathbb{U}}^l)$ be the criterion quantifying the improvement of the global uncertainty of $\tilde{\mathbb{U}}^l$ by adding $\mathbf{x}$ to the current training set $\mathcal{X}$:

$$\mathbf{x}^* = \underset{\mathbf{x} \in \text{supp}(\mathbf{\Omega}^d)}{\text{argmax}} \left(AN(\mathcal{X}, \mathbf{x}, \tilde{\mathbb{U}}^l) \right) = \underset{\mathbf{x} \in \text{supp}(\mathbf{\Omega}^d)}{\text{argmax}} \left\{ \sum_{i=1}^{\text{Card}(\tilde{\mathbb{U}}^l)} |\widehat{\sigma}(\tilde{\mathbf{u}}_{(i)}, \mathcal{X}) - \widehat{\sigma}(\tilde{\mathbf{u}}_{(i)}, \mathcal{X}, \mathbf{x})| \right\} \tag{9.8}$$

with

- $\widehat{\sigma}(\tilde{\mathbf{u}}, \mathcal{X})$ the standard deviation of the prediction at $\tilde{\mathbf{u}}$ related to the Kriging model built from the current training set $\mathcal{X}$,
- $\widehat{\sigma}(\tilde{\mathbf{u}}, \mathcal{X}, \mathbf{x})$ the standard deviation of the prediction at $\tilde{\mathbf{u}}$ related to the Kriging model built from the extended training set $\{\mathcal{X}, \mathbf{x}\}$[Balesdent et al., 2013]. We have:

$$\widehat{\sigma}^2 \left(\tilde{\mathbf{u}}, \mathcal{X}, \mathbf{x} \right) = \sigma^2_{Z'} (1 - \mathbf{r}'(\tilde{\mathbf{u}}, \mathcal{X}, \mathbf{x})^{\mathrm{T}} \mathbf{R}'^{-1}(\mathcal{X}, \mathbf{x}) \mathbf{r}'(\tilde{\mathbf{u}}, \mathcal{X}, \mathbf{x}) \Big) \tag{9.9}$$

with

$$\mathbf{r}'(\tilde{\mathbf{u}}, \mathcal{X}, \mathbf{x}) = [\mathbf{r}'(\tilde{\mathbf{u}}, \mathcal{X})^{\mathrm{T}}, \text{Corr}(\tilde{\mathbf{u}}, \mathbf{x})]^{\mathrm{T}} \tag{9.10}$$

and

$$\mathbf{R}'(\mathcal{X}, \mathbf{x}) = \begin{bmatrix} \text{Corr}(\mathbf{x}_{(1)}, \mathbf{x}_{(1)}) & \cdots & \text{Corr}(\mathbf{x}_{(1)}, \mathbf{x}_{(p)}) & \text{Corr}(\mathbf{x}_{(1)}, \mathbf{x}) \\ \vdots & \ddots & \vdots & \vdots \\ \text{Corr}(\mathbf{x}_{(p)}, \mathbf{x}_{(1)}) & \cdots & \text{Corr}(\mathbf{x}_{(p)}, \mathbf{x}_{(p)}) & \text{Corr}(\mathbf{x}_{(p)}, \mathbf{x}) \\ \text{Corr}(\mathbf{x}, \mathbf{x}_{(1)}) & \cdots & \text{Corr}(\mathbf{x}, \mathbf{x}_{(p)}) & \text{Corr}(\mathbf{x}, \mathbf{x}) \end{bmatrix}. \tag{9.11}$$

Since $g(\cdot)$ is unknown, $\sigma^2_{Z'}$ is approximated by σ^2_Z which is the estimated process standard deviation for the training set $\mathcal{X}$. This approximation may induce an error which is expected to be small when $\text{Card}(\mathcal{X})$ is large enough. This standard deviation may also be assumed to be known and kept constant [Cornford et al., 2005]. The optimization of the criterion AN enables to find the sample points with the biggest influence on the total standard deviation of the uncertain set. CMA-ES algorithm is used to optimize the refinement criterion, since this latter may be multimodal and present local minima. This optimization strategy has also been exploited in a similar context in [Picheny, 2009; Janusevskis and Le Riche, 2013; Balesdent et al., 2013].
This refinement process is included in the initial CE algorithm for IS probability estimation (the step 2 of "classical CE") and in the step 4 of the proposed algorithm (section 9.3.1.2) for re-estimating the probability with a change in input parameter distribution value):

1. Construct a Kriging surrogate model of the limit state function $g(\cdot)$ from the current training set $\mathcal{X}$,
2. Predict $\widehat{g}(\mathbf{u}_{(1)}, \mathcal{X}), \ldots, \widehat{g}(\mathbf{u}_{(M)}, \mathcal{X})$ using the metamodel, compute the confidence domain and determine $\tilde{\mathbb{U}}$,
3. While $\text{Card}(\tilde{\mathbb{U}}) \neq 0$
   (a) Optimize the criterion AN with CMA-ES to determine $\mathbf{x}^*$,
   (b) Evaluate $g(\mathbf{x}^*)$ and add it to the current training set, $M \leftarrow M + 1$,
   (c) Re-estimate the parameters of the Kriging model from the new training set,
   (d) Predict $\widehat{g}(\mathbf{u}_{(1)}, \mathcal{X}), \ldots, \widehat{g}(\mathbf{u}_{(M)}, \mathcal{X})$ using the surrogate model, compute the confidence domain and determine $\tilde{\mathbb{U}}$.

This approach allows to reduce the number of points to evaluate on $g(\cdot)$ at the intermediary iterations and to have an accuracy of $\eta_S = 1.96$ (95%) for the probability estimation at the final iteration of the CE algorithm. The relative part of the IS estimator variance due to the use of the Kriging surrogate model may be determined by deriving the probability of misclassification of a sample as described in [Balesdent et al., 2013]. To distinguish the probability estimated with the exact function $g(\cdot)$ and with the surrogate model, the following notation is adopted: $\widehat{\mathbb{P}}_{\max} = \max_{\mathbf{e} \in \boldsymbol{\Upsilon}} \mathbb{P}_{\mathbf{e}}^{\text{CE}}(\hat{g}(\mathbf{U}, \mathcal{X}) > 0)$ (same for $\widehat{\mathbb{P}}_{\min}$).
Since the rare event probability estimation calculated by IS is a multivariate integral estimation, it is a random variable. Therefore, the optimization process to compute the probability bounds has to be able to handle noisy objective functions. Optimization of noisy functions is a key problem as illustrated in chapter 5. Moreover, to our knowledge, no derivation of the sensitivity of the probability of failure computed by IS-CE has been derived with respect to epistemic uncertainty variables. Therefore, in this part, CMA-ES algorithm is used to find the probability bounds at it is an unconstrained noisy optimization problem. The different steps of the proposed approach to find the bounds on the probability estimate are illustrated in Figure 9.2.

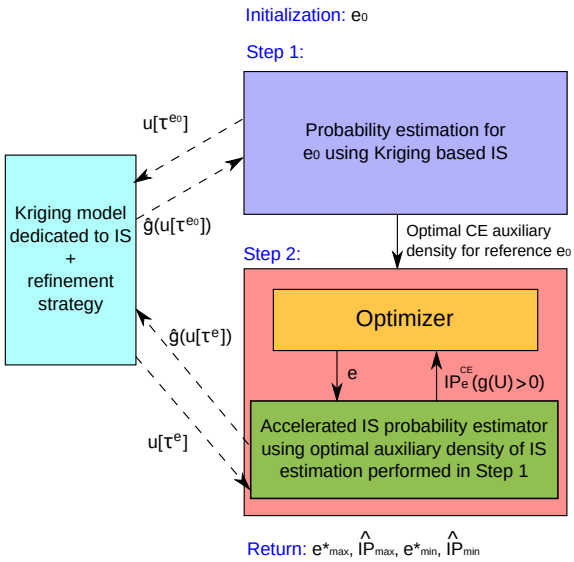

Figure 9.1: Proposed approach to propagate the epistemic uncertainty on input distribution parameters to the rare event probability estimate with a reduced computational cost

9.4 Analytical application cases

In order to evaluate the efficiency of the proposed method, the current one has been compared with two "classical engineering methods" on two test-cases of different complexities (one analytical toy case, one academic analytical test case). The classical methods used for determining the probability bounds $\mathbb{P}_{\max}$ and $\mathbb{P}_{\min}$ are the following:

- use of Crude Monte Carlo (CMC) simulations for both probability estimations and probability bound calculation (CMC-CMC) with the exact function $g(\cdot)$,
- use of classical IS for probability estimation (without Kriging) and CMC for probability bound determination (CMC-IS) with the exact function $g(\cdot)$.

For that purpose, a hundred samples of $\boldsymbol{e}$ have been generated with CMC for each bound determination using a uniform distribution $\mathcal{U}$ in $\boldsymbol{\Upsilon}$. For each sample, the corresponding probability $\mathbb{P}(\cdot)$ has been computed by using a huge CMC estimation in the first case and by using classical IS in the second case. $\mathbb{P}_{\max}$ (and respectively $\mathbb{P}_{\min}$) is then defined as the maximum (respectively the minimum) of the obtained set of probability estimates. $\mathbb{P}_{\max}$ is the bound on the probability that is the most interesting to design a complex system as it is in general a requirement to respect.
In order to compare the different methods, the optimization process by CMA-ES of the proposed method has been stopped at the 100^{th} iteration to perform the comparison with the same computational budget for the probability bound determination process in terms of number of probability estimations (of course, the computational budgets involved to perform the probability estimations are not the same and depend on the methods). The parameter Λ of the probability estimation algorithm has been chosen in such a way that the standard deviation of the probability estimate

is below 10%.

9.4.1 Ackley test case

9.4.1.1 Description

The input-output function of the toy case corresponds to an Ackley-like modified function. The traditional Ackley function [Ackley, 1987] has been modified in order to be consistent with the level of probability of failure (Fig. 9.2). This function is a classical multimodal non linear and non convex optimization benchmark function and is relevant to evaluate the efficiency of algorithm to find $\boldsymbol{e}$ that maximizes or minimizes the probability estimate. The expression of the limit state function is given in Eq.(9.14). The considered uncertain parameters are the means of the multivariate Gaussian input distribution. The covariance matrix is fixed and is equal to identity. The probability of failure calculated with the classical CE for the reference value of $\boldsymbol{e}$ is 6.3×10^{-5}.

$$S = 0 \tag{9.12}$$

$$\mathbf{U} \sim \mathcal{N}(\boldsymbol{e}, I_2) \tag{9.13}$$

$$g : \left| \begin{array}{l} \mathbb{R}^2 \to \mathbb{R} \\ x \to -10 + \frac{1}{y}\left(-a \exp\left(-b\sqrt{\frac{\sum_{i=1}^{2}(u^{(i)} - \kappa)^2}{l}} \right) - \exp\left(\frac{b}{l} \cos\left(c \sum_{i=1}^{2}(u^{(i)} - \kappa)^2 \right) \right) + d \right) \end{array} \right. \tag{9.14}$$

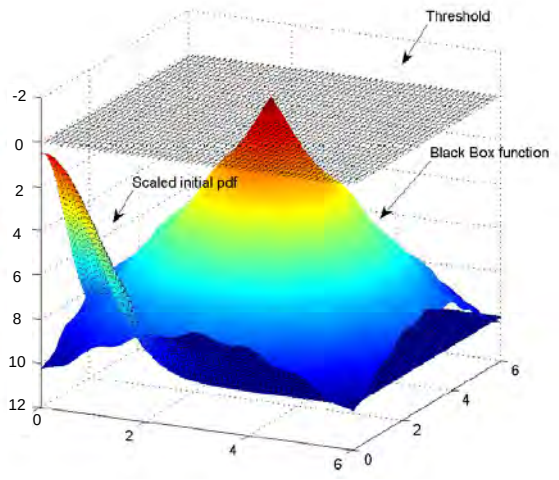

Figure 9.2: Aclkey function, threshold and initial PDF

with $a = 20$, $b = 0.2$, $c = 2\pi$, $d = a + \exp(1) + 5.7$, $y = 0.8$, $\kappa = 2.5$ and $l = 2$. The bounds on the input distribution parameters are: $\mathbf{e}_{\min} = [-1, -1]^T$ and $\mathbf{e}_{\max} = [4, 4]^T$. The bounds on these parameters are very large and non realistic in practice. These variation domains have been

arbitrary chosen large in order to test the ability of the proposed algorithm to find the lower and upper bounds on the probability estimate in critical conditions. The maximum of the function is located at $(2.5, 2.5)$.

9.4.1.2 Results

The results obtained for this test case are illustrated in Figures 9.3-9.9 and summarized in Table 9.5. The estimated bounds on the probability interval are $\widehat{\mathbb{P}}_{\min} = 1.65 \times 10^{-7}$ and $\widehat{\mathbb{P}}_{\max} = 3.14 \times 10^{-2}$, and correspond to $\boldsymbol{e} = [-1.00, -1.00]^T$ and $\boldsymbol{e} = [2.48, 2.49]^T$, that is consistent with the reality (Fig. 9.3-9.9). Indeed, the parameters that give the lower bound are located at the opposite of the maximum of the Ackley function and at the bounds of the input parameter variation domain. On the other hand, the input parameters that provide the maximal probability are located near the coordinates of the maximum of the transfer function. In that way, the combination of these parameters allows to sample a maximum of points over the threshold and consequently allows to maximize the failure probability.

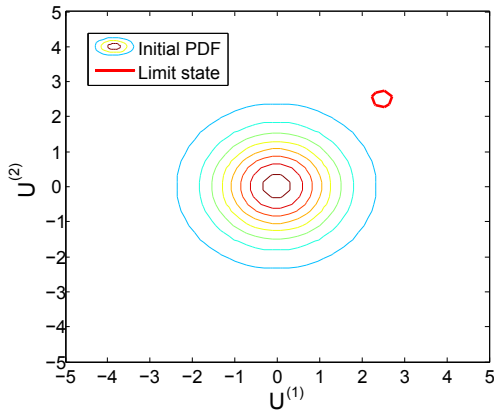

Figure 9.3: Initial PDF and limit state function

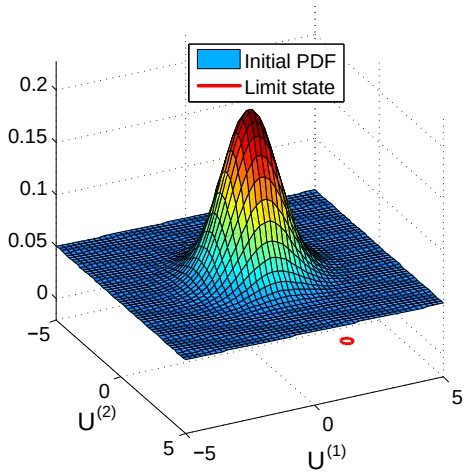

Figure 9.4: Initial PDF in 3D and limit state function

Table 9.5: Synthesis of the Ackley test case

	Proposed method	CMC-CMC	CMC-IS
Number of samples required by CE for estimating the probability with reference $\boldsymbol{e}_0$	1.20×10^4	10^6	1.20×10^4
Number of samples evaluated on $g(\cdot)$ for estimating the probability with reference $\boldsymbol{e}_0$ using Kriging	290	/	/
Estimation of $\widehat{\mathbb{P}}_{\boldsymbol{e}_0}(g(\mathbf{U}) > 0)$	6.32×10^{-5}	6.35×10^{-5}	6.33×10^{-5}
Std deviation of the probability estimate for reference $\boldsymbol{e}_0$	2.29%	12.5%	4.43%
$\widehat{\mathbb{P}}_{\max}$	3.14×10^{-2}	2.85×10^{-2}	2.88×10^{-2}
$\boldsymbol{e}$ corresponding to $\widehat{\mathbb{P}}_{\max}$	$[2.48, 2.49]^T$	$[2.44, 2.20]^T$	$[2.29, 2.17]^T$
Number of points evaluated on $g(\cdot)$ to find $\widehat{\mathbb{P}}_{\max}$	274	10^8	1.20×10^6
Std deviation of $\mathbb{P}_{\max}$	2.17%	0.58%	4.29%
$\widehat{\mathbb{P}}_{\min}$	1.65×10^{-7}	5.00×10^{-6}	1.67×10^{-6}
$\boldsymbol{e}$ corresponding to $\widehat{\mathbb{P}}_{\min}$	$[-1.00, -1.00]^T$	$[-0.42, -0.60]^T$	$[-0.49, -0.80]^T$
Number of points evaluated on $g(\cdot)$ to find $\widehat{\mathbb{P}}_{\min}$	201	10^8	1.20×10^6
Std deviation of $\widehat{\mathbb{P}}_{\min}$	2.03%	45%	4.88%
Average number of points evaluated on $g(\cdot)$ to provide an estimation of $\mathbb{P}$ during the probability bound calculation	2.37	10^6	1.20×10^4

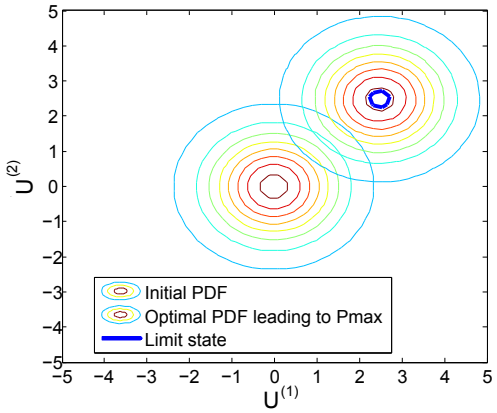

Figure 9.6: Optimal PDF with $\mathbf{e} = [2.48, 2.49]^T$ leading to $\widehat{\mathbb{P}}_{\max}$

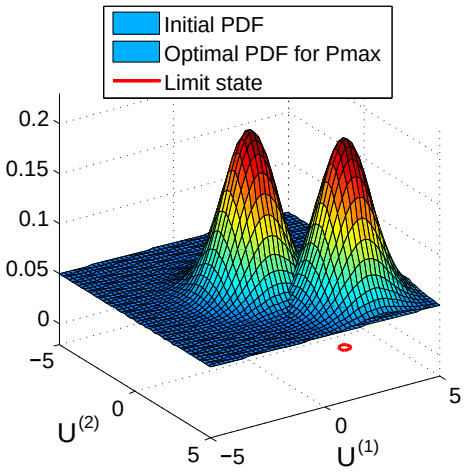

Figure 9.7: Optimal PDF in 3D with $\mathbf{e} = [2.48, 2.49]^T$ leading to $\widehat{\mathbb{P}}_{\max}$

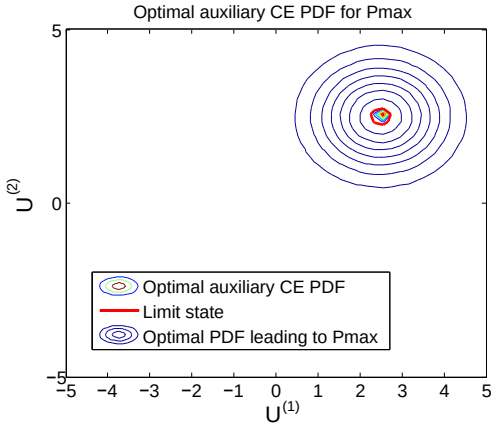

Figure 9.8: Optimal CE auxiliary PDF used to compute leading to $\widehat{\mathbb{P}}_{\max}$

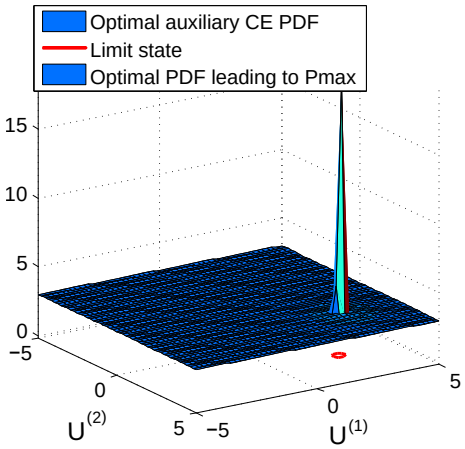

Figure 9.9: Optimal CE auxiliary PDF in 3D used to compute leading to $\widehat{\mathbb{P}}_{\max}$

In this test-case, the Ackley function is relatively smooth and low dimensional. The Kriging surrogate performs well to model the function and only a few number of reevaluations of $g(\cdot)$ are required for re-estimating the probability with a change in $\boldsymbol{e}$.

In order to evaluate the efficiency of the proposed method, estimations of $\mathbb{P}_{\max}$ and $\mathbb{P}_{\min}$ have been performed using "classical methods", *i.e.* using CMC for both probability estimations and probability bound calculation (CMC-CMC), and classical IS for probability estimation and CMC for probability bound determination (CMC-IS). For that purpose, a hundred samples of $\boldsymbol{\theta}$ have been generated with CMC, and for each of them,

In order to evaluate the efficiency of the proposed method, the estimations of $\mathbb{P}_{\max}$ and $\mathbb{P}_{\min}$ have been performed with the two classical methods. For this case, the simulation budget of the probability estimation by CMC-CMC has been fixed to 10^6. The results obtained with CMC-CMC and

CMC-IS are summarized in Table 9.5. Concerning the estimation of the probability for the reference $\boldsymbol{e}_0$, all the methods provide the same estimation of the probability but the standard deviation of proposed and classical IS are much lower that CMC, that points out a better accuracy of the estimation. Since the simulation budget for each CMC probability estimation is 10^6, the probabilities lower than 10^{-6} are not affordable with this technique (and the probabilities lower than 10^{-5} are very imprecise), consequently the lower bound on the probability estimate cannot be estimated using a total simulation budget of 10^8. The proposed method requires 765 (=290+274+201) evaluations of $g(\cdot)$ to determine the probability bounds. CMC-IS requires 1.20×10^6 samples to estimate the bounds, but the lower bound cannot be determined accurately because the simulation budget of 100 probability estimations is not sufficient in this case. As we can see, the proposed approach clearly outperforms CMC based procedures, in terms of calculation cost and quality of the found results. In this case, the average number of points really evaluated on the input-output function to provide an estimation of the probability during the optimization process is very low and less than 3.

9.4.2 Non-linear oscillator

9.4.2.1 Description

The second analytical test case is a one-degree-of-freedom non-linear oscillator. This example is used in [Rajashekhar and Ellingwood, 1993; Gomes and Awruch, 2004] but has been modified in such a way that the failure corresponds to a rare event. The dimension of the input space is 6 and the different variables are distributed according to 6 Gaussian distributions. The means of c_1, c_2, r and m, and the standard deviations of t_1 and F_1 are supposed to be uncertain.

$$S = 0 \tag{9.15}$$

$$\mathbf{U} = [c_1, c_2, r, m, t_1, F_1]^{\mathrm{T}} \sim \left[\mathcal{N}(e^{(1)}, 0.1^2), \mathcal{N}(e^{(2)}, 0.01^2), \mathcal{N}(e^{(3)}, 0.05^2), \mathcal{N}(e^{(4)}, 0.05^2), \mathcal{N}\left(1, {e^{(5)}}^2\right), \mathcal{N}\left(1, {e^{(6)}}^2\right)\right]^{\mathrm{T}} \tag{9.16}$$

$$g : \left| \begin{array}{l} \mathbb{R}^6 \to \mathbb{R} \\ \mathbf{u} = [c_1, c_2, r, m, t_1, F_1]^{\mathrm{T}} \to -1 - 3r - \left| \dfrac{2F_1}{c_1 + c_2} \sin\left(\sqrt{\dfrac{c_1 + c_2}{m}} \dfrac{t_1}{2}\right) \right| \end{array} \right. \tag{9.17}$$

The means (respectively variances) are supposed to vary by 2% (respectively 10%) around their reference value (Table 9.10). The probability of failure calculated with the classical CE for the reference value of $\boldsymbol{e}$ is 3.32×10^{-6}.

Table 9.10: Variation domain of the uncertain parameters

Parameter	Variation domain
$\mathbb{E}(c_1)$	[0.98, 1.02]
$\mathbb{E}(c_2)$	[0.098,0.102]
$\mathbb{E}(m)$	[0.98,1.02]
$\mathbb{E}(r)$	[0.49,0.51]
$\sigma(t_1)$	[0.18,0.22]
$\sigma(F_1)$	[0.18,0.22]

9.4.2.2 Results

The results obtained for the oscillator test-case are given in Table 9.11.
The proposed method requires approximately 1755 evaluations of the exact limit state function in order to determine the two bounds of the probability estimate interval, that represents approximately 7 evaluations of the function per probability estimation during the optimization process, which is very low. The estimated bounds on the probability correspond to the bounds of the

uncertain parameter variation domain $\boldsymbol{e}$.
Concerning CMC-CMC, since the dimension of the input-parameter variation domain is 6, the method consisting in performing a huge CMC of the parameters to estimate the bounds is clearly not affordable here. Indeed, with a total simulation budget of 10^9 for the input-output function evaluations, only 100 combinations of the parameters can be evaluated if 10^7 samples per parameter combination are used for estimating the probability by the CMC at lower level. As in the previous example, the proposed method outperforms CMC-CMC and CMC-IS in terms of quality of the results and number of evaluations of the input-output function. One can notice here that CMC-CMC and CMC-IS provide quite different estimations of $\widehat{\mathbb{P}}_{\min}$ for quasi-identical $\boldsymbol{e}$. This is due to the rareness of the considered event corresponding to the simulation budget used in CMC-CMC, that implies very inaccurate results for such range of probability (very high variance of the estimation). The accuracies of the probability estimates $\widehat{\mathbb{P}}_{\boldsymbol{e}_0}$, $\widehat{\mathbb{P}}_{\min}$ and $\widehat{\mathbb{P}}_{\max}$ (illustrated by the standard deviation) are in the same order of magnitude (around 5%) for the proposed and CMC-IS methods. This is due to the use of IS which performs well to estimate the considered probabilities. However, the difference in terms of probability value of $\widehat{\mathbb{P}}_{\min}$ (2.68×10^{-7} vs. 4.96×10^{-7}) may be explained by the found values of $\boldsymbol{e}$ corresponding to $\widehat{\mathbb{P}}_{\min}$, which are different for the two methods. The determination by optimization (proposed method) is more efficient to find the optimal $\boldsymbol{e}$ corresponding to $\widehat{\mathbb{P}}_{\min}$, than CMC. An analog reasoning may be used to explain the difference in the $\widehat{\mathbb{P}}_{\max}$ values.

9.5 Limitations of the proposed approach

The proposed approach presents several limits. Due to the use of CE to solve reliability analysis problems, multiple failure regions are not intrinsically taken into account. Several techniques have been proposed to extend CE to multiple failure zones [Kurtz and Song, 2013]. An alternative to CE could be to use NAIS to perform IS (section 2.4.3). Moreover, due to the use of Kriging surrogate model, the reliability analysis problem that may be solved are limited to low dimensional problem as Kriging present some computational cost and accuracy issues in high dimensions [Shan and Wang, 2010]. The proposed method decreases the computational cost compared to classical techniques, however, it presents a higher level of complexity in terms of implementation and tuning compared to CMC classically used in UMDO which may complicate its use within this framework. Further investigations are required to incorporate the proposed technique within UMDO.

Table 9.11: Synthesis of the oscillator test-case using proposed method, CMC-CMC and CMC-IS

	Proposed method	CMC-CMC	CMC-IS
Number of samples required by CE for estimating the probability with reference $\boldsymbol{e}_0$	1.40×10^4	10^7	1.40×10^4
Number of samples evaluated on $g(\cdot)$ for estimating the probability with reference $\boldsymbol{e}_0$ using Kriging	341	/	/
Estimation of $\widehat{\mathbb{P}}_{\boldsymbol{e}_0}(g(\mathbf{U}) > 0)$	3.33×10^{-6}	3.37×10^{-6}	3.32×10^{-6}
Std deviation of the probability estimate for reference $\boldsymbol{e}_0$	5.34%	17.8%	5.45%
$\widehat{\mathbb{P}}_{\max}$	2.22×10^{-5}	1.45×10^{-5}	1.38×10^{-5}
$\boldsymbol{e}$ corresponding to $\widehat{\mathbb{P}}_{\max}$	$[0.98, 0.10, 0.98, 0.49, 0.22, 0.21]^T$	$[0.99, 0.10, 1.00, 0.49, 0.21, 0.21]^T$	$[0.99, 0.10, 1.00, 0.49, 0.21, 0.21]^T$
Number of points evaluated on $g(\cdot)$ to find $\widehat{\mathbb{P}}_{\max}$	662	10^9	1.40×10^6
Std deviation of the $\widehat{\mathbb{P}}_{\max}$ estimate	4.39%	8.30%	5.30%
$\widehat{\mathbb{P}}_{\min}$	2.68×10^{-7}	4.00×10^{-7}	4.96×10^{-7}
$\boldsymbol{e}$ corresponding to $\widehat{\mathbb{P}}_{\min}$	$[1.02, 0.10, 1.02, 0.51, 0.18, 0.18]^T$	$[1.00, 0.10, 0.99 0.50, 0.18, 0.19]^T$	$[1.01, 0.10, 1.00, 0.50, 0.18, 0.18]^T$
Number of points evaluated on $g(\cdot)$ to find $\widehat{\mathbb{P}}_{\min}$	752	10^9	1.40×10^6
Std deviation of the $\widehat{\mathbb{P}}_{\min}$ estimate	6.04%	50.0%	6.10%
Average number of points evaluated on $g(\cdot)$ to provide an estimation of P during the probability bound calculation	7.07	10^7	1.40×10^4

9.6 Conclusion

In this chapter, a method for propagating parameter uncertainty on the input distributions to the rare event probability estimation has been proposed. To this end, an approach to reevaluate the IS estimation due to a change in the input distribution parameters has been developed. It allows to reduce the computational cost of the probability evaluations. The proposed method involves a surrogate model with controlled error, adapted to IS, in order to reduce the number of the exact function evaluations. A parametric IS method is adopted with an accelerated version of CE in which the auxiliary density is initialized in accordance to the previous CE estimation for another

epistemic uncertainty value decreasing the computational cost. Moreover, a dedicated optimization algorithm (CMA-ES) is used in order to estimate the probability bounds in the presence of noise inherent to the use of IS. The proposed approach has been compared with two engineering methods involving CMC and classical IS on two analytical test cases. The developed method requires fewer calls to the exact limit state function and provides better estimation of the probability bounds. In chapter 11 this approach will be applied on a launch vehicle analysis problem involving a safety zone determination for a stage fallout.
In the next chapter, another reliability analysis method is proposed to handle epistemic uncertainty directly affecting the limit state function.

- Context:
  - Reliability analysis in the presence of mixed aleatory/epistemic uncertainties,
  - Epistemic uncertainty on the hyper-parameters of the aleatory distributions,
  - State-of-the-art methods are either computationally expensive (CMC) or limited to simple problem (FORM), see chapter 4.
- Contributions:
  - Development of a new reliability analysis method based on an accelerated version of CE combined with an adapted Kriging model to IS and a dedicated refinement strategy.
  - Application and comparison of the proposed approach on two analytical test cases, highlighting its efficiency to propagate epistemic uncertainty to failure probability.
- Actionable information:
  - Useful for problems that present modeling uncertainty in the hyper-parameters of the aleatory distributions,
  - Essential to ensure system design reliability based on our present uncertain modeling knowledge,
  - Accurate reliability estimation could be used to re-optimize the safety margins.
- Perspectives:
  - Extend the approach to handle multiple failure regions,
  - Extend the technique to solve high dimensional problems (>10),
  - Incorporate the method within the UMDO context.

Chapter 10

Reliability analysis in the presence of mixed aleatory/epistemic uncertainties

Contents

Chapter goals

- Develop a reliability analysis method in the presence of epistemic uncertainty affecting the system limit state function,
- Apply and compare the proposed approach to reference techniques on an analytical test case.

10.1 Introduction and problem statement

In the previous chapter, a technique has been presented to take into account epistemic uncertainty affecting the hyper-parameters of PDF distributions in reliability assessment problems. This chapter is devoted to the presentation of a reliability analysis method dedicated to the presence of epistemic uncertainty modifying the limit state of the system. Lack of knowledge or simplification assumptions may introduce model uncertainties that have to be taken into account to accurately estimate the reliability of a system. These uncertainties directly affect the modeling of the system dynamics and therefore the limit state function delimiting safe from failure regions. When these epistemic uncertainties are modeled with interval formalism, dedicated techniques have to be employed. Indeed, the failure probability is not unique and depends on the values taken by epistemic uncertainty . To characterize the probability of failure, it is possible to determine its domain of variation. The proposed approach to solve this type of problem consists of a two steps sequential loop. Firstly, an Interval Analysis (IA) which includes Probability Analysis (PA) based on Subset Simulation combined with a Kriging surrogate model of the limit state function is performed. Secondly, the metamodel refinement is performed to ensure efficient probability bound estimations. This surrogate model is constructed in the joint aleatory/epistemic uncertain space in order to accurately represent the limit state function in the area of interest *i.e.* in the vicinity of the threshold, in high probability content regions and around the epistemic variable values leading to the minimal and maximal failure probabilities. The Kriging model does not need to be accurate in the whole epistemic uncertain space or in low probability content regions but just around the optimal epistemic variable values, *i.e.* the values leading to the probability bounds. The Kriging prediction variance enables to control the surrogate model error and to refine it. The refinement strategy is based on a modification of the Generalized Max-min [Lacaze and Missoum, 2014b] to take into account the presence of epistemic uncertainty.
Consider a d-dimensional random vector $\mathbf{U}$ defined on the sampling space $\mathbf{\Omega}$ by a jointPDF $\phi(\cdot)$ and a w-dimensional vector $\mathbf{e} = [e^{(1)}, \ldots, e^{(w)}]$. $\mathbf{e}$ represents epistemic uncertainties defined using intervals: $\mathbf{e} \in \mathbf{\Upsilon} = \{\mathbf{e} \in \mathbb{R}^w |\ e^{(i)} \in \left[e^{(i)}_{\min}, e^{(i)}_{\max}\right]\ \forall i \in \{1, \ldots, w\}\}$. Consider a system characterized by a limit state function $g : \mathbf{\Omega} \times \mathbf{\Upsilon} \to \mathbb{R}$ assumed to be a deterministic continuous input-output function. The reliability analysis of the system consists in determining its probability of failure defined as $\mathbb{P}(g(\mathbf{U}, \mathbf{e}) > S)$ with $S = 0$ the threshold. Due to the complexity of the physical phenomena involved in the simulation of $g(\cdot)$, it is supposed that $g(\cdot)$ is non linear and presents multiple failure regions. In the presence of mixed aleatory and epistemic uncertainties impacting the system, the failure probability is not unique and depends on the values taken by $\mathbf{e}$. To characterize the probability of failure, it is possible to determine its domain of variation by finding the lower and upper bounds:

$$\begin{cases} \mathbb{P}_{\min} = \min\limits_{\mathbf{e} \in \mathbf{\Upsilon}}\ \mathbb{P}(g(\mathbf{U}, \mathbf{e}) > 0) \\ \mathbb{P}_{\max} = \max\limits_{\mathbf{e} \in \mathbf{\Upsilon}}\ \mathbb{P}(g(\mathbf{U}, \mathbf{e}) > 0) \end{cases} \tag{10.1}$$

The determination of the probability bounds requires an optimization problem solving. In this chapter, gradient-based optimization techniques are favored due to their fast convergence properties and their scalability when gradients are available. In order to use gradient-based optimization algorithms, a sensitivity estimation of the probability of failure with respect to epistemic uncertain variables $\mathbf{e}$ is proposed in the first section of this chapter. The sensitivity will be latter used in IA to find the bounds on the probability of failure. For this purpose, an analytical derivation

based on the properties of the indicator function $\mathbb{1}_{(\cdot)}$ is proposed (section 10.2). Estimators for the sensitivity using CMC simulation and Subset Simulation are subsequently derived. In addition, the numerical implementation of the proposed sensitivities requires the approximation of a Dirac distribution (section 10.2.2). In section 10.2.3, the sensitivity estimates are compared to a case where the exact sensitivities are available. This section also discusses the choice of a parameter involved in the approximation of the Dirac distribution. Then, in section 10.3, using these sensitivities, the proposed sequential method and the different steps to estimate the failure probability bounds with reduced computational cost is detailed. Finally, in section 10.4 the proposed reliability assessment technique is compared to a reference approach which consists in an analytical test case to demonstrate the effectiveness of the proposed approach.

10.2 Sensitivity of the probability of failure with respect to decision variables

In this section the sensitivities are derived for a decision variable vector $\mathbf{z}$ (which may be for instance deterministic design variables or epistemic uncertain variables). In the next sections, the considered decision variables in IA will be the epistemic uncertain variable vector $\mathbf{e}$. In its most general form, a probability of failure is defined as:

$$\mathbb{P}(\mathbf{z}, \boldsymbol{\theta}) = \int_{\Omega_f(\mathbf{z})} \phi^{\boldsymbol{\theta}}(\mathbf{u}) \mathrm{d}\mathbf{u} \tag{10.2}$$

where $\mathbf{z} \in \mathbb{R}^n$ are decision variables (*e.g.* design variables) and $\boldsymbol{\theta} \in \mathbb{R}^p$ are hyper-parameters of the PDF $\phi^{\boldsymbol{\theta}}(\cdot)$ of the random variables $\mathbf{U} \in \boldsymbol{\Omega}$, with $\boldsymbol{\Omega}$ the sampling space. Ω_f stands for the failure domain. Note that $\boldsymbol{\theta}$ only influences the joint distribution while $\mathbf{z}$ only influences the definition of the failure domain Ω_f. Beyond reliability assessment, such a probability of failure also appears in Reliability-based Design Optimization (RDBO) [Youn et al., 2004; Aoues and Chateauneuf, 2010] or in UMDO problems. When gradient-based techniques are used to solve UMDO problems, the sensitivities of $\mathbb{P}(\cdot)$ with respect to the decision variables are needed [Zou and Mahadevan, 2006; Lee et al., 2011]. Sensitivities of $\mathbb{P}(\cdot)$ with respect to $\boldsymbol{\theta}$ have been derived for various reliability analysis techniques [Zou and Mahadevan, 2006; Song et al., 2009; Dubourg et al., 2011]. However, to our knowledge, there are no existing derivations of sensitivities with respect to decision variables, such as deterministic design variables or epistemic uncertain variables.

The difficulty stems from the dependence of the failure domain on the decision variables. In many approaches, probabilities of failure are calculated based on a fixed failure domain. For methods involving the estimation of the gradient of the probability of failure, this has confined current UMDO and RDBO techniques to problems that exclude deterministic design variables or gradient-based optimization algorithms. Sensitivities of the probability of failure with respect to deterministic variables would therefore substantially extend previous gradient-based RDBO techniques and offer new perspectives in UMDO.

The objective of this section is to propose a formulation of the sensitivity of the failure probability with respect to the decision variable vector $\mathbf{z}$. For this purpose, an analytical derivation based on the properties of the indicator function $\mathbb{1}_{(\cdot)}$ is proposed (section 10.2). Estimators for the sensitivity using CMC simulation and Subset Simulation (section 10.2.1) are subsequently derived. In addition, the numerical implementation of the proposed formulation requires the approximation of a Dirac distribution (section 10.2.2). In section 10.2.3, the sensitivity estimates are compared

to a case where the exact sensitivities are available. This section also discusses the choice of a parameter involved in the approximation of the Dirac distribution.
In most applications, the failure domain is expressed as:

$$\Omega_f(\mathbf{z}) = \{\mathbf{u} \in \mathbf{\Omega} |\, g(\mathbf{u}, \mathbf{z}) > 0\} \tag{10.3}$$

which depends on random variable vector $\mathbf{U}$ and decision variable vector $\mathbf{z}$. This leads to another well known expression of the probability of failure:

$$\mathbb{P}(\mathbf{z}) = \int_{\Omega} \mathbb{1}_{g(\mathbf{u},\mathbf{z})>0} \phi(\mathbf{u}) \mathrm{d}\mathbf{u} \tag{10.4}$$

For the sake of clarity and without loss of generality, $\boldsymbol{\theta}$ was omitted. According to the differentiation rules under the integral symbol using the theory of distributions [Schwartz, 1957; Jones, 1982], the sensitivity of $\mathbb{P}(\cdot)$ with respect to the variable $z^{(k)}$, k^{th} coordinate of $\mathbf{z}$ reads:

$$\begin{aligned} \left.\frac{\partial \mathbb{P}}{\partial z^{(k)}}\right|_{\mathbf{z}} &= \frac{\partial}{\partial z^{(k)}} \int_{\Omega} \mathbb{1}_{g(\mathbf{u},\mathbf{z})>0} \phi(\mathbf{u}) \mathrm{d}\mathbf{u} \\ &= \int_{\Omega} \frac{\partial}{\partial z^{(k)}} \mathbb{1}_{g(\mathbf{u},\mathbf{z})>0} \phi(\mathbf{u}) \mathrm{d}\mathbf{u} \end{aligned} \tag{10.5}$$

From the theory of distributions, the derivative of the indicator function is:

$$\frac{\mathrm{d}\mathbb{1}_{y\geq 0}}{\mathrm{d}y} = -\frac{\mathrm{d}\mathbb{1}_{y\leq 0}}{\mathrm{d}y} = \delta_y = \begin{cases} +\infty & \text{if } y = 0 \\ 0 & \text{otherwise} \end{cases} \tag{10.6}$$

where δ is the Dirac distribution. Hence, Eq.(10.5) becomes:

$$\left.\frac{\partial \mathbb{P}}{\partial z^{(k)}}\right|_{\mathbf{z}} = \int_{\Omega} \left.\frac{\partial g}{\partial z^{(k)}}\right|_{\mathbf{u},\mathbf{z}} \delta_{g(\mathbf{u},\mathbf{z})} \phi(\mathbf{u}) \mathrm{d}\mathbf{u} \tag{10.7}$$

Note that Eq.(10.7) involves the derivative of $g(\cdot)$. Such derivatives are always available if $g(\cdot)$ is replaced by an approximation $\widehat{g}(\cdot)$ such as an adequate metamodel.

10.2.1 Sensitivity estimators

In practice, the integrals involved in Eq.(10.4) and Eq.(10.7) are intractable. In order to evaluate the integral in Eq.(10.4), sampling-based techniques are typically used. The CMC estimator is defined as:

$$\mathbb{P}(\mathbf{z}) \approx \frac{1}{M} \sum_{i=1}^{M} \mathbb{1}_{g(\mathbf{u}_{(i)},\mathbf{z})>0} \tag{10.8}$$

where $\mathbb{U} = \left\{\mathbf{u}_{(1)}, \ldots, \mathbf{u}_{(M)}\right\}$ is a CMC sample of size M distributed according to $\phi(\cdot)$. From Eq.(10.7), the CMC estimator of $\frac{\partial \mathbb{P}}{\partial z^{(k)}}$ is:

$$\left.\frac{\partial \mathbb{P}}{\partial z^{(k)}}\right|_{\mathbf{z}} \approx \frac{1}{M} \sum_{i=1}^{M} \left.\frac{\partial g}{\partial z^{(k)}}\right|_{\mathbf{u}_{(i)},\mathbf{z}} \delta_{g(\mathbf{u}_{(i)},\mathbf{z})} \tag{10.9}$$

However, in the case of a rare event probability estimation, CMC simulations are intractable. For this reason, a wide variety of variance reduction techniques have been introduced over the years [Rubinstein and Kroese, 2011]. Among them, the Subset Simulation (SS) [Au and Beck, 2001; Song et al., 2009] derives a small probability of failure as a product of larger conditional ones. Specifically, given a failure domain Ω_f, let $\Omega_{f_0} \equiv \Omega \supset \Omega_{f_1} \supset \cdots \supset \Omega_{f_\lambda} \equiv \Omega_f$ be a decreasing sequence of $\lambda + 1$ failure domains where:

$$\Omega_{f_i}(\mathbf{z}) = \{\, \mathbf{u} |\, g_i(\mathbf{u}, \mathbf{z}) > 0\} \qquad \forall i = \{1, \ldots, \lambda\} \tag{10.10}$$

Eq.(10.4) can be expressed as:

$$\mathbb{P}(\mathbf{z}) = \prod_{i=1}^{\lambda} \mathbb{P}_i(\mathbf{z}) \tag{10.11}$$

where:

$$\mathbb{P}_1(\mathbf{z}) = \int_\Omega \mathbb{1}_{g_1(\mathbf{u},\mathbf{z})>0} \phi(\mathbf{u}) \mathrm{d}\mathbf{u} \tag{10.12}$$

and for $\forall i = \{2, \ldots, \lambda\}$:

$$\mathbb{P}_i(\mathbf{z}) = \int_\Omega \mathbb{1}_{g_i(\mathbf{u},\mathbf{z})>0} \tau_{i-1}\left(\mathbf{u} | \Omega_{f_{i-1}}(\mathbf{z})\right) \mathrm{d}\mathbf{u} \tag{10.13}$$

with $\tau_{i-1}\left(\mathbf{u} | \Omega_{f_{i-1}}(\mathbf{z})\right)$ the conditional auxiliary PDF associated to the failure domain $\Omega_{f_i}(\mathbf{z})$ defined as [Song et al., 2009].

$$\tau_{i-1}\left(\mathbf{u} | \Omega_{f_{i-1}}(\mathbf{z})\right) = \frac{\mathbb{1}_{g_{i-1}(\mathbf{u},\mathbf{z})>0}}{\prod_{j=1}^{i-1} \mathbb{P}_j(\mathbf{z})} \phi(\mathbf{u}) \tag{10.14}$$

Therefore:

$$\begin{aligned} \mathbb{P}_i(\mathbf{z}) &= \int_\Omega \mathbb{1}_{g_i(\mathbf{u},\mathbf{z})>0} \frac{\mathbb{1}_{g_{i-1}(\mathbf{u},\mathbf{z})>0}}{\prod_{j=1}^{i-1} \mathbb{P}_j(\mathbf{z})} \phi(\mathbf{u}) \mathrm{d}\mathbf{u} \\ &= \int_\Omega \frac{\mathbb{1}_{g_i(\mathbf{u},\mathbf{z})>0}}{\prod_{j=1}^{i-1} \mathbb{P}_j(\mathbf{z})} \phi(\mathbf{u}) \mathrm{d}\mathbf{u} \qquad \forall i = \{2, \ldots, \lambda\} \end{aligned} \tag{10.15}$$

Based on SS, the sensitivity of $\mathbb{P}(\cdot)$ is:

$$\left.\frac{\partial \mathbb{P}}{\partial z^{(k)}}\right|_{\mathbf{z}} = \mathbb{P}(\mathbf{z}) \sum_{i=1}^{\lambda} \frac{1}{\mathbb{P}_i(\mathbf{z})} \left.\frac{\partial \mathbb{P}_i}{\partial z^{(k)}}\right|_{\mathbf{z}} \tag{10.16}$$

For the first SS sub-domain, we have:

$$\left.\frac{\partial \mathbb{P}_1}{\partial z^{(k)}}\right|_{\mathbf{z}} = \int_\Omega \left.\frac{\partial g_1}{\partial z^{(k)}}\right|_{\mathbf{u},\mathbf{z}} \delta_{g_1(\mathbf{u},\mathbf{z})} \phi(\mathbf{u}) \mathrm{d}\mathbf{u} \tag{10.17}$$

and for any subsequent step $i > 1$:

$$\begin{aligned}\left.\frac{\partial \mathbb{P}_i}{\partial z^{(k)}}\right|_{\mathbf{z}} &= \int_\Omega \frac{\partial}{\partial z^{(k)}}\left[\frac{\mathbb{1}_{g_i(\mathbf{u},\mathbf{z})>0}}{\prod_{j=1}^{i-1}\mathbb{P}_j(\mathbf{z})}\right]\phi(\mathbf{u})\mathrm{d}\mathbf{u} \\ &= \int_\Omega \left.\frac{\partial g_i}{\partial z^{(k)}}\right|_{\mathbf{u},\mathbf{z}} \frac{\delta_{g_i(\mathbf{u},\mathbf{z})}}{\prod_{j=1}^{i-1}\mathbb{P}_j(\mathbf{z})}\phi(\mathbf{u})\mathrm{d}\mathbf{u} \\ &\quad + \frac{\frac{\partial}{\partial z^{(k)}}\left[\prod_{j=1}^{i-1}\mathbb{P}_j(\mathbf{z})\right]}{\prod_{j=1}^{i-1}\mathbb{P}_j^2(\mathbf{z})}\int_\Omega \mathbb{1}_{g_i(\mathbf{u},\mathbf{z})>0}\phi(\mathbf{u})\mathrm{d}\mathbf{u}\end{aligned} \tag{10.18}$$

Noting the three following relations:

$$\int_\Omega \mathbb{1}_{g_i(\mathbf{u},\mathbf{z})>0}\phi(\mathbf{u})\mathrm{d}\mathbf{u} = \prod_{j=1}^{i}\mathbb{P}_j(\mathbf{z}) \tag{10.19}$$

$$\frac{\partial}{\partial z^{(k)}}\left[\prod_{j=1}^{i-1}\mathbb{P}_j(\mathbf{z})\right] = \prod_{j=1}^{i-1}\mathbb{P}_j(\mathbf{z})\sum_{j=1}^{i-1}\frac{1}{\mathbb{P}_j(\mathbf{z})}\left.\frac{\partial \mathbb{P}_j}{\partial z^{(k)}}\right|_{\mathbf{z}} \tag{10.20}$$

$$\phi(\mathbf{u}) = \frac{\prod_{j=1}^{i-1}\mathbb{P}_j(\mathbf{z})}{\mathbb{1}_{g_{i-1}(\mathbf{u},\mathbf{z})>0}}\tau_{i-1}\left(\mathbf{u}|\Omega_{f_{i-1}}(\mathbf{z})\right)\ \ \forall \mathbf{u}\in\Omega_{f_{i-1}}(\mathbf{z})\ , \tag{10.21}$$

where $\phi(\cdot)$ is defined only on $\Omega_{f_{i-1}}(\mathbf{z})$ and that the support of $\tau_{i-1}\left(\cdot|\Omega_{f_{i-1}}(\mathbf{z})\right)$ is $\Omega_{f_{i-1}}(\mathbf{z})$, the i^{th} intermediate sensitivity is:

$$\begin{aligned}\left.\frac{\partial \mathbb{P}_i}{\partial z^{(k)}}\right|_{\mathbf{z}} &= \int_\Omega \left.\frac{\partial g_i}{\partial z^{(k)}}\right|_{\mathbf{u},\mathbf{z}} \delta_{g_i(\mathbf{u},\mathbf{z})}\tau_{i-1}\left(\mathbf{u}|\Omega_{f_{i-1}}(\mathbf{z})\right)\mathrm{d}\mathbf{u} \\ &\quad + \mathbb{P}_i(\mathbf{z})\sum_{j=1}^{i-1}\frac{1}{\mathbb{P}_j(\mathbf{z})}\left.\frac{\partial \mathbb{P}_j}{\partial z^{(k)}}\right|_{\mathbf{z}}\end{aligned} \tag{10.22}$$

Each of these derivatives may be estimated using the result of a SS. Given $\underline{\mathbb{U}}$ a SS sample defined as $\underline{\mathbb{U}} = \left\{\mathbf{u}^{\{1\}},\ldots,\mathbf{u}^{\{\lambda\}}\right\}$ such that:

$$\mathbf{u}^{\{1\}} \sim \tau_0\left(\cdot|\Omega_{f_0}(\mathbf{z})\right) \equiv \phi(\cdot) \tag{10.23}$$

$$\mathbf{u}^{\{i\}} \sim \tau_{i-1}\left(\cdot|\Omega_{f_{i-1}}(\mathbf{z})\right) \qquad \forall i = \{2,\ldots,\lambda\}\ , \tag{10.24}$$

the estimators of the sensitivities Eq.(10.17) and Eq.(10.22) are:

$$\left.\frac{\partial \mathbb{P}_1}{\partial z^{(k)}}\right|_{\mathbf{z}} \approx \frac{1}{M_1}\sum_{l=1}^{M_1}\left.\frac{\partial g_1}{\partial z^{(k)}}\right|_{\mathbf{u}_{(l)}^{\{1\}},\mathbf{z}}\delta_{g_1\left(\mathbf{u}_{(l)}^{\{1\}},\mathbf{z}\right)} \tag{10.25}$$

$$\begin{aligned}\left.\frac{\partial \mathbb{P}_i}{\partial z^{(k)}}\right|_{\mathbf{z}} \approx \frac{1}{M_i}\sum_{l=1}^{M_i}\left.\frac{\partial g_i}{\partial z^{(k)}}\right|_{\mathbf{u}_{(l)}^{\{i\}},\mathbf{z}}\delta_{g_i\left(\mathbf{u}_{(l)}^{\{i\}},\mathbf{z}\right)} + \\ \mathbb{P}_i(\mathbf{z})\sum_{j=1}^{i-1}\frac{1}{\mathbb{P}_j(\mathbf{z})}\left.\frac{\partial \mathbb{P}_j}{\partial z^{(k)}}\right|_{\mathbf{z}}\end{aligned} \tag{10.26}$$

Combining all the intermediate sensitivities, we finally get:

$$\left.\frac{\partial \mathbb{P}}{\partial z^{(k)}}\right|_{\mathbf{z}} = \mathbb{P}(\mathbf{z}) \sum_{i=1}^{\lambda} \left\{ \frac{1}{\mathbb{P}_i(\mathbf{z})} \cdot \left[\frac{1}{M_i} \sum_{l=1}^{M_i} \left.\frac{\partial g_i}{\partial z^{(k)}}\right|_{\mathbf{u}_{(l)}^{\{i\}},\mathbf{z}} \delta_{g_i\left(\mathbf{u}_{(l)}^{\{i\}},\mathbf{z}\right)} \right.\right.$$
$$\left.\left. + \mathbb{P}_i(\mathbf{z}) \sum_{j=1}^{i-1} \frac{1}{\mathbb{P}_j(\mathbf{z})} \left.\frac{\partial \mathbb{P}_j}{\partial z^{(k)}}\right|_{\mathbf{z}} \right] \right\} \tag{10.27}$$

10.2.2 Approximation of the Dirac distribution

The presence of a Dirac distribution in Eq. 10.27 makes the numerical computation of the sensitivities intractable. To overcome this hurdle, the Dirac distribution is approximated using a smooth function $\hat{\delta}$ such that $\lim_{\sigma \to 0} \hat{\delta}_y(\sigma) = \delta_y$. This approach has been widely used in the past, *e.g.* for Gaussian approximation [Yoo and Lee, 2014]. Five candidates are considered in this work:

Gaussian $\hat{\delta}_y(\sigma) = \frac{1}{\sigma\sqrt{2\pi}} \exp^{-\frac{y^2}{2\sigma^2}} = \frac{1}{\sigma}\phi_{\mathcal{N}}\left(\frac{y}{\sigma}\right)$

Truncated Gaussian $\hat{\delta}_y(\sigma) = \frac{\frac{1}{\sigma}\phi_{\mathcal{N}}\left(\frac{y}{\sigma}\right)}{\Phi_{\mathcal{N}}(1) - \Phi_{\mathcal{N}}(-1)} \mathbb{1}_{-\sigma \leq y \leq \sigma}$

Sinc $\hat{\delta}_y(\sigma) = \frac{\sin\left(\frac{y}{\sigma}\right)}{y\pi}$

Bump $\hat{\delta}_y(\sigma) = \frac{1}{A\sigma} \exp^{-\frac{1}{1-\left(\frac{y}{\sigma}\right)^2}} \mathbb{1}_{-\sigma \leq y \leq \sigma}$

$A = \int_{-1}^{1} \exp^{-\frac{1}{1-y^2}} \mathrm{d}y$

Poisson $\hat{\delta}_y(\sigma) = \frac{\sigma}{\pi(\sigma^2 + y^2)}$

$\phi_{\mathcal{N}}(\cdot)$ and $\Phi_{\mathcal{N}}(\cdot)$ the PDF and CDF of the Gaussian distribution. All these functions include a scalar parameter σ which defines the "width" of the Dirac approximation. The choice of the approximation as well as σ is of prime importance. Ideally, one would like σ to tend to zero. However, because we are using sampling-based methods, only a finite amount of information is available. For this reason, an "optimal" value of σ needs to be chosen.

10.2.3 Numerical experiments. Selection of the shape parameter.

The optimal value of σ and the choice of Dirac approximation might be problem dependent. Statistically, the optimal choice is the one that minimizes the error between the actual and the estimated sensitivity. Knowing the true sensitivity, traditional performance metrics of an estimator may be computed, such as normalized bias ($Bias$), standard deviation (Std) and root mean square error ($RMSE$):

$$Bias\ (\%) = 100 \times \frac{\left|\mathbb{E}\left[\tilde{\psi}\right] - \psi\right|}{\psi} \tag{10.28}$$

$$Std\ (\%) = 100 \times \frac{\sqrt{\mathbb{E}\left[\tilde{\psi}^2\right] - \mathbb{E}\left[\tilde{\psi}\right]^2}}{\psi} \tag{10.29}$$

$$RMSE\ (\%) = 100 \times \frac{\sqrt{\mathbb{E}\left[\left(\tilde{\psi} - \psi\right)^2\right]}}{\psi} \tag{10.30}$$

where ψ is the actual sensitivity as defined in Eq.(10.35) and $\tilde{\psi}$ is an estimator of ψ, as defined in Eq.(10.9). At this point, it is important to recall that the estimator of the sensitivity encompasses two levels of approximation:

$$\begin{aligned}\left.\frac{\partial \mathbb{P}}{\partial z^{(k)}}\right|_{\mathbf{z}} &= \int_\Omega \left.\frac{\partial g}{\partial z^{(k)}}\right|_{\mathbf{u},\mathbf{z}} \delta_{g(\mathbf{u},\mathbf{z})}\phi(\mathbf{u})\mathrm{d}\mathbf{u} \\ &\approx \int_\Omega \left.\frac{\partial g}{\partial z^{(k)}}\right|_{\mathbf{u},\mathbf{z}} \hat{\delta}_{g(\mathbf{u},\mathbf{z})}\phi(\mathbf{u})\mathrm{d}\mathbf{u} \qquad (10.31) \\ &\approx \frac{1}{M}\sum_{i=1}^{M} \left.\frac{\partial g}{\partial z^{(k)}}\right|_{\mathbf{u}_{(i)},\mathbf{z}} \hat{\delta}_{g(\mathbf{u}_{(i)},\mathbf{z})} \qquad (10.32)\end{aligned}$$

Because CMC estimators are unbiased, Eq.10.32 only introduces *variance* in the estimator. On the other hand, Eq.10.31 is an analytical approximation, and only introduces *bias* on the estimator. Although the variance could be estimated using the standard error, the bias is not strictly speaking statistical. Therefore it cannot be quantified statistically, such as with leave one out approaches. The "optimal" σ is obtained through experiments. Although not optimal for *any* problem, this *educated guess* of σ would lead to better results than an arbitrary one. As a demonstrative case, consider the following linear analytical limit state, for which analytical sensitivities may be derived:

$$g(u, z) = u + z - d > 0 \tag{10.33}$$

where $U \sim \mathcal{N}(0, 1)$. Because the limit state function is linear, the probability of failure and its derivative may be obtained exactly:

$$\mathbb{P}(z) = 1 - \Phi_{\mathcal{N}}(d - z) \tag{10.34}$$

$$\left.\frac{\mathrm{d}\mathbb{P}}{\mathrm{d}z}\right|_z = \phi_{\mathcal{N}}(d - z) \tag{10.35}$$

The number of CMC samples (M) is defined to ensure a 5% coefficient of variation on the probability of failure:

$$M(z) = \left\lceil \left(\frac{\sqrt{1 - \mathbb{P}(z)}}{\sqrt{\mathbb{P}(z)} \times 0.05} \right)^2 \right\rceil \tag{10.36}$$

where $\mathbb{P}(\cdot)$ is defined by Eq.(10.34) and $\lceil\cdot\rceil$ the ceiling function.
σ is a function of the number of samples (*i.e.* the amount of information) available, which is in turn influenced by the value of $\mathbb{P}(\cdot)$. For this reason, a parameter α is introduced to define a fraction M_r of the available samples so that $M_r = \lceil \mathbb{P}(z) \times M \times \alpha \rceil$, where $\mathbb{P}(\cdot)$ is estimated using Eq. 10.8. Because the optimal value of σ is also dependent on the variation domain of $g(\cdot)$, the following quantities are defined. Let $\boldsymbol{\upsilon}$ be the vector of responses such that $\upsilon^{(i)} = g\left(\mathbf{u}_{(i)}, \mathbf{z}\right)$, $|\boldsymbol{\upsilon}|$ the vector of absolute values of $\boldsymbol{\upsilon}$ and the rank operator such that $\upsilon^{[1]} = \min(\boldsymbol{\upsilon}^{(i)})$ and $\upsilon^{[M]} = \max(\boldsymbol{\upsilon}^{(i)})$, $i \in \{1, \ldots, M\}$. σ is therefore defined as $\upsilon^{[M_r]}$ so that only the M_r closest points from the limit

Table 10.1: Normalized bias ($Bias$), standard error (Std) and root mean square error ($RMSE$) at $\alpha = \alpha_{opt}$ and $\alpha = 0.5$. Gaussian approximation.

$\mathbb{P}(\cdot)$	10^{-1}	10^{-2}	10^{-3}	10^{-4}
$\alpha_{opt}\|\alpha$	0.94|0.50	0.59|0.50	0.53|0.50	0.50|0.50
$Bias(\alpha_{opt})\|Bias(\alpha)$	2.52|1.54	2.62|1.94	2.30|2.03	2.55|2.55
$Std(\alpha_{opt})\|Std(\alpha)$	3.40|5.15	4.74|5.18	4.89|5.04	5.22|5.22
$RMSE(\alpha_{opt})\|RMSE(\alpha)$	4.23|5.36	5.41|5.52	5.40|5.43	5.80|5.80

state have function value within $\pm\sigma$. These points are the most relevant to the calculation of the sensitivity of $\mathbb{P}(\cdot)$ because they will potentially lead to a variation of $\mathbb{1}_{g(\mathbf{u},\mathbf{z})\leq 0}$.
The experiments is reproduced for four values of d such that $\mathbb{P}(\cdot)$ equals 10^{-1}, 10^{-2}, 10^{-3}, and 10^{-4}. For SS, each probability step (here, 10^{-1}) is estimated using CMC (w.r.t a conditional distribution). Figure 12.10 shows the plots of normalized bias Eq.10.28, standard error Eq.10.29 and root mean square error Eq.10.30 for the example introduced in Eq.10.33. Expectations in Eqs.(10.28-10.30) are calculated out of 300 repetitions. The experiment is repeated for 4 levels of probability. Two immediate conclusions arise:

- The Poisson approximation shows a poor performance compared to the other approximations,
- The Sinc approximation provides inconsistent results.

Out of the three remaining approximations, the Gaussian one has the lowest variance across the experiments. Note that this is a very favorable feature for optimization. In gradient-based optimization, the variance in the sensitivities will impair the convergence properties more than the bias. For these reasons, the Gaussian approximation is elected.
From the results in Figure 12.10, in the case of a Gaussian approximation, a graphical inspection shows that a value of $\alpha = 0.5$ is a satisfactory choice for the minimization of $RMSE$. This value can be compared to the solution of the following optimization problem:

$$\alpha_{opt} = \arg\min_{\alpha} \quad RMSE(\alpha) \tag{10.37}$$

Table 10.1 shows normalized bias Eq.10.28, standard error Eq.10.29 and root mean square error Eq.10.30 for $\alpha = \alpha_{opt}$ and $\alpha = 0.5$. Except for the case $\mathbb{P}(\cdot) = 10^{-1}$, $\alpha = 0.5$ yields similar results to $\alpha = \alpha_{opt}$. For $\mathbb{P}(\cdot) = 10^{-1}$ it yields to an increase in the $RMSE$ of about 1%.

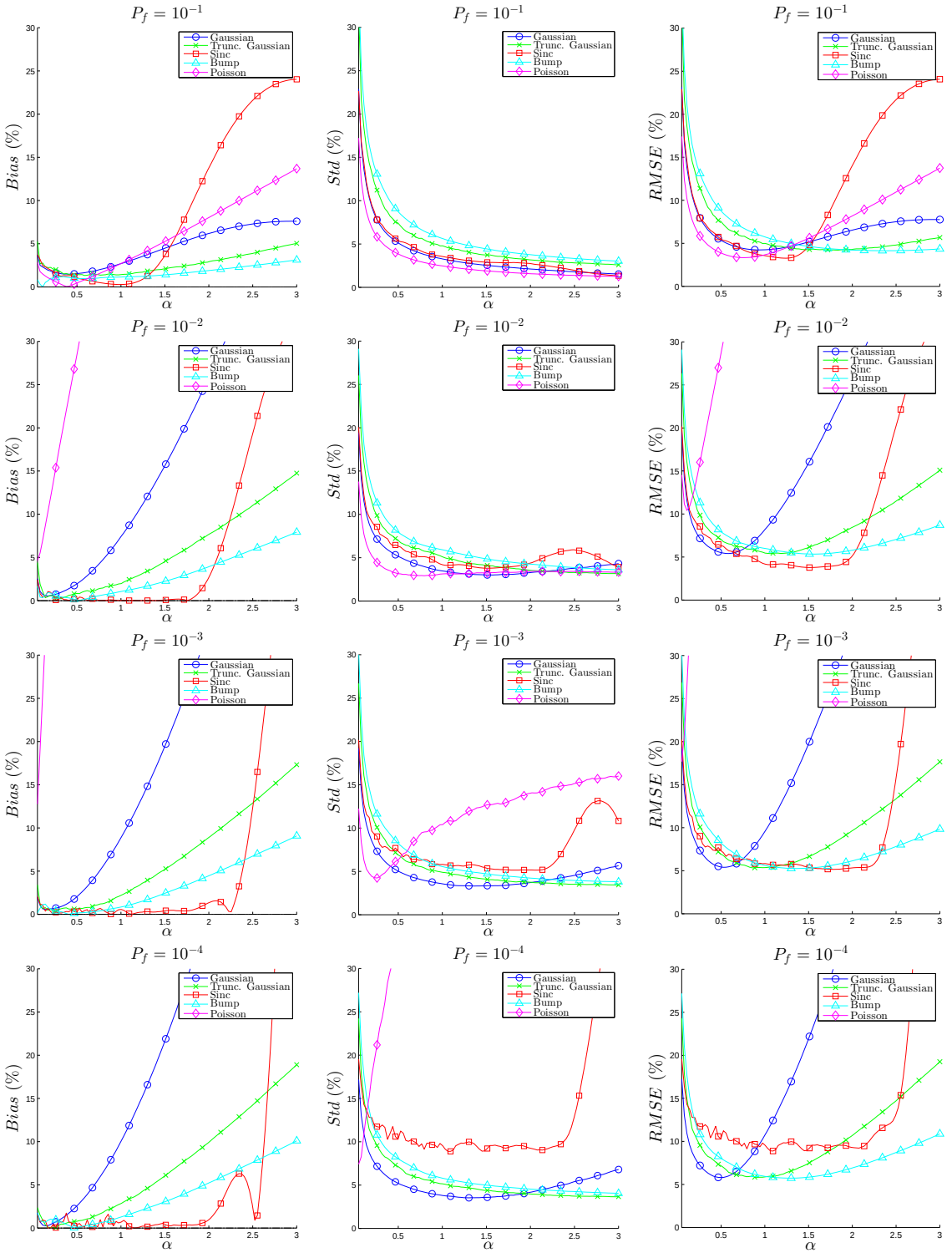

Figure 10.2: Normalized bias ($Bias$), standard error (Std) and root mean square error ($RMSE$) for 4 level of probability of failure.

10.3 Proposed method for mixed aleatory/epistemic reliability analysis

The sensitivity of the probability of failure with respect to decision variables will be used to solve IA where the decision variables are the epistemic uncertain variables. In this section, instead of solving both equations in Eqs.(10.1), we focus on the computation of the maximum probability of failure $\mathbb{P}_{\max}$ as it may be used to evaluate the system safety. The same analysis may be derived for $\mathbb{P}_{\min}$. In order to compute the maximal probability of failure, a sequential approach (Fig. 10.3) of IA and surrogate model refinement is proposed. Subset Simulation is used to evaluate the probability of failure as it is efficient to estimate rare event probability [Au and Beck, 2001] and is able to handle multiple failure regions and non linear limit state function. Kriging surrogate model of the limit state function is used in order to decrease the number of calls to the expensive code. To take into account the presence of mixed aleatory and epistemic uncertainties, the Kriging surrogate model is constructed in the joint aleatory-espistemic uncertain space $\mathbf{\Omega} \times \mathbf{\Upsilon}$ and a dedicated refinement method is derived from the Generalized Max-min [Lacaze and Missoum, 2014b]. The sequential approach enables to refine the Kriging model only around the epistemic variable values, in high probability content regions leading to $\mathbb{P}_{\max}$ and not on the entire epistemic and aleatory uncertain spaces, limiting the number of evaluations of $g(\cdot)$. The proposed approach is detailed in the following sections.

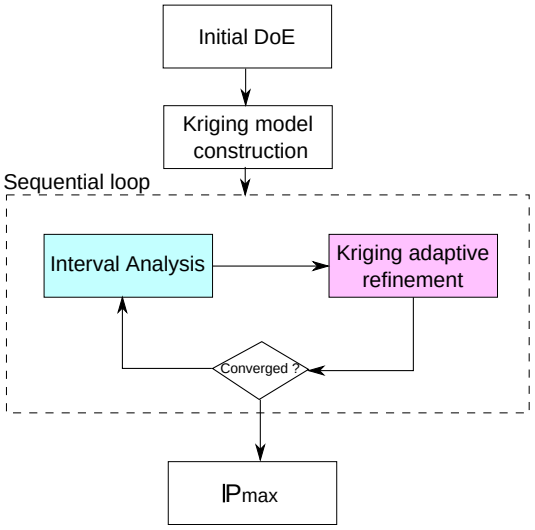

Figure 10.3: Flowchart of the proposed process for reliability analysis in the presence of mixed aleatory/epistemic uncertainties

10.3.1 Training set and Kriging construction

The first step of the proposed approach is to construct an initial training set composed of p samples $\mathcal{X} = \{(\mathbf{u}_{(1)}, \mathbf{e}_{(1)}), \ldots, (\mathbf{u}_{(p)}, \mathbf{e}_{(p)})\} \in \mathbf{\Omega} \times \mathbf{\Upsilon}$ and to build a Kriging surrogate model in the joint

aleatory/epistemic uncertain space $\mathbf{\Omega} \times \mathbf{\Upsilon}$ based on the DoE. The exact limit state function $g(\cdot)$ is evaluated on the DoE $\boldsymbol{g}_p(\mathcal{X}) = \left[g(\mathbf{u}_{(1)}, \mathbf{e}_{(1)}), \ldots, g(\mathbf{u}_{(p)}, \mathbf{e}_{(p)})\right]^{\mathrm{T}}$. Then, a Kriging surrogate model is built based on the training set and its parameters are determined by Maximum Likelihood Estimation. The Kriging prediction for any $(\mathbf{u}, \mathbf{e}) \in \mathbf{\Omega} \times \mathbf{\Upsilon}$ is given by

$$\hat{g}(\mathbf{u}, \mathbf{e}, \mathcal{X}) = m(\mathbf{u}, \mathbf{e}) + \mathbf{r}(\mathbf{u}, \mathbf{e}, \mathcal{X})^{\mathrm{T}} \mathbf{R}^{-1} \left(\mathcal{X}\right)\left(\boldsymbol{g}_p(\mathcal{X}) - \mathbf{m}_p(\mathcal{X})\right), \tag{10.38}$$

and the associated prediction variance

$$\sigma^2(\mathbf{u}, \mathbf{e}, \mathcal{X}) = \sigma_Z^2 \left(1 - \mathbf{r}(\mathbf{u}, \mathbf{e}, \mathcal{X})^{\mathrm{T}} \mathbf{R}^{-1}(\mathcal{X}) \mathbf{r}(\mathbf{u}, \mathbf{e}, \mathcal{X})\right). \tag{10.39}$$

The Kriging surrogate model built in the joint aleatory/epistemic uncertain space is used instead of the exact limit state function to compute the probability of failure. Based on the prediction variance, the Kriging model is refined in the joint uncertain space in order to ensure an accurate probability estimation (low variance) for the epistemic variable values leading to a maximal failure probability. The interval analysis step is detailed in section 10.3.2.

10.3.2 Interval analysis and probability estimation

IA consists in solving an optimization problem in order to find the epistemic variable value leading to the maximal failure probability $\mathbb{P}_{\max} = \max_{\mathbf{e} \in \mathbf{\Upsilon}} \mathbb{P}(g(\mathbf{U}, \mathbf{e}) > 0)$. Instead of computing the probability with the real limit state function, the problem is reformulated such that $\hat{\mathbb{P}}_{\max} = \max_{\mathbf{e} \in \mathbf{\Upsilon}} \mathbb{P}(\hat{g}(\mathbf{U}, \mathbf{e}, \mathcal{X}) > 0)$. The surrogate model used for IA is the Kriging model constructed from the DoE at the first sequential loop iteration ($t = 1$) or the refined Kriging model at the next iterations ($t \geq 2$).
At the j^{th} IA iteration, the probability of failure for an epistemic variable value $\mathbf{e}^{[j]}$ is given by:

$$\mathbb{P}\left(\mathbf{e}^{[j]}\right) = \mathbb{P}(g(\mathbf{U}, \mathbf{e}^{[j]}) > 0) = \int_{\{\mathbf{u} | g(\mathbf{u}, \mathbf{e}^{[j]}) > 0\}} \phi(\mathbf{u}) \mathrm{d}\mathbf{u} \tag{10.40}$$

$$= \int_{\mathbf{\Omega}} \mathbb{1}_{g(\mathbf{u}, \mathbf{e}^{[j]}) > 0} \phi(\mathbf{u}) \mathrm{d}\mathbf{u} \simeq \hat{\mathbb{P}}\left(\mathbf{e}^{[j]}\right) \tag{10.41}$$

$$\hat{\mathbb{P}}\left(\mathbf{e}^{[j]}\right) = \int_{\mathbf{\Omega}} \mathbb{1}_{\hat{g}(\mathbf{u}, \mathbf{e}^{[j]}, \mathcal{X}) > 0} \phi(\mathbf{u}) \mathrm{d}\mathbf{u} \tag{10.42}$$

Eq.(10.42) approximates the failure probability $\mathbb{P}\left(\mathbf{e}^{[j]}\right)$ due to the use of the Kriging surrogate model. Eq.(10.42) is computed by Subset Simulation (see Section 2.4.4)

$$\hat{\mathbb{P}}\left(\mathbf{e}^{[j]}\right) = \int_{\mathbf{\Omega}} \mathbb{1}_{\hat{g}(\mathbf{u}, \mathbf{e}^{[j]}, \mathcal{X}) > 0} \phi(\mathbf{u}) \mathrm{d}\mathbf{u}, \tag{10.43}$$

$$= \prod_{i=1}^{\lambda} \mathbb{P}\left(\mathbf{U} \in \hat{\Omega}_{f_i}\left(\mathbf{e}^{[j]}\right) | \mathbf{U} \in \hat{\Omega}_{f_{i-1}}\left(\mathbf{e}^{[j]}\right)\right), \tag{10.44}$$

with $\hat{\Omega}_{f_i}(\mathbf{e}^{[j]}) = \{\mathbf{u} | \hat{g}(\mathbf{u}, \mathbf{e}^{[j]}, \mathcal{X}) > S_i\} \quad \forall i \in \{1, \ldots, \lambda\}$ the failure domain associated to the Kriging model and S_i the intermediate thresholds.

Finally, using Subset Simulation and Kriging, IA consists in solving the following optimization problem:

$$\max \quad \prod_{i=1}^{\lambda} \mathbb{P}\left(\mathbf{U} \in \hat{\Omega}_{f_i}(\mathbf{e}) | \mathbf{U} \in \hat{\Omega}_{f_{i-1}}(\mathbf{e})\right) \tag{10.45}$$

$$\text{w.r.t.} \quad \mathbf{e} \in \boldsymbol{\Upsilon} \tag{10.46}$$

The optimal failure probability is noted $\hat{\mathbb{P}}_{\max}$. An important point is to estimate the error introduced by the use of a surrogate model instead of the exact limit state function. By using the Kriging prediction variance it is possible to determine pseudo-confidence bounds [Deheeger and Lemaire, 2007; Dubourg et al., 2011] on the estimated failure probability:

$$\hat{\mathbb{P}}^{+}_{\max}(\mathbf{e}) = \mathbb{P}\left[\hat{g}(\mathbf{U}, \mathbf{e}, \mathcal{X}) - \eta\sigma(\mathbf{U}, \mathbf{e}, \mathcal{X}) > 0\right] \tag{10.47}$$

$$\hat{\mathbb{P}}^{-}_{\max}(\mathbf{e}) = \mathbb{P}\left[\hat{g}(\mathbf{U}, \mathbf{e}, \mathcal{X}) + \eta\sigma(\mathbf{U}, \mathbf{e}, \mathcal{X}) > 0\right] \tag{10.48}$$

with η a parameter defining the confidence level of the Kriging model (for instance $\eta_S = 1.96$ defines a confidence level of 95%).
To conclude, at the iteration $[t]$ of the sequential loop, IA provides the epistemic variable value $\mathbf{e}^{*[t]}$ leading to the maximization of the failure probability $\hat{\mathbb{P}}_{\max} = \hat{\mathbb{P}}\left(\mathbf{e}^{*[t]}\right)$. Moreover, it is possible to determine pseudo-confidence bounds on $\hat{\mathbb{P}}_{\max} \in \left[\hat{\mathbb{P}}^{-}_{\max}\left(\mathbf{e}^{*[t]}\right), \hat{\mathbb{P}}^{+}_{\max}\left(\mathbf{e}^{*[t]}\right)\right]$. In order to ensure an accurate estimation of $\hat{\mathbb{P}}_{\max}$, it is necessary to refine the Kriging model constructed from the initial training set. The refinement strategy must be adapted to the estimation of the sought $\hat{\mathbb{P}}_{\max}$. It must focus on the regions around the epistemic vector value leading to $\hat{\mathbb{P}}_{\max}$, in the vicinity of the limit state boundaries and in high probability content regions. The refinement strategy is detailed in the section 10.3.3.

10.3.3 Refinement strategy of the Kriging surrogate model

The second step of the sequential loop is the Kriging model refinement strategy. This strategy is used to update the Kriging constructed in the joint aleatory-epistemic uncertain space and is based on the Generalized Max-min (GMm) method developed for Reliability Analysis [Lacaze and Missoum, 2014b]. The original GMm takes into account the joint PDF of the aleatory variables to generate samples in regions with high probability content on the limit state boundaries while populating sparse regions of the space. In order to consider the presence of aleatory and epistemic uncertainties, a modification of the original GMm is proposed. The refinement strategy has to reduce the Kriging prediction variance around the epistemic vector values leading to $\hat{\mathbb{P}}_{\max}$ while reducing the Kriging prediction variance in regions with high probability content around the predicted limit state boundaries. The Kriging model does not need to be accurate in regions in which the epistemic variable values lead to low failure probability. The Kriging prediction variance allows to ensure that despite the Kriging error for some epistemic variable values, they do not lead to $\hat{\mathbb{P}}_{\max}$. The refinement strategy at the iteration $[t]$ of the sequential loop consists of the following optimization

problem:

$$\max_{\mathbf{u},\mathbf{e}} \quad (\phi(\mathbf{u})\phi_{\mathcal{U}}(\mathbf{e}))^{\frac{1}{d+w}} \min_{i=1,\dots,M_s} \| (\mathbf{u}_{(i)}, \mathbf{e}_{(i)}) - (\mathbf{u}, \mathbf{e}) \| \tag{10.49}$$

$$\text{s.t.} \quad \hat{g}(\mathbf{u}, \mathbf{e}, \mathcal{X}) = 0 \tag{10.50}$$

$$\hat{\mathbb{P}}(\mathbf{e}) \geq \hat{\mathbb{P}}^{-}_{\max}\left(\mathbf{e}^{*[t]}\right) \tag{10.51}$$

$$\mathbf{e} \in \boldsymbol{\Upsilon} \tag{10.52}$$

$$\mathbf{u} \in \boldsymbol{\Omega} \tag{10.53}$$

This optimization formulation allows one to sample on the approximated limit state boundaries Eq.(18.51) following the joint PDF $\phi(\cdot)$ for the aleatory variables and according to a uniform PDF $\phi_{\mathcal{U}}(\cdot)$ for the epistemic variables while exploring sparse regions. Eq.(18.52) forces the generation of a new sample in the epistemic regions such that the failure probability $\hat{\mathbb{P}}(\mathbf{e})$ is at least equal to the inferior bound of the maximum probability found in IA $\hat{\mathbb{P}}^{-}_{\max}\left(\mathbf{e}^{*[t]}\right)$ at the iteration $[t]$. $\hat{\mathbb{P}}(\mathbf{e})$ is estimated by Subset Sampling as in IA. At the first iterations of the sequential loop, the uncertainty on the Kriging model is high due to the limited sample size in the training set resulting in a large prediction variance $\sigma^2(\mathbf{u}, \mathbf{e}, \mathcal{X})$. The pseudo-confidence bounds are function of the prediction variance, if the prediction variance is large therefore the bounds around $\hat{\mathbb{P}}_{\max}$ are large enabling to sample in the whole epistemic space Eq.(18.52). The refinement of the Kriging leads to a reduction of prediction variance in the vicinity of the threshold Eq.(18.51), in high probability content regions Eq.(18.50) and in regions of the epistemic space corresponding to $\hat{\mathbb{P}}_{\max}$ Eq.(18.52). Therefore, during the successive sequential loops the solving of the refinement optimization problem results in adding samples in the epistemic region leading to the maximal probability of failure and not on the entire epistemic space. Once a new refinement sample $(\mathbf{u}, \mathbf{e})_{\text{mGMm}}$ is found by the modified GMm (mGMm), the exact limit state function $g(\cdot)$ is evaluated $g\left((\mathbf{u}, \mathbf{e})_{\text{mGMm}}\right)$ and added to the existing DoE $\boldsymbol{g}_{M_s}(\mathcal{X})$. The Kriging model is re-constructed based on the new augmented DoE. After a new sample has been added, the sequential process goes back to the IA. The sequential loop stopping criteria are detailed in section 10.3.4.

10.3.4 Convergence criteria

The sequential loop at iteration $[t]$ is stopped if the three following termination criteria are simultaneously satisfied:

- $A = \| \mathbf{e}^{*[t+n-1]} - \mathbf{e}^{*[t+n]} \| \leq \epsilon_{\mathbf{e}} \ \forall n \in \{1, \dots, q\}$,
- $B = \left| \hat{\beta}\left(\mathbf{e}^{*[t+n-1]}\right) - \hat{\beta}\left(\mathbf{e}^{*[t+n]}\right) \right| \leq \epsilon_{\beta} \ \forall n \in \{1, \dots, q\}$,
- $cv = \log_{10}\left(\frac{\hat{\mathbb{P}}^{+}_{\max}(\mathbf{e}^{*[t]})}{\hat{\mathbb{P}}^{-}_{\max}(\mathbf{e}^{*[t]})}\right) \leq \epsilon$,

with β the reliability index which is linked to the failure probability by: $\mathbb{P} = \Phi_{\mathcal{N}(0,1)}(-\beta)$ where $\Phi_{\mathcal{N}(0,1)}(\cdot)$ is the CDF of a standard normal distribution. For numerical reasons, all the optimizations are performed using the reliability index β. The first criterion ensures that q times in a row the same epistemic realization is given by the IA with an $\epsilon_{\mathbf{e}}$ tolerance. The second criterion ensures that the probability of failure is stabilized q times in a row and the last criterion controls the bounds on the maximal probability of failure due to the Kriging error. $\epsilon = 1$ is a minimum requirement to

ensure that the failure probability estimation with Kriging surrogate model is at least in the order of magnitude of the exact result. The proposed sequential loop is summarized in the Algorithm 3.

Algorithm 3 Proposed sequential reliability analysis process

1) Set $t = 1$, set q for the convergence criteria, set $\epsilon_{\mathbf{e}}, \epsilon_\beta, \epsilon$, set $n = 0$, perform an initial DoE with p samples and construct a Kriging surrogate model.
while $A > \epsilon_{\mathbf{e}}$ and $B > \epsilon_\beta$ and $cv > \epsilon$ and $n < q$ **do**
  2-1) Perform an IA by solving Eq.(10.46) to determine $\hat{\mathbb{P}}_{\max}$. Compute the pseudo confidence bounds Eqs.(10.47-10.48)
  2-2) Perform a Kriging surrogate model refinement by solving the modified GMm, Eqs.(18.50-18.54)
  2-3) Evalutate the exact limit state function $g(\cdot)$ on the sample determined by the refinement strategy. Add the point to the existing DoE
  if $A \leq \epsilon_{\mathbf{e}}$ and $B \leq \epsilon_\beta$ and $cv \leq \epsilon$ **then**
    $n \leftarrow n + 1$
  else
    $n = 0$
  end if
  $t \leftarrow t + 1$
end while
4) **return** $\hat{\mathbb{P}}_{\max}$, $\mathbf{e}^*$ and the pseudo confidence bounds.

10.4 Analytical test case

In order to evaluate the efficiency of the proposed method, a comparison with FORM-UUA [Du et al., 2005; Du, 2008] (section 4.4.2) is performed on an analytical problem. The optimization solving involved in the IA and the PA for FORM-UUA method are solved with a Sequential Quadratic Programming (SQP) algorithm with a convergence tolerance of 10^{-3} on the objective function and the constraints. A multi-start approach (10 different initialization) is used to avoid the risk of local convergence. A multi-start SQP is also used to solve the Kriging refinement strategy. In the proposed approach, the sensitivity of the probability of failure with respect to decision variables required by SQP is estimated according to the method developed in the previous section [Lacaze et al., 2015]. The initial DoE for the Kriging model is performed using Latin Hypercube Sampling. The analytical problem involves two independent aleatory variables $\mathbf{U} \sim \mathcal{N}(\mathbf{0}, \mathbf{I})$ and one epistemic variable $e \in [0, 5]$. The limit state function $g(\cdot)$ is defined as follows:

$$\begin{cases} p(e) = -\frac{1}{8}e^2 + 3.22 \\ r(e) = -\frac{1}{40}e^2 + 3.5 \\ g(\mathbf{u}, e) = {u^{(1)}}^2 - 4p(e)(u^{(2)} - r(e)) \end{cases} \tag{10.54}$$

The failure boundary (Fig. 10.5) is defined by $\{(\mathbf{u}, e) \in \mathbf{\Omega} \times \Upsilon | g(\mathbf{u}, e) = 0\}$ in which the parabola parameters p and r are impacted by the epistemic uncertainty. In the aleatory/epistemic uncertain space, the MPP coordinates are $[0.0, 2.88, 5.0]^{\mathrm{T}}$. The maximum failure probability arises for $e = 4.72$ as identified by performing an IA with the exact limit state function. The initial DoE is constituted

of 15 samples in the joint aleatory/epistemic uncertain space (Fig. 10.9). The Subset Simulation is performed with 90000 samples per step on $\hat{g}(\cdot)$. The proposed sequential loop is stopped when $q = 3$ iterations in a row, $A \leq \epsilon_e$, $B \leq \epsilon_\beta$ and $cv \leq \epsilon$ are simultaneously satisfied with $\epsilon_e = 10^{-3}$, $\epsilon_\beta = 10^{-2}$ and $\epsilon = 0.25$.

Table 10.4: Uncertain input variables for the analytical problem

Uncertain variables	Type	Definition
$U^{(1)}$	Aleatory	$\mathcal{N}(0,1)$
$U^{(2)}$	Aleatory	$\mathcal{N}(0,1)$
e	Epistemic	$[0,5]$

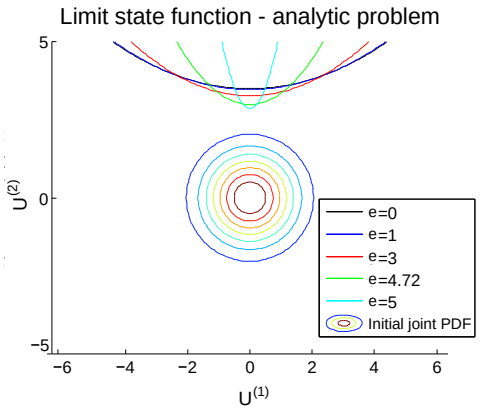

Figure 10.5: Limit state boundary as a function of aleatory/epistemic uncertainties

The solving of the problem with the proposed method and FORM-UUA is repeated 10 times with different initializations. The results of the reliability analysis for the analytical problem are summarized in Table 10.6. The epistemic variable value leading to a maximum probability e^* is 4.72 (Fig. 10.8) for the proposed method and $e^* = 5.00$ for FORM-UUA (Fig. 10.13). As expected, the FORM-UUA method identifies the MPP in the joint aleatory/epistemic uncertain space (Figs. 10.13,10.14) but due to the non linearity of the limit state function, it does not identify the epistemic realization leading to a maximal probability. Moreover, FORM-UUA over-estimates the probability of failure by locally linearizing $g(\cdot)$. In the proposed approach, at first the Kriging model does not represent correctly the limit state function ($cv = 1.5$) (Fig. 10.9) and the IA identifies $e^* = 5.00$ as the epistemic variable value leading to $\mathbb{P}_{\max}$ (Fig. 10.8). After the successive surrogate model refinements, IA identifies $e^* = 4.72$ as the optimal epistemic variable value and the kriging model accurately represent the exact limit state function in the region (Fig. 10.10). The optimal reliability index is $\hat{\beta}_{\max}(e^*) = 3.175$ which corresponds to a maximal probability of failure of $\hat{\mathbb{P}}_{\max}(e^*) = 7.49 \times 10^{-4}$. Subset Simulation succeeds to capture the non linearity of the limit state function (Fig. 10.12). The pseudo confidence bounds around $\hat{\mathbb{P}}_{\max}(e^*)$ are $[7.39 \times 10^{-4}, 7.62 \times 10^{-4}]$

Table 10.6: Analytical problem results (average over 10 repetitions, in parenthesis the Relative Standard Deviation (RSD) - $\sigma(\hat{\mathbb{P}}_{\max})/\mathbb{E}(\hat{\mathbb{P}}_{\max})$)

	Proposed Method	FORM-UUA
e^*	4.720 (3.1%)	5.000 (4.4%)
$\hat{\beta}_{\max}(e^*)$	3.175 (5.3%)	2.875 (4.4%)
$\hat{\mathbb{P}}_{\max}(e^*)$	7.49×10^{-4} (5.3%)	2.00×10^{-3} (4.4%)
$[\hat{\beta}^-_{95\%}(e^*), \hat{\beta}^+_{95\%}(e^*)]$	[3.170, 3.179] (5.6%)	–
$[\hat{\mathbb{P}}^-_{\max_{95\%}}(e^*), \hat{\mathbb{P}}^+_{\max_{95\%}}(e^*)]$	$[7.39 \times 10^{-4}, 7.62 \times 10^{-4}]$ (5.6%)	–
cv	0.014 (4.8%)	–
$N_{g-calls}$	15+13=28 (3.3%)	114 (6.8%)
$N_{seq-loop}$	13 (3.3%)	7 (6.8%)

(Fig. 10.7) which corresponds to a ratio of $cv = 0.014$ (Fig. 10.11). The number of calls to the exact limit state function $N_{g-calls}$ is 28 for the proposed approach (15 for the initial DoE and 13 for the refinement strategy) whereas FORM-UUA requires 114 calls to $g(\cdot)$. The number of sequential loop $N_{seq-loop}$ is 13 for the proposed approach and 7 for FORM-UUA.

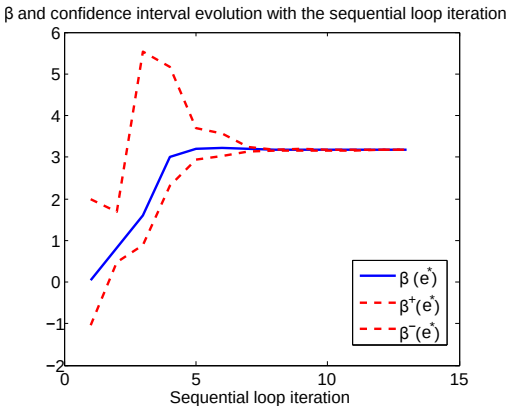

Figure 10.7: Reliability index and pseudo confidence bounds at 95%

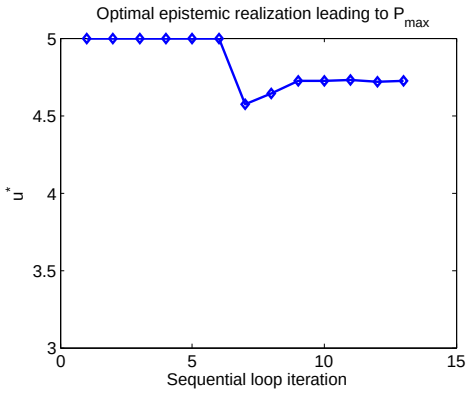

Figure 10.8: Optimal epistemic realization leading to $\mathbb{P}_{\max}$

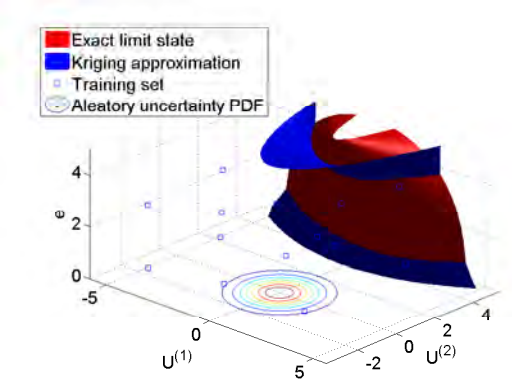

Figure 10.9: Initial training set, exact limit state and kriging approximation

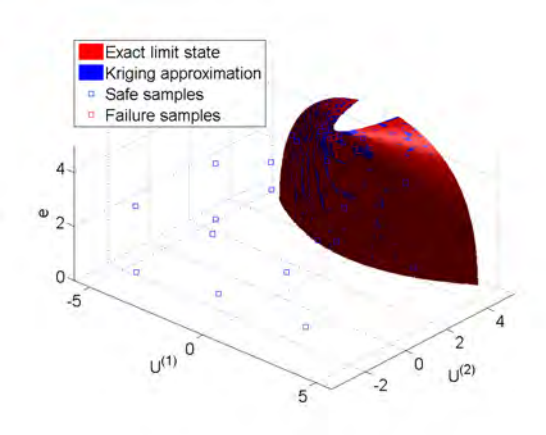

Figure 10.10: Final training set, exact limit state and kriging approximation

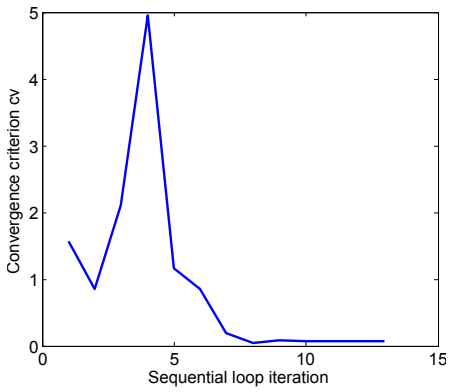

Figure 10.11: Convergence criterion cv

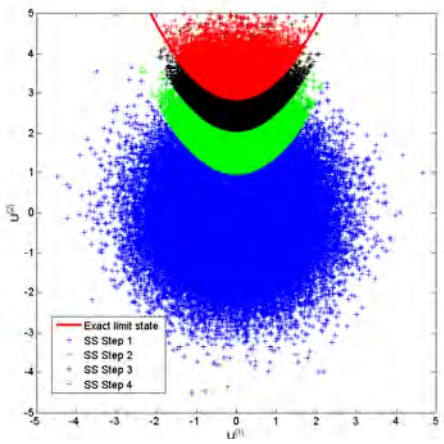

Figure 10.12: Subset Sampling samples for $e^* = 4.72$

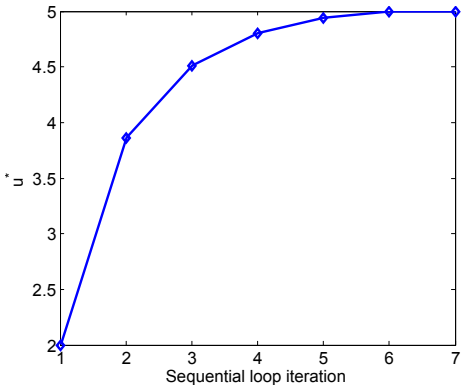

Figure 10.13: IA results, FORM-UUA method

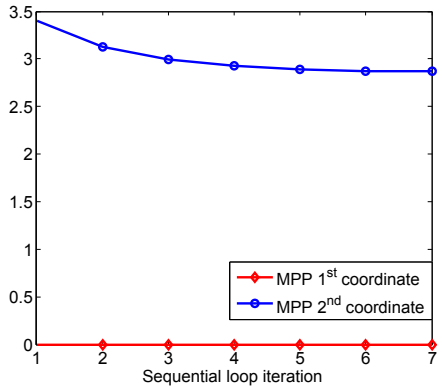

Figure 10.14: PA results, FORM-UUA method

10.5 Limitations of the proposed approach

The proposed approach presents several limits. As in the previous chapter, the reliability analysis problems that may be solved with the proposed technique are limited to low dimensional problems due to the Kriging (under 15 variables). Moreover, the complexity and the computational cost may limit its use within the UMDO framework. Further investigations are required to incorporate the proposed technique within the UMDO context. The derivation of the sensitivity of $\mathbb{P}(\cdot)$ enables to use gradient-based approaches to propagate epistemic uncertainty and to find the bounds of the probability of failure. However, further investigations have to be performed to ensure the robustness of the Dirac distribution approximation and gradient estimations for various test cases.

10.6 Conclusion

In this chapter, firstly an expression of the sensitivity of probability of failure with respect to decision variables has been derived. Estimators have been proposed based on CMC and SS. Numerical concerns regarding the approximation of the Dirac distribution have been addressed. Experiments seem to show that Gaussian approximation should be favored with a value of $\alpha = 0.5$. However, this result might not always be true and an automatic tuning algorithm to find the optimal α (i.e., σ) as in [Morio et al., 2013] might be investigated. Then, in a second time, a new method to perform reliability analysis in the presence of epistemic uncertainty affecting the limit state function has been developed. The approach allows one to estimate failure probability involving multiple failure regions and non linear limit state functions. For this purpose, a sequential strategy has been proposed in order to determine the probability bounds based on Subset Simulation and Kriging surrogate model to reduce the number of calls to the computationally expensive function. The proposed sequential loop consists of two steps: the Interval Analysis with Probability Analysis with the use of the surrogate model and the refinement of the Kriging model. The surrogate model is constructed in the joint aleatory/epistemic uncertain space in order to accurately represent the limit state function only in the areas of interest, *i.e.* in the vicinity of the threshold, in high probability content regions and around the epistemic vector values leading to the failure probability

bounds. A modification of the original Generalized Max-min is proposed for the Kriging refinement strategy to take into account the epistemic uncertainty. The proposed method has been compared to FORM-UUA on an analytical problem illustrating its efficiency in terms of number of calls to the exact function and the determination of the probability maximal bound.
In the next chapter, this method is applied to a reliability analysis problem concerning a launch vehicle stage fallout.

- Context:
  - Reliability analysis in the presence of mixed aleatory/epistemic uncertainties,
  - Epistemic uncertainty directly affecting the limit state function,
  - State-of-the-art methods are either computationally expensive (CMC) or limited to simple problem (FORM), see chapter 4.
- Contributions:
  - Development of a new reliability analysis method involving a sequential loop of failure probability bound estimation and surrogate model refinement. It is based on Subset Simulation combined with Kriging model and a dedicated refinement strategy based on GMm.
  - Development of sensitivity of the failure probability with respect to decision variables with CMC and SS techniques.
  - Application and comparison of the proposed approach with respect to FORM-UUA on one analytical test case, highlighting its efficiency to propagate epistemic uncertainty to failure probability.
- Actionable information:
  - Useful for problems that present modeling uncertainty of the failure domains,
  - Essential to ensure system design reliability based on our present uncertainty modeling knowledge,
  - Accurate reliability analysis could be used to re-optimize the safety margins.
- Perspectives:
  - Extend the technique to solve high dimensional problems,
  - Needs further investigation on the influence of the sensitivities of $\mathbb{P}(\cdot)$ on the optimizer convergence,
  - Incorporate the method within the UMDO context.

Chapter 11

Application of reliability analysis methods to launch vehicle trajectory analysis

Contents

Chapter goals

- Apply the developed reliability analysis methods in the presence of mixed aleatory/epistemic uncertainties on two launch vehicle test cases,
- Compare the results with reference techniques.

11.1 Introduction

All the launches operated from Kourou (French Guyana) have to comply with the French Space Operation Act which sets up regime of authorization and verification of space operations in order to protect people, properties, public health and environment. The stage fall back operation on Earth has to comply with requirements for the protection of life and infrastructures. During the design of a launch vehicle, constraints have to be imposed during trajectory optimization for a specific mission to ensure the stage fallout in safe conditions and in an adequate zone. The estimation of launch vehicle fallout safety zone is a crucial problem in aerospace because it potentially involves

dramatic repercussions on the population and the environment. For that purpose, an efficient estimation of the probability that a launch vehicle stage falls at a distance greater than a given safety limit is strategic for the qualification of such vehicles. In the following, two test cases of stage fallout are considered:

- The first problem considers the fallout of a first solid propulsion stage with epistemic uncertainty on the hyper-parameters of the PDF defining aleatory uncertainty (section 11.2).
- The second problem considers the fallout of a second solid propulsion stage with epistemic uncertainty affecting directly the system dynamics in addition to the aleatory uncertainty (section 11.3).

11.2 Reliability analysis in the presence of epistemic uncertainty on the hyper-parameters of PDF

This test case focuses on the fallout of a first solid propulsion stage of a launch vehicle which lifts off from the Kourou spaceport (French Guyana). Its mass at its separation is about 35 tons. The jettison conditions are an altitude of 112 kilometers and a flight path angle of 15 degrees. At the end of its mission, the solid stage falls into the sea at some distance of a predicted position. This position is determined from the nominal fallout conditions when no perturbation of the re-entry appears.
The launch vehicle stage fall-back is modeled as an input-output function $g(\cdot)$ with an input uncertain vector $\mathbf{U}$ of dimension 4 characterized by $\phi^{\mathbf{e}}(\cdot)$ and one output $Y = g(\mathbf{U})$, representing the orthodromic distance between the estimated launch stage fall-back position and the predicted one. The probability that the distance to the predicted impact position exceeds 0.65km is predicted: $\mathbb{P}(g(\mathbf{U}) > 0.65) = \mathbb{P}(g(\mathbf{U}) - 0.65 > 0)$. The different components of $\mathbf{U}$ are:

- meteorological condition (1 input: Mc). The variation of the considered meteorological conditions is the wind variation during the fall-back which influences the impact position,
- the error in the orientation estimation (1 input: Eo) of the launcher stage that influences the ballistic fallout of the stage,
- launch vehicle mass (1 input: m). The mass of the different parts of the launch vehicle is also slightly random during the fall-back, because the propellant may not be totally burnt during the powered flight,
- the flight path angle between the vertical axis and the velocity vector (1 input: γ). This angle characterizes the orientation of the stage with respect to the velocity vector at the stage separation and thus influences its ballistic fall-back phase and consequently the impact position.

A 3 dimensional model with rotating round Earth is used. The dynamics of the launch vehicle stage re-entry is detailed in appendix 17. All the input parameters are distributed according to independent Gaussian laws $\phi^{\mathbf{e}}(\cdot)$. The means of the meteorogical condition, the error of orientation, the launch vehicle mass and slope angle are supposed to be uncertain, their variances are being fixed. The domain of variation of the uncertain parameters is +/- 10% around their reference values (the values of Table 11.1 are nondimensionalized). The probability of reference calculated by CE for $\boldsymbol{e}_0$ which is the baseline of PDF uncertain parameters is equal to 1.98×10^{-5}.

Table 11.1: Variation domains of the uncertain parameters

Parameter	Variation domain
$\mathbb{E}(Mc)$	$[-1.1,-0.9]$
$\mathbb{E}(Eo)$	$[0.9,1.1]$
$\mathbb{E}(m)$	$[0.45,0.55]$
$\mathbb{E}(\gamma)$	$[-2.2,-1.8]$

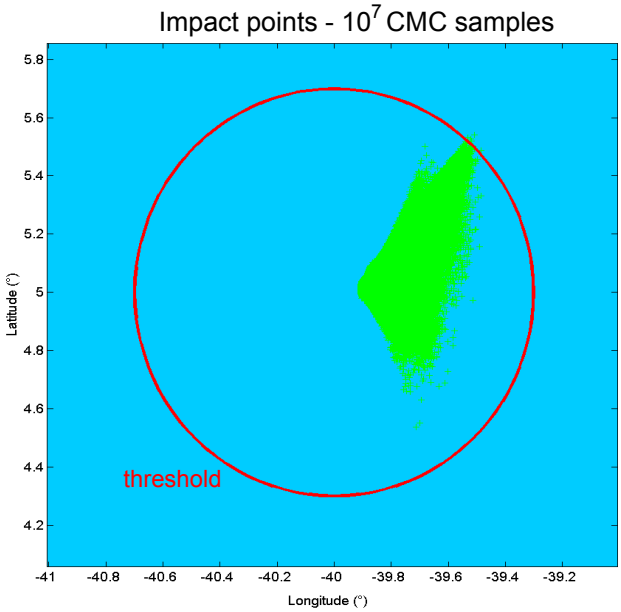

Figure 11.2: Stage fallout zone, threshold and impact points, 10^7 CMC samples

11.2.0.1 Results

In comparison with the two analytical test cases, the input-output function involved in this test-case is non smoothed and non-linear, that explains the more important number of points required to approximate this function by Kriging model and consequently the greater number of samples evaluated on $g(\cdot)$ to estimate the probability with reference $\boldsymbol{e}_0$ using CE.

Table 11.3: Synthesis of the launch vehicle fall-back problem

	Proposed method	CMC-CMC	CMC-IS
Number of samples required by CE for estimating the probability with reference $\boldsymbol{e}_0$	2.80×10^4	10^6	2.80×10^4
Number of samples evaluated on $g(\cdot)$ for estimating the probability with reference $\boldsymbol{e}_0$ using Kriging	1196	/	/
Estimation of $\widehat{\mathbb{P}}_{\boldsymbol{e}_0}(g(\mathbf{U}) > 0)$	1.96×10^{-5}	1.95×10^{-5}	1.98×10^{-5}
Std deviation of the probability estimate for reference $\boldsymbol{e}_0$	4.91%	22.6%	4.80%
$\widehat{\mathbb{P}}_{\max}$	7.47×10^{-5}	6.50×10^{-5}	6.22×10^{-5}
$\boldsymbol{e}$ corresponding to $\widehat{\mathbb{P}}_{\max}$	$[-1.10, 1.10, 0.55, -1.80]^T$	$[-1.06, 1.09, 0.54, -2.10]^T$	$[-0.96, 1.10, 0.55, -2.06]^T$
Number of points evaluated on $g(\cdot)$ to find $\widehat{\mathbb{P}}_{\max}$	7089	10^8	$2.8.10^6$
Std deviation of $\widehat{\mathbb{P}}_{\max}$	5.00%	12.4%	5.03%
$\mathbb{P}_{\min}$	3.14×10^{-6}	7.00×10^{-6}	5.69×10^{-6}
$\boldsymbol{e}$ corresponding to $\widehat{\mathbb{P}}_{\min}$	$[-0.90, 0.90, 0.45, -2.20]^T$	$[-1.02, 0.92, 0.48, -2.10]^T$	$[-0.97, 0.92, 0.46, -2.04]^T$
Number of points evaluated on $g(\cdot)$ to find $\widehat{\mathbb{P}}_{\min}$	6791	10^8	2.80×10^6
Std deviation of $\widehat{\mathbb{P}}_{\min}$	5.59 %	37.80%	5.82%
Average number of points evaluated on $g(\cdot)$ to provide an estimation of $\widehat{\mathbb{P}}$ during the probability bound calculation	69.4	10^6	2.80×10^4

The conclusions of this test case are similar to the analytical cases. Figures 11.4 and 11.5 illustrate the difficulty to accurately estimate the probability of failure with CMC. CE succeeds to identify the failure regions and to center the auxiliary optimal PDF at the center of the failure zone in order

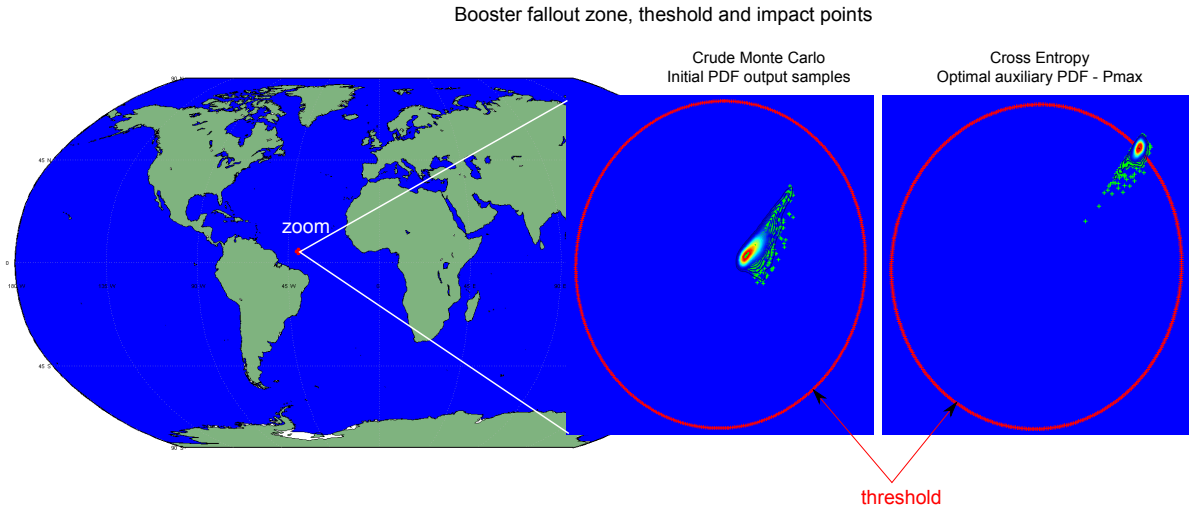

Figure 11.4: Impact points of the launch vehicle stage, CMC and optimal auxiliary CE densities for $\widehat{\mathbb{P}}_{\max}$

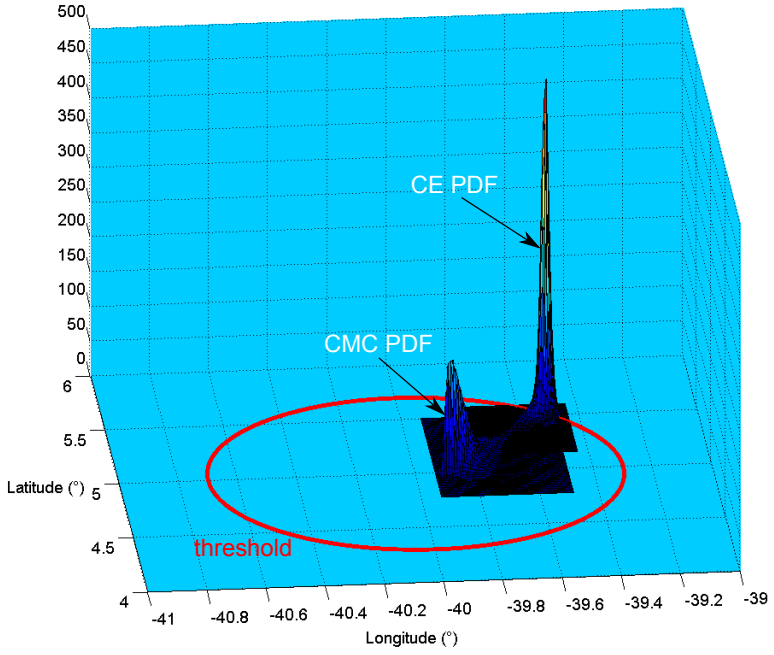

Figure 11.5: CMC and optimal auxiliary CE densities for $\widehat{\mathbb{P}}_{\max}$

to efficiently estimate the probability of failure. The proposed method finds a better optimum than CMC-CMC and CMC-IS in terms of computation cost and quality of the results. Indeed, the proposed method provides more optimal bounds (higher maximum and lower minimum) on the probability estimate with 15076 ($= 1196 + 7089 + 6791$) evaluations of $g(\cdot)$, that represents in average 69.4 evaluations of $g(\cdot)$ per probability estimation during the optimization process instead of 2.80×10^4 required by using classical IS. Moreover, because the range of probability of $\widehat{\mathbb{P}}_{\min}$ and the simulation budget used in CMC-CMC are not compatible, this method fails to find the probability and its results are very imprecise, due to the high standard deviation of this estimator for evaluating such low probabilities.
In the next section, another test case of launch vehicle stage fallout is considered but with epistemic uncertainty directly affecting the launch vehicle dynamics model.

11.3 Reliability analysis in the presence of epistemic uncertainty affecting the limit state function

For this test case, a launch vehicle of approximatively 150t is considered. It lifts off from the Kourou spaceport and aims at delivering a payload (1.5t) in polar orbit (circular at 700km). It is composed of three solid propulsion stages. The first and the second stages fall back into the Atlantic Ocean (Fig. 11.8) and the third stage is injected into orbit with the payload. The fall-back zone of the second stage is considered in this test case. The second stage separation dynamics occurs approximately at an altitude of 164 km and a velocity of 3.7 km/s. A three degree of freedom model is used and the second stage state is characterized by the altitude $h(m)$, the velocity $v(km/s)$, the flight path angle γ(rad), the longitude λ(rad), the latitude ϕ(rad), the azimuth ψ(rad) and the mass $m(kg)$. The 2^{nd} stage dry mass is about 2660 kg and the nominal state of the 2^{nd} stage at the separation is given by $[h, v, \gamma, \lambda, \phi, \psi, m] = [164420, 3687.5, 0.332, -0.922, 0.133, -0.027, 2660]$. At the end of its mission, the rocket stage falls into the ocean at some orthodromic distance of a predicted position (which is the position in nominal conditions).
The launch vehicle stage fallout is modeled as an input-output function $g(\cdot)$ with an aleatory vector $\mathbf{U}$ of five independent Gaussian inputs $\phi(\cdot)$ and one epistemic variable e (Fig. 11.8). The output of $g(\cdot)$ represents the orthodromic distance between the predicted position and the exact launch stage fallout one. In this case study, we aim at estimating the probability that the distance to the predicted impact position exceeds 20 km. The disciplines involved in this test case are represented in Figure 11.7. The propulsion discipline provides the engine characteristics (thrust, specific impulse, *etc.*) for the propulsive ascent phase. The sizing discipline provides the masses and geometries of the different stages. The aerodynamics provides the aerodynamics coefficients used to compute the forces during the ascent and the fallout phases. Eventually, the ascent trajectory corresponds to the trajectory from Kourou to the orbit while the fallout trajectory discipline is the uncontrolled 2^{nd} stage fallout.
The aleatory uncertainties impact the separation state of the 2^{nd} stage (Table 11.6). The level and modeling of uncertainty for this test case have been defined with expert at Onera on the launch vehicle separation and re-entry. The stage separation altitude $U^{(1)}$ and velocity $U^{(2)}$ are perturbed depending on weather conditions during the ascent atmospheric flight. The flight path angle $U^{(3)}$ and the azimuth $U^{(4)}$ characterize the orientation of the stage with respect to the velocity vector at the stage separation influencing its ballistic re-entry and consequently its impact position. The mass of the stage $U^{(5)}$ is also random during the fallout due to the residual propellant mass not

Table 11.6: Uncertain variables for the stage fallout problem

Uncertain variables	Type	Definition
Separation altitude error (m)	Aleatory	$\mathcal{N}(0, 0.01)$
Separation velocity error (km/s)	Aleatory	$\mathcal{N}(0, 0.01)$
Flight path angle separation error (rad)	Aleatory	$\mathcal{N}(0, 0.03)$
Azimuth separation error (rad)	Aleatory	$\mathcal{N}(0, 0.00175)$
Stage dry mass error (kg)	Aleatory	$\mathcal{N}(0, 70)$
1^{st} stage propulsion mass flow rate parameter error	Epistemic	$[0, 1]$

consumed during the flight. The epistemic uncertainty impacts the mass flow rate profile during the combustion of the 1^{st} stage (Fig. 11.9). The uncertainty associated to the mass flow rate of a solid propulsion motor is very difficult to characterize and the tail of the mass flow rate profile depends on the nozzle erosion, combustion instabilities, surface combustion rate, *etc.* All these physical phenomena are not well understood and the existing models are limited due to this lack of knowledge [Kuo et al., 1984]. The mass flow rate tail uncertainty models only provide bounds on the mass flow rate tail. This latter is parameterized by a dimensionless coefficient representing the epistemic uncertainty $u \in [0, 1]$ (Fig. 11.9). The uncertainty on the mass flow rate tail influences the propulsion phase, the stage separation state and therefore the stage impact point.
In the proposed approach, the initial training set is constituted of 60 samples in the joint aleatory/epistemic uncertain space. The Subset Simulation is performed with 90000 samples per step on $\hat{g}(\cdot)$. The proposed sequential loop is stopped when 3 iterations in a row, $A \leq \epsilon_e$, $B \leq \epsilon_\beta$ and $cv \leq \epsilon$ are simultaneously !ed with $\epsilon_e = 10^{-2}$, $\epsilon_\beta = 10^{-2}$ and $\epsilon = 0.37$. The solving of the problem is repeated 10 times.
For comparison, the maximal probability of failure computed with the exact limit state function function using SS of 90000 samples per step (quantile at 10%) and SQP algorithm is $2.90{\times}10^{-4}$ and is reached for the epistemic realization $e^* = 0.490$. The results of the reliability analysis for the stage fallout problem are summarized in Table 11.10. SS distributions with the epistemic uncertainty fixed to its optimal value e^* (Figs. 11.19-11.23) illustrate the presence of multiple regions leading to the threshold exceedance, in particular on the velocity (Fig. 11.20) and the flight path angle (Fig. 11.19) input spaces. The proposed sequential loop requires 72 iterations in order to converge. The presence of multiple regions make the problem more complex than the analytical problem as the surrogate model has to be accurate in different regions of the input aleatory space. The maximal probability of failure computed with the proposed approach is 2.91×10^{-4} and is reached for the epistemic realization $e^* = 0.494$. The pseudo confidence interval of the maximal probability is $[2.42 \times 10^{-4}, 5.57 \times 10^{-4}]$. Due to the presence of multiple regions, FORM-UUA identifies a maximal probability of 6.41×10^{-5} (Fig. 11.15) and the associated epistemic realization $e^*_{FORM} = 0.450$ (Fig. 11.14) which under estimates the potential risk. FORM-UUA algorithm has been initialized at different epistemic uncertain variable values. In comparison, a Subset Sampling at the optimal epistemic value $e = e^*$ with the exact limit state function $g(\cdot)$ instead of the Kriging model provides a probability of failure of 2.93×10^{-4}. The optimization problem to estimate $\hat{\mathbb{P}}_{\max}$ results in a number of exact limit state function evaluations of 1114 for FORM-UUA as opposed to 72 for the proposed approach. CMC method is not adapted to estimate the stage fallout probability in this

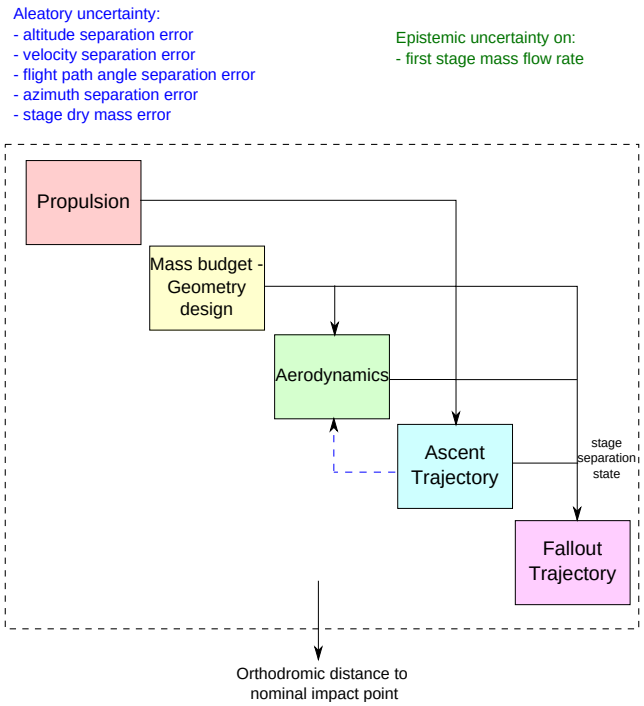

Figure 11.7: Disciplines involved in the stage fallout reliability problem

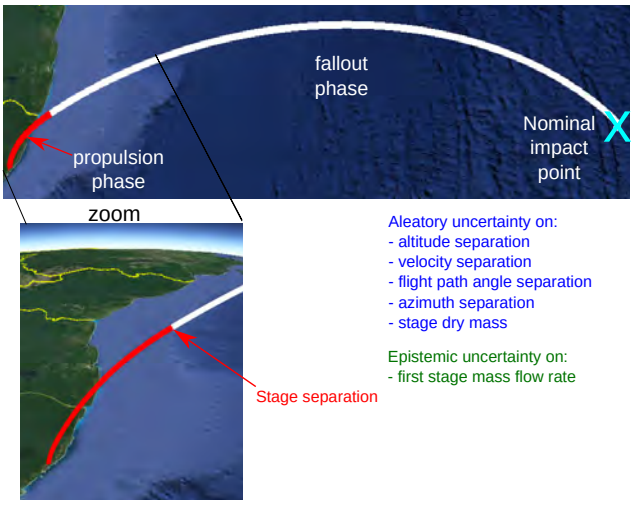

Figure 11.8: 2nd stage separation and impact point in nominal conditions

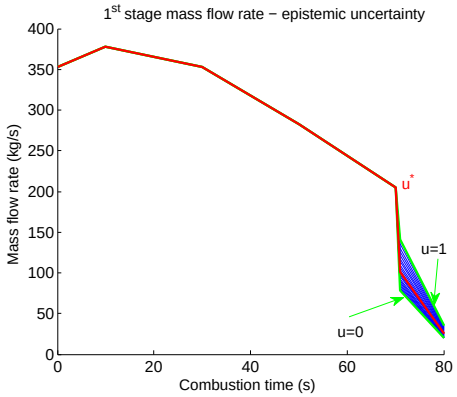

Figure 11.9: 1st stage mass flow rate epistemic uncertainty

Table 11.10: Stage fallout results (average over 10 repetitions, in parenthesis the Relative Standard Deviation (RSD) - $\sigma/\mathbb{E}$)

	Proposed Method	FORM-UUA
e^*	0.494 (6.5%)	0.450 (20.7%)
$\hat{\beta}_{max}(e^*)$	3.44 (10.1%)	3.83 (20.7%)
$\hat{\mathbb{P}}_{max}(e^*)$	2.91×10^{-4} (10.1%)	6.41×10^{-5} (20.7%)
$[\hat{\beta}^-_{95\%}(e^*), \hat{\beta}^+_{95\%}(e^*)]$	[3.26, 3.49] (9.4%)	–
$[\hat{\mathbb{P}}^-_{max_{95\%}}(e^*), \hat{\mathbb{P}}^+_{max_{95\%}}(e^*)]$	$[2.42 \times 10^{-4}, 5.57 \times 10^{-4}]$ (5.6%)	–
cv	0.363 (8.8%)	–
$N_{g-calls}$	60+72=78 (8.7%)	1114 (31.1%)
$N_{seq-loop}$	72 (8.7%)	7 (14.3%)

test case. Indeed, CMC does not succeed to sample in high probability content regions around the limit state function (threshold) as illustrated in Figure 11.16 whereas Subset Sampling does. The latitude and longitude impact point joint PDF obtained with CMC to estimate the probability of failure is monomodal centered on the nominal impact point (Fig. 11.17) whereas it is multiple with Subset Simulation (Fig. 11.18) centered on the threshold in the two high probability content regions.

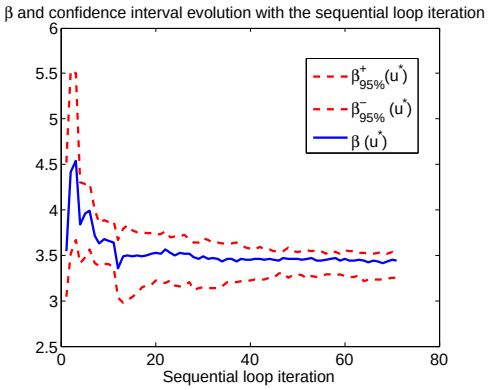

Figure 11.11: Reliability index and pseudo confidence bounds at 95%

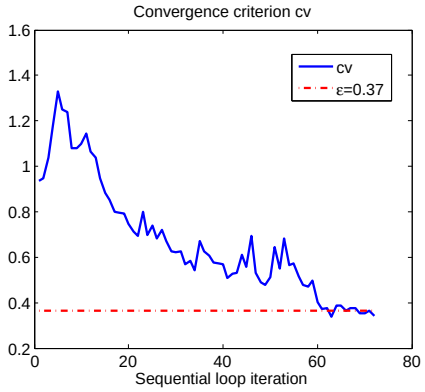

Figure 11.12: Convergence criterion *cv*

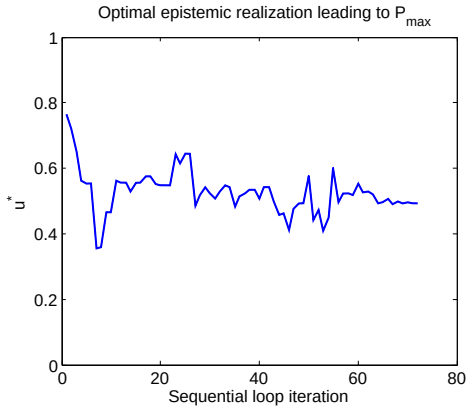

Figure 11.13: Optimal epistemic realization leading to $\widehat{\mathbb{P}}_{\max}$

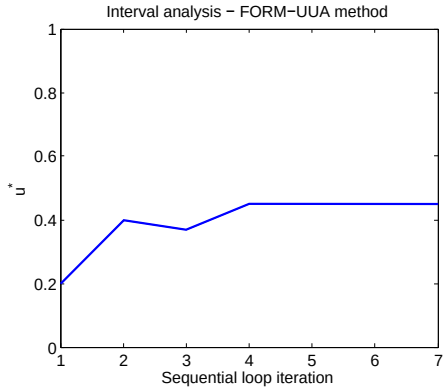

Figure 11.14: Interval Analysis for the stage fallout, FORM-UUA method

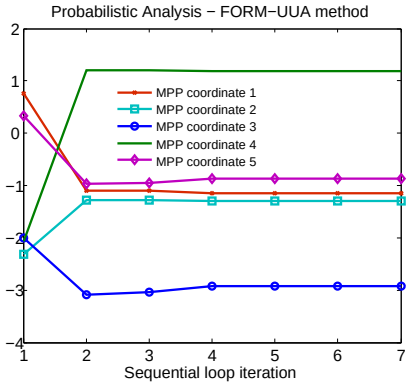

Figure 11.15: PA for the stage fallout, FORM-UUA method

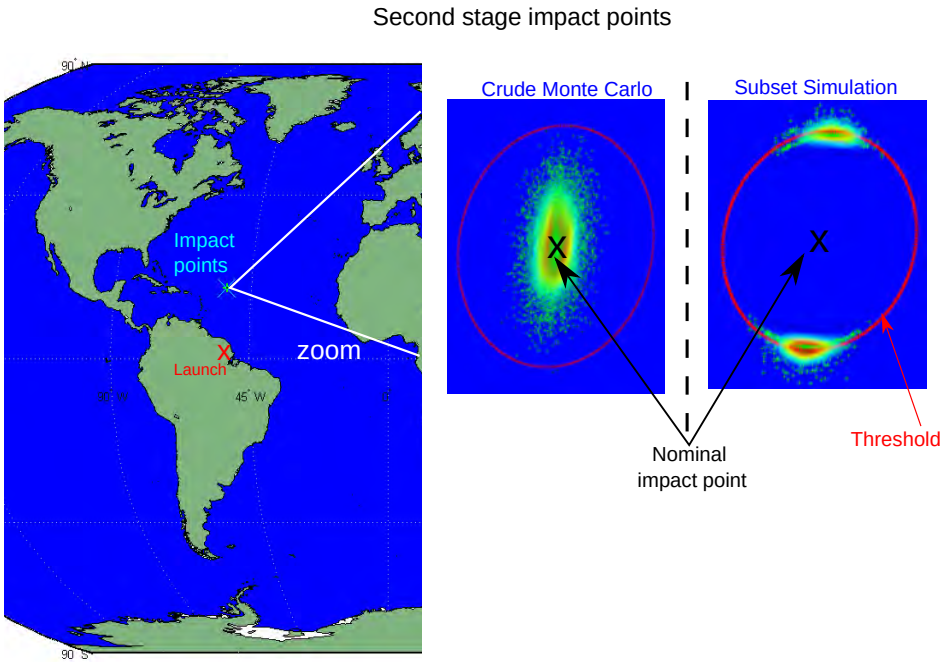

Figure 11.16: Impact points of the launch vehicle 2^{nd} stage

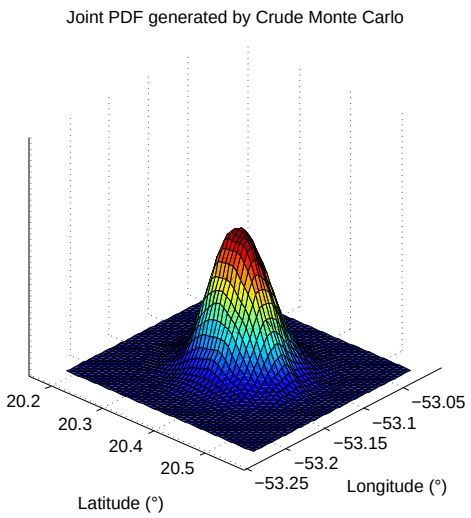

Figure 11.17: Crude Monte Carlo latitude and longitude impact point joint PDF

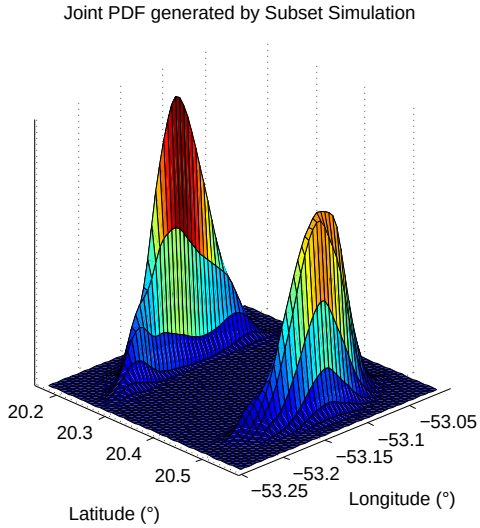

Figure 11.18: Subset Simulation latitude and longitude impact point joint PDF

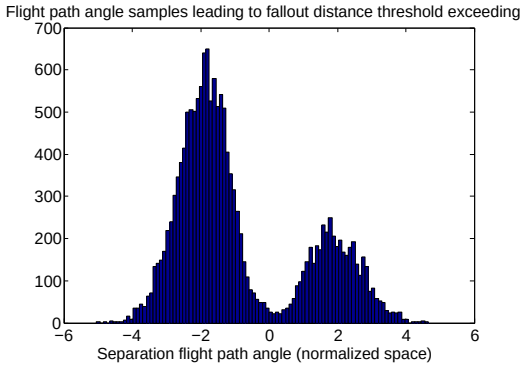

Figure 11.19: Histogram of the sample points used for flight path angle dimension in SS

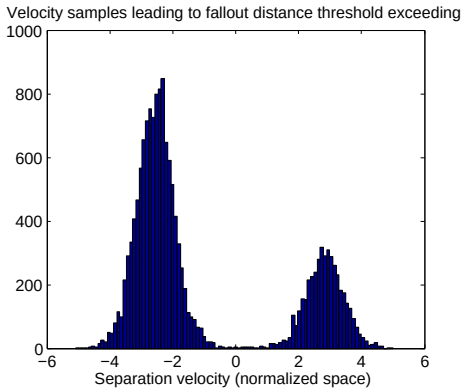

Figure 11.20: Histogram of the sample points used for velocity dimension in SS

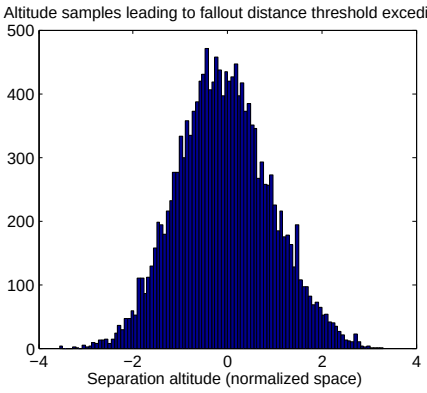

Figure 11.21: Histogram of the sample points used for altitude dimension in SS

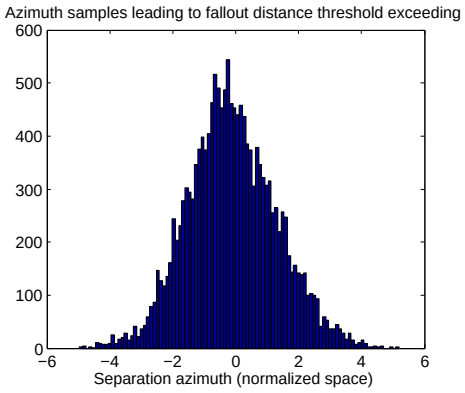

Figure 11.22: Histogram of the sample points used for azimuth dimension in SS

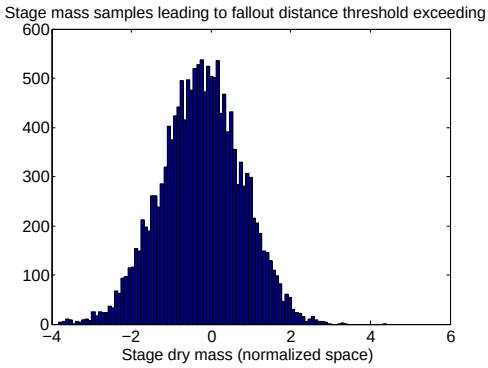

Figure 11.23: Histogram of the sample points used for dry mass dimension in SS

11.4 Conclusion of the chapter

In this chapter, two launch vehicle test cases have been presented to illustrate the developed methods to handle both epistemic and aleatory uncertainties. These test cases are representative of design constraints that have to be considered during the design of a launch vehicle. In the first problem, epistemic uncertainty on the hyper-parameters of the aleatory uncertainty (meteorological conditions, stage orientation, stage mass and flight path angle) are investigated. In the second problem, epistemic uncertainty directly impacting the launch vehicle dynamics is investigated (during the propulsive phase, uncertainty on the mass flow rate tail). The estimation of the probability bounds require less calls to the limit state function with the proposed methods than with the reference approaches.

This chapter highlights the difficulty to accurately estimate probability of failure in the presence of both aleatory and epistemic uncertainties at an affordable cost. Dedicated approaches have to be

developed and involve several methodologies: sampling techniques, surrogate modeling, refinement strategies, optimization. The accurate estimation of system reliability is essential in the conceptual design phase as it will drive the designer toward different solutions according to their reliability and performance. However, at this design phase, the uncertainty modeling is often not perfectly known and taking it into account is essential to guarantee the adequacy between the estimation of the failure probability and the present uncertainty knowledge. Moreover, accurate estimation of the reliability may be used to reoptimize the safety factors and margins used to prevent failure in order to avoid conservative design which decrease the system performance.

11.5 Conclusion of part III

In this part III of the thesis, two new methods to perform reliability analysis for complex systems in the presence of aleatory and epistemic uncertainties have been proposed. To be able to deal with mixed aleatory/epistemic uncertainties, the methods combine rare event estimation techniques (either IS or SS) with surrogate model (Kriging) and dedicated refinement techniques.

- To handle epistemic uncertainty in the hyper-parameters of PDF, an accelerated IS probability estimator based on CE is combined with a Kriging model dedicated to IS and a refinement strategy. CMA-ES algorithm is used to solve the optimization problems to find the bounds of the failure probability. The acceleration of the IS estimation results from the re-use of failure samples generated for another epistemic uncertainty value avoiding to restart the CE algorithm from the beginning.
- To handle epistemic uncertainty directly affecting the system dynamics, a sequential approach is implemented with SS combined with a Kriging model dedicated to SS and a refinement strategy. The surrogate model is constructed in the joint aleatory/epistemic uncertain space in order to accurately represent the limit state function only in the area of interest, *i.e.* in the vicinity of the threshold, in high probability content regions and around the epistemic vector values leading to the failure probability bounds. A gradient-based algorithm combined with a proposed method to estimate the sensitivity of $\mathbb{P}(\cdot)$ with respect to decision variables is used to solve the optimization problems.

Both probability estimation techniques allow to handle non linear limit state function. In addition, SS technique enables to handle multiple failure regions which may occur in reliability analysis problem as illustrated in section 11.3.
When performing reliability analysis, the information about the input aleatory uncertainty and the limit state function delimiting safe for failure domains are essential. The probability of failure directly results from these information. However, in practice in the industry, these information are often limited and not perfectly known due to the difficulty to collect the information. The proposed reliability analysis methods allow to take into account the potential uncertainty in the input aleatory variable modeling or in the limit state function. It allows to ensure that the estimated probability of failure account for the modeling uncertainty based on our present uncertainty knowledge. This accurate reliability analyses could be used to re-optimize the safety margins that are used to design systems accounting for all the unknown uncertainty in order to find the safety margins that ensure the system reliability and non over conservative design.

However, several limits have to be pointed out. First, even if the proposed methods reduce the number of calls to the limit state function compared to classical techniques used in UMDO (CMC, IS) or extend the domains of application (multiple failure regions impossible with FORM), the computational cost is still high ($\sim$ 15 hours for the launch vehicle test cases). Using these methods in an UMDO problem solving seems complicated considering the induced computational cost (repeated calls to reliability analysis techniques). Moreover, the proposed methods by combining several tools (surrogate model, optimization algorithm, rare event estimation) increase the complexity of the probability estimation compared to the classical approaches. Incorporating them in UMDO would require knowledge on all these aspects to ensure the accurate estimation of the constraints and the respect of the requirements.

Contributions to Uncertainty-based Multidisciplinary Design Optimization, application to launch vehicle design

- Context:
  - Reliability analysis in the presence of mixed aleatory/epistemic uncertainties,
  - Rare event probability estimation.
- Contributions:
  - Development of a new reliability assessment technique to handle epistemic uncertainty on the hyper-parameters of PDF,
  - Development of a new reliability analysis method to handle epistemic uncertainty affecting the system dynamics,
  - Combination of rare event estimation techniques (IS and SS) with Kriging model of the limit state and dedicated refinement strategies,
  - Development of sensitivity estimators of the failure probability with respect to decision variables with CMC and SS techniques,
  - Application of the proposed methods on two test cases involving the fallout of a launch vehicle stage.
- Actionable information:
  - Appropriate for problems that present uncertainty on the modeling of the input PDF or the system dynamics which influences the probability of failure,
  - Essential to ensure system design reliability based on our present uncertainty modeling knowledge,
  - Accurate reliability analysis could be used to re-optimize the safety margins.

Part IV

Evolutionary strategy for constraint handling in a noisy environment, applications to launch vehicle design

Chapter 12

Adaptation of CMA-ES algorithm for constraint handling in a noisy environment

Contents

Chapter goals

- Develop a constraint handling method for evolutionary algorithm CMA-ES,
- Apply and compare the proposed approach to reference techniques on analytical test cases.

12.1 Introduction

In the two previous parts II and III interdisciplinary coupling handling method and reliability assessment techniques in the presence of mixed aleatory/epistemic uncertainty have been proposed. The design of a complex system with UMDO methodologies requires to solve an optimization problem in the presence of uncertainty and constraints. In this part, only aleatory uncertainty is considered. As highlighted in chapter 5, dedicated optimization algorithms have been developed to solve these complex optimization problems. Population-based algorithms present advantages to optimize functions in the presence of uncertainty. The population-based optimization algorithms

are less dependent on the quality of candidate solutions and the impact of uncertainty. They move from one set of solutions to the next one and consequently are not so much affected when an outlier solution receives a particularly good objective function value through stochastic influence. Among the population-based algorithms, Evolution strategy approaches such as Covariance Matrix Adaptation - Evolutionary Strategy (CMA-ES) have demonstrated efficient optimization capacities in the presence of uncertainty [Nissen and Propach, 1998; Hansen et al., 2003; Hansen, 2009]. However, as outlined in chapter 5, although CMA-ES efficiently solves optimization problem in the presence of uncertainty, the handling of constraints presents some issues. Classical handling contraint methods rely on penalization (death penalty [Schwefel and Rudolph, 1995], weighted penalization [Collange et al., 2010b; De Melo and Iacca, 2014]) are problem dependent techniques which require tuning parameters for the weighted penalization approach.

In this chapter, a modification of CMA-ES algorithm is proposed in order to incorporate the constraint handling directly in the generation mechanisms of the population of candidates. The proposed technique is adapted from the modification of (1+1)-CMA-ES [Arnold and Hansen, 2012] to handle the constraints. The update mechanisms of the parameterized sampling distribution used to generate the candidate solutions are modified. CMA-ES algorithm generates candidates according to a Gaussian distribution parameterized by a covariance matrix. This covariance matrix represent an iso-probable hypervolume of search in the design space in which the candidates may be sampled. The proposed constraint handling method allows to reduce the semi-principal axes of the probable search hypervolume in the directions violating the constraints in accordance with the information provided by the candidates.
In section 12.2, the proposed constraint handling method is developed explaining the search hypervolume update mechanisms. Moreover, several adjustments of the parameters update mechanisms are detailed in order to take into account possible specific situations during the optimization. In section 12.3, the proposed approach is compared to existing constraint handling techniques (death penalty, penalized CMA-ES and modified (1+1)-CMA-ES) on three analytical optimization problems to highlight the efficiency and the robustness of the algorithm.
In chapter 13, the proposed handling constraint method is used to design a two stage solid propulsion launch vehicle.
This work has been performed in collaboration with R. Chocat (Institut Francais de Mécanique Avancée), Mathieu Balesdent (Onera) and Sebastien Defoort (Onera).

12.2 Adaptation of CMA-ES(λ, μ) for constraint handling

Let us consider the following UMDO problem:

$$\begin{aligned} \min \quad & \Xi\left[f(\mathbf{z}, \mathbf{Y}(\mathbf{z}, \mathbf{U}), \mathbf{U})\right] && (12.1)\\ \text{w.r.t.} \quad & \mathbf{z} \\ \text{s.t.} \quad & \mathbb{K}\left[\mathbf{g}(\mathbf{z}, \mathbf{Y}(\mathbf{z}, \mathbf{U}), \mathbf{U})\right] \leq 0 && (12.2)\\ & \mathbf{z}_{\min} \leq \mathbf{z} \leq \mathbf{z}_{\max} && (12.3) \end{aligned}$$

A coupled approach is used to focus on the optimization algorithm and not on the interdisciplinary coupling satisfaction. To solve this UMDO problem, the optimization algorithm has to take into account the presence of uncertainty and the constraints. Noise in the optimization results from

the numerical approximation of the measure of uncertainty $\Xi[\cdot]$ and $\mathbb{K}[\cdot]$ by sampling techniques (CMC, IS, SS, *etc.*).
In this part of the thesis, we propose to solve this UMDO problem with a modified version of CMA-ES algorithm. The proposed approach of CMA-ES(λ, μ) for constraint handling is based on the same approach as modified (1+1)-CMA-ES (section 5.5.3). However, it is necessary to adapt it to take into account the specificities of CMA-ES(λ, μ). Indeed, CMA-ES(λ, μ) generates a population instead of a single offspring candidate. Thus, each offspring candidate may potentially violate one or several constraints. Moreover, the selection of the μ best candidates is based on the rank of the objective function. However, these best candidates may also violate the constraints. Depending on whether the μ best candidates are feasible or not, or if only a fraction of them is feasible, or on the number of violated constraints, the covariance matrix used to generate the offspring candidates has to be modified in order to avoid the future generation of unfeasible offspring candidates.
As explained in chapter 5, CMA-ES(λ, μ) generates the population at iteration $[k+1]$ by sampling a multivariate normal distribution:

$$\mathbf{z}_t^{[k+1]} \sim \mathbf{m}^{[k]} + \sigma^{[k]} \mathcal{N}\left(0, \mathbf{C}^{[k]}\right), \text{ for } t = 1, ..., \lambda \tag{12.4}$$

with $\mathbf{z}_t^{[k+1]} \in \mathbb{R}^n$ an offspring candidate generated from a mean vector $\mathbf{m}^{[k]}$, a step size $\sigma^{[k]}$ and a multivariate normal distribution $\mathcal{N}(0, \mathbf{C}^{[k]})$ with zero mean and a covariance matrix $\mathbf{C}^{[k]} \in \mathbb{R}^n \times \mathbb{R}^n$. λ is the size of the population generated at each iteration $[k]$. The normal distribution is characterized by a positive definite covariance matrix $\mathbf{C}^{[k]}$ in order to allow homothetic transformations and rotations of the probable search hypervolume. The search hypervolume engendered by an iso-probability contour of the multivariate normal distribution $\mathcal{N}(0, \mathbf{C})$ may be represented by a n-dimensional ellipsoid (Fig. 12.1).

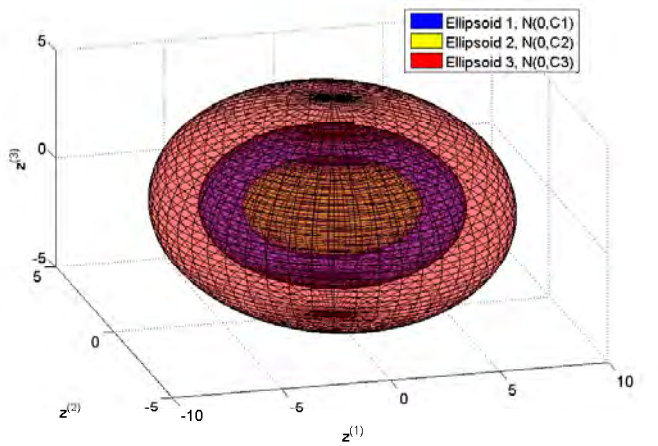

Figure 12.1: Different ellipsoids in dimension 3 defining the probable search hypervolume depending on the covariance matrix $\mathbf{C}_i$ at an iso-probability level of 95%.

The hyper-volumes represented in Figure 12.1 represent the volume in which the offspring candidates will be generated with an iso-probability contour of 95%. This volume is parameterized by

the covariance matrix $\mathbf{C}$. In the proposed approach, the constraint handling method allows to reduce the semi-principal axes of the search ellipsoid in the directions violating the constraints. The eigenvalues of the covariance matrix $\mathbf{C}$ control the length of the semi-principal axes. The decrease of the eigenvalues reduces the semi-principal axis lengths. The direction of the eigenvectors are not modified in order to keep the direction of search and to adapt it to the presence of constraints. The covariance matrix, which is symmetric positive definite, may be decomposed according to:

$$\mathbf{C} = \mathbf{PDDP}^T = \mathbf{PD}^2\mathbf{P}^T \tag{12.5}$$

where $\mathbf{P}$ is an orthogonal matrix such that: $\mathbf{PP}^T = \mathbf{P}^T\mathbf{P} = \mathbf{I}$. The columns of $\mathbf{P}$ form an orthogonal basis of eigenvectors of $\mathbf{C}$. $\mathbf{D} = \text{diag}(\sqrt{\text{vp}_1}, ..., \sqrt{\text{vp}_n})$ is a diagonal matrix with the square roots of eigenvalues of $\mathbf{C}$. As illustrated in Figure 12.2, the square roots of the covariance matrix eigenvalues $\sqrt{\text{vp}_i}$ are proportional to the semi-principal axis lengths of the ellipsoid defining the sampling hypervolume.

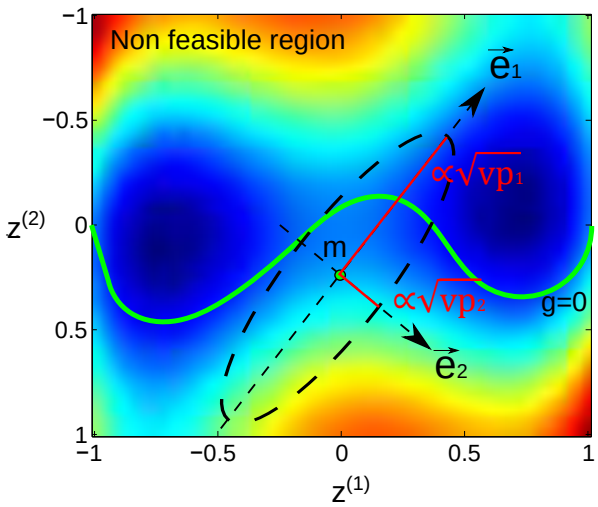

Figure 12.2: Parametrization of the ellipsoid defining the probable search hypervolume.

At the generation $[k]$, if any of the τ constraints is violated by any of the μ best offspring candidates, the covariance matrix is modified according to Algorithm 4.
with:

$$\sqrt{\widetilde{\text{vp}}_i^{[k]}} = \left(\sqrt{\text{vp}_i^{[k]}} \sum_{j=1}^{\tau} \frac{\sum_{l=1}^{\mu} \mathbb{1}_{g_j(\mathbf{z}_{(l)}^{[k]})>0} w_{lj} \text{Proj}_{\vec{e}_i} \left[\mathbf{z}_{(l)}^{[k]} - \mathbf{m}^{[k]} \right]}{\sum_{t=1}^{\mu} \mathbb{1}_{g_j(\mathbf{z}_{(t)}^{[k]})>0} w_{tj}} \right) \tag{12.9}$$

The covariance matrix is diagonalized Eq.(12.6) and the eigenvalues $\text{vp}_i^{[k]}$ of the covariance matrix $\mathbf{C}^{[k]}$ are modified. The new eigenvalues are the former eigenvalues minus a term $\widetilde{\text{vp}}_i^{[k]}$ taking into account the violation of the constraints. $\sqrt{\widetilde{\text{vp}}_i^{[k]}}$, Eq.(12.9), is a function of the former eigenvalues $\sqrt{\text{vp}_i^{[k]}}$, of the indicator function of the constraint $\mathbb{1}_{g_j(\mathbf{z}_{(l)}^{[k]})>0}$, of the weighting coefficients w_{ij} and

Algorithm 4 Proposed CMA-ES(λ, μ) covariance matrix modificiation

$$\text{3.3.1) Diagonalize } \mathbf{C}^{[k]} \text{such that } \mathbf{P}\mathbf{D}^{[k]^2}\mathbf{P}^T = \mathbf{C}^{[k]} \tag{12.6}$$

$$\text{3.3.2) } \mathbf{S}^{[k]} \leftarrow \mathbf{P}\mathbf{D}^{[k]^2}\mathbf{P}^T - \gamma\mathbf{P}\text{diag}\left(\sqrt{\widetilde{\text{vp}}_1^{[k]}}, ..., \sqrt{\widetilde{\text{vp}}_n^{[k]}}\right)^2\mathbf{P}^T \tag{12.7}$$

$$\text{3.3.3) } \mathbf{C}^{[k]} \leftarrow \left[\frac{\det(\mathbf{C}^{[k]})}{\det(\mathbf{S}^{[k]})}\right]^{1/n}\mathbf{S}^{[k]} \tag{12.8}$$

of the projection $\text{Proj}_{\vec{e_i}}\left[\mathbf{z}_{(l)}^{[k]} - \mathbf{m}^{[k]}\right]$ of the distance between an ordered candidate violating the constraints $\mathbf{z}_{(l)}^{[k]}$ and the mean point $\mathbf{m}^{[k]}$ in the direction of the eigenvector $\vec{e_i}$ corresponding to the eigenvalue $\text{vp}_i^{[k]}$. γ is a parameter similar to β in (1+1)-CMA-ES. For $\gamma = 0$ the proposed algorithm is similar to the classical CMA-ES(λ, μ). For each constraint g_j, the μ_{cj} candidates among the μ best candidates that violate the constraint are ranked according to the constraint value. The weighting coefficients w_{ij} for each constraint g_j are defined according to the same rule as for the recombination process for the calculation of $\mathbf{m}^{[k]}$:

$$w_{ij} = \frac{\ln(\mu_{cj} + 1) - \ln(i)}{\mu_{cj}\ln(\mu_{cj} + 1) - \sum_{k=1}^{n}\ln(k)} \tag{12.10}$$

and $\sum_{i=1}^{\mu} w_{ij} = 1$ where: $w_{1j} \geq \cdots \geq w_{\mu j} \geq 0$. w_{1j} is associated to the candidate that violates the most the constraint g_j and $w_{1\mu_c}$ with the candidate that violates the less the constraint. For the candidates among the μ best that do not violate the constraint, the indicator function is equal to zero and therefore these candidates do not participate in the modification of the covariance matrix. The projection of the violation distance along the eigenvector (Fig. 12.3) allows to reduce the covariance matrix in the direction orthogonal to the constraint boundaries.
Eq.(12.8) allows to keep the hypervolume of the ellipsoid constant before and after the modification of the covariance matrix in order to avoid premature convergence. The volume of the ellipsoid is reduced in the direction orthogonal to the constraints but is increased in the direction tangential to the constraints (Fig. 12.4). The modified CMA-ES(λ, μ) algorithm for constraint handling is detailed in Algorithm 5.
In order to illustrate the effect of the modified algorithm, if one of the μ best candidates violates a constraint, the evolution of the ellipsoid between the generations $[k]$ and $[k+1]$ is illustrated in Figure 12.4. The modification of $\mathbf{C}^{[k]}$ allows homothetic transformations in order to avoid to generate candidates in the non feasible zone.
Several adjusments have been made in order to take into account specific situations/

- If the mean vector $\mathbf{m}^{[k]}$ after the combination process is not feasible, instead of reducing the covariance matrix, the ellipsoid hypervolume is increased in order to generate candidates in the feasible zone. Therefore, the ellipsoid hypervolume is increased according to:

$$\mathbf{S}^{[k]} \leftarrow \mathbf{P}\mathbf{D}^{[k]^2}\mathbf{P}^T + \gamma\mathbf{P}\text{diag}\left(\sqrt{\widetilde{\text{vp}}_1^{[k]}}, ..., \sqrt{\widetilde{\text{vp}}_n^{[k]}}\right)^2\mathbf{P}^T \tag{12.11}$$

  The mean vector is displaced to the best feasible candidate generated at the next generation.

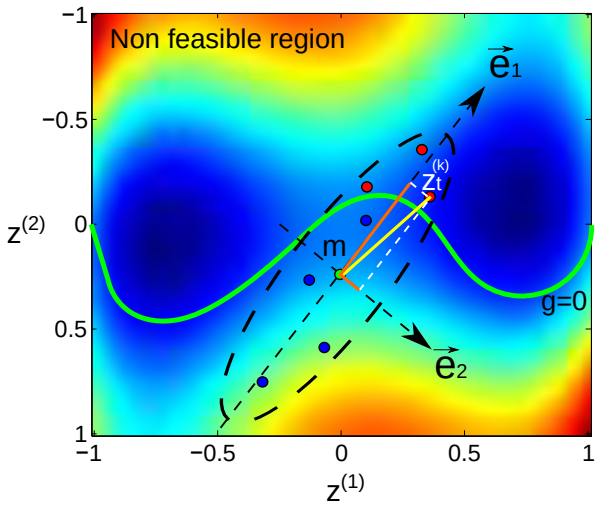

Figure 12.3: Violation of the constraint and projection over the eigenvectors, blue=feasible, red=unfeasible candidates.

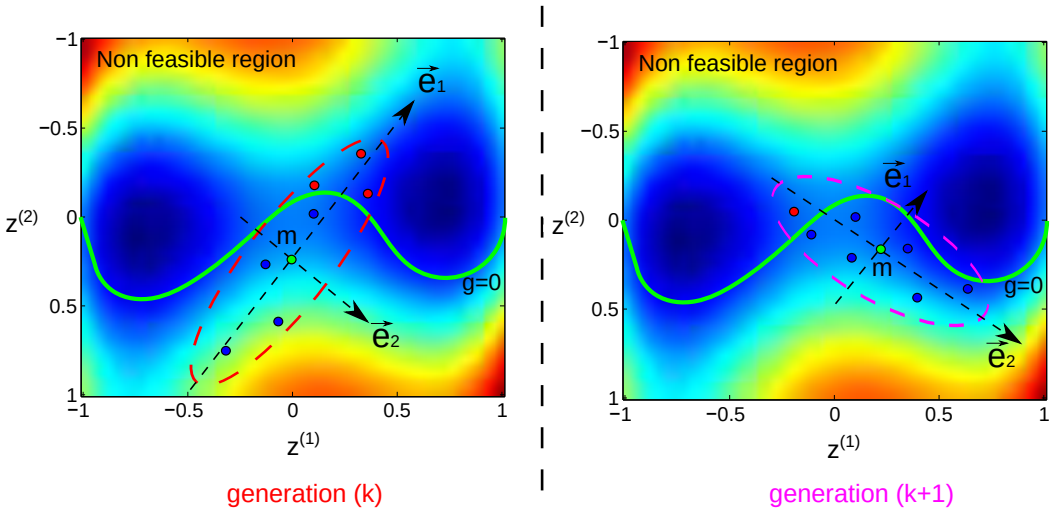

Figure 12.4: Evolution of the covariance matrix due to the constraint violation, blue=feasible, red=unfeasible candidates.

- To avoid stagnation and non exploration of the algorithm when the μ best candidates are all generated in the non feasible space n_μ times in a row, the algorithm does not select the μ best candidates according to the objective function but the μ best candidates in the feasible space in order to update the algorithm parameters ($\mathbf{m}$, $\mathbf{C}$ and σ) and to continue the design space exploration and convergence to the optimum.

Algorithm 5 Proposed modified CMA-ES(λ, μ) for constraint handling

1) Initialize the covariance matrix $\mathbf{C}^{[0]} = \mathbf{I}$, the step size $\sigma^{[0]}$ and the selection parameters [Hansen et al., 2003]
2) Initialize the mean vector $\mathbf{m}^{[0]}$ to a random candidate, $k \leftarrow 0$
while CMA-ES convergence criterion is not reached **do**
  3-1) Generate λ new offspring candidates according to: $\mathbf{z}_t^{[k+1]} \sim \mathbf{m}^{[k]} + \sigma^{[k]}\mathcal{N}(0, \mathbf{C}^{[k]})$, $t \in \{1, ..., \lambda\}$
  3-2) Evaluate candidates and sort them based on the objective function
  if all the μ best candidates are infeasible **then**
    Modify the covariance matrix according to Algorithm 4. Return to step 3.1)
  else
    if all the μ best candidates are feasible
    Determine the mean vector given the weightings of the μ best candidates: $\mathbf{m}^{[k+1]} = \sum_{i=1}^{\mu} w_i \mathbf{z}_{(i)}^{[k+1]}$
    Update covariance matrix $\mathbf{C}^{[k+1]}$ according to [Hansen et al., 2003] **end if**
  else
    if at least one of the μ best candidates is infeasible and at least one is feasible
    Modify the covariance matrix according to Algorithm 4.
    Use the feasible candidates to determine the mean vector $\mathbf{m}^{[k+1]}$
    Use the feasible candidates to update covariance matrix $\mathbf{C}^{[k+1]}$ according to [Hansen et al., 2003] **end if**
  end if
  3-3) Update the step size $\sigma^{[k+1]}$ according to [Hansen et al., 2003], $k \leftarrow k + 1$
end while
4) **return** best candidate $\mathbf{z}_{best}$

- CMA-ES may sometimes converge to a local solution. To overcome this issue, a bi-population based approach has been adopted in CMA-ES [Hansen, 2009] to start the algorithm with a higher size population and after several iteration, the λ default size population is used. The population is increased for the k_{ipop} first iterations in order to sufficiently explore the design space and learn about the objective function before going to the λ default size.

The modified CMA-ES(λ, μ) allows to take into account the constraints without degrading the objective function by penalization and avoids to tune the penalization parameters. Moreover, the proposed algorithm relies on the same update and selection mechanisms of the original CMA-ES(λ, μ) and it keeps the invariance and unbiased design principles of CMA-ES(λ, μ) [Hansen et al., 2003]. In the next sections, the proposed algorithm is tested on a benchmark of analytical functions and on the design of a two stage rocket in order to evaluate its performances.

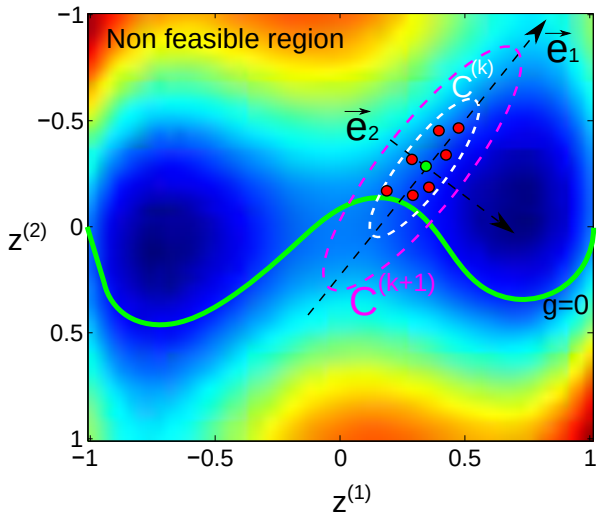

Figure 12.5: Modification of the covariance matrix due to the mean vector constraint violation, blue=feasible, red=unfeasible candidates.

12.3 Benchmark on analytical optimization problems

The proposed modified CMA-ES(λ, μ) is tested and compared to a penalized version of CMA-ES(λ, μ) with a constant penalization function, to the death penalty applied to CMA-ES(λ, μ) and to the modified (1+1)-CMA-ES on a benchmark of three analytical functions. The benchmark consists of a modified Six Hump Camel problem in 2 dimensions, the G04 optimization problem [Hansen, 2009] in 5 dimensions and a modified Rosenbrock problem in 20 dimensions. These optimization problems are used in order to evaluate the proposed algorithm efficiency for different design space dimensions and different types of and numbers of inequality constraints (linear, non linear). In the following, the benchmark problems are introduced with the results. A discussion and a synthesis of the results for all the tests is provided in section 4.4.

In the three problem formulations, the expected value is computed by CMC method. A sample of 1000 points is used to estimate the expected value of the objective function. For each method (Modified CMA-ES(λ, μ), Death Penalty CMA-ES(λ, μ), Penalization CMA-ES(λ, μ), Modified (1+1)-CMA-ES) the optimization is repeated 50 times. The initialization is chosen randomly in the design space and the same initialization and the same random number seed are used for the four optimization algorithms. The same stopping criterion is used for all the algorithms: the distance in the design space between the mean vector and the best point found $\| \mathbf{m}^{[k]} - \mathbf{z}^* \|^2 < 10^{-3}$ must be lower than a tolerance 20 times in a row.

12.3.1 Modified Six Hump Camel problem

A modified version of the Six Hump Camel problem is used in order to introduce uncertainty and three inequality constraints. The formulation of the problem is the following:

$$\begin{aligned}
\min \quad & \mathbb{E}\left[f_{6-hump}(z^{(1)}, z^{(2)}) + f_{6-hump}\left(z^{(1)}\cos(u) + z^{(2)}\sin(u) - z^{(1)}\sin(u) \right.\right. \\
& \left.\left. + z^{(2)}\cos(u)\right)\right] \qquad (12.12) \\
\text{w.r.t.} \quad & \mathbf{z} = [z^{(1)}, z^{(2)}] \\
\text{s.t.} \quad & g_1(z^{(1)}, z^{(2)}) = z^{(1)} + z^{(2)}/4 - 0.52 \leq 0 \qquad (12.13) \\
& g_2(z^{(1)}, z^{(2)}) = z^{(1)} + 0.01z^{(2)} - 0.7 + 0.30\cos(60{z^{(1)}}^{2/6}) \leq 0 \qquad (12.14) \\
& g_3(z^{(1)}, z^{(2)}) = z^{(1)} - z^{(2)}/4 - 0.45 \leq 0 \qquad (12.15) \\
& \mathbf{z}_{\min} \leq \mathbf{z} \leq \mathbf{z}_{\max} \qquad (12.16)
\end{aligned}$$

with $\mathbf{z} \in [-3, 3] \times [-2, 2]$, $f_{6-hump}(z_1, z_2) = (4 - 2.1z_1^2 + z_1^4/3) + z_1 z_2 + (4z_2^2 - 4)z_2^2$ and U a random variable distributed according to a normal distribution $U \sim \mathcal{N}(0, 0.05)$.

Table 12.6: Results of modified Six Hump Camel problem. Average over 50 optimizations (in parenthesis the Relative Standard Deviation (RSD) - $\sigma/\mathbb{E}$)

Results	Modified CMA-ES(λ, μ)	Death Penalty CMA-ES(λ, μ)	Penalization CMA-ES(λ, μ)	Modified (1+1)-CMA-ES
Objective function (global optimum [1])	-1.875(0.80%)	-1.875(0.89%)	-1.874(0.88%)	-1.865(0.88%)
Objective function (local optimum [2])	-0.347(0.75%)	-0.347(0.84%)	-0.347(0.79%)	-0.348(0.85%)
Constraint functions	-4.72×10^{-4} (96%)	-2.57×10^{-4} (75%)	-6.43×10^{-4} (68%)	-4.86×10^{-4} (127%)
Number of objective function +constraint evaluations	1211(13%)	1395(12%)	1618(12%)	781(16%)
Percentage of convergence to the global minimum	37%	22%	33%	48%
Percentage of convergence to the local minimum	63%	78%	67%	52%

[1] Statistics based on the optimizations that converged to the global optimum.
[2] Statistics based on the optimizations that converged to the local optimum.

Representations of the function and the constraints are provided in Figure 12.8. The problem has one local optimum and one global optimum. The results are presented in Table (12.6) and the convergence curves for one optimization are given in Figure (12.9).

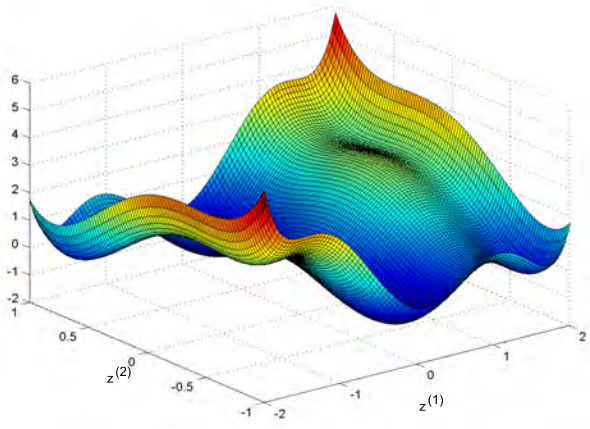

Figure 12.7: Modified Six Hump Camel 3D function.

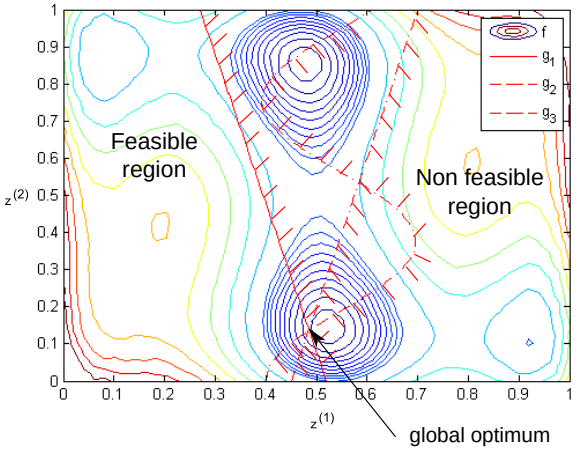

Figure 12.8: Iso-contour of the expected value of Modified Six Hump Camel function, constraints and global optimum.

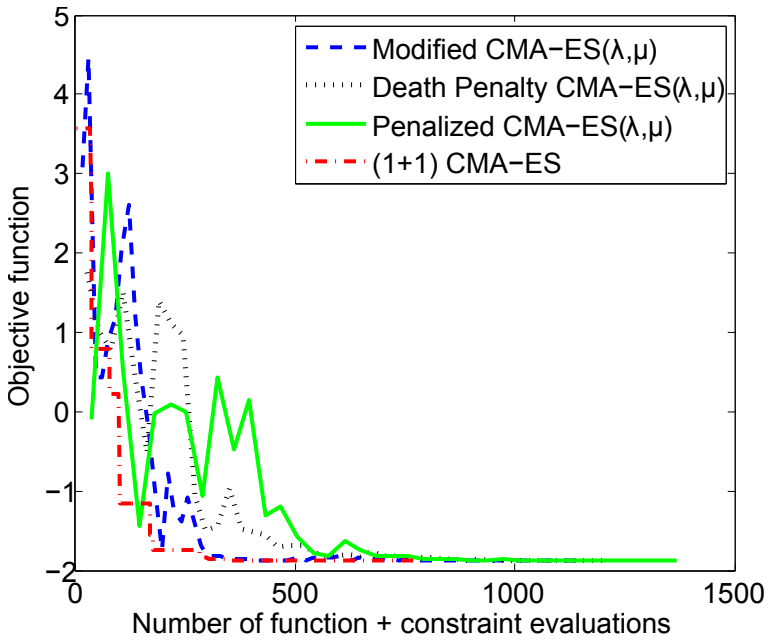

Figure 12.9: Convergence curves of the Six Hump Camel problem in 2 dimensions, based on one optimization run.

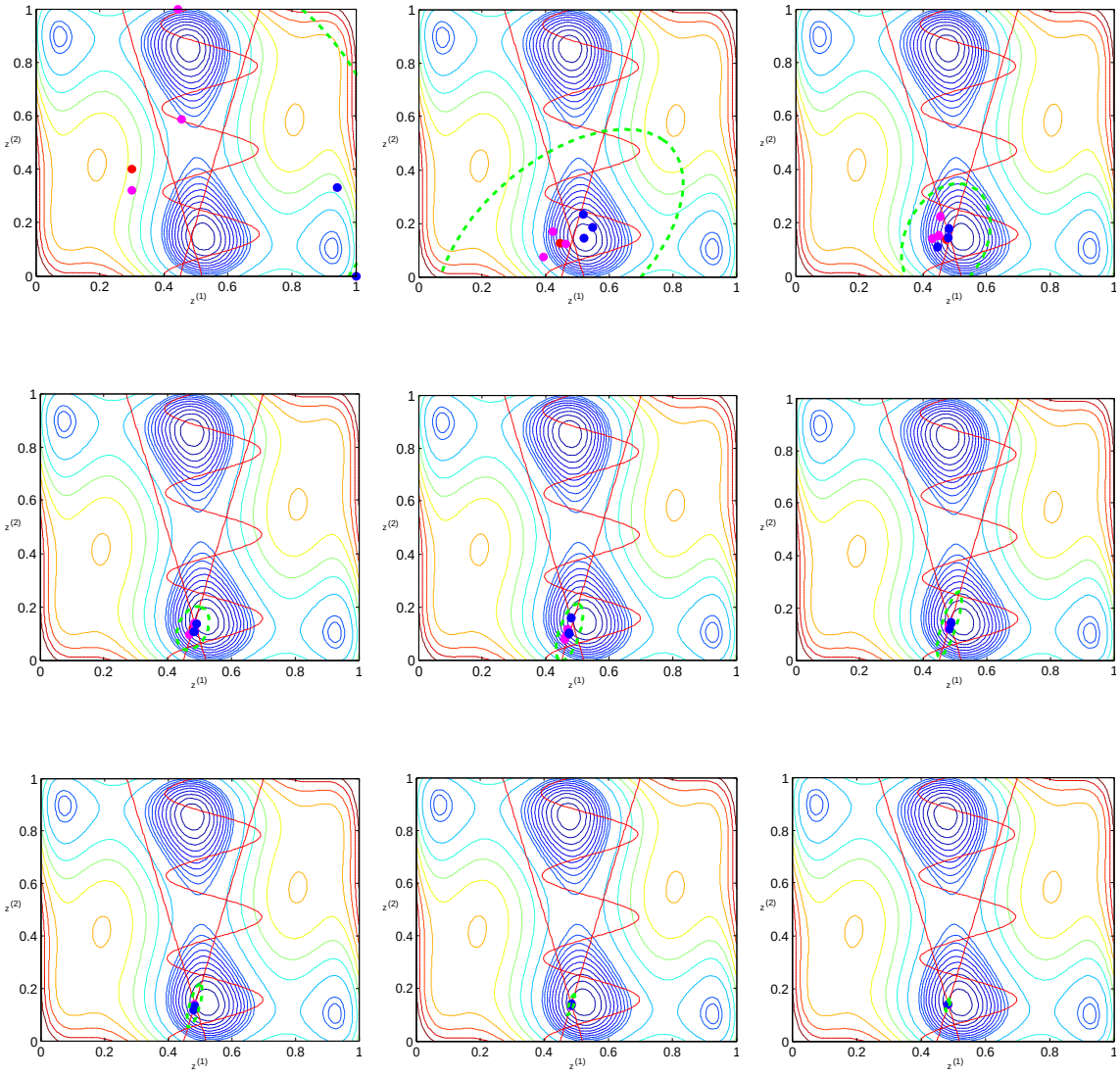

Figure 12.10: Six hump camel optimization, iso-probability search volume in green, μ best candidate in blue, mean point in red, other candidates in pink, a plot every 18 modified CMA-ES iterations.

12.3.2 G04 optimization problem

The G04 optimization problem [Hansen, 2009] involves 6 inequality constraints and is defined as follows:

$$\begin{aligned}
\min \quad & G_{04}(\mathbf{z}) = 5.3578547 \times z^{(3)^2} + 0.8356891 \times z^{(1)} * z^{(5)} + 37.293239 \times z^{(1)} \\
& \qquad -40792.141 \qquad (12.17) \\
\text{w.r.t.} \quad & \mathbf{z} = [z^{(1)}, z^{(2)}, z^{(3)}, z^{(4)}, z^{(5)}] \\
\text{s.t.} \quad & g_1(\mathbf{z}) = u(\mathbf{z}) - 92 \leq 0 \qquad (12.18) \\
& g_2(\mathbf{z}) = -u(\mathbf{z}) \leq 0 \qquad (12.19) \\
& g_3(\mathbf{z}) = v(\mathbf{z}) - 110 \leq 0 \qquad (12.20) \\
& g_4(\mathbf{z}) = -v(\mathbf{z}) + 90 \leq 0 \qquad (12.21) \\
& g_5(\mathbf{z}) = w(\mathbf{z}) - 25 \leq 0 \qquad (12.22) \\
& g_6(\mathbf{z}) = -w(\mathbf{z}) + 20 \leq 0 \qquad (12.23) \\
& \mathbf{z}_{\min} \leq \mathbf{z} \leq \mathbf{z}_{\max} \qquad (12.24)
\end{aligned}$$

with $\mathbf{z} \in \mathbb{R}^5$, $\mathbf{z_{min}} = [78, 33, 27, 27, 27]$, $\mathbf{z_{max}} = [102, 45, 45, 45, 45]$ and:

$$\begin{aligned}
u(\mathbf{z}) &= 85.334407 + 0.0056858 \times z^{(2)} \times z^{(5)} + 0.0006262 \times z^{(1)} \times z^{(4)} \\
&\quad -0.0022053 \times z^{(3)} \times z^{(5)} \qquad (12.25) \\
v(\mathbf{z}) &= 80.51249 + 0.0071317 \times z^{(2)} \times z^{(5)} + 0.0029955 \times z^{(1)} \times z^{(2)} \\
&\quad +0.0021813 \times z^{(3)^2} \qquad (12.26) \\
w(\mathbf{z}) &= 9.300961 + 0.0047026 \times z^{(3)} \times z^{(5)} + 0.0012547 \times z^{(1)} \times z^{(3)} \\
&\quad +0.0019085 \times z^{(3)} \times z^{(4)} \qquad (12.27)
\end{aligned}$$

Table 12.11: Results of G04 optimization problem. Average over 50 optimizations (in parenthesis the RSD - $\sigma/\mathbb{E}$).

Results	Modified CMA-ES(λ, μ)	Death Penalty CMA-ES(λ, μ)	Penalization CMA-ES(λ, μ)	Modified (1+1)-CMA-ES
Objective function	$-30487(0.48\%)$	$-28105(6.10\%)$	$-28758(12\%)$	$-30452(0.46\%)$
Number of objective function +constraint evaluations	1618(33%)	9120(40%)	13139(107%)	7048(93%)

The results are presented in Table (12.11) and the convergence curves for one optimization are given in Figure 12.12.

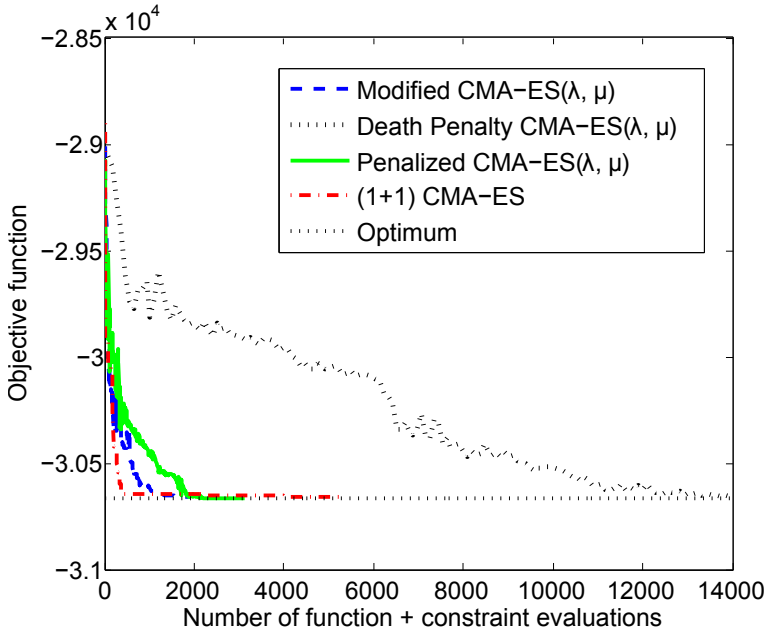

Figure 12.12: Convergence curves of the G04 optimization problem, based on one optimization run.

12.3.3 Modified Rosenbrock problem

The Rosenbrock optimization problem has been modified in order to incorporate uncertainty and an inequality constraint. The problem is formulated as following:

$$\min \quad \mathbb{E}\left[100\sum_{i=1}^{n-1}\left(z^{(i+1)}-z^{(i)^2}\right)^2+\sum_{i=1}^{n-1}\left(1-z^{(i)}\right)^2+U\right] \tag{12.28}$$

$$\text{w.r.t.} \quad \mathbf{z}=\left[z^{(1)},...,z^{(20)}\right]$$

$$\text{s.t.} \quad g(\mathbf{z})=2-\prod_{i=1}^{n}z^{(i)}\leq 0 \tag{12.29}$$

$$\tag{12.30}$$

with n=20, $\mathbf{z}\in\mathbb{R}^{20}$ and U a random variable distributed according to $U\sim\mathcal{U}(-0.1,0.0)$ a uniform distribution.
The results are presented in Table (12.15) and the convergence curves for one optimization are given in Figure 12.14.

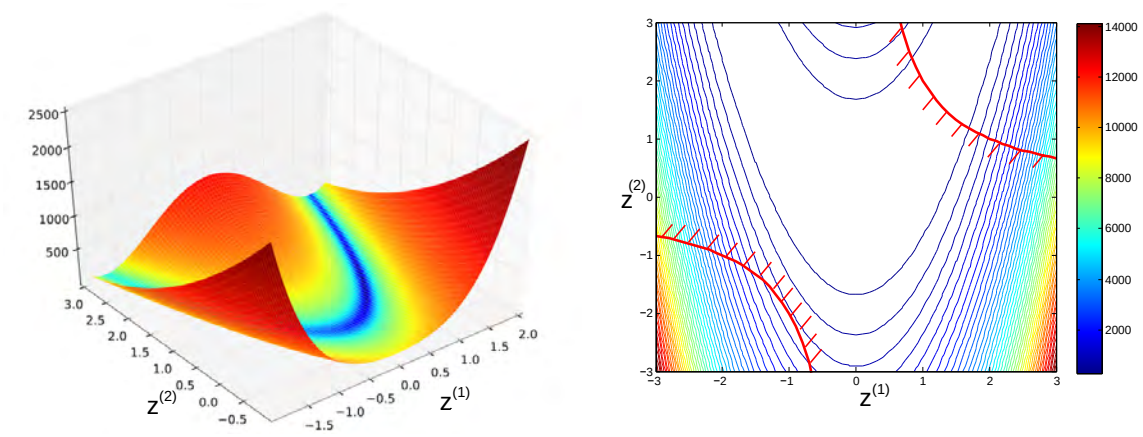

Figure 12.13: Expected value of modified Rosenbrock function and the constraints in 2 dimensions.

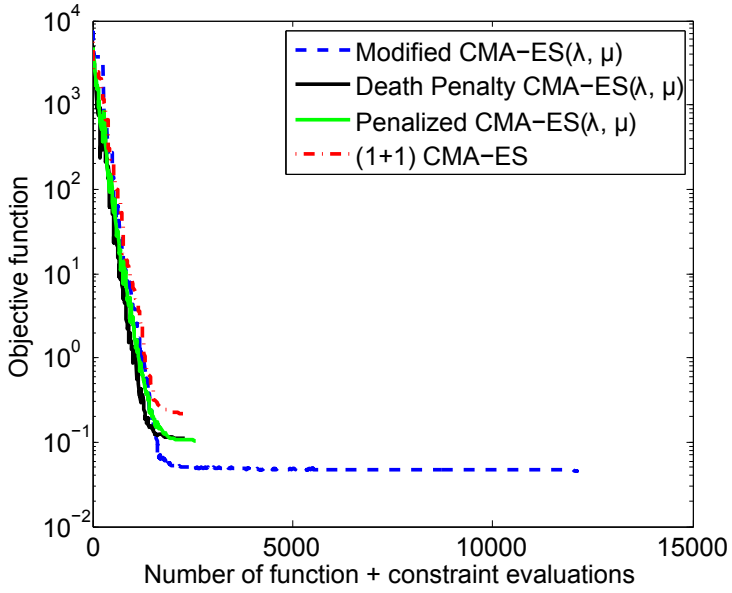

Figure 12.14: Convergence curves of the modified Rosenbrock problem in 20 dimensions, based on one optimization run.

12.3.4 Results and synthesis

The analytical test cases involve different dimensions (2, 5 and 20) and different number of constraints (1, 3 and 6) in order to evaluate the efficiency of the proposed Modified CMA-ES(λ, μ) on various optimization problems. A qualitative synthesis of the obtained results is given in Figure

Table 12.15: Results of constrained Rosenbrock problem. Average over 50 optimizations (in parenthesis the RSD - $\sigma/\mathbb{E}$).

Results	Modified CMA-ES(λ, μ)	Death Penalty CMA-ES(λ, μ)	Penalization CMA-ES(λ, μ)	Modified (1+1)-CMA-ES
Objective function	0.046(0.12%)	0.109(42.77%)	0.096(26%)	0.0841(53.85%)
Constraint functions	$-5.05 * 10^{-4}$(96%)	-0.74(75%)	1.45(68%)	-0.4294(127%)
Number of objective function +constraint evaluations	12798(11%)	2708(33%)	2689(49%)	3481(28%)

12.16. For all the three criteria (number of evaluations, robustness to initialization and value of the optimum), the lower value the better the quality of the method for the given criterion.
The Six Hump Camel problem has one local optimum and one global optimum. All the optimization algorithms converge either to the local or the global optimum. It illustrates the robustness property of the algorithms with respect to the initialization (relative standard deviation $\sim 0.85\%$ for all the algorithms). The found optima are all feasible. Modified (1+1)-CMA-ES converges in 48% of the optimization runs to the global optimum and the proposed Modified CMA-ES (λ, μ) in 37% of the cases. The penalization and the death penality approaches converge only in 33% and 22% of the optimization runs to the global optimum. The number of calls to the objective function and the constraints is in increasing order: Modified (1+1)-CMA-ES (781), Modified CMA-ES(λ, μ) (1211), Death Penalty CMA-ES(λ, μ) (1395) and Penalization CMA-ES(λ, μ) (1618). Modified (1+1)-CMA-ES is more efficient in this test case due to the low dimension and the simplicity of the optimization problem. The proposed Modified CMA-ES(λ, μ) provides better results than the penalization and the death penalty approaches.
In the G04 problem, only the proposed Modified CMA-ES(λ, μ) and the Modified (1+1)-CMA-ES converge to the global minimum (with sufficient robustness with respect to the initialization). The number of calls to the objective function and the constraints is lower in the proposed algorithm (1618) compared to Modified (1+1)-CMA-ES (7048) and the relative standard deviation is lower in the proposed approach. Moreover, the proposed approach converges efficiently to the global optimum. The Death Penalty and the penalization approaches do not succeed to reach the global optimum and are not robust to the initialization.
In the modified Rosenbrock problem, only the proposed Modified CMA-ES(λ, μ) reaches the global optimum (with sufficient robustness (RSD : 0.12%) to the initialization). All the other algorithms are not robust to the initialization and do not converge to the global optimum. The number of calls to the objective function and the constraints is larger for the proposed approach (12798) compared the other algorithms.
Consequently, from the benchmark, in small dimensions (< 8), the Modified (1+1)-CMA-ES provides good results in terms of convergence to the global optimum and robustness with respect to the

initialization, however, as expected, in large dimensions, it presents issues to converge to the global optimum. The proposed Modified CMA-ES(λ, μ) succeeds in small and large dimensions (up to 20) to find the global optimum. Moreover, this algorithm appears as robust to the initialization. In the next section, the proposed algorithm is used to design a two stage solid rocket and is compared to the existing CMA-ES based optimization algorithms.

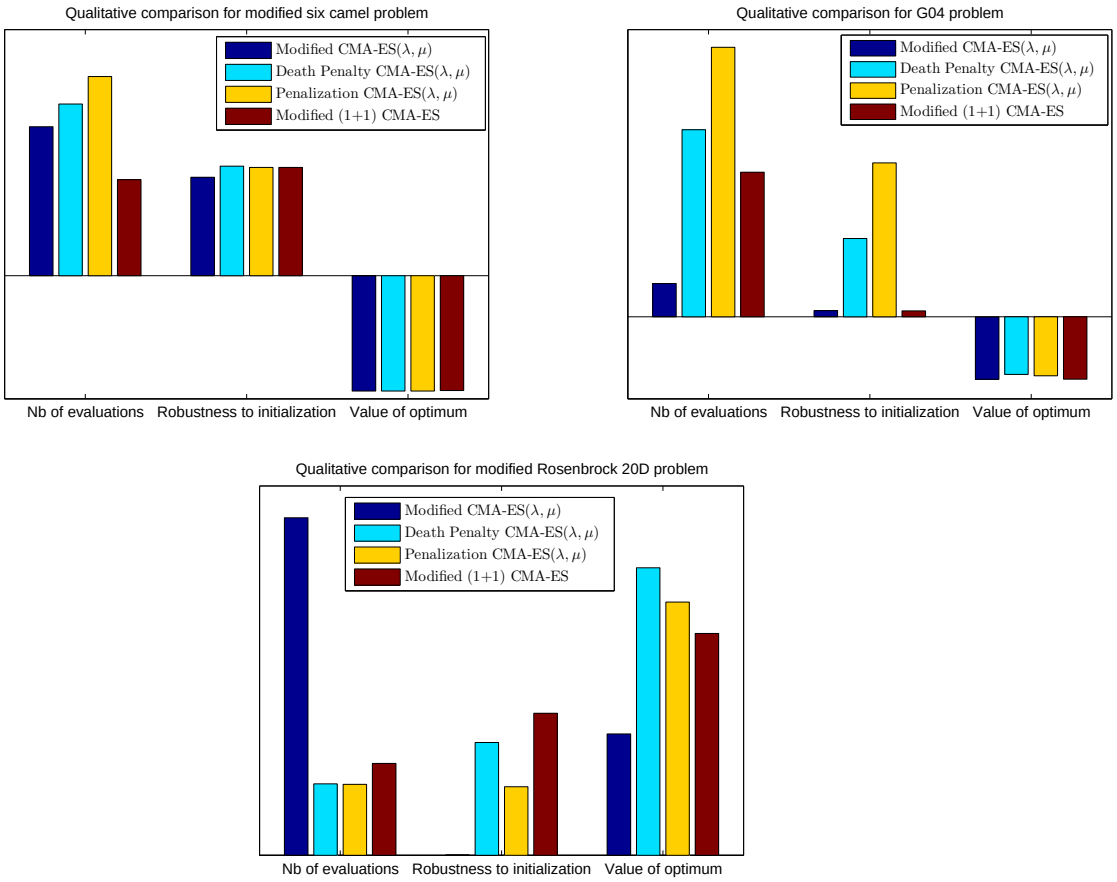

Figure 12.16: Qualitative results obtained for the different test cases (the smaller the better).

12.4 Conclusion

The design of complex systems often induces a constrained optimization problem under uncertainty. Dedicated optimization algorithms are required to solve these types of problems. In this chapter, an adaptation of the optimization algorithm CMA-ES(λ, μ) which is based on Evolutionary Strategy has been proposed in order to efficiently handle the constraints. CMA-ES(λ, μ) generates the candidate population according to the sampling of a parameterized Gaussian distribution $\mathcal{N}(0, \mathbf{C})$ where $\mathbf{C}$ is a covariance matrix. In this chapter, the search hypervolume engendered by an iso-probability contour of the multivariate normal distribution used to generate the candidate population is modified. The constraint handling method allows to reduce the semi-principal axes of the iso-probable search ellipsoid in the directions violating the constraints by decreasing the eigenvalues of the covariance matrix $\mathbf{C}$. The proposed approach has been tested and compared to three CMA-ES methods with three analytical optimization problems highlighting the efficiency of the algorithm and the robustness with respect to the initialization. A better optimum has been found with the proposed approach with respect to the existing CMA-ES based optimization algorithms.

Chapter 13

Modified CMA-ES - launch vehicle application

Contents

Chapter goals

- Apply and compare the proposed approach to reference techniques on a launch vehicle design test case.

13.1 Introduction

In the previous chapter 12, a modification of CMA-ES algorithm has been proposed in order to incorporate the constraint handling and to generate a probable research taking into account the constraint violation in accordance with the information provided by the candidates. The proposed technique has been compared to classical penalization methods of CMA-ES(λ, μ) and to the modified version of (1+1)-CMA-ES, outlining the robustness and efficiency of the proposed approach. In this chapter, the proposed handling constraint method is used to design a two stage solid propulsion launch vehicle. The modeling of the launch vehicle is different from chapter 8 in order to use less computationally intensive models and therefore enables numerical comparison between the

different optimization algorithms. For instance, the trajectory simulation is replaced by a measure corresponding to the propulsive speed increment characterizing the vehicle performance. The models used here are still representative of the vehicle dynamics but with a lower degree of fidelity.

13.2 Two stage solid propulsion rocket design

A multidisciplinary design problem consisting in maximizing the propulsive velocity increment ΔV provided by a two stage rocket under geometrical and physical feasibility constraints is solved. The propulsive speed increment is one of the important performance metrics of a launch vehicle and is similar to the range for an aircraft. The conceptual design models use simplified analysis of a two stage cylindrical solid propellant rocket motor. The multidisciplinary analysis involves four disciplines: the propulsion, the mass and sizing, the structure and the performance and constraint assessment (Fig. 13.1). At the early design phase, model uncertainties exist and have to be taken into account. Two uncertainties are considered: the density of the propellant ρ and the ultimate strength σ for the rocket case material.

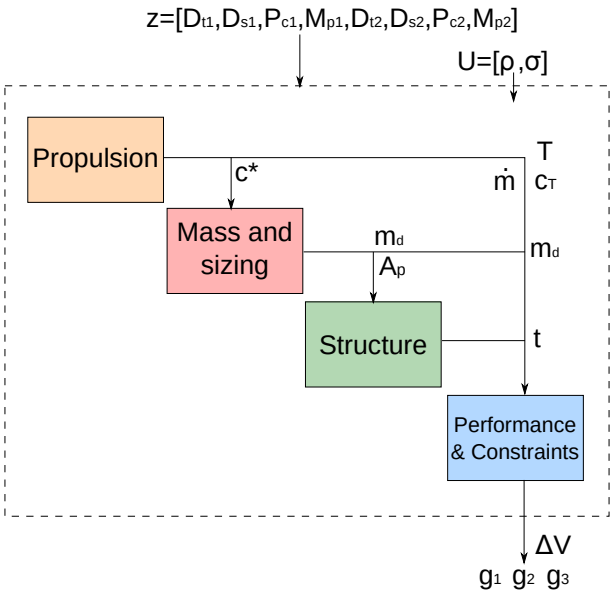

Figure 13.1: Design Structure Matrix for the two stage solid rocket.

The problem is formulated as follows:

$$\begin{aligned}
&\max && \mathbb{E}\left[\Delta V(\mathbf{z},\mathbf{U})\right] && (13.1)\\
&\text{w.r.t.} && \mathbf{z} = [D_{t1}, D_{s1}, P_{c1}, M_{p1}, D_{t2}, D_{s2}, P_{c2}, M_{p2}] &\\
&\text{s.t.} && \mathbb{P}_f\left[g_1(\mathbf{z},\mathbf{U}) \geq 0\right] \leq 10^{-2} && (13.2)\\
& && \mathbb{P}_f\left[g_2(\mathbf{z},\mathbf{U}) \geq 0\right] \leq 10^{-2} && (13.3)\\
& && \mathbb{P}_f\left[g_3(\mathbf{z},\mathbf{U}) \geq 0\right] \leq 10^{-2} && (13.4)\\
& && \mathbf{z}_{\min} \leq \mathbf{z} \leq \mathbf{z}_{\max} && (13.5)
\end{aligned}$$

with: $\mathbf{U} = [U^{(1)}, U^{(2)}]$ with $U^{(1)} \sim \mathcal{N}(1, 0.02)$ the uncertainty of the density of the propellant (ρ) and $U^{(2)} \sim \mathcal{N}(1, 0.05)$ the uncertainty of the ultimate strength limit (σ) for the rocket case material. The design variables are described in Table 13.2. An overview of the disciplines is provided in the next sections.

Table 13.2: Design variables for the two-stage rocket.

Variables	Symbol	Domain of definition	Baseline
1^{st} stage nozzle throat diameter	D_{t1}	$[0.05, 1]$ m	0.75m
2^{nd} stage nozzle throat diameter	D_{t2}	$[0.05, 1]$ m	0.75m
1^{st} stage nozzle exit diameter	D_{s1}	$[0.5, 1.4]$ m	1m
2^{nd} stage nozzle exit diameter	D_{s2}	$[0.5, 1.4]$ m	1m
1^{st} stage combustion pressure	P_{c1}	$[1, 500]$ bar	100bar
2^{nd} stage combustion pressure	P_{c2}	$[1, 500]$ bar	100bar
1^{st} stage propellant mass	M_{p1}	$[2000, 15000]$ kg	8000kg
2^{nd} stage propellant mass	M_{p1}	$[2000, 15000]$ kg	8000kg

13.2.1 Disciplinary models

13.2.1.1 Propulsion

The propulsion discipline computes for a given set of propellant characteristics (density ρ, combustion speed, flame temperature T_c, heat capacity ratio γ), the thrust T, the mass flow rate $\dot{m}$, the thrust coefficient c_τ , the characteristic velocity c^* and the specific impulse I_{sp}. Moreover, it is assumed that the flow through the nozzle is isentropic with a perfect gas and steady. The thrust coefficient c_τ depends entirely on the nozzle characteristics D_t, D_s and the heat capacity ratio γ:

$$c_\tau = \left[\frac{2\gamma^2}{\gamma-1}\left(\frac{2}{\gamma+1}\right)^{\frac{\gamma+1}{\gamma-1}}\left[1-\left(\frac{P_e}{P_c}\right)^{\frac{\gamma-1}{\gamma}}\right]\right]^{\frac{1}{2}} + \frac{(P_e - P_a)\times A_e}{A_t \times P_c} \tag{13.6}$$

where P_c is the combustion chamber pressure, P_e is the nozzle exit pressure, P_a is the local atmospheric pressure, A_e is the nozzle exit area and A_t is the nozzle throat area. Moreover, the characteristic velocity c^* depends on the flame temperature according to:

$$c^* = \frac{\sqrt{\gamma \times R \times T_c}}{\gamma\left(\frac{2}{\gamma+1}\right)^{\frac{\gamma+1}{2(\gamma-1)}}} \tag{13.7}$$

with $R = 8314/M_c$ the gas constant. The specific impulse is derived from c_τ and c^*:

$$I_{sp} = \frac{c^* \times c_\tau}{g_0} \tag{13.8}$$

and furthermore, we have the thrust of the solid rocket motor given by:

$$T = g_0 \times q \times I_{sp} \tag{13.9}$$

with q the mass flow rate. The discipline takes nozzle shape D_t, D_s and combustion pressure P_c as inputs. The used propellant is the butargols with polybutadiene binder without aluminium additive. See the appendices for more details on the models.

13.2.1.2 Mass and Sizing

The mass and sizing discipline computes the dry mass m_d and the geometry of the two stage solid propulsion rocket. The dry mass involves the mass of the rocket case, the mass of the nozzle and the pyrotechnic igniter. The rocket geometry consists of the initial combustion area, the packaging ratio and the size of the central channel. The mass models used are derived from conceptual design phases models developed by Castellini [Castellini, 2012]. See the appendices for more details on the models.

13.2.1.3 Structure

The structure discipline computes the tank wall thickness (t) which are sized under the combustion pressure based on the material characteristics (density, ultimate tensile strength limit) and rocket geometry to be used by the mass discipline. Moreover, it computes the stress in the rocket case. The motorcase thickness t is given by:

$$t = \frac{P_b \times R_c}{F_{tu}} \tag{13.10}$$

where P_b is the burst pressure determined based on the maximum expected operating pressure [Humble et al., 1995], R_c is the case radius and F_{tu} is the ultimate tensile strength of case material. The material used for the motorcase is the 4130 steel alloy ($\rho_c = 7830\ kg/m^3$, $F_{tu} = 0.862\ GPa$).

13.2.1.4 Performance and constraints

The performance metric is the propulsive speed increment ΔV and the expected value of ΔV is the objective function to be maximized. CMC based on 1000 samples is used to compute the expected value of the propulsive velocity increment. The propulsive velocity increment is given by:

$$\Delta V = g_0 I_{sp} \ln\left(\frac{m_i}{m_f}\right) \tag{13.11}$$

with m_i the initial mass and m_f the final mass of the launch vehicle.
Three constraints are considered for each stage:

- $g_1(\cdot)$ which ensures packaging ratio (Propellant volume / Available volume) that has to be inferior to 87%,

- $g_2(\cdot)$ which ensures that central channel diameter is 30% greater than the nozzle throat diameter,
- $g_3(\cdot)$ which ensures that combustion area is greater than the minimum feasible (area of central channel walls).

The probabilities of failure for the three constraints have to be inferior to 1%. The probabilities of failure are computed with a CMC of 10^4 samples, numerically corresponding to a relative standard error ($\sigma/\mathbb{E}$) of the probability estimation in the order of 5%. See the appendices for more details on the models.

13.2.2 Results

The optimization process for each algorithm is repeated 10 times. All the optimizations start from the same baseline given in Table 13.2. The same stopping criterion is used for all the optimization algorithms: the distance in the design space between the mean vector and the best point found $\| \mathbf{m}^{(k)} - \mathbf{z}_{best} \|^2 < 10^{-3}$ must be under a tolerance 20 times in a row. The convergence curves of the algorithms are given in Figure 13.5. The dimension of the launch vehicle design problem is 8 with 6 constraints. The different algorithms do not converge exactly to the same optimum. Modified CMA-ES (λ, μ) provides a better optimum in terms of propulsive speed increment: $6234.1 m/s$ with a better robustness to the repetition of the optimization process. Modified CMA-ES (λ, μ) and Penalization CMA-ES (λ, μ) share a close optimum. The difference in terms of propulsive increment is due to the higher chamber pressure, the different distributions of propellant masses between the two stages and a different nozzle geometry for the first stage in the Modified CMA-ES (λ, μ). The sensitivity of the propulsive increment to the chamber pressure, the mass of propellant and the nozzle geometry is important resulting into a difference into the optimization results. The proposed algorithm converges on the average with 1127 discipline evaluations. The other optimization algorithms converge with the same order of number of discipline evaluations ($\sim$ 1750). Four constraints are active at the optimum which constrained the design and make complex the optimization. The better optimum found by the proposed approach is essential as it has a better propulsive speed increment which could be used to increase the payload mass. Figure 13.3 illustrates the difference between the optimal solutions found by the different algorithms. The grain geometry and the optimal rocket found by modified CMA-ES are represented in Figure 13.6.

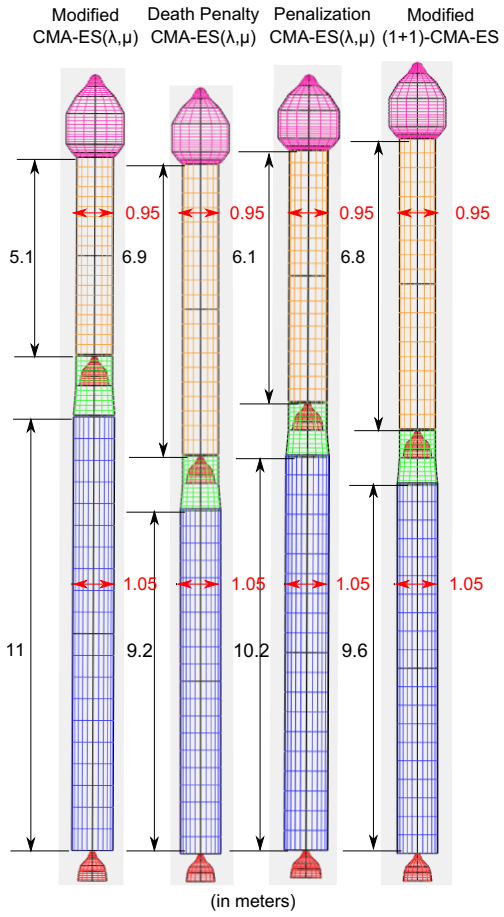

Figure 13.3: Optimal launch vehicle design for the four optimizers.

Table 13.4: Results of the two stage rocket optimization. Average over 10 optimizations (in parenthesis the RSD - $\sigma/\mathbb{E}$).

Results	Modified CMA-ES(λ, μ)	Death Penalty CMA-ES(λ, μ)	Penalization CMA-ES(λ, μ)	Modified (1+1)-CMA-ES
Design Variables	[0.321, 0.9081, 205.46, 12428.1, 0.637, 1.288, 21.08, 7911.2]	[0.449, 1.240, 64.12, 10781.4, 0.535, 1.112, 32.85, 9726.6]	[0.283, 0.7131, 181.83, 12462.5, 0.571, 1.39, 26.20, 9316.9]	[0.3558, 0.9961, 199.87, 11750.2, 0.5476, 1.314, 31.78, 9723.6]
Objective function	6234.1 (0.95%)	6093.2 (1.55%)	6097.4 (1.43%)	6080.1 (1.19%)
Constraint functions	[−0.01, −0.0023, −0.0014, −0.01, −0.0023, −0.0032]	[−0.01, −0.025, −0.01, −0.01, −0.01, −0.0037]	[−0.01, −0.0079 −0.0053, −0.01, −0.0054, −0.0067]	[−0.01, −0.0086, −0.0037, −0.01, −0.0028, −0.0046]
Number of discipline evaluations	1127 (0.73%)	1758 (0.88%)	1813 (1.54%)	1675 (0.94%)

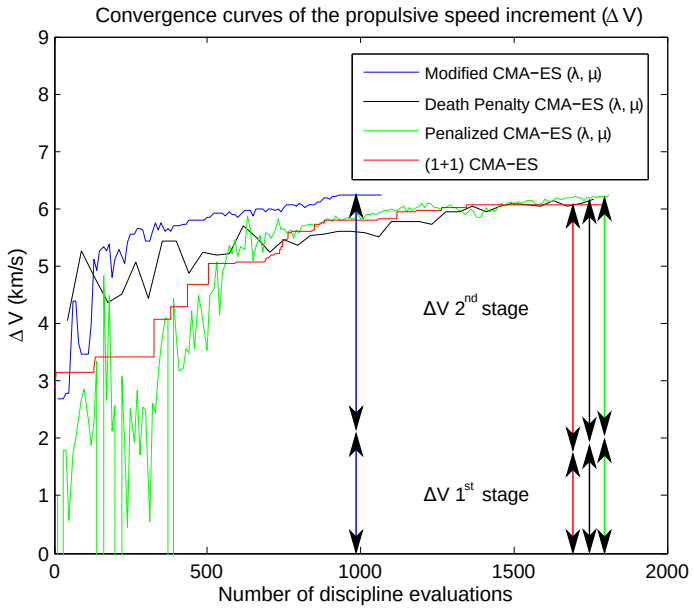

Figure 13.5: Convergence curves of the propulsive speed increment for the two stage solid propulsion rocket.

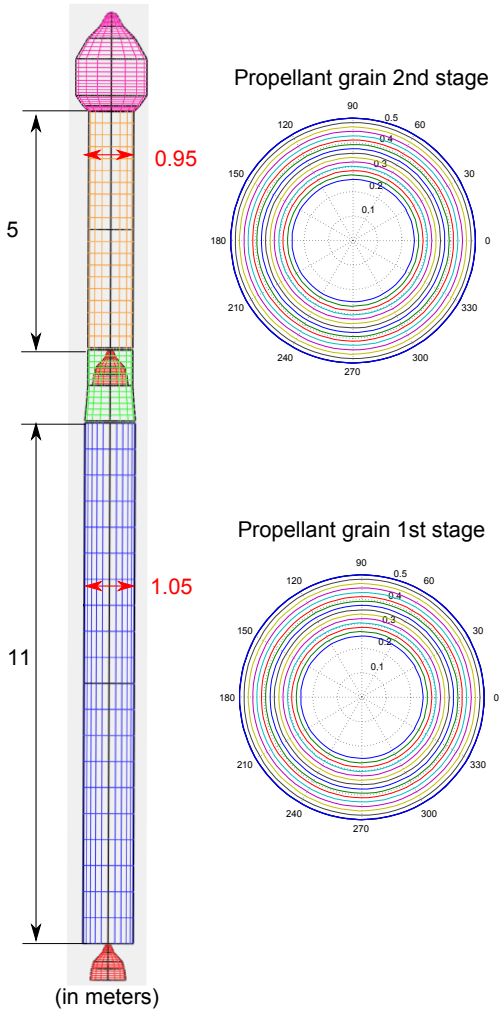

Figure 13.6: Optimal two stage booster design with modified CMA-ES(λ, μ) and solid grain propellant configuration.

13.3 Conclusion

This chapter deals with the design of a two stage solid rocket with the proposed modifications of CMA-ES(λ, μ). A multidisciplinary optimization problem is solved in the presence of uncertainty and constraints. The design problem involves four disciplines: the propulsion, the sizing and mass, the structure and the launch vehicle performance. The solving of the associated UMDO problem has been performed with the proposed modified CMA-ES(λ, μ), death penalty CMA-ES(λ, μ), penalized CMA-ES(λ, μ) and modified (1+1)-CMA-ES. A better optimum has been found with the proposed approach with respect to the existing CMA-ES based optimization algorithms resulting in a potential increase in the payload mass. The robustness of the proposed constraint handling is highlighted over the repetitions of the problem solving both in terms of objective function value and number of calls to the disciplines. However, CMA-ES may present local convergence [Hansen et al., 2003] as illustrated in the Rosenbrock, G04 and launch vehicle design problems, and the current approaches to avoid that is a restart procedure. Further investigations on local convergence issues have to be performed in order to ensure algorithm global convergence.

Modified CMA-ES(λ, μ) has been proposed in order to make robust the constraint handling approach and to avoid the existing problem dependent methods. The proposed approach does not dependent on the type of problem to be solved, it only modifies the covariance matrix update mechanism in order to take into account the constraint violations by the candidates. This approach is interesting for the optimization of complex system which may present local minima and nonlinear dynamics with a non-gradient-based algorithm. In practice, CMA-ES requires a large number of function evaluation ($> 10^3$) compared to gradient-based algorithms but its robustness to the presence of uncertainty make this algorithm interesting to solve UMDO problems in the early design phases when the disciplines involve low fidelity analysis models. Moreover, CMA-ES has been extended in order to include discrete variable handling which is an interesting capability in the context of launch vehicle design. Indeed, in the proposed test cases, design variables such as number of stages, number of boosters, number of engines *etc.* have been fixed *a priori* but further investigations to include the control of this type of variable in a MDO framework is primordial to discriminate launch vehicles with different architectures.

- Context:
  - Constrained optimization problem solving in the presence of uncertainty,
  - Covariance Matrix Adaptation - Evolutionary Strategy (CMA-ES),
  - State-of-the-art methods are problem dependent techniques.
- Contributions:
  - Development of a new update mechanism of the covariance matrix used to generate the candidate population to take into account the presence of the constraints,
  - Application and comparison of the proposed approach on three analytical test cases, highlighting its efficiency solve constrained optimization problems in the presence of uncertainty,
  - Application and comparison on a launch vehicle design problem emphasizing its robustness in solving constrained UMDO problems.
- Actionable information:
  - Useful for constrained UMDO problem solving which present local minima and non-linear dynamics,
  - Does not require problem dependent parameter setting,
  - Might be extended to handle discrete variables for MDO problems.
- Perspectives:
  - Develop a method to avoid CMA-ES local convergence,
  - Compare to other UMDO optimization algorithms such as Multi-Agents Systems [Jaeger et al., 2015] or stochastic gradient [Andrieu et al., 2007].
  - Extend the approach to problems involving mixed continuous and discrete variables.

Conclusion and perspectives

This thesis is focused on the development of methodologies for Multidisciplinary Design Analysis and Optimization in the presence of uncertainty enabling the design of complex systems such as launch vehicles at the early design phases. The contributions of this work are related to three important topics in UMDO.

13.4 Interdisciplinary coupling

Firstly, the thesis focused on interdisciplinary coupling satisfaction in the presence of uncertainty. From the analysis of the different existing UMDO formulations and their handling of interdisciplinary couplings, a new approach has been proposed. The method allows to decouple the disciplines in order to avoid computationally expensive MDA at each iteration while ensuring multidisciplinary feasibility for the optimal systems for all the simulated realizations of the uncertain variables (corresponding to uncertain events). To this end, a surrogate model-based method has been developed. The metamodels represent at the convergence of the UMDO process, the functional relationships between the disciplines as would do MultiDisciplinary Analysis (MDA) under uncertainty. This approach enables decomposition strategies for the design process. Based on this technique, two UMDO formulations have been proposed. The first one is a single-level UMDO formulation derived from Individual Discipline Feasible (IDF) formulation named IDF-PCE. Polynomial Chaos Expansions (PCE) of the interdisciplinary coupling mappings are built all along the system-level optimization. The PCE coefficients are controlled by the system-level optimizer in addition with the design variables characterizing the system architecture. The coupling constraints are expressed through an integral form and are added to the system-level optimization problem in order to guarantee multidisciplinary feasibility for all the simulated realizations of the uncertain variables for the optimal system at the UMDO process convergence. Three techniques (Crude Monte Carlo, quadrature, PCE) have been proposed to estimate the multidimensional interdisciplinary coupling constraints. The proposed approaches transform the original complex infinite-dimensional problem into a finite-dimensional problem while ensuring a numerically equivalence in terms of coupling satisfaction between coupled and decoupled design strategies.
The second proposed formulation is a multi-level UMDO approach derived from the Stage-Wise decomposition for Optimal Rocket Design (SWORD) exploiting a transverse decomposition of the design process of launch vehicles according to the different flight phases instead of the classical disciplinary decomposition according to the disciplines. The proposed method named Multi-level Hierarchical Optimization under Uncertainty (MHOU) is a semi-decoupled hierarchical method that removes all the feedback interdisciplinary couplings in order to avoid expensive disciplinary loops

through MDA. The formulation relies on two levels of optimization and the surrogate model-based technique to ensure the multidisciplinary feasibility at the convergence of the UMDO processes. These two formulations have been tested and compared with MDF on an analytical test case and on two launch vehicle design problems. These test cases illustrated the efficiency of the proposed approach (especially MHOU) compared to MDF for the design of launch vehicles. Moreover, they highlighted the benefit of taking account uncertainty at the early design phases in order to ensure the robustness and reliability of the optimal launch vehicles with respect to uncertain events. Nevertheless, these studies have shown that the use of decoupled design strategies in the presence of uncertainty make the solving of the optimization problem more complex compared to deterministic decoupled MDO strategies.
These approaches are useful for designing a complex system with a decomposed design process involving engineering teams of different fields. In practice, industrial companies are organized according to the different competence (propulsion, aerodynamics, *etc.*) which are sometimes even not at the same location. Decomposed design procedure allows to offer engineering team autonomy while ensuring system design consistency at the end of the design process. One of the main constraints in terms of system design consistency is the interdisciplinary coupling satisfaction which guarantees that the different teams performed analyses with the same shared characteristics (diameters, thrusts, pressures, temperatures, *etc.*). The proposed approaches maintain the system design consistency in the presence of uncertainty which is a novelty compared to the state-of-the-art methods.

13.5 Reliability analysis

Secondly, the thesis focused on reliability analysis in the presence of mixed aleatory and epistemic uncertainties. From the analysis of the different existing reliability analysis methods in the presence of mixed aleatory and epistemic uncertainties, two new reliability assessment techniques have been proposed. In the early design phases, in addition to the aleatory uncertainty modeled with the probability formalism, epistemic uncertainty is present due to lack of knowledge, simplification hypotheses and low fidelity simulation models. Epistemic uncertainty is often modeled with interval formalism. Two types of problems have been considered: epistemic uncertainty on the hyper-parameters of the PDF defining the aleatory uncertainty and epistemic uncertainty directly affecting the system failure limit state function.
The proposed method to solve the first problem combines Importance Sampling (IS) using Cross Entropy (CE) with an adaptive Kriging model used to replace the expensive limit state function, and an optimization algorithm (CMA-ES) aiming at determining the bounds of the probability of failure. This approach allows to handle rare event probability calculations and possible non linear limit state. Moreover, CE algorithm has been modified in order to accelerate the calculation of a probability of failure for a new epistemic uncertain variable value based on a previous calculation. Furthermore, a dedicated refinement strategy of the Kriging model has been used in order to ensure an accurate estimation of the probability bounds and the precision of the Kriging model in high probability content regions around the failure threshold.
The proposed methodology to solve the second problem is based on an iterative sequential loop which combines Subset Simulation with an adaptive Kriging model and an optimization algorithm. The first step of the process involves an interval analysis including the probability estimation using the Kriging model of the limit state function. The second step consists of a refinement strategy for

the metamodel adapted to the presence of epistemic uncertainty. The refinement strategy ensures the accuracy of the Kriging model in the regions of high probability content around the failure threshold and around the epistemic variable values leading to the probability bounds. In order to determine the bounds of the failure probability with a gradient-based algorithm, an approach has been developed to compute the sensitivity of the probability of failure with respect to the epistemic variables that directly affect the limit state function. An analytical derivation based on the properties of the indicator function has been proposed. Estimators for the sensitivity using Crude Monte Carlo and Subset Simulation have been derived in addition to the numerical implementation.
The developed reliability analysis methods have been tested and compared to reference approaches on analytical test cases and on launch vehicle analysis problems. During the design of a launch vehicle, constraints have to be imposed during the trajectory optimization to ensure the stage fallout in safe conditions in an adequate zone. The launch vehicle analysis problem consists in estimating the probability that a stage falls at a distance greater than a given safety margin to a nominal impact point. Both the analytical test cases and the launch vehicle problems have illustrated the efficiency of the proposed techniques compared to the existing methods. However, due to the complexity of the proposed approach and the induced computational cost, a direct implementation in a design problem such as in a UMDO process requires further investigations.
Reliability analysis is an essential study to be performed during the design of a new system. The result of reliability analysis directly depends on the modeling of input aleatory uncertainty and the limit state function. In practice, at the early design phases, the uncertainty modeling and the limit state function suffer from epistemic uncertainty, industrial companies have difficulties in getting, aggregating and analyzing uncertainties in order to use these data for future system design. Therefore, the knowledge about uncertainty is often limited and taking into account these limitations is essential in order to accurately assess the probability of failure of the system. The proposed approaches are useful for this type of problem because they allows to account for that potential lack of knowledge into the failure probability estimation and therefore make the calculation only based on the known information.

13.6 Optimization with evolutionary strategy

Thirdly, the thesis focused on evolutionary strategy optimization algorithms (and more particularly CMA-ES) in the presence of constraints and uncertainty. An UMDO problem requires to solve a constrained optimization problem in the presence of uncertainty. The analysis of the different existing optimization algorithms adapted to UMDO problems outlined the efficiency of CMA-ES but also its difficulties to handle constraints. The classical techniques based on penalization require fine tuning and are problem dependent. A new method modifying the mechanism used to generate the population of candidates has been proposed in order to account for the presence of constraints. The proposed technique modifies the update mechanism of the covariance matrix in order to take into account the violation of the constraints and to reduce the search hypervolume in the directions where unfeasible candidates have been found. The proposed approach has been tested and compared to reference methods on three analytical optimization problems and one launch vehicle design problem highlighting the efficiency of the new algorithm compared to the classical constraint handling techniques for CMA-ES.
The efficiency of solving of UMDO problems directly results from the optimizer algorithm capability

to converge quickly to an optimum. In practice, the presence of uncertainty and constraints make more complex the optimization solving and deterministic algorithms are not adapted to these problems. The proposed approach is useful to solve constrained UMDO problems without requiring tuning of problem dependent parameters. The state-of-the-art CMA-ES techniques are problem dependent and the proposed methods modify the covariance matrix update mechanism which is independent of the type of problem solved.

13.7 Perspectives

In order to further improve the proposed UMDO methods presented in this thesis, some extensions may be proposed. In this thesis, contributions in terms of problem formulation and coupling handling, in terms of reliability analysis and in terms of optimization algorithms dedicated to UMDO have been proposed. An important extension could be to combine all the developed methods into a new UMDO process. It would be interesting to design a new launch vehicle with a decomposition strategy and to incorporate stage fallout constraint estimation with the developed techniques while using the modified CMA-ES. However, the computational cost would make the solving of this design problem difficult. Further improvements are required to mature UMDO methodologies:

Interdisciplinary coupling satisfaction
In this thesis, no MultiDisciplinary Analysis has been performed in the proposed decomposition design strategies. However, the developed method to handle interdisciplinary couplings has shown limitations in the case of the increase of the number of uncertain variables. An hybrid formulation propagating uncertainties with a decoupled approach while authorizing MDA to ensure multidisciplinary feasibility could be an intermediate solution between coupled and decoupled strategies. The propagation of uncertainty would allow to evaluate the disciplines in parallel. It would allow to avoid expensive discipline loops during uncertainty propagation. Moreover, MDA would be used to ensure multidisciplinary feasibility as some semi-decoupled approaches do for deterministic MDO (for instance CSSO or BLISS). Moreover, in this thesis, IDF-PCE and MHOU formulations only manage uncertainty that is modeled with the probability formalism. An extension of the proposed UMDO to other uncertain formalisms such as Evidence theory or Possibility theory would be very interesting but requires an adequate handling of interdisciplinary couplings which has to be developed. Moreover, a comparison of UMDO methods and results with safety factor-based approaches could be interesting to either re-set the value of the safety factors or to confirm the historical choices.

Reliability analysis
Additionally, improvements of the proposed reliability analysis methods to further reduce their computational costs could be interesting in order to incorporate them in UMDO formulations. The proposed methods are able to handle low dimensional problems, but it would be valuable to improve the techniques for high dimensional problems. The main difficulties are due to the surrogate models which present accuracy and computational cost issues in high dimensions. More adapted surrogate models such as Support Vector Regression could be investigated for high dimensional problems. Performing sensitivity analysis of the probability of failure could also be an interesting way of improvement in order to determine the most influential parameters for the probability of failure and to decrease the problem dimension by fixing the non influential ones. Moreover, a work on

uncertainty modeling to find the most appropriate formalism among the existing ones based on the available information for each uncertain parameters could be interesting to improve the fidelity of the reliability analysis results with respect to the uncertainty information knowledge.

Optimization algorithms

Finally, the proposed UMDO formulations have been tested on the design of classical launch vehicles involving only continuous design variables. It would be very interesting to incorporate the handling of discrete variables (such as the number of boosters, the number of stages, *etc.*) and categorical variables (the type of propellant solid, liquid or hybrid, the type of material, *etc.*). Moreover, developing some optimization techniques to handle variable-size design space problems would be very beneficial within the context of launch vehicle design. It would allow to extend the types of launch vehicle architecture studied by allowing the introduction of new design variables and constraints during the optimization process and therefore enhance the decision maker choice. Moreover, only single objective problems have been treated in this thesis. It would be interesting to extend the proposed methods to multi-objective problems (for instance minimization of the launch vehicle cost while maximizing the payload mass). This would offer the possibility to design a family of launch vehicles dedicated to different missions (low Earth orbit, Geostationary Transfer Orbit, *etc.*). Eventually, integrating multi-fidelity approaches in order to control and reduce the impact of epistemic uncertainty in the optimization process could be investigated within the context of UMDO.

Appendices

Chapter 14

Appendix A - Dry mass sizing module

The dry mass module aims at estimating the mass of the different parts of the launch vehicle to calculate the Gross Lift-Off Weight (GLOW). All the mass models used in this thesis are derived from engineering models for the conceptual design of launch vehicles developed by Castellini [Castellini, 2012].
Three inputs from other disciplines are required to compute the GLOW:

- Propulsion outputs: thrust, specific impulse, solid propellant grain geometry, chamber pressure, *etc.*
- Sizing outputs: geometry of all the different parts of the launch vehicle (tank volume, stage length, launcher surface, engine size, *etc.*)
- Trajectory outputs: the maximal axial load subjected by the launch vehicle during the flight.

Figure 14.1 presents the mass tree of all the involved components to compute the launch vehicle GLOW. In the following, only the input variables and the parameters of the launch vehicle main components are given. For the detailed engineering models please refer to [Castellini, 2012].

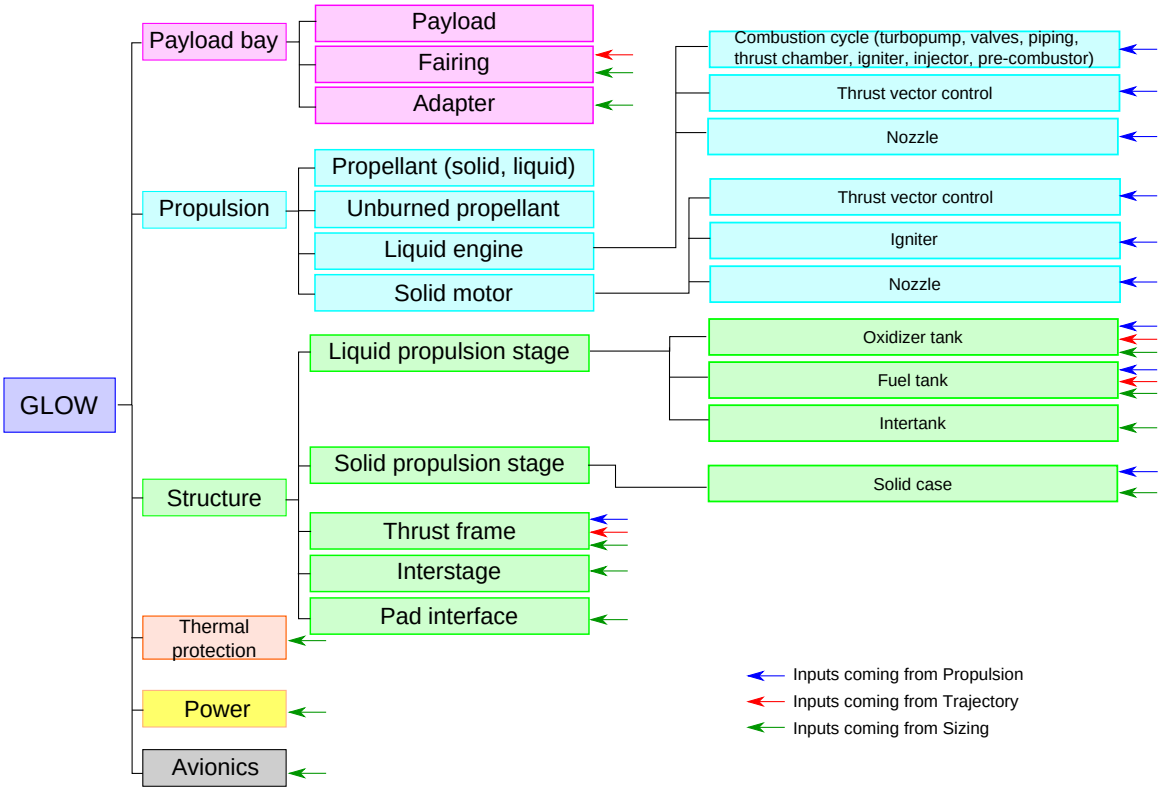

Figure 14.1: GLOW computations with all the involved components

14.1 Liquid propulsion system masses

For a liquid propellant stage, the dry mass of the stage is the sum of the following elements:

- tanks,
- liquid engine (turbo-pumps, valves, piping, thrust chamber, igniter, pressuring systems, injector, pre-combustor, *etc.*) depending on the type of engine cycle,
- thrust vector control,
- intertank (if no common bulkhead),
- thrust frame,
- nozzle,

All the models are detailed in [Castellini, 2012], only the different module and parameters are given in the following.

14.1.1 Tanks

- Selected material: Aluminum alloy (density $\rho = 2800kg.m^{-3}$, ultimate strength $\sigma_r = 400MPa$),

- Structural safety margin: 1.25,

- Propellant densities: $\rho_{LOx} = 1141kg.m^{-3}$, $\rho_{LH2} = 71kg.m^{-3}$.

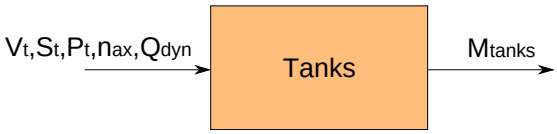

Figure 14.2: Tank mass module

Table 14.3: Tank mass input variables.

Symbol	Input variables
V_t	Propellant volume (m^3)
S_t	Tank surface (m^2)
P_t	Tank pressure (bar)
n_{ax}	Maximal axial load (m^2/s)
Q_{dyn}	Maximal dynamic pressure (Pa)

Unused propellants are considered for several reasons: propellant trapped in pipes, valves, wetting tank walls (linear model from 0.8%-0.4% for 0 to 500t of propellants) unbalance in mixture ratio, cryogenics boil-off, and due to propellant flight reserves. According to [Castellini, 2012] the propellant flight reserves are in the order of 0.5% for lower stages and 1.5% for upper stages. These flight reserves may be consumed in the presence of uncertainty to try to inject the payload into the appropriate orbit.

14.1.2 Liquid engine

In the liquid engine mass depending on the cycle type, the following elements are included:

- Stage combustion:
  - Pre-combustors
  - Turbopumps
  - Valves and piping
  - Injector and igniter
  - Thrust chamber

- Expander cycle:
  - Turbopumps
  - Valves and piping
  - Injector and igniter
  - Thrust chamber
- Gas generator:
  - Gas generators
  - Turbopumps
  - Valves and piping
  - Injector and igniter
  - Thrust chamber

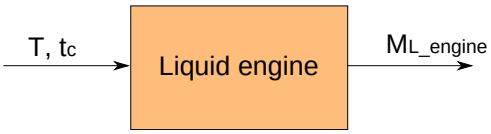

Figure 14.4: Liquid engine module

Table 14.5: Liquid input variables.

Symbol	Input variables
T	Thrust (N)
t_c	Type of cycle

The liquid engine mass models are based on mass regressions from more than 30 existing engines (for instance Vulain-2, Merlin-1C, SSME, RD-180, Vinci, HM-7B, *etc.*) of different cycle types and different couples of propellants (cryo-storable, cryo-cryo, storable-storable).

14.1.3 Thrust vector control

Two possible types of thrust vector control are considered: either hydraulic actuation or electro-mechanic actuation system. In both type, the thrust vector control mass may be approximated considering a function of the vacuum thrust of the engine. The thrust vector control models are applicable to both liquid and solid propellant stages.

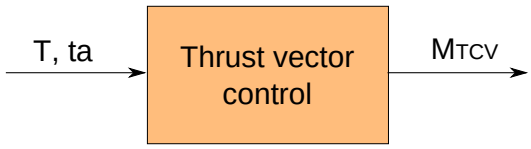

Figure 14.6: Liquid engine module

Table 14.7: Thrust vector control variables.

Symbol	Input variables
T	Thrust (N)
t_a	Type of actuation

14.1.4 Intertank

If the oxidizer and the fuel tanks do not have a common bulkhead, the following model is used for the intertank mass:

Figure 14.8: Intertank module

Table 14.9: Intertank variables.

Symbol	Input variables
D	Stage diameter (m)
S	Lateral surface (m^2)
t_i	Type of intertank

Depending if the intertank is for a lower or an upper stage, a different mass model is used. An identical model (with different coefficients) is used for interstage and pad interface mass calculation.

14.1.5 Thrust frame

The thrust frame structure is the structure where the liquid engine is fixed.

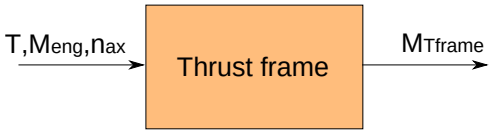

Figure 14.10: Thrust frame module

Table 14.11: Thrust frame variables.

Symbol	Input variables
T	Engine thrust (N)
$M_{L-engine}$	Engine mass (kg)
n_{ax}	Maximal axial load (m^2/s)

14.1.6 Nozzle

A conical nozzle with a constant thickness is considered in the model used. The half angle is fixed to a value of 15°. Nickel-based materials are used for the nozzle with a density of $8000kg.m^{-3}$ and the ultimate strength of $\sigma_r = 310MPa$.

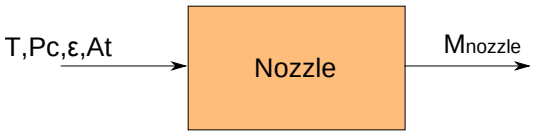

Figure 14.12: Nozzle module

Table 14.13: Nozzle variables.

Symbol	Input variables
T	Engine thrust (N)
P_c	Chamber pressure (bar)
ϵ	Nozzle expansion ratio
A_t	Throat area (m^2)

This model is also developed in [Humble et al., 1995].

14.2 Solid motor

The main differences with the liquid propulsion stage is the motor case and the igniter module. Spherical domes for the solid grain are assumed for the solid case. Moreover, another important difference comes from the fact that the main structural mass of solid propellant stage is determined by the chamber pressure and no couplings is taken into consideration with the trajectory through flight loads. In the used models, these loads are neglected, implying that compression stresses may be sustained by the solid case which is sized by the chamber pressure.

14.2.1 Solid case

The Al-7075 alloy ($\rho = 2730 kg.m^{-3}$, $\sigma_r = 505 MPa$) is used for the solid case material.

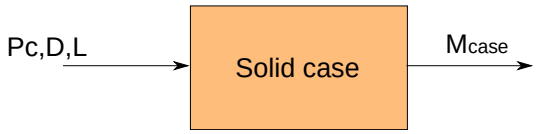

Figure 14.14: Solid case module

Table 14.15: Solid case variables.

Symbol	Input variables
P_c	Chamber pressure (bar)
D	Solid case diameter (m)
L	Solid case length (m)

14.2.2 Igniter

The igniter mass is a function of the cavity volume inside the solid case with the grain propellant. The mass of the igniter is given by [Castellini, 2012]:

$$M_{igniter} = 20.62 V_{cav}^{0.7368}$$

This model is derived from available data for Solid Rocket Motor of Ariane 5 and Vega launchers.

14.3 Launch vehicle

Finally several components such as avionics or Electrical Power Systems (EPS) mass estimation are based on the surface of the whole launch vehicle S_{tot} [Castellini, 2012]:

$$M_{avionics} = K_{RL} \times 0.25 \times (246.76 + 1.3183 \times S_{tot})$$

and

$$M_{EPS} = K_{RL} \times 0.82 \times M_{avionics}$$

where K_{RL} accounts for the redundancy level in the avionics systems: no redundancy ($K_{RL} = 0.7$), critical components only ($K_{RL} = 1.0$) or fully redundant ($K_{RL} = 1.3$).

Chapter 15

Appendix B - Propulsion module

15.1 Liquid propulsion

The liquid propulsion discipline is based on Chemical Equilibrium with Applications (CEA) which is a thermochemical simulation software developed by NASA [Gordon and McBride, 1996]. In particular, CEA has a rocket mode to simulate the combustion of gas in a combustion chamber and the gas expansion in a nozzle. CEA computes chemical equilibrium compositions and properties of complex mixtures such as in rocket combustion. It includes databases of more than 2000 species with their transport and thermodynamic properties. The conditions for chemical reaction equilibrium are stated in terms of minimization of Gibbs or Helmholtz energy or the maximization of the entropy. In the different test cases, temperature and pressure are used to characterize the thermodynamics state therefore, Gibbs energy is minimized as temperature and pressure are its natural variables. The condition for chemical equilibrium is the minimization of free energy since each species may be treated independently without specification of a set of reaction *a priori*. The system of equations to solve the equilibrium and to obtain the chemical composition are non linear and iterative methods (such as descent Newton-Raphson algorithm) are used.
CEA involves theoretical performance of rocket engine calculations adapted to conceptual and preliminary design phases and the following assumptions are made:

- Ideal gas and homogeneous mixture without interactions between the species,
- Isentropic expansion in the nozzle,
- Adiabatic and complete combustion,
- Zero velocity at the combustion chamber entrance,
- Constant area of the cross section in the combustion chamber,
- Non isentropic, irreversible combustion process,
- Finite Area Combustor or Infinite Area Combustor.

CEA simulation requires three inputs to compute the characteristics of the liquid rocket engine (Table 15.1):

- Chamber pressure P_c,
- Nozzle expansion ratio $\epsilon = \frac{A_e}{A_t}$, the ratio between the nozzle exit area and the nozzle throat area,
- Mixture ratio $O/F = \frac{q_{ox}}{q_f}$, the ratio between the mass flow rate of the oxidizer and the mass flow rate of the fuel.

Table 15.1: CEA Input variables.

Symbol	Input variables
P_c	Chamber pressure (bar)
ϵ	Nozzle expansion ratio
O/F	Mixture ratio

Moreover, to simulate the gas combustion in the chamber and its expansion in the nozzle, CEA takes as input several parameters:

- Storage temperature of the propellants,
- Reactant chemical composition,
- Frozen composition expansion or shifting chemical equilibrium through the nozzle.

The outputs of CEA simulations enable to compute several rocket engine characteristics:

- Characteristic velocity $c^* = \frac{P_c A_t}{q}$ with q the mass flow rate at the throat area,
- Thrust coefficient $c_\tau = \frac{T}{P_c A_t}$ with T the nominal thrust,
- Specific impulse $I_{sp} = \frac{c^* c_\tau}{g_0}$,
- Nozzle exhaust gas specific heats ratio γ_e, gas temperature T_e, pressure P_e.

From the following outputs, the rocket engine thrust may be easily derived. To correct the theoretical results provided by CEA, efficiency factors are considered: η_{comb} the combustion efficiency and η_{noz} the nozzle efficiency. Typical values for these efficiencies may be found in [Castellini, 2012].

15.2 Solid propulsion

For solid rocket motor, the propellant display in the motor case has an impact on all the macroscopic characteristics of the motor (specific impulse, thrust, chamber pressure *etc.*). Therefore, dedicated models have to be developed to set up the geometry of the solid grain section. Thomas Coquet (Onera), based on the work of [Ricciardi, 1989] and [Hartfield et al., 2003], developed a grain geometry analysis model coupled with CEA to compute the solid motor characteristics based on several parameters. A large number of configurations for the grain geometry are available (Fig. 15.2).

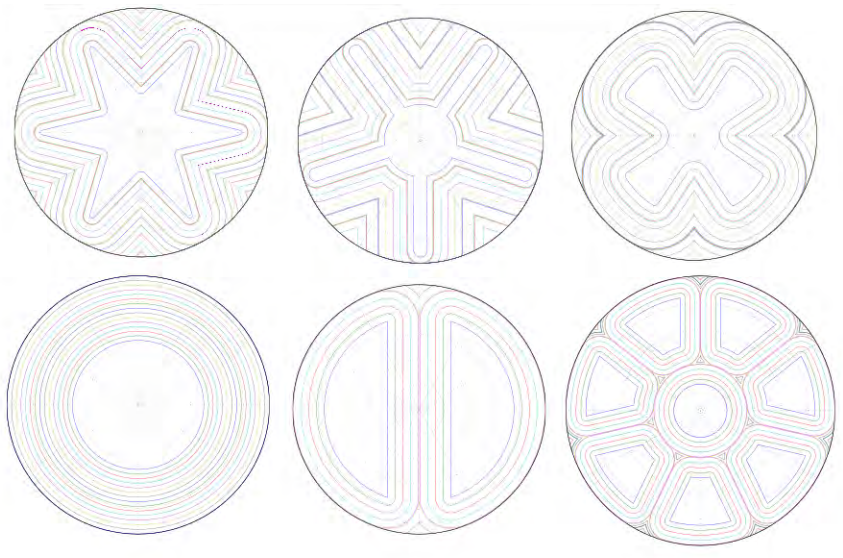

Figure 15.2: Curves of iso-combustion depth for different grain configurations

In practice, two classical configurations have been used in the thesis, the cylindrical and the star grain configurations (Figs. 15.3,15.4).

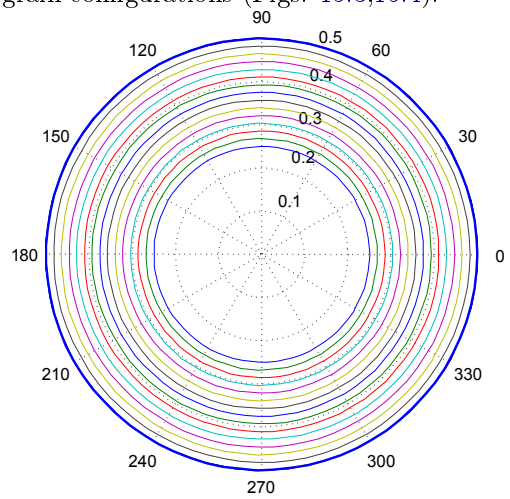

Figure 15.3: Curves of iso-combustion depth for the circle grain

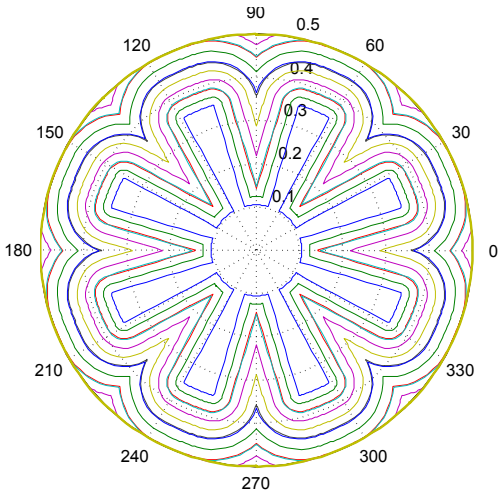

Figure 15.4: Curves of iso-combustion depth for the star grain

A general star model has been developed by A. Ricciardi [Ricciardi, 1989] and modified by T. Coquet. Seven parameters are required to define the star geometry (Table 15.5).
The half branch of the star is divided into 14 zones depending on the depth of combustion and

Table 15.5: Grain geometry parameters.

Symbol	Variables ad parameters
R	grain radius (m)
W_c	depth of combustion (m)
N	number of branch
r_1	radius of curvature superior (m)
r_2	radius of curvature inferior (m)
ξ	angle for non circular part (rad)
η	half angle between the branch (rad)

the initial parameters. Then, a series of zone configurations are defined depending on the initial parameters of the star. For instance, in Figure 15.6 the different zones associated to this particular configuration are illustrated: zone 10, 13 14 and 4.

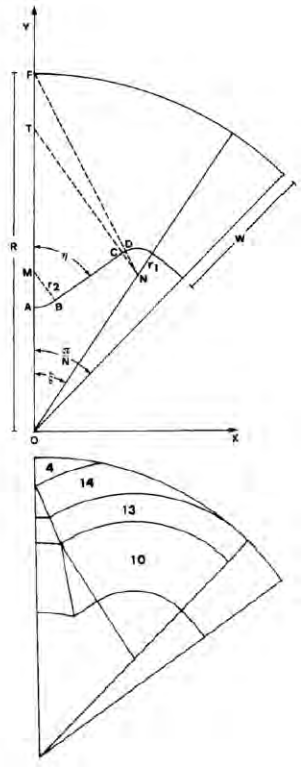

Figure 15.6: Example of star geometry configuration

To simulate the solid propellant combustion, two assumptions are used in addition to the CEA

hypotheses:

- Stationary regime, no propellant accumulation in the combustion chamber,
- 2D model.

Table 15.7: Solid propellant combustion variables.

Symbol	Variables
η_{comb}	combustion efficiency
η_{noz}	nozzle efficiency
A_t	throat area (m^2)
W_c	depth of combustion (m)
v_r	regression rate (m/s)
P_c	chamber pressure (bar)
m	propellant mass (m)
c^*	characteristic exhaust velocity (m/s)
c_τ	thrust coefficient
A_b	burn area (m^2)
M_e	Mach nozzle exit
$v_{r0,th}$	throat erosion velocity (m/s)
P_e	nozzle exit pressure (bar)
γ	ratio of specific heats
ϵ	nozzle expansion ratio
a	burn rate coefficient (cm/s)
n	burn rate exponent

The parameters involved in the modeling of the solid propellant combustion are summarized in Table 15.7. The differential system of equations modeling the combustion dynamics of the solid propellant grain is discretized according to a first order Euler method. The following system of differential equations models the propellant combustion:

$$\frac{dW_c}{dt} = v_r \tag{15.1}$$

$$\frac{dm}{dt} = -\rho A_b v_r \tag{15.2}$$

$$\frac{dA_t}{dt} = -2\sqrt{\pi A_t}\left(v_{r0,th}\sqrt{\frac{A_{t,i}}{A_t}}\right)^{0.2}\left(\frac{P_c}{P_{c,i}}\right)^{0.8} \tag{15.3}$$

$$\tag{15.4}$$

Some parameters are interpolated from CEA simulation results:

$$c^* = \eta_{comb} c^*_{CEA}(P_c) \tag{15.5}$$

$$\gamma = \gamma_{CEA}(P_c) \tag{15.6}$$

$$\tag{15.7}$$

Moreover, the following relations are used:

$$P_c = \left(\frac{a\rho c^* A_b}{A_t}\right)^{\frac{1}{1-n}} \tag{15.8}$$

$$v_r = aP_c^n \tag{15.9}$$

$$\epsilon = \epsilon_i \frac{A_{t,i}}{A_t} \tag{15.10}$$

$$\tag{15.11}$$

If we note P_b the perimeter of the combustion area and A_p the port area, we have the following relation:

$$P_b = \frac{dA_p}{dW_c}$$

Eventually, the output characteristics of the solid motor are interpolated from CEA simulation results:

$$c_\tau = c_{\tau CEA}(P_c, \epsilon) \tag{15.12}$$

$$P_e = P_{eCEA}(P_c, \epsilon) \tag{15.13}$$

$$M_e = M_{eCEA}(P_c, \epsilon) \tag{15.14}$$

$$Isp = IspCEA(P_c, \epsilon) \tag{15.15}$$

$$\tag{15.16}$$

The solid propellant used the different solid motor test cases is the TP-H-3340 constituted of 18% of Aluminum, 71% of Ammonium Perchlorate (AP) and 11% of Hydroxyl-terminated Polybutadiene (HTPB).

Chapter 16

Appendix C - Aerodynamics module

The aerodynamics module involves Missile DATCOM [Blake, 1998] developed for the USAF by McDonnell Douglas. Missile DATCOM is a preliminary design and analysis computer program of missile and launch vehicle aerodynamics based on their geometry and flight conditions. It is based on analytical and semi-empirical methods encompassing a wide range of geometries, configurations and flight conditions. Missile DATCOM is used to compute the aerodynamics coefficients (drag C_D and lift C_L coefficients) for different launch vehicle geometries and different Mach and angle of attack conditions. Three inputs are required to compute the aerodynamics coefficients by Missile DATCOM:

- A vector of Mach and angle of attack values. These values are used in the trajectory discipline to interpolate the aerodynamics coefficients. During the ODE integration, from the current position and velocity of the launcher, the aerodynamics coefficients are interpolated from the Missile DATCOM simulations in order to estimate the aerodynamics forces.
- Boundary layer information, which is assumed to be turbulent with a Roughness Height Rating of 250 commonly used in aerospace surfaces [Castellini, 2012].
- The geometry of the axi-symetric launch vehicle.

Missile DATCOM presents some limitations for launch vehicles with boosters [Castellini, 2012]. All the considered launch vehicles in this thesis are without boosters. Missile DATCOM validation has been performed on Ariane 5 and Vega launch vehicle. In the following, the geometry (Fig. 16.1) and the drag coefficient (16.2) for Vega are provided and compared to an actual profile given in [Castellini, 2012] with an angle of attack of 0°.

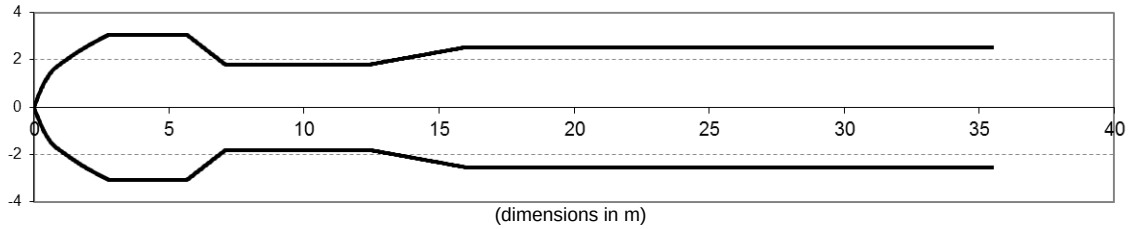

Figure 16.1: Geometry of Vega launch vehicle

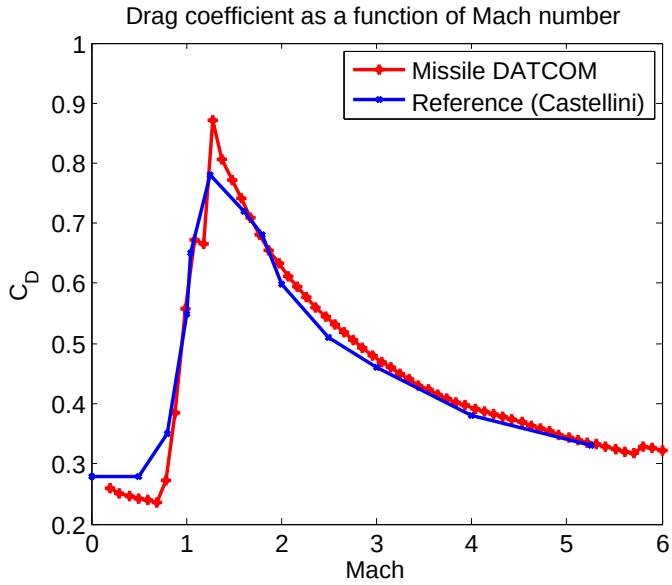

Figure 16.2: Reference [Castellini, 2012] and Missile DATCOM drag coefficients for Vega launch vehicle

Chapter 17

Appendix D - Trajectory module

The trajectory model used in this thesis are derived from a three dimensional model with rotating round Earth (radius 6371km). The trajectory model used the following 3D dynamics equations, written in an Earth-centered, rotating Earth referential.

$$\dot{r} = V\sin(\gamma) \tag{17.1}$$

$$\dot{V} = \frac{T\cos(\theta-\gamma)-D}{m} - g(r)\sin(\gamma) + \omega_E^2 r\cos(\phi)(\sin(\gamma)\cos(\phi) - \cos(\gamma)\sin(\phi)\cos(\psi)) \tag{17.2}$$

$$\dot{\gamma} = \frac{[L+T\sin(\theta-\gamma)]\cos(\mu)}{mV} + \left(\frac{V}{r} - \frac{g(r)}{V}\right)\cos(\gamma) + 2\omega_E\sin(\psi)\cos(\phi) + \frac{\omega_E^2 r\cos(\phi)(\cos(\gamma)\cos(\phi)+\sin(\gamma)\sin(\phi)\cos(\psi))}{V} \tag{17.3}$$

$$\dot{\lambda} = \frac{V\cos(\gamma)\sin(\psi)}{r\cos(\phi)} \tag{17.4}$$

$$\dot{\phi} = \frac{V\cos(\gamma)\cos(\psi)}{r} \tag{17.5}$$

$$\dot{\psi} = \frac{[L+T\sin(\theta-\gamma)]\sin(\mu)}{mV\cos(\gamma)} + \frac{V\cos(\gamma)\sin(\psi)\tan(\phi)}{r} + 2\omega_E(\sin(\phi) - \cos(\psi)\cos(\phi)\tan(\gamma)) + \frac{\omega_E^2 r\sin(\phi)\cos(\phi)\sin(\psi)}{V\cos(\gamma)} \tag{17.6}$$

$$\dot{m} = -q \tag{17.7}$$

The sequence of the trajectory is illustrated in Figure 17.3. The sequence is composed of a vertical flight to leave the launch area protecting the installations, a pitch-over maneuver corresponding to optimum orientation of the launcher in the trajectory plane, a flight at zero incidence angle (the thrust is in the direction of the velocity, also called gravity turn phase) and a controlled exo-atmospheric flight to reach the injection orbit.
The used referential is given in Figure 17.2 and the Table 17.1 explains the notations used. The trajectory discipline consists of an optimization problem. The optimal control is performed with a direct method [Betts, 1998]. The objective of trajectory optimization is to minimize the distance

Table 17.1: Trajectory variables and parameters.

Symbol	Variables ad parameters
r	radius (m)
V	norm of the velocity vector $(m.s^{-1})$
γ	flight path angle (rad)
ϕ	latitude (rad)
λ	longitude (rad)
ψ	flight path heading (rad)
μ	bank angle (rad)
θ	pitch angle (rad)
ω_E	angular velocity of the Earth (rad/s)
T	thrust (N)
D	drag (N)
L	lift (N)
$g(r)$	gravity acceleration at r (m/s^2)
m	launch vehicle mass (kg)
q	mass flow rate (kg/s)

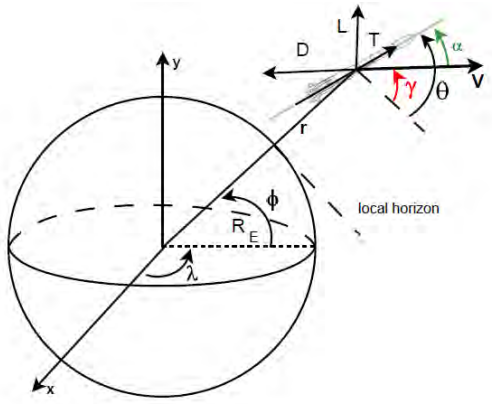

Figure 17.2: Earth-centered, Earth-fixed reference frame

between the real injection point and the given target injection point. The trajectory optimization consists to define crossing points for the pitch angle θ and to modify them to satisfy the specifications of the mission. In order to reduce the computation volume, the pitch angle is calculated by piecewise linear functions. The trajectory discipline computes the loads (axial load factor, dynamic pressure) required to simulate the mass budget and geometry design discipline. A zero lift model is used for the aerodynamics and the trajectory.

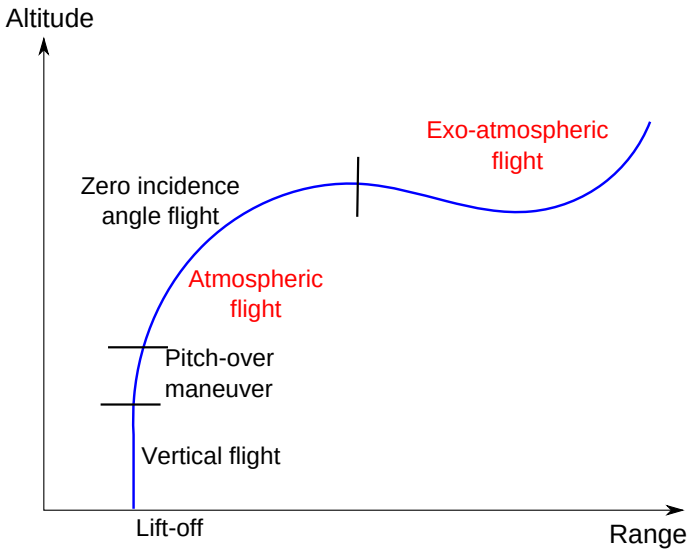

Figure 17.3: Trajectory sequence

The dynamic pressure P_{dyn} during the flight is given by:

$$P_{\text{dyn}} = \frac{1}{2}\rho(r)V^2$$

with $\rho(r)$ the air density as a function of the altitude. Using a spherical Earth, the density of the air is given by:

$$\rho(r) = \rho_0 \exp(-\frac{r - R_E}{h_{ref}})$$

with:

- $\rho_0 = 1.22557 kg.m^3$
- $h_{ref} = 7254.24m$

Moreover, the axial load factor n_f is given by:

$$n_f = \frac{g_0.q.Isp(r) - \frac{1}{2}\rho(r).S_{ref}.V^2.C_D.\cos(\theta - \gamma)}{m.g_0}$$

with:

- S_{ref}: the aerodynamic reference surface,
- C_D: the drag coefficient

Eventually, during the flight, the fairing is jetisoned when the aerothermal flux gets below $1135 W/m^2$. The aerothermal flux is determined by the following relationship:

$$\phi_A = \frac{1}{2}\rho(r)V^3$$

The ODE dynamics equations are numerically integrated with a 4^{th} order Runge Kutta solver.

For the stage fallout dynamics, in the system of differential equations, the thrust T and the mass flow rate q are both equal to zero. The orthodromic distance used to compute the distance between the nominal impact point characterized by (ϕ_N, λ_N) and the exact impact (ϕ_I, λ_I) is given by:

$$d_{orthodromic} = R_E \times \arccos(\sin(\phi_N)\sin(\phi_I) + \cos(\lambda_N)\cos(\lambda_I)\cos(\Delta_\lambda))$$

where Δ_λ is the absolute difference between the two points on Earth and R_E the Earth radius.

Chapter 18

Appendix E - Résumé étendu de la thèse

Contents

Introduction

Les lanceurs sont des éléments clés pour garantir un accès indépendant à l'espace pour de nombreux pays tels que les États-Unis, la Russie, l'Europe, *etc.* Les agences spatiales développent leurs stratégies en fonction des capacités de leurs lanceurs dans les domaines d'exploration spatiale, d'observation de la Terre ou de vols habités. La conception de lanceurs est un projet au long terme impliquant des budgets importants et un processus organisationnel complexe. Les agences spatiales telles que la NASA et l'ESA qui financent en partie de tels projets insistent sur la nécessité de réduire les coûts de développement et d'utilisation ainsi que l'importance d'améliorer les performances des lanceurs [Zeitlin et al., 2012]. Améliorer le processus de conception des systèmes aérospatiaux est essentiel pour obtenir des capacités de lancement efficaces à bas coût et à haute fiabilité. La conception d'un tel système est un processus multidisciplinaire complexe: l'objectif est de trouver l'architecture et les caractéristiques du lanceur qui fournissent une performance optimale tout en assurant ainsi un niveau minimum de fiabilité [Jaeger et al., 2013].
La conception de lanceurs implique de nombreuses disciplines et fait classiquement intervenir des modèles de propulsion, d'aérodynamique, de trajectoire, de dimensionnement, de structure, *etc.* L'évaluation de la performance d'un lanceur résulte d'une analyse couplée des disciplines qui implique de faire des compromis entre des objectifs disciplinaires antagonistes afin d'atteindre un équilibre optimal entre la fiabilité, la sécurité, le coût et la performance du système. Les approches classiques de conception de lanceurs consistent en une boucle d'optimisation disciplinaire où, à chaque itération, chaque discipline est ré-optimisée à partir des nouvelles données fournies par les disciplines optimisées précédemment. Cependant, en raison de possibles objectifs disciplinaires antagonistes, il est difficile de rechercher des compromis entre ces disciplines. Par exemple, la discipline aérodynamique va chercher à diminuer la trainée lors du vol endo-atmosphérique en diminuant le diamètre de l'étage, alors que la discipline structure va chercher à augmenter ce diamètre pour des raisons de stabilité et de résistance aux efforts.
En conséquence, la conception de lanceurs requiert des méthodologies dédiées pour gérer la complexité du problème à résoudre. L'optimisation multidisciplinaire (MDO pour Multidisciplinary Design Optimization) est un domaine de recherche visant à développer des méthodologies d'ingénierie de conception dédiées à la résolution de problèmes multidisciplinaires complexes [Sobieszczanski-Sobieski and Haftka, 1997]. La MDO gère le problème de conception dans son intégralité en incluant la gestion des interactions entre les disciplines contrairement aux approches classiques. Les méthodes de MDO tirent avantage des synergies et des couplages entre les disciplines impliquées dans le processus de conception pour diminuer le coût de calcul et/ou améliorer la performance du système optimal [Balesdent et al., 2012a]. Cependant, la complexité des problèmes d'optimisation à résoudre se trouve significativement augmentée à cause de la gestion simultanée de toutes les disciplines. Pour maîtriser cette complexité, plusieurs formulations MDO ont été développées [Cramer et al., 1994; Balling and Sobieszczanski-Sobieski, 1996; Alexandrov, 1997; Kroo, 1997].
Dans l'industrie aérospatiale, le développement d'un nouveau système suit différentes phases de conception (phase d'avant-projet, phase préliminaire, phase détaillée, phase de fabrication). Pour un lanceur, il a été établi que la phase d'avant-projet est décisive pour le succès du processus de conception dans son ensemble et qu'au moins 80% des coûts de développement sont figés lors de cette phase. En phase d'avant-projet, le domaine de recherche pour le lanceur optimal est étendu car peu de caractéristiques du lanceur sont figées [Zang et al., 2002]. Les approches par MDO sont intéressantes car elles permettent de gérer des espaces étendus de conception dans un environnement multidisciplinaire. Martins *et al.* [Martins and Lambe, 2013] expliquent que les

ingénieurs, en utilisant la MDO dans les phases d'avant-projet, pourraient améliorer la performance du système et diminuer le temps de développement, et ce en évitant de possibles re-conceptions durant les phases ultérieures. Lors des phases avant-projet, des modèles basse fidélité sont principalement utilisés et de nombreuses méconnaissances existent. Ces modèles basse fidélité sont employés à cause du grand nombre d'architectures du système qui doivent être évaluées pour explorer l'espace de recherche. Cette exploration requiert une simulation répétée des disciplines qui serait impossible à effectuer avec des modèles hautes fidélités pour des raisons de coût de calculs. De plus, afin d'augmenter la performance des systèmes de lancement et de diminuer leurs coûts, de nouvelles technologies (nouveaux types d'ergols comme le mélange oxygène et méthane, nouveaux moteurs réallumables) et de nouvelles architectures (réutilisabilité du premier étage des lanceurs) sont étudiées. Cependant, notamment en raison de la maturité des ces technologies et de l'utilisation de modèles basse fidélité, un haut niveau d'incertitudes est présent lors des phases d'avant-projet. Ainsi, incorporer la gestion des incertitudes en MDO en phase d'avant-projet est essentiel pour offrir les améliorations suivantes [Zang et al., 2002]:

- réduire la durée du processus de conception, les coûts de développement et les risques associés,
- augmenter la robustesse du lanceur vis-à-vis des incertitudes durant les phases de développement (*e.g.* simplification des phénomènes physiques pris en compte) et des incertitudes durant les lancements (*e.g.* rafales de vent),
- améliorer les performances du système tout en respectant les contraintes de fiabilité.

La prise en compte des incertitudes se fait souvent au travers de marges de sécurité qui peuvent mener à des systèmes très conservatifs avec des performances diminuées. L'optimisation multidisciplinaire sous incertitudes (UMDO pour Uncertainty-based Multidisciplinary Design Optimization) vise à résoudre des problèmes MDO en présence d'incertitudes. Les méthodes UMDO sont récentes et toujours en développement car elles n'ont pas encore atteint la maturité nécéssaire pour identifier le système optimal et estimer de façon efficace ses performances et sa fiabilité [Zang et al., 2002].
Incorporer la gestion des incertitudes dans les approches de MDO introduit de nombreux défis. Dans les phases d'avant-projet, être capable de concevoir un système en prenant en compte les interactions interdisciplinaires et les incertitudes est difficile en raison des coûts de calculs prohibitifs associés. Trois défis complémentaires peuvent être identifiés comme clefs pour résoudre efficacement les problèmes UMDO.

- *La gestion des couplages interdisciplinaires en présence d'incertitudes.*
  La plupart des formulations UMDO existantes sont dérivées de la formulation MultiDiscipline Feasible (MDF) et utilisent des analyses multidisciplinaires (MDA pour MultiDisciplinary Analysis) pour assurer la faisabilité multidisciplinaire. Pour garantir la cohérence multidisciplinaire du système, un système couplé d'équations doit être résolu. Les approches basées sur des MDA impliquent des boucles entre les disciplines afin d'identifier les variables de couplage satisfaisant le système d'équations. La combinaison de MDA avec la propagation d'incertitudes résulte en une explosion du coût de calcul. Pour contourner les appels répétés aux disciplines imposées par les MDA, des stratégies de décomposition du processus de conception ont été proposées [Du and Chen, 2001; Du et al., 2008; Ghosh et al., 2014] visant à évaluer en parallèle les disciplines et non de façon consécutive. Cependant, la gestion des couplages entre les disciplines pose alors problème. En effet, les approches existantes dans la littérature

[Du and Chen, 2001; Du et al., 2008; Ghosh et al., 2014] ne garantissent pas la satisfaction des couplages pour tous les événements incertains qui pourraient se produire. Elles assurent la satisfaction des couplages uniquement pour quelques instantiations particulières (par exemple au point le plus probable de défaillance). Cependant, afin de maintenir l'équivalence entre les approches classiques (dites couplées) et les approches découplées (visant à éliminer les boucles entre les disciplines) il est nécéssaire d'assurer la faisabilité multidisciplinaire quel que soit l'événement incertain qui pourrait se produire durant la conception (*e.g.* erreur de modélisation) ou l'exploitation du système (*e.g.* rafales de vent). De plus, dans la littérature, tous les processus de conception de lanceurs en présence d'incertitudes considèrent une décomposition du processus selon les disciplines impliquées telles que la propulsion, la trajectoire, l'aérodynamique, *etc.* Des stratégies de décomposition selon les étages du lanceur ont été proposées afin de résoudre des problèmes MDO déterministes [Balesdent et al., 2012a]. Cependant, ces approches n'ont pas été étendues à la présence d'incertitudes. Une décomposition par étage du processus de conception afin de résoudre des problèmes de UMDO pour les lanceurs pourrait bénéficier des mêmes avantages que l'approche déterministe. Cette approche repose sur un processus multi-niveaux pour faciliter la convergence de l'optimiseur du niveau système tout en évitant les boucles disciplinaires imposées par l'utilisation de MDA.

- *L'analyse de fiabilité pour des systèmes complexes.*
  Un autre défi important lors de la résolution d'un problème UMDO est d'assurer la fiabilité du système optimal vis-à-vis des incertitudes. L'analyse de fiabilité consiste à estimer la probabilité de défaillance du système au vu des incertitudes considérées. La probabilité de défaillance du système optimal ne doit pas dépasser un certain seuil défini par le cahier des charges. En phase d'avant-projet, deux types d'incertitudes sont existent: les incertitudes aléatoires et épistémiques [Thunnissen, 2003]. La combinaison des incertitudes aléatoires et épistemiques nécessite des méthodes d'analyse de fiabilité dédiées. La plupart des approches existantes sont basées sur Crude Monte Carlo (CMC) [Rubinstein and Kroese, 2011] ou bien sur First Order Reliability Method (FORM) [Madsen, 1986; Bjerager, 1990] qui sont facilement utilisables mais dont le champ d'utilisation est limité. En effet, FORM n'est efficace que si la fonction de défaillance est linéarisable et CMC induit des coûts de calcul prohibitifs pour des défaillances rares ($< 10^{-4}$). La détermination de zones de sureté de retombée d'étage de lanceurs est essentiel lors de leur conception et implique un problème d'analyse de fiabilité non linéarisable avec des événements rares. Ainsi, pour résoudre ce type de problème, d'autres approches sont nécessaires.

- *L'optimisation sous contraintes en présence d'incertitudes avec des approches évolutionnaires.*
  Afin de résoudre les problèmes UMDO, des algorithmes d'optimisation sont nécessaires. Ils doivent avoir au moins deux caractéristiques. Tout d'abord, ils doivent être efficaces malgré la présence d'incertitudes. Ensuite, ils doivent gérer la présence de contraintes afin d'assurer la satisfaction des spécifications du cahier des charges pour le système optimal. Les approches classiques basées sur le gradient peuvent présenter des difficultés à converger à cause des erreurs possibles sur l'estimation des gradients dues aux incertitudes. Les algorithmes basés sur des populations d'individus [Hansen et al., 2003; Jin and Branke, 2005] sont intéressants grâce à leurs capacités à gérer des environnements incertains. Cependant, la plupart de ces algorithmes utilisent des techniques de pénalisation de la fonction objectif par les contraintes qui requièrent le réglage de paramètres et qui sont dépendants du problème. Covariance Matrix Adaptation - Evolution Strategy (CMA-ES) est un algorithme évolutionnaire

qui se démarque en présence d'incertitudes comme illustré dans de nombreux parangonnages [Auger and Hansen, 2009; Hansen, 2009] mais dont la gestion des contraintes par pénalisation introduit des limitations [Collange et al., 2010a].

Cette thèse est centrée sur l'élaboration de nouvelles méthodes d'analyse et d'optimisation multidisciplinaire en présence d'incertitudes permettant la conception de systèmes complexes en phase d'avant-projet tels que des lanceurs.

Trois contributions sont à distinguer dans cette thèse.

1. Tout d'abord, deux nouvelles formulations UMDO avec satisfaction des couplages interdisciplinaires pour toutes les réalisations des variables incertaines ont été élaborées. Pour cela, une nouvelle technique basée sur un métamodèle paramétrique (polynôme du chaos) des relations de couplage, dont les paramètres sont contrôlés au niveau système par l'optimiseur a été développée. Grâce à une nouvelle contrainte de satisfaction des couplages interdisciplinaires, à la convergence du problème d'optimisation, les métamodèles représentent les relations de couplage comme le ferait une analyse multidisciplinaire, assurant donc la faisabilité multidisciplinaire. Cette technique permet la décomposition du processus de conception et ainsi l'évaluation en parallèle des disciplines. Cette approche a été utilisée pour les deux formulations UMDO proposées. La première est une formulation mono-niveau inspirée de l'Individual Discipline Feasible (IDF) et adaptée à la présence d'incertitudes. Cette approche, intitulée Individual Discipline Feasible - Polynomial Chaos Expansion (IDF-PCE) permet d'assurer la faisabilité multidisciplinaire pour le système optimal tout en utilisant une stratégie découplée au niveau du processus de conception.

   La deuxième formulation est une approche multi-niveaux inspirée de SWORD (pour Stage-Wise decomposition for Optimal Rocket Design [Balesdent et al., 2012a]) adaptée à la présence d'incertitudes et qui maintient l'équivalence mathématique avec les approches couplées en terme de faisabilité multidisciplinaire. Cette formulation intitulée Multi-Hierarchical Optimization under Uncertainty (MHOU) repose sur une optimisation multi-niveaux des disciplines et est particulièrement adaptée à la conception de lanceurs. Cette approche transforme le problème initial de conception de lanceurs en un problème plus simple au travers d'une décomposition par étages qui sont optimisés hiérarchiquement.

2. Ensuite, deux approches d'analyse de fiabilité ont été développées pour gérer la présence d'incertitudes à la fois aléatoires et épistemiques. Pour réaliser ce type d'analyse spécifique, deux approches combinant de l'échantillonnage adaptatif avec un modèle de substitution et une stratégie de raffinement ont été développées. Ces deux techniques sont différenciées par l'impact des incertitudes épistémiques. Dans le premier problème, les incertitudes épistémiques portent sur les hyper-paramètres de lois des densités de probabilité des variables aléatoires (*e.g.* la moyenne d'une variable distribuée selon une Gaussienne est seulement connue dans un intervalle). Dans le deuxième problème, les incertitudes épistémiques influencent directement l'état du système et donc l'état limite qui constitue la séparation entre le domaine de défaillance et de non défaillance. Les approches proposées utilisent un modèle par Krigeage de l'état limite afin de limiter le nombre d'évaluations de la fonction exacte et une stratégie de raffinement pour garantir une estimation précise et fiable de la probabilité

de défaillance. Par ailleurs, les méthodes d'échantillonnage adaptatif (Importance Sampling, Subset Sampling) permettent de réduire la variance de l'estimateur de la probabilité.

3. Enfin, une modification de l'algorithme CMA-ES a été développée pour gérer efficacement les contraintes dans les problèmes UMDO. Cette adaptation permet d'éviter l'utilisation de techniques fondées sur la pénalisation de la fonction objectif. Cette méthode introduit une modification des mécanismes de mise à jour de la matrice de covariance qui paramétrise une distribution Gaussienne. Cette distribution est utilisée pour la génération d'une population d'individus et sa mise à jour permet de modifier l'espace de recherche et de converger vers la solution optimale. La modification de CMA-ES permet de tenir compte de la violation des contraintes par certaines solutions candidates pour modifier la matrice de covariance afin de ne plus générer de solutions candidates dans les zones non faisables.

Pour ces trois contributions, chaque nouvelle méthode proposée est comparée aux approches de références existantes dans la littérature sur des cas tests analytiques et des applications de conception et d'analyse de lanceurs.
Le manuscrit est organisé en quatre parties.
La première partie dresse un panorama des méthodes utilisées en UMDO et leurs applications à la conception de lanceurs. Le chapitre 1 présente les concepts clefs en MDO déterministe et les principales formulations existantes pour résoudre ces problèmes. Dans le chapitre 2, plusieurs caractéristiques essentielles concernant le traitement des incertitudes sont introduites afin de poser les bases essentielles des méthodologies UMDO. Ce chapitre inclut la définition des incertitudes, les différents formalismes mathématiques existants ainsi que les méthodes de propagation d'incertitudes associées. Le chapitre 3 concerne la présentation des méthodes UMDO existantes et plus particulièrement la gestion des couplages interdisciplinaires en présence d'incertitudes. Le chapitre 4 est dévolu à la présentation des techniques d'analyse de fiabilité en présence d'incertitudes mixtes à la fois aléatoires et épistémiques. Enfin, le chapitre 5 détaille les différents algorithmes d'optimisation existants pour résoudre des problèmes UMDO sous contraintes. Au regard de cette étude de la littérature, le chapitre 5 présente quelques voies possibles d'amélioration des méthodologies UMDO existantes qui seront détaillées dans les parties II, III et IV.
La seconde partie de la thèse se concentre sur le développement et l'analyse de deux formulations d'UMDO. Le chapitre 6 présente la formulation Individual Discipline Feasible - Polynomial Chaos Expansion (IDF-PCE). Une méthode de gestion des couplages interdisciplinaires en présence d'incertitudes est introduite afin de permettre une stratégie de conception par un processus découplé pour les disciplines. Une comparaison avec l'approche MDF classiquement utilisée pour résoudre des problèmes UMDO est également réalisée pour un cas test analytique. Dans le chapitre 7, une formulation multi-niveaux nommée Multi-level Hierarchical Optimization under Uncertainty (MHOU) est introduite. Cette formulation est particulièrement adaptée aux lanceurs et décompose le processus de conception selon les étages du lanceur. Enfin, dans le chapitre 8, deux cas tests de conception de lanceurs sont réalisés pour comparer les formulations développées avec l'approche MDF.
La troisième partie de la thèse se concentre sur l'analyse de fiabilité de systèmes en présence d'incertitudes aléatoires et épistémiques. Le chapitre 9 présente une méthode d'analyse de fiabilité permettant de propager les incertitudes épistémiques affectant les hyper-paramètres de lois qui définissent les densités de probabilité des incertitudes aléatoires, à la probabilité de défaillance du système. Le chapitre 10 présente une méthode d'analyse de fiabilité en présence d'incertitudes aléatoires et épistémiques affectant directement l'état limite de défaillance. Enfin, dans le chapitre

11, les méthodes d'analyse de fiabilité développées sont testées sur deux cas tests de rentrée d'étage de lanceurs.
La dernière partie de ce manuscrit est dévolue à la modification de l'algorithme CMA-ES afin de tenir compte de la présence de contraintes dans la résolution des problèmes UMDO. Dans le chapitre 12, l'adaptation de CMA-ES pour la gestion des contraintes est présentée. Une comparaison de la méthode proposée avec des approches classiques de gestion des contraintes est également réalisée sur plusieurs cas tests analytiques. Enfin, dans le chapitre 13, la méthode proposée est comparée à des approches classiques sur un cas test de conception d'un lanceur.
Les annexes présentent les modèles disciplinaires utilisés dans les différents cas tests.

18.1 Panorama des méthodes UMDO

18.1.1 MDO déterministe

Cette section a pour but de présenter les différents concepts et méthodes utilisé en UMDO. Pour cela, les approches MDO déterministes existantes sont présentées puis dans un second temps les différences dues à la prise en compte des incertitudes en MDO seront détaillées. Ensuite, brièvement, les techniques UMDO existantes de gestion des couplages seront introduites, puis les méthodes d'analyse de fiabilité en présence d'incertitudes mixtes aléatoires et épistémiques et enfin les algorithmes d'optimisation en présence de contraintes et d'incertitudes.

La formulation générale d'un problème MDO déterministe impliquant N disciplines est la suivante [Balesdent et al., 2012b]:

$$\begin{aligned}
\min \quad & f(\mathbf{z},\mathbf{y},\mathbf{x}) && (18.1)\\
\text{p.r.à} \quad & \mathbf{z},\mathbf{y},\mathbf{x} && \\
\text{s.à} \quad & \mathbf{g}(\mathbf{z},\mathbf{y},\mathbf{x}) \leq 0 && (18.2)\\
& \mathbf{h}(\mathbf{z},\mathbf{y},\mathbf{x}) = 0 && (18.3)\\
& \forall (i,j) \in \{1,...,N\}^2 \; i \neq j, \; \mathbf{y}_{ij} = \mathbf{c}_{ij}(\mathbf{z}_i,\mathbf{y}_{.i},\mathbf{x}_i) && (18.4)\\
& \forall i \in \{1,...,N\}^2, \; \mathbf{r}_i(\mathbf{z}_i,\mathbf{y}_{.i},\mathbf{x}_i) = 0 && (18.5)\\
& \mathbf{z_{min}} \leq \mathbf{z} \leq \mathbf{z_{max}} && (18.6)
\end{aligned}$$

avec:

- $\mathbf{z}$: le vecteur des variables de conception (*e.g.* masses, diamètre),
- $\mathbf{x}$: le vecteur des variables d'état évoluant durant les analyses disciplinaires afin de trouver un équilibre pour satisfaire les équations d'état,
- $\mathbf{y}$: le vecteur des variables de couplage en entrée des disciplines (*e.g.* impulsion spécifique), utilisées pour relier les différentes disciplines,
- $f(\cdot)$: fonction objectif. Dans la conception de lanceurs, la fonction objectif est souvent un critère de masse (*e.g.* minimisation de la masse totale au décollage) ou un critère de coût,
- $\mathbf{g}(\cdot)$: la fonction de contraintes d'inégalité (*e.g.* contrainte de pression de combustion),

- $\mathbf{h}(\cdot)$: les fonctions de contrainte d'égalité (*e.g.* altitude d'injection sur orbite),
- $\mathbf{c}$: les fonctions de couplage, servant à calculer les variables de couplage sortant des différentes disciplines,
- $\mathbf{r}(\cdot)$: les fonctions de résidus, servant à évaluer la satisfaction des équations d'état.

Afin de résoudre un problème MDO, il est nécessaire de satisfaire:

- le cahier des charges, c'est-à-dire respecter la satisfaction des contraintes imposées par les fonctions $\mathbf{g}(\cdot)$ et $\mathbf{h}(\cdot)$,
- la faisabilité disciplinaire, c'est-à-dire la satisfaction du système d'équations d'état Eqs.(18.5) en trouvant les valeurs des variables d'état $\mathbf{x}$ telles que les équations soient satisfaites. Dans la suite, on supposera qu'une analyse interne aux disciplines gère la faisabilité disciplinaire, ainsi il ne sera plus fait référence aux variables et équations d'état,
- la faisabilité multidisciplinaire, c'est-à-dire la satisfaction du système d'équations Eqs.(18.4) en déterminant les valeurs des variables de couplage d'entrée des disciplines telles que le système d'équations soit satisfait Eqs.(18.7).

La satisfaction de la faisabilité multidisciplinaire est un point essentiel des approches MDO. Deux types d'approches existent pour la satisfaction des couplages interdisciplinaires.

- **Approches couplées**:
  Une analyse multidisciplinaire (MDA pour MultiDisciplinary Analysis) est réalisée à chaque itération de l'optimiseur système afin de satisfaire le système d'équations suivant:

$$\begin{cases} \mathbf{y}_{ij} = \mathbf{c}_{ij}(\mathbf{z}_i, \mathbf{y}_{.i}) \\ \mathbf{y}_{ji} = \mathbf{c}_{ji}(\mathbf{z}_j, \mathbf{y}_{.j}) \end{cases} \tag{18.7}$$

  Le système d'équations est classiquement résolu par point fixe ou par une optimisation auxiliaire [Coelho et al., 2009]. Ainsi, la formulation Multi Discipline Feasible (MDF) [Balling and Sobieszczanski-Sobieski, 1996] utilise cette approche à chaque itération du niveau système (Fig. 18.1):

$$\begin{aligned} \min \quad & f\left(\mathbf{z}, \mathbf{y}(\mathbf{z})\right) && (18.8) \\ \text{p.r.à} \quad & \mathbf{z} \\ \text{s.à} \quad & \mathbf{g}\left(\mathbf{z}, \mathbf{y}(\mathbf{z})\right) \leq 0 && (18.9) \\ & \mathbf{h}\left(\mathbf{z}, \mathbf{y}(\mathbf{z})\right) = 0 && (18.10) \\ & \mathbf{z_{min}} \leq \mathbf{z} \leq \mathbf{z_{max}} && (18.11) \end{aligned}$$

  L'optimiseur contrôle les variables de conception $\mathbf{z}$ et à chaque itération, une analyse multidisciplinaire est utilisée pour trouver les variables de couplage satisfaisant Eqs.(18.7). La formulation MDF est simple à mettre en œuvre mais, en raison des boucles entre les disciplines nécessaires aux MDA, le temps de calcul est important. Cette formulation est la formulation MDO la plus utilisée. D'autres formulations telles que Concurrent SubSpace Optimization (CSSO) [Sobieszczanski-Sobieski, 1988] ou Bi-Level Intregrated System Synthesis (BLISS) [Sobieszczanski-Sobieski et al., 1998] utilisent également des MDA pour satisfaire les couplages interdisciplinaires.

- **Approches découplées**:
  Cette approche vise à supprimer les boucles disciplinaires imposées par la MDA et à introduire des contraintes d'égalité Eq.(18.4) sur les variables de couplage entre les entrées et les sorties des disciplines au niveau système. L'optimiseur système, en plus de contrôler les variables de conception **z**, gère également les variables de couplage d'entrée des disciplines **y** (Fig. 18.2). Des formulations comme Individual Discipline Feasible (IDF) [Balling and Sobieszczanski-Sobieski, 1996], All At Once (AAO) [Balling and Sobieszczanski-Sobieski, 1996] ou Collaborative Optimization (CO) [Braun et al., 1996] reposent sur ce principe. Ces formulations ont été introduites afin de concevoir un système complexe par une stratégie découplée et ainsi diminuer les coûts de calcul en évitant les boucles disciplinaires et en introduisant potentiellement plusieurs niveaux d'optimisation. En revanche, ces formulations sont plus complexes à mettre en oeuvre.

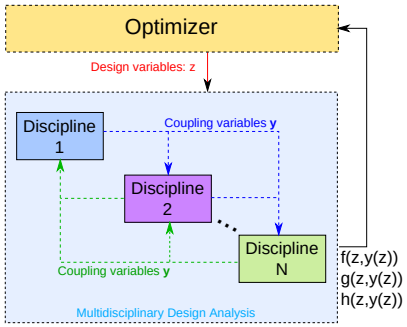

Figure 18.1: Multidisciplinary Design Optimization, approche **couplée**

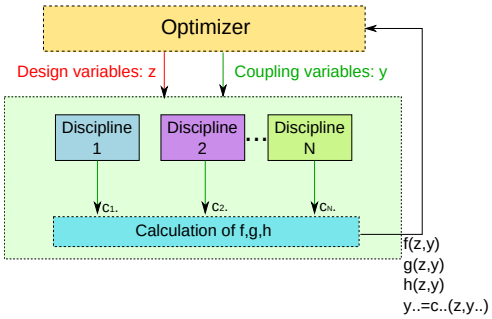

Figure 18.2: Multidisciplinary Design Optimization, approche **découplée**

Les formulations évoquées jusqu'à présent sont suffisamment générales pour être adaptables à n'importe quel problème de conception. Cependant, la conception de lanceurs présente des particularités comme la prédominance de la discipline trajectoire dans le processus de conception. L'exploitation de cette particularité a été proposée au travers des formulations Stage Wise decomposition for Optimal Rocket Design (SWORD) [Balesdent et al., 2012a]. Dans ces approches, la conception de lanceurs est décomposée par rapport à l'étagement et non plus classiquement selon les disciplines (propulsion, trajectoire, *etc.*). Ainsi les sous-systèmes considérés sont le premier étage, le deuxième étage, *etc.* Ces formulations ont été comparées à la formulation MDF et présentent de meilleures caractéristiques de convergence et de qualité d'optimum.

18.1.2 Introduction d'incertitudes en MDO

Dans la littérature, deux types d'incertitudes sont distingués [Thunnissen, 2003]:

- les incertitudes *aléatoires*: elles correspondent à la variabilité inhérente du système physique considéré et/ou de son environnement. Les incertitudes aléatoires ne peuvent pas être réduites par la collecte de plus d'informations ou de données. Les incertitudes aléatoires sont aussi appelées incertitudes stochastiques ou incertitudes irréductibles. Un exemple d'incertitudes aléatoires est la présence, la direction et l'amplitude d'une rafale de vent.

- les incertitudes *épistémiques*: elles correspondent à des méconnaissances, des simplifications de modélisation et peuvent être réduites par la collecte de plus d'informations. Les incertitudes épistémiques sont aussi appelées incertitudes de modélisation ou incertitudes réductibles. Par exemple, un modèle d'écoulement d'un fluide construit sous certaines hypothèses simplificatrices telles que l'incompressibilité du fluide, l'absence de couches limites, l'absence de turbulence pour modéliser un écoulement dans une tuyère représente avec une basse fidélité la réalité physique de l'écoulement.

La distinction entre ces deux types d'incertitudes est essentielle car des formalismes mathématiques adaptés à chaque type existent. Les incertitudes aléatoires sont traditionnellement modélisées par le formalisme des probabilités. D'autres formalismes existent pour représenter les incertitudes épistémiques tels que la théorie de l'évidence [Dempster, 1967; Shafer, 1976] ou le formalisme des intervalles [Moore et al., 2009] qui sont parfois plus adaptés pour représenter fidèlement les informations disponibles. En effet, les ingénieurs ne disposent souvent que de domaines de variation pour les paramètres incertains. Ainsi, le formalisme des intervalles est particulièrement adapté car aucune hypothèse sur la distribution des incertitudes à l'intérieur de l'intervalle n'est nécessaire (contrairement à une distribution uniforme).

L'introduction d'incertitudes dans les problèmes MDO mène à une nouvelle formulation générale dite UMDO (pour Uncertainty-based Multidisciplinary Design Optimization). On se place pour le moment dans le cadre d'incertitudes uniquement aléatoires modélisées avec le formalisme des probabilités. La formulation générale d'un problème UMDO est donnée par [Yao et al., 2011]:

$$
\begin{aligned}
\min \quad & \Xi\left[f(\mathbf{z}, \boldsymbol{\theta}_{\boldsymbol{Y}}, \mathbf{U})\right] && (18.12)\\
\text{p.r.à} \quad & \mathbf{z}, \boldsymbol{\theta}_{\boldsymbol{Y}} && \\
\text{s.à} \quad & \mathbb{K}\left[\mathbf{g}(\mathbf{z}, \boldsymbol{\theta}_{\boldsymbol{Y}}, \mathbf{U})\right] \leq 0 && (18.13)\\
& \forall i \neq j, \forall \mathbf{u} \in \boldsymbol{\Omega},\ \mathbf{y}_{ij}(\boldsymbol{\theta}_{\boldsymbol{Y}ij}, \mathbf{u}_i) = \mathbf{c}_{ij}(\mathbf{z}_i, \mathbf{y}_{.i}(\boldsymbol{\theta}_{\boldsymbol{Y}.i}, \mathbf{u}_{.i}), \mathbf{u}_i) && (18.14)\\
& \mathbf{z}_{\min} \leq \mathbf{z} \leq \mathbf{z}_{\max} && (18.15)
\end{aligned}
$$

D'importantes différences existent entre les formulations déterministes et sous incertitudes:

- $\mathbf{U}$ est le vecteur d'incertitudes d'entrée du système. On note $\mathbf{U}_i$ le vecteur incertain d'entrée de la discipline i. La $k^{\text{ème}}$ réalisation générée par Crude Monte Carlo (CMC) du vecteur aléatoire $\mathbf{U}$ est notée $\mathbf{u}_{(k)}$. On note $\phi(\cdot)$ la densité de probabilité (PDF) jointe du vecteur incertain $\mathbf{U}$.

- Ξ est la mesure d'incertitudes de la fonction objectif (*e.g.* l'espérance mathématique).

- $\mathbb{K}$ est la mesure d'incertitudes pour le vecteur des fonctions de contraintes d'inégalité. On distingue deux types de mesure pour les contraintes:

  - Mesure de robustesse: $\mathbb{K}\left[\mathbf{g}(\mathbf{z}, \boldsymbol{\theta}_{\boldsymbol{Y}}, \mathbf{U})\right] = \mathbb{E}\left[\mathbf{g}(\mathbf{z}, \boldsymbol{\theta}_{\boldsymbol{Y}}, \mathbf{U})\right] + \eta\sigma\left[\mathbf{g}(\mathbf{z}, \boldsymbol{\theta}_{\boldsymbol{Y}}, \mathbf{U})\right]$ avec $\mathbb{E}[\cdot]$ l'espérance mathématique, $\sigma[\cdot]$ l'écart type et $\eta \in \mathbb{R}^+$ un paramètre de restriction de l'espace faisable.
  - Mesure de fiabilité: pour la $i^{\text{ème}}$ composante du vecteur $\mathbf{g}(\cdot)$, avec $\mathbb{P}$ la mesure de

probabilité,

$$\mathbb{K}_i\left[g_i(\mathbf{z},\boldsymbol{\theta}_{\boldsymbol{Y}},\mathbf{U})\right] = \mathbb{P}\left[g_i(\mathbf{z},\boldsymbol{\theta}_{\boldsymbol{Y}},\mathbf{U})>0\right] - \mathbb{P}_{t_i} = \int_{\mathcal{I}_i}\phi(\mathbf{u})\mathrm{d}\mathbf{u} - \mathbb{P}_{t_i}$$

avec $\mathcal{I}_i = \{\mathbf{u}\in\boldsymbol{\Omega} | g_i(\mathbf{z},\boldsymbol{\theta}_{\boldsymbol{Y}},\mathbf{u})>0\}$ et $\mathbb{P}_{t_i}$ le seuil maximal pour la probabilité de défaillance.

Par ailleurs, on ne considère que des contraintes d'inégalité $\mathbf{g}(\cdot)$. Pour la conception de lanceurs, les contraintes d'égalité en présence d'incertitudes sont usuellement transformées en contraintes d'inégalité grâce à des tolérances (*e.g.* tolérances à l'injection sur orbite).

- $\mathbf{Y}$ est le vecteur des variables de couplage d'entrée des disciplines. En raison de la présence des variables incertaines $\mathbf{U}$, les variables de couplage sont elles-mêmes incertaines. Dans les formulations UMDO découplées, les variables de couplage d'entrée des disciplines doivent être gérées par l'optimiseur. Cependant, $\mathbf{Y}$ est un vecteur aléatoire, il s'agit d'un vecteur de fonctions. Afin d'éviter les problèmes d'optimisation en dimension infinie, l'optimiseur ne contrôle pas directement les variables de couplage mais plutôt des paramètres déterministes $\boldsymbol{\theta}_{\boldsymbol{Y}}$ modélisant les variables de couplage d'entrée des disciplines. Ces paramètres peuvent être des réalisations, des moments statistiques, des paramètres de PDF, *etc.*

Comme pour les formulations MDO déterministes, deux types de formulation UMDO peuvent être distingués pour la gestion des couplages:

- Satisfaction des couplages interdisciplinaires par une approche couplée (avec MDA),

- Satisfaction des couplages interdisciplinaires par une approche découplée.

Dans les sections suivantes, les méthodes de gestion des couplages dans les formulations UMDO sont brièvement décrites.

18.1.2.1 Approches couplées

Comme en approche déterministe, la formulation MDF en présence d'incertitudes est la formulation UMDO la plus utilisée. Les couplages interdisciplinaires sont gérés par des simulations CMC pour propager les incertitudes et, pour chaque échantillon, le système d'équations de satisfaction des couplages est résolu par MDA [Oakley et al., 1998; Koch et al., 2002; Jaeger et al., 2013]. La formulation MDF en présence d'incertitudes est donnée par (Fig. 18.3):

$$\begin{aligned} \min \quad & \Xi\left[f(\mathbf{z},\mathbf{Y}(\mathbf{z},\mathbf{U}),\mathbf{U})\right] && (18.16)\\ \text{p.r.à} \quad & \mathbf{z} \\ \text{s.à} \quad & \mathbb{K}\left[\mathbf{g}(\mathbf{z},\mathbf{Y}(\mathbf{z},\mathbf{U}),\mathbf{U})\right] \leq 0 && (18.17)\\ & \mathbf{z}_{\min} \leq \mathbf{z} \leq \mathbf{z}_{\max} && (18.18) \end{aligned}$$

Pour chaque échantillon CMC, le système d'équations suivant est résolu par MDA:

$$\forall\, \mathbf{u}\in\boldsymbol{\Omega},\ \forall (i,j)\in\{1,...,N\}^2\ i\neq j,\ \mathbf{y}_{ij} = \mathbf{c}_{ij}(\mathbf{z}_i,\mathbf{y}_{.i},\mathbf{u}) \qquad (18.19)$$

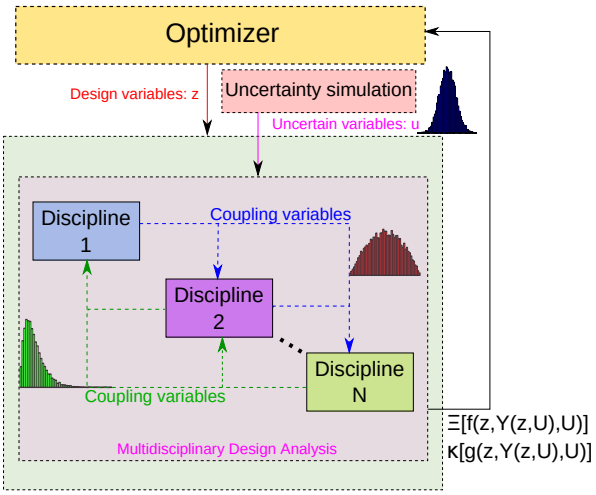

Figure 18.3: Multi Discipline Feasible en présence d'incertitudes

MDF en présence d'incertitudes permet d'assurer la faisabilité multidisciplinaire pour toutes les réalisations des variables incertaines garantissant ainsi une estimation précise de la performance et des contraintes du système. Cependant, la combinaison de l'optimisation, de la propagation d'incertitudes et des analyses multidisciplinaires induit un coût de calcul prohibitif. MDF en présence d'incertitudes est considérée comme la formulation de référence dû à la satisfaction intrinsèque des couplages interdisciplinaires. Afin de réduire les coûts de calcul, des méthodes couplées (System Uncertainty Analysis et Concurrent SubSystem Uncertainty Analysis [Du and Chen, 2002; Du et al., 2002]) fondées sur des métamodèles des relations de couplage ont été proposées.
Afin de réduire le nombre d'appels aux disciplines, des formulations UMDO découplées ont été proposées en espérant d'obtenir les mêmes avantages que pour les formulations MDO déterministes.

18.1.2.2 Approches découplées

Deux types de gestion des couplages ont été proposés pour des formulations UMDO découplées:

- *Égalité des moments statistiques.* Des approches découplées inspirées de CO ont été proposées [Du and Chen, 2001; McAllister and Simpson, 2003; Liu et al., 2006; Ghosh et al., 2014] dans lesquelles la satisfaction des couplages interdisciplinaires s'effectue grâce à des contraintes d'égalité au niveau système entre les moments statistiques calculés pour les variables de couplage d'entrée des disciplines et les moments statistiques des variables de couplage de sortie des disciplines. Par exemple, Du *et al.* ont proposé la formulation Hierarchical Approach to Collaborative Multidisciplinary Robust Design [Du and Chen, 2001] dans laquelle l'optimiseur système gère l'espérance mathématique $\boldsymbol{\mu_Y}$ et l'écart type $\boldsymbol{\sigma_Y}$ des variables de couplage d'entrée $\mathbf{Y}$. L'avantage de ces approches est de ne pas avoir recours aux MDA et d'être similaire aux formulations MDO déterministes découplées. En revanche, la satisfaction des couplages interdisciplinaires n'est assurée que pour les deux premiers moments statistiques des variables de couplage et non pour toutes les réalisations des variables incertaines

comme pour MDF en présence d'incertitudes.

- *Sequential Optimization and Reliability Assessment (SORA).* SORA repose sur une approche séquentielle pour résoudre les problèmes UMDO afin de décomposer la phase d'optimisation du système de la phase d'analyse de fiabilité. En effet, l'analyse de fiabilité est particulièrement coûteuse dans le processus UMDO. Afin d'en limiter le nombre, l'approche séquentielle repose sur deux étapes principales: une optimisation MDO déterministe du système avec les incertitudes fixées au point le plus probable de défaillance $\mathbf{u}^*$ et une deuxième étape d'analyse de fiabilité (Fig. 18.4). L'analyse de fiabilité est réalisée à l'optimum trouvé par l'optimisation déterministe en utilisant FORM (First Order Reliability Method), afin d'identifier dans l'espace incertain le point le plus probable de défaillance (MPP). Si le système optimal trouvé ne satisfait pas les contraintes de défaillance, un nouveau problème d'optimisation déterministe est formulé tenant compte du nouveau point le plus probable de défaillance. Dans cette approche, la satisfaction des couplages interdisciplinaires s'effectue au point le plus probable de défaillance. Les variables de couplage d'entrée et de sortie des disciplines doivent avoir la même valeur au MPP. SORA permet de découpler les disciplines et de réduire le coût de calcul par rapport à la formulation MDF. En revanche, elle ne permet pas d'assurer la satisfaction des couplages interdisciplinaires pour toutes les réalisations des variables incertaines comme avec MDF.

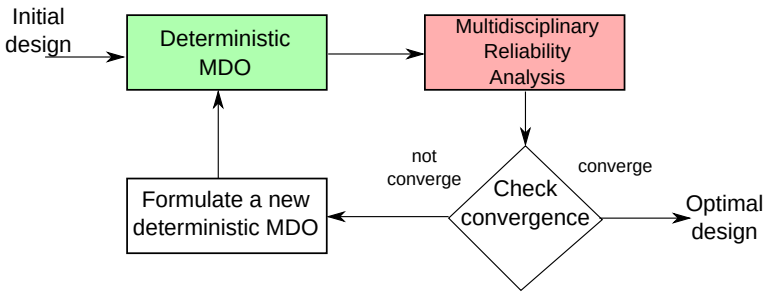

Figure 18.4: Procédure SORA pour résoudre un problème UMDO [Du et al., 2008]

Outre la gestion des couplages interdisciplinaires, l'analyse de fiabilité est un point important dans les formulations UMDO. Des méthodes d'analyse de fiabilité en présence d'incertitudes aléatoires ont été proposées telles que CMC, FORM [Madsen, 1986; Bjerager, 1990], IS (Importance Sampling) [Engelund and Rackwitz, 1993; L'Ecuyer et al., 2009; Kroese and Rubinstein, 2012b], SS (Subset Sampling) [Au and Beck, 2001] , *etc.* Les techniques d'IS et de SS ont été développées dans le cadre de calcul de probabilités de défaillance impliquant des évènements rares. Par ailleurs, ces techniques ont été couplées avec des modèles de substitution et des stratégies de raffinement [Schueremans and Van Gemert, 2005; Picheny, 2009; Vazquez and Bect, 2009; Echard et al., 2011; Li et al., 2012; Bect et al., 2012a; Baudoui et al., 2012; Balesdent et al., 2013; Dubourg et al., 2013] afin de réduire les coûts de calcul. Cependant, en phase d'avant-projet, la présence d'incertitudes à la fois aléatoires et épistémiques requiert des méthodes d'analyse de fiabilité adaptées. Dans la section suivante, les approches existantes sont brièvement présentées.

18.1.3 Analyse de fiabilité en présence d'incertitudes aléatoires et épistémiques

Dans la littérature, l'impact des incertitudes épistémiques est classé en deux catégories:

- les hyper-paramètres de loi des densités de probabilité sont affectés par des incertitudes épistémiques (*e.g.* la moyenne d'une distribution Gaussienne n'est pas connue exactement mais uniquement sur un intervalle),
- l'état limite délimitant le domaine de défaillance est directement affecté par des incertitudes épistémiques.

18.1.3.1 Incertitudes épistémiques sur les hyper-paramètres de lois des variables incertaines

On considère un vecteur aléatoire $\mathbf{U}$ de dimension d défini sur l'espace $\mathbf{\Omega}$ par une PDF jointe $\phi^{\mathbf{e}}(\cdot)$ indexée par un vecteur paramètre $\mathbf{e} = [e^{(1)}, \ldots, e^{(w)}]^{\mathrm{T}} \in \mathbb{R}^w$. $\mathbf{e}$ est affecté par des incertitudes épistémiques et seul le domaine de variation de ses composantes est connu $\mathbf{\Upsilon} = \{\mathbf{e} \in \mathbb{R}^w | e^{(i)} \in [e^{(i)}_{\min}, e^{(i)}_{\max}] \; \forall i \in \{1, \ldots, w\}\}$. On considère un système caractérisé par une fonction état limite $g : \mathbf{\Omega} \to \mathbb{R}$ supposée continue, étant une boîte noire et coûteuse à évaluer. En présence d'incertitudes aléatoires et épistémiques, la probabilité de défaillance du système n'est pas unique et dépend de la valeur prise par $\mathbf{e}$ (Figs. 18.5,18.6). Afin de caractériser la probabilité de défaillance, il est possible de déterminer ses bornes de variation:

$$\begin{cases} \mathbb{P}_{\min} = \min\limits_{\mathbf{e} \in \mathbf{\Upsilon}} \; \mathbb{P}_{\mathbf{e}}(g(\mathbf{U}) \leq 0) \\ \mathbb{P}_{\max} = \max\limits_{\mathbf{e} \in \mathbf{\Upsilon}} \; \mathbb{P}_{\mathbf{e}}(g(\mathbf{U}) \leq 0) \end{cases} \tag{18.20}$$

La détermination des valeurs des variables épistémiques menant aux bornes de la probabilité de défaillance implique la résolution de problèmes d'optimisation et des analyses de fiabilité Eqs.(18.20).

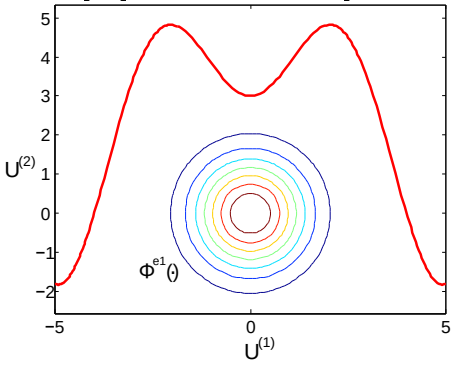

Figure 18.5: Analyse de fiabilité avec $\phi^{\mathbf{e1}}(\cdot)$

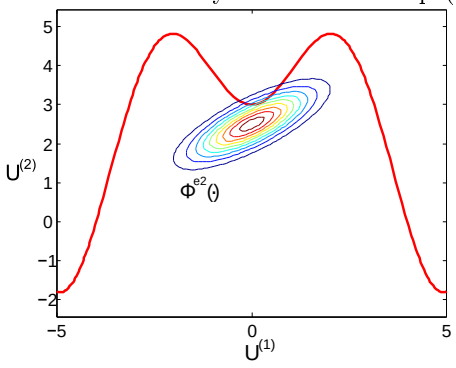

Figure 18.6: analyse de fiabilité avec $\phi^{\mathbf{e2}}(\cdot)$

Des approches basées sur CMC [Zhang et al., 2010] ou FORM [Qiu et al., 2008] ont été proposées pour résoudre ce type de problèmes au travers d'une double boucle. À chaque itération de l'optimiseur, une analyse de fiabilité par CMC ou FORM est réalisée. Cependant, le coût de calcul engendré par ce type d'approche est prohibitif. Afin d'éviter ces deux niveaux de calcul, CMC ainsi que IS ont été étendus à la prise en compte directe d'intervalles. Néanmoins, ces méthodes permettent

aux variables épistémiques de prendre différentes valeurs en fonction des réalisations des variables aléatoires, ce qui n'est pas possible dans le problème considéré. Par ailleurs, des méthodes basées sur FORM ont été développées pour prendre en compte directement les variables décrites par un intervalle. Cependant, comme FORM repose sur une linéarisation locale de la fonction objectif et l'hypothèse de l'unicité de la zone de défaillance, le type de problèmes traités est limité. Dans le cas des lanceurs, les contraintes de fiabilité sur la retombée des étages n'entrent pas dans ce cadre.

18.1.3.2 Incertitudes épistémiques affectant l'état limite de défaillance

On considère le même cadre qu'au paragraphe précédent avec cette fois un système caractérisé par une fonction état limite $g : \mathbf{\Omega} \times \mathbf{\Upsilon} \rightarrow \mathbb{R}$ supposée continue, étant une boîte noire et coûteuse à évaluer. Ce problème est différent du précédent car les incertitudes épistémiques $\mathbf{e}$ n'affectent pas les densités de probabilité des variables aléatoires mais directement l'état limite de défaillance (Fig.18.7), ici la fonction $g(\cdot)$ dépend directement de $\mathbf{e}$. Afin de caractériser la probabilité de défaillance, il est nécessaire de déterminer ses bornes de variation:

$$\begin{cases} \mathbb{P}_{\min} = \min\limits_{\mathbf{e}\in\mathbf{\Upsilon}} \ \mathbb{P}(g(\mathbf{U},\mathbf{e}) \leq 0) \\ \mathbb{P}_{\max} = \max\limits_{\mathbf{e}\in\mathbf{\Upsilon}} \ \mathbb{P}(g(\mathbf{U},\mathbf{e}) \leq 0) \end{cases} \tag{18.21}$$

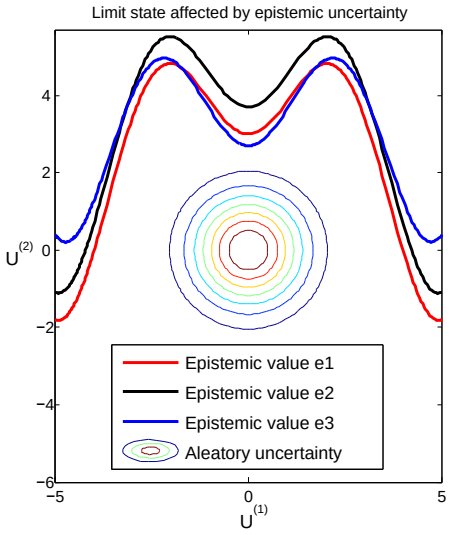

Figure 18.7: État limite affecté par des incertitudes épistémiques

Pour ce type de problèmes, des approches basées sur CMC [Yang et al., 2014] ou FORM [Du, 2008; Du et al., 2005] ont été proposées. Cependant, elles souffrent des mêmes limitations que celles exposées précédemment.

Afin de résoudre un problème UMDO, des algorithmes d'optimisation maîtrisant à la fois la présence d'incertitudes et de contraintes sont nécessaires. Plusieurs algorithmes ont été développés à ces fins et sont brièvement décrits dans la section suivante.

18.1.4 Optimisation numérique en présence de contraintes et d'incertitudes

De nombreux algorithmes et techniques ont été proposés afin de gérer les incertitudes et les contraintes dans les problèmes d'optimisation. Ainsi, pour maîtriser la présence d'incertitudes plusieurs approches ont été développées:

- Ré-échantillonage [Branke and Schmidt, 2003; Jin and Branke, 2005]: cette approche consiste à ré-evaluer la fonction objectif et les contraintes pour une même valeur des variables de conception $\mathbf{z}$ et à utiliser une mesure statistique pour la valeur de la fonction objectif et des contraintes (*e.g.* l'espérance mathématique).
- Modèle de substitution [Branke and Schmidt, 2003; Jin, 2005]: des métamodèles de la fonction objectif et des contraintes sont construits. De façon générale, les métamodèles lissent les fonctions modélisées atténuant ainsi le bruit et diminuant l'impact des incertitudes.
- Algorithmes à base de population d'individus [Nissen and Propach, 1998; Hansen et al., 2003; Jin and Branke, 2005]: ces algorithmes reposent sur une population d'individus pour trouver l'optimum de la fonction. Ils peuvent modifier la taille de la population afin de couvrir des zones plus importantes pour obtenir plus d'information et ainsi diminuer l'impact des incertitudes. Comme ces algorithmes ne reposent pas sur un seul candidat, ils sont moins affectés par les incertitudes.

Les algorithmes à base de population (Particle Swarm Optimization [Eberhart and Kennedy, 1995], Ant Colony [Dorigo and Birattari, 2010], Genetic Algorithm [Holland, 1975], *etc.*) sont particulièrement intéressants pour résoudre des problèmes UMDO qui sont souvent non linéaires, non convexes avec de multiples optima locaux et en présence d'incertitudes. Parmi les algorithmes à base de population, l'algorithme Covariance Matrix Adaptation - Evolutionary Strategy (CMA-ES) [Hansen et al., 2003] est particulièrement efficace pour les problèmes d'optimisation en présence d'incertitudes comme illustré dans plusieurs parangonnages [Hansen, 2009; Hansen et al., 2010].

CMA-ES est un algorithme développé pour résoudre les problèmes non contraints. Il repose sur un modèle paramétrique de distribution de la population (une densité multivariée paramétrique) afin d'explorer l'espace de conception. Avec CMA-ES(λ, μ), à chaque itération, λ candidats sont générés à partir de μ parents. À la génération suivante, les nouveaux μ parents sont sélectionnés parmi les λ enfants par rapport à leurs classements vis-à-vis de la fonction objectif. Ainsi à l'itération $[k+1]$, les enfants sont générés selon:

$$\mathbf{z}_t^{[k+1]} \sim \mathbf{m}^{[k]} + \sigma^{[k]} \mathcal{N}\left(0, \mathbf{C}^{[k]}\right), \text{ pour } t = 1, ..., \lambda \tag{18.22}$$

avec $\mathbf{z}_t^{[k+1]} \in \mathbb{R}^n$ un candidat enfant généré à partir du vecteur moyen $\mathbf{m}^{[k]}$, du pas $\sigma^{[k]}$ et d'une distribution normale $\mathcal{N}\left(0, \mathbf{C}^{[k]}\right)$ paramétrée par une matrice de covariance $\mathbf{C}^{[k]}$. Cette matrice de covariance permet d'effectuer des transformations homothétiques et des rotations de l'espace de recherche (Fig. 18.8). La mise à jour de la matrice de covariance tient compte des itérations passées et des μ meilleurs candidats de la génération actuelle. Le vecteur moyen caractérise le centre de la prochaine distribution et est déterminé par une pondération des μ meilleurs candidats. Les mécanismes de mise à jour sont détaillés dans [Hansen et al., 2003].

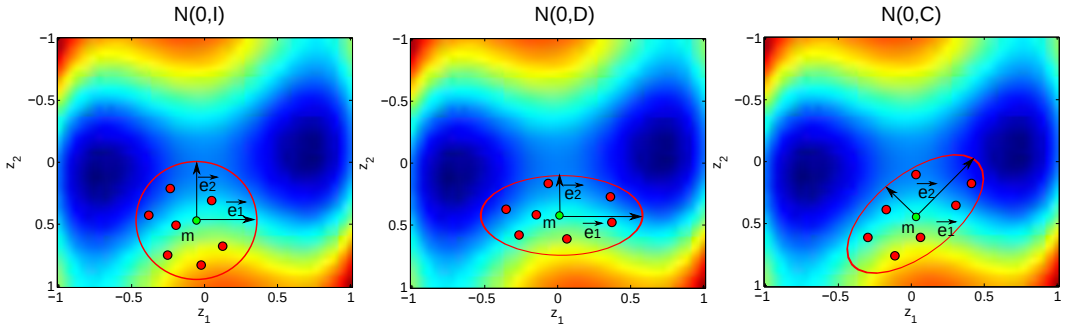

Figure 18.8: Espace de recherche pour différentes matrices de covariance

CMA-ES a été étendu pour la prise en compte d'incertitudes [Hansen et al., 2009]. De nombreux mécanismes assurent la robustesse de l'algorithme face à la présence d'incertitudes: la population, la combinaison pondérée des candidats, l'utilisation d'un classement plutôt que la valeur de la fonction objectif d'un candidat, *etc.* Cependant, si les incertitudes sont trop importantes elles peuvent perturber la convergence. Lorsque le bruit est trop élevé, les mécanismes de sélection et de mise à jour des paramètres sont modifiés. Les candidats sont ré-évalués et suivant la modification de leur rang, l'espace de recherche est agrandi ou rétréci afin d'assurer la collecte d'une quantité suffisante d'information malgré la présence d'incertitudes.
Le principal inconvénient de CMA-ES est qu'il ne prend pas en compte les contraintes. Comme la plupart des heuristiques évolutionnaires, le traitement des contraintes dans l'algorithme CMA-ES peut s'effectuer avec des méthodes basées sur la pénalisation de la fonction objectif [Collange et al., 2010b; Beyer and Finck, 2012; De Melo and Iacca, 2014] ou sur des métamodèles des fonctions de contraintes [Kramer et al., 2009]. Cependant, ces techniques requièrent un réglage fin qui dépend du problème traité. Une approche alternative a été proposée pour (1+1)-CMA-ES [Arnold and Hansen, 2012] qui est une version simplifiée de CMA-ES(λ, μ) avec un unique enfant et la sélection s'effectue uniquement entre le parent et l'enfant. La mise à jour de la matrice de covariance a été modifiée afin de tenir compte de la violation des contraintes et ainsi changer l'espace de recherche pour l'itération suivante afin de limiter la génération possible d'un enfant dans l'espace non faisable (Fig. 18.9).
(1+1)-CMA-ES est efficace pour les problèmes unimodaux mais présente des difficultés pour les problèmes multimodaux et en grande dimension [Arnold and Hansen, 2012].

18.1.5 Conclusion et voies d'amélioration

Au regard du bref état de l'art réalisé des méthodes UMDO existantes, nous pouvons identifier plusieurs voies d'amélioration possibles. Trois pistes seront explorées dans la suite de cette thèse afin de résoudre quelques limitations évoquées dans l'état de l'art:

1. Le développement d'une approche permettant la gestion des couplages interdisciplinaires dans les formulations UMDO découplées afin de garantir la faisabilité multidisciplinaire quelle que soit la réalisation des variables incertaines. Pour maintenir l'équivalence mathématique entre les approches couplées et découplées, il est nécessaire d'assurer un couplage fonctionnel entre

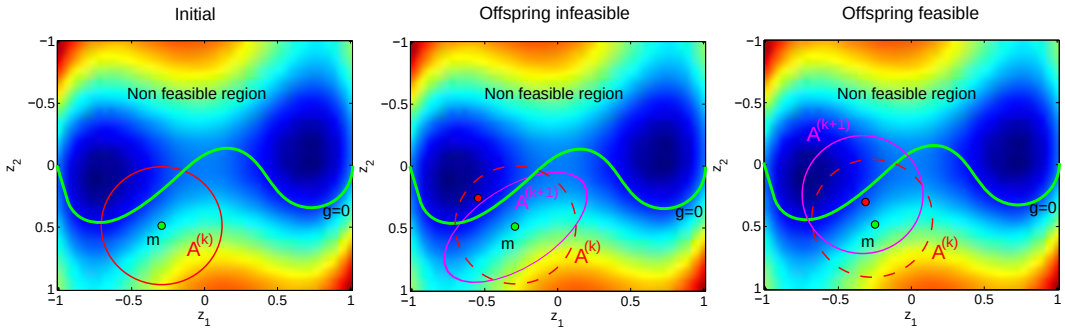

Figure 18.9: Le point vert est le parent et le point rouge l'enfant généré. Sur la gauche, le cercle trait plein représente l'espace de recherche paramétré par $\mathbf{A}^{[k]}$. Au centre, l'ellipse rose représente la mise à jour de la matrice de covariance $\mathbf{A}^{[k+1]}$ en tenant compte de la violation de la contrainte par l'enfant. À droite, l'enfant ne violant pas la contrainte, la matrice de covariance est mise à jour classiquement.

les disciplines. De plus, adapter les formulations SWORD afin de prendre en compte la gestion d'incertitudes permettrait de bénéficier des mêmes avantages qu'en approche déterministe.

2. Le développement de méthodes d'analyse de fiabilité tenant compte de la présence à la fois d'incertitudes aléatoires et épistémiques afin de pouvoir traiter des problèmes avec des états limites non linéaires et plusieurs zones de défaillance. Par ailleurs, ces méthodes doivent être adaptées aux calculs de probabilité impliquant des évènements rares comme par exemple pour l'analyse de retombée d'un étage de lanceur en dehors de sa zone nominale.

3. Le développement d'une technique permettant la gestion des contraintes pour l'algorithme CMA-ES afin de ne pas utiliser les approches par pénalisation dont le réglage dépend du problème à résoudre.

Dans la suite, ces trois points seront détaillés respectivement dans les sections 18.2, 18.3 et 18.4.

18.2 Formulations UMDO avec satisfaction fonctionnelle des couplages interdisciplinaires

Dans cette section, nous présentons une méthode permettant la satisfaction des couplages interdisciplinaires pour toutes les réalisations des variables incertaines. Deux formulations UMDO découplées sont proposées, une mono-niveau Individual Discipline Feasible - Polynomial Chaos Expansion (IDF-PCE) et une multi-niveaux Multi-level Hierarchical Optimization under Uncertainty. Dans cette section on considère que toutes les incertitudes sont modélisées par des variables aléatoires avec le formalisme des probabilités.

18.2.1 Satisfaction des couplages interdisciplinaires

Afin de supprimer l'utilisation de MDA, les processus de conception décomposés visent à découpler les disciplines. Pour garantir la faisabilité multidisciplinaire, deux défis doivent être résolus:

- Les variables de couplage d'entrée des disciplines $\mathbf{Y}$ doivent être gérées par l'optimiseur système. Les variables de couplage sont des fonctions et les problèmes d'optimisation en dimension infinie sont difficiles à résoudre.
- Des contraintes d'égalité doivent être imposées entre les variables de couplage d'entrée des disciplines et celles de sortie des disciplines au niveau système. L'égalité entre deux variables aléatoires correspond à une égalité entre deux fonctions ce qui est difficile à gérer dans un problème UMDO.

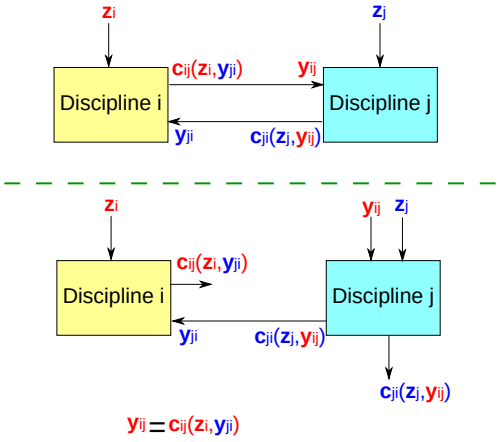

Figure 18.10: Couplage entre deux disciplines i et j

En MDO déterministe, afin de garantir la faisabilité multidisciplinaire pour une formulation découplée, une contrainte d'égalité doit être imposée au niveau système. En considérant le couplage scalaire entre les disciplines i et j comme représenté sur la Figure 18.10, la contrainte suivante est imposée au niveau système afin d'assurer la faisabilité multidisciplinaire:

$$y_{ij} = c_{ij}(\mathbf{z}_i, y_{ji})$$

Cependant, en présence d'incertitudes, la contrainte d'égalité doit être imposée entre deux variables aléatoires. Deux variables aléatoires sont égales si et seulement si les fonctions correspondantes possèdent les mêmes espaces de départ et d'arrivée et si chaque aléa possède la même image. Ainsi, assurer la satisfaction des couplages pour toutes les réalisations des variables incertaines revient à imposer un nombre infini de contraintes d'égalité. Par exemple, pour le même couplage en présence d'incertitudes:

$$\forall \mathbf{u} \in \mathbf{\Omega},\ y_{ij} = c_{ij}(\mathbf{z}_i, y_{ji}, \mathbf{u}_i)$$

Afin de ne pas résoudre un problème d'optimisation avec un nombre infini de contraintes, on propose d'introduire une nouvelle forme de contrainte interdisciplinaire, pour un problème possédant

N disciplines:

$$\forall (i,j) \in \{1,...,N\}^2 \; i \neq j, \; \mathbf{J}_{ij} = \int_{\mathbf{\Omega}} \left[\mathbf{c}_{ij}(\mathbf{z}_i, \mathbf{y}_{.i}, \mathbf{u}_i) - \mathbf{y}_{ij}\right]^2 \phi(\mathbf{u}) \mathrm{d}\mathbf{u} = 0 \tag{18.23}$$

Afin de satisfaire Eq.(18.23), les variables de couplage d'entrée des disciplines doivent être égales aux variables de couplage de sortie des disciplines pour toutes les réalisations des variables incertaines (sauf éventuellement sur un espace de mesure nulle). Si cette contrainte d'égalité est satisfaite, alors l'équivalence mathématique avec les approches couplées est maintenue.
Néanmoins, afin de découpler les disciplines, les variables de couplage d'entrée $\mathbf{Y}$ doivent être gérées par l'optimiseur au niveau système. Afin de permettre à l'optimiseur de gérer un nombre fini de variables, chaque variable de couplage est remplacée par un métamodèle représentant les relations fonctionnelles entre les disciplines:

$$y_{ij} \rightarrow \hat{y}_{ij}\left(\mathbf{u}, \boldsymbol{\alpha}^{(ij)}\right) \tag{18.24}$$

avec $\boldsymbol{\alpha}^{(ij)}$ des paramètres du métamodèle. Ces paramètres sont contrôlés par l'optimiseur système en plus des variables de conception $\mathbf{z}$. Dans les formulations proposées par la suite, chaque variable de couplage qui est découplée est remplacée par un métamodèle dont les paramètres sont gérés par l'optimiseur système et une contrainte d'égalité sous forme intégrale est imposée. Les métamodèles fournissent une représentation fonctionnelle de la dépendance entre les variables de couplage d'entrée des disciplines et les variables incertaines. Ainsi, le problème d'optimisation en dimension infinie est transformé en un problème d'optimisation en dimension finie, dont la dimension correspond au nombre de paramètres des métamodèles plus le nombre de variables de conception.
On se propose de représenter les relations fonctionnelles de couplage par des polynômes du chaos (PCE pour Polynomial Chaos Expansion) [Eldred, 2009] car ces métamodèles présentent de nombreux avantages pour l'analyse et la propagation d'incertitudes. En effet, les PCE sont des modèles réduits dédiés à la représentation de fonctions qui dépendent de variables aléatoires. Un PCE utilisé pour modéliser une fonction $y_{ij} : \mathbf{\Omega} \rightarrow \mathbb{R}$ telle que $\mathbb{E}[y_{ij}(\mathbf{U}^2)] < +\infty$ est une approximation polynomiale qui consiste à décomposer la fonction y_{ij} sur une base polynomiale orthogonale [Eldred, 2009; Hosder, 2012]:

$$\hat{y}_{ij}\left(\mathbf{u}, \boldsymbol{\alpha}^{(ij)}\right) = \sum_{k=1}^{d_{\mathrm{PCE}}} \alpha_{(k)}^{(ij)} \Psi_k(\mathbf{u}) \tag{18.25}$$

avec d_{PCE} le degré de décomposition du PCE et $\Psi_k(\cdot)$ un polynôme de la base orthogonale choisie en fonction de la distribution des variables incertaines d'entrée [Eldred, 2009]. Afin de conserver un métamodèle simple, la dépendance en $\mathbf{z}$ n'est pas présente, les coefficients des PCE sont appris pour un $\mathbf{z}$ spécifique correspondant à l'optimum du problème UMDO.
Les formulations proposées dans la suite reposent sur cette technique pour la gestion des couplages interdisciplinaires. En même temps que l'optimiseur système gère les variables de conception, il contrôle également les coefficients des PCE modélisant les variables de couplage d'entrée des disciplines afin de ne pas faire intervenir de MDA. De plus, les contraintes intégrales permettent d'assurer la faisabilité multidisciplinaire à l'optimum du problème d'UMDO. En effet, à l'optimum, les métamodèles des relations de couplage représentent les relations fonctionnelles entre les disciplines comme le ferait une analyse multidisciplinaire en présence d'incertitudes. La technique proposée permet d'éviter de faire des MDA à chaque itération.

18.2.2 Individual Discipline Feasible - Polynomial Chaos Expansion

La première formulation proposée est dérivée de la formulation IDF déterministe. Il s'agit d'une formulation mono-niveau découplée (Fig. 18.11):

$$\begin{aligned}
\min \quad & \Xi\left[f(\mathbf{z},\boldsymbol{\alpha},\mathbf{U})\right] && (18.26)\\
\text{p.r.à} \quad & \mathbf{z},\boldsymbol{\alpha} \\
\text{s.t.} \quad & \mathbb{K}\left[\mathbf{g}(\mathbf{z},\boldsymbol{\alpha},\mathbf{U})\right] \leq 0 && (18.27)\\
& \forall (i,j) \in \{1,...,N\}^2,\ i \neq j, \\
& \mathbf{J}_{ij} = \int_{\mathbf{\Omega}} \left[\mathbf{c}_{ij}\left(\mathbf{z}_i, \hat{\mathbf{y}}_{.i}\left(\mathbf{u},\boldsymbol{\alpha}^{(.i)}\right),\mathbf{u}_i\right) - \hat{\mathbf{y}}_{ij}\left(\mathbf{u},\boldsymbol{\alpha}^{(ij)}\right)\right]^2 \phi(\mathbf{u})\mathrm{d}\mathbf{u} = \mathbf{0} && (18.28)\\
& \mathbf{z}_{\min} \leq \mathbf{z} \leq \mathbf{z}_{\max} && (18.29)
\end{aligned}$$

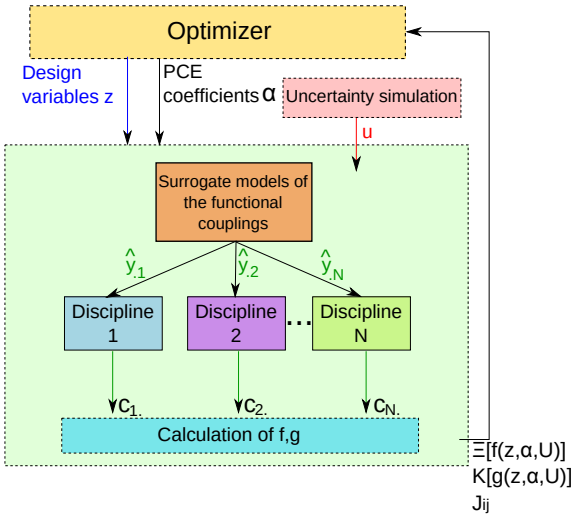

Figure 18.11: IDF-PCE avec les métamodèles des relations fonctionnelles de couplage

avec $\mathbf{J}_{ij}$ la contrainte interdisciplinaire des couplages de la discipline i vers la discipline j et $\hat{\mathbf{y}}_{.i}\left(\mathbf{u},\boldsymbol{\alpha}^{(.i)}\right)$ les PCE de toutes les variables de couplage d'entrée de la discipline i. La figure 18.11 illustre le processus d'IDF-PCE. L'optimiseur système gère les variables de conception $\mathbf{z}$ et les coefficients des PCE $\boldsymbol{\alpha}$. L'approche proposée permet de simuler les disciplines en parallèle et ainsi de décomposer le processus de conception. La contrainte Eq.(18.28) permet d'assurer à la convergence du problème UMDO la faisabilité multidisciplinaire du système pour toutes les réalisations des variables incertaines.
Afin de calculer les intégrales multidimensionnelles nécessaires à l'évaluation de la fonction objectif (la mesure $\Xi[\cdot]$ peut-être par exemple l'espérance mathématique $\mathbb{E}[\cdot]$), des contraintes $\mathbb{K}[\cdot]$ (robustes ou fiables) et des contraintes de couplage interdisciplinaire, quatre techniques sont utilisées:

- Approximation par CMC,

- Approximation par quadrature,
- Décomposition des variables de couplage de sortie des disciplines à l'aide d'une deuxième série de PCEs,
- Subset Simulation (SS) couplée avec des Support Vector Machines (SVM) pour le calcul des contraintes faisant intervenir des calculs de fiabilité.

Pour plus de détails se référer au chapitre 6. La formulation IDF-PCE a été comparée à la formulation MDF sur un cas test analytique présenté au chapitre 6.

18.2.3 Multi-level Hierarchical Optimization under Uncertainty

La deuxième formulation proposée est dérivée de la formulation SWORD déterministe dédiée à la conception de lanceurs. La formulation a été généralisée pour la conception de n'importe quel système et adaptée à la prise en compte d'incertitudes. Il s'agit d'une formulation multi-niveaux découplée de façon hiérarchique (Fig. 18.2.3). Seules les variables de couplage de retour (feedback coupling variables) sont supprimées. La formulation présuppose que la fonction objectif $\Xi[f(\cdot)]$ est décomposable comme la somme de contributions de sous-systèmes $\Xi[f(\cdot)] = \sum_{k=1}^{N} \Xi[f_k(\cdot)]$ avec $\Xi[f_k(\cdot)]$ la fonction objectif du $k^{\text{ème}}$ sous-système. Par exemple, la masse totale du lanceur au décollage (GLOW pour Gross Lift-Off Weight) est décomposable comme la somme de la masse totale de chaque étage. De nombreux systèmes peuvent être décomposés selon ce principe (contributions des sous-systèmes au coût total du système, à la masse totale, aux dimensions totales, *etc.*). La formulation MHOU est donnée par:

- Niveau système:

$$\min \quad \sum_{k=1}^{N} \Xi\left[f_k(\mathbf{z}_{sh}, \mathbf{z}_k^*, \boldsymbol{\alpha}, \mathbf{U})\right] \tag{18.30}$$

$$\text{p.r.à} \quad \mathbf{z}_{sh} \in \mathcal{Z}_{sh}, \boldsymbol{\alpha}$$

$$\text{s.à} \quad \mathbb{K}\left[\mathbf{g}(\mathbf{z}_{sh}, \mathbf{z}_k^*, \boldsymbol{\alpha}, \mathbf{U})\right] \leq 0 \tag{18.31}$$

$$\forall (k,j) \in \{1,...,N\}^2,\ j \neq k\ \mathbf{J}_{kj}(\mathbf{z}_{sh}, \mathbf{z}_k^*, \boldsymbol{\alpha}) = 0 \tag{18.32}$$

$$\forall k \in \{1,...,N\},\ \mathbb{K}\left[\mathbf{g}_k(\mathbf{z}_{sh}, \mathbf{z}_k^*, \boldsymbol{\alpha}, \mathbf{U})\right] \leq 0 \tag{18.33}$$

- Niveau sous-système:

$k = N$

$$\text{tant que} \quad k > 0$$

$$\text{étant donné} \quad \mathbf{y}_{Nk}, \ldots, \mathbf{y}_{(k+1)k}$$

Pour le $k^{\text{ème}}$ sous-système

$$\min \quad \Xi\left[f_k(\mathbf{z}_{sh}, \mathbf{z}_k, \boldsymbol{\alpha}, \mathbf{U})\right] \tag{18.34}$$

$$\text{p.r.à} \quad \mathbf{z}_k \in \mathcal{Z}_k$$

$$\text{s.à} \quad \mathbb{K}\left[\mathbf{g}_k(\mathbf{z}_{sh}, \mathbf{z}_k, \boldsymbol{\alpha}, \mathbf{U})\right] \leq 0 \tag{18.35}$$

$$\forall j \in \{1,...,N\},\ j \neq k\ \mathbf{J}_{kj} =$$

$$\int_{\boldsymbol{\Omega}} \left[\mathbf{c}_{kj}\left(\mathbf{z}_{sh}, \mathbf{z}_k, \hat{\mathbf{y}}_{.k}\left(\mathbf{u}, \boldsymbol{\alpha}^{(.k)}\right), \mathbf{u}_k\right) - \hat{\mathbf{y}}_{kj}\left(\mathbf{u}, \boldsymbol{\alpha}^{(kj)}\right)\right]^2 \phi(\mathbf{u}) \mathrm{d}\mathbf{u} = \mathbf{0} \tag{18.36}$$

$$k \leftarrow k - 1$$

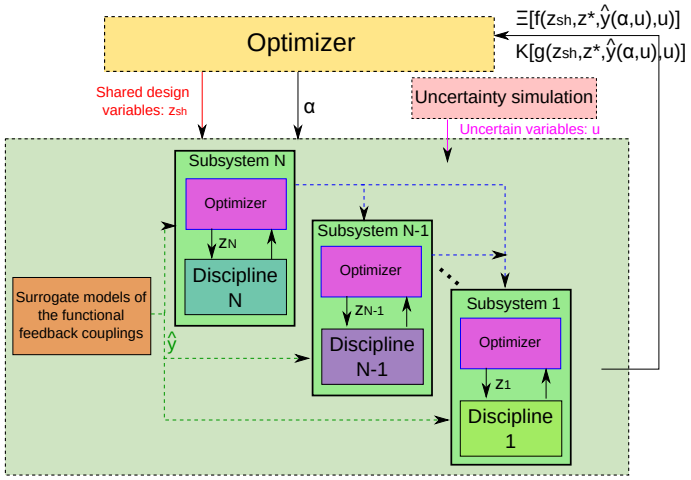

Figure 18.12: Multi-level Hierarchical Optimization under Uncertainty (MHOU)

où $\mathbf{z}_k$ est le vecteur des variables de conception relatif au sous-système k et $\mathbf{z}_{sh}$ est le vecteur des variables de conception partagé par plusieurs sous-systèmes. L'optimiseur du sous-système k gère uniquement les variables de conception $\mathbf{z}_k$. L'optimiseur système contrôle le vecteur des variables de conception partagées et les coefficients des PCE. Les contraintes de couplages interdisciplinaires permettent d'assurer la faisabilité multidisciplinaire du système optimal. Cette formulation est particulièrement adaptée à la conception de lanceurs constitués de plusieurs étages. L'étage supérieur est tout d'abord optimisé en tenant compte de toutes les disciplines impliquées dans sa conception, ensuite les étages intermédiaires et enfin le premier étage. Les variables de couplage découplées correspondent à l'état du lanceur à la séparation des étages (*e.g.* altitude, vitesse, pente).

18.2.4 Applications à la conception de lanceurs

Ces deux formulations ont été appliquées à deux cas tests de conception de lanceurs. Le cas test pour la méthode IDF-PCE est brièvement décrit dans la suite. Pour plus de concision, le cas test lanceur pour la formulation MHOU ainsi qu'une comparaison avec IDF-PCE n'est pas présenté ici et est décrit chapitre 8. Le cas test IDF-PCE est décrit ici car il illustre la prédominance de la discipline trajectoire et l'impact des incertitudes sur l'injection de la charge utile. Le cas test IDF-PCE consiste à concevoir un lanceur bi-étage à propulsion liquide afin de placer une charge utile de 4000kg sur une orbite de transfert géostationnaire depuis Kourou (injection au périgée à 250 km). Quatre disciplines sont prises en compte: la propulsion, le dimensionnement, l'aérodynamique et la trajectoire (Fig. 18.13). Les modèles utilisés sont des modèles simplifiés, classiquement utilisés en phase d'avant-projet. Les variables de conception sont le diamètre du 1$^{\text{er}}$ étage D_1, la masse d'ergol du 1$^{\text{er}}$ étage M_{p1}, la poussée du 1$^{\text{er}}$ étage T_1, le rapport de mélange du 1$^{\text{er}}$ étage OF_1, le diamètre du 2$^{\text{ème}}$ étage D_2, la masse d'ergol du 2$^{\text{ème}}$ étage M_{p2} et enfin le coefficient de détarage du moteur du 2$^{\text{ème}}$ étage Der.
Les trois incertitudes considérées dans ce cas test portent sur l'impulsion spécifique du 1$^{\text{er}}$ étage, sur la masse sèche du 2$^{\text{ème}}$ étage et sur la poussée du 2$^{\text{ème}}$ étage. La formulation du problème de MDF est la suivante:

$$\begin{aligned} \min \quad & \mathbb{E}\left[\text{GLOW}\left(\mathbf{z},\mathbf{U}\right)\right] && (18.37)\\ \text{w.r.t.} \quad & \left[D_1, M_{p1}, T_1, OF_1, D_2, M_{p2}, Der\right]^{\mathrm{T}} \\ \text{s.t.} \quad & \mathbb{P}_f(\mathbf{z},\mathbf{U}) \leq 5\times 10^{-2} && (18.38)\\ & \mathbf{z}_{\min} \leq \mathbf{z} \leq \mathbf{z}_{\max} && (18.39) \end{aligned}$$

avec $\mathbb{P}_f(\mathbf{z},\mathbf{U}) = 1 - \mathbb{P}\left[(247.5 \leq H_t \leq 252.5) \cap (9.703 \leq V_t \leq 9.723) \cap (-0.4 \leq \gamma_t \leq 0.4)\right]$ avec H_t, V_t et γ_t l'altitude, la vitesse et la pente de l'orbite visée. Cette probabilité de défaillance correspond à la probabilité de ne pas réussir la mission en injectant sur une mauvaise orbite. Elle est calculée par SS couplée avec un métamodèle SVM de l'état limite.
La formulation IDF-PCE est la suivante:

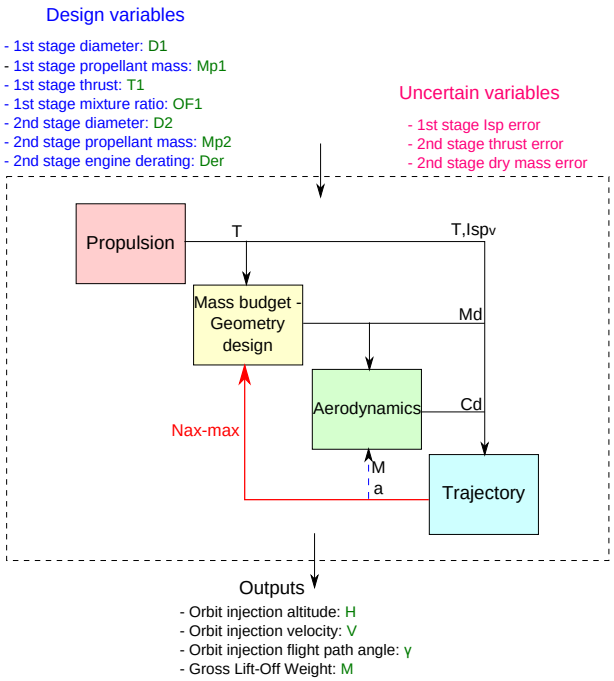

Figure 18.13: Conception d'un lanceur bi-étage

$$\min \quad \mathbb{E}\left[\mathrm{GLOW}\left(\mathbf{z},\mathbf{U}\right)\right] \tag{18.40}$$

$$\text{w.r.t.} \quad \left[D_1, M_{p1}, T_1, OF_1, D_2, M_{p2}, Der\right]^{\mathrm{T}}, \boldsymbol{\alpha}$$

$$\text{s.t.} \quad \mathbb{P}_f(\mathbf{z},\mathbf{U}) \leq 5\times 10^{-2} \tag{18.41}$$

$$J^{\mathrm{CMC}} = \sum_{k=1}^{M_s}\left[c_{N_{ax_{max}}}\left(\mathbf{z}, \hat{y}_{N_{ax_{max}}}\left(\mathbf{u}_{(k)},\boldsymbol{\alpha}\right),\mathbf{u}\right) - \hat{y}_{N_{ax_{max}}}\left(\mathbf{u}_{(k)},\boldsymbol{\alpha}\right)\right]^2 \leq \epsilon \tag{18.42}$$

$$\mathbf{z}_{\min} \leq \mathbf{z} \leq \mathbf{z}_{\max} \tag{18.43}$$

avec un calcul des intégrales multidimensionnelles par CMC. Le couplage de retour entre la discipline trajectoire et la discipline dimensionnement correspond au facteur de charge axial maximal et est supprimé afin de ne pas avoir à réaliser de boucles entre les disciplines. Le facteur de charge est décomposé selon un produit de polynômes d'Hermite d'ordre total d'expansion de degré 2 correspondant à 10 coefficients PCE.

Résultats Les deux méthodes convergent vers le même optimum à la fois en terme de variables de conception que de valeur de la fonction objectif et de la contrainte de défaillance. En revanche, l'approche proposée permet de réduire par 11 le nombre d'appels aux différentes disciplines en évitant l'utilisation de MDA (Figs. 18.14,18.15). De plus, ce cas test illustre l'importance de la

prise en compte des incertitudes en phase d'avant-projet comme illustré sur les Figures 18.16 à 18.19.

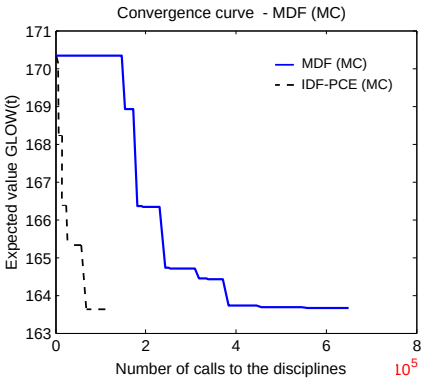

Figure 18.14: Courbes de convergence

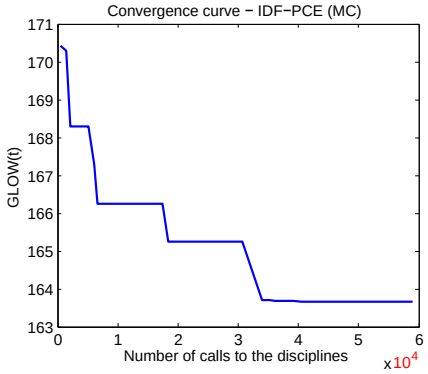

Figure 18.15: Courbe de convergence d'IDF-PCE

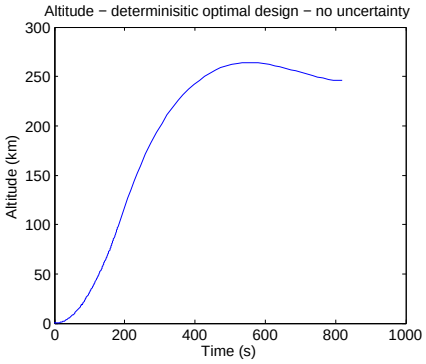

Figure 18.16: Trajectoire pour un lanceur optimal avec MDF déterministe

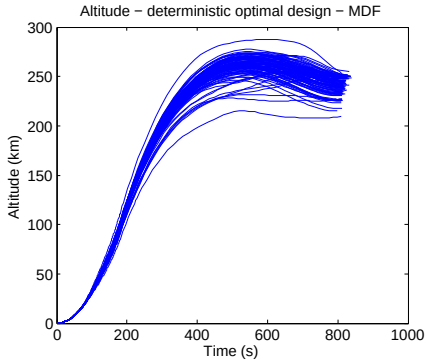

Figure 18.17: Analyse de robustesse pour le lanceur déterministe trouvé

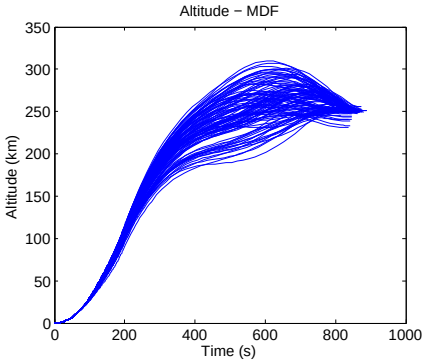

Figure 18.18: Altitude du lanceur optimal - MDF en présence d'incertitudes

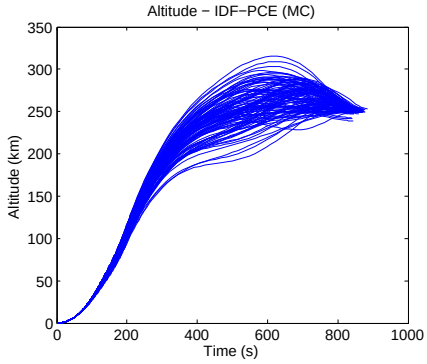

Figure 18.19: Altitude du lanceur optimal - IDF-PCE en présence d'incertitudes

Lorsque le lanceur est conçu par une approche MDF sans prise en compte des incertitudes on obtient un lanceur qui injecte sur la bonne orbite (Fig.18.16). En revanche, lorsque l'on soumet ce lanceur aux incertitudes considérées on constate qu'il n'est pas robuste et l'injection sur une orbite à 250km n'est pas précis (Fig. 18.17). Cependant, si l'on prend en compte les incertitudes dès le début de la phase de conception, alors plus d'ergol est prévu pour le lancement afin de pouvoir assurer une injection robuste sur l'orbite voulue (Figs. 18.18-18.19)
De plus, l'approche proposée assure la faisabilité multidisciplinaire du lanceur optimal pour toutes les réalisations des variables incertaines comme le fait la formulation MDF. Par exemple la Figure 18.20 présente la distribution de l'erreur de couplage entre le facteur de charge d'entrée de la discipline dimensionnement et le facteur de charge simulé en sortie de la discipline trajectoire.

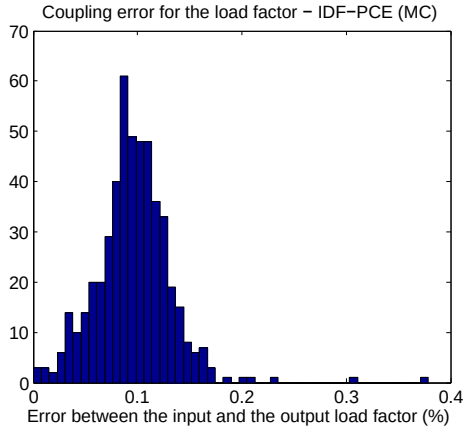

Figure 18.20: Distribution de l'erreur de couplage pour le facteur de charge axial maximal

18.2.5 Conclusion

La méthode de gestion des couplages interdisciplinaires proposée permet d'assurer numériquement une satisfaction des couplages similaire entre les approches couplées et découplées. Cette technique repose sur le remplacement des variables de couplage d'entrée des disciplines par un métamodèle (Polynôme du chaos) dont les coefficients qui le paramétrisent sont gérés par l'optimiseur système avec les variables de conception. Le degrée de décomposition des PCE fixe le degrée de précision de la satisfaciton des couplages. Une nouvelle contrainte de satisfaction des couplages permet de garantir la faisabilité multidisciplinaire pour toutes les réalisations des variables incertaines. Deux formulations ont été développées à l'aide de cette technique de gestion des couplages: une mono-niveau (Individual Discipline Feasible - Polynomial Chaos Expansion) permettant l'évaluation en parallèle des disciplines et la suppression d'analyse multidisciplinaire et une multi-niveaux (Multi-level Hierarchical Optimization under Uncertainty) particulièrement adaptée à la conception de lanceurs. Ces deux formulations ont été comparées à la formulation de référence MDF sur un cas test analytique et des cas tests lanceurs et permettent de diminuer le nombre d'appels aux disciplines et ainsi le temps de calcul. Par ailleurs, ces formulations permettent d'assurer la robustesse du lanceur aux incertitudes vis-à-vis de l'injection sur orbite de la charge utile.

Outre la gestion des couplages interdisciplinaires, l'analyse de fiabilité est une tâche importante des processus UMDO. Dans la section suivante, deux techniques d'analyse de fiabilité en présence d'incertitudes à la fois aléatoires et épistémiques sont proposées.

18.3 Méthodes d'analyse de fiabilité en présence d'incertitudes aléatoires et épistémiques

Assurer la fiabilité du système optimal obtenu est essentiel dans la conception de systèmes complexes. On se place dans le cadre de la présence d'incertitudes à la fois aléatoires et épistémiques. On s'intéresse aux deux cas de figure existant dans la littérature:

- Incertitudes épistémiques sur les hyper-paramètres des PDF caractérisant les variables aléatoires,
- Incertitudes épistémiques affectant directement l'état limite de défaillance.

18.3.1 Incertitudes épistémiques sur les hyper-paramètres des PDF

On considère le problème posé en section 18.1.3.1. L'objectif est de calculer les bornes supérieures et inférieures du domaine de variation de la probabilité de défaillance Eqs.(18.44).

$$\begin{cases} \mathbb{P}_{\min} = \min\limits_{\mathbf{e}\in\boldsymbol{\Upsilon}} \ \mathbb{P}_{\mathbf{e}}(g(\mathbf{U}) \leq 0) \\ \mathbb{P}_{\max} = \max\limits_{\mathbf{e}\in\boldsymbol{\Upsilon}} \ \mathbb{P}_{\mathbf{e}}(g(\mathbf{U}) \leq 0) \end{cases} \tag{18.44}$$

Par ailleurs, on considère que le calcul de la probabilité de défaillance fait intervenir des évènements rares. Afin de limiter le nombre d'appels à la fonction état limite $g(\cdot)$, on propose d'utiliser une méthode d'échantillonnage préférentiel (Importance Sampling avec l'algorithme de Cross Entropy [Rubinstein and Kroese, 2004]) avec un modèle de substitution de $g(\cdot)$ (par Krigeage [Matheron, 1963; Sasena, 2002]).
Afin d'avoir une estimation précise de la probabilité de défaillance, l'estimation de probabilité par Importance Sampling (IS) vise à remplacer la densité $\phi^{\mathbf{e}}(\cdot)$ par une densité auxiliaire plus adaptée pour générer des échantillons dans les zones de défaillance. Une probabilité de défaillance calculée par IS pour une valeur $\mathbf{e}$ des variables épistémiques est estimée de la façon suivante:

$$\hat{\mathbb{P}}_{\mathbf{e}}^{IS} = \frac{1}{M}\sum_{i=1}^{M} \mathbb{1}_{g(\mathbf{u}_{(i)})>0} \frac{\phi^{\mathbf{e}}(\mathbf{u}_{(i)})}{\tau(\mathbf{u}_{(i)})} \tag{18.45}$$

avec M le nombre d'échantillons, $\mathbb{1}_{g(\mathbf{u}_{(i)})>0}$ la fonction indicatrice, $\phi^{\mathbf{e}}(\cdot)$ la densité de tirage initiale et $\tau(\cdot)$ la densité de tirage auxiliaire. L'algorithme de Cross Entropy (CE) est un processus adaptatif visant à déterminer la densité auxiliaire qui se rapproche le plus de la densité auxiliaire optimale (qui minimise la variance de l'estimateur IS mais est inaccessible en pratique). Pour cela, CE est fondé sur l'optimisation d'une densité auxiliaire paramétrique afin de déterminer la valeur des paramètres $\boldsymbol{\theta}$ qui permet de minimiser la distance de Kullback-Leibler avec la densité auxiliaire optimale. Ce processus de détermination des paramètres est adaptatif et fait intervenir des seuils de défaillance intermédiaires avec la résolution d'un problème d'optimisation à chaque seuil pour trouver la densité auxiliaire optimale jusqu'à atteindre le seuil de défaillance final.

Afin de calculer les bornes Eqs.(18.44), il est nécessaire d'estimer de façon efficace la probabilité de défaillance un grand nombre de fois (pour chaque valeur des variables épistémiques $\mathbf{e}$ proposée par l'optimiseur). Pour cela, on se propose de modifier l'initialisation de l'algorithme CE et d'utiliser les estimations des probabilités de défaillance précédentes. On considère qu'une itération complète de l'algorithme CE a été réalisée pour une valeur $\mathbf{e}_0$ des variables épistémiques partant de la densité $\phi^{\mathbf{e}_0}(\cdot)$ pour trouver la densité auxilaire optimale. A la convergence de CE, on dispose ainsi de la densité auxiliaire optimale $\tau_{\boldsymbol{\theta}^*}(\cdot)$ pour $\mathbf{e}_0$. Cette densité permet de générer des échantillons dans la zone de défaillance et ainsi d'estimer de façon précise la probabilité de défaillance. Lorsque l'optimiseur fournit une nouvelle valeur $\mathbf{e}$ pour les variables épistémiques, on propose d'utiliser cette densité optimale ainsi que les échantillons générés précédemment pour initialiser CE. On dispose ainsi directement d'une densité générant des échantillons dans la zone de défaillance. L'algorithme CE est alors utilisé pour trouver la densité optimale pour la valeur $\mathbf{e}$ à moindre coût de calcul par rapport à une initialisation de l'algorithme avec $\phi^{\mathbf{e}}(\cdot)$.

De plus, afin de réduire de façon significative le nombre d'appels à la fonction état limite $g(\cdot)$, un modèle de substitution $\widehat{g}(\cdot)$ de cette fonction est construit et amélioré à l'aide d'une stratégie de raffinement [Balesdent et al., 2013].
Enfin, afin de résoudre les deux problèmes d'optimisation pour trouver les bornes de la probabilité de défaillance, CMA-ES est utilisé car la fonction objectif est bruitée (estimation par IS) et il n'existe pas à notre connaissance de dérivation du gradient de la probabilité de défaillance calculé par CE par rapport aux variables épistémiques.

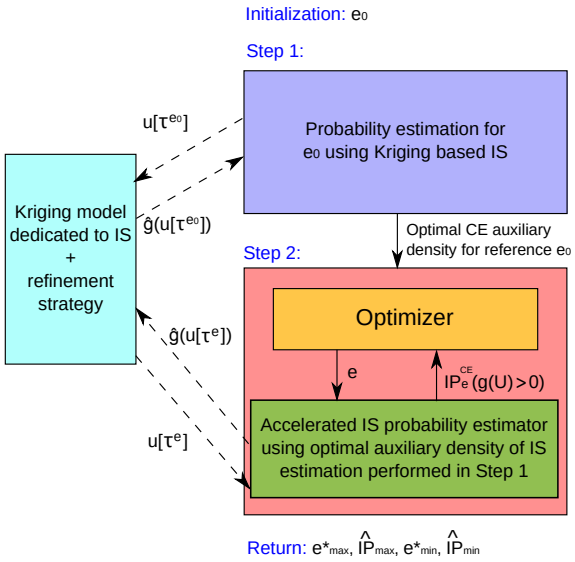

Figure 18.21: Approche proposée pour le calcul des bornes de la probabilité de défaillance avec des incertitudes épistémiques affectant les PDF des variables aléatoires avec un coût de calcul réduit

La méthode proposée est illustrée Figure 18.21 et permet de réduire le nombre d'appels à la fonction état limite exacte tout en assurant une estimation précise de la probabilité de défaillance. Cette

approche a été testée sur deux cas tests analytiques par rapport à deux méthodes de référence et est plus efficace que ces approches tant sur la qualité de l'optimum que sur la précision (faible variance de l'estimée de la probabilité de défaillance). Cette méthode a été testée sur un cas test lanceur (voir chapitre 11).

18.3.2 Incertitudes épistémiques affectant directement l'état limite

On considère le problème posé en section 18.1.3.2. L'objectif est de calculer les bornes supérieures et inférieures du domaine de variation de la probabilité de défaillance:

$$\begin{cases} \mathbb{P}_{\min} = \min\limits_{\mathbf{e}\in\boldsymbol{\Upsilon}} \ \mathbb{P}(g(\mathbf{U},\mathbf{e}) \leq 0) \\ \mathbb{P}_{\max} = \max\limits_{\mathbf{e}\in\boldsymbol{\Upsilon}} \ \mathbb{P}(g(\mathbf{U},\mathbf{e}) \leq 0) \end{cases} \tag{18.46}$$

Dans ce problème l'état limite de défaillance est directement impacté par la présence d'incertitudes épistémiques. On considère par la suite uniquement le calcul de la borne supérieure du domaine de variation de la probabilité de défaillance car c'est cette valeur qui est déterminante dans la conception d'un système (respect du cahier des charges). Néanmoins, l'approche proposée est adaptable au calcul de la borne inférieure. Par ailleurs, on considère que le calcul de la probabilité de défaillance fait intervenir des évènements rares. Afin de limiter le nombre d'appels à la fonction état limite $g(\cdot)$, on propose d'utiliser une méthode d'échantillonnage adaptatif (Subset Sampling) avec un modèle de substitution de $g(\cdot)$ (par Krigeage). Le Subset Sampling (SS) est utilisé car cette technique d'estimation d'évènements rares permet de tenir compte de plusieurs zones de défaillance pour des états limites non linéaires.
La méthode proposée repose sur une approche séquentielle avec une phase d'estimation de la borne de probabilité de défaillance maximale à l'aide d'un métamodèle et d'une phase de raffinement du modèle de substitution (Fig. 18.22).
Pour déterminer la borne maximale de la probabilité de défaillance, on se propose d'utiliser un algorithme par gradient pour leur rapidité de convergence. Pour cela, une technique permettant l'estimation du gradient de la probabilité de défaillance par rapport aux variables épistémiques $\mathbf{e}$ a été dérivée. La probabilité de défaillance s'exprime par:

$$\mathbb{P}(\mathbf{e}) = \int_{\Omega_f(\mathbf{e})} \phi(\mathbf{u})\mathrm{d}\mathbf{u} \tag{18.47}$$

avec le domaine de défaillance $\Omega_f(\mathbf{e}) = \{\mathbf{u} \in \boldsymbol{\Omega} | \, g(\mathbf{u},\mathbf{e}) \leq 0\}$ qui dépend des variables épistémiques. La probabilité peut se réécrire avec la fonction indicatrice:

$$\mathbb{P}(\mathbf{e}) = \int_{\Omega} \mathbb{1}_{g(\mathbf{u},\mathbf{e})\leq 0}\phi(\mathbf{u})\mathrm{d}\mathbf{u} \tag{18.48}$$

Ainsi, pour pouvoir utiliser un algorithme d'optimisation à base de gradient, il est nécessaire de calculer:

$$\begin{aligned} \left.\frac{\partial \mathbb{P}}{\partial e^{(k)}}\right|_{\mathbf{e}} &= \frac{\partial}{\partial e^{(k)}} \int_{\Omega} \mathbb{1}_{g(\mathbf{u},\mathbf{e})\leq 0}\phi(\mathbf{u})\mathrm{d}\mathbf{u} \\ &= \int_{\Omega} \frac{\partial}{\partial e^{(k)}} \mathbb{1}_{g(\mathbf{u},\mathbf{e})\leq 0}\phi(\mathbf{u})\mathrm{d}\mathbf{u} \end{aligned} \tag{18.49}$$

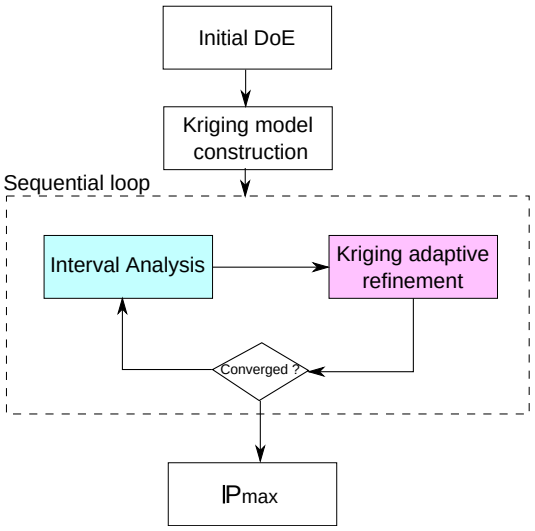

Figure 18.22: Processus de détermination de la borne supérieure de la probabilité de défaillance en présence d'incertitudes épistémiques affectant directement l'état limite

Pour cela, deux techniques sont proposées: calcul de l'Eq.(18.49) par CMC ou par SS. Le calcul du gradient de la probabilité de défaillance fait intervenir la distribution de Dirac qu'il est nécessaire d'approximer. Pour cela, plusieurs approches ont été comparées et une technique fondée sur une distribution Gaussienne avec le réglage d'un paramètre σ est proposée. L'estimation du gradient de la probabilité de défaillance est utilisée par l'algorithme d'optimisation afin de trouver la borne maximale de défaillance.

Par ailleurs, pour l'estimation de la probabilité de défaillance, on se propose de construire le modèle de Krigeage dans l'espace joint incertain aléatoire/épistémique. Pour chaque valeur des variables épistémiques, une estimation de la probabilité de défaillance par SS est réalisée avec le Krigeage. Afin d'assurer une estimation précise de la probabilité de défaillance, un raffinement du métamodèle, qui a été construit à partir d'un plan d'expérience, est nécessaire. Pour cela, un problème d'optimisation a été mis en place afin de trouver le points dans l'espace joint aléatoire/épistémique permettant de réduire l'incertitude du modèle de substitution. Ce problème d'optimisation est dérivé du Generalized Max-min [Lacaze and Missoum, 2014a] et adapté à la prise en compte d'incertitudes épistémiques. La résolution du problème d'optimisation à l'itération $[t]$ de la boucle séquentielle permet de trouver un point tel qu'il soit :

- proche du seuil de défaillance grâce à la contrainte $\hat{g}(\mathbf{u}, \mathbf{e}, \mathcal{X}) = 0$ avec $\mathcal{X}$ le plan d'expérience du Krigeage,
- dans les régions à haut niveau de PDF $(\phi(\mathbf{u})\phi_{\mathcal{U}}(\mathbf{e}))^{\frac{1}{d+w}}$ avec $\phi(\cdot)$ la densité jointe des variables aléatoires, $\phi_{\mathcal{U}}(\cdot)$ la densité uniforme pour les variables épistémiques, d la dimension du vecteur de variables aléatoires et w celle du vecteur des variables épistémiques,
- autour de la valeur des variables épistémiques menant à la probabilité de défaillance maximale

$\hat{\mathbb{P}}(\mathbf{e}) \geq \hat{\mathbb{P}}^{-}_{\max}\left(\mathbf{e}^{*[t]}\right)$ avec $\hat{\mathbb{P}}(\mathbf{e})$ la probabilité de défaillance pour le vecteur $\mathbf{e}$ et $\hat{\mathbb{P}}^{-}_{\max}\left(\mathbf{e}^{*[t]}\right)$ la borne inférieure de la probabilité de défaillance maximale pour la valeur des variables épistémiques menant à la probabilité de défaillance maximale trouvée lors de l'Interval Analysis. Cette borne inférieure tient compte de l'incertitude du métamodèle,

- suffisamment éloigné des M_s points existants dans le plan d'expérience $\min_{i=1,\dots,M_s} \parallel (\mathbf{u}_{(i)}, \mathbf{e}_{(i)}) - (\mathbf{u}, \mathbf{e}) \parallel$.

Le problème d'optimisation trouve des solutions qui ne raffinent pas dans tout l'espace épistémique mais uniquement dans les zones d'intérêt pour le calcul des bornes de probabilité de défaillance. L'estimation de la variance de la prédiction par Krigeage permet de contrôler l'erreur de ce dernier et son impact sur l'estimée de la probabilité de défaillance. Le problème d'optimisation pour le raffinement du Krigeage est donné par:

$$\max_{\mathbf{u},\mathbf{e}} \quad (\phi(\mathbf{u})\phi_{\mathcal{U}}(\mathbf{e}))^{\frac{1}{d+w}} \min_{i=1,\dots,M_s} \parallel (\mathbf{u}_{(i)}, \mathbf{e}_{(i)}) - (\mathbf{u}, \mathbf{e}) \parallel \tag{18.50}$$

$$\text{s.t.} \quad \hat{g}(\mathbf{u}, \mathbf{e}, \mathcal{X}) = 0 \tag{18.51}$$

$$\hat{\mathbb{P}}(\mathbf{e}) \geq \hat{\mathbb{P}}^{-}_{\max}\left(\mathbf{e}^{*[t]}\right) \tag{18.52}$$

$$\mathbf{e} \in \boldsymbol{\Upsilon} \tag{18.53}$$

$$\mathbf{u} \in \boldsymbol{\Omega} \tag{18.54}$$

La méthode proposée (Fig.18.22) permet de réduire le nombre d'appels à la fonction état limite exacte tout en assurant une estimation précise de la probabilité de défaillance. Cette approche a été testée sur un cas test analytique par rapport à une méthode de référence (FORM-UUA) et est plus efficace que cette dernière tant sur la qualité de l'optimum que sur la précision (faible variance de l'estimée de la probabilité de défaillance). Par ailleurs, cette méthode a été testée sur un cas test lanceur présenté à la section 18.3.3.

18.3.3 Application à l'analyse de lanceurs

Dans cette section, le cas test lanceur est présenté avec des variables épistémiques impactant l'état limite de défaillance. Pour plus de concision, le cas test lanceur impliquant des variables épistémiques affectant les hyper-paramètres de loi des variables aléatoires n'est pas présenté ici et est décrit chapitre 11.
On considère un lanceur composé de plusieurs étages à propulsion solide et on s'intéresse à la retombée du deuxième étage dans l'océan. On souhaite déterminer la probabilité pour l'étage de retomber à une distance de plus de 20km du point de retombée nominal. Les variables incertaines considérées sont présentées dans le tableau 18.23.
Le débit massique du profile de la queue de poussée d'un étage à propulsion solide est difficile à modéliser et des incertitudes de modélisation existent. En effet, le profile de la queue de poussée d'un étage solide dépend de l'érosion de la tuyère, des instabilités de combustion, du taux de combustion de la surface d'ergol solide, *etc.* En pratique, ces phénomènes physiques sont complexes et en phase d'avant-projet, les modèles utilisés ne permettent de fournir qu'un domaine de variation possible pour le profile de la queue de poussée de l'étage.
Afin de simuler la phase ascensionnelle et la retombée du lanceur, les disciplines de propulsion, de dimensionnement, d'aérodynamique, de trajectoire montée et descente sont impliquées (Fig.18.24) dans le calcul de la distance orthodromique d'impact de l'étage au point nominal.

Table 18.23: Variables incertaines pour le problème de retombée de l'étage

Variables incertaines	Type	Définition
Erreur altitude séparation (m)	Aléatoire	$\mathcal{N}(0, 0.01)$
Erreur vitesse séparation (km/s)	Aléatoire	$\mathcal{N}(0, 0.01)$
Erreur pente séparation (rad)	Aléatoire	$\mathcal{N}(0, 0.03)$
Erreur azimuth séparation (rad)	Aléatoire	$\mathcal{N}(0, 0.00175)$
Erreur masse sèche (kg)	Aléatoire	$\mathcal{N}(0, 70)$
Erreur débit massique 1^{er} étage	Epistémique	$[0, 1]$

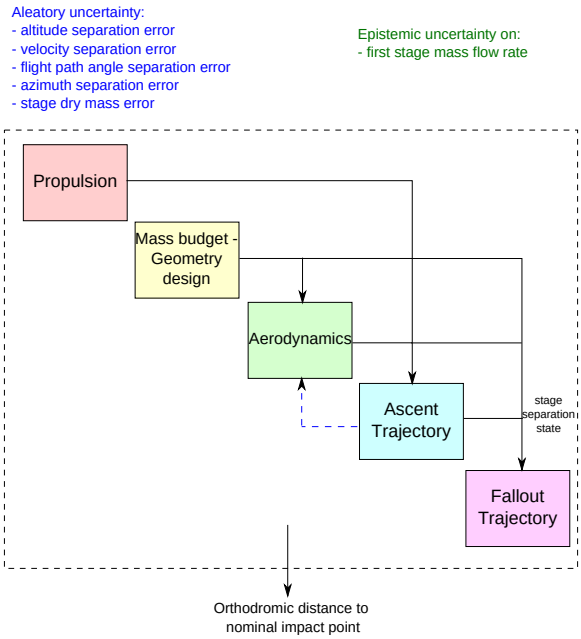

Figure 18.24: Disciplines impliquées dans le calcul de probabilités de défaillance

L'approche proposée permet de calculer les bornes de la probabilité de défaillance en raison de l'incertitude de modélisation sur la queue de poussée du premier étage. Elle permet de faire moins d'appels à la fonction état limite (impliquant toutes les disciplines) que l'approche de référence (dérivée de FORM) et permet de trouver une meilleure valeur pour la borne supérieure. Par ailleurs, l'importance de l'utilisation du Subset Sampling est illustrée par la figure 18.26. En effet, deux zones de défaillances principales existent et CMC ne parvient pas à générer des points dans l'espace de défaillance alors que l'approche utilisant le Subset Sampling permet une estimation précise de la probabilité de défaillance. L'utilisation du modèle de Krigeage permet de réduire le coût de calcul en appelant le moins de fois possible les disciplines.

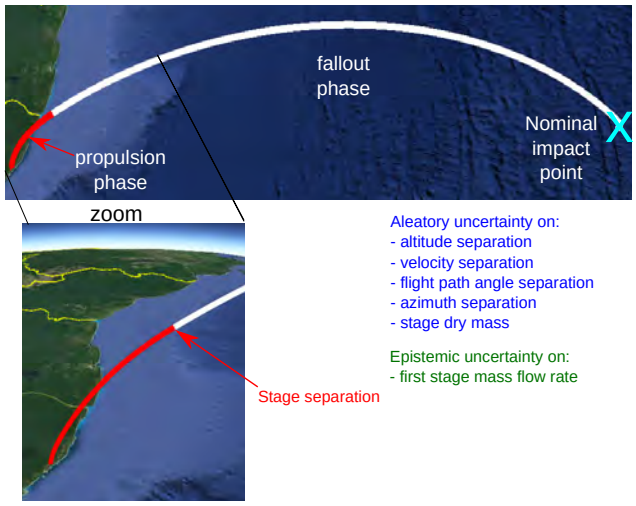

Figure 18.25: Séparation et point d'impact nominal du 2ème étage

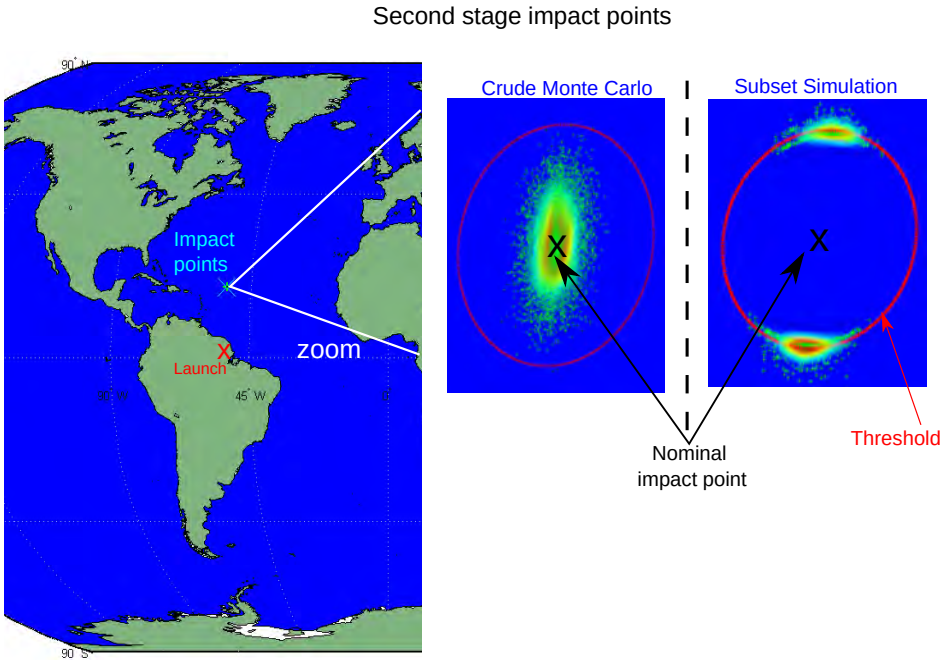

Figure 18.26: Points d'impact du 2ème étage du lanceur

18.3.4 Conclusion

Dans cette section, deux méthodes d'analyse de fiabilité en présence d'incertitudes à la fois aléatoires et épistémiques ont été proposées. Ces méthodes reposent sur l'utilisation d'une technique d'estimation de probabilité impliquant des évènements rares (Importance Sampling ou Subset Sampling) combinée à l'utilisation d'un métamodèle de la fonction état limite (Krigeage) et d'une stratégie de raffinement afin d'être précis uniquement dans les zones désirées. Ces approches ont été comparées à des méthodes de référence sur des cas tests analytiques et sur des cas tests d'analyse de retombée d'étage de lanceurs. Les approches proposées permettent d'obtenir de meilleurs bornes sur les probabilités de défaillance avec un nombre plus faible d'appels à la fonction état limite exacte.
Outre la gestion des couplages interdisciplinaires et l'analyse de fiabilité, un autre élément important afin de résoudre un problème UMDO est l'optimisation. La section suivante se focalise sur l'adaptation de l'algorithme CMA-ES à la prise en compte de contraintes.

18.4 Gestion des contraintes pour CMA-ES

18.4.1 Modification de la mise à jour de la matrice de covariance

Comme expliqué dans la section 18.1.4, l'algorithme CMA-ES [Hansen et al., 2003] n'est pas adapté à la prise en compte de contraintes. Seules des techniques par pénalisation de la fonction objectif existent et sont à régler pour chaque problème d'optimisation.
Dans cette section, on se propose de modifier l'algorithme CMA-ES à partir de la méthode développée pour (1+1)-CMA-ES [Arnold and Hansen, 2012]. La particularité de CMA-ES est qu'il définit un volume de recherche dans lequel il génère une population d'individus à l'aide d'une loi Gaussienne paramétrée par une matrice de covariance $\mathbf{C}$. Cette matrice de covariance peut générer différents hyper-volumes et, par des homothéties et des rotations, privilégier des zones de l'espace de recherche afin de converger vers l'optimum.

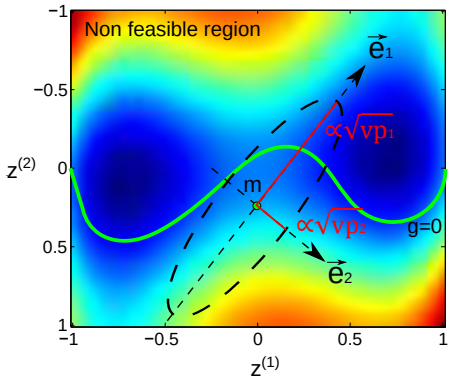

Figure 18.27: Paramétrage de l'ellipsoïde de recherche de candidats définie par une matrice de covariance.

Pour tenir compte de la génération de candidats enfreignant les contraintes, une technique modi-

fiant la mise à jour de la matrice de covariance est proposée. En effet, la matrice de covariance est caractérisée par ses valeurs propres et ses vecteurs propres. L'hyper-volume de recherche et la zone de génération de candidats sont donc fonction des valeurs propres de la matrice $\mathbf{C}$ (Fig.18.27).

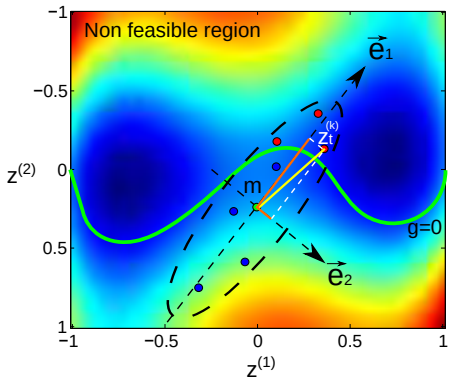

Figure 18.28: Violation de la contrainte et projection sur les vecteurs propres, candidats bleu=faisables, rouge=non faisables.

Lorsqu'un candidat enfreint une ou plusieurs contraintes, à l'aide de projections de la distance entre le candidat et le point moyen $\mathbf{m}$ sur les vecteurs propres, les valeurs propres de la matrice de covariance sont modifiées afin de réduire la possibilité de générer des futurs candidats dans ces directions (Fig.18.28). En réduisant les valeurs propres de la matrice de covariance selon les directions adéquates, on réduit l'espace de recherche dans les zones enfreignant les contraintes et ainsi la possibilité de générer des candidats dans ces espaces (Fig.18.29).

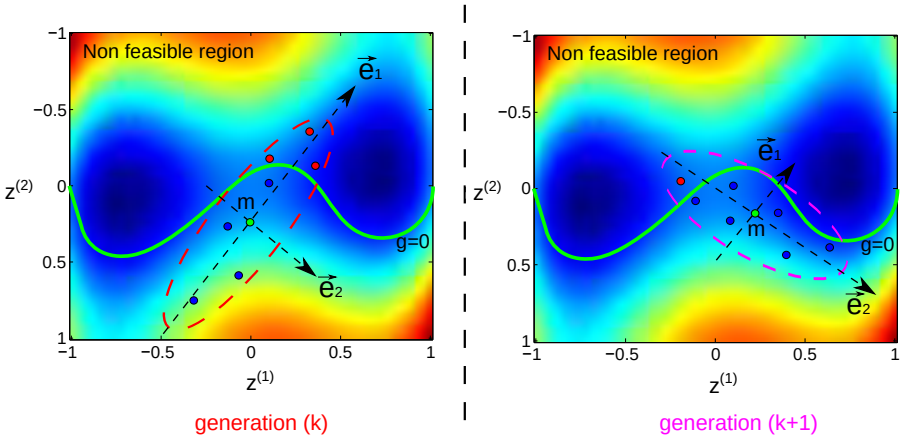

Figure 18.29: Évolution de la matrice de covariance dûe à la violation de la contrainte entre deux itérations, candidats bleu=faisables, rouge=non faisables.

18.4.2 Applications: cas tests analytiques et conception de lanceur

Cette technique a été utilisée et comparée à des méthodes de référence (death penalty, penalization, modified (1+1)-CMA-ES) sur trois cas tests analytiques:

- Modified Six Hump Camel,
- G04 optimization problem,
- Modified Rosenbrock problem.

La Figure 18.30 illustre la convergence de l'algorithme proposé vers l'optimum pour le problème Modified Six Hump Camel. On constate que l'algorithme converge bien vers l'optimum global, sature des contraintes et que la matrice de covariance s'adapte à la présence des contraintes.
La Figure 18.31 illustre un bilan qualitatif des résultats sur les trois cas tests analytiques (nombre d'évaluations des fonctions, robustesse à l'initialisation, valeur de l'optimum).
Par ailleurs, CMA-ES modifié a été utilisé pour l'optimisation d'un lanceur à propulsion solide bi-étage afin de maximiser l'incrément de poussée fourni par le lanceur. En comparaison des méthodes de références, CMA-ES modifié permet d'obtenir un meilleur incrément de vitesse avec un nombre restreint d'appels aux fonctions objectif et contraintes (voir chapitre 13 pour plus de détails).

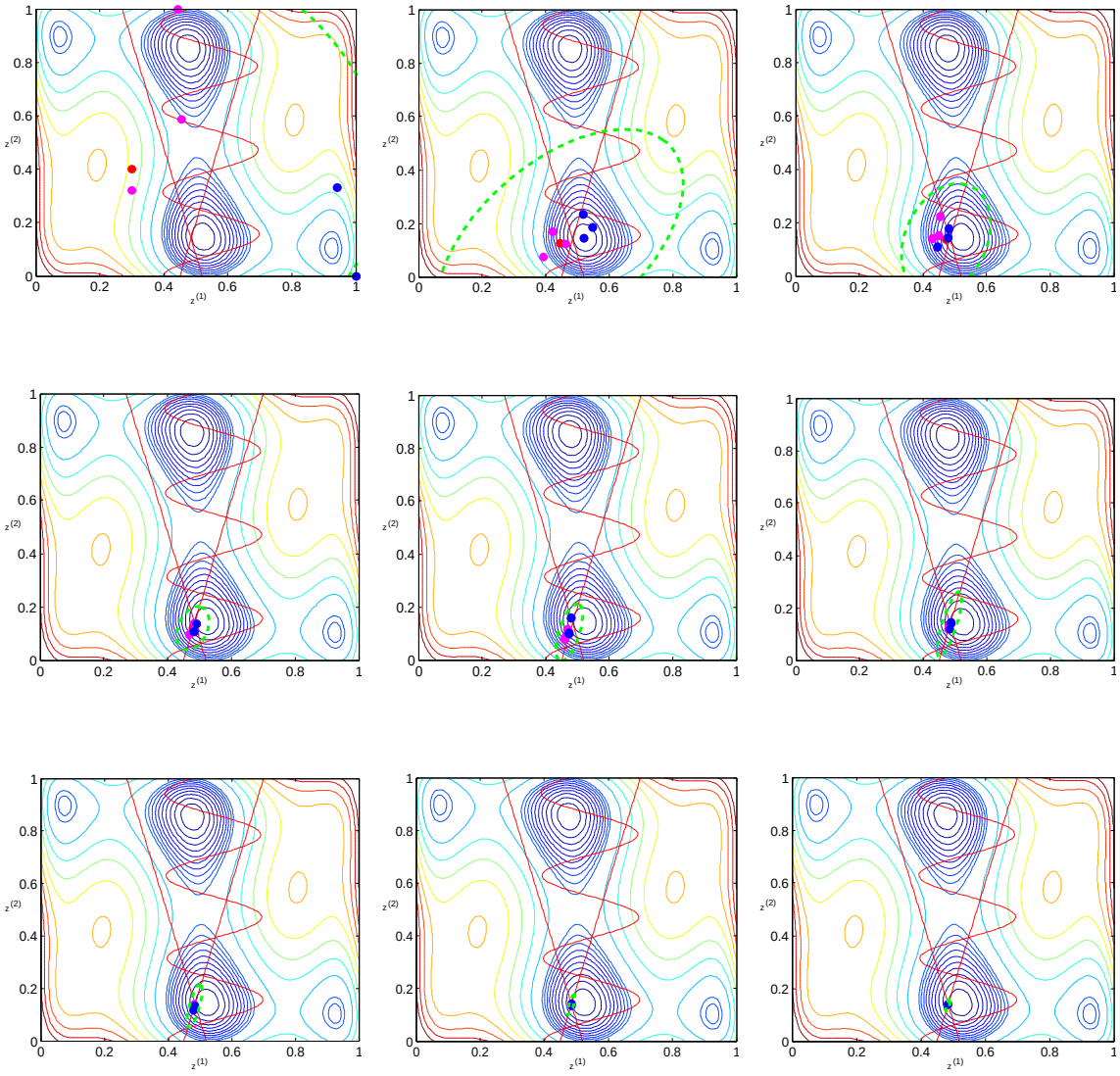

Figure 18.30: Optimisation du problème Modified Six Hump Camel avec l'algorithme proposé, la représentation du volume de recherche paramètré par la matrice de covariance en vert, μ meilleurs candidats en bleu, point moyen en rouge, autres candidats en rose, une figure toutes les 18 itérations.

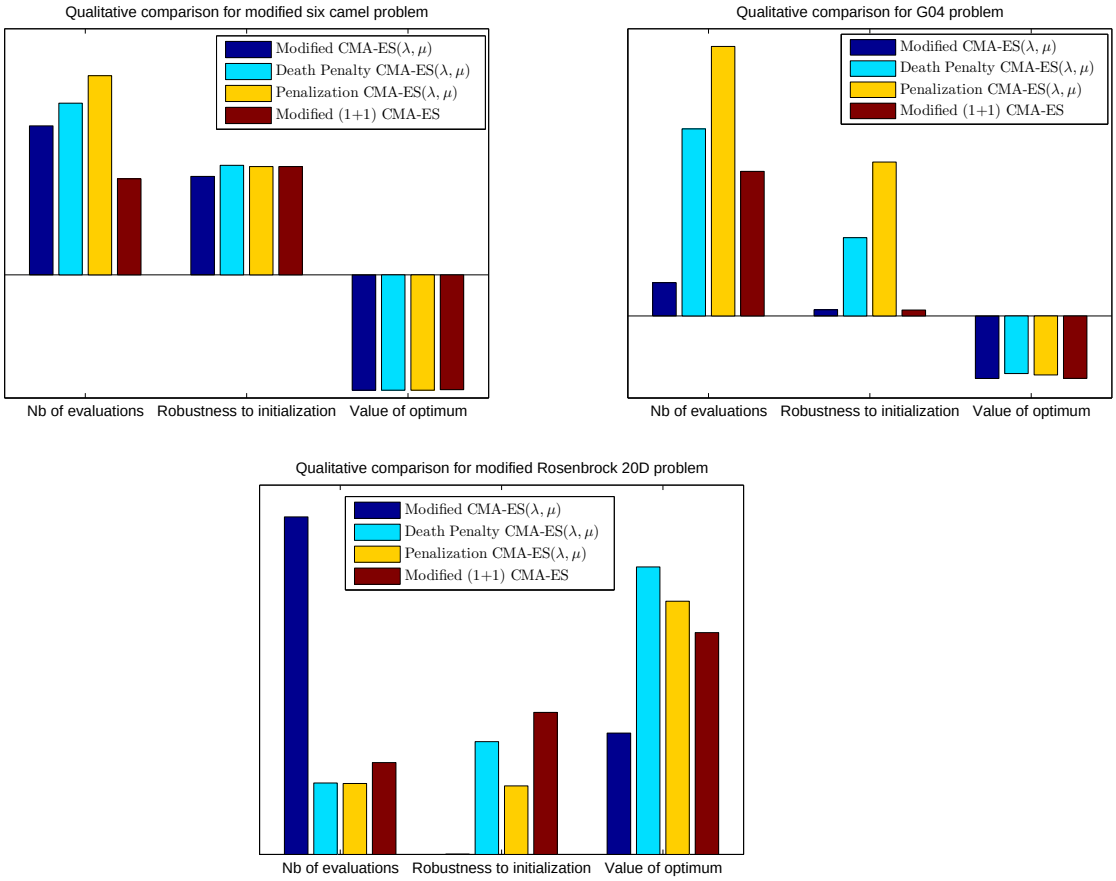

Figure 18.31: Comparaison qualitative pour les cas tests analytiques. Plus la valeur est faible, plus la méthode est performante.

18.5 Conclusion et perspectives

Cette thèse est centrée sur le développement de méthodes MDO en présence d'incertitudes en phase d'avant-projet permettant la conception de systèmes complexes tels que les lanceurs. Les contributions de cette thèse portent sur trois thématiques importantes en UMDO:

1. Tout d'abord, nous avons travaillé sur la satisfaction des couplages interdisciplinaires en présence d'incertitudes pour les formulations UMDO découplées. Les disciplines sont découplées afin de supprimer les analyses multidisciplinaires (MDA) qui requièrent des simulations répétées des disciplines. D'après l'étude des formulations UMDO existantes et leurs gestions des couplages, une nouvelle technique a été proposée afin de satisfaire les couplages quelle que soit la réalisation des variables incertaines. Pour cela, une approche fondée sur un métamodèle paramétrique (polynôme du chaos) des relations de couplage, dont les paramètres sont contrôlés au niveau système par l'optimiseur, a été développée. Le métamodèle est con-

struit tout au long de l'optimisation du système. Grâce à une contrainte de satisfaction des couplages interdisciplinaires, à la convergence du problème d'optimisation, les métamodèles représentent les relations de couplage comme le ferait une analyse multidisciplinaire (MDA) assurant ainsi la faisabilité multidisciplinaire. Cette technique permet la décomposition du processus de conception et ainsi l'évaluation en parallèle des disciplines. Cette approche a été utilisée pour deux formulations UMDO développées: une mono-niveau Individual Discipline Feasible - Polynomial Chaos Expansion (IDF-PCE) et une multi-niveaux Multi-level Hierarchical Optimization under Uncertainty (MHOU). Quatre techniques pour calculer les intégrales multidimensionnelles ont été utilisées: Crude Monte Carlo, les quadratures, les PCE et le Subset Sampling couplé à des Support Vector Machines pour le calcul de probabilités de défaillance.

MHOU est une formulation dérivée de la formulation Stage-Wise decomposition for Optimal Rocket Design exploitant une décomposition transverse du processus de conception des lanceurs en décomposant selon les phases de vol plutôt que par une décomposition par discipline. MHOU est une formulation UMDO permettant une décomposition hiérarchique du problème de conception afin de supprimer les couplages de retour et ainsi les boucles disciplinaires. Cette formulation repose sur un niveau d'optimisation sous-système et d'un niveau d'optimisation système chargé de coordonner le processus de conception et d'assurer la faisabilité multidisciplinaire.

Les deux formulations proposées ont été appliquées et comparées sur des cas tests analytiques et des cas tests de conception de lanceurs. Les approches proposées ont permis d'illustrer leur efficacité par rapport à la méthode de référence MDF. Par ailleurs, les cas test ont mis en avant l'importance de la prise en compte des incertitudes en phase d'avant-projet. Cependant, les études effectuées ont montré que l'utilisation de stratégies découplées pour la conception en présence d'incertitudes rend très complexe la résolution de tels problèmes en comparaison avec les approches déterministes.

2. Dans la seconde partie de cette thèse, deux méthodes d'analyse de fiabilité en présence d'incertitudes aléatoires et épistémiques ont été proposées. En phase d'avant-projet, la présence d'incertitudes épistémiques résulte des méconnaissances, des hypothèses simplificatrices et de l'utilisation de modèles de basse fidélité. Deux types de problèmes ont été considérés: des incertitudes épistémiques sur les hyper-paramètres des PDF caractérisant les incertitudes aléatoires et des incertitudes épistémiques affectant directement l'état limite.

   La première technique combine l'Importance Sampling utilisant la Cross Entropy avec un Krigeage et une stratégie de raffinement du métamodèle. Cette approche permet de calculer les bornes de la probabilité de défaillance impliquant des évènements rares. L'estimation par Cross Entropy a été modifiée afin d'accélérer le calcul de probabilités de défaillance pour une nouvelle valeur des variables épistémiques à partir des calculs précédents. De plus, afin d'assurer l'estimation des bornes de la probabilité de défaillance, une stratégie de raffinement pour avoir un Krigeage précis dans les zones proches du seuil de défaillance et dans les hautes densités de probabilité a été utilisée.

   Pour le deuxième problème, une méthode combinant Subset Simulation, Krigeage et une stratégie de raffinement a été proposée. Afin de tenir compte de la présence à la fois d'incertitudes aléatoires et épistémiques, le Krigeage est construit et raffiné dans l'espace joint incertain pour assurer une estimation précise de la probabilité de défaillance. Par

ailleurs, pour trouver les bornes du domaine de variation de la probabilité de défaillance, un algorithme par gradient a été utilisé et une technique d'estimation du gradient de la probabilité de défaillance par rapport à des variables de décision (comme les variables épistémiques) a été développée. Une expression analytique fondée sur des propriétés de la fonction indicatrice a été proposée avec son implémentation numérique à l'aide de Crude Monte Carlo et Subset Sampling pour estimer le gradient de la probabilité de défaillance. Les deux techniques d'analyse de fiabilité ont été testées sur des cas tests analytiques et deux cas tests de retombée d'étage de lanceurs. Les méthodes proposées ont présenté de meilleurs résultats que les approches de référence (Crude Monte Carlo, FORM). Cependant, en raison de la complexité de mise en œuvre, une implémentation directe pour résoudre des problèmes UMDO nécessite de plus amples investigations.

3. Dans la troisième partie de cette thèse, une modification de l'algorithme d'optimisation évolutionnaire CMA-ES a été proposée afin de gérer les contraintes. Pour résoudre les problèmes de UMDO, les algorithmes d'optimisation doivent pouvoir gérer la présence d'incertitudes et de contraintes. CMA-ES est un algorithme d'optimisation pour des problèmes non contraints et des techniques de pénalisation de la fonction objectif par les contraintes sont souvent utilisées. Une nouvelle approche inspirée d'une méthode pour (1+1)-CMA-ES a été proposée visant à modifier la mise à jour de la matrice de covariance qui paramétrise une distribution Gaussienne utilisée pour générer une population de candidats. Les mécanismes de mise à jour ont été modifiés afin de tenir compte de la violation par certains candidats des contraintes et ainsi de réduire le volume de recherche de solution dans les directions où les candidats violent les contraintes. Cette approche a été testée sur plusieurs cas tests analytiques et sur un cas test de conception de lanceur à propulsion solide illustrant l'efficacité de la méthode de gestion des contraintes proposée par rapport aux approches de référence.

Afin d'améliorer les méthodes UMDO proposées dans cette thèse, plusieurs extensions des travaux peuvent être proposées. Dans cette thèse, des méthodes pour la gestion des couplages interdisciplinaires, pour l'analyse de fiabilité et pour l'optimisation ont été proposées. Il serait utile de les combiner afin de développer une nouvelle formulation UMDO. Cela permettrait de concevoir un lanceur par une stratégie de conception décomposée tout en incluant l'estimation de la probabilité de défaillance pour la retombée d'étages avec les techniques proposées et en optimisant le système avec l'algorithme CMA-ES modifié. Cependant, le coût calculatoire qui serait induit semble trop important à l'heure actuelle et des améliorations des méthodes sont nécessaires pour perfectionner les méthodologies UMDO.

Gestion des couplages interdisciplinaires

Dans cette thèse, aucune MDA n'a été réalisée dans les formulations découplées proposées. Cependant, les méthodes pour gérer les couplages interdisciplinaires ont montré des limitations dans le cas où le nombre de variables incertaines augmente. Une approche hybride permettant la propagation des incertitudes par une approche découplée afin de paralléliser l'évaluation des disciplines et l'utilisation de MDA pour satisfaire le système d'équations interdisciplinaires pourrait être une alternative intéressante. Cela permettrait d'éviter les boucles disciplinaires pour la propagation des incertitudes mais faciliterait la gestion des couplages comme le font certaines formulations MDO déterministes telles que CSSO ou BLISS. De plus, dans cette thèse, les formulations proposées ne permettent que de modéliser les incertitudes à l'aide du formalisme des probabilités. Une extension

afin de gérer d'autres formalismes d'incertitudes (comme la théorie de l'évidence) serait utile pour modéliser les incertitudes avec les informations disponibles.

Analyse de fiabilité
Les techniques proposées sont efficaces en faible dimension mais des difficultés apparaissent en grande dimension. Ainsi, les métamodèles (comme le Krigeage) sont peu performants en grande dimension. Un travail sur des métamodèles et des stratégies de raffinement en grande dimension pour de l'analyse de fiabilité serait intéressant. L'utilisation d'autres métamodèles plus adaptés aux grandes dimensions tels que les Support Vector Regression pourrait être une piste à explorer. Par ailleurs, utiliser des techniques d'analyse de sensibilité des probabilités de défaillance permettrait d'identifier les paramètres les plus influents afin de réduire la dimension du problème d'estimation de probabilité de défaillance. De plus, des travaux sur les formalismes et la modélisation des incertitudes semblent essentiels afin de réaliser des analyses de fiabilité qui soient les plus fidèles possible aux informations disponibles sur les incertitudes.

Optimisation numérique
Enfin, les formulations proposées ont été testées sur des problèmes de conception classiques impliquant des lanceurs consommables sans boosters avec des variables de conception continues. Il serait intéressant d'étendre les techniques existantes à la gestion de variables discrètes (nombre de boosters, nombre d'étages, *etc.*) et catégorielles (type d'ergol, solide, liquide, hybride, type de matériaux, *etc.*). Cela permettrait d'enrichir le type d'architecture de lanceur analysée dans une même étude. De plus, seuls des cas tests avec des problèmes mono-objectifs ont été étudiés. Il serait utile d'élargir les méthodes afin de résoudre des problèmes multi-objectifs (*e.g.* maximisation de la masse de la charge utile tout en minimisant le coût de lancement). Cela offrirait la possibilité d'étudier des familles de lanceurs dédiées à différentes missions (orbites basse, géostationnaire, *etc.*). Enfin, l'utilisation de stratégies multi-fidélité pour contrôler les incertitudes épistémiques introduites lors des phases avant-projet semble être une piste d'exploration intéressante pour résoudre des problèmes UMDO.

List of publications

Book chapters:

- Contribution to two chapters of: An Estimation of rare event probabilities in complex aerospace and other systems, J. Morio, M. Balesdent. Elsevier (August 2015)
  - Chapter 8 : Methods for high dimensional and computationally intensive models,
  - Chapter 10 : Estimation of launch vehicle stage fallout zone.
- Contribution to a chapter of: *Modeling and Optimization in Space Engineering, Vol 2.* Fasano, Giorgio, Pinter, Janos D. (Eds.) (2016)
  - Chapter: Space vehicle design taking into account multidisciplinary design optimization aspects and mixed epistemic / aleatory uncertainties

Publications in international journals:

- *Accepted:*
  - Decoupled MDO formulation for interdisciplinary coupling satisfaction under uncertainty. L. Brevault, M. Balesdent, N. Bérend, R. Le Riche. *AIAA Journal* (Accepted, July 2015)
  - Modified Covariance Matrix Adaptation - Evolution Strategy algorithm for constrained optimization under uncertainty, application to rocket design. R. Chocat, L. Brevault, M. Balesdent, S. Defoort. *International Journal for Simulation and Multidisciplinary Design Optimization* 2015, 6, A1.
  - Probability of failure sensitivity with respect to decision variables. S. Lacaze, L. Brevault, M. Balesdent, S. Missoum. *Structural and Multidisciplinary Optimization*, 52(2):375-381 Springer,
  - Rare Event Probability Estimation in the Presence of Epistemic Uncertainty on Input Probability Distribution Parameters. M. Balesdent, J. Morio, L. Brevault. *Methodology and Computing in Applied Probability* (2014) Springer, published online. DOI : 10.1007/s11009-014-9411-x

Contributions to Uncertainty-based Multidisciplinary Design Optimization, application to launch vehicle design

Publications in international journals:

- *Submitted:*
  - Kriging based sequential reliability analysis in the presence of mixed aleatory and epistemic uncertainties. L. Brevault, S. Lacaze, M. Balesdent, S. Missoum. Submited to *Structural Safety* (Feb. 2015).

Publications in international conferences:

- Multi-level hierarchical MDO formulation with functional coupling satisfaction under uncertainty, application to sounding rocket design. L. Brevault, M. Balesdent, N. Bérend, R. Le Riche. *WCSMO-11*, Sydney, Australia, June 2015. **Early Career Researcher Fellowships award**.
- A Sampling-based RBDO Algorithm with Local Refinement and Efficient Gradient Estimation. S. Lacaze, L. Brevault, S. Missoum, M. Balesdent. *12th International Conference on Applications of Statistics and Probability in Civil Engineering*, Vancouver, Canada, July, 2015.
- Decoupled UMDO formulation for interdisciplinary coupling satisfaction under uncertainty. L. Brevault, M. Balesdent, N. Bérend, R. Le Riche. *15th AIAA/ISSMO Multidisciplinary Analysis and Optimization Conference*, Atlanta, GA, USA, June 2014. **Best student paper award**.
- Challenges and future trends in Uncertainty-Based Multidisciplinary Design Optimization for space transportation system design. L. Brevault, M. Balesdent, N. Bérend, R. Le Riche. *5th EUCASS*, Munich, Germany, May 2013.
- Comparison of different global sensitivity analysis methods for aerospace vehicle optimal design. L. Brevault, M. Balesdent, N. Bérend, R. Le Riche. *WCSMO-10*, Orlando, FL, USA, May 2013.

Bibliography

Ackley, D. H. (1987). *A connectionist machine for genetic hillclimbing*. Kluwer Boston Inc., Hingham, MA. 187

Agarwal, H., Renaud, J. E., Preston, E. L., and Padmanabhan, D. (2004). Uncertainty quantification using evidence theory in multidisciplinary design optimization. *Reliability Engineering & System Safety*, 85(1):281–294. 82

Ahn, J. and Kwon, J. (2006). An efficient strategy for reliability-based multidisciplinary design optimization using bliss. *Structural and Multidisciplinary Optimization*, 31(5):363–372. 90

Alexandrov, N. and Lewis, R. (2000). *Algorithmic Perspectives on Problem Formulations in MDO*. NASA Langley Technical Report Server. 39

Alexandrov, N. M. (1997). Multilevel methods for MDO. *Multidisciplinary Design Optimization: State of the Art*, pages 79–89. 15, 26, 32, 39, 294

Allison, J., Kokkolaras, M., Zawislak, M., and Papalambros, P. Y. (2005). On the use of analytical target cascading and collaborative optimization for complex system design. In *6th World Congress on Structural and Multidisciplinary Optimization, Rio de Janeiro, June 2005*, pages 3091–3100. Citeseer. 33

Andrieu, L., Cohen, G., and Vázquez-Abad, F. J. (2007). Stochastic programming with probability constraints. *arXiv preprint arXiv:0708.0281*. 105, 263

Aoues, Y. and Chateauneuf, A. (2010). Benchmark study of numerical methods for reliability-based design optimization. *Structural and multidisciplinary optimization*, 41(2):277–294. 199

Arnold, D. V. and Hansen, N. (2012). A (1+ 1)-CMA-ES for constrained optimisation. In *Proceedings of the fourteenth international conference on Genetic and evolutionary computation conference, New York, NY, USA*, pages 297–304. ACM. 111, 112, 113, 236, 309, 327

Arras, K. O. (1998). An introduction to error propagation: Derivation, meaning and examples. *Autonomous Systems Lab, Swiss Federal Institute of Technology Lausanne, Tech. Rep. EPFL-ASL-TR-98-01 R*, 3:1998. 56

Arrow, K. J., Hurwicz, L., and Uzawa, H. (1958). Studies in linear and non-linear programming. 105

Askey, R. and Wilson, J. A. (1985). *Some basic hypergeometric orthogonal polynomials that generalize Jacobi polynomials*, volume 319. American Mathematical Soc. 55, 56, 57

Au, S.-K. and Beck, J. L. (2001). Estimation of small failure probabilities in high dimensions by subset simulation. *Probabilistic Engineering Mechanics*, 16(4):263–277. doi:10.1016/S0266-8920(01)00019-4. 68, 129, 178, 201, 207, 305

Audet, C. and Dennis Jr, J. E. (2002). Analysis of generalized pattern searches. *SIAM Journal on Optimization*, 13(3):889–903. 153, 154

Auger, A. and Hansen, N. (2009). Benchmarking the (1+ 1)-CMA-ES on the BBOB-2009 noisy testbed. In *Proceedings of the 11th Annual Conference Companion on Genetic and Evolutionary Computation Conference: Late Breaking Papers*, pages 2467–2472. ACM. 18, 106, 111, 113, 115, 297

Balesdent, M. (2011). *Multidisciplinary design optimization of launch vehicles*. PhD thesis, Ecole Centrale de Nantes. 17, 35, 113

Balesdent, M., Bérend, N., and Dépincé, P. (2012a). Stagewise multidisciplinary design optimization formulation for optimal design of expendable launch vehicles. *Journal of Spacecraft and Rockets*, 49:720–730. 15, 19, 39, 40, 41, 120, 143, 145, 148, 294, 296, 297, 301

Balesdent, M., Bérend, N., Dépincé, P., and Chriette, A. (2012b). A survey of multidisciplinary design optimization methods in launch vehicle design. *Structural and Multidisciplinary Optimization*, 45(5):619–642. 26, 27, 32, 33, 34, 39, 41, 299

Balesdent, M., Morio, J., and Marzat, J. (2013). Kriging-based adaptive importance sampling algorithms for rare event estimation. *Structural Safety*, 44:1–10. 56, 70, 71, 73, 78, 181, 183, 184, 185, 305, 321

Balesdent, M., Morio, J., and Marzat, J. (2015). Recommendations for the tuning of rare event probability estimators. *Reliability Engineering & System Safety*, 133:68–78. doi:10.1016/j.ress.2014.09.001. 68

Balling, R. J. and Sobieszczanski-Sobieski, J. (1996). Optimization of coupled systems-a critical overview of approaches. *AIAA journal*, 34(1):6–17. 15, 30, 32, 33, 34, 36, 39, 294, 300, 301

Basudhar, A. (2011). *Computational optimal design and uncertainty quantification of complex systems using explicit decision boundaries*. PhD thesis, University of Arizona. 76

Basudhar, A., Dribusch, C., Lacaze, S., and Missoum, S. (2012). Constrained efficient global optimization with support vector machines. *Structural and Multidisciplinary Optimization*, 46(2):201–221. doi:10.1007/s00158-011-0745-5. 56, 70, 78

Basudhar, A. and Missoum, S. (2008). Adaptive explicit decision functions for probabilistic design and optimization using support vector machines. *Computers & Structures*, 86(19):1904–1917. 73

Basudhar, A. and Missoum, S. (2010). An improved adaptive sampling scheme for the construction of explicit boundaries. *Structural and Multidisciplinary Optimization*, 42(4):517–529. 73, 76

Baudoui, V. (2012). *Optimisation robuste multiobjectifs par modèles de substitution*. PhD thesis, ISAE-Institut Supérieur de l'Aéronautique et de l'Espace. 59, 81

Baudoui, V., Klotz, P., Hiriart-Urruty, J.-B., Jan, S., and Morel, F. (2012). LOcal Uncertainty Processing (LOUP) method for multidisciplinary robust design optimization. *Structural and Multidisciplinary Optimization*, 46(5):1–16. 71, 305

Bect, J., Ginsbourger, D., Li, L., Picheny, V., and Vazquez, E. (2012a). Sequential design of computer experiments for the estimation of a probability of failure. *Statistics and Computing*, 22(3):773–793. 71, 305

Bect, J., Ginsbourger, D., Li, L., Picheny, V., and Vazquez, E. (2012b). Sequential design of computer experiments for the estimation of a probability of failure. *Statistics and Computing*, 22(3):773–793. 73

Bernardo, J. M. and Smith, A. F. (2009). *Bayesian theory*, volume 405. John Wiley & Sons. 52

Berveiller, M., Sudret, B., and Lemaire, M. (2005). Non linear non intrusive stochastic finite element method-application to a fracture mechanics problem. In *Proc. 9th Int. Conf. Struct. Safety and Reliability (ICOSSAR2005), Rome, Italie*. 77

Berveiller, M., Sudret, B., and Lemaire, M. (2006). Stochastic finite element: a non intrusive approach by regression. *European Journal of Computational Mechanics/Revue Européenne de Mécanique Numérique*, 15(1-3):81–92. 77

Bettis, B. R., Hosder, S., and Winter, T. (2011). Efficient uncertainty quantification in multidisciplinary analysis of a reusable launch vehicle. *17th AIAA International Space Planes and Hypersonic Systems and Technologies Conference, San Francisco, USA, April 2011*. 93

Betts, J. T. (1998). Survey of numerical methods for trajectory optimization. *Journal of guidance, control, and dynamics*, 21(2):193–207. 289

Beyer, H.-G. and Finck, S. (2012). On the design of constraint Covariance Matrix self-Adaptation Evolution Strategies including a cardinality constraint. *Evolutionary Computation, IEEE Transactions on*, 16(4):578–596. 111, 309

Bianchi, L., Dorigo, M., Gambardella, L. M., and Gutjahr, W. J. (2009). A survey on metaheuristics for stochastic combinatorial optimization. *Natural Computing: an international journal*, 8(2):239–287. 109

Bichon, B. J., Eldred, M. S., Swiler, L. P., Mahadevan, S., and McFarland, J. M. (2008a). Efficient global reliability analysis for nonlinear implicit performance functions. *AIAA journal*, 46(10):2459–2468. doi:10.2514/1.34321. 69

Bichon, B. J., Eldred, M. S., Swiler, L. P., Mahadevan, S., and McFarland, J. M. (2008b). Efficient global reliability analysis for nonlinear implicit performance functions. *AIAA journal*, 46(10):2459–2468. 73

Birattari, M., Balaprakash, P., and Dorigo, M. (2005). Aco/f-race: Ant colony optimization and racing techniques for combinatorial optimization under uncertainty. In *MIC 2005: The 6th Metaheuristics International Conference*, pages 107–112. Vienna, Austria. 109

Bjerager, P. (1990). On computation methods for structural reliability analysis. *Structural Safety*, 9(2):79–96. 62, 296, 305

Blair, J., Ryan, R., and Schutzenhofer, L. (2001). *Launch vehicle design process: characterization, technical integration, and lessons learned*. NASA, Langley Research Center. 13, 15, 16

Blake, W. B. (1998). Missile datcom: User's manual-1997 fortran 90 revision. Technical report, DTIC Document. 153, 287

Blatman, G. and Sudret, B. (2008). Sparse polynomial chaos expansions and adaptive stochastic finite elements using a regression approach. *Comptes Rendus Mécanique*, 336(6):518–523. 77

Blatman, G. and Sudret, B. (2011). Adaptive sparse polynomial chaos expansion based on least angle regression. *Journal of Computational Physics*, 230(6):2345–2367. 77, 143

Boer, P. T. D., Kroese, D. P., Mannor, S., and Rubinstein, R. Y. (2005). A tutorial on the cross-entropy method. *Annals of Operations Research*, 134(1):19–67. 180

Bouchon-Meunier, B. and Nguyen, H. T. (1996). *Les incertitudes dans les systèmes intelligents*. Presses universitaires de France. 46

Bourinet, J.-M., Deheeger, F., and Lemaire, M. (2011a). Assessing small failure probabilities by combined subset simulation and support vector machines. *Structural Safety*, 33(6):343–353. doi:10.1016/j.strusafe.2011.06.001. 70, 78

Bourinet, J.-M., Deheeger, F., and Lemaire, M. (2011b). Assessing small failure probabilities by combined subset simulation and support vector machines. *Structural Safety*, 33(6):343–353. 73, 76

Branke, J. and Schmidt, C. (2003). Selection in the presence of noise. In *Genetic and Evolutionary Computation Conference Chicago, IL, USA*. 104, 105, 308

Braun, R. and Kroo, I. (1995). Development and application of the collaborative optimization architecture in a multidisciplinary design environment. *Multidisciplinary Design Optimization: State of the Art*, 80:98. 40

Braun, R., Moore, A., and Kroo, I. (1996). Use of the collaborative optimization architecture for launch vehicle design. In *6th Symposium on Multidisciplinary Analysis and Optimization, Bellevue, USA, Sept. 1996*, pages 306–318. 33, 39, 87, 301

Braun, R. D. (1996). *Collaborative optimization: an architecture for large-scale distributed design*. PhD thesis. 26, 39, 40

Breitkopf, P. and Coelho, R. F. (2013). *Multidisciplinary design optimization in computational Mechanics*. John Wiley & Sons. 26, 30, 32, 39, 40, 106, 110, 113

Breitung, K. (1984). Asymptotic approximations for multinormal integrals. *Journal of Engineering Mechanics*, 110(3):357–366. 63

Brown, N. F. and Olds, J. R. (2006). Evaluation of multidisciplinary optimization techniques applied to a reusable launch vehicle. *Journal of Spacecraft and Rockets*, 43(6):1289–1300. 39, 40

Bruns, M. C. (2006). *Propagation of imprecise probabilities through black box models*. PhD thesis, Georgia Institute of Technology. 60

Bucklew, J. A. (2004). *Introduction to Rare Event Simulation*. Springer, New York, USA. 65

Castellini, F. (2012). *Multidisciplinary design optimization for expendable launch vehicles*. PhD thesis, Politecnico de Milano. 41, 150, 153, 164, 256, 273, 274, 275, 279, 282, 287, 288

Charania, A., Bradford, J. E., Olds, J. R., and Graham, M. (2002). System level uncertainty assessment for collaborative RLV design. In *2002 JANNNAF, Destin, USA, April 2002*. 93

Chiralaksanakul, A. and Mahadevan, S. (2007). Decoupled approach to multidisciplinary design optimization under uncertainty. *Optimization and Engineering*, 8(1):21–42. 90

Choi, K. K., Du, L., and Youn, B. D. (2005). Integration of reliability-and possibility-based design optimizations using performance measure approach. Technical report, SAE Technical Paper. 47

Choi, S.-K., Grandhi, R. V., and Canfield, R. A. (2004). Structural reliability under non-gaussian stochastic behavior. *Computers & structures*, 82(13):1113–1121. 77

Choudhary, R., Malkawi, A., and Papalambros, P. (2005). Analytic target cascading in simulation-based building design. *Automation in construction*, 14(4):551–568. 26

Clarke, S. M., Griebsch, J. H., and Simpson, T. W. (2005). Analysis of support vector regression for approximation of complex engineering analyses. *Journal of mechanical design*, 127(6):1077–1087. 73

Coelho, R. F., Breitkopf, P., Knopf-Lenoir, C., and Villon, P. (2009). Bi-level model reduction for coupled problems. *Structural and Multidisciplinary Optimization*, 39(4):401–418. 28, 30, 300

Coello, C. A. (2000). Constraint-handling using an evolutionary multiobjective optimization technique. *Civil Engineering Systems*, 17(4):319–346. 108

Collange, G., Delattre, N., Hansen, N., Quinquis, I., and Schoenauer, M. (2010a). Multidisciplinary optimization in the design of future space launchers. *Multidisciplinary Design Optimization in Computational Mechanics*, pages 459–468. 18, 111, 115, 297

Collange, G., Reynaud, S., and Hansen, N. (2010b). Covariance matrix adaptation evolution strategy for multidisciplinary optimization of expendable launcher family. In *13th AIAA/ISSMO Multidisciplinary Analysis Optimization Conference. Fort-Worth, TX*. 108, 111, 236, 309

Conn, A. R., Gould, N. I., and Toint, P. L. (2000). *Trust region methods*, volume 1. Siam. 37

Cormier, T., Scott, A., Ledsinger, L., McCormick, D., Way, D., and Olds, J. (Sept. 2000). Comparison of collaborative optimization to conventional design techniques for a conceptual rlv. In *8th AIAA/ISSMO Multidisciplinary Analysis and Optimization Conference, Long Beach, California, USA*. 40

Corne, D., Dorigo, M., and Glover, F. (1999). The ant colony optimization meta-heuristic. *New Ideas in Optimization. McGraw Hill, New York*. 107

Cornford, D., Csató, L., and Opper, M. (2005). Sequential, bayesian geostatistics: a principled method for large data sets. *Geographical Analysis*, 37(2):183–199. 184

Cramer, E. J., Dennis, Jr, J., Frank, P. D., Lewis, R. M., and Shubin, G. R. (1994). Problem formulation for multidisciplinary optimization. *SIAM Journal on Optimization*, 4(4):754–776. 15, 34, 36, 294

Cristianini, N. and Shawe-Taylor, J. (2000). *An introduction to support vector machines and other kernel-based learning methods*. Cambridge university press, New York, USA. 73

Culioli, J.-C. and Cohen, G. (1995). Stochastic optimization subject to expectation constraints. *Comptes rendus de l'Academie des sciences. Serie 1, Mathematique.*, 320(6):753–756. 105

Davis, P. J. and Rabinowitz, P. (2007). *Methods of numerical integration*. Courier Dover Publications. 54, 55, 56, 126

de Mello, T. H. and Rubinstein, R. Y. (2002). *Rare event estimation for static models via cross-entropy and importance sampling*. John Wiley, New York, USA. 66

De Melo, V. V. and Iacca, G. (2014). A modified Covariance Matrix Adaptation Evolution Strategy with adaptive penalty function and restart for constrained optimization. *Expert Systems with Applications*, 41(16):7077–7094. 106, 108, 111, 236, 309

Deheeger, F. and Lemaire, M. (2007). Support vector machine for efficient subset simulations: 2SMART method. In *10th International Conference on Application of Statistics and Probability in Civil Engineering, Proceedings and Monographs in Engineering, Water and Earth Sciences*, pages 259–260. 76, 209

DeMiguel, A.-V. and Murray, W. (2000). An analysis of collaborative optimization methods. In *Proceedings of the 8th AIAA/USAF/NASA/ISSMO symposium on multidisciplinary analysis and optimization, AIAA paper*, volume 4720. 34

DeMiguel, V. and Murray, W. (2006). A local convergence analysis of bilevel decomposition algorithms. *Optimization and Engineering*, 7(2):99–133. 39

Dempster, A. P. (1967). Upper and lower probabilities induced by a multivalued mapping. *The annals of mathematical statistics*, 38(2):325–339. 47, 81, 96, 302

Der Kiureghian, A. and Dakessian, T. (1998). Multiple design points in first and second-order reliability. *Structural Safety*, 20(1):37–49. 64

Devolder, O., Glineur, F., and Nesterov, Y. (2010). Solving infinite-dimensional optimization problems by polynomial approximation. pages 31–40. 122

Ditlevsen, O. and Madsen, H. O. (1996). *Structural reliability methods*, volume 178. Wiley New York. 63

Dorigo, M. and Birattari, M. (2010). Ant colony optimization. In *Encyclopedia of Machine Learning*, pages 36–39. Springer. 106, 107, 108, 308

Du, X. (2008). Unified uncertainty analysis by the first order reliability method. *Journal of mechanical design*, 130:091401. doi:10.1115/1.2943295. 18, 100, 211, 307

Du, X. and Chen, W. (2001). A hierarchical approach to collaborative multidisciplinary robust design. *Department of Mechanical Engineering, University of Illinois at Chicago*. 17, 87, 88, 120, 295, 296, 304

Du, X. and Chen, W. (2002). Efficient uncertainty analysis methods for multidisciplinary robust design. *AIAA journal*, 40(3):545–552. 84, 85, 86, 120, 304

Du, X. and Chen, W. (2004). Sequential optimization and reliability assessment method for efficient probabilistic design. *Journal of Mechanical Design*, 126:225. 89

Du, X. et al. (2002). *Efficient methods for engineering design under uncertainty*. PhD thesis, Graduate College, University of Illinois at Chicago. 84, 86, 120, 304

Du, X., Guo, J., and Beeram, H. (2008). Sequential optimization and reliability assessment for multidisciplinary systems design. *Structural and Multidisciplinary Optimization*, 35(2):117–130. 17, 18, 81, 84, 89, 90, 120, 295, 296, 305

Du, X., Sudjianto, A., and Huang, B. (2005). Reliability-based design with the mixture of random and interval variables. *Journal of mechanical design*, 127(6):1068–1076. doi:10.1115/1.1992510. 18, 51, 99, 211, 307

Duan, K.-B. and Keerthi, S. S. (2005). Which is the best multiclass svm method? an empirical study. In *Multiple Classifier Systems*, pages 278–285. Springer. 73

Dubourg, V. (2011a). *Adaptive surrogate models for reliability analysis and reliability-based design optimization*. PhD thesis, Université Blaise Pascal-Clermont-Ferrand II. 73

Dubourg, V. (2011b). *Méta-modèles adaptatifs pour l'analyse de fiabilité et l'optimisation sous contrainte fiabiliste*. PhD thesis, Université Blaise Pascal-Clermont-Ferrand II. 64

Dubourg, V., Sudret, B., and Bourinet, J.-M. (2011). Reliability-based design optimization using kriging surrogates and subset simulation. *Structural and Multidisciplinary Optimization*, 44(5):673–690. doi: 10.1007/s00158-011-0653-8. 69, 199, 209

Dubourg, V., Sudret, B., and Deheeger, F. (2013). Metamodel-based importance sampling for structural reliability analysis. *Probabilistic Engineering Mechanics*. doi:10.1016/j.probengmech.2013.02.002. 69, 71, 91, 129, 305

Eberhart, R. C. and Kennedy, J. (1995). A new optimizer using particle swarm theory. In *Proceedings of the sixth international symposium on micro machine and human science*, volume 1, pages 39–43. New York, NY. 76, 106, 108, 308

Echard, B. (2012). *Kriging-based reliability assessment of structures submitted to fatigue*. PhD thesis, Université Blaise Pascal. 72

Echard, B., Gayton, N., and Lemaire, M. (2011). AK-MCS : An active learning reliability method combining Kriging and Monte Carlo Simulation. *Structural Safety*, 33:145–154. 71, 305

Efron, B., Hastie, T., Johnstone, I., Tibshirani, R., et al. (2004). Least angle regression. *The Annals of statistics*, 32(2):407–499. 143

El Majd, B. A., Desideri, J.-A., and Habbal, A. (2010). Optimisation de forme fluide-structure par un jeu de nash. *Revue Africaine de la Recherche en Informatique et Mathématiques Appliquées*, (13):3–15. 28

Eldred, M. (2009). Recent advances in non-intrusive polynomial chaos and stochastic collocation methods for uncertainty analysis and design. In *AIAA Structures, Structural Dynamics, and Materials Conference, Palm Springs, CA*. 55, 56, 57, 123, 126, 312

Eldred, M. and Burkardt, J. (2009). Comparison of non-intrusive polynomial chaos and stochastic collocation methods for uncertainty quantification. In *Proceedings of the 47th AIAA Aerospace Sciences Meeting and Exhibit, number AIAA-2009-0976, Orlando, FL*, volume 123, page 124. 57, 58

Engelund, S. and Rackwitz, R. (1993). A benchmark study on importance sampling techniques in structural reliability. *Structural Safety*, 12(4):255–276. 64, 305

Faravelli, L. (1989). Response-surface approach for reliability analysis. *Journal of Engineering Mechanics*, 115(12):2763–2781. 70

Felippa, C. A., Park, K., and Farhat, C. (2001). Partitioned analysis of coupled mechanical systems. *Computer methods in applied mechanics and engineering*, 190(24):3247–3270. 31

Ferson, S., Ginzburg, L., and Akcakaya, R. (1996). Whereof one cannot speak: when input distributions are unknown. *Risk Analysis (to appear)*. 47

Ferson, S., Kreinovich, V., Ginzburg, L., Myers, D. S., and Sentz, K. (2002). *Constructing probability boxes and Dempster-Shafer structures*, volume 835. Sandia National Laboratories. 98

Ferson, S., Kreinovich, V., Hajagos, J., Oberkampf, W., and Ginzburg, L. (2007). *Experimental uncertainty estimation and statistics for data having interval uncertainty*. 51, 52

Gang, C., Zi-Ming, W., Min, X., and Si-Lu, C. (2005). Genetic algorithm optimization of rlv reentry trajectory. *Proceedings of the AIAA/CIRA 13th International Space Planes and Hypersonic Systems and Technologies AIAA-2005-3269*. 39, 40

Gao, J. B., Gunn, S. R., Harris, C. J., and Brown, M. (2002). A probabilistic framework for svm regression and error bar estimation. *Machine Learning*, 46(1-3):71–89. 73

Gardner, W. A. (1984). Learning characteristics of stochastic-gradient-descent algorithms: A general study, analysis, and critique. *Signal Processing*, 6(2):113–133. 18, 105

Ghosh, S., Lee, C. H., and Mavris, D. N. (June 2014). Covariance matching collaborative optimization for uncertainty-based multidisciplinary aircraft design. *15th AIAA/ISSMO Multidisciplinary Analysis and Optimization Conference, Atlanta, USA, June 2015*. 17, 83, 87, 88, 295, 296, 304

Giassi, A., Bennis, F., and Maisonneuve, J.-J. (2004). Multidisciplinary design optimisation and robust design approaches applied to concurrent design. *Structural and Multidisciplinary Optimization*, 28(5):356–371. 81

Gomes, H. and Awruch, A. (2004). Comparison of response surface and neural network with other methods for structural reliability analysis. *Structural Safety*, 26:49–67. 192

Gordon, S. and McBride, B. J. (1996). *Computer program for calculation of complex chemical equilibrium compositions and applications*. NASA. 150, 152, 281

Gutjahr, W. J. (2003). *A converging ACO algorithm for stochastic combinatorial optimization*. Springer. 109

Gutjahr, W. J. (2004). *S-ACO: An ant-based approach to combinatorial optimization under uncertainty*. Springer. 109

Haftka, R. T. and Watson, L. T. (2005). Multidisciplinary design optimization with quasiseparable subsystems. *Optimization and Engineering*, 6(1):9–20. 33

Hansen, E. and Walster, G. W. (2003). *Global optimization using interval analysis: revised and expanded*, volume 264. CRC Press. 60

Hansen, N. (2009). Benchmarking a BI-population CMA-ES on the BBOB-2009 noisy testbed. In *Proceedings of the 11th Annual Conference Companion on Genetic and Evolutionary Computation Conference: Late Breaking Papers, Montreal, Québec, Canada, 2009*, pages 2397–2402. ACM. 18, 106, 109, 111, 113, 181, 236, 241, 242, 247, 297, 308

Hansen, N., Auger, A., Ros, R., Finck, S., and Pošík, P. (2010). Comparing results of 31 algorithms from the black-box optimization benchmarking BBOB-2009. In *Proceedings of the 12th annual conference companion on Genetic and evolutionary computation*, pages 1689–1696. ACM. 109, 308

Hansen, N., Müller, S., and Koumoutsakos, P. (2003). Reducing the time complexity of the derandomized Evolution Strategy with Covariance Matrix Adaptation (CMA-ES). *Evolutionary Computation*, 11(1):1–18. 18, 104, 105, 106, 109, 110, 236, 241, 262, 296, 308, 327

Hansen, N., Niederberger, A. S., Guzzella, L., and Koumoutsakos, P. (2009). A method for handling uncertainty in evolutionary optimization with an application to feedback control of combustion. *Evolutionary Computation, IEEE Transactions on*, 13(1):180–197. 111, 309

Hartfield, R., Jenkins, R., Burkhalter, J., and Foster, W. (2003). A review of analytical methods for solid rocket motor grain analysis. *AIAA Paper*, 4506:2003. 282

Hasofer, A. M. and Lind, N. C. (1974). Exact and invariant second-moment code format. *Journal of the Engineering Mechanics division*, 100(1):111–121. 63

Hastings, W. K. (1970). Monte Carlo sampling methods using markov chains and their applications. *Biometrika*, 57(1):97–109. 68

Helton, J. C. and Davis, F. J. (2003). Latin hypercube sampling and the propagation of uncertainty in analyses of complex systems. *Reliability Engineering & System Safety*, 81(1):23–69. 54

Helton, J. C., Johnson, J. D., and Oberkampf, W. L. (2004). An exploration of alternative approaches to the representation of uncertainty in model predictions. *Reliability Engineering & System Safety*, 85(1):39–71. doi:10.1016/j.ress.2004.03.025. 47

Henderson, R., Martins, J.R.R.A, and Perez, R. (2012). Aircraft conceptual design for optimal environmental performance. *Aeronautical Journal*, 116(1175):1. 26

Hirmajer, T., Balsa-Canto, E., and Banga, J. (2008). Dotcvp: Dynamic optimization toolbox with cvp approach for handling continuous and mixed-integer do problems. *Technical report*. 132

Holland, J. H. (1975). *Adaptation in natural and artificial systems: An introductory analysis with applications to biology, control, and artificial intelligence*. University of Michigan Press. 106, 108, 308

Hosder, S. (2012). Stochastic response surfaces based on non–intrusive polynomial chaos for uncertainty quantification. *International Journal of Mathematical Modelling and Numerical Optimisation*, 3(1):117–139. 56, 312

Hu, C. and Youn, B. D. (2011). Adaptive-sparse polynomial chaos expansion for reliability analysis and design of complex engineering systems. *Structural and Multidisciplinary Optimization*, 43(3):419–442. 77

Huang, H., An, H., Wu, W., Zhang, L., Wu, B., and Li, W. (2014). Multidisciplinary design modeling and optimizationfor satellite with maneuver capability. *Structural and Multidisciplinary Optimization*, 50(5):883–898. 26

Huang, H.-Z., Yu, H., Zhang, X., Zeng, S., and Wang, Z. (2010). Collaborative optimization with inverse reliability for multidisciplinary systems uncertainty analysis. *Engineering Optimization*, 42(8):763–773. 88

Humble, R. W., Henry, G. N., Larson, W. J., et al. (1995). *Space propulsion analysis and design*, volume 1. McGraw-Hill New York. 256, 278

Hurtado, J. E. (2004a). An examination of methods for approximating implicit limit state functions from the viewpoint of statistical learning theory. *Structural Safety*, 26(3):271–293. doi:10.1016/j.strusafe.2003.05.002. 56, 70

Hurtado, J. E. (2004b). An examination of methods for approximating implicit limit state functions from the viewpoint of statistical learning theory. *Structural Safety*, 26(3):271–293. 73

Hurtado, J. E. (2013). Assessment of reliability intervals under input distributions with uncertain parameters. *Probabilistic Engineering Mechanics*, 32:80–92. 98

Hurtado, J. E. and Alvarez, D. A. (2001). Neural-network-based reliability analysis: a comparative study. *Computer methods in applied mechanics and engineering*, 191(1):113–132. doi:10.1016/S0045-7825(01)00248-1. 70

Hurtado, J. E. and Alvarez, D. A. (2010). An optimization method for learning statistical classifiers in structural reliability. *Probabilistic Engineering Mechanics*, 25(1):26 – 34. 76

Hwang, J. T., Lee, D. Y., Cutler, J. W., and Martins, J.R.R.A (2013). Large-scale MDA of a small satellite using a novel framework for the solution of coupled systems and their derivatives. In *Proceedings of the 54th AIAA/ASME/ASCE/AHS/ASC Structures, Structural Dynamics, and Materials Conference*. 26

Jaeger, L., Gogu, C., Segonds, S., and Bes, C. (2013). Aircraft multidisciplinary design optimization under both model and design variables uncertainty. *Journal of Aircraft*, pages 1–11. 13, 17, 83, 294, 303

Jaeger, L., Segonds, S., and Bes, C. (2015). Methodology based on multiagent for solving multidisciplinary optimization problem under uncertainty. *Journal of Aerospace Information Systems*, 12(2):290–298. 106, 263

Janusevskis, J. and Le Riche, R. (2013). Simultaneous kriging-based estimation and optimization of mean response. *Journal of Global Optimization*, 55(2):313–336. 184

Jiang, C., Han, X., Li, W., Liu, J., and Zhang, Z. (2012). A hybrid reliability approach based on probability and interval for uncertain structures. *Journal of Mechanical Design*, 134(3):031001. doi:10.1115/1.4005595. 100

Jin, Y. (2005). A comprehensive survey of fitness approximation in evolutionary computation. *Soft computing*, 9(1):3–12. 105, 308

Jin, Y. and Branke, J. (2005). Evolutionary optimization in uncertain environments-a survey. *Evolutionary Computation, IEEE Transactions on*, 9(3):303–317. 18, 104, 105, 296, 308

Jones, D. R., Schonlau, M., and Welch, W. J. (1998). Efficient global optimization of expensive black-box functions. *Journal of Global optimization*, 13(4):455–492. doi:10.1023/A:1008306431147. 101

Jones, D. S. (1982). *The Theory of Generalised Functions*. Cambridge University Press. Cambridge Books Online. 200

Karaboga, D. (2005). An idea based on honey bee swarm for numerical optimization. Technical report, Technical report-tr06, Erciyes university, engineering faculty, computer engineering department. 106

Kaymaz, I. (2005). Application of kriging method to structural reliability problems. *Structural Safety*, 27(2):133–151. 70, 78

Keane, A. and Nair, P. (2005). *Computational approaches for aerospace design: the pursuit of excellence*. Wiley & Sons. 31

Kennedy, G.J. and Martins, J.R.R.A (2014). A parallel aerostructural optimization framework for aircraft design studies. *Structural and Multidisciplinary Optimization*, 50(6):1079–1101. 28

Kenway, G.K.W., Kennedy, G.J., and Martins, J.R.R.A (2014). Scalable parallel approach for high-fidelity steady-state aeroelastic analysis and adjoint derivative computations. *AIAA journal*, 52(5):935–951. 26, 28

Kiefer, J., Wolfowitz, J., et al. (1952). Stochastic estimation of the maximum of a regression function. *The Annals of Mathematical Statistics*, 23(3):462–466. 18, 105

King, J. M., Grandhi, R. V., and Benanzer, T. W. (2012). Quantification of epistemic uncertainty in re-usable launch vehicle aero-elastic design. *Engineering Optimization*, 44(4):489–504. 93

Kiureghian, A. D. and Ditlevsen, O. (2009). Aleatory or epistemic? does it matter? *Structural Safety*, 31(2):105–112. doi:10.1016/j.strusafe.2008.06.020. 46

Klir, G. J. (2005). *Uncertainty and information: foundations of generalized information theory*. Wiley-Interscience. 46, 47, 52

Koch, P. N., Wujek, B., Golovidov, O., and Simpson, T. W. (2002). Facilitating probabilistic multidisciplinary design optimization using kriging approximation models. In *9th AIAA/ISSMO Symposium on Multidisciplinary Analysis & Optimization (September 2002). AIAA paper*, volume 5415. 17, 83, 303

Kolmogorov, A. (1950). *Foundations of the Theory of Probability*. Chelsea, New York. First published in German in 1933. 47, 48

Kramer, O., Barthelmes, A., and Rudolph, G. (2009). Surrogate constraint functions for CMA Evolution Strategies. In *KI 2009: Advances in Artificial Intelligence*, pages 169–176. Springer. 108, 309

Krause, P. and Clark, D. (1993). *Representing uncertain knowledge: an artificial intelligence approach*. Kluwer Academic Publishers. 46

Kreinovich, V. and Ferson, S. A. (2004). A new cauchy-based black-box technique for uncertainty in risk analysis. *Reliability Engineering & System Safety*, 85(1):267–279. 59

Kroese, D. P. and Rubinstein, R. Y. (2012a). Monte carlo methods. *Wiley Interdisciplinary Reviews: Computational Statistics*, 4(1):48–58. 62

Kroese, D. P. and Rubinstein, R. Y. (2012b). Monte-Carlo methods. *Wiley Interdisciplinary Reviews: Computational Statistics*, 4(1):48–58. 64, 305

Kroo, I. (1997). MDO for large-scale design. *Multidisciplinary design optimization: state-of-the-art. SIAM, Philadelphia*, pages 22–44. 15, 294

Kuo, K. K., Summerfield, M., et al. (1984). *Fundamentals of solid-propellant combustion*, volume 90. American Institute of Aeronautics and Astronautics New York. 223

Kurtz, N. and Song, J. (2013). Cross-entropy-based adaptive importance sampling using gaussian mixture. *Structural Safety*, 42:35–44. 193

Kuschel, N. and Rackwitz, R. (1997). Two basic problems in reliability-based structural optimization. *Mathematical Methods of Operations Research*, 46(3):309–333. 129

Lacaze, S., Brevault, L., Missoum, S., and Balesdent, M. (2015). Probability of failure sensitivity with respect to decision variables. *Structural and Multidisciplinary Optimization*, 52(2):375–381. 211

Lacaze, S. and Missoum, S. (2014a). A generalized max-min sample for surrogate update. *Structural and Multidisciplinary Optimization*, 49(4):683–687. 76, 323

Lacaze, S. and Missoum, S. (2014b). A generalized max-min sample for surrogate update. *Structural and Multidisciplinary Optimization*, 49(4):683–687. doi:10.1007/s00158-013-1011-9. 129, 198, 207, 209

Larson, J. M. (2012). *Derivative free optimization of noisy functions*. PhD thesis, University of Colorado. 106, 132

L'Ecuyer, P., Mandjes, M., and Tuffin, B. (2009). Importance sampling in rare event simulation. In Rubino, G. and Tuffin, B., editors, *Rare Event Simulation using Monte Carlo Methods*, pages 17–38. John Wiley & Sons, Ltd. 64, 305

Lee, I., Choi, K. K., and Zhao, L. (2011). Sampling-based rbdo using the stochastic sensitivity analysis and dynamic kriging method. *Structural and Multidisciplinary Optimization*, 44(3):299–317. 199

Li, H.-s., Lü, Z.-z., and Yue, Z.-f. (2006). Support vector machine for structural reliability analysis. *Applied Mathematics and Mechanics*, 27:1295–1303. 75

Li, L., Bect, J., and Vazquez, E. (2010a). A numerical comparison of two sequential Kriging-based algorithms to estimate a probability of failure. In *Uncertainty in Computer Model Conference, Sheffield, UK, July, 12-14, 2010*. 71

Li, L., Bect, J., and Vazquez, E. (2012). Bayesian Subset Simulation: a Kriging-based subset simulation algorithm for the estimation of small probabilities of failure. In *Proceedings of PSAM 11 and ESREL 2012, 25-29 June 2012, Helsinki, Finland*. 71, 305

Li, L., Jing, S., and Liu, J. (2010b). A hierarchical hybrid strategy for reliability analysis of multidisciplinary design optimization. In *Computer Supported Cooperative Work in Design (CSCWD), 2010 14th International Conference on*, pages 525–530. IEEE. 90

Li, L., Liu, J. H., and Liu, S. (2013). An efficient strategy for multidisciplinary reliability design and optimization based on csso and pma in sora framework. *Structural and Multidisciplinary Optimization*, pages 1–14. 90

Lin, P. T. and Gea, H. C. (2013). Reliability-based multidisciplinary design optimization using probabilistic gradient-based transformation method. *Journal of Mechanical Design*, 135(2):021001. 129

Liu, H., Chen, W., Kokkolaras, M., Papalambros, P. Y., and Kim, H. M. (2006). Probabilistic analytical target cascading: a moment matching formulation for multilevel optimization under uncertainty. *Journal of Mechanical Design*, 128(2):991–1000. 83, 87, 88, 120, 129, 304

Madsen, H. (1986). *0., Krenk, S. and Lind, NC Methods of Structural Safety*. Prentice-Hall. 62, 296, 305

Mahadevan, S. (2000). *Probability, reliability, and statistical methods in engineering design*. Wiley. 84

Martins, J.R.R.A and Lambe, A. (2013). Multidisciplinary design optimization: a survey of architectures. *AIAA journal*, 51(9):2049–2075. 15, 32, 34, 39, 294

Matheron, G. (1963). Principles of geostatistics. *Economic geology*, 58(8):1246–1266. doi:10.2113/gsecongeo.58.8.1246. 70, 178, 183, 320

McAllister, C. D. and Simpson, T. W. (2003). Multidisciplinary robust design optimization of an internal combustion engine. *Journal of mechanical design*, 125(1):124–130. 26, 83, 87, 304

McCormick, D. J. (2001). *Distributed uncertainty analysis techniques for conceptual launch vehicle design*. PhD thesis, Georgia Institute of Technology. 93

Melchers, R. (1989). Importance sampling in structural systems. *Structural safety*, 6(1):3–10. 129

Metropolis, N., Rosenbluth, A. W., Rosenbluth, M. N., Teller, A. H., and Teller, E. (1953). Equation of state calculations by fast computing machines. *The journal of chemical physics*, 21(6):1087–1092. 68

Mezura-Montes, E. and Coello, C. A. (2011). Constraint-handling in nature-inspired numerical optimization: past, present and future. *Swarm and Evolutionary Computation*, 1(4):173–194. 108

Moore, R. E., Kearfott, R. B., and Cloud, M. J. (2009). *Introduction to interval analysis*. Siam. 47, 52, 81, 302

Morio, J. (2012). Extreme quantile estimation with nonparametric adaptive importance sampling. *Simulation Modelling Practice and Theory*, 27:76–89. 67, 68

Morio, J. and Balesdent, M. (2015). *Estimation of Rare Event Probabilities In Complex Aerospace And Other Systems*. Elsevier. 62, 67, 73

Morio, J., Jacquemart, D., Balesdent, M., and Marzat, J. (2013). Optimisation of interacting particle systems for rare event estimation. *Computational Statistics & Data Analysis*, 66(0):117 – 128. 215

Nataf, A. (1962). Détermination des distributions dont les marges sont données (in french). *Comptes rendus de l'Académie des Sciences*, 225:42–43. 63, 89

Neddermeyer, J. C. (2009). Computationally efficient nonparametric importance sampling. *Journal of the American Statistical Association*, 104:788–802. 67

Nguyen, N.-V., Choi, S.-M., Kim, W.-S., Lee, J.-W., Kim, S., Neufeld, D., and Byun, Y.-H. (2013). Multidisciplinary unmanned combat air vehicle system design using multi-fidelity model. *Aerospace Science and Technology*, 26(1):200–210. 26

Niederreiter, H. and Spanier, J. (2000). *Monte Carlo and Quasi-Monte Carlo Methods*. Springer. 179

Nissen, V. and Propach, J. (1998). On the robustness of population-based versus point-based optimization in the presence of noise. *Evolutionary Computation, IEEE Transactions on*, 2(3):107–119. 105, 236, 308

Noton, A. R. M. (2013). *Introduction to variational methods in control engineering*. Elsevier. 122

Oakley, D. R., Sues, R. H., and Rhodes, G. S. (1998). Performance optimization of multidisciplinary mechanical systems subject to uncertainties. *Probabilistic Engineering Mechanics*, 13(1):15–26. 17, 83, 303

Ortega, J. M. (1973). Stability of difference equations and convergence of iterative processes. *SIAM Journal on Numerical Analysis*, 10(2):268–282. 30

Pate-Cornell, M. (1986). Probability and uncertainty in nuclear safety decisions. *Nuclear Engineering and Design*, 93(2):319–327. 46

Peri, D. and Campana, E. F. (2003). Multidisciplinary design optimization of a naval surface combatant. *Journal of Ship Research*, 47(1):1–12. 26

Picheny, V. (2009). *Improving accuracy and compensating for uncertainty in surrogate modeling.* PhD thesis, University of Florida. 71, 184, 305

Picheny, V., Ginsbourger, D., Roustant, O., Haftka, R. T., and Kim, N.-H. (2010). Adaptive designs of experiments for accurate approximation of a target region. *Journal of Mechanical Design*, 132(7):071008. 69, 73

Platt, J. C. (1999). Probabilistic outputs for support vector machines and comparisons to regularized likelihood methods. In *Advances in large margin classifiers*, pages 61–74. MIT Press. 73

Poles, S. and Lovison, A. (2009). A polynomial chaos approach to robust multiobjective optimization. *Proceedings of Hybrid and Robust Approaches to Multiobjective Optimization*. 57

Price, K., Storn, R. M., and Lampinen, J. A. (2006). *Differential evolution: a practical approach to global optimization*. Springer. 106

Qiu, Z., Yang, D., and Elishakoff, I. (2008). Probabilistic interval reliability of structural systems. *International Journal of Solids and Structures*, 45(10):2850–2860. 97, 98, 306

Rackwitz, R. (2001). Reliability analysis a review and some perspectives. *Structural Safety*, 23(4):365–395. 89

Rackwitz, R. and Flessler, B. (1978). Structural reliability under combined random load sequences. *Computers & Structures*, 9(5):489–494. 63

Rafique, A. F., LinShu, H., Kamran, A., and Zeeshan, Q. (2010). Multidisciplinary design of air launched satellite launch vehicle: Performance comparison of heuristic optimization methods. *Acta Astronautica*, 67(7):826–844. 93

Rajashekhar, M. and Ellingwood, B. (1993). A new look at the response surface approach for reliability analysis. *Structural Safety*, 12(3):205–220. 192

Ranjan, P., Bingham, D., and Michailidis, G. (2008). Sequential experiment design for contour estimation from complex computer codes. *Technometrics*, 50(4):527–541. 73

Rasmussen, N. C. (1974). *Reactor safety study: An assessment of accident risks in US commercial nuclear power plants*. NTIS. 46

Rattray, M. and Shapiro, J. (1998). Noisy fitness evaluation in genetic algorithms and the dynamics of learning. *R. K. Belew and M. D. Vose, Eds. San Mateo, CA: Morgan Kaufmann*, pages 117–139. 105

Ricciardi, A. (1989). Complete geometrical analysis of cylindrical star grains. In *AIAA, ASME, SAE, and ASEE, Joint Propulsion Conference, 25 th, Monterey, CA*, page 1989. 282, 283

Ricciardi, A. (1992). Generalized geometric analysis of right circular cylindrical star perforated and tapered grains. *Journal of Propulsion and Power*, 8(1):51–58. 163

Rosenblatt, M. (1952). Remarks on a multivariate transformation. *The annals of mathematical statistics*, 23(3):470–472. 63, 89

Rubinstein, R. Y. and Kroese, D. P. (2004). *The Cross-Entropy method: a unified approach to combinatorial optimization, Monte-Carlo simulation and machine learning*. Springer Science & Business Media. 66, 67, 180, 320

Rubinstein, R. Y. and Kroese, D. P. (2011). *Simulation and the Monte Carlo method*, volume 707. John Wiley & Sons. 201, 296

Sankararaman, S. and Mahadevan, S. (2012). Likelihood-based approach to multidisciplinary analysis under uncertainty. *Journal of Mechanical Design*, 134(3):031008–031012. 31, 91, 92

Sasena, M. J. (2002). *Flexibility and efficiency enhancements for constrained global design optimization with kriging approximations*. PhD thesis, University of Michigan. 70, 71, 183, 320

Schittkowski, K. (1986). Nlpql: A fortran subroutine solving constrained nonlinear programming problems. *Annals of operations research*, 5(2):485–500. 74

Schlüter, M. and Gerdts, M. (2010). The oracle penalty method. *Journal of Global Optimization*, 47(2):293–325. 108, 132

Schueremans, L. and Van Gemert, D. (2005). Use of Kriging as Meta-model in simulation procedures for structural reliability. In *9th International conference on structural safety and reliability, Rome*, pages 2483–2490. 71, 305

Schwartz, L. (1957). *Théorie des Distributions: Vol.: 1*. Hermann & Cie. 200

Schwefel, H.-P. and Rudolph, G. (1995). *Contemporary evolution strategies*. Springer. 108, 236

Shafer, G. (1976). *A mathematical theory of evidence*, volume 1. Princeton university press Princeton. 47, 96, 302

Shan, S. and Wang, G. G. (2010). Survey of modeling and optimization strategies to solve high-dimensional design problems with computationally-expensive black-box functions. *Structural and Multidisciplinary Optimization*, 41(2):219–241. 193

Shawe-Taylor, J. and Cristianini, N. (2004). *Kernel methods for pattern analysis*. Cambridge university press. 73

Silverman, B. W. (1986). *Density estimation for statistics and data analysis*, volume 26. CRC press. 62

Smolyak, S. (1963). Quadrature and interpolation formulas for tensor products of certain classes of functions. In *Dokl. Akad. Nauk SSSR*, volume 4, page 111. 56

Sobieszczanski-Sobieski, J. (1988). Optimization by decomposition: a step from hierarchic to non-hierarchic systems. 33, 300

Sobieszczanski-Sobieski, J., Agte, J., and Sandusky, R. (1998). Bi-level integrated system synthesis (bliss). langley research center, hampton, virginia. *NASA Technical Report TM-1998-208715*. 33, 37, 300

Sobieszczanski-Sobieski, J., Agte, J. S., and Sandusky, R. R. (2000). Bilevel integrated system synthesis. *AIAA journal*, 38(1):164–172. 37

Sobieszczanski-Sobieski, J. and Haftka, R. (1997). Multidisciplinary aerospace design optimization: survey of recent developments. *Structural and Multidisciplinary Optimization*, 14(1):1–23. 15, 26, 294

Sobol, I. M. (1994). *A primer for the Monte Carlo method*. CRC press. 62

Socha, K. and Dorigo, M. (2008). Ant colony optimization for continuous domains. *European journal of operational research*, 185(3):1155–1173. 108

Sokolowski, J. and Zolesio, J.-P. (1992). *Introduction to shape optimization*. Springer. 122

Song, H., Choi, K. K., Lee, I., Zhao, L., and Lamb, D. (2013). Adaptive virtual support vector machine for reliability analysis of high-dimensional problems. *Structural and Multidisciplinary Optimization*, 47(4):479–491. 73

Song, S., Lu, Z., and Qiao, H. (2009). Subset simulation for structural reliability sensitivity analysis. *Reliability Engineering & System Safety*, 94(2):658–665. 199, 201

Soundappan, P., Nikolaidis, E., Haftka, R. T., Grandhi, R., and Canfield, R. (2004). Comparison of evidence theory and bayesian theory for uncertainty modeling. *Reliability engineering & System safety*, 85(1):295–311. 52

Steinwart, I. and Christmann, A. (2008). *Support vector machines*. Springer, New York, USA. 73

Sudret, B. (2007). Uncertainty propagation and sensitivity analysis in mechanical models–contributions to structural reliability and stochastic spectral methods. *Habilitation à Diriger la Recherches, Université Blaise Pascal, Clermont-Ferrand, France*. 77

Sudret, B. and Der Kiureghian, A. (2002). Comparison of finite element reliability methods. *Probabilistic Engineering Mechanics*, 17(4):337–348. 77

Summerfield, M. (1951). A theory of unstable combustion in liquid propellant rocket systems. *Journal of the American Rocket Society*, 21(5):108–114. 161

Sutton, G. P. and Biblarz, O. (2010). *Rocket propulsion elements*. John Wiley & Sons. 153

Swiler, L. P., Paez, T. L., and Mayes, R. L. (2009). Epistemic uncertainty quantification tutorial. In *Proceedings of the 27th International Modal Analysis Conference*. 59

Tedford, N. P. and Martins, J.R.R.A (2006). On the common structure of mdo problems: a comparison of architectures. In *Proceedings of the 11th AIAA/ISSMO multidisciplinary analysis and optimization conference, Portsmouth, VA, AIAA*, volume 7080, page 2006. 30

Tedford, N. P. and Martins, J.R.R.A (2010). Benchmarking multidisciplinary design optimization algorithms. *Optimization and Engineering*, 11(1):159–183. 33

Thunnissen, D. P. (2003). Uncertainty classification for the design and development of complex systems. In *3rd annual predictive methods conference*, pages 1–16. 46, 296, 301

Tou, J. T. and Gonzalez, R. C. (1974). *Pattern recognition principles*. Addison Wesley, London, UK. 73

Vapnik, V. (2000a). *The nature of statistical learning theory*. springer. 58, 125

Vapnik, V. N. (2000b). The nature of statistical learning theory. statistics for engineering and information science. *Springer-Verlag*. 74

Vapnik, V. N. and Vapnik, V. (1998). *Statistical learning theory*, volume 2. Wiley, New York, USA. 56, 73

Vazquez, E. and Bect, J. (2009). A Sequential Bayesian algorithm to estimate a probability of failure. In *15th IFAC, Symposium on System Identification (SYSID'09), 5 pages, Saint-Malo, France, July 6-8*. 71, 305

Walley, P. (1996). Measures of uncertainty in expert systems. *Artificial intelligence*, 83(1):1–58. 96

Wand, M. P. and Jones, M. C. (1994). *Kernel smoothing*. Crc Press. 59, 67

Wang, Y., Yu, X., and Du, X. (2012). Reliability analysis with svm and gradient information at MPP. In *Proceedings of the seventh China-Japan-Korea joint symposium on optimization of structural and mechanical systems, Huanshang, China, June*. 76

Wiener, N. (1938). The homogeneous chaos. *American Journal of Mathematics*, pages 897–936. 56

Xiao, N.-C., Huang, H.-Z., Wang, Z., Pang, Y., and He, L. (2011). Reliability sensitivity analysis for structural systems in interval probability form. *Structural and Multidisciplinary Optimization*, 44(5):691–705. doi:10.1007/s00158-011-0652-9. 100

Xiong, F., Chen, W., Xiong, Y., and Yang, S. (2011). Weighted stochastic response surface method considering sample weights. *Structural and Multidisciplinary Optimization*, 43(6):837–849. 57

Xiong, F., Liu, Y., and Yang, S. (2012). A new probabilistic distribution matching patc formulation using polynomial chaos expansion. *Engineering Optimization*, 44(7):843–858. 120

Xiong, F., Sun, G., Xiong, Y., and Yang, S. (2014). A moment-matching robust collaborative optimization method. volume 28, pages 1365–1372. Springer. 88

Yang, X., Liu, Y., Gao, Y., Zhang, Y., and Gao, Z. (2014). An active learning kriging model for hybrid reliability analysis with both random and interval variables. *Structural and Multidisciplinary Optimization, Publication pending*, pages 1–14. doi:10.1007/s00158-014-1189-5. 101, 307

Yao, W., Chen, X., Huang, Y., and van Tooren, M. (2013). An enhanced unified uncertainty analysis approach based on first order reliability method with single-level optimization. *Reliability Engineering & System Safety*, 116(0):28–37. 100

Yao, W., Chen, X., Luo, W., van Tooren, M., and Guo, J. (2011). Review of uncertainty-based multidisciplinary design optimization methods for aerospace vehicles. *Progress in Aerospace Sciences*, 47(6):450–479. 17, 46, 80, 81, 302

Yao, W., Chen, X., Ouyang, Q., and Van Tooren, M. (2012). A surrogate based multistage-multilevel optimization procedure for multidisciplinary design optimization. *Structural and multidisciplinary optimization*, 45(4):559–574. 93

Yao, W., Guo, J., Chen, X., and van Tooren, M. (2010). Utilizing uncertainty multidisciplinary design optimization for conceptual design of space systems. In *Proc. of the 8th Conference on Systems Engineering Research, Hoboken, NJ, USA*. 93

Yeniay, O., Unal, R., and Lepsch, R. A. (2006). Using dual response surfaces to reduce variability in launch vehicle design: a case study. *Reliability Engineering & System Safety*, 91(4):407–412. 93

Yi, S.-I., Shin, J.-K., and Park, G. (2008). Comparison of MDO methods with mathematical examples. *Structural and Multidisciplinary Optimization*, 35(5):391–402. 33

Yoo, D. and Lee, I. (2014). Sampling-based approach for design optimization in the presence of interval variables. *Structural and Multidisciplinary Optimization*, 49(2):253–266. 203

Youn, B. D., Choi, K. K., Yang, R.-J., and Gu, L. (2004). Reliability-based design optimization for crashworthiness of vehicle side impact. *Structural and Multidisciplinary Optimization*, 26(3):272–283. 199

Zadeh, L. A. (1978). Fuzzy sets as a basis for a theory of possibility. *Fuzzy sets and systems*, 1(1):3–28. 81

Zadeh, P. M. and Toropov, V. V. (2002). Multi-fidelity multidisciplinary design optimization based on collaborative optimization framework. In *AIAA 2002-5504, Proc. 9th AIAA/ISSMO Symp. Multidisciplinary Analysis & Optimization*. 34

Zaman, K. and Mahadevan, S. (2013). Robustness-based design optimization of multidisciplinary system under epistemic uncertainty. *AIAA Journal*, 51(5):1021–1031. 93

Zaman, K., McDonald, M., Mahadevan, S., and Green, L. (2011). Robustness-based design optimization under data uncertainty. *Structural and Multidisciplinary Optimization*, 44(2):183–197. 93

Zang, T. A., Hemsch, M. J., Hilburger, M. W., Kenny, S. P., Luckring, J. M., Maghami, P., Padula, S. L., and Stroud, W. J. (2002). *Needs and opportunities for uncertainty-based multidisciplinary design methods for aerospace vehicles*. NASA, Langley Research Center. 15, 16, 17, 42, 294, 295

Zeitlin, N. P., Schaefer, S., Brown, B., Clements, G., and Fawcett, M. (2012). NASA ground and launch systems processing technology area roadmap. In *Aerospace Conference, 2012 IEEE*, pages 1–19. IEEE. 13, 294

Zhang, H. (2012). Interval importance sampling method for finite element-based structural reliability assessment under parameter uncertainties. *Structural Safety*, 38(0):1–10. 98

Zhang, H., Mullen, R. L., and Muhanna, R. L. (2010). Interval monte carlo methods for structural reliability. *Structural Safety*, 32(3):183–190. 97, 98, 306

Zhang, J. and Zhang, B. (2013a). A collaborative approach for multidisciplinary systems reliability design and optimization. *Advanced Materials Research*, 694:911–914. 90

Zhang, J. and Zhang, B. (2013b). A collaborative strategy for reliability-based multidisciplinary design optimization. In *Computer Supported Cooperative Work in Design (CSCWD), 2013 IEEE 17th International Conference on*, pages 104–109. IEEE. 90

Zhang, P. (1996). Nonparametric importance sampling. *Journal of the American Statistical Association*, 91(435):1245–1253. 67

Zhang, X. and Huang, H.-Z. (2010). Sequential optimization and reliability assessment for multidisciplinary design optimization under aleatory and epistemic uncertainties. *Structural and Multidisciplinary Optimization*, 40(1-6):165–175. 47

Zhou, K., Doyle, J. C., Glover, K., et al. (1996). *Robust and optimal control*, volume 40. Prentice hall New Jersey. 122

Zou, T. and Mahadevan, S. (2006). A direct decoupling approach for efficient reliability-based design optimization. *Structural and Multidisciplinary Optimization*, 31(3):190–200. 199

École Nationale Supérieure des Mines de Saint-Étienne

NNT: 2015 EMSE 0792

Loïc Brevault

Contributions to Multidisciplinary Design Optimization under uncertainty, application to launch vehicle design

Speciality: Applied Mathematics

Keywords: Multidisciplinary Design Optimization, Uncertainty, Launch vehicle design, Surrogate model, Reliability analysis

Abstract :
Launch vehicle design is a Multidisciplinary Design Optimization problem whose objective is to find the launch vehicle architecture providing the optimal performance while ensuring the required reliability. In order to obtain an optimal solution, the early design phases are essential for the design process and are characterized by the presence of uncertainty due to the involved physical phenomena and the lack of knowledge on the used models. This thesis is focused on methodologies for multidisciplinary analysis and optimization under uncertainty for launch vehicle design. Three complementary topics are tackled. First, two new formulations have been developed in order to ensure adequate interdisciplinary coupling handling. Then, two new reliability techniques have been proposed in order to take into account the various natures of uncertainty, involving surrogate models and efficient sampling methods. Eventually, a new approach of constraint handling for optimization algorithm "Covariance Matrix Adaptation - Evolutionary Strategy" has been developed to ensure the feasibility of the optimal solution. All the proposed methods have been compared to existing techniques in literature on analysis and design test cases of launch vehicles. The results illustrate that the proposed approaches allow the improvement of the efficiency of the design process and of the reliability of the found solution.

École Nationale Supérieure des Mines de Saint-Étienne

NNT: 2015 EMSE 0792

Loïc Brevault

Contributions à l'optimisation multidisciplinaire sous incertitudes, application à la conception de lanceurs

Spécialité: Mathématiques appliquées

Mots Clefs: Optimisation Multidisciplinaire, Incertitudes, Lanceurs, Conception, Analyse de fiabilié, Métamodèle

Résumé:
La conception de lanceurs est un problème d'optimisation multidisciplinaire dont l'objectif est de trouver l'architecture du lanceur qui garantit une performance optimale tout en assurant un niveau de fiabilité requis. En vue de l'obtention de la solution optimale, les phases d'avant-projet sont cruciales pour le processus de conception et se caractérisent par la présence d'incertitudes dues aux phénomènes physiques impliqués et aux méconnaissances existantes sur les modèles employés. Cette thèse s'intéresse aux méthodes d'analyse et d'optimisation multidisciplinaire en présence d'incertitudes afin d'améliorer le processus de conception de lanceurs. Trois sujets complémentaires sont abordés. Tout d'abord, deux nouvelles formulations du problème de conception ont été proposées afin d'améliorer la prise en compte des interactions disciplinaires. Ensuite, deux nouvelles méthodes d'analyse de fiabilité, permettant de tenir compte d'incertitudes de natures variées, ont été proposées, impliquant des techniques d'échantillonnage préférentiel et des modèles de substitution. Enfin, une nouvelle technique de gestion des contraintes pour l'algorithme d'optimisation "Covariance Matrix Adaptation - Evolutionary Strategy" a été développée, visant à assurer la faisabilité de la solution optimale. Les approches développées ont été comparées aux techniques proposées dans la littérature sur des cas tests d'analyse et de conception de lanceurs. Les résultats montrent que les approches proposées permettent d'améliorer l'efficacité du processus d'optimisation et la fiabilité de la solution obtenue.

Office National d'Études et de Recherches Aérospatiales
Chemin de la Hunière et des Joncherettes – BP 80100
91123 PALAISEAU Cedex
Tél. : +33 1 80 38 60 60 - Fax : +33 1 80 38 65 10
http://www.onera.fr